

JOURNAL OF AGRICULTURAL SCIENCES

TARIM BİLİMLERİ DERGİSİ

ANKARA UNIVERSITY FACULTY OF AGRICULTURE

e-ISSN 2148-9297

JIAS



Year 24

Volume 30

Issue 03

Ankara University
Faculty of Agriculture

JOURNAL OF AGRICULTURAL SCIENCES

**TARIM BİLİMLERİ
DERGİSİ**

e-ISSN: 2148-9297

Ankara - TÜRKİYE



e-ISSN 2148-9297

**JOURNAL OF
AGRICULTURAL SCIENCES**

TARIM BİLİMLERİ DERGİSİ
ANKARA UNIVERSITY FACULTY OF AGRICULTURE

Product Information

Publisher	Ankara University, Faculty of Agriculture
Owner (On Behalf of Faculty)	Prof. Dr. Hasan Huseyin ATAR
Editor-in-Chief	Prof. Dr. Halit APAYDIN
Journal Administrator	Salih OZAYDIN
Library Coordinator	Dr. Can BESIMOGLU
IT Coordinator	Lecturer Murat KOSECAVUS
Graphic Design	Ismet KARAASLAN
Date of Online Publication	23.07.2024
Frequency	Published four times a year
Type of Publication	Double-blind peer-reviewed, widely distributed periodical
Aims and Scope	JAS publishes high quality original research articles that contain innovation or emerging technology in all fields of agricultural sciences for the development of agriculture.
Indexed and Abstracted in	Clarivate Science Citation Index Expanded (SCIE) Elsevier Scopus TUBITAK-ULAKBIM-TRDizin CAB International EBSCO FAO-AGRIS SOBIAD OpenAire BASE IFIS CNKI

Management Address

Journal of Agricultural Sciences - Tarım Bilimleri Dergisi
Ankara University Faculty of Agriculture Publication Department 06110
Diskapi/Ankara-Türkiye
Telephone : +90 312 596 14 24 | Fax : +90 312 317 67 24
E-mail: tbdeditor@ankara.edu.tr | <http://jas.ankara.edu.tr/>



e-ISSN 2148-9297

JOURNAL OF
AGRICULTURAL SCIENCES

TARIM BİLİMLERİ DERGİSİ
ANKARA UNIVERSITY FACULTY OF AGRICULTURE

Editor-in-Chief Halit APAYDIN, Ankara University, Ankara, TÜRKİYE

Managing Editor Muhittin Onur AKCA, Ankara University, Ankara, TÜRKİYE

Ahmet ULUDAG, Canakkale Onsekiz Mart University, TÜRKİYE

Akasya TOPCU, Ankara University, TÜRKİYE

Ali Adnan HAYALOĞLU, Inonu University, TÜRKİYE

Ali UNLUKARA, Erciyes University, TÜRKİYE

Anna Maria DE GIROLAMO, Italian National Research
Council, ITALY

Belgin COSGE ŞENKAL, Yozgat Bozok University, TÜRKİYE

Bilal RASOOL, Government College University Faisalabad,
Punjab, PAKISTAN

Burhan OZKAN, Akdeniz University, TÜRKİYE

Claudia Di BENE, Research Centre for Agriculture and
Environment, ITALY

Duygu SEMİZ, Ankara University, TÜRKİYE

Engin YENİCE, Ankara University, TÜRKİYE

Erhan MUTLU, Akdeniz University, TÜRKİYE

Farhat JABEEN, Government College University, PAKISTAN

Fatma Sezer ŞENOL DENİZ, Gazi University, TÜRKİYE

Fazıl SEN, Van Yuzuncu Yil University, TÜRKİYE

Filiz ERTUNC, Ankara University, TÜRKİYE

Giuseppe BADAGLIACCA, Mediterranean University of
Reggio Calabria, ITALY

Giuseppe GAVAZZI, University of Milan, ITALY

Giuseppe PULIGHE, CREA Research Centre for Agricultural
Policies and Bioeconomy, ITALY

Gunars LACIS, Latvia University of Life Sciences and Techn.,
Dobele, LATVIA

Habib ALI, Khwaja Fareed University of Eng. and Inf., Rahim Yar
Khan, PAKISTAN

Hasan YETİM, Istanbul Sebahattin Zaim University, TÜRKİYE

Ismail KARACA, Isparta University of Applied Sciences,
TÜRKİYE

Isil ÇAKCI, Ankara University, TÜRKİYE

Julia MALYSH, All-Russian Institute for Plant Protection,
RUSSIA

Karina BATISTA, Instituto de Zootecnia, BRAZIL

Mahmut ELP, Kastamonu University, TÜRKİYE

Mine TURKTAS, Gazi University, TÜRKİYE

Mehmet Emin CALISKAN, Nigde Omer Halisdemir University,
TÜRKİYE

Muhammad SULTAN, Bahauddin Zakariya University, Multan,
PAKISTAN

Panagiotis SIMITZIS, Agricultural University of Athens,
GREECE

Peter SCHAUSBERGER, University of Vienna, AUSTRIA

Renata BAZOK, University of Zagreb, CROATIA

Sefa TARHAN, Tokat Gaziosmanpaşa University, TÜRKİYE

Selen DEVİREN SAYGIN, Ankara University, TÜRKİYE

Semra DEMİR, Van Yuzuncu Yil University, TÜRKİYE

Serpil SAHİN, Middle East Technical University, TÜRKİYE

Stanislav TRDAN, University of Ljubljana, SLOVENIA

Tuba SANLI, Ankara University, TÜRKİYE

Turkan AKTAS, Namık Kemal University, TÜRKİYE

Umut TOPRAK, Ankara University, TÜRKİYE

Yang LI, Shihezi University, CHINA

Yonca YUCEER, Canakkale Onsekiz Mart University,
TÜRKİYE

Advisory Board

Cengiz SAYIN, Akdeniz University, Antalya, TÜRKİYE

Fahrettin GÖĞÜŞ, Gaziantep University, Gaziantep, TÜRKİYE

Fazlı OZTURK, Ankara University (Em.), Ankara, TÜRKİYE

Ensar BASPINAR, Ankara University, Ankara, TÜRKİYE

Sultan COBANOGLU, Ankara University (Em.), Ankara, TÜRKİYE



e-ISSN 2148-9297

JOURNAL OF
AGRICULTURAL SCIENCES

TARIM BİLİMLERİ DERGİSİ
ANKARA UNIVERSITY FACULTY OF AGRICULTURE

CONTENTS

2024, 30(3)

Invited reviews:

- 413 **Review of Process and Extraction Effects on the Bioavailability of Anthocyanins in Grapes**
Zehra Gulsunoglu-Konuskan, Sena Bakir, Tilahun A. Teka, Ayla Elmi Kashtiban, Atefeh Karimidastjerd
- 424 **The Use of Medical Foods to Fight Chronic Diseases: A Narrative Review**
Hilal Meral, Aslıhan Demirdöven
- 436 **Predatory Protists: The Key Players in the Quest for Sustainable Agricultural Practices**
Seda Ozer Bodur, Mayu Fujino, Rasit Asiloglu

Research articles:

- 444 **Characterization and antimicrobial properties of silver nanoparticles biosynthesized from cornelian cherry (*Cornus mas* L.)**
Tuğçe Özeşer, Nural Karagozlu
- 458 ***Aronia melanocarpa* (Michaux) Elliot Fruit Juice Attenuates Acetaminophen-induced Hepatotoxicity on Larval Zebrafish Model**
Çiğdem Bilgili, Gülçin Çakan Akdoğan
- 464 **Machine Learning-based for Automatic Detection of Corn-Plant Diseases Using Image Processing**
Khaled Adil Dawood Idress, Omsalma Alsadig Adam Gadalla, Yeşim Benal Öztekin, Geoffrey Prudence Baitu
- 477 **Effects of 24-Epibrassinolide on Shoot tip Cultures Under NaCl Stress in Tomato (*Solanum lycopersicum* L.)**
Emel Yılmaz-Gökdoğan, Betül Burun
- 488 **The Photochemical and Antioxidant Defence Strategies of Two Maize Genotypes Exposed to Zinc Toxicity at the Seedling Stage**
Yasemin Ekmekçi, Şeküre Çulha Erdal, Şeniz Ünalın Okar, Nuran Çiçek, Deniz Tanyolaç
- 501 **Instrumental use of Marine Bacteria to Stimulate Growth in Seaweed**
Pham Thi Mien, Phan Minh-Thu, Bui Thi Ngoc Trieu, Nguyen Minh Hieu, Dao Viet Ha
- 513 **A comprehensive Assessment of Sunflower Genetic Diversity Against *Macrophomina phaseolina***
Nemanja Ćuk, Sandra Cvejić, Velimir Mladenov, Milan Jocković, Miloš Krstić, Brankica Babec, Siniša Jocić, Boško Dedić
- 526 **Agricultural Land-based Functional Model for Effective Rural Land Management in Türkiye**
Orhan Ercan
- 546 **Health Risk Assessment of Metals via Consumption of Rapa Whelk (*Rapana venosa*) from the Black Sea**
Baris Bayrakli, Murat Yigit, Mutlu Altuntas, Masashi Maita
- 562 **Hemp Seed Priming via Different Agents to Alleviate Temperature Stress**
Sibel Day, Nilüfer Koçak-Şahin, Burak Önel

- 570 Creation of Gold Nanoparticles with the Use of *Nigella sativa* L. Plant Extract Derived from Agricultural Waste Components and Its Potential as a Biomedical Agent**
Mehmet Fırat Baran
- 584 Molecular Characterization and Dose-Response to 2,4-D Herbicide in *Convolvulus arvensis* Populations in Türkiye**
Yücel Karaman, Nihat Tursun, Hikmet Murat Sipahiođlu
- 594 Comparative Assessment of Solar Dryer with Thermal Energy Storage System and Heat Pump Dryer in Terms of Performance Parameters and Food Analysis**
Özlem Timurtas, Gökkan Gürlek



Review of Process and Extraction Effects on the Bioavailability of Anthocyanins in Grapes

Zehra Gulsunoglu-Konuskan^{a*} , Sena Bakir^b , Tilahun A. Teka^c , Ayla Elmi Kashtiban^d ,
Atefeh Karimidastjerd^e 

^aIstanbul Aydin University, Faculty of Health Science, Nutrition and Dietetics Department, 34295, Istanbul, TURKEY

^bRecep Tayyip Erdogan University, Tourism Faculty, Department of Gastronomy and Culinary Arts, 53400, Rize, TURKEY

^cJimma University, Department of Postharvest Management, College of Agriculture and Veterinary Medicine, 307, Jimma, ETHIOPIA

^dUrmia University, Faculty of Agriculture, Department of Food Science and Technology, Urmia, IRAN

^eYildiz Technical University, Faculty of Chemical and Metallurgical Engineering, Food Engineering Department, 34220, Istanbul, TURKEY

ARTICLE INFO

Review Article

Corresponding Author: Zehra Gulsunoglu-Konuskan, E-mail: zehragulsunoglu@aydin.edu.tr

Received: 12 July 2023 / Revised: 27 December 2023 / Accepted: 10 January 2024 / Online: 23 July 2024

Cite this article

Gulsunoglu-Konuskan Z, Bakir S, Teka T A, Kashtiban A E, Karimidastjerd A (2024). Review of Process and Extraction Effects on the Bioavailability of Anthocyanins in Grapes. *Journal of Agricultural Sciences (Tarim Bilimleri Dergisi)*, 30(3):413-423. DOI: 10.15832/ankutbd.1326299

ABSTRACT

Grapes are widely consumed worldwide in various forms, including fresh and dried, or processed into products like juice, vinegar, wine, and so on. Anthocyanins, mainly found in grapes, are responsible for various health-promoting effects and contribute to their colours such as red, purple, and blue. Although grapes contain a high quantity of anthocyanins, their bioavailability is considered limited. Anthocyanins may be absorbed by the gastrointestinal wall, undergo intensive first-pass metabolism, and emerge as metabolites in systemic circulation. A significant percentage of some anthocyanins can enter the large intestine and undergo breakdown

induced by digestive system microorganisms. Several factors, such as pH, temperature, light, and solvents, can affect anthocyanin bioavailability, and processing grapes into products may impact their bioavailability. Considering the high market share of grapes and grape products, it is important to understand the effects of processing on anthocyanin bioavailability. This review discusses changes in the bioavailability of anthocyanins found in grapes and grape products during food processing, the effect of extraction conditions on bioavailability, as well as the health-promoting effects of grapes and grape products.

Keywords: Metabolism, Absorption, Grape products, Anthocyanins, Process conditions

1. Introduction

Grapes are very popular and one of the most produced crops around the world. According to the Food and Agriculture Organization of the United Nations (FAO), China, Italy, Spain, France, the United States of America, and Turkey are leading grape producers (FAO 2021). Different products can be made from grapes, such as non-alcoholic fermented juices like hardaliye (a traditional Turkish beverage based on red grapes) and non-fermented beverages such as grape juice, alcoholic fermented beverages like wines, concentrated grape juice (doshab, pekmez or molasses) and grape spreads like grape jelly, jam, preserves, butter, and marmalade (Kaya & Maskan 2003; Aladeboyeje & Şanlı 2021). All these grape-derived products may contain different types and quantities of anthocyanins due to various processing steps, such as fermentation, evaporation, drying, and so on.

The quantity and quality of anthocyanins in grapes and their products differ significantly from those found in other anthocyanin-rich fruits and vegetables due to factors such as the regulation of the anthocyanin biosynthetic pathway, the diversity of anthocyanin molecules, and the influence of rootstock on anthocyanin content (Alenazi et al. 2019). The main dietary sources of anthocyanins include red-coloured fruits, some vegetables and red wine. According to the FAO, the main anthocyanin-rich fruits and vegetables are produced annually in quantities of approximately 0.9 million tons for blueberries, 4 million tons for strawberries, 3.2 million tons for sour cherries and cherries, 0.7 million tons for raspberries, 4 million tons for plums and blackthorn, 1.7 million tons for eggplant, 0.5 million tons for cranberries, and 70 million tons for grapes (FAO 2021). The annual production of grapes is quite high compared to other anthocyanin-rich foods. Additionally, grapes have potential distinctive uses in food applications, setting them apart from other food sources.

Grapes and other grape-derived products have enormous potential for diverse biofunctional roles due to containing bioactive compounds, mainly anthocyanins, phenolic acids, flavonoids, stilbenes, and lipids. The health benefits of grapes have been

proven in several research studies, and they can reduce the risk of cardiovascular disease, cancer, and obesity, and have anti-inflammatory, antimicrobial, and antioxidative properties (Lee et al. 2017; Henriques et al. 2020; Sabra et al. 2021). The health benefits of anthocyanins are strongly influenced by their bioavailability.

The term “bioavailability” is defined by the Food and Drug Administration (FDA) as “*the rate and extent to which the active ingredient or moiety is absorbed and becomes available at the site of action*” (FDA 2001). Although anthocyanins constitute a significant class of phenolic compounds in grapes, their bioavailability is extremely low (Han et al. 2019). The low bioavailability of anthocyanins is mainly connected to poor absorption in the gastrointestinal tract. Moreover, this limitation may be related to low water solubility due to anthocyanins being present in foods as polymers or as glycosylated forms that bond covalently to food matrices (Polia et al. 2022). Most anthocyanins consumed through foods are conjugated, digested by the colon bacteria, and eliminated in urine and feces, resulting in low bioavailability (De Rosso et al. 2012; Fang 2015). Additionally, anthocyanin degradation occurs due to several environmental conditions, including temperature, light, solvents, changes in chemical structure, and pH fluctuations during processing. The purpose of this review is to inform readers about how the extraction method and its byproducts affect anthocyanin bioavailability in grapes and their products. The health benefits of anthocyanins in grapes are also reviewed.

2. Anthocyanins found in grapes and health benefits

Anthocyanins are a major class of flavonoids and possess diverse biological functions. Anthocyanins are water-soluble pigments that give blue, purple, and red colours to grape cultivars, and are primarily present in grape skin. Hundreds of anthocyanins have been identified until now. Delphinidin-, cyanidin-, petunidin-, peonidin- and malvidin-3-*O*-glucoside are the predominant anthocyanins found in *Vitis vinifera* grapes (Han et al. 2019). In contrast, other grape species, such as *V. labrusca*, contain both anthocyanin 3-monoglucoside and 3,5-diglucosides when compared to *V. vinifera* (de Castilhos et al. 2015). The anthocyanin content of grapes varies with grape variety, and is influenced by several environmental factors such as soil type, climate, and management practices (Han et al. 2019).

Anthocyanins have various bioactive properties beneficial to human health, including the prevention of cardiovascular diseases and possess antioxidant, anti-cancer, anti-inflammatory, antidiabetic, and anti-obesity activities, as well as neuroprotective effects and improving eye and brain health. Not only grape and grape products but also grape by-products, which are left over mainly from wine and juice industries, contain beneficial phenolic chemicals, including anthocyanins. In cholesterol-fed rabbits, the administration of grape seed proanthocyanidin extract at a concentration of 0.1% resulted in a 30%–50% reduction in atherosclerosis. This effect was primarily attributed to the inhibition of low-density lipoprotein (LDL) oxidation, and a 25% reduction in malondialdehyde levels, an index of lipid oxidation, in the aorta (Yamakoshi et al. 1999). In Caco-2 cells pretreated with red grape skin anthocyanins, glucose transporter 2 (GLUT2) expression increased compared to controls, suggesting that persistent consumption of anthocyanins may improve their bioavailability. Additionally, the anthocyanins in red grape skin inhibited glucose uptake by interfering with it (Faria et al. 2009).

The effects of anthocyanin-rich diets on transcription factors and genes/proteins involved in antioxidant and anti-inflammatory defence may be related to the presence of native anthocyanins in the brain, heart, and other tissues. Trials with sour cherries, grapes, blueberries, and bilberries demonstrated this process (Seymour et al. 2011; 2013). More specifically, anthocyanins play a role in brain function as they can pass the blood-brain barrier. Grape anthocyanins (8 mg/kg body weight dose) were identified in the brains of rats at a concentration of 192 ng/g barely 10 min after being introduced into the stomach, according to Passamonti et al. (2005). In a recent study, the researchers found out that giving rats a commercial anthocyanin extract made from grape skins (200 mg/kg for 25 days) had a preventative effect on behavioural alterations in a rat model of streptozotocin-induced dementia in sporadic Alzheimer's disease. The extract had protective properties against reactive oxygen species (ROS) and antioxidant enzymes, including superoxide dismutase, catalase, and glutathione peroxidase (Pacheco et al. 2018). In a subsequent study, where streptozotocin was injected into rats along with grapes, Jankowski et al. (2000) observed a significant drop in sugar levels in urine and blood serum. The authors proposed that anthocyanins reduce collagen, lipoproteins, and glycoprotein production, and elastase and adenosine deaminase activity, both of which are elevated in diabetics (Jankowski et al. 2000).

3. Bioavailability and metabolism of anthocyanins

Since anthocyanins are naturally present in many plant-based meals, a balanced diet inherently includes a significant amount of them (Hornedo-Ortega et al. 2021). In particular, consuming foods rich in anthocyanins, like grapes, was associated with reduced risk of several diseases (Mattioli et al. 2020). However, anthocyanin health benefits were linked to their metabolic byproducts. Bioavailability typically refers to the proportion of a nutrient that becomes accessible at its intended location for action after absorption from the gastrointestinal tract. It can also refer to the fraction of the nutrient that is absorbed and ready for use in physiological processes and storage (Fernández-García et al. 2009). Therefore, for anthocyanins to exert their metabolic functions, they must be bioavailable, requiring digestion and absorption as well as metabolism (Iglesias-Carres et al. 2019). Additionally, the bioavailability of anthocyanins can be influenced by their transport through the gut epithelium (Kamiloglu et al. 2015). Anthocyanins display a noteworthy level of stability and are capable of being absorbed during the gastric phase, with

only a small proportion undergoing hydrolysis. After simulated stomach digestion, there was a modest decrease in anthocyanin stability in the gastrointestinal cavity. Alkaline conditions and microbiota in the intestine can catabolize anthocyanins into different compounds like phenolic acids and aldehydes, making the intestine a major site for anthocyanin metabolism and absorption (Soares et al. 2018). This tendency is more pronounced in red wine anthocyanins, and this could be related to the complexity of anthocyanin structure (Oliveira et al. 2019). Data indicates that anthocyanins are highly affected by the intestinal system, whereas they remain relatively unaffected in the stomach. Cyanidin, the precursor pigment for other anthocyanins, can be transformed into them by phase I and phase II reactions. Cyanidin can be converted into peonidin due to methylation at the C-3' position, which can be catalyzed by 3'-*O*-methyltransferase (Yuzuak & Xie 2022). Methylation reactions are classified as phase II reactions that occur in mammals and increase the bioavailability, stability and biological properties (Gulsunoglu-Konuskan & Kilic-Akyilmaz 2021). 3'-5'-*O*-methyltransferase catalyzes delphinidin into petunidin, and petunidin into malvidin as a result of methylation (Pomar et al. 2005). Hydroxylation is one of the most common reactions to increase antioxidant potential due to the number and the position of -OH groups (Gulsunoglu-Konuskan & Kilic-Akyilmaz 2021). According to reports, the hydroxylation of cyanidin to delphinidin is also possible by the action of 3'-hydroxylase (Pomar et al. 2005). Additionally, protocatechuic and vanillic acid can form from cyanidin and peonidin glycosides. However, phenolic metabolites of delphinidin, malvidin, and petunidin glycosides are not stable and can be broken into smaller molecules (Fang 2015). The conversion mechanism of major grape anthocyanins is shown in Figure 1.

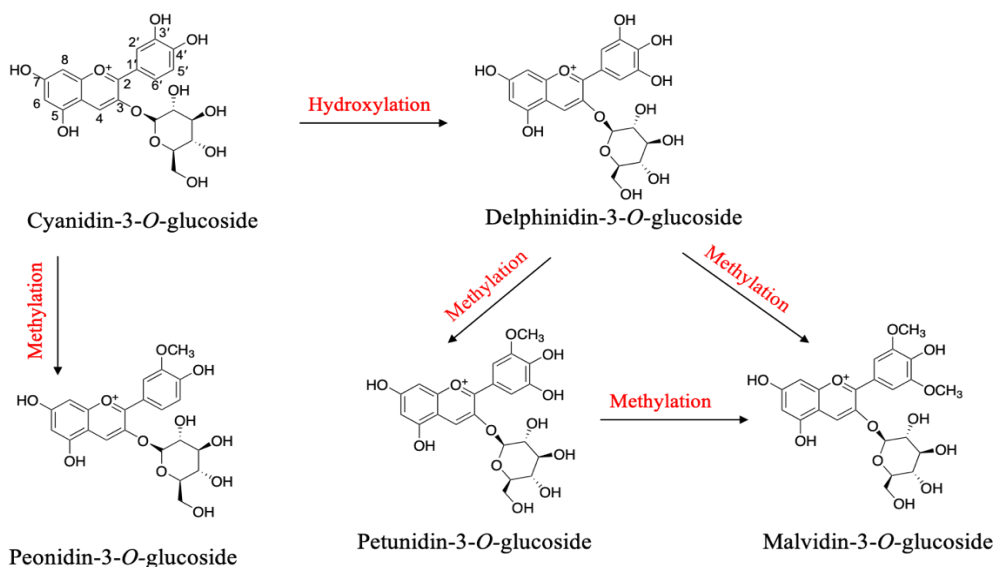


Figure 1- Schematic representation of conversion pathways for grape anthocyanins

The insoluble fraction yields a larger percentage of recovered anthocyanins (in some instances, the insoluble fraction yields all of the anthocyanins), implying that the food matrix may alter the action of digestive settings; thereby, preserving anthocyanins from degradation (Pineda-Vadillo et al. 2017). Gut bacteria may break down acylated anthocyanins more quickly than nonacylated anthocyanins. In obese mice administered a 12-week chronic dose of a Concord grape supplement rich in acylated anthocyanins, total anthocyanins in their fecal matter increased by a factor of ten compared to feces collected during the period of the late test week when antibiotics were given to suppress gut microbiota. The difference was more significant than that observed after administering nonacylated anthocyanin-rich berry supplements (Overall et al. 2017).

Compared to conventional grape-administered rats, the blood profile of rats administered organic grapes showed greater metabolite concentrations at two hours and lower metabolite concentrations at 24 hours. Consequently, the bioactivity of phenolic compounds may be influenced by their serum kinetic behaviour (Iglesias-Carres et al. 2019). Under gastrointestinal pH and temperature circumstances, the stability of anthocyanins and their breakdown products from Cabernet sauvignon red wine were investigated, and it was observed that anthocyanins can be degraded to phenolic acids under small intestine conditions when whole grapes are consumed (Yang et al. 2018). The decreased stability of anthocyanins during the intestinal phase of digestion can be attributed to factors such as the alkaline pH of the solution, leading to an increase in non-flavylium cation forms of anthocyanins. Additionally, the binding of anthocyanins to proteins and bile salts contributes to the formation of indigestible complexes, resulting in their subsequent precipitation (McDougall et al. 2005; Fleschhut et al. 2006). The pharmacokinetics and excretive profiles of phenolic metabolites were examined in 10 participants after the acute administration of a drink produced from red grape pomace. Only a few anthocyanin derivatives were tentatively discovered in trace amounts in 0–3 h urine samples from some volunteers and were consequently ignored (Castello et al. 2018). In a crossover study, 9 healthy volunteers consumed a single oral dosage of 400 mL red grape juice or red wine with dose-adjusted anthocyanin content (283.5 mg or 279.6 mg, respectively). Plasma and urine excretion both contained anthocyanin glycosides. Plasmatic antioxidant activity was also measured after the meal. Biokinetic criteria for single anthocyanins, such as AUC (the total area from zero to infinity), C_{max} (maximum plasma concentration), t_{max} (time to reach C_{max}), and the elimination rate $t_{1/2}$, were computed based on plasma

content. Total anthocyanin excretion in urine differed significantly, accounting for 0.18% (red wine) and 0.23% (red grape juice) of the administered dose, respectively. Additionally, when juice was consumed instead of wine, plasmatic antioxidant activity increased to higher levels. Red grape juice appeared to have better intestinal absorption of anthocyanins than red wine, suggesting a possible synergistic effect with the juice's glucose content (Bitsch et al. 2004).

Based on the findings of these studies, the concentrations of anthocyanins analyzed in both plasma and urine samples from the specific matrices and subjects were comparable, indicating a lack of significant differences. This suggests that the anthocyanins undergo minimal alterations from their entry into the bloodstream to their elimination through urine. Furthermore, anthocyanins exhibit rapid excretion within a 24-hour timeframe and possess a low absorption rate of less than 1%. Consequently, the glycosylated forms of anthocyanins were found to be more efficiently absorbed, leading to increased bioavailability.

4. Effects of processing methods on bioavailability of anthocyanin in grapes

The bioavailability of anthocyanins is influenced by key factors such as food matrix, food processing, enzymes involved in metabolism, and transport (Eker et al. 2019). Anthocyanins are highly reactive molecules and thus sensitive to degradation by exposure to oxygen, light, temperature, pH, and enzymes, affecting their chemistry, stability, and colour (Enaru et al. 2021). Degradation of anthocyanins can occur during food processing, extraction, and storage. Therefore, processing methods like heating, mechanical procedures, and domestic processes may contribute to anthocyanin degradation, potentially altering their antioxidant properties and bioavailability (Patras et al. 2010). Studies investigating the effect of thermal or non-thermal processing conditions on the bioavailability of anthocyanins found in grape and grape products are given in Table 1.

Table 1- Effect of processing on bioavailability of anthocyanins in grapes and grape products

Product type	Grape species	Anthocyanin intake	Experiment	Major findings	Reference
Grape juice	<i>V. labrusca</i>	17.5±22.5 μ mol mv-3-glu/100 mL	Human trials	Glycemia ↓ Blood levels of uric acid ↓ Plasma lipid peroxidation ↓ Plasma antioxidant capacity ↑	(Copetti et al. 2018)
Red grape juice	ND	283.5 mg/400 mL	Human trials	C_{max} (ng/mL)=100.1 T_{max} (h)=0.5 AUC ₀₋₁₈₀ (ng/mL.h)=168.4	(Bitsch et al. 2004)
Grape juice	<i>V. labrusca</i> Concord	238±6 μ mol/350 mL	<i>In vitro</i>	C_{max} (ng/mL)=1.0–2.0 nmol/L T_{max} (h)=1.3–33 Recovery in ileal effluent=47±9 μ mol Urinary excretion=612 nmol (0.26% of total anthocyanins)	(Stalmach et al. 2012)
Red wine	<i>V. vinifera</i> L. cv Syrah	126.27±14.73 mg mv-3-glu/L	<i>In vitro</i>	26% of anthocyanins released in mouth Anthocyanin content in stomach ↓ 36% pn-3-glu, 40% pt-3-aglu released in intestine	(Lingua et al. 2018)
Red wine	<i>V. labrusca</i>	66.7±10.2 μ mol mv-3-glu/100 mL	Human trials	Glycemia ↓ Blood levels of uric acid ↑ Plasma lipid peroxidation ↓ Plasma antioxidant capacity ↑	(Copetti et al. 2018)
Port red wine	ND	48.94±0.08 mg/100 mL	Human trials	C_{max} (mg/mL)=5.9±0.73 T_{max} (min)=90±17 AUC ₀₋₁₂₀ (mg/mL.min)=500.64±62.52	(Fernandes et al. 2017)
Red wine	<i>V. vinifera</i> Blaufrankisch (Lemberger)	279.6mg/400 mL	Human trials	C_{max} (ng/mL)=42.9 T_{max} (h)=1.5 AUC ₀₋₁₈₀ (ng/mL.h)=100.8	(Bitsch et al. 2004)
Grape extract	<i>V. vinifera</i>	3.85 g cyn-3-gal/kg	<i>In vivo</i>	Urinary anthocyanin concentration=33.2 nmol/L In plasma highest peaks= pt-3,5-diglu, mv-3,5-diglu	(He et al. 2006)
Red grape	<i>V. vinifera</i> L. cv Syrah	334.63±22.53 mg mv-3-glu/kg fw	<i>In vitro</i>	22% of anthocyanins released in mouth 45% of anthocyanins released in stomach 44% del-3-glu, 26% pn-3-glu, 53% pn-3-aglu released in intestine	(Lingua et al. 2018)

AUC: area under the curve of total anthocyanins, C_{max} : maximum plasma concentration, cyn-3-gal: cyanidin-3-galactoside, del-3-glu: delphinidin-3-glucoside, mv-3,5-diglu: malvinidin-3,5-diglucoside, mv-3-glu: malvinidin-3-glucoside, pn-3-aglu: peonidin-3-acetylglucoside, pn-3-glu: peonidin-3-glucoside, pt-3-aglu: petunidin-3-acetylglucoside, pt-3,5-diglu: petunidin-3,5-diglucoside, T_{max} : time to reach maximum C_{max} .

4.1. Maceration, pressing and fermentation

Maceration is the stage in which anthocyanins in grape skins are transferred to must and wine. Maceration and fermentation are not separate processes (Morata et al. 2021). Anthocyanins are transferred through diffusion from seeds and grape skins to wine during fermentation. The highest amount of anthocyanins is extracted during the first few days of maceration, after which no more extraction is usually observed, despite 30–40% of anthocyanins remaining in the crushed skins. Studies indicate anthocyanin extraction occurs in the first seven days of maceration from grape skins (Romero-Cascales et al. 2005). However, the highest anthocyanin extraction was accomplished during the first six days of fermentative maceration by freezing with dry-ice techniques (Busse-Valverde et al. 2011).

Fermentation and aging of the wine result in the chemical transformation of anthocyanins, providing pigments that can be more stable than the original anthocyanins (Ruta & Farcasanu 2019). In addition, a large number of differential metabolites were identified during the fermentation of wine and two in the post-fermentation process (Ai et al. 2021). Therefore, high amounts of anthocyanins are extracted from fermented grapes using moderate temperatures and short-time extraction (Vergara-Salinas et al. 2013). Anthocyanin concentrations in red wine range from 90 to 400 mg/L, depending on the age of the wine (Waterhouse 2002). The grapes of the *V. vinifera* variety include common wine grapes such as Cabernet sauvignon and Merlot, containing mainly anthocyanidin monoglycosides, especially malvidin-3-*O*-glucoside. Anthocyanidin diglycosides are primarily found in wine grape cultivars other than *V. vinifera*. *V. vinifera* hybrid cultivars contain monoglycosides and diglycosides of anthocyanidin (De Rosso et al. 2012). These anthocyanins contribute to the organoleptic and chemical properties of grapes and wines because of their interaction with other phenolic compounds as well as with proteins and polysaccharides.

The intestinal absorption of anthocyanins from red grape juice was improved compared to red wine, a phenomenon that can be explained by the synergistic effect of glucose content in the juice (Bitsch et al. 2004). Bub et al. (2001) reported that the C_{max} of malvidin-3-*O*-glucoside after drinking red wine or dealcoholized red wine was not substantially different (288 ± 127 nmol.h/L and 214 ± 124 nmol.h/L, respectively) and was approximately two times lower than that recorded after drinking red grape juice (662 ± 210 nmol.h/L). However, C_{max} was reached after 20 minutes for red wine, while it took 90 and 180 minutes to reach this value for dealcoholized red wine and red grape juice, respectively. This difference could be attributed to the possibility that the alcohol content may increase the absorption of malvidin-3-*O*-glucoside (Bub et al. 2001). The bioavailability of flavanol-anthocyanin dimer (+)-catechin-malvidin-3-*O*-glucoside, an anthocyanin derivative found in grape skins and red wine, was investigated with an intestinal model barrier by using Caco-2 cells to examine transepithelial transportation. The research showed that the Caco-2 cell barrier model can be successfully crossed by anthocyanins and flavanols, as well as dimeric complexes that contain both anthocyanins and flavanols (Fernandes et al. 2012).

4.2. Drying

Raisins are grape products dried using the heat of the sun, solar drying or oven drying (Jeszka-Skowron & Czarczyńska-Goślińska 2020). The drying of grapes, whether pretreated with olive oil or not to produce raisins, resulted in quantitative and qualitative changes in the anthocyanin composition. However, reaching a firm conclusion regarding the variability in anthocyanin bioavailability, specifically identifying the responsible metabolizing enzymes or bacteria, is challenging (Eker et al. 2019). It was confirmed that raisins dried after treatment with olive oil preserve more anthocyanins and proanthocyanidins than raisins not treated with olive oil (Olivati et al. 2019). This could be related to the behaviour of olive oil as an edible film on the surface of raisins, protecting them from environmental conditions.

4.3. Evaporation

The purpose of evaporating grape juice is to sterilize it, extend its shelf-life and make sweet and flavoured products that can be healthier than sugar. “Pekmez” (molasses) is the traditional name of boiled juice prepared from different berry fruits such as grape and mulberry in Turkey (Bozkurt et al. 1999). Similar to pekmez, a special evaporated grape juice named “doshab” in Iran is produced by boiling and concentrating grape juice by adding “doshab soil” (Aliakbarlu et al. 2014). Another concentrated grape product is “saba” produced in Italy to make balsamic vinegar. Tagliazucchi et al. (2013) studied the effects of cooking temperature (85 ± 2 °C) at different times on the polyphenols and anthocyanin in two different grapes. The degradation of anthocyanin was reported as more than 92% for each monomer, and the highest decrease in anthocyanin concentration occurred within the first 30 min of heating, especially for the nonacylated ones. Even though they might be less stable, nonacylated anthocyanins are more bioavailable *in vivo* than acylated anthocyanins in human investigations (Fernandes et al. 2015).

A new method in the winemaking industry is the evaporation of intermediate wine that is rich in alcohol (Ozturk & Anli 2014). This step is a pre-fermentation heat treatment technique commonly criticized for unacceptable sensory properties. Eker et al. (2019) reported that thermal treatment, such as evaporation, causes an increase in the bioaccessibility and bioavailability of anthocyanins while decreasing their concentrations. In spite of the observation of the decrease in the amount of anthocyanins, thermal treatments crack cell membranes, releasing cytoplasmic substances and increasing the absorption of anthocyanins (Barba et al. 2016; Celli & Brooks 2017). This indirectly provides higher bioaccessibility of these bioactive compounds before

absorption by human digestion (Leong & Oey 2012). Overall, based on the literature reviewed, different factors contribute to the variability in anthocyanin bioavailability, including processing methods.

4.4. Fruit juice production

Grape juice is known to be a rich source of anthocyanins. In grapes, anthocyanins are primarily located in the skin and also in the flesh depending on the variety (Benmezziane et al. 2016; He et al. 2010). Delphinidin-3-*O*-glucoside, peonidin-3-*O*-glucoside, peonidin-3,5-*O*-diglucoside, malvidin, malvidin-3-*O*-glucoside, and malvidin-3,5-*O*-diglucoside are reported to be the major anthocyanins in different varieties of grape juice (Oh et al. 2008). Non-fermented red grape juice is usually characterized by malvidin-3-*O*-glucoside as a major anthocyanin (Cahyana et al. 2019).

Anthocyanins are known to be sensitive to heat and physicochemical factors. Therefore, processes used to make grape juice, such as thermal and enzymatic treatments, grapefruit juice processing, contact time between juice and grape solid constituents (skins and seeds), pressing, and food matrix, may lead to a degradation of anthocyanins and alter their antioxidant properties (Ioannou et al. 2012; Weber & Larsen 2017). Sulphur dioxide and tartaric acid supplementation also impact the quantity and type of phenolic compounds in grape juice (Cosme et al. 2018).

In addition to processing factors that influence the bioavailability of anthocyanins, evidence suggests that anthocyanin intake could be improved by consuming smoothies and grape juices (Kuntz et al. 2015). This implies that dietary matrices, such as red wine and red grape juice, affect the bioavailability of anthocyanins. After grape juice production, anthocyanins detach and become free from interactions with other biomolecules such as proteins, bio membranes, and DNA constituents (Fernandes et al. 2019). It is reported that the structural differences and physicochemical properties of anthocyanins greatly interfere with their absorption and digestion (Crozier et al. 2009).

Bub et al. (2001) found that several variables contribute to anthocyanin bioavailability, including fecal excretion, intestinal degradation at neutral pH, gut microbiota metabolism, fast accumulation in distinct tissues, or ring fission metabolism after consuming red wine, dealcoholized red wine, and red grape juice. Furthermore, low plasma and urine quantities suggest that anthocyanins are absorbed slowly and metabolized quickly (Murkovic et al. 2001). Furthermore, grape juice's high sugar content may interfere with the intestinal absorption of these chemicals, lowering anthocyanin bioavailability (Frank et al. 2003). In another research conducted by Stalmach et al. (2012), healthy individuals who consumed Concord grape juice were investigated. Urinary excretion of anthocyanins ranged from 5.7 nmol for peonidin-3-*O*-glucoside to 368 nmol petunidin-*O*-glucuronide during a 24-hour period, and anthocyanin excretion amounted to 612 nmol, which is equivalent to 0.26% intake. Similar to other studies, researchers also claimed that grape juice anthocyanins were stable under acidic conditions in the presence of pepsin, with an average recovery of 88% for the 25 anthocyanins, lowering to 24% following simulated digestion with pancreatin and bile extract. Malvidin, peonidin, and cyanidin glycosides, with recoveries of 57%, 48% and 37% respectively, were more stable than petunidin (14%) and delphinidin (5.5%) glycosides (the only two anthocyanins detected in plasma). According to reports, the conversion of anthocyanins into reversible pseudo foundations, quinoidal foundations, and chalcones, as well as hydrolysis to various phenolic acids, for instance 3,4-dihydroxybenzoic acid (also known as protocatechuic acid), are contributing factors to anthocyanin loss under neutral pH and alkaline conditions (Stalmach et al. 2012).

5. Effects of extraction methods on bioavailability of anthocyanins in grape

Anthocyanins can be extracted from plant-based materials using various extraction techniques and solvents. Anthocyanins are dominantly found in the form of flavylium cations, giving a red colour in acidic solutions (pH 1–3). The flavylium cations convert to carbinol and chalcone, and chemical degradation occurs at pH above 4 (Fang, 2014). Under highly acidic conditions, flavylium cations remain stable. Consequently, extraction solvents used for anthocyanin extraction contain mineral and organic acids (Revilla et al. 1998). The use of an acid solvent may produce anthocyanidins, which have high bioavailability compared to their glycosylated form but are less stable in comparison (Eker et al. 2019).

Various extraction methods were suggested to obtain anthocyanin-rich extracts, typically based on organic solvents with different polarities such as methanol, ethanol, acetone, water, or mixtures in acidic or neutral conditions. In a study by Lapornik et al. (2005), red, black, and grape marc byproducts were examined for solvent-based extraction of polyphenol and anthocyanin. They applied water as a solvent along with 70% ethanol and 70% methanol. The effects of plant substance, solvent, and extraction duration (1, 12, and 24 hours) on extraction productivity and various anthocyanins were examined. Alcohol extraction was found to be superior, showing higher polyphenol and anthocyanin content compared to classic maceration. Ethanol and methanol extracts of red and black currants had twice as much anthocyanin and polyphenols, while grape marc alcohol extracts consisted of a higher amount of phenolic compounds, seven times more than water extracts. Extraction time was not effective on the water extracts of red and black currants, while it was effective for grape marc water extracts, indicating an increase in phenolic compound extraction with higher extraction time. Methanol was slightly better than ethanol, but the difference was not great. However, ethanol is considered more appropriate in the food industry. Black currant marc had the highest antioxidant activity, whereas red currant marc had the lowest.

Traditional extraction methods are considered obsolete due to their use of large amounts of organic solvents, low efficiency, time-consuming nature, and degradation of phenolic compounds (Drosou et al. 2015; Liu et al. 2018). The utilization of innovative non-thermal technologies has proven to be an effective approach for extracting anthocyanins from grapes, leading to enhanced yield, faster processing, and maintaining antioxidant capacity (Morata et al. 2021). Several extraction methods have been widely employed for extracting anthocyanins, including supercritical fluid extraction, microwave-assisted extraction, ultrasound-assisted extraction, pulsed electric fields, high-pressure liquid extraction, high-voltage electrical discharge, and enzyme-assisted extraction (Tena & Asuero 2022). Extraction of anthocyanins using a pulsed electric field increased the antioxidant activity by four-fold, three-fold with high hydrostatic pressure and two-fold with ultrasonics compared to conventional extraction (Corrales et al. 2009). Subcritical water at 100 to 110 °C enables the extraction of anthocyanins from dried red grape skin (Ju & Howard 2005). The extraction of anthocyanins from grapes using a natural deep eutectic solvent (NaDES) (chloride, choline and citric acid) recovered 54% of anthocyanins from red grape pomace (Iannone et al. 2021).

Elmi Kashtiban & Esmaili (2019) compared solvent extraction for phenolic compounds from black grape skins with subcritical water extraction. Subcritical water extraction is an innovative method performed at lower temperatures and higher pressures compared to solvent extraction. They concluded that subcritical water extraction was a more efficient method. They also used ultrasound as pretreatment before subcritical water extraction and it was also found to be effective. The optimum conditions for subcritical water extraction of grape phenolic compounds were temperature of 150 °C, pressure of 40 bar, and a time of 30 minutes without using any organic solvents. They observed that temperature was the most important parameter for subcritical water extraction.

Bonfigli et al. (2017) compared conventional and ultrasound extraction of grape pomace anthocyanins using a mixture of 50% ethanol-water. In both methods anthocyanin extraction straightly increased, as ultrasound-assisted extraction increased the mass transfer rate in the first stage of extraction (washing stage). In conventional solvent extraction, 80% of anthocyanins were obtained in the first 600 seconds, whereas in the ultrasound-assisted extraction method, 90% of anthocyanins were extracted in the same time. Ultrasound waves create cavities in cell walls, modifying the structure of materials and their physical and chemical characteristics. As a result, this simplified the release of bioactive compounds and increased mass transfer, while the extraction diminished with time passing. Elmi Kashtiban & Esmaili (2019) achieved similar results, realizing that ultrasound pretreatment before subcritical water extraction methods increased the extraction yield of polyphenolic compounds. Bonfigli et al. (2017) also observed that as the temperature increased, the extraction yield also went up.

Cvjetko Bubalo et al. (2016) conducted a study on the extraction of anthocyanins in red grape skin using deep eutectic solvents (DES), combined with microwave-assisted extraction and ultrasound-assisted extraction. They tested five different choline chloride-based DES (ChCl-based containing glycerol (ChGyl), oxalic acid (ChOa), sorbose (ChSor), malic acid (ChMa), and proline and malic acid (ChProMa)) as possible extraction solvents using conventional solvent extraction with a shaker at 65 °C as the optimal temperature. Their conclusion was that ChOa with 25% water was the best solvent. They observed that the extraction yield increased more with ultrasound-assisted extraction compared to microwave-assisted extraction and conventional solvent extraction, respectively. These findings align with similar conclusions reached by other studies, such as Esclapez et al. (2011) and Mandal et al. (2007). Bi et al. (2013) evaluated temperature as the main parameter in the extraction of anthocyanins with DES. They used alcoholic and ChCl-based DES and realized that ChCl/1,4-butanediol was the best DES for the extraction of bioactive compounds.

Panić et al. (2019) studied the extraction of anthocyanins from grape pomace using NaDES. Based on the literature, the structure and stability of anthocyanins depend on the pH value, remaining stable within the range of pH 2–7 (Cheynier et al. 2012; Cvjetko Bubalo et al. 2016; Bosiljkov et al. 2017). Previous studies showed that organic acid-based NaDES can effectively separate anthocyanins. Panić et al. (2019) used 8 different NaDES compositions: choline chloride/citric acid, choline chloride/malic acid, choline chloride/proline/malic acid, proline/malic acid, betaine/malic acid, betaine/citric acid, malic acid/glucose/glycerol, malic acid/glucose. The NaDES solutions were prepared by adding 25% (v/v) water to reduce viscosity and enhance mass transfer between liquid and solid phases (Cvjetko Bubalo et al. 2016). Low-frequency ultrasound and multimode microwave were employed individually and concurrently, and it was concluded that the optimal extraction conditions were achieved with concurrent ultrasound/microwave-assisted extraction using 30% water (v/v).

Corrales et al. (2009) investigated the extraction of anthocyanins from red grape skins using high hydrostatic pressure. They studied four parameters (pressure, time, temperature, and % ethanol) to determine the optimal conditions. Pressure exhibited a selective effect on anthocyanin extraction; for instance, at a pressure of 200 MPa, the highest levels of total anthocyanin monoglycosides were acquired, while the optimal pressure for the extraction of acylglycosides was 600 MPa. They realized that time was not a significant factor in anthocyanin extraction. However, the extraction yield was higher when higher ethanol concentrations were applied, as the highest anthocyanin recovery was obtained when pure ethanol was used. Spigno et al. (2007) obtained similar results for anthocyanin extraction using pure ethanol. Corrales et al. (2009) found that the best extraction temperature was 50–70 °C.

Monrad et al. (2010) investigated subcritical solvent extraction of anthocyanins from freeze-dried ground Sunbelt red grape pomace using an accelerated solvent extractor (ASE). They applied the following variables: pressure was constant (6.8 MPa),

temperature (40, 60, 80, 100, 120, and 140 °C), and four combined water-ethanol solvents (10, 30, 50, and 70% ethanol). Conventional solvent extraction (methanol/water/formic acid; 60:37:7, v/v/v) was compared with subcritical solvent extraction. Temperature was identified as having a significant effect on total anthocyanins using ASE, while the solvent and temperature interaction effect was insignificant. Optimum temperatures were determined to be 80, 100, and 120 °C. The solvent mixture was also found to have a significant effect with higher ethanol concentrations (50–70%), resulting in the extraction of the greatest amount of anthocyanins from grape pomace. This coincides with several investigations that obtained similar results by applying 50–95% ethanol-water solvents for polyphenol extraction from grapes. The researchers realized that a higher ethanol concentration >70% led to an insignificant resumption of anthocyanins (Lapornik et al. 2005; Luque-Rodríguez et al. 2007; Makris et al. 2008). Optimal extraction conditions (70% ethanol, 103.7 °C) were identified using regression and response surface methods. The study revealed the extraction of diverse anthocyanins, such as petunidin-3-*O*-monoglucoside, petunidin-3-*O*-monoglucoside, petunidin-3-(6-*O*-*p*-coumaroyl)-5-*O*-diglucoside, cyanidin-3-*O*-(6-*O*-*p*-coumaroyl)-monoglucoside, and petunidin-3-*O*-(6-*O*-*p*-coumaroyl)-monoglucoside, with the conventional method. The researchers concluded that employing both methods together yielded more anthocyanins. They detected 12 peaks of anthocyanins conditionally, with malvidin-3,5-*O*-diglucoside and peonidin-3-(6-*O*-coumaroyl)-5-*O*-diglucoside being the highest peaks. Pomar et al. (2005) detected 3-monoglucosides (acylated with coumaric, acetic, and caffeic acid) derivatives from 50 red table grape cultivars, while Monrad et al. (2010) also found several acylated diglycosides in Sunbelt grape pomace.

6. Conclusions

Anthocyanin metabolism after oral intake follows a unique pattern compared to other flavonoids. While anthocyanins can be absorbed in the stomach and intestine, they are among the least bioavailable bioactive compounds within the spectrum of flavonoids. This limited bioavailability is attributed to the highly reactive nature of anthocyanins, which exhibit different structural forms depending on the pH of the aqueous solution. The preservation of anthocyanins and their antioxidant activity from environmental conditions and during processing steps is crucial for developing new processes, such as encapsulation, which enable the stabilization of anthocyanins. To fully comprehend the bioavailability of anthocyanins in grape and grape products, additional *in vivo* research is required.

References

- Ai J, Wu Q, Battino M, Bai W & Tian L (2021). Using untargeted metabolomics to profile the changes in roselle (*Hibiscus sabdariffa* L.) anthocyanins during wine fermentation. *Food Chemistry* 364: 130425
- Aladeboyeje O & Şanlı N Ö (2021). Fermented Traditional Probiotic Beverages of Turkish Origin: A Concise Review. *International Journal of Life Sciences and Biotechnology* 4(3): 546-564
- Alenazi M M, Shafiq M, Alobeed R S, Alsdon A A, Abbasi N A, Ali I & Javed I (2019). Application of abscisic acid at veraison improves red pigmentation and accumulation of dietary antioxidants in red table grapes cv. Red Globe at harvest. *Scientia Horticulturae* 257: 108672
- Aliakbarlu J, Khalili S, Mohammadi S & Naghili H (2014). Physicochemical properties and antioxidant activity of Doshab (a traditional concentrated grape juice). *International Food Research Journal* 21: 367–371
- Barba F J, Nikmaram N, Roohinejad S & Khelifa A (2016). Bioavailability of glucosinolates and their breakdown products: Impact of processing. *Frontiers in Nutrition* 3: 1–35
- Benmeziane F, Cadot Y, Djamaï R & Djermoun L (2016). Determination of major anthocyanin pigments and flavonols in red grape skin of some table grape varieties (*Vitis vinifera* sp.) by high-performance liquid chromatography–photodiode array detection (HPLC-DAD). *Oeno One* 50: 125–135
- Bi W, Tian M & Row K H (2013). Evaluation of alcohol-based deep eutectic solvent in extraction and determination of flavonoids with response surface methodology optimization. *Journal of Chromatography A* 1285: 22–30
- Bitsch R, Netzel M, Frank T, Strass G & Bitsch I (2004). Bioavailability and biokinetics of anthocyanins from red grape juice and red wine. *Journal of Biomedicine and Biotechnology* 4: 293–298
- Bonfigli M, Godoy E, Reinheimer M A & Scenna N J (2017). Comparison between conventional and ultrasound-assisted techniques for extraction of anthocyanins from grape pomace. Experimental results and mathematical modeling. *Journal of Food Engineering* 207: 56–72
- Bosiljkov T, Dujmić F, Cvjetko Bubalo M, Hribar J, Vidrih R, Brnčić M, Zlatić E, Redovniković I R & Jokić S (2017). Natural deep eutectic solvents and ultrasound-assisted extraction: Green approaches for extraction of wine lees anthocyanins. *Food and Bioprocess Technology* 102: 195–203
- Bozkurt H, Gögüş F & Eren S (1999). Nonenzymic browning reactions in boiled grape juice and its models during storage. *Food Chemistry* 64: 89–93
- Bub A, Watzl B, Heeb D, Rechkemmer G & Briviba K (2001). Malvidin-3-glucoside bioavailability in humans after ingestion of red wine, dealcoholized red wine and red grape juice. *European Journal of Nutrition* 40: 113–120
- Busse-valverde N, Encarna G, Jose M L & Bautista-ortín A B (2011). The Extraction of Anthocyanins and Proanthocyanidins from Grapes to Wine during Fermentative Maceration Is Affected by the Enological Technique. *Journal of Agricultural and Food Chemistry* 59: 5450–5455
- Cahyana Y, Gordon M H & Gibson T M (2019). Urinary Excretion of Anthocyanins following Consumption of Strawberry and Red Grape Juice. *International Journal for Vitamin and Nutrition Research* 89: 29–36
- Castello F, Costabile G, Bresciani L, Tassotti M, Naviglio D, Luongo D, Ciciola P, Vitale M, Vetrani C, Galaverna G, Brighenti F, Giacco R, Del rio D & Mena P (2018). Bioavailability and pharmacokinetic profile of grape pomace phenolic compounds in humans. *Archives of Biochemistry and Biophysics* 646: 1–9

- de Castilhos M B M, Corrêa O L dos S, Zanus M C, Maia J D G, Gómez-Alonso S & García-Romero E (2015). Pre-drying and submerged cap winemaking: Effects on polyphenolic compounds and sensory descriptors. Part II: BRS Carmem and Bordô (*Vitis labrusca* L.). *Food Research International* 76: 697–708
- Celli G B & Brooks M S (2017). Impact of extraction and processing conditions on betalains and comparison of properties with anthocyanins — A current review. *Food Research International* 100: 501–509
- Cheyrier V, Gomez C & Ageorges A (2012). Flavonoids: Anthocyanins. In: M L Leo & F T Nollet (Eds.), *Handbook of Analysis of Active Compounds in Functional Foods*, CRC Press pp. 379–403
- Copetti C, Franco F W, Machado E D R, Soquetta M B, Quatrin A, Ramos V D M & Penna N G (2018). Acute consumption of bordo grape juice and wine improves serum antioxidant status in healthy individuals and inhibits reactive oxygen species production in human neuron-like cells. *Journal of Nutrition and Metabolism* pp. 1–11
- Corrales M, García A F, Butz P & Tauscher B (2009) Extraction of anthocyanins from grape skins assisted by high hydrostatic pressure. *Journal of Food Engineering* 90: 415–421
- Cosme F, Pinto T & Vilela A (2018). Phenolic Compounds and Antioxidant Activity in Grape Juices: A Chemical and Sensory View. *Beverages* 4: 22
- Crozier A, Jaganath I B, Clifford M N (2009). Dietary phenolics: Chemistry, bioavailability and effects on health. *Natural Products Reports*, 26(8): 1001-1043. <https://doi.org/10.1039/b802662a>.
- Cvjetko Bubalo M, Čurko N, Tomašević M, Kovačević Ganić K & Radojčić Redovniković I (2016). Green extraction of grape skin phenolics by using deep eutectic solvents. *Food Chemistry* 200: 159–166
- De Rosso M, Tonidandel L, Larcher R, Nicolini G, Ruggeri V, Dalla Vedova A (2012). Study of anthocyanic profiles of twenty-one hybrid grape varieties by liquid chromatography and precursor-ion mass spectrometry. *Analytica Chimica Acta* 732: 120–129
- Drosou C, Kyriakopoulou K, Bimpilas A, Tsimogiannis D, Krokida M (2015). A comparative study on different extraction techniques to recover red grape pomace polyphenols from vinification byproducts. *Ind Crops Prod* 75: 141–149
- Eker M E, Aaby K, Budic-Leto I, Rimac S, Brnčić B, Nehir El S (2019). A review of factors affecting anthocyanin bioavailability: Possible implications for the inter-individual variability. *Foods* 9(1): 2
- Elmi Kashitaban A & Esmaili M (2019). Extraction of phenolic compounds from Siah-Sardasht grape skin using subcritical water and ultrasound pretreatment. *Journal of Food Processing and Preservation* 43: 1–10
- Enaru B, Dreţcanu G, Pop T D, Stănilă A & Diaconeasa Z (2021). Anthocyanins: Factors Affecting Their Stability and Degradation. *Antioxidants* 10: 1967
- Esclapez M D, García-Pérez J V, Mulet A & Cárcel J A (2011). Ultrasound-Assisted Extraction of Natural Products. *Food Engineering Reviews* 3: 108–120
- Fang J (2014). Bioavailability of anthocyanins. *Drug Metabolism Reviews* 46(4): 508–520. <https://doi.org/10.3109/03602532.2014.978080>
- Fang J (2015). Classification of fruits based on anthocyanin types and relevance to their health effects. *Nutrition* 31: 1301–1306
- FAO. FAOSTAT online database. FAOSTAT Online Database 2021. <https://www.fao.org/faostat/en/#data/QCL> (accessed December 22, 2023).
- Faria A, Pestana D, Azevedo J, Martel F, de Freitas V & Azevedo I (2009). Absorption of anthocyanins through intestinal epithelial cells—Putative involvement of GLUT2. *Molecular Nutrition and Food Research* 53: 1430–1437
- FDA (Food and Drug Administration). Title 21 Code of Federal Regulations (CFR) Part 320. National Archives and Records Administration, USA, 2001
- Fernandes I, Faria A, de Freitas V, Calhau C, Mateus N (2015). Multiple-approach studies to assess anthocyanin bioavailability. *Phytochemistry Reviews* 14: 899–919
- Fernandes I, Marques C, Évora A, Cruz L, de Freitas V, Calhau C, Faria A & Mateus N (2017). Pharmacokinetics of Table and Port Red Wine Anthocyanins: A Crossover Trial in Healthy Men. *Food and Function* 8(5): 2030–2037
- Fernandes I, Marques C, Évora A, Faria A, Calhau C, Mateus N & de Freitas V (2019). Anthocyanins: Nutrition and Health. In: J M Merillon & K G Ramawat (Eds.), *Bioactive molecules in food*, Springer Cham, Switzerland AG pp. 1097-1133
- Fernandes I, Nave F, Gonçalves R, de Freitas V & Mateus N (2012). On the bioavailability of flavanols and anthocyanins: Flavanol–anthocyanin dimers. *Food Chemistry* 135: 812–818
- Fernández-García E, Carvajal-Lérida I & Pérez-Gálvez A (2009). In vitro bioaccessibility assessment as a prediction tool of nutritional efficiency. *Nutrition Research* 29: 751–760
- Fleschhut J, Kratzer F, Rechkemmer G & Kulling S E (2006). Stability and biotransformation of various dietary anthocyanins in vitro. *European Journal of Nutrition* 45: 7–18
- Frank T, Netzel M, Strass G, Bitsch R & Bitsch I (2003). Bioavailability of Anthocyanidin-3-Glucosides Following Consumption of Red Wine and Red Grape Juice. *Canadian Journal of Physiology and Pharmacology* 81(5): 423–435. doi:10.1139/y03-038
- Gulsunoglu-Konuskan Z & Kilic-Akyilmaz M (2021). Microbial Bioconversion of Phenolic Compounds in Agro-industrial Wastes: A Review of Mechanisms and Effective Factors. *Journal of Agricultural and Food Chemistry* 70(23): 6901-6910
- Han F, Yang P, Wang H, Fernandes I, Mateus N & Liu Y (2019). Digestion and absorption of red grape and wine anthocyanins through the gastrointestinal tract. *Trends in Food Science and Technology* 83: 211–224
- He F, Mu L, Yan G L, Liang N N, Pan Q H, Wang J, Reeves M J & Duan C Q (2010). Biosynthesis of anthocyanins and their regulation in colored grapes. *Molecules* 15: 9057–9091
- He J, Magnuson B A, Lala G, Tian Q, Schwartz S J & Giusti M M (2006). Intact Anthocyanins and Metabolites in Rat Urine and Plasma After 3 Months of Anthocyanin Supplementation. *Nutrition and Cancer* 54: 3–12
- Henriques J F, Serra D, Dinis T C P & Almeida L M (2020). The Anti-Neuroinflammatory Role of Anthocyanins and Their Metabolites for the Prevention and Treatment of Brain Disorders. *International Journal of Molecular Sciences* 21(22): 1-31
- Hornedo-Ortega R, Rasines-Perea Z, Jourdes A B C, Teissedre P L, Jourdes M (2021). Anthocyanins: Dietary Sources, Bioavailability, Human Metabolic Pathways, and Potential Anti-Neuroinflammatory Activity. *OpenIntech*.
- Iannone A, Sapone V, Di L, Cicci A (2021). Extraction of Anthocyanins from Grape (*Vitis vinifera*) Skins Employing Natural Deep Eutectic Solvents (NaDES). *Chemical Engineering Transactions* 87: 469–474
- Iglesias-Carres L, Mas-Capdevila A, Bravo FI, Aragonès G, Arola-Arnal A & Muguerza B (2019). A comparative study on the bioavailability of phenolic compounds from organic and nonorganic red grapes. *Food Chemistry* 30(299): 125092

- Ioannou I, Hafsa I, Hamdi S, Charbonnel C & Ghoul M (2012). Review of the effects of food processing and formulation on flavonol and anthocyanin behaviour. *Journal of Food Engineering* 111: 208–217
- Jankowski A, Jankowska B & Niedworok J (2000). The effects of anthocyanin dye from grapes on experimental diabetes. *Folia Medica Cracoviensia* 41: 5–15
- Jeszka-skowron M & Czarzyńska-Goślińska B (2020). Raisins and the other dried fruits: Chemical profile and health benefits. *The Mediterranean Diet* pp. 229–238
- Ju Z & Howard LR (2005). Subcritical water and sulfured water extraction of anthocyanins and other phenolics from dried red grape skin. *Journal of Food Science* 70: 270–276
- Kamiloglu S, Capanoglu E, Grootaert C & Camp J Van (2015). Anthocyanin Absorption and Metabolism by Human Intestinal Caco-2 Cells — A Review. *International Journal of Molecular Sciences* 16(9): 21555–21574
- Kaya S & Maskan A (2003). Water vapor permeability of pestil (a fruit leather) made from boiled grape juice with starch. *Journal of Food Engineering* 57: 295–299
- Kuntz S, Rudloff S, Asseburg H, Borsch C, Frohling B, Unger F, Dold S, Spengler B, Römpf A & Kunz C (2015). Uptake and bioavailability of anthocyanins and phenolic acids from grape / blueberry juice and smoothie in vitro and in vivo. *British Journal of Nutrition* 113(7): 1044-1055
- Lapornik B, Prošek M & Wondra AG (2005). Comparison of extracts prepared from plant by-products using different solvents and extraction time. *Journal of Food Engineering* 71: 214–222
- Lee Y-M, Yoom Y, Yoon H & Song S (2017). Dietary Anthocyanins against Obesity and Inflammation. *Nutrients* 9: 1–15
- Leong S Y & Oey I (2012) Effects of processing on anthocyanins, carotenoids and vitamin C in summer fruits and vegetables. *Food Chemistry* 133: 1577–1587
- Lingua M S, Wunderlin D A & Baroni M V (2018). Effect of Simulated Digestion on the Phenolic Components of Red Grapes and Their Corresponding Wines. *Journal of Functional Foods* 44: 86–94
- Liu Q, Tang G Y, Zhao C N, Feng X L, Xu X Y & Cao S Y (2018). Comparison of antioxidant activities of different grape varieties. *Molecules* 23: 1–17
- Luque-Rodríguez J M, Luque de Castro M D & Pérez-Juan P (2007). Dynamic superheated liquid extraction of anthocyanins and other phenolics from red grape skins of winemaking residues. *Bioresource Technology* 98: 2705–2713
- Makris D P, Boskou G, Chiou A & Andrikopoulos N K (2008). An investigation on factors affecting recovery of antioxidant phenolics and anthocyanins from red grape (*Vitis vinifera* L.) pomace employing water/ethanol-based solutions. *American Journal of Food Technology* 3: 164–173
- Mandal V, Mohan Y, Hemalatha S (2007). Microwave Assisted Extraction – An Innovative and Promising Extraction Tool for Medicinal Plant Research. *Pharmacognosy Reviews* 1(1): 7-18
- Mattioli R, Francioso A, Mosca L & Silva P (2020). Anthocyanins : A Comprehensive Review of Their Chemical Properties and Health Effects on Cardiovascular and Neurodegenerative Diseases. *Molecules* 25: 1–42
- McDougall G J, Dobson P, Smith P, Blake A & Stewart D (2005). Assessing potential bioavailability of raspberry anthocyanins using an in vitro digestion system. *Journal of Agricultural and Food Chemistry* 53: 5896–5904
- Monrad J K, Howard L R, King J W, Srinivas K & Mauromoustakos A (2010). Subcritical solvent extraction of anthocyanins from dried red grape pomace. *Journal of Agricultural and Food Chemistry* 58: 2862–2868
- Morata A, Escott C, Loira I, Carmen L, Palomero F & Gonz C (2021). Emerging Non-Thermal Technologies for the Extraction of Grape Anthocyanins. *Antioxidants* 10(12): 1863
- Murkovic M, Mülleder U, Adam U & Pfannhauser W (2001). Detection of anthocyanins from elderberry juice in human urine. *Journal of the Science of Food and Agriculture* 81: 934–937
- Oh Y S, Lee J H, Yoon S H, Oh C H, Choi D S, Choe E & Jung M Y (2008). Characterization and quantification of anthocyanins in grape juices obtained from the grapes cultivated in Korea by HPLC/DAD, HPLC/MS, and HPLC/MS/MS. *Journal of Food Science* 73: 378–389
- Olivati C, Paula Y, Nishiyama D O, Souza T De, Janzanti N S, Aparecida M, Gomes E, Hermosin-Gutierrez I, Silva R & Lago-Vansela E S (2019). Effect of the pre-treatment and the drying process on the phenolic composition of raisins produced with a seedless Brazilian grape cultivar. *Food Research International* 116: 190–199
- Oliveira H, Perez-Gregório R, de Freitas V, Mateus N, Fernandes I (2019). Comparison of the in vitro gastrointestinal bioavailability of acylated and non-acylated anthocyanins: Purple-fleshed sweet potato vs red wine. *Food Chemistry* 276: 410–418
- Overall J, Bonney S, Wilson M, Beermann A, Grace M, Esposito D, Lila M A & Komarnytsky S (2017). Metabolic Effects of Berries with Structurally Diverse Anthocyanins. *International Journal of Molecular Sciences* 18: 422
- Ozturk B & Anli E (2014). Different techniques for reducing alcohol levels in wine : A review. *BIO Web of Conferences* 3: 2–9
- Pacheco S M, Soares M S P, Gutierrez J M, Gerzson M F B, Carvalho F B, Azambuja J H, Schetinger M R C, Stefanello F M & Spanevello R M (2018). Anthocyanins as a Potential Pharmacological Agent to Manage Memory Deficit, Oxidative Stress and Alterations in Ion Pump Activity Induced by Experimental Sporadic Dementia of Alzheimer's Type. *The Journal of Nutritional Biochemistry* 56: 193–204
- Panić M, Gunjević V, Cravotto G & Redovniković I R (2019). Enabling technologies for the extraction of grape-pomace anthocyanins using natural deep eutectic solvents in up-to-half-litre batches extraction of grape pomace anthocyanins using NADES. *Food Chemistry* 300: 125185
- Passamonti S, Vrhovsek U, Vanzo A & Mattivi F (2005). Fast access of some grape pigments to the brain. *Journal of Agricultural and Food Chemistry* 53: 7029–7034
- Patras A, Brunton NP, O'Donnell C & Tiwari BK (2010). Effect of thermal processing on anthocyanin stability in foods; mechanisms and kinetics of degradation. *Trends in Food Science and Technology* 21: 3–11
- Pineda-Vadillo C, Nau F, Guerin-Dubiard C, Jardin J, Lechevalier V, Sanz-Buenhombre M, Guadarrama A, Toth T, Csavajda E, Hingyi H, Karakaya S, Sibakov J, Capozzi F, Bordoni A & Dupont D (2017). The food matrix affects the anthocyanin profile of fortified egg and dairy matrices during processing and in vitro digestion. *Food Chemistry* 214: 486–496
- Polia F, Pastor-belda M, Mart A, Horcajada M & Tom F A (2022). Technological and Biotechnological Processes to Enhance the Bioavailability of Dietary (Poly)phenols in Humans. *Journal of Agricultural and Food Chemistry* 70(7): 2092–2107
- Pomar F, Novo M & Masa A (2005). Varietal differences among the anthocyanin profiles of 50 red table grape cultivars studied by high performance liquid chromatography. *Journal of Chromatography A* 1094: 34-41

- Revilla E, Ryan J M & Martín-Ortega G (1998). Comparison of Several Procedures Used for the Extraction of Anthocyanins from Red Grapes. *Journal of Agricultural and Food Chemistry* 46: 4592–4597
- Romero-Cascales I, Fernandez-Fernandez J I, Lopez-Roca J M & Gomez-Plaza E (2005). The maceration process during winemaking extraction of anthocyanins from grape skins into wine. *European Food Research and Technology* 221: 163–167
- Ruta L L & Farcasanu I C (2019). Anthocyanins and Anthocyanin-Derived Products in. *Antioxidants* 8: 1–13
- Sabra A, Netticadan T & Wijekoon C (2021). Grape bioactive molecules and the potential health benefits in reducing the risk of heart diseases. *Food Chemistry X*:100149
- Seymour E M, Tanone I I, Urcuyo-Llanes D E, Lewis S K, Kirakosyan A & Kondoleon M G (2011). Blueberry intake alters skeletal muscle and adipose tissue peroxisome proliferator-activated receptor activity and reduces insulin resistance in obese rats. *Journal of Medicinal Food* 14: 1511–1518
- Seymour E M, Wolforth J, Bosak K, Kondoleon M, Mehta V & Brickner P (2013). Effect of tart cherry versus PPAR agonist pioglitazone on stroke-related phenotypes and inflammation. *The FASEB Journal* 27: 7
- Soares S, Garcia-Estévez I, Ferrer-Galego R, Brás NF, Brandão E, Silva M, et al. (2018). Study of human salivary proline-rich proteins interaction with food tannins. *Food Chemistry* 243:175-185
- Spigno G, Tramelli L & De Faveri D M (2007). Effects of extraction time, temperature and solvent on concentration and antioxidant activity of grape marc phenolics. *Journal of Food Engineering* 81: 200–208
- Stalmach A, Edwards C A, Wightman J D & Crozier A (2012). Gastrointestinal stability and bioavailability of (poly)phenolic compounds following ingestion of Concord grape juice by humans. *Molecular Nutrition and Food Research* 56: 497–509
- Tagliacozzi D, Verzelloni E, Helal A & Conte A (2013). Effect of grape variety on the evolution of sugars, hydroxymethylfurfural, polyphenols and antioxidant activity during grape must cooking. *International Journal of Food Science and Technology* 48: 808–816
- Tena N & Asuero A G (2022). Up-To-Date Analysis of the Extraction Methods for Anthocyanins: Principles of the Techniques, Optimization, Technical Progress, and Industrial Application. *Antioxidants* 11(2): 286
- Vergara-salinas J R, Bulnes P, Agosin E & Pe J R (2013). Effect of Pressurized Hot Water Extraction on Antioxidants from Grape Pomace before and after enological fermentation. *Journal of Agricultural Food and Chemistry* 61(28): 6929–6936
- Waterhouse A L (2002). Wine phenolics. *Annals of the New York Academy of Sciences* 957(1): 21–36
- Weber F & Larsen L R (2017). Influence of fruit juice processing on anthocyanin stability. *Food Research International* 100: 354–365
- Yamakoshi J, Kataoka S, Koga T & Ariga T (1999). Proanthocyanidin-rich extract from grape seeds attenuates the development of aortic atherosclerosis in cholesterol-fed rabbits. *Atherosclerosis* 142: 139–149
- Yang P, Yuan C, Wang H, Han F, Liu Y, Wang L & Liu Y (2018). Stability of Anthocyanins and Their Degradation Products from Cabernet Sauvignon Red Wine under Gastrointestinal pH and Temperature Conditions. *Molecules* 23: 354
- Yuzuak S & Xie D (2022). Anthocyanins from muscadine (*Vitis rotundifolia*) grape fruit. *Current Plant Biology* 30: 100243



Copyright © 2024 The Author(s). This is an open-access article published by Faculty of Agriculture, Ankara University under the terms of the [Creative Commons Attribution License](https://creativecommons.org/licenses/by/4.0/) which permits unrestricted use, distribution, and reproduction in any medium or format, provided the original work is properly cited.



The Use of Medical Foods to Fight Chronic Diseases: A Narrative Review

Hilal Meral^{a*} , Ashhan Demirdöven^a 

^aFood Engineering Department, Faculty of Engineering and Architecture, Tokat Gaziosmanpaşa University, Tokat, TURKEY

ARTICLE INFO

Review Article

Corresponding Author: Hilal Meral, E-mail: hilal.meral@gop.edu.tr

Received: 08 September 2023 / Revised: 12 December 2023 / Accepted: 11 January 2024 / Online: 23 July 2024

Cite this article

Meral H, Demirdöven A (2024). The Use of Medical Foods to Fight Chronic Diseases: A Narrative Review. *Journal of Agricultural Sciences (Tarım Bilimleri Dergisi)*, 30(3):424-435. DOI: 10.15832/ankutbd.1357154

ABSTRACT

Chronic diseases cannot be treated completely, and, therefore, often require repeated treatments. This issue leads to long-term drug utilization. However, medical foods can offer alternative natural drugs in the management and treatment of chronic diseases. Medical foods are specially formulated food to meet the particular nutritional requirements of patients affected by certain diseases. They play an important role in nutritional support for patients in clinical applications such as deglutition, dyspepsia or eating disorders. Moreover, they considerably enhance the quality of living of patients by reducing drug usage, preventing complications that may arise through the overreliance of drugs, and reducing the expenses of treatments. The nutritive value of medical foods can be regulated and personalized depending on the disease. Since they

are not drugs, they exempt from regulations applying to drugs. Each medical food is formulated specifically for the relevant chronic disease. However, there are no studies in the literature that provide examples of medical foods for different diseases available in the market. The examination and compilation of medical foods, including examples from the market, is vital both in terms of creating new products and filling the gap in the relevant literature. Consequently, the aim of this review is to explain the use of medical foods for Alzheimer's, Parkinson's, anxiety and sleep disorder, pain syndrome, cancer, congenital metabolic disorders, diabetes mellitus, and indicate why should be used as a nutritional supplement for these chronic diseases.

Keywords: Food, Medical nutrition therapy, Disease, Treatment, Dietary management

1. Introduction

Today, the world is facing a notable increase in the number of people suffering from complex and chronic diseases such as diabetes, Alzheimer's, cancer, and autism. An examination of the existing medical research shows a noticeable shift, where the primary objective of treating patients has evolved into a pursuit of comprehensive healing. This paradigm shift implies that while patients' symptoms may persist, they can be managed over the course of their lives with an escalating regimen of drugs. What patients truly require is a therapeutic approach that aims to promote healing by addressing the root cause of their diseases. It is in this context that the significance of functional medicine becomes apparent. Functional medicine adopts an individualized and integrative methodology, encompassing the understanding and exploration of preventive measures and the management of chronic diseases. Functional medicine does not refuse conventional medicine, but it uses conventional medicine as a basis on which to add new aspects in the consideration, prevention, and management of chronic disease (Nikogosian 2022). One specific aspect investigated within the realm of functional medicine is the dietary pattern of a patient. At this point, the importance of the term of “medical food” in the treatment of chronic diseases emerges.

Medical foods first entered the market under the regulatory oversight of the Food and Drug Administration (FDA) in the United States in 1972. One of the first examples of medical foods was “Lofenalac”, which was used for the dietary management of patients in the treatment of phenylketonuria (PKU), an inborn disease of metabolism. In 1988, the Orphan Drug Act was rearranged to create a legal definition for the term medical food (Holmes et al. 2021). In 1990, the Nutritional Labeling and Education Act (NLEA) exempted medical foods from the health claims and nutrition labeling requirements. The legal definition refers to the “specific dietary management of a disease or condition” whereas the NLEA refer to the “dietary management of a patient with a specific disease or condition”. This distinction is important as not all food produced for patients is medical food (Bagchi 2019). In 1996, the FDA reevaluated the regulatory norms of medical foods and published an announcement with a detailed definition for the term “medical food” (Parker 2005). After the FDA withdrew the announcement in 2004 due to constraints in resources, it released a final guide in 2016 to ensure that manufacturers better understood the regulations concerning medical foods (Lewis & Jackson 2019). The document “Guidance for Industry: Frequently Asked Questions About Medical Foods, Second Edition” clarifies the term “medical food” via a question-and-answer format (FDA 2016).

Medical foods are produced for special medical purposes according to a particular recipe to address the specific dietary needs of patients suffering from metabolic disorders or other chronic diseases. According to the FDA's definition, medical food is a "food formula generated for the specific dietary management of a disease or condition for which distinctive nutritional needs have been determined by medical evaluation that has been formulated for consumption or enteral administration under the supervision of a physician" (Lange et al. 2019a; FDA 2022). Most foodstuffs are grouped, whether they are "sugar-free", "low fat", "lactose-free", "gluten-free" or "organic" produced. However, uncertainty remains regarding the differences of health-related foods from dietary/nutritional supplements and conventional foods in the market, throughout various medical disciplines and especially among consumers (Markowitz et al. 2020). For a better understanding of the differences, commonly known food terms using for different food stuffs and their definitions are provided in the Table 1. Although all the food items can be used to improve health conditions, medical foods must be consumed under medical supervision in the specific dietary management of certain diseases (Shi et al. 2020).

The current review aims to elucidate the definition of medical foods, highlight their distinctions from pharmaceutical drugs, and provide illustrative examples of medical food applications in conditions such as Alzheimer's, Parkinson's, anxiety and sleep disorders, pain syndromes, cancer, congenital metabolic disorders, and diabetes mellitus.

Table 1- Food Terms and Definitions (Markowitz et al. 2020)

Term	Definition
Functional Food	Products used in combination with enhanced, fortified or enriched foods that offer health benefits when consumed in a certain diet.
Fortified Food	A conventional food which is enriched by adding extra micronutrients to it.
Enriched Food	Food product in which essential nutrients lost during processing are added back.
Dietary Supplements	A product which is manufactured to support the diet with components like plant extracts, vitamins, amino acids, minerals, various dietary fiber and/or a combination of these components. Unlike medical foods, it is not used under physician supervision or for the treatment of any specific disease.
Food for Special Dietary Use (FSDU)	A product used to meet dietary needs due to a physiological, pathological or other condition, including disease, pregnancy etc. It is not used under medical supervision, and it does not make health claims.
Drug	Any substance (except food) which is used to treat, prevent, or cure a disease.
Medical Food	Food formulated for consumption under the supervision of a physician to meet nutritional needs which are identified by a clinical study of patients.

2. The Differences Between Medical Foods and Drugs

Medical foods have an important place in enteral nutrition but are not defined as drugs. Enteral nutrition supplemented with medical foods can reduce the adverse effects of long-term drug utilization, incidence of some complications, shorten the length of hospital stay, and decrease the economic losses resulting from illness (Seron-Arbeloa et al. 2013; Przyrembel et al. 2015). Healthcare professionals do not desire the depletion of certain nutrients when considering the long-term health consequences of prescription drugs continuously used by patients for the treatment of chronic diseases (Meletis & Zabriskie 2007). Vitamin B₁₂ deficiency caused through the use of an oral hypoglycemic agent, coenzyme Q₁₀ deficiency that occurs through the use of statins, vitamin B, calcium and magnesium deficiencies arising from the frequent use of antibiotics are some examples of loss of nutrients due to drug use. Consequently, the use of medical foods and dietary supplements is thought to be effective in prohibiting drug-related nutritional losses (Valuck & Ruscin 2004).

Medical foods are exempt from FDA laws and requirements for drugs. However, medical foods are liable to all the FDA requirements determined for conventional and functional foods, such as good manufacturing practices. There is a misunderstanding that medical foods can only be given to patients through prescriptions; unlike medical drugs, over the counter delivery of medical foods is not prohibited. It is forbidden to include the inscription "Rx" in prescription medical drugs on the label of a medical food. In addition, medical foods produced for dietary management should be labeled to indicate that they are specific to the relevant patient or disease and meet the nutritional requirements necessary for managing that disease. All ingredients used in the formulation of medical foods should meet FDA requirements and be generally recognized as safe (GRAS). Medical foods are exempt from nutritional content and health claims requirements (Fung et al. 2018; Markowitz et al. 2020; Li et al. 2021).

While foods for special medical purposes (FSMPs) are expressed as medical foods in some non-European Union (non-EU) countries (e.g., USA, Argentina), they are also expressed as enteral nutrition in some countries (e.g., Brazil). Since the 1970s, these specialty medical foods or FSMPs, were subject to drug regulations due to the lack of advanced regulatory rules. However, in recent years, medical foods have been characterized in more detail within the scope of food laws (Domínguez Díaz et al. 2020). The re-evaluation of medical food regulations has allowed for a new phase of development in medical food industry. In China, however, medical foods are not subject to the FDA regulations that apply to drugs (Bagchi 2019). Products regarded as medical foods in the USA are regulated as FSMPs in the EU (Domínguez Díaz et al. 2020). In Turkey, the registration,

permission, import procedures, control, and inspection of establishments for producing and selling medical foods are carried out by the Ministry of Health and the Ministry of Agriculture and Forestry, in accordance with the provisions of the “Turkish Food Codex Regulation on Dietary Foods for Special Medical Purposes”. As per the regulations (Official Gazette No. 24640), the product should be used under the supervision of a physician, and the target consumer group for the product should be stated on the packaging. In addition, packaging information should be created without using nutrition and health claims (TFC 2001; Domínguez Díaz et al. 2020).

3. Medical Foods Treatment on Different Diseases

Simple dietary changes can be effective in the management of many chronic diseases. In this narrative review, we will emphasize neurodegenerative diseases (Alzheimer's & Parkinson), anxiety & sleep disorders, pain syndromes, cancer, congenital metabolic disorders, and diabetes mellitus. These are chronic diseases where diet and medical food use have proven effective, and they affect a significant number of patients.

3.1. Neurodegenerative diseases

Alzheimer's disease (AD), a multifactorial neurodegenerative disease, is the most common cause of dementia in the world. The greatest known risk factor for the disease is old age, and most Alzheimer's patients are over the age of 65. Treatments to prevent or delay disease progression are not yet available that provide a significant improvement in the condition of patients. The current treatment options are primarily aimed at treating clinical symptoms that only offer symptomatic relief and promote healthy brain aging (Ohnuma et al. 2016).

One important risk factor for Alzheimer's is nutrition. Current evidence suggests that embracing prudent dietary patterns may be linked to a decelerated cognitive decline and a reduced risk of AD and related dementias, even though the precise mechanisms remain unclear. One potential mechanism involves the impact of specific dietary constituents on neural resources, thereby enhancing cognitive health and resilience. For instance, adopting healthier dietary patterns has been associated with the homeostatic formation of hippocampal neurons - an impairment often observed in the early stages of Alzheimer's dementias (Ellouze et al. 2023). An unhealthy diet, like a high-fat, low protein intake, high glycemic load, and high cholesterol or Western diet, is a significant risk factor for neurodegeneration, increasing A β peptide stores and neurodegeneration biomarkers in AD. Conversely, adopting a healthy diet like Dietary Approaches to Stop Hypertension (DASH), Mediterranean, or low-fat diets has neuroprotective effects, reducing oxidative stress, inflammation, and A β peptide accumulation. The Mediterranean and DASH diets, rich in potassium, calcium, magnesium, and fiber, with low sodium and saturated fat, exhibit anti-inflammatory effects and help protect against AD (Hoscheidt et al. 2022). The Mediterranean diet (MD) benefits cerebral perfusion, especially in early AD stages, while the Western diet heightens AD risk, impacting metabolic health, reducing cerebral perfusion, and impairing cognition (Xu et al. 2023). Therefore, by fortifying cognitive resilience over time, these dietary elements may contribute to enhanced cognitive trajectories in later life. Various dietary approaches provide symptomatic benefits for AD and fulfill the criteria for approval as medical food by providing components that meet the special nutritional needs of the patients. When considering the developments in symptomatology and regional brain atrophy in Alzheimer's disease (AD), studies have accelerated on various types of medical foods. These include products that provide ketone bodies as an alternative energy source for neurons, contain precursors believed to improve synaptic function, and address oxidative stress associated with memory loss (Atri 2019; Lange et al. 2019a). In a study conducted on Alzheimer's disease patients, it was determined that the medical food called *Axona*, which contains medium chain fatty acids, yielded positive results in patients with mild AD (Sharma et al. 2014). Another medical food that has shown success in treating the disease is *Souvenaid*, which improves memory efficiency in Alzheimer's patients. *Souvenaid* contains phosphatide precursors and other cofactors such as eicosapentaenoic acid (EPA), phospholipids, vitamin E, vitamin C, selenium, vitamin B₁₂ (Scheltens 2010). Many other methodological shortcomings complicate the interpretation of the current findings of medical food trials in AD (Table 2). In addition, dietary patterns such as the Mediterranean diet show promise in the prevention of AD, but large-scale clinical studies using valid, sensitive and reliable assessment tools are needed to determine the efficiency of them (Morley et al. 2018; Omar 2019).

The second most common neurodegenerative illness is Parkinson's disease (PD), a slowly progressing disorder in the brain linked to the loss of dopaminergic neurons, resulting in involuntary movements, balance disorders, and ataxia. Non-motor symptoms in PD patients include anosmia, autonomic disorders, cognitive deficits, psychological disorders, and sleep disturbances (Postuma et al. 2012; Lange et al. 2019a). Various genetic and environmental factors contribute to the occurrence of PD (Simon et al. 2020; Gonzalez-Latapi et al. 2021), with age being the most significant and well-established factor in its development. The brain, particularly susceptible to oxidative stress in old age, is believed to play a crucial role in the dysfunction of the dopaminergic system (Aslan et al. 2019; Kaya & Soyukibar 2022; Özdemir 2022). Neuropathological clinical trials reveal the accumulation of α -synuclein proteins, known as Lewy bodies, in the central, autonomic, and peripheral nervous systems of PD patients. These bodies destroy relevant nerve cells and intercellular junctions, halting the exchange of neurotransmitters (Armstrong & Okun 2020). There is still no definitive treatment for PD, but the basis of treatment is the administration of drugs that increase dopamine levels or directly stimulate dopamine receptors (Aarsland et al. 2021; Bloem et al. 2021). Specific macronutrients and micronutrients, which are environmental factors in the etiology of PD, are an effective parameter in the management and progression of the disease and therefore in its treatment. In a study on potential nutritional risk factors in PD,

those who consumed foods rich in vegetables, seeds, nuts, xanthophylls, xanthine, and lutein had a lower frequency of the disease compared to the control group (Ishihara & Brayne 2005; Gaenslen et al. 2008). It was determined in a similar study conducted with a group of 4,524 individuals aged 40-79 years without a diagnosis of PD that the consumption of milk had a positive effect on the progress of the disease, while the consumption of niacin-rich meat and meat products had a negative effect (Sääksjärvi et al. 2013). Dietary polyphenols which have antioxidant and anti-inflammatory properties, such as resveratrol, anthocyanins, catechins, theaflavins, and curcumin may have neuroprotective potential in PD (Farooqui & Farooqui 2017; Singh et al. 2020; Giuliano et al. 2021). Omega-3 polyunsaturated fatty acids that allow for the continuation of neurobiological functions, play an important role in the neurodegenerative process in PD with actions that alleviate oxidative stress and neurotrophic factors. Studies have shown that docosanoids and elovonoids from omega-3 fatty acids contribute to inflammatory responses and neuroprotection (Bazan 2018; Lange et al. 2019b). Considering potential mechanisms leading to neurodegeneration in PD oxidative stress, antioxidant components such as vitamins C, D, E and carotenoids can prevent oxidative stress and act as a neurotrophic factor. A study has shown that a diet rich in vitamin D, in particular, can induce an increase in dopamine levels in the brain. This is achieved by facilitating the transition of the dopamine precursor, tyrosine, into the cerebrospinal fluid and by stimulating the expression of tyrosine hydroxylase, a key enzyme in dopamine synthesis (Yeshokumar et al. 2015; Hughes et al. 2016; Bivona et al. 2019; Miclea et al. 2020). In this sense, preliminary tests of medical foods in PD are based on a ketogenic diet (KD) composition. The KD is defined by its emphasis on high fat intake and low carbohydrate consumption, encouraging the production of ketones for energy. A high-carbohydrate diet can induce dopamine increase in the brain by facilitating the transition of dopamine precursor tyrosine into the cerebrospinal fluid (Yeshokumar et al. 2015). In addition, a KD contributes positively to PD by improving the energy metabolism of central neurons and mitochondrial biogenesis and by controlling neurotransmitters (Rudy et al. 2020). Studies have indicated a significant association between high adherence to the MD and overall reductions in the mean age of onset, incidence, progression, and motor symptom manifestations of PD, along with an increase in cognitive function (Bianchi et al. 2023). MD is a diet rich in olive oil, unrefined cereals, fruits, and vegetables; a moderate to high intake of fish; a moderate consumption of dairy products, predominantly cheese and yogurt; moderate wine consumption; and a low consumption of red meat products. The MD exerts an anti-inflammatory effect by reducing oxidative stress, C-reactive protein (CRP), fasting insulin, adiponectin levels, and neuroinflammation. Additionally, it improves gut microbiota and metabolic syndrome, leading to a reduction in α -synuclein aggregation and early neuronal degeneration. This improvement is presumed to occur both in the gut and various areas of the brain (Molsberry et al. 2020).

3.2. Anxiety & Sleep disorder

Sleep, a highly regulated function in which different groups of neurons are affected, is necessary for the normal and healthy functioning of the human body and is associated with the regulation of learning, memory and emotional state. Sleep disorders can be seen as a disease on their own or as a symptom of another physical or mental illness. One of these mental illnesses is anxiety (Adell 2004; Arenas et al. 2019), a psychological disorder which includes symptoms such as irritability, difficulty concentrating, sensitivity to sound, and restlessness. Anxiety and sleep disorders have long been known to be interrelated. The majority of those suffering from anxiety disorders have chronic or periodic sleep problems. At this point, it is important to emphasize the necessity of restorative sleep for central nervous system disorders, including anxiety, as it significantly influences feelings of depression (Groff et al. 2022). Sleep is regulated by several neurotransmitters, including serotonin and acetylcholine, which are released sufficiently and at appropriate times. Agents and drugs used for anxiety and sleep disorders interfere and regulate neurotransmitters. However, they may cause side effects such as lethargy, depression, and dysmnasia. Therefore, in recent years, medical foods for anxiety and sleep disorders have been introduced in the market. Medical foods formulated for anxiety and sleep disorders consist of serotonin and acetylcholine precursors that increase amino acid intake and neurotransmitter release. The produced serotonin and acetylcholine commence sleep and support delta sleep. Firstly, 5-hydroxytryptophan is converted to serotonin to induce sleep, then choline is converted to acetylcholine for delta sleep (España & Scammell 2004). In a study conducted by Md et al. (2012), 111 subjects using *Sentra*, a medical food formulated for anxiety, were monitored for 30 days. The subjects provided informed consent and completed an initial sleep survey. Their study found that medical food reduces the time to fall asleep, reduces drowsiness in the morning and improves sleep quality. Therefore, the study has proven that the use of *Sentra* contributes positively to depression and anxiety. A similar study utilized various ingredients including Ginkgo biloba as an uptake stimulator, choline, glutamic acid as a precursor of glutamate, cocoa as an adenosine antagonist, and grape seed extract as a source of polyphenols. These ingredients were used in the production of a medical food called *GABADone*, which is a combination of amino acids. It has been indicated that the produced medical food decreases the sleep latency and increases the duration and quality of sleep (Shell et al 2010). In summary, studies in the literature show that some amino acids affect sleep cycles and therefore central nervous system functions, including depression and anxiety (Glenn et al. 2019; Zhao et al. 2020).

3.3. Pain syndromes

Chronic pain syndrome is defined as pain in which the etiology is not very clear, and which usually lasts longer than 6 months or that relapses frequently (Martikainen et al. 2018). Chronic pain, unlike acute pain, may not derived from damaged tissue. It is thought to be associated with pain memory in the related centers of the brain and sensitive areas around the backbone. In other words, nerve cells can send pain signals without the presence of tissue damage in the affected area (Martikainen et al. 2018). In this type of pain, besides biological approaches, psychodynamic perspectives are also crucial. Therefore, some chronic pain may

be psychological in origin. Although chronic pain treatment methods vary according to the type and location of the pain, the use of medication is usually recommended at the first stage (Shim et al. 2019). In addition to drug use, psychological and physiotherapeutic methods are also frequently used chronic pain treatment methods. However, chronic pain syndrome, which usually does not completely respond medical treatment, can best be treated with a multidisciplinary approach (manual therapy, physical therapy, aqua therapy, occupational therapy, psychotherapy, and certain new therapies). Physical therapy and other approaches may increase treatment costs (Shim et al. 2019). In this multidisciplinary approach, nutrition and medical foods in the specific dietary management of the patients plays an important role. The production of medical foods containing specific amino acids and neurotransmitters required to reduce chronic pain syndrome, which occurs depending on the frequency and volume of the pain signals in the nervous system, has increased in recent years. One of these medical foods currently available is *Percura* which formulates with biogenic amins, amino acids, and botanicals inducing the production of neurotransmitters to decrease signals throughout the pain pathways. The key ingredients of this medical food are choline bitartrate as a precursor of acetylcholine, inositol for the development and functioning of peripheral nerves, osteogenesis, and reproductive functions, L-arginine as an ingredient for producing nitrite oxide a neurotransmitter substance, L-ornithine for improving the sympathetic nerve outflows, and creatine monohydrate as a source of intracellular energy. In a clinical outcome study of *Percura*, it was found that patients with peripheral neuropathy experienced a reduction in pain and numbness at a rate of 82-89% over a 21-day period (Shell et al. 2016). *Trepadone* is another medical food specifically designed to address the specific amino acid requirements needed in the reduction of chronic pain syndromes associated with joint disorders. It contains chondroitin sulfate, glucosamine sulfate, L-histidine, and whey protein, which stimulate the production of serotonin, γ -aminobutyric acid (GABA), nitric oxide, glutamate and histamine neurotransmitters. It has been scientifically proven that these ingredients support the cellular or physiological activities needed to restore metabolic balance (Shell et al. 2016; Taylor et al. 2021). Although there are examples of medical foods on the market, there are limited studies showing the effectiveness of medical foods containing specific amino acids and neurotransmitter precursors on chronic pains. For this reason, further studies on the subject are required.

3.4. Cancer

Cancer is a disease in which some of the body's cells grow uncontrollably and spread to other parts of the body. Nutrition plays a crucial role as a risk factor in the deaths of cancer patients, accounting for 20-40% of direct causes of death. Therefore, enteral nutrition therapy is an important part of cancer treatment (Mao et al. 2018). The primary nutritional problem, and likely also the most impactful on prognosis, is myolysis. Myolysis in cancer patients may lead to cachexia and anorexia over time. Cachexia is characterized by involuntary weight loss and anorexia on top of skeleton mass loss (Arends et al. 2017; Muscaritoli et al. 2021). Several studies have shown that muscle mass can be improved and losses can be reduced with a daily protein intake of >1.5 g/kg body weight in patients with cancer cachexia, and this effect may be more significant when combined with exercise. In this sense, protein-enriched medical foods such as *ProtiMedic Amino Plus* can be used in the dietary management of cancer patients (Blasiak et al. 2020).

Medical foods designed for cancer patients are widely used nutritional agents and have an important place in medical nutrition therapy. For example, to maintain the nitrogen balance, the protein content of medical foods for cancer patients may be increased and thus cachexia can be prevented. Antioxidants such as vitamin E, vitamin C and selenium can retard the formation and development of cancer by preventing lipid peroxidation. Since the cancer disease weakens the immune system of patients, immunomodulatory agents such as arginine, glutamine, n-3 fatty acids, and nucleotides can be used in medical food formulas (Rosenthal et al. 2016; Xu et al. 2016).

3.5. Medical foods for congenital metabolic disorders

Congenital Metabolic Disorders (CMD) are expressed as inherited disorders that occur in carbohydrate, protein or fat metabolism due to a particular enzyme defect. CMD is divided into three categories as intoxication disorders, energy metabolism disorders and disorders of complex molecules. Treatment methods for this disease are determined by considering the defective enzyme and the damaged metabolic reaction. Although the most effective treatment modalities for CMD are organ transplantation and gene therapy, their applicability is more difficult due to immune rejection issues, donor availability, and immature gene therapy. At this point, medical foods produced specifically for CMD can be effective in relieving the symptoms and reducing their incidence by limiting the uptake and accumulation of the relevant reaction substrate (Camp et al. 2012).

A common CMD is phenylketonuria (PKU), which is one of the most common congenital metabolic diseases requiring nutritional therapy. PKU is an amino acid metabolism disorder that occurs as a result of the inability to break down phenylalanine due to the deficiency of the enzyme phenylalanine hydroxylase, which converts phenylalanine to tyrosine. Since the accumulation of phenylalanine in blood and tissue causes permanent damage to the nerves, reducing its level is crucial, especially for children (Camp et al. 2012). Medical foods used in the treatment of PKU are divided into two groups according to their differences based on components. While one group contains all other nutrients, foods that do not contain phenylalanine at all or contain negligible amounts; the other group can be expressed as foods that have been modified to be low in protein. Various studies on the subject have shown that medical foods with a low phenylalanine formula can improve the health status of children with PKU (Chen et al. 2015; MacDonald et al. 2020; Mtewa et al. 2020). Specified medical food formulas that do not contain

disease-causing protein derivatives should be used in other amino acid metabolism disorders such as non-ketonic hyperglycinemia, tyrosinemia, and maple syrup urine disease (McCandless et al. 2021; Chong et al. 2022).

Another CMD is lactose intolerance. Lactose is a disaccharide found in both cow and human milk and is the primary energy source that supports growth in infants. But in some cases, lactase deficiency causes problems in the digestion of lactose. For this reason, medical food product prescriptions are designed to be lactose-free. The main difference between lactose-free infant formulas and standard infant formulas is that lactose-free formulas have glucose instead of lactose as the source of the carbohydrate (Lynch et al. 2020). Medical foods are produced for infants in the case of special disorders or conditions according to their nutritional requirements. Therefore, infant formulas are designed to provide ease of administration to infants for nutritional and medical purposes (Mtewa et al. 2020). Medical foods are widely used for premature infants as well as lactose intolerance. According to a statement made by the World Health Organization (WHO), infants born before 37 weeks are defined as premature (Chen et al. 2020; WHO 2022). These infants need a special diet because they have an immature gastrointestinal system due to preterm birth. Premature infant formulas are created to support the growth and development of preterm newborn and low birth weight babies (babies' weight <1500 g). Formulas containing cow's milk protein in their composition contain very high amounts of calcium and phosphorus. They are designed to match the higher calcium and phosphorus levels children need as they grow, similar to the levels found in whole milk (Chen et al. 2020; Sanadgol Nezami et al. 2021).

3.6. *Diabetes mellitus*

Diabetes Mellitus (DM) is a chronic metabolic disease characterized by persistent hyperglycemia, resulting from the insufficient or decreased effectiveness of insulin. The disease can be classified into two groups: Type-1 (insulin-dependent) and Type-2 (insulin-independent). Type-1 involves the complete destruction of pancreas β -cells, leading to an absolute insulin deficiency, while Type-2 is characterized by chronic hyperglycemia due to impaired insulin secretion or receptor function (Li et al. 2018; WHO 2022). The incidence of diabetes is rising globally, with approximately 592 million estimated cases by 2035. Type-2 diabetes accounts for 90% of all diabetes cases (Atkinson et al. 2014; Guariguata et al. 2014). The disease poses a significant economic burden and, if untreated, can lead to life-threatening complications affecting various organs. Treatment approaches include hypoglycemic drugs, insulin therapy, and surgical procedures. Ideal treatment focuses on achieving good glycemic control and correcting accompanying metabolic conditions (Tümer & Çolak 2012; Kaur et al. 2017). The American Diabetes Association (ADA) recommends a balanced diet, incorporating oral antidiabetic drugs and insulin, if necessary, along with regular exercise for Type-2 diabetes management. Medical foods are attracting more attention in diabetes treatment, as they offer nutritional support to help control blood sugar levels, and clinical trials exploring the use of medical foods in diabetes treatment are on the rise (ADA 2018). Representative examples of medical food products produced for DM patients are provided in Table 2.

When examining the compositions of medical foods produced for diabetes patients, healthcare professionals encourage individuals to consume various fiber-containing foods such as whole grains, fruits, and vegetables, since these foods provide vitamins, minerals, fiber, and other substances considered important for health. Studies conducted on the use of fibrous foods with patients with Type-1 diabetes show that fibrous structure has a positive effect on glycemia. In Type-2 diabetes patients, it has been determined that high fiber intake provides metabolic benefits on glycemic control, hyperinsulinemia and plasma lipids (Gao et al. 2020). For this reason, there is no harm in consuming fructose, which is naturally found in fruits, vegetables and other foods, depending on the level of intake, and the consumption of products rich in dietary fibers is encouraged (Satija et al. 2016; Torres et al. 2020). Agrawal et al. (2014) reported an association between vegetarian diet consumption and the occurrence of Type-2 diabetes in a nationally representative sample of 156 participants aged 20-49 years. It has been determined that the risk of diabetes in individuals who adhere to any vegetarian diet is statistically significantly lower. The similar results obtained in this study was found to be consistent with another study conducted by Chiu et al. (2014). Epidemiological studies comparing the prevalence of Type-2 diabetes among vegetarians and non-vegetarians have shown that vegetarians have a lower risk of Type-2 diabetes. This can be partially explained by lower weight, higher intakes of dietary fiber and plant-derived protein, lower intakes of saturated fat and a lack of protein from meat and eggs in the diet. Studies have shown that vegetarian diets, especially vegan diets, are effective tools in glycemic control and these diets are traditionally recommended for patients with diabetes (Pawlak 2017).

4. Medical Foods on Different Diseases in Global Market

The global medical foods industry is experiencing sustained growth due to the increasing recognition of the significance of nutrition in maintaining health and overall well-being. The market size of medical foods was assessed at \$21.38 billion in 2022 and is anticipated to increase from \$22.62 billion in 2023 to \$35.3 billion by 2032. The higher prevalence of chronic diseases, the aging global population, and a growing demand for customized nutrition are driving the market growth (Gotadki 2023). Representative examples of medical food products commercially available for different chronic diseases are given Table 2.

Table 2- Medical Foods in Global Market

<i>Medical Food</i>	<i>Composition</i>	<i>Efficacy</i>	<i>Findings</i>	<i>Reference</i>
<u>ALZHEIMER</u>				
Axona	Caprylic triglyceride (Medium chain triglycerides), caseinate, maltodextrin, whey protein, soy lecithin, magnesium phosphate.	Provides an energy source that the brain can use as an alternative to glucose to support the formation and function of synapses in the brain.	Ketone bodies occurring from the metabolism of medium chain triglycerides induce hyperketonemia, and thus ensure an alternate glucose substrate.	Sharma et al. 2014
Souvenaid	Omega-3 fatty acids, vitamin B ₁₂ , vitamin C, uridine monophosphate, choline, phospholipids, vitamin E, vitamin B ₆ , and folic acid.	The components in Souvenaid are effective in forming synapses between cell membranes.	Souvenaid has been scientifically proven to lead to improvements when taken daily for 3 years in the early diagnosis of Alzheimer's disease.	Soininen et al. 2021
Prevagen	Apoaequorin, vitamin D ₃ , microcrystalline cellulose, maltodextrin, magnesium stearate, salt, sugar, soy peptones, and modified corn starch.	Apoaequorin is a photoprotein naturally found in jellyfish. It improves memory, thinking speed, and overall cognition	It is thought that the calcium-binding ability of Prevagen is beneficial in preventing forgetfulness. This is because calcium disorder plays a part in the onset and progression of AD.	Grossman et al. 2022
Cerefolin	L-methylfolate calcium (Metafolin), methylcobalamin, algae powder, N-acetylcysteine.	L-methylfolate, an activated folate, influence memory, and protecting cognitive health.	Cerefolin is a prescription dietary supplement containing B vitamins. It is aimed at preventing and/or treating memory issues and forgetfulness caused by vitamin B12 and/or folate deficiency.	Spence et al. 2017
<u>CANCER</u>				
Nutrisource® Fiber	Partially hydrolyzed guar gum, soy, milk, and egg products.	It ensures soluble fiber to support digestive health and intestinal system and can be mixed with pudding, yoghurt, juices etc.	It should be used under the supervision of a physician to ensure that the ingredients do not affect the patient's health or cancer treatments.	Ravasco 2019
Medtrition ProSource	Water, protein (from collagen hydrolysate and whey isolate), maltodextrin, fructose, phosphoric acid, natural flavors, L-tryptophan, and milk.	The product, which is lactose-free and gluten-free, and contains 10 grams of protein, can be consumed orally or by tube.	Enriched medical foods as nutritional content are important for patients who have difficulty in swallowing in the last stages of cancer.	Liu et al. 2018
Boost® Nutritional Pudding	Maltodextrin, canola, high oleic sunflower and corn oil, milk protein concentrate, modified cornstarch, riboflavin, β-carotene, other vitamins and minerals.	It is produced to supply energy with 230 nutrients to facilitate the conversion of food into energy. It does not contain any artificial sweeteners.	Antioxidants, such as vitamins C and E, bind free radicals and prevent them from reacting with healthy cells. Therefore, antioxidant-rich formulas are recommended for cancer patients receiving chemotherapy.	Imran et al. 2020
Impact Advanced Recovery®	Water, sugar, calcium caseinate (milk), fish oil (anchovy, sardine), citric acid, maltodextrin, β-carotene, vitamin K ₁ , biotin, vitamin D ₃ , vitamin B ₁₂ , riboflavin.	This formula can help patients recover quickly after surgery and prevents the harmful effects that may occur due to malnutrition.	The importance of medical foods and supplements that strengthen the immune systems of cancer patients during the difficult treatment process is increasing.	Chen et al. 2021

Table 2(Continued)- Medical Foods in Global Market

<i>Medical Food</i>	<i>Composition</i>	<i>Efficacy</i>	<i>Findings</i>	<i>Reference</i>
<u>CMD</u>				
Vitabite	Lactose (milk), vegetable oil (fractionated palm kern oil), sugar, natural and artificial flavoring, carob flour, soy lecithin, and nuts.	A chocolate with high energy and low protein content is preferred for patients who require a protein-restricted diet due to an IEM.	The consumption of Vitabite, whose compositions are appropriately formulated for the disease, positively affects the course of the disease.	Rocha et al. 2021
PKU Start™	Carbohydrate, fat, essential and non-essential amino acids, trace elements, vitamins, arachidonic acid, docosahexaenoic acid, and minerals.	It is phenylalanine free formula food for PKU and must be used under doctor's supervision.	It is very important to use specially formulated medical foods that do not contain phenylalanine in order to prevent neurological diseases that may occur due to disease.	Van Calcar 2022
SMA LF®	Glucose, sunflower oil, soya lecithin, citric acid, phenylalanine, antioxidants (tocopherol-rich extract, ascorbyl palmitate), and L-carnitine	It is a lactose-free medical formula for babies with lactose intolerance. It is suitable for babies up to 18 months.	Lactose-free formulas are available to meet health and nutritional needs lactose intolerant. Reduced-lactose and lactose-free formulas can affect the course and reduce the duration of diarrhea.	Dipasquale et al. 2020
Similac NeoSure	Non-fat milk, corn syrup solids, lactose, soy oil, whey protein concentrate, coconut oil, β-carotene, lutein, potassium citrate, inositol, calcium carbonate, and soy lecithin.	It provides comprehensive nutrition for babies born prematurely (<37 weeks). This special formula has increased protein, vitamins, and minerals.	Nutrition can be difficult for many premature babies. At this point, it is crucial to produce medical food that babies can easily consume with premature formulas.	Lubbe 2018
<u>DIABETES</u>				
Diabetisource® AC	Water, corn syrup, soy protein, canola oil, green pea, green bean puree, and less than 2% of fructose, peach puree, FOS (soluble fiber), orange juice, refined fish oil, guar gum (soluble fiber), and soy fiber (insoluble fiber)	It is a tube feeding mixture that includes pureed fruits and vegetables to provide a source of carbohydrates for the diet management of diabetes.	In recent years, has become a growing global concern. The use of formulas rich in omega-3 fatty acids in diabetes reduces the risk of complications and prevents the occurrence of side effects that may arise with the use of medical drugs	Gao et al. 2020
Glytrol®	Water, maltodextrin, calcium-potassium caseinate (milk), modified corn starch and less than 2% of canola oil, safflower oil, pea fiber, FOS, soy lecithin, inulin (from chicory), L-carnitine, vitamins and minerals.	Glytrol® is medical food including easily digestible carbohydrate mixtures to regulate blood glucose. It contains soluble prebiotic fiber admixtures to promote a healthy digestive system.	Research studies show that the high fiber content of the diet has a high potential for preventing Type-2 diabetes. Therefore, this medical food is effective in diabetes management.	Torres et al. 2020
Boost Glucose Control® Max	Water, milk protein isolate, and less than 2% of sunflower oil, vitamins and minerals, cellulose gel, inulin, salt, calcium caseinate, whey protein concentrate, sucralose, carrageenan, and vanilla extract.	It contains 30 g of protein. For this reason, it is effective in preventing muscle weakness and keeping the fasting glucose level in balance.	It is clinically proven to produce a lower blood sugar response as a normal nutritional drink in patients with Type-2 diabetes.	Moore 2018
Betacell Glucofix	Cinnamon, gymnema, berberine, bitter melon and turmeric.	Glucofix is designed to regulate glucose metabolism, to provide ideal sugar values and to create an antioxidant source for the body.	Glucofix consists of a mixture of natural herbal ingredients that are effective on blood sugar. It is stated in various studies that the herbal materials in the product composition are effective in the treatment of diabetes	Awuchi 2019

CMD: Congenital metabolic disorder.

4. Conclusions

Chronic diseases last for an extended period of time, cannot be completely treated and, therefore, often require repeated treatments, and the extended use of pharmacological drugs. Standard treatments, while effective, come with a high financial cost and a range of side effects, including weight gain, hypertension, peripheral edema, anemia, nephropathy, and gastrointestinal issues. As an alternative approach, medical foods appear to be a promising avenue in the management and treatment of chronic diseases. Medical foods, formulated specifically for the treatment of certain diseases or disorders, offer a distinct advantage over conventional diets. When the nutritional requirements of a disease or condition cannot be adequately met through a regular diet alone, the use of medical foods becomes imperative. Despite their potential, the awareness of medical foods in society remains insufficient, emphasizing the need for further research to bridge this knowledge gap. This review has aimed to elucidate the term of medical food and underscore its importance by providing illustrative examples of its application in the treatment of various chronic diseases, including neurodegenerative diseases, anxiety and sleep disorders, pain syndromes, cancer, congenital metabolic disorders, and diabetes. The need remains to develop new medical food prescriptions and increase commercial production as natural alternatives to costly pharmaceutical products for both public health and the current gaps in literature. It is evident that more comprehensive studies are required to raise societal awareness regarding the vital role of medical foods in treating chronic diseases effectively through dietary intervention. The recommendation from the authors is to prioritize future exploratory and meta-analysis studies in this field. This approach aims to achieve a more precise estimation of the global impact on the health of patients and individuals. In addition, legal procedures for the production, distribution and processing of medical foods need to be detailed and there is a pressing need for specialized training programs to cultivate expertise in the field. These initiatives will not only ensure the adherence to regulatory standards but also contribute to the proficiency of professionals involved in the medical food industry.

Abbreviations

AD	Alzheimer's disease
ADA	American Diabetes Association
DASH	Dietary approaches to stop hypertension
DM	Diabetes mellitus
FDA	Food and Drug Administration
FSMPs	Foods for special medical purposes
GABA	γ -aminobutyric acid
CMD	Congenital metabolic disorders
KD	Ketogenic diet
MD	Mediterranean diet
PD	Parkinson's disease
PKU	Phenylketonuria
WHO	World Health Organization

References

- Aarsland D, Batzu L, Halliday G M, Geurtsen G J, Ballard C, Ray Chaudhuri K & Weintraub D (2021). Parkinson disease-associated cognitive impairment. *Nature Reviews Disease Primers* 7(1): 47. <https://doi.org/10.1038/s41572-021-00280-3>
- ADA- American Diabetes Association (2018). Updates to the standards of medical care in diabetes 2018. *Diabetes Care* 41(9): 2045-2047. <https://doi.org/10.2337/dc18-su09>
- Adell A (2004). Antidepressant properties of substance P antagonists: relationship to monoaminergic mechanisms? *Current Drug Targets-CNS & Neurological Disorders* 3(2): 113-121. <https://doi.org/10.2174/1568007043482516>
- Agrawal S, Millett C J, Dhillon P K, Subramanian S V & Ebrahim S (2014). Type of vegetarian diet, obesity and diabetes in adult Indian population. *Nutrition Journal* 13: 1-18. <https://doi.org/10.1186/1475-2891-13-89>
- Arenas D J, Thomas A, Wang J & DeLisser H M (2019). A systematic review and meta-analysis of depression, anxiety, and sleep disorders in US adults with food insecurity. *Journal of General Internal Medicine* 34: 2874-2882. <https://doi.org/10.1007/S11606-019-05202-4>
- Arends J, Bachmann P, Baracos V, Barthelemy N, Bertz H, Bozzetti F & Preiser J C (2017). ESPEN guidelines on nutrition in cancer patients. *Clinical Nutrition* 36(1): 11-48. <https://doi.org/10.1016/j.clnu.2016.07.015>
- Armstrong M J & Okun M S (2020). Diagnosis and treatment of Parkinson disease: a review. *Jama* 323(6): 548-560. <https://doi.org/10.1001/jama.2019.22360>
- Aslan S N & Karahalil B (2019). Oksidatif stres ve Parkinson Hastalığı. *Journal of Faculty of Pharmacy of Ankara University* 43: 94-116. <https://doi.org/10.33483/jfpau.519964>
- Atkinson M A, Eisenbarth G S & Michels A W (2014). Type 1 diabetes. *The Lancet* 383(9911): 69-82. [https://doi.org/10.1016/S0140-6736\(13\)60591-7](https://doi.org/10.1016/S0140-6736(13)60591-7)
- Atri A (2019). Current and Future Treatments in Alzheimer's Disease, *Seminars in Neurology* 39(2): 227-240. <https://doi.org/10.1055/S-0039-1678581>
- Awuchi C G (2019). Medicinal plants: the medical, food, and nutritional biochemistry and uses. *International Journal of Advanced Academic Research* 5(11): 220-241
- Bagchi D (2019). Understanding medical foods under FDA regulations. In: D Bagchi (Eds.), *Nutraceutical and Functional Food Regulations in the United States and Around the World*, Academic Press, US, pp. 203-235.
- Bazan N G (2018). Docosanoids and elovanoids from omega-3 fatty acids are pro-homeostatic modulators of inflammatory responses, cell damage and neuroprotection. *Molecular Aspects of Medicine* 64: 18-33. <https://doi.org/10.1016/j.mam.2018.09.003>

- Bianchi V E, Rizzi L & Somaa F (2023). The role of nutrition on Parkinson's disease: a systematic review. *Nutritional Neuroscience* 26(7): 605-628. <https://doi.org/10.1080/1028415X.2022.2073107>.
- Bivona G, Gambino C M, Iacolino G & Ciaccio M (2019). Vitamin D and the nervous system. *Neurological Research* 41(9): 827-835. <https://doi.org/10.1080/01616412.2019.1622872>
- Blasiak J, Chojnacki J, Pawlowska E, Szczepanska J & Chojnacki C (2020). Nutrition in cancer therapy in the elderly—an epigenetic connection? *Nutrients* 12(11): 3366. <https://doi.org/10.3390/nu12113366>
- Bloem B R, Okun M S & Klein C (2021). Parkinson's disease. *The Lancet* 397(10291): 2284-2303. [https://doi.org/10.1016/S0140-6736\(21\)00218-X](https://doi.org/10.1016/S0140-6736(21)00218-X)
- Camp K M, Lloyd-Puryear M A & Huntington K L (2012). Nutritional treatment for inborn errors of metabolism: indications, regulations, and availability of medical foods and dietary supplements using phenylketonuria as an example. *Molecular Genetics and Metabolism* 107(1-2): 3-9. <https://doi.org/10.1016/j.ymgme.2012.07.005>
- Chen C, Yin Q, Wu H, Cheng L, Kwon J I, Jin J & Che H (2020). Different effects of premature infant formula and breast milk on intestinal microecological development in premature infants. *Frontiers in Microbiology* 10: 3020. <https://doi.org/10.3389/FMICB.2019.03020/FULL>
- Chen H, Cao S, Pei B, Li Y & Wei H (2015). Effects of Enteral Nutrition Powder in Children with Phenylketonuria under One Year. *China Pharmacy* pp.4968-4970
- Chen Q H, Wu B K, Pan D, Sang L X & Chang B (2021). Beta-carotene and its protective effect on gastric cancer. *World Journal of Clinical Cases* 9(23): 6591. <https://doi.org/10.12998/wjcc.v9.i23.6591>
- Chiu T H, Huang H Y, Chiu Y F, Pan W H, Kao H Y, Chiu J P & Lin C L (2014). Taiwanese vegetarians and omnivores: dietary composition, prevalence of diabetes and IFG. *PLoS One* 9(2): e88547. <https://doi.org/10.1371/JOURNAL.PONE.0088547>
- Chong L, Kalvala J, Chadborn N & Ojha S (2022). Breastfeeding in infants diagnosed with phenylketonuria (Protocol). *Cochrane Database of Systematic Reviews* 2022(8). <https://doi.org/10.1002/14651858.CD015243>
- Dipasquale V, Serra G, Corsello G & Romano C (2020). Standard and specialized infant formulas in Europe: making, marketing, and health outcomes. *Nutrition in Clinical Practice* 35(2): 273-281. <https://doi.org/10.1002/ncp.10261>
- Domínguez Díaz L, Fernández-Ruiz V & Cámara M (2020). The frontier between nutrition and pharma: The international regulatory framework of functional foods, food supplements and nutraceuticals. *Critical Reviews in Food Science and Nutrition* 60(10): 1738-1746. <https://doi.org/10.1080/10408398.2019.1592107>
- Ellouze I, Sheffler J, Nagpal R & Arjmandi B (2023). Dietary patterns and Alzheimer's disease: An updated review linking nutrition to neuroscience. *Nutrients* 15(14): 3204. <https://doi.org/10.3390/nu15143204>
- España R A & Scammell T E (2004). Sleep neurobiology for the clinician. *Sleep* 27(4): 811-820. <https://doi.org/10.1093/sleep/27.4.811>
- Farooqui T, Farooqui A A (2017). Neuroprotective effects of phytochemicals in neurological disorders. In T Farooqui & A A Farooqui (Eds.), *John Wiley & Sons, New York*, pp. 561-580
- FDA (2016). Center for Food Safety and Applied Nutrition. Guidance for industry: frequently asked questions about medical foods. Retrieved in April, 18, 2023 from <https://www.fda.gov/regulatory-information/search-fda-guidance/documents/guidance-industry-frequently-asked-questions-about-medical-foods-second-edition/>
- FDA (2022). Draft guidance for industry: frequently asked questions about medical foods. Retrieved in April, 18, 2023 from <https://www.fda.gov/regulatory-information/search-fda-guidance%20documents/guidance-industry-frequently-asked-questions-about-medical-foods-second-edition/>
- Fung F, Wang H S & Menon S (2018). Food safety in the 21st century. *Biomedical Journal* 41(2): 88-95. <https://doi.org/10.1016/j.bj.2018.03.003>
- Gaenslen A, Gasser T & Berg D (2008). Nutrition and the risk for Parkinson's disease: review of the literature. *Journal of Neural Transmission* 115: 703-713. <https://doi.org/10.1007/S00702-007-0005-4>
- Gao L, Lin L, Shan N, Ren C Y, Long X, Sun Y H & Wang L (2020). The impact of omega-3 fatty acid supplementation on glycemic control in patients with gestational diabetes: a systematic review and meta-analysis of randomized controlled studies. *The Journal of Maternal-Fetal & Neonatal Medicine* 33(10): 1767-1773. <https://doi.org/10.1080/14767058.2018.1526916>
- Giuliano C, Cerri S & Blandini F (2021). Potential therapeutic effects of polyphenols in Parkinson's disease: In vivo and in vitro pre-clinical studies. *Neural Regeneration Research* 16(2): 234. <https://doi.org/10.4103/1673-5374.290879>
- Glenn J M, Madero E N & Bott N T (2019). Dietary protein and amino acid intake: links to the maintenance of cognitive health. *Nutrients* 11(6): 1315. <https://doi.org/10.3390/nu11061315>
- Gonzalez-Latapi P, Bayram E, Litvan I & Marras C (2021). Cognitive impairment in Parkinson's disease: epidemiology, clinical profile, protective and risk factors. *Behavioral Sciences* 11(5): 74. <https://doi.org/10.3390/bs11050074>
- Gotadki R (2023). Global Medical Foods Market Overview. Retrieved in April, 25, 2023 from <https://www.marketresearchfuture.com/reports/medical-foods-market-4915/>
- Groff M L, Choi B, Lin T, McIlraith I, Hutnik C & Malvankar-Mehta M S (2022). Anxiety, depression, and sleep-related outcomes of glaucoma patients: systematic review and meta-analysis. *Canadian Journal of Ophthalmology*. <https://doi.org/10.1016/j.cjco.2022.02.010>
- Grossman S, Nathan J P, Siuzdak A, Liang J & Sprycha C (2022). Prevagen®: Analysis of Clinical Evidence and Its Designation as a “# 1 Pharmacist Recommended Brand”. *The Senior Care Pharmacist* 37(8): 335-338
- Guariguata L, Whiting D R, Hambleton I, Beagley J, Linnenkamp U & Shaw J E (2014). Global estimates of diabetes prevalence for 2013 and projections for 2035. *Diabetes Research and Clinical Practice* 103(2): 137-149. <https://doi.org/10.1016/j.diabres.2013.11.002>
- Holmes J L, Biella A, Morck T, Rostorfer J & Schneeman B (2021). Medical foods: Science, regulation, and practical aspects. Summary of a workshop. *Current Developments in Nutrition* 5(1): 172. <https://doi.org/10.1093/cdn/nzaa172>
- Hoscheidt S, Sanderlin A H, Baker L D, Jung Y, Lockhart S, Kellar D & Craft S (2022). Mediterranean and Western diet effects on Alzheimer's disease biomarkers, cerebral perfusion, and cognition in mid-life: A randomized trial. *Alzheimer's & Dementia* 18(3): 457-468. <https://doi.org/10.1002/alz.12421>
- Hughes K C, Gao X, Kim I Y, Rimm E B, Wang M, Weisskopf M G & Ascherio A (2016). Intake of antioxidant vitamins and risk of Parkinson's disease. *Movement Disorders* 31(12): 1909-1914. <https://doi.org/10.1002/mds.26819>
- Imran M, Ghorat F, Ul-Haq I, Ur-Rehman H, Aslam F, Heydari M & Rebezov M (2020). Lycopene as a natural antioxidant used to prevent human health disorders. *Antioxidants* 9(8): 706. <https://doi.org/10.3390/antiox9080706>

- Ishihara L & Brayne C (2005). A systematic review of nutritional risk factors of Parkinson's disease. *Nutrition Research Reviews* 18(2): 259-282. <https://doi.org/10.1079/NRR2005108>
- Kaur R, Dahiya L & Kumar M (2017). Fructose-1, 6-bisphosphatase inhibitors: a new valid approach for management of type 2 diabetes mellitus. *European Journal of Medicinal Chemistry* 141: 473-505. <https://doi.org/10.1016/j.ejmech.2017.09.029>
- Kaya D & Soyukibar T E (2022). Parkinson Hastalığı ve Parkinsonizm. *The Journal of Turkish Family Physician* 13(4): 182-192. <https://doi.org/10.15511/tjtfp.22.00482>
- Lange K W, Guo J, Kanaya S, Lange K M, Nakamura Y & Li S (2019a). Medical foods in Alzheimer's disease. *Food Science and Human Wellness* 8(1): 1-7. <https://doi.org/10.1016/j.fshw.2019.02.002>
- Lange K W, Nakamura Y, Chen N, Guo J, Kanaya S, Lange K M & Li S (2019b). Diet and medical foods in Parkinson's disease. *Food Science and Human Wellness* 8(2): 83-95. <https://doi.org/10.1016/j.fshw.2019.03.006>
- Lewis C A, Jackson M C (2019). In Nutraceutical and Functional Food Regulations in the United States and Around the World. In J R Bailey (Eds.), Academic Press, US, 203 pp
- Li S, Ho C T & Lange K W (2021). Medical foods in USA at a glance. *Journal of Future Foods* 1(2): 141-145. <https://doi.org/10.1016/j.jfutfo.2022.01.003>
- Li X, Jiang X, Sun J, Zhu C & Bai W (2018). Recent advances of medical foods in China: The opportunities and challenges under standardization. *Food and Chemical Toxicology* 119: 342-354. <https://doi.org/10.1016/j.fct.2018.02.024>
- Liu Z, Ren Z, Zhang J, Chuang C C, Kandaswamy E, Zhou T & Zuo L (2018). Role of ROS and nutritional antioxidants in human diseases. *Frontiers in Physiology* 9: 477. <https://doi.org/10.3389/FPHYS.2018.00477/FULL>
- Lubbe W (2018). Clinicians guide for cue-based transition to oral feeding in preterm infants: An easy-to-use clinical guide. *Journal of Evaluation in Clinical Practice* 24(1): 80-88. <https://doi.org/10.1111/jep.12721>
- Lynch R, Burke A, Byrne J & Buckin V (2020). Osmolality and molar mass of oligosaccharides in breast milks and infant formula during hydrolysis of lactose. Application of high-resolution ultrasonic spectroscopy. *Food Chemistry* 322: 126645. <https://doi.org/10.1016/j.foodchem.2020.126645>
- MacDonald A, Van Wegberg A M J, Ahring K, Beblo S, Bélanger-Quintana A, Burlina A & Van Spronsen F J (2020). PKU dietary handbook to accompany PKU guidelines. *Orphanet Journal of Rare Diseases* 15(1): 1-21. <https://doi.org/10.1186/S13023-020-01391-Y>
- Mao X Y, Jin M Z, Chen J F, Zhou H H & Jin W L (2018). Live or let die: Neuroprotective and anti-cancer effects of nutraceutical antioxidants. *Pharmacology & Therapeutics* 183: 137-151. <https://doi.org/10.1016/j.pharmthera.2017.10.012>
- Markowitz J S, Gurley P C & Gurley B J (2020). Medical foods—A closer look at the menu: A brief review and commentary. *Clinical Therapeutics* 42(7): 1416-1423. <https://doi.org/10.1016/j.clinthera.2020.05.011>
- Martikainen I K, Hagelberg N, Jääskeläinen S K, Hietala J & Pertovaara A (2018). Dopaminergic and serotonergic mechanisms in the modulation of pain: In vivo studies in human brain. *European Journal of Pharmacology* 834: 337-345.
- McCandless S, Frederick S R, William B J, Cara M, Benjamin S (2021). Laboratory Diagnosis of Inborn Errors of Liver Metabolism. In F J Suchy, R J Sokol & W F Balistreri (Eds.), *Liver Disease in Children*. Cambridge University Press, UK, pp. 401 - 416
- Md W E S, Md L A M, Crc D H B B C & Md D S S (2012). Sentra PM (a medical food) and trazodone in the management of sleep disorders. *Journal of Central Nervous System Disease* 4 pp. <https://doi.org/10.4137/JCNSD.S9381>
- Meletis C D & Zabriskie N (2007). Common nutrient depletions caused by pharmaceuticals. *Alternative & Complementary Therapies* 13(1): 10-17. <https://doi.org/10.1089/act.2006.13102>
- Miclea A, Bagnoud M, Chan A & Hoepner R (2020). A brief review of the effects of vitamin D on multiple sclerosis. *Frontiers in Immunology* 11: 781. <https://doi.org/10.3389/FIMMU.2020.00781/FULL>
- Molsberry S, Bjornevik K, Hughes K C, Healy B, Schwarzschild M & Ascherio A (2020). Diet pattern and prodromal features of Parkinson disease. *Neurology* 95(15): 2095-2108. <https://doi.org/10.1212/WNL.0000000000010523>
- Moore M D (2018). Food as medicine: diet, diabetes management, and the patient in twentieth century Britain. *Journal of the History of Medicine and Allied Sciences* 73(2): 150-167. <https://doi.org/10.1093/jhmas/jry008>
- Morley J E, Farr S A & Nguyen A D (2018). Alzheimer disease. *Clinics in Geriatric Medicine* 34(4): 591-601. <https://doi.org/10.1016/j.cger.2018.06.006>
- Mtewa A G, Kasali M F, Bekele T, Obura B (2020). Medical Foods and Infant Formulas. In: C Egbuna, G Dable Tupas (Eds.), *Functional Foods and Nutraceuticals*. Springer, Switzerland, pp. 509-525. https://doi.org/10.1007/978-3-030-42319-3_23
- Muscaritoli M, Arends J, Bachmann P, Baracos V, Barthelemy N, Bertz H & Bischoff S C (2021). ESPEN practical guideline: Clinical Nutrition in cancer. *Clinical Nutrition* 40(5): 2898-2913. <https://doi.org/10.1016/j.clnu.2021.02.005>
- Nikogosian A (2022). Functional Medicine, South West Functional Medicine. Retrieved in April, 21, 2023 from <https://southwestfunctionalmedicine.com/about-functional-medicine/>
- Ohnuma T, Toda A, Kimoto A, Takebayashi Y, Higashiyama R, Tagata Y & Arai H (2016). Benefits of use, and tolerance of, medium-chain triglyceride medical food in the management of Japanese patients with Alzheimer's disease: a prospective, open-label pilot study. *Clinical Interventions in Aging* pp. 29-36. <https://doi.org/10.2147/CIA.S95362>
- Omar S H (2019). Mediterranean and MIND diets containing olive biophenols reduces the prevalence of Alzheimer's disease. *International Journal of Molecular Sciences* 20(11): 2797. <https://doi.org/10.3390/ijms20112797>
- Özdemir H (2022). Parkinson Hastalığı "Geçmişten Geleceğe". Turkey Clinics Publishing House, Turkey
- Parker F R (2005). Department of Health and Human Services, US Food and Drug Administration: Authority and Responsibility. In: F R Parker (Eds.), *FDA Administrative Enforcement Manual*, CRC Press, US, pp. 21-60
- Pawlak R (2017). Vegetarian diets in the prevention and management of diabetes and its complications. *Diabetes Spectrum* 30(2): 82-88. <https://doi.org/10.2337/ds16-0057>
- Postuma R B, Aarsland D, Barone P, Burn D J, Hawkes C H, Oertel W & Ziemssen T (2012). Identifying prodromal Parkinson's disease: pre-motor disorders in Parkinson's disease. *Movement Disorders* 27(5): 617-626. <https://doi.org/10.1002/mds.24996>
- Przyrembel H, Siani A, Turck D & Van A (2015). EFSA Panel on Dietetic Products, Nutrition and Allergies (NDA) on foods for special medical purposes in the context of Article 3 of Regulation (EU) No 609 EFSA Supporting Publications 12. <https://doi.org/10.2903/sp.efsa.2015.EN-904>
- Ravasco P (2019). Nutrition in cancer patients. *Journal of Clinical Medicine* 8(8): 1211. <https://doi.org/10.3390/jcm8081211>

- Rocha J C, Bausell H, Bélanger-Quintana A, Bernstein L, Gökmen-Özel H, Jung A & Heddrich-Ellerbrok M (2021). Development of a practical dietitian road map for the nutritional management of phenylketonuria (PKU) patients on pegvaliase. *Molecular Genetics and Metabolism Reports* 28: 100771. <https://doi.org/10.1016/j.ymgmr.2021.100771>
- Rosenthal M D, Carrott P W, Patel J, Kiraly L & Martindale R G (2016). Parenteral or enteral arginine supplementation safety and efficacy. *The Journal of Nutrition* 146(12): 2594S-2600S. <https://doi.org/10.3945/jn.115.228544>
- Rudy L, Carmen R, Daniel R, Artemio R & Moisés R O (2020). Anticonvulsant mechanisms of the ketogenic diet and caloric restriction. *Epilepsy Research* 168: 106499. <https://doi.org/10.1016/j.eplepsyres.2020.106499>
- Sääksjärvi K, Knekt P, Lundqvist A, Männistö S, Heliövaara M, Rissanen H & Järvinen R (2013). A cohort study on diet and the risk of Parkinson's disease: the role of food groups and diet quality. *British Journal of Nutrition* 109(2): 329-337. <https://doi.org/10.1017/S0007114512000955>
- Sanadgol Nezami M, Feizbakhsh A & Bagheri Garmarudi A (2021). Detection of soybean powder and rice flour adulterations in premature formula by ATR-FTIR spectroscopy and chemometrics. *Iranian Journal of Science and Technology, Transactions A: Science* 45(3): 857-865. <https://doi.org/10.1007/S40995-021-01072-W>
- Satija A, Bhupathiraju S N, Rimm E B, Spiegelman D, Chiuve S E, Borgi L & Hu F B (2016). Plant-based dietary patterns and incidence of type 2 diabetes in US men and women: results from three prospective cohort studies. *PLoS Medicine* 13(6): e1002039. <https://doi.org/10.1371/JOURNAL.PMED.1002039>
- Scheltens, P, Kamphuis P J, Verhey F R, Rikkert M G O, Wurtman R J, Wilkinson D & Kurz A (2010). Efficacy of a medical food in mild Alzheimer's disease: A randomized, controlled trial. *Alzheimer's & Dementia* 6(1): 1-10. <https://doi.org/10.1016/j.jalz.2009.10.003>
- Seron-Arbeloa C, Zamora-Elson M, Labarta-Monzon L & Mallor-Bonet T (2013). Enteral nutrition in critical care. *Journal of Clinical Medicine Research* 5(1): 1. <https://doi.org/10.4021/jocmr1210w>
- Sharma A, Bemis M & Desilets A R (2014). Role of medium chain triglycerides (Axona®) in the treatment of mild to moderate Alzheimer's disease. *American Journal of Alzheimer's Disease & Other Dementias* 29(5): 409-414. <https://doi.org/10.1177/1533317513518650>
- Shell W E, Pavlik S, Roth B, Silver M, Breitstein M L, May L & Silver D (2016). Reduction in pain and inflammation associated with chronic low back pain with the use of the medical food theramine. *American Journal of Therapeutics* 23(6): e1353. <https://doi.org/10.1097/MJT.0000000000000068>
- Shell W, Bullias D, Charuvastra E, May L A & Silver D S (2010). A randomized, placebo-controlled trial of an amino acid preparation on timing and quality of sleep. *American Journal of Therapeutics* 17(2): 133-139. <https://doi.org/10.1097/MJT.0b013e31819e9eab>
- Shi C, Wang P, Airen S, Brown C, Liu Z, Townsend J H & Jiang H (2020). Nutritional and medical food therapies for diabetic retinopathy. *Eye and Vision* 7(1): 1-16. <https://doi.org/10.1186/S40662-020-00199-Y>
- Shim H, Rose J, Halle S & Shekane P (2019). Complex regional pain syndrome: a narrative review for the practising clinician. *British Journal of Anaesthesia* 123(2): e424-e433. <https://doi.org/10.1016/j.bja.2019.03.030>
- Simon D K, Tanner C M & Brundin P (2020). Parkinson disease epidemiology, pathology, genetics, and pathophysiology. *Clinics in Geriatric Medicine* 36(1): 1-12. <https://doi.org/10.1016/j.cger.2019.08.002>
- Singh A, Tripathi P, Yadawa A K & Singh S (2020). Promising polyphenols in Parkinson's disease therapeutics. *Neurochemical Research* 45: 1731-1745. <https://doi.org/10.1007/S11064-020-03058-3>
- Soininen H, Solomon A, Visser P J, Hendrix S B, Blennow K, Kivipelto M & LipiDiDiet Clinical Study Group (2021). 36-month LipiDiDiet multinutrient clinical trial in prodromal Alzheimer's disease. *Alzheimer's & Dementia* 17(1): 29-40. <https://doi.org/10.1002/alz.12172>
- Spence J, Chintapenta M, Kwon H I & Blaszczyk A T (2017). A brief review of three common supplements used in Alzheimer's disease. *The Consultant Pharmacist* 32(7): 412-414. <https://doi.org/10.4140/TCP.n.2017.412>
- Taylor S S, Noor N, Urits I, Paladini A, Sadhu M S, Gibb C & Viswanath O (2021). Complex regional pain syndrome: a comprehensive review. *Pain and Therapy* 10(2): 875-892. <https://doi.org/10.1007/S40122-021-00279-4>
- TFC (2001). Communiqué on Dietary Foods for Special Medical Purposes. Retrieved in April, 25, 2023 from <https://www.titck.gov.tr/mevzuat/turk-gida-kodeksi-ozel-tibbi-amacli-diyet-gidalar-teblihi-27122018172804/>
- Torres N, Avila-Nava A, Medina-Vera I & Tovar A R (2020). Dietary fiber and diabetes. *Science and Technology of Fibers in Food Systems* 201-218. https://doi.org/10.1007/978-3-030-38654-2_9
- Tümer G & Çolak R (2012). Tip 2 diabetes mellitusda tibbi beslenme tedavisi. *Journal of Experimental and Clinical Medicine* 29(1): 12-15. <https://doi.org/10.5835/jecm.omu.29.s1.004>
- Valuck R J & Ruscin J M (2004). A case-control study on adverse effects: H2 blocker or proton pump inhibitor use and risk of vitamin B12 deficiency in older adults. *Journal of Clinical Epidemiology* 57(4): 422-428. <https://doi.org/10.1016/j.jclinepi.2003.08.015>
- Van Calcar S (2022). Tetrahydrobiopterin Therapy for Phenylketonuria. In L E Bernstein, F Rohr & J R Helm (Eds.), *Nutrition Management of Inherited Metabolic Diseases*, Springer, New York, pp. 127-151
- Weinstein D A, Steuerwald U, De Souza C F & Derks T G (2018). Inborn errors of metabolism with hypoglycemia: glycogen storage diseases and inherited disorders of gluconeogenesis. *Pediatric Clinics* 65(2): 247-265. <https://doi.org/10.1016/j.pcl.2017.11.005>
- WHO (2022). Diabetes. Retrieved in March, 12, 2023 from <http://www.who.int/mediacentre/factsheets/fs312/en/>
- Xu R, Ding Z, Zhao P, Tang L, Tang X & Xiao S (2016). The effects of early post-operative soluble dietary fiber enteral nutrition for colon cancer. *Nutrients* 8(9): 584. <https://doi.org/10.3390/nu8090584>
- Xu Lou I, Ali K & Chen Q (2023). Effect of nutrition in Alzheimer's disease: A systematic review. *Frontiers in Neuroscience* 17: 1147177. <https://doi.org/10.3389>
- Yeshokumar A K, Saylor D, Kornberg M D & Mowry E M (2015). Evidence for the importance of vitamin D status in neurologic conditions. *Current Treatment Options in Neurology* 17: 1-13. <https://doi.org/10.1007/S11940-015-0380-3>
- Zhao M, Tuo H, Wang S & Zhao L (2020). The effects of dietary nutrition on sleep and sleep disorders. *Mediators of Inflammation*. <https://doi.org/10.1155/2020/3142874>





Predatory Protists: The Key Players in the Quest for Sustainable Agricultural Practices

Seda Ozer Bodur^a , Mayu Fujino^a , Rasit Asiloglu^{b*} 

^aGraduate School of Science and Technology, Niigata University, Niigata, JAPAN

^bInstitute of Science and Technology, Niigata University, Niigata, JAPAN

ARTICLE INFO

Review Article

Corresponding Author: Rasit Asiloglu, E-mail: asiloglu@agr.niigata-u.ac.jp

Received: 06 March 2024 / Revised: 07 May 2024 / Accepted: 11 May 2024 / Online: 23 July 2024

Cite this article

Bodur S O, Fujino M, Asiloglu R (2024). Predatory Protists: The Key Players in the Quest for Sustainable Agricultural Practices. *Journal of Agricultural Sciences (Tarim Bilimleri Dergisi)*, 30(3):436-443. DOI: 10.15832/ankutbd.1447822

ABSTRACT

To overcome the global problem of food shortage while supporting sustainable life on Earth, we must appreciate the critical importance of soil microorganisms—the key drivers of essential ecosystem services such as nutrient cycling and plant productivity. Protists are one of the major microbial groups in soil ecosystem including primary producers, decomposers, predators, and symbionts. The diverse morphologies and feeding strategies of predatory protists, including amoebae, ciliates, and flagellates, contribute to their versatility in capturing prey. Particularly, trophic interactions between protists and bacteria play a crucial role in regulating bacterial communities in the soil. Protists selectively prey on bacteria, influencing community composition, and enhancing microbial

activity. The impact extends to nutrient cycling, secondary metabolite production, and even antibiotic resistance in soil bacterial communities. Despite recent advances, the field of applied protistology remains underexplored, necessitating further research to bridge the gap between theoretical potential and practical application. We call for increased scientific attention, research efforts, and practical implementations to fully harness the benefits of soil protistology for future agricultural practices. In this article, we introduced the frequently overlooked essential roles of predatory protists in soil ecosystem and their potential usage in sustainable agriculture.

Keywords: Predatory Protist, Soil Protists, Sustainable Agriculture, Trophic Interactions, Plant Growth, Applied Protistology

1. Introduction

Food shortage is one of the most critical global problems. The FAO (Food and Agriculture Organization) predicts that we have to increase overall food production by 70% to feed the world population in 2050, which is challenging with the current agricultural practices (*e.g.*, agrochemicals) (FAO 2024). To overcome the global problem of food shortage while supporting sustainable life on Earth, we must appreciate the critical importance of soil microorganisms—the key drivers of essential ecosystem services such as nutrient cycling and plant productivity (Trivedi et al. 2020). A better understanding of plant-microbe interaction could revolutionize agriculture through manipulating the plant microbiome to sustainably increase crop production (Jansson et al. 2023). Among the soil microbiome, bacteria, fungi, and archaea are well-studied, while protists, the vast majority of eukaryotes, are largely neglected (Gao et al. 2019).

Protists represents the majority of eukaryotes. Indeed, all eukaryotes except fungi, plants, and animals are protists. They are predominantly microscopic, unicellular, and ubiquitous (Adl et al. 2012). Protists includes primary producers, decomposers, predators, and symbionts (Geisen et al. 2017). The predators are taxonomically most diverse functional group of protists, constitutes more than half of the protist diversity (Gao et al. 2019). Their preys include bacteria, archaea, fungi, and even nematodes, which allows them to control soil biodiversity and the population of microorganisms, enhance microbial activity, and promote nutrient cycling and plant productivity (Geisen et al. 2018; Gao et al. 2019; Xiong et al. 2020; Guo et al. 2021). Degradation of organic matter is an important role of decomposer protists, which accelerates nutrient cycling (Geisen et al. 2018). Photoautotrophic protists, mainly algae, play key roles in the global soil carbon balance.

The 6% of the net primary production of the whole terrestrial vegetation come from the carbon fixed by the soil algae (Jassey et al. 2022). Plant pathogenic protists (mainly belonging to Oomycetes) cause enormous negative impacts on agricultural production, while negative effect on the health of animals and microorganisms caused by animal and microbial parasites belonging to protists (Gilbert & Parker 2023). Taken together, soil biodiversity, nutrient cycling, and agricultural productivity are controlled by protists and protist communities are sensitive to environmental factors such as soil physicochemical properties,

the rhizosphere effect, organic and inorganic fertilizers, especially nitrogen (Asiloglu et al. 2015; 2016; 2021a; 2021b; Asiloglu 2022; Bodur et al. 2024).

Despite their enormous ecological impact, not everyone today recognizes that protists are the essential component of the microbial world (Caron et al. 2009). This review article explains the basics of predatory protists targeting those who are not specialized in protistology research area. In this article, we aimed to introduce recent studies on predatory protists focusing on their potential in sustainable agriculture. We explained the functional importance of predatory protists, their trophic relationships with their prey communities, and the services they provide to soil and plant health, followed by a highlight on their potential use in sustainable agriculture.

2. Predatory Protists

Predatory protists, a diverse group of microorganisms, play a crucial role in ecosystems by consuming other microorganisms including bacteria, fungi, other protists, and even nematodes. Their morphology and feeding types vary, allowing diverse trophic interactions with their prey. The outcome of the trophic interactions has profound effects on soil health, nutrient turnover, and plant productivity (Geisen et al. 2018; Gao et al. 2019).

2.1. Morphology and feeding types

Predatory protists are heterotrophs that rely on external sources for nutrients which is obtained through phagotrophy. Predatory protists extract the essential nutrients from their prey by capturing and internalizing their prey. Predatory protists exhibit a range of morphological features with different motility and feeding styles, which results in a variety of ways to consume their prey. Although exceptions are not rare, in general protists' morphology is an important indicator for how they capture their prey. The three major morphological groups are amoebae (naked amoebae and testate amoeba), ciliates, and flagellates (Figure 1).

Amoebae have the ability to alter its shape by extending and retracting pseudopods (Figure 1A). The pseudopodia allow an extraordinary advantage enabling them to navigate their environment with unparalleled precision; therefore, pseudopodia play a crucial role in amoeba's feeding strategy. Thanks to pseudopods, amoeba can reach into small pores that are inaccessible to larger predators such as ciliates. This unique adaptation demonstrates amoeba's ability to exploit the tiniest of resources to survive. Although they are grouped together morphologically, amoeba are not monophyletic as they belong to several taxonomic groups such as Amoebozoa, Rhizaria, and Excavata (Jan 2008; Nikolaev et al. 2024). The major difference between amoeba and the other two morphologic groups, ciliates and flagellates, is that amoeba can crawl on the surface of soil particles, ciliates and flagellates can swim in the water-filled soil pores.

Ciliates are the only monophyletic group of predatory protists belonging to Ciliophara (Gao et al. 2016). They are distinguished with their short hair-like organelles called cilia, which extend from the cell's surface enabling ciliates to perform a wide range of functions (Figure 1B). Ciliates rhythmically move their cilia to swim in aquatic environments or water-filled soil pores. In addition to swimming, cilia are also useful for navigating surfaces and exploring their environment. Ciliates exhibit an exceptional ability, filter-feeding, using their cilia to create water currents that draw in their prey. This filtering process allows ciliates to capture and consume vast amounts of prey microorganisms, effectively serving as efficient predators in their ecosystems. On the other hand, filter-feeding makes ciliates less selective on their prey (Asiloglu et al. 2020). It should be noted that not all ciliates are filter-feeders. Besides cilia's role in prey capturing, cilia also play a crucial role in sensation, while enabling ciliates to detect environmental changes and actively interact with their surroundings.

Another morphological group of predatory protists is flagellates (Figure 1C). They are fast swimmer thanks to their whip-like flagella. The flagella's propulsive action allows flagellates to swiftly explore their surroundings, actively seeking out essential resources; nutrients or prey. Some flagellates exhibit raptorial feeding abilities, using their flagella to capture prey with impressive ability. This predatory strategy allows them to actively pursue and trap smaller microorganisms, making them both fast hunters and elusive. Besides, the flagella allow them to easily escape potential danger (Nielsen & Kiørboe 2021), allowing them to thrive in a variety of ecological environments. Flagellates are polyphyletic, meaning they belong to several taxonomic supergroups of protists. In addition to the three main morphological groups, there is a group of protists that can transform between amoeboid forms and flagellate forms called amoeboflagellates (Mitchell 2007).

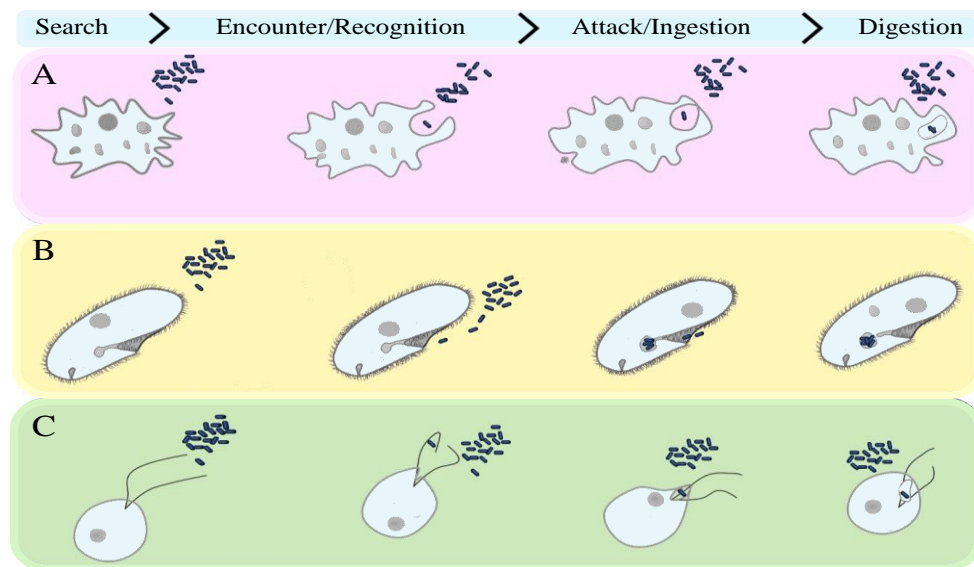


Figure 1- Schematic view of predatory protists' feeding types. A, Amoeba utilizes pseudopodia for precise navigation and resource capture through phagotrophy; B, Ciliate engages in filter-feeding using cilia, creating water currents to capture and consume prey microorganisms; C, Flagella demonstrates fast-swimming and raptorial feeding abilities using whip-like flagella for prey capture.

2.2. Microbial trophic interaction

Predatory protists engage in complex trophic interactions with various microorganisms, influencing ecosystem dynamics. They have diverse impact on their prey communities depending on the prey type.

2.2.1. Trophic interaction with bacteria

Understanding how protists and bacteria interact in soil is crucial for revealing the complex dynamics of the soil ecosystems. Numerous studies have been conducted on the regulation of bacterial communities concerning various biotic and abiotic factors. When considering trophic levels in ecology, most of these factors primarily constitute the provision of nutrients to bacteria, which are primarily bottom-up factors. The famous ecology paper by Hairston and colleagues (1960) argued that the abundance of prey is controlled by predators, introducing the concept of top-down control. Pernthaler (2005), emphasized structure of microbial communities is shaped by both protistan predation (top-down control) and competition for organic carbon and nutrients (bottom-up control) in aquatic ecosystem. Recent studies have highlighted the significance of top-down regulation by predatory protists on soil bacterial communities, surpassing the impact of bottom-up factors such as nutrient availability. Asiloglu et al. (2021c) studied the top-down and bottom-up factors controlling soil bacterial communities, which revealed that the soil bacterial communities are strongly controlled by predatory protists rather than the bottom-up nutrients in rice field soil. Fujino et al. (2023) revealed a substantial role of protists in shaping the composition of the active bacterial community, emphasizing the pronounced top-down influence of predatory protists on bacterial communities, especially Proteobacteria and Bacteroidota, and likely activities within the soil ecosystems.

Trophic interactions between protists and bacteria significantly influence the overall community composition in soil (Figure 2A). Additionally, most of protists exhibit selective feeding behaviours, preying on specific microbial taxa within the bacterial community (Gonzalez et al. 1990; Verity 1991; Šimek et al. 1994). A study by Matz et al. (2002) showed that bacterial phenotypic traits affect the feeding preferences of the heterotrophic nanoflagellate, *Spumella* sp. Pernthaler (2005) emphasized that protists exhibit selective feeding, favour certain bacterial species over the others. Murase & Frenzel (2008) compared the edibility of different methanotrophs for soil protist in rice field soil. The study found that protist showed a grazing preference for different methanotrophs, with some strains being more edible than others. This suggests that selective grazing by protists may impact not only bacteria but also the methanotrophic community of archaea. Taking together protist have a species-specific effect on bacterial communities, thus the presence of protist species in soil ecosystem is important to understand how soil microbiome is shaped. In addition, Asiloglu et al. (2020) showed that mix culture of protists has a bigger impact on bacterial communities than single protists species, suggesting that the effect of protists may be much more than expected in the soil ecosystem where hundreds of protist species inhabits.

Prey traits play crucial role in the survival, thus endurance and diversification of bacteria. Important bacterial traits include but not limited to prey size, prey motility, prey biochemical composition, cell surface characteristics, and prey's ability to produce toxins, form microcolonies and biofilm (Jürgens & Massana 2008). Matz & Kjelleberg (2005) studied the dietary niche breadth on eight protist isolates and 20 bacterial species. The researchers found that each protist showed a distinct feeding pattern

depending on the bacterial traits. In addition to these direct interactions based on bacterial traits, protists can also respond to volatile organic compounds (VOCs) produced by bacteria. A recent study demonstrated that predatory protists can sense bacterial volatile organic compounds (VOCs) and likely to use them to locate and select prey in soil ecosystems (Schulz-Bohm et al. 2017). This selectivity may be a critical factor in detecting distinct bacterial species and thus shaping the composition of bacterial communities.

Protists exert influence not only by reducing specific bacterial populations through selective predation, but also several bacterial species benefit the protist predation through reduced bacterial competition and release of nutrients (Figure 2B) (Clarholm, M., 1985; Bonkowski et al. 2000; Creevy et al. 2016). Previously, Asiloglu et al. (2020) showed that co-inoculation of protists and a plant growth promoting rhizobacteria (PGPR), *Azospirillum* sp. B510, enhanced the survival of PGPR, most likely through regulating the bacterial communities. Understanding how protists affect its environment is essential for comprehending the broader implications for nutrient cycling, ecosystem stability, and plant-microbe interactions.

Beyond shaping bacterial community structure, trophic interactions with protists impact the bacterial activity (Figure 2C). This influence extends to the production of secondary metabolites and plant growth hormones (Krome et al. 2010). Some protists can directly prey upon plant pathogens and contribute to disease suppression. (Guo et al. 2022). For instance, they can enhance the production of antibiotics in PGPRs. Recent studies show that soil protists, as the key predators of soil bacteria, play an important role in driving the abundance and diversity of antibiotic resistance in soil bacterial communities (Nguyen et al. 2023). The researchers inoculated soil microcosms with low, medium, and high concentrations of indigenous soil protist suspensions. They found that an increase in protistan predation pressure was strongly associated with a higher abundance and diversity of soil antibiotic resistance genes.

Taken together, protists regulate bacterial communities and activities in species-specific manner depending on the bacterial traits. The trophic relationships between soil predatory protists and bacteria are a cornerstone in the intricate web of soil ecology. The interdependence between these microorganisms not only shapes the composition of bacterial communities but also has far-reaching effects on ecosystem functionality. Further research in this field will contribute to our understanding of soil ecosystem dynamics, providing valuable insights for sustainable agriculture, environmental conservation, and microbial ecology.

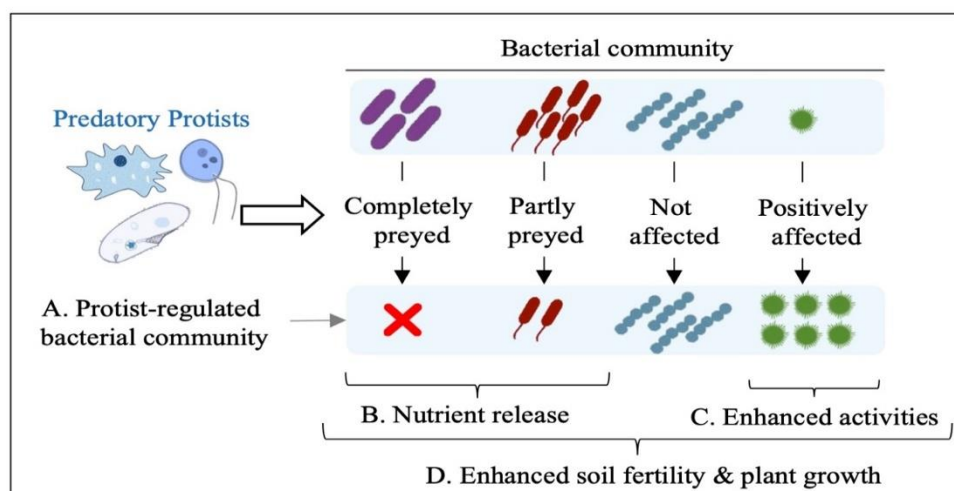


Figure 2- Effects of predators of bacteria (predatory protists) in the soil ecosystem. A, Predatory protists selectively feed on bacteria and alter their community composition; B, Nutrients are released from the preyed bacterial biomass into the soil; C, Predatory protists enhance activities of several bacterial species; D, Consequently, the soil fertility and plant growth are enhanced by the predatory protists

2.2.2. Trophic interaction with fungi

Although protists are considered mainly bacterivorous, it has been long recognized that protists feed on fungi as well (Heal 1963; Old & Darbyshire 1978; Bunting et al. 1979). Nevertheless, most of the studies focused on protist-bacteria interaction and fungivorous protists are mainly ignored until recently. Geisen et al. (2016) re-visited the protist-fungi interaction and showed that many bacterivorous protists also feed on fungi, which makes it possible for protists to affect fungal communities and activities. In addition to bacterivorous protists that feed on fungi, obligate fungivorous protists are abundant in soils (Geisen et al. 2016). For instance, *Lecythium terrestris* is identified by Dumack et al. (2016) as a fungivorous and algivorous protist, feeding on fungi and algae in soil environments. Huang et al. (2021) studied effects of different biotic and abiotic factors on fungal communities in paddy soils across climatic zones. The study showed that among the several biotic and abiotic factors, protists are the most important factor shaping fungal communities. In addition, studies showed that the trophic relationship between predatory protists and fungi is driven by biotic and abiotic factors such as land use intensification (Xue et al. 2023), organic

fertilizer addition (Hu et al. 2024), the rhizosphere effect (Wang et al. 2024). Even though not directly proven, studies suggested that these protists might control fungal communities. Protist-fungi interaction is a relatively new research area open to discoveries. Understanding these interactions is essential for unravelling the dynamics of soil microbial communities and their influence on ecosystem functioning.

2.2.3. Trophic interaction with nematode and other microorganisms

Intriguingly, predatory protists can interact with other microorganisms like nematodes. This trophic relationship can have cascading effects on soil food webs and nutrient dynamics, highlighting the interconnectedness of microorganisms in the soil ecosystem. Geisen et al. (2015) investigated the predatory behaviour of a common soil amoeba on nematodes. In this study they showed feeding procedure of *Cryptodiffugia operculata* on the nematode *Acrobeloides buetschlii*. The findings revealed a specific attack pattern of the protist, wherein the amoeba immobilized nematodes by attaching to their tails and anterior ends. Subsequently, other amoebae cooperatively immobilized the nematode. This cooperative feeding process involved multiple amoebae disintegrating and absorbing the nematode prey within 12 hours. Additionally, the study underlined that protist could serve as potential biocontrol agents against plant pathogenic nematodes.

In addition to all these, there are various findings that protists prey on other protists. In a study (Seppey et al. 2017) proposing that phagotrophic protists play a significant role in contribute to an alternative pathway for nutrient cycling in soil ecosystems by consuming algae.

2.3. Protists and soil health

Soil protists, like all other soil microorganisms, are essential for soil fertility and ecosystem functioning. They exert various impacts on soil health by influencing nutrient turnover, microbial communities, as well as activities related to nutrient decomposition and mineralization. In soil ecosystems, predatory protists serve a fundamental role in nutrient turnover, as outlined by the microbial loop concept (Clarholm M 1985; Bonkowski 2004). By preying on diverse microorganisms, protists release the excess nutrients. As nitrogen is excreted as a waste product from protist-consumed microbial biomass, protists are known to increase nitrogen availability in soil (Sherr et al. 1983; Bonkowski et al. 2000).

By increasing nutrient availability (Figure 2B) protist leads to increase microorganism activity. The predatory activity of protists on bacteria and fungi, they influence the composition and abundance of these microbial populations (Figure 2C). This control over microbial communities can have far-reaching impact for the functioning of the soil ecosystems. Jousset (2017) has been suggested that heterotrophic protists increase the activity and survival of PGPR. Asiloglu et al. (2020) showed that protist enhance the survival of *Azospirillum* sp. which is one of the most widely used commercial biofertilizer. Additionally, some studies are showing that the protist stimulates the production of siderophores, an iron-chelating compound, by *Pseudomonas* (Levrat et al. 1992), the cyclic biosynthesis of an antibiotic lipopeptide (Mazzola et al. 2009), and the anti-phytopathogenic compound 2,4-diacetylphloroglucinol (Jousset & Bonkowski 2010; Jousset et al. 2011).

The regulation of specific microbial groups by protists can indirectly influence bacterial activities (Figure 2D) such as nitrogen mineralization and carbon mineralization (Kuikman et al. 1991; Hervey & Greaves 1941; Ratsak et al. 1996; Rønn et al. 2001). The first evidence for an effect of protists on the sulfur cycle showed by Murase and colleague (2006). The protists are thought to influence SO_4^{2-} reduction directly by grazing on SO_4^{2-} reducing bacteria or indirectly via creating more reduced soil conditions by stimulating the overall microbial activities. Gluconic acid plays a crucial role in phosphorous mineralization, serving as an efficient strategy for *Enterobacter* to avoid protist grazing, that was demonstrated by Gómez et al. (2010). In addition, protists feed on dormant bacteria leading to increase the relative abundance of the active bacteria. Taking together protists are considered as an important compound for soil fertility.

2.4. Protists and plant productivity

Protists are one of the most abundant microorganisms in rhizosphere (Murase & Asiloglu 2023) that densely inhabit the plant roots (Asiloglu & Murase 2017; Bonkowski et al. 2004). Plant health is influenced by especially the rhizosphere soil microbiome, in which protists are one of the most abundant microorganisms. The interactions between predatory protists and microorganisms have implications for plant productivity (Bonkowski 2004; Rosenberg et al. 2009). A pivotal aspect of this influence is the enhancement of nutrient availability through protist predation, a critical factor in meeting the nutritional needs of plants. Xiong et al. (2020) and Gao et al. (2019) showed the importance of protist, which is one of the main groups of the rhizosphere, as top-down controllers of functioning linked to plant health. The research by Guo et al. (2021) emphasizes the positive impact of cercozoan protists on plant growth. Additionally, gluconic acid which is produced by enterobacter against *Colpoda steini* (Gómez et al. 2010), has been proven to increase fertility by they participate actively in mobilizing phosphorus between sparingly soluble mineral phosphates and the soil solution, thus increasing the fertility of phosphorus deficient soils (Rodríguez & Fraga 1999).

The production of plant hormones by PGPR is known to stimulate plant growth. Bonkowski & Brandt (2002) showed that the presence of *Acanthamoeba castellanii* correlated with a greater and more branched root system in watercress seedlings. This

change was accompanied by an increase in the ratio of auxin, indole-3-acetic acid (IAA) producing rhizospheric bacteria in the presence of protists. This has been attributed to changes in the composition and activity of the microbial community. Kreuzer et al. (2006), supported this information by showing that *Acanthamoeba castellanii* can stimulate rice root growth and elongate lateral roots. The effects of a rhizosphere bacterial community and *A. castellanii* on root branching and on IAA metabolism in *Lepidium sativum* and *Arabidopsis thaliana* were investigated by Krome et al. (2010). In the study, concentrations of bioactive-free IAA in *Lepidium sativum* shoots were strongly increased by the predation activity of protists on bacteria. Increased nitrate concentrations by presence of amoeba in the rhizosphere are thought to cause the accumulation of cytokinin in plants and interactions with free auxin and resulted to increasing root growth.

The enhanced nutrient turnover facilitated by protists has the potential to improve plant health by increasing plant resistance to disease and stress. Moreover, protists actively contribute to the suppression of plant pathogens, creating a protective effect on plants (Guo et al. 2022). Not only bacteria but also fungal pathogens impacted by protist. The study by Bahroun et al. (2021) showed that bacterivorous protist has been shown to induce soil suppressiveness against the fungal pathogen *Fusarium oxysporum*. However, very less is known about protist-fungi interaction.

Overall, by enhancing nutrient availability, altering microbial community composition, influencing root development, and fortifying plants against pathogens, protists emerge as key players in the intricate relationship of factors shaping plant productivity.

3. Application of Predators in Sustainable Agriculture

The application of microorganisms and the knowledge about them has been used for centuries in curing diseases, improving food production, and protecting the environment from pollution. The application of soil protists in agriculture is promising as they can improve agricultural yield while, potentially, reducing the input of chemical fertilizers or pesticides. In applied protistology, predatory protists deserve special attention as they can be applied as biostimulants and biocontrol agents. Various strategies can be employed for the application of predatory protists, similar to the methods used for bacterial and fungal biocontrol agents. While specific application methods were not explicitly tested, there is potential efficacy in approaches like seed coating or introducing protists into irrigation water and drip irrigation systems. Notably, predatory protists serve as catalysts for the decomposition of organic matter. Consequently, there is a prospective application of protists in organic fertilizers, including biochar and compost, to optimize their effects when integrated into agricultural fields. However, applied protistology has received little attention despite its vast potential. The relatively few applied protistology researches in the last decade that were mainly conducted in Europe and the United States obtained exciting results. For instance, recently, protist-based biostimulants and plant protection products can be seen in the European market (Protoplus, ECOstyle, Belgium).

As different protists have distinct impact on the bacterial community composition, soil fertility, and the plant health (Gao et al. 2019), selection of protist species to be applied should be considered carefully. For instance, depending on the predatory protists' feeding types (Figure 1), their usage can be varied. Protists such as ciliates with filter-feeding behaviour can feed on huge number of bacteria in a short time (Figure 1B), resulting in higher nutrient turnover rates and lower selective impact on bacterial community composition. On the other hand, protists such as amoeba and flagellates (Figure 1A and C) feed on relatively less bacteria than ciliates, while having a higher selectivity on the prey bacteria. Therefore, filter-feeders can be beneficial for overall soil health due to higher nutrient turnover rates, while the protists with the other feeding types (Figure 1) can be used to manipulate soil microbial communities and functionalities.

4. Conclusions

This review highlights the roles of predatory protist in soil microbial ecosystems, which has been overlooked for many years. Briefly we introduced the trophic interaction between predatory protists and microbiomes and their impact on soil health and plant productivity, which indicate a robust potential for the use of predatory protists in sustainable agriculture. However, uncertainties exist regarding the adoption of this new perspective in practice and its integration into standard agricultural practices. Methods for implementing protist-based solutions have not been clearly defined yet. Despite exciting recent findings, limited scientific interest in protistology hampers progress in this field. There is a need for increased scientific attention and participation to bridge the gap between the potential benefits of soil protistology and tangible, applicable solutions. At this juncture, more research is needed on how protist-based solutions can be integrated into agricultural practices, the impact of this integration on agricultural productivity and sustainability, and the scientific community's allocation of more resources to this field. Encouraging the scientific community to understand the significance of soil protistology and engage in further research can play a crucial role in shaping future sustainable agricultural practices.

References

- Adl S M, Simpson A G, Lane C E, Lukeš J, Bass D, Bowser S S & Spiegel F W (2012). The revised classification of eukaryotes. *Journal of eukaryotic microbiology* 59(5): 429-514
- Asiloglu R (2022). Biochar–microbe interaction: more protist research is needed. *Biochar* 4(1): 72



- Asiloglu R & Murase J (2016). Active community structure of microeukaryotes in a rice (*Oryza sativa* L.) rhizosphere revealed by RNA-based PCR-DGGE. *Soil Science and Plant Nutrition* 62(5-6): 440-446
- Asiloglu R & Murase J (2017). Microhabitat segregation of heterotrophic protists in the rice (*Oryza sativa* L.) rhizosphere. *Rhizosphere* 4: 82-88
- Asiloglu R, Honjo H, Saka N, Asakawa S & Murase J (2015). Community structure of microeukaryotes in a rice rhizosphere revealed by DNA-based PCR-DGGE. *Soil Science and Plant Nutrition* 61(5): 761-768
- Asiloglu R, Kenya K, Samuel S O, Sevilir B, Murase J, Suzuki K & Harada N (2021c). Top-down effects of protists are greater than bottom-up effects of fertilisers on the formation of bacterial communities in a paddy field soil. *Soil Biology and Biochemistry* 156: 108186
- Asiloglu R, Samuel S O, Sevilir B, Akca M O, Acar Bozkurt P, Suzuki K & Harada N (2021a). Biochar affects taxonomic and functional community composition of protists. *Biology and Fertility of Soils* 57: 15-29
- Asiloglu R, Shiroishi K, Suzuki K, Turgay O C & Harada N (2021b). Soil properties have more significant effects on the community composition of protists than the rhizosphere effect of rice plants in alkaline paddy field soils. *Soil Biology and Biochemistry* 161: 108397
- Asiloglu R, Shiroishi K, Suzuki K, Turgay O C, Murase J & Harada N (2020). Protist-enhanced survival of a plant growth promoting rhizobacteria, *Azospirillum* sp. B510, and the growth of rice (*Oryza sativa* L.) plants. *Applied Soil Ecology* 154: 103599
- Bahroun A, Jousset A, Mrabet M, Mhamdi R & Mhadhbi H (2021). Protists modulate *Fusarium* root rot suppression by beneficial bacteria. *Applied Soil Ecology* 168: 104158
- Bodur S O, Samuel S O, Suzuki K, Harada N & Asiloglu R (2024). Nitrogen-based fertilizers differentially affect protist community composition in paddy field soils. *Soil Ecology Letters* 6(3): 230221
- Bonkowski M (2004). Protozoa and plant growth: the microbial loop in soil revisited. *New Phytologist* 162(3): 617-631
- Bonkowski M & Brandt F (2002). Do soil protozoa enhance plant growth by hormonal effects? *Soil Biology and Biochemistry* 34(11): 1709-1715
- Bonkowski M, Griffiths B & Scrimgeour C (2000). Substrate heterogeneity and microfauna in soil organic 'hotspots' as determinants of nitrogen capture and growth of ryegrass. *Applied Soil Ecology* 14(1): 37-53
- Bunting L A, Neilson J B & Bulmer G S (1979). *Cryptococcus neoformans*: gastronomic delight of a soil amoeba. *Sabouraudia* 17(3): 225-232.
- Caron D A, Worden A Z, Countway P D, Demir E & Heidelberg K B (2009). Protists are microbes too: a perspective. *The ISME journal* 3(1): 4-12
- Clarholm M (1985). Interactions of bacteria, protozoa and plants leading to mineralization of soil nitrogen. *Soil Biology and Biochemistry* 17(2): 181-187
- Creevy A L, Fisher J, Puppe D & Wilkinson D M (2016). Protist diversity on a nature reserve in NW England—With particular reference to their role in soil biogenic silicon pools. *Pedobiologia* 59(1-2): 51-59
- Dumack K, Müller M E & Bonkowski M (2016). Description of *Lecythium terrestris* sp. nov. (Chlamydomphryidae, Cercozoa), a soil dwelling protist feeding on fungi and algae. *Protist* 167(2): 93-105
- Fujino M, Suzuki K, Harada N & Asiloglu R (2023). Protists modulate active bacterial community composition in paddy field soils. *Biology and Fertility of Soils* 59(7): 709-721
- Gao F, Warren A, Zhang Q, Gong J, Miao M, Sun P & Song W (2016). The all-data-based evolutionary hypothesis of ciliated protists with a revised classification of the phylum Ciliophora (Eukaryota, Alveolata). *Scientific Reports* 6(1): 24874
- Gao Z, Karlsson I, Geisen S, Kowalchuk G & Jousset A (2019). Protists: puppet masters of the rhizosphere microbiome. *Trends in Plant Science* 24(2): 165-176
- Geisen S, Koller R, Huenninghaus M, Dumack K, Urich T & Bonkowski M (2016). The soil food web revisited: diverse and widespread mycophagous soil protists. *Soil Biology and Biochemistry* 94: 10-18
- Geisen S, Mitchell E A, Adl S, Bonkowski M, Dunthorn M, Ekelund F & Lara E (2018). Soil protists: a fertile frontier in soil biology research. *FEMS Microbiology Reviews*, 42(3): 293-323
- Geisen S, Mitchell E A, Wilkinson D M, Adl S, Bonkowski M, Brown M W & Lara E (2017). Soil protistology rebooted: 30 fundamental questions to start with. *Soil Biology and Biochemistry* 111: 94-103
- Geisen S, Rosengarten J, Koller R, Mulder C, Urich T & Bonkowski M (2015). Pack hunting by a common soil amoeba on nematodes. *Environmental microbiology* 17(11): 4538-4546
- Gómez W, Buela L, Castro L T, Chaparro V, Ball M M & Yarzabal L A (2010). Evidence for gluconic acid production by *Enterobacter* intermedium as an efficient strategy to avoid protozoan grazing. *Soil Biology and Biochemistry* 42(5): 822-830
- Gonzalez J M, Sherr E B & Sherr B F (1990). Size-selective grazing on bacteria by natural assemblages of estuarine flagellates and ciliates. *Applied and Environmental Microbiology* 56(3): 583-589
- Guo S, Tao C, Jousset A, Xiong W, Wang Z, Shen Z & Geisen S (2022). Trophic interactions between predatory protists and pathogen-suppressive bacteria impact plant health. *The ISME Journal* 16(8): 1932-1943
- Guo S, Xiong W, Hang X, Gao Z, Jiao Z, Liu H & Geisen S (2021). Protists as main indicators and determinants of plant performance. *Microbiome* 9: 1-11
- Hairton N G, Smith F E & Slobodkin L B (1960). Community structure, population control, and competition. *The american naturalist* 94(879): 421-425
- Heal O W (1963). Soil fungi as food for amoebae. *Soil organisms* pp. 289-297
- Hervey R J & Greaves J E (1941). Nitrogen Fixation by *Azotobacter Chroococcum* in the Presence Of Soil Protozoa. *Soil Science* 51(2): 85-100
- Ratsak C H, Maarsen K A & Kooijman S A L M (1996). Effects of protozoa on carbon mineralization in activated sludge. *Water Research* 30(1): 1-12
- Hu X, Gu H, Liu J, Wei D, Zhu P, Zhou B & Wang G (2024). Different long-term fertilization regimes affect soil protists and their top-down control on bacterial and fungal communities in Mollisols. *Science of The Total Environment* 908: 168049
- Huang X, Wang J, Dumack K, Liu W, Zhang Q, He Y & Li, Y (2021). Protists modulate fungal community assembly in paddy soils across climatic zones at the continental scale. *Soil Biology and Biochemistry* 160: 108358
- Jan P (2008). The twilight of Sarcodina: a molecular perspective on the polyphyletic origin of amoeboid protists. *Protistology* 5(4): 281-302
- Jansson J K, McClure R & Egbert R G (2023). Soil microbiome engineering for sustainability in a changing environment. *Nature Biotechnology* 41(12): 1716-1728
- Jassey V E, Hamard S, Lepère C, Céréghino R, Corbara B, Küttim M & Carrias J F (2022). Photosynthetic microorganisms effectively contribute to bryophyte CO₂ fixation in boreal and tropical regions. *ISME Communications* 2(1): 64

- Jousset A (2017). Application of protists to improve plant growth in sustainable agriculture. *Rhizotrophs: Plant growth promotion to bioremediation* pp. 263-273
- Jousset A & Bonkowski M (2010). The model predator *Acanthamoeba castellanii* induces the production of 2, 4, DAPG by the biocontrol strain *Pseudomonas fluorescens* Q2-87. *Soil Biology and Biochemistry* 42(9): 1647-1649
- Jousset A, Rochat L, Lanoue A, Bonkowski M, Keel C & Scheu S (2011). Plants respond to pathogen infection by enhancing the antifungal gene expression of root-associated bacteria. *Molecular Plant-Microbe Interactions* 24(3): 352-358
- Jürgens K & Massana R (2008). Protistan grazing on marine bacterioplankton. *Microbial ecology of the oceans* 383-441
- Kreuzer K, Adamczyk J, Iijima M, Wagner M, Scheu S & Bonkowski M (2006). Grazing of a common species of soil protozoa (*Acanthamoeba castellanii*) affects rhizosphere bacterial community composition and root architecture of rice (*Oryza sativa* L.). *Soil Biology and Biochemistry* 38(7): 1665-1672
- Krome K, Rosenberg K, Dickler C, Kreuzer K, Ludwig-Müller J, Ullrich-Eberius C & Bonkowski M (2010). Soil bacteria and protozoa affect root branching via effects on the auxin and cytokinin balance in plants. *Plant and Soil* 328: 191-201
- Kuikman P J, Lekkerkerk L J A & Van Veen J A (1991). Carbon Dynamics of a Soil Planted with Wheat under an Elevated Atmospheric CO₂. *Advances in soil organic matter research: The impact on agriculture and the Environment* 267 pp
- Levrat P, Pussard M & Alabouvette C (1992). Enhanced bacterial metabolism of a *Pseudomonas* strain in response to the addition of culture filtrate of a bacteriophagous amoeba. *European journal of protistology* 28(1): 79-84
- Matz C & Kjelleberg S (2005). Off the hook—how bacteria survive protozoan grazing. *Trends in microbiology* 13(7): 302-307
- Matz C, Boenigk J, Arndt H & Jürgens K (2002). Role of bacterial phenotypic traits in selective feeding of the heterotrophic nanoflagellate *Spumella* sp. *Aquatic microbial ecology* 27(2): 137-148
- Mazzola M, De Bruijn I, Cohen M F & Raaijmakers J M (2009). Protozoan-induced regulation of cyclic lipopeptide biosynthesis is an effective predation defense mechanism for *Pseudomonas fluorescens*. *Applied and Environmental Microbiology* 75(21): 6804-6811
- Mitchell D R (2007). The evolution of eukaryotic cilia and flagella as motile and sensory organelles. *Eukaryotic membranes and cytoskeleton: Origins and evolution* pp. 130-140
- Murase J & Asiloglu R (2023). Protists: the hidden ecosystem players in a wetland rice field soil. *Biology and Fertility of Soils* pp. 1-15
- Murase J & Frenzel P (2008). Selective grazing of methanotrophs by protozoa in a rice field soil. *FEMS microbiology ecology* 65(3): 408-414
- Murase J, Noll M & Frenzel P (2006). Impact of protists on the activity and structure of the bacterial community in a rice field soil. *Applied and environmental microbiology* 72(8): 5436-5444
- Nguyen T B A, Bonkowski M, Dumack K, Chen Q L, He J Z & Hu H W (2023). Protistan predation selects for antibiotic resistance in soil bacterial communities. *The ISME Journal* 17(12): 2182-2189
- Nielsen L T & Kjørboe T (2021). Foraging trade-offs, flagellar arrangements, and flow architecture of planktonic protists. *Proceedings of the National Academy of Sciences* 118(3): e2009930118
- Nikolaev S I, Berney C, Fahrni J F, Bolivar I, Polet S, Mylnikov A P & Pawlowski J (2004). The twilight of Heliozoa and rise of Rhizaria, an emerging supergroup of amoeboid eukaryotes. *Proceedings of the National Academy of Sciences* 101(21): 8066-8071
- Old K M & Darbyshire J F (1978). Soil fungi as food for giant amoebae. *Soil Biology and Biochemistry* 10(2): 93-100
- Pernthaler J (2005). Predation on prokaryotes in the water column and its ecological implications. *Nature Reviews Microbiology* 3(7): 537-546
- Ratsak C H, Maarsen K A & Kooijman S A L M (1996). Effects of protozoa on carbon mineralization in activated sludge. *Water Research* 30(1): 1-12
- Rodríguez H & Fraga R (1999). Phosphate solubilizing bacteria and their role in plant growth promotion. *Biotechnology advances* 17(4-5): 319-339
- Rønn R M, Griffiths B S & Young I M (2001). Protozoa, nematodes and N-mineralization across a prescribed soil textural gradient. *Pedobiologia* 45(6): 481-495
- Rosenberg K, Bertaux J, Krome K, Hartmann A, Scheu S & Bonkowski M (2009). Soil amoebae rapidly change bacterial community composition in the rhizosphere of *Arabidopsis thaliana*. *The ISME Journal* 3(6): 675-684
- Schulz-Bohm K, Geisen S, Wubs E J, Song C, de Boer W & Garbeva P (2017). The prey's scent—volatile organic compound mediated interactions between soil bacteria and their protist predators. *The ISME journal* 11(3): 817-820
- Seppéy C V, Singer D, Dumack K, Fournier B, Belbahri L, Mitchell E A & Lara E (2017). Distribution patterns of soil microbial eukaryotes suggests widespread alivory by phagotrophic protists as an alternative pathway for nutrient cycling. *Soil Biology and Biochemistry* 112: 68-76
- Sherr B F, Sherr E B & Berman T (1983). Grazing, growth, and ammonium excretion rates of a heterotrophic microflagellate fed with four species of bacteria. *Applied and Environmental Microbiology* 45(4): 1196-1201
- Šimek K, Vrba J & Hartman P (1994). Size-selective feeding by *Cyclidium* sp. on bacterioplankton and various sizes of cultured bacteria. *FEMS microbiology ecology* 14(2): 157-167
- Trivedi P, Leach J E, Tringe S G, Sa T & Singh B K (2020). Plant–microbiome interactions: from community assembly to plant health. *Nature reviews microbiology* 18(11): 607-621
- Verity P G (1991). Feeding in planktonic protozoans: evidence for non-random acquisition of prey. *The Journal of protozoology* 38(1): 69-76.
- Wang B, Chen C, Xiao Y M, Chen K Y, Wang J, Zhao S & Zhou G Y (2024). Trophic relationships between protists and bacteria and fungi drive the biogeography of rhizosphere soil microbial community and impact plant physiological and ecological functions. *Microbiological Research* 280: 127603
- Xiong W, Song Y, Yang K, Gu Y, Wei Z, Kowalchuk G A & Geisen S (2020). Rhizosphere protists are key determinants of plant health. *Microbiome* 8: 1-9
- Xue P, Minasny B, McBratney A, Jiang Y & Luo Y (2023). Land use effects on soil protists and their top-down regulation on bacteria and fungi in soil profiles. *Applied soil ecology* 185: 104799





Characterization and antimicrobial properties of silver nanoparticles biosynthesized from cornelian cherry (*Cornus mas L.*)

Tuğçe Özeşer^a , Nural Karagozlu^{a*} 

^aManisa Celal Bayar University, Engineering Faculty, Food Engineering Department, Manisa, TÜRKİYE

ARTICLE INFO

Research Article

Corresponding Author: Nural Karagozlu, E-mail: nural.karagozlu@cbu.edu.tr

Received: 25 July 2023 / Revised: 18 November 2023 / Accepted: 10 January 2024 / Online: 23 July 2024

Cite this article

Özeşer T, Karagozlu N(2024). Characterization and antimicrobial properties of silver nanoparticles biosynthesized from cornelian cherry (*Cornus mas L.*). *Journal of Agricultural Sciences (Tarım Bilimleri Dergisi)*, 30(3):444-457. DOI: 10.15832/ankutbd.1332427

ABSTRACT

Nanoparticles produced by green synthesis has been increasingly gaining popularity, especially because they are eco-friendly and low cost. In the present article, silver nanoparticles (AgNPs) were synthesized from the extracts prepared using cornelian cherry (*Cornus mas L.*) at two different temperatures. The properties of obtained AgNPs were determined through UV-Vis spectroscopy, SEM, EDX, FTIR, and XRD analyses, and their antimicrobial effects on four pathogenic bacteria were investigated. The analysis results conducted using UV-spectrophotometry, SEM, EDX, FTIR, and XRD on AgNPs prepared from extracts obtained at two different temperatures (20 °C and 60 °C) were similar. The groups playing a role in nanoparticle formation were determined to be C=C, C=O, and C-O, and it was also concluded that the two different extraction temperatures had no significant effect on nanoparticle synthesis and

characterization. The cherry extract's antimicrobial activity was effective against *Staphylococcus aureus*, *Listeria monocytogenes*, and *Salmonella Typhi*, while it didn't show activity against *Escherichia coli* O157:H7. The AgNPs at concentration of 25 mg/mL created inhibition zones of 9 mm, 9 mm, and 7 mm for *L.monocytogenes*, *S.aureus*, and *S.Typhi*, respectively, at 20 °C. It was seen that 25 mg/mL AgNPs synthesized at 60 °C formed 9 mm and 8 mm inhibition zones in *S.aureus* and *L.monocytogenes* cultures, respectively, whereas they showed no inhibiting activity against *S.Typhi*, and *E.coli* O157:H7. It has been seen that 20 °C has ease of application in two different temperatures applied in the preparation of silver nanoparticles and is a good alternative to chemical methods.

Keywords: Silver nanoparticles, Antimicrobial effects, Cornelian cherry, *Cornus mas L.*, Green synthesis

1. Introduction

Particles with sizes below 100 nm are referred to as nanoparticles, and metals whose sizes are reduced through various methods can acquire different properties (Rai & Bai 2011; Wang et al. 2011). Metal nanoparticles can be obtained through physical and chemical methods. Nevertheless, these methods possess drawbacks, including elevated costs, slow production rates, increased energy demands, and the potential of toxicity. Therefore, in recent years, a biological method called green synthesis has gained importance and has been used for nanoparticle synthesis. This method offers advantages over other methods, including low cost, rapid production, ease of acquisition, eco-friendliness, low energy requirements, non-toxicity of the resulting nanoparticles, biocompatibility, and ease of sustainability. Biological agents such as bacteria, yeast, fungi, algae, and plants are used as reducing and stabilizing agents in nanoparticle synthesis, and the synthesis is achieved through the reduction of metal salts facilitated by the metabolites they contain (Arshadi et al. 2018; Rezvani et al. 2019). During the synthesis of nanoparticles, various metabolites contained within plants play a crucial role in the reduction of silver ions. Vitamins, proteins, amino acids, and polysaccharides found in these plants facilitate the formation of nanoparticles, while alkaloids, terpenes, glycosides, and flavonoids are involved in the reduction of silver ions and the stability of nanoparticles (Arya et al. 2019; Paiva-Santos et al. 2021). The primary component responsible for nanoparticle formation, as reported by Ceylan et al. (2021) in their study with three *Sideritis* species, is chlorogenic acid, whereas Ekrikaya et al. (2021), in their research with berries, identified ellagic acid as the key compound. The synthesis process is rooted in the reduction of metal salts using plant extracts. Various factors such as synthesis time, pH, reaction temperature and duration, metal type and concentration, and extract-to-metal salt ratio affect the characteristics of nanoparticles, such as size and shape (Arya et al. 2019; Rana et al. 2020; Alkhattaf 2021; Paiva-Santos et al. 2021).

The use of silver in nanoparticle synthesis has increased compared to other metals due to its lower toxicity and antimicrobial effects, leading to extensive research in the fields of food and healthcare (Silver 2003; Rai et al. 2011). Silver nanoparticles (AgNPs) are known for their optical, catalytic, and electrical properties, in addition to their remarkable oxidative resistance, high stability, surface reactivity, and the ease with which their surfaces can be modified (Paiva-Santos et al. 2021). Furthermore, the antimicrobial activity of AgNPs is noteworthy. AgNPs weaken the cell wall through electrostatic interactions, enter the bacterial

cell, inhibit bacterial growth, and cause cell death. Several studies have been conducted to illustrate the electrostatic attraction between positively charged nanoparticles (NPs) and negatively charged bacterial cells. These NPs have been observed to accumulate within the cell membrane, potentially penetrating and causing damage to the cell wall or membrane. It is hypothesized that silver ions bind to thiol groups (-SH) and subsequently induce deactivation within the cell membrane. Furthermore, it is suggested that silver ions may denature the DNA molecule by disrupting the hydrogen bonds between the two strands of DNA and intercalating between purine and pyrimidine base pairs. Factors including nanoparticle size, shape, surface charge, nanoparticle concentration, bacterial species, and the bacterial counts impact antimicrobial activity (Cao et al. 2001; Ghaedi et al. 2015; Abbasi et al. 2016; Arya et al. 2019; Hernandez Morales et al. 2019).

Nanotechnology as a packaging material in food production has gained importance in reducing energy consumption, improving gas barrier properties, and reducing CO₂ emissions to preserve human and environmental health (Baysal 2020). With the increasing interest of consumers in healthier, minimally processed, additive-free food products, producers have started to utilize nanotechnology to meet these demands by extending the shelf life of food, preserving food nutritional values, and developing new products. A study indicated that using AgNPs in fruit storage can extend the shelf life by catalyzing the ethylene gas and slowing respiration (Polat & Fenercioğlu 2014).

It has also been shown that nanoparticles could find applications in the fields of food and healthcare, thanks to their low toxicity and antimicrobial properties. (Ceylan et al. 2021). The application areas of AgNPs in the food industry include food packaging materials, ensuring food safety, and water disinfection. However, with the growing interest in AgNPs synthesized through biological methods, research is also being conducted on improving the texture and aroma properties of food, extending the shelf life of food, and preserving food nutritional values (Sürengil & Kılınc 2011).

In this study, silver nanoparticles (AgNPs) were synthesized using cornelian cherry (*Cornus mas* L.), a shrub-like plant belonging to the *Cornaceae* family of the *Umbelliflorae* order, which grows in Central and Southeastern Europe, including Ukraine, Georgia, Armenia, the Czech Republic, Slovakia, Turkey, Serbia, Austria, and Poland. Cornelian cherry is a red oval-shaped fruit with different species. Cornelian cherry is one of the fruits that naturally grow in Turkey and it has been used in folk medicine for centuries mainly in Anatolia to prevent some diseases (Celep et al. 2012). It contains phenolic compounds, mineral substances, vitamin C, anthocyanins, flavonoids, and polyphenols. It also exhibits antioxidant and anti-inflammatory properties (Stankovic et al. 2014; Salejda et al. 2018). Cornelian cherry (*Cornus mas* L.) fruit, naturally growing in Anatolia, was selected for this study owing to its economic significance and its observed antimicrobial properties. In contemporary times, silver, a historical agent for infection control and preservation, has garnered attention as it has not been synthesized in cranberries to date. It was aimed to determine the basic properties of AgNPs synthesized from extracts obtained from *Cornus mas* L. fruit at two different extraction temperatures, which have yet to be used in previous studies. The antimicrobial activity of the obtained AgNPs against some foodborne pathogenic bacteria, including *Staphylococcus aureus*, *Listeria monocytogenes*, *Salmonella* Typhi, and *Escherichia coli* O157:H7, was also investigated. For this purpose, the properties of AgNPs obtained from extracts prepared at two different temperatures, 20 °C and 60 °C, were determined using UV-Vis spectrophotometry, FTIR, EDX, XRD, and SEM, and their antimicrobial properties were investigated using the paper disc method on some foodborne pathogenic bacteria.

2. Material and Methods

2.1. Materials

The cornelian cherry fruit (*Cornus mas* L.) used in the study was freshly obtained from a local market in August. The cherries were washed, deseeded, dried in a rotary tray dryer at 65 °C, and grinded. The dried cherries were stored in glass jars in a cool and dark environment until further use.

2.2. Method

2.2.1. Preparation of cornelian cherry extract

Room temperatures (20 °C) and 60 °C were applied to prepare the cornelian cherry extract. 10 g of dried cherries were mixed with 100 mL of distilled water. The mixture was agitated in an orbital shaker at 135 rpm for 30 minutes and then kept in a dark environment for 24 hours. The obtained cornelian cherry extract was filtered through Whatman No.1 filter paper and centrifuged at 4100 rpm for 15 minutes (NÜVE NF 800R). The supernatant was collected to obtain the extract for further use (Figures 1 and 2).

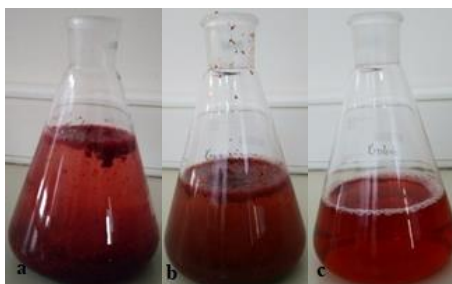


Figure 1- (a) Cornelian cherry extract prepared at 20 °C, (b) extract after 24 hours, (c) filtered extract



Figure 2- (a) Cornelian cherry extract prepared at 60 °C, (b) extract after 24 hours, (c) filtered extract

2.2.2. Silver nanoparticle synthesis

For the synthesis of AgNPs, 10 mL of cornelian cherry (*Cornus mas* L.) extract was mixed with 90 mL of 1 mM AgNO₃ (Carlo Erba, 423952) solution and agitated in a shaker incubator at room temperature, 135 rpm, for 90 minutes, in a light-protected environment. Subsequently, it was kept in a dark environment for 24 hours, and color change was observed (Figure 3 and Figure 4). Spectrum analysis was performed using UV spectroscopy.

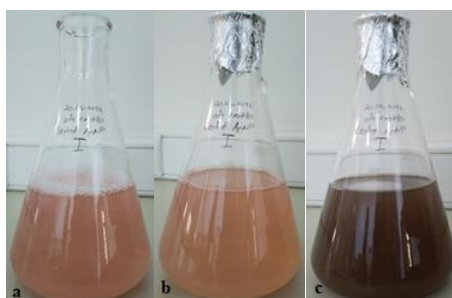


Figure 3- AgNP solution obtained from cornelian cherry extract prepared at 20 °C (a) 0 min, (b) 90 min, (c) 24 hours



Figure 4- AgNP solution obtained from cornelian cherry extract prepared at 60 °C (a) 0 min, (b) 90 min, (c) 24 hours

For the purification of AgNPs, centrifugation was performed at 4100 rpm for 25 minutes, and the supernatant was discarded. The precipitate was washed several times by adding distilled water. After this process, the AgNPs were transferred to Petri dishes, dried in a vacuum oven at 65 °C, and stored in a dark environment at room conditions (Figure 5).

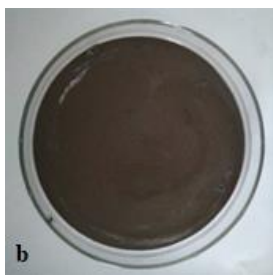


Figure 5- Cornelian cherry AgNPs after drying

2.2.3. Characterization of synthesized silver nanoparticles

The spectrophotometric analysis of the extract and nanoparticles was performed using a Shimadzu UV-1601 UV-Vis spectrophotometer in the wavelength range of 200-1000 nm. Spectrum acquisition was conducted against pure water at a medium speed.

Scanning Electron Microscopy (SEM) to determine the morphological structure of AgNPs while Energy-Dispersive X-ray Spectroscopy (EDX) was utilized to confirm the presence of silver (ZEISS GeminiSEM 500). Carbon tape was used in the SEM analysis, and the gold coating was applied under a vacuum to ensure the conductivity of the nanoparticles. ImageJ software determined particle size, and a histogram graph was plotted using the Statistical Package for the Social Sciences (SPSS) program.

Fourier Transform Infrared Spectroscopy (FTIR, Thermo Scientific Nicolet IS20) analysis was performed in the range of 4000-400 cm^{-1} to determine the functional groups responsible for the reduction in the extracts and involved in AgNP synthesis.

X-Ray Diffraction (XRD) analyses were carried out in the PANalytical EMPYREAN instrument in the range of $5^\circ \leq 2\theta \leq 85^\circ$ to determine the crystal structure and size of AgNPs. The Debye-Scherrer equation, $D = K\lambda / (\beta \cos \theta)$, was used to calculate the particle size, where D represents the particle size (nm), K is a constant value (0.9), λ is the X-ray wavelength (\AA) (1.54060), β is the half-width at the maximum peak value (FWHM) (rad), and θ is the angle of the maximum peak height (rad).

2.2.4. Determination of antimicrobial properties of synthesized silver nanoparticles

For the evaluation of the antimicrobial properties of AgNPs synthesized from cornelian cherry (*Cornus mas* L.) through green synthesis, *Staphylococcus aureus* (ATCC 12600), *Listeria monocytogenes* (ATCC 7644), *Salmonella* Typhi (ATCC 14028), and *Escherichia coli* O157:H7 (ATCC 25922) bacteria were used. The cultures were obtained from the Department of Dairy Technology, Faculty of Agriculture, Ege University. The cultures were activated in 10 mL of Tryptic Soy Broth (Merck, 105459) and incubated at 37 °C for 24 hours. From this culture, 0.1 mL was transferred to a Petri dish, and approximately 15 mL of Tryptic Soy Agar (TSA, Merck, 105458) was added to prepare the medium for antimicrobial testing.

AgNPs were prepared at 10 and 25 mg/mL concentrations, and their antimicrobial activity was determined using the paper disk method. The nanoparticle solution was prepared using sterile distilled water and allowed to stand in an ultrasonic water bath for 1 hour for a homogeneous distribution. The AgNP solution was impregnated onto filter paper disks (Whatman No.1) and placed on the agar plates. A chloramphenicol antibiotic disk (Bioanalyse, 30 μg) was used for the positive control, and the extract concentration was prepared at a 1:1 ratio for the negative control.

2.2.5. Statistical analysis

The study was conducted in two parallel sets with three replicates each. The obtained microbiological analysis results were analyzed using the MANOVA (Multivariate Analysis of Variance) test in the SPSS program, and values below $p < 0.05$ were considered statistically significant.

3. Results and Discussion

3.1. Determination of Properties of Silver Nanoparticles Obtained from Cornelian Cherry Extract

The properties of the AgNPs were determined through UV spectroscopy, SEM, EDX, FTIR, and XRD analyses. The silver nanoparticles (AgNPs) were obtained through biological synthesis using cornelian cherry (*Cornus mas* L.) extract at two different temperatures, 20 °C, and 60 °C. A color change from pink to brown was observed in nanoparticle synthesis at both temperatures, and the synthesis started after 24 hours.

The visible color change is the initial indicator that the biological synthesis of nanoparticles has begun. The synthesis time of nanoparticles depends on the pH of the environment. When the pH is low (acidic environment), the reaction starts later, and

the synthesis time can be longer (Alkhattaf 2021). Due to the pH value of 3 in the cornelian cherry extract, the color change occurred after 24 hours and shifted from pink to brown.

The spectrum analysis results of the extracts prepared at 20 °C and 60 °C revealed maximum absorbance peaks at 510 nm and 512 nm, respectively. The spectrum results of the AgNP solution derived from these extracts yielded the maximum peaks for the both temperatures at 500 nm (Figure 6 and Figure 7).

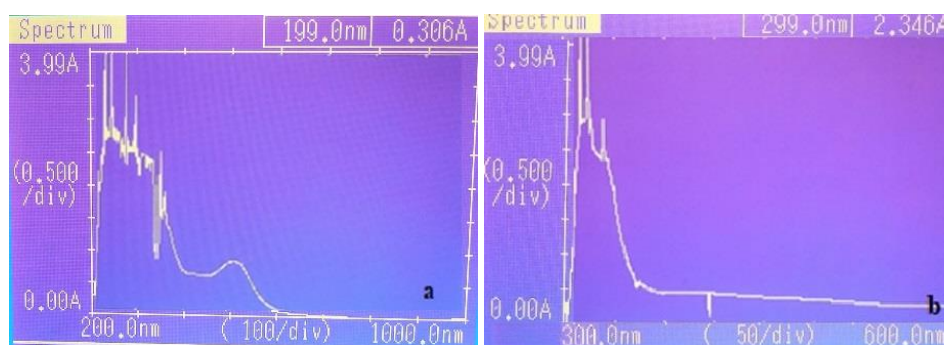


Figure 6- Spectrum graph of (a) cornelian cherry extract and (b) cornelian cherry AgNP solution prepared at 20 °C

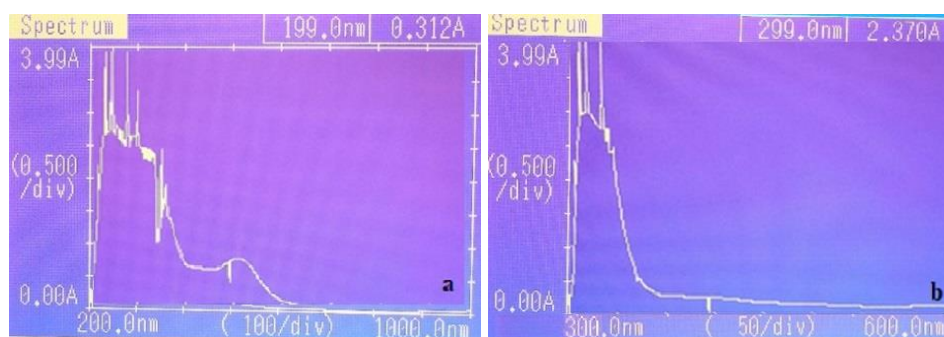


Figure 7- Spectrum graph of (a) cornelian cherry extract and (b) cornelian cherry AgNP solution prepared at 60 °C

In a study using *Cornus sanguinea* fruit similar to cornelian cherry, AgNPs obtained at room temperature showed a maximum absorbance peak at 510 nm (David et al. 2020). In this study, the result obtained at 20 °C was similar to our study; The temperature application of 60 °C showed a minor difference in the peak. In another cornelian cherry study, the maximum absorbance peak was observed at 418 nm (Filip et al. 2019). AgNPs derived from *Mangifera indica* fruit exhibited a maximum absorbance peak at 450 nm (Ameen et al. 2019). In a different study, *Rosa canina* fruit extract was obtained by heating for 5 minutes, and nanoparticles synthesized at 85 °C showed a maximum absorbance peak at 422 nm (Gulbagca et al. 2019). *Citrus sinensis* peels were used to synthesize AgNPs, and nanoparticle synthesis was carried out at two different temperatures, 25 °C and 60 °C, after boiling the extract in pure water for 2 minutes. The resulting nanoparticles exhibited maximum absorbance peaks at 445 nm for 25 °C and 424 nm for 60 °C, according to spectrophotometric analysis (Kaviya et al. 2011). As can be seen from the studies, the difference in fruit variety causes the change of the peaks.

In the morphology of nanoparticles, SEM analyses are used quite effectively for the size and shape of the nanomaterial (Ghaedi et al. 2015). SEM analysis of the AgNPs obtained from cornelian cherry extract at 20 °C and 60 °C. The SEM results and histogram graphs are presented in Figure 8 and Figure 9, respectively. The average sizes of AgNPs synthesized from the extracts at 20 °C and 60 °C were determined to be 50.86 nm and 61.17 nm, respectively. The AgNPs obtained at both temperatures exhibited spherical shapes.

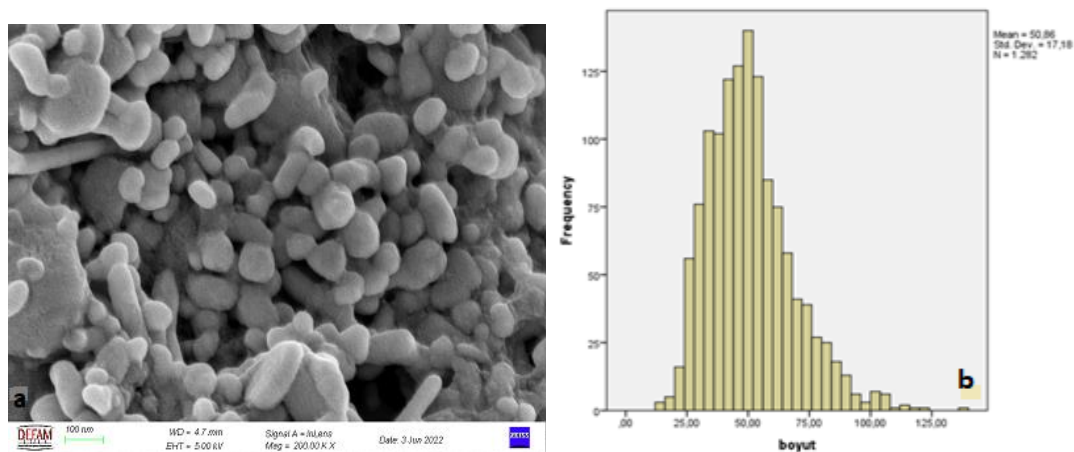


Figure 8- SEM results of nanoparticles obtained from the extract at 20 °C: (a) 200.00 K X, (b) histogram graph of nanoparticle size

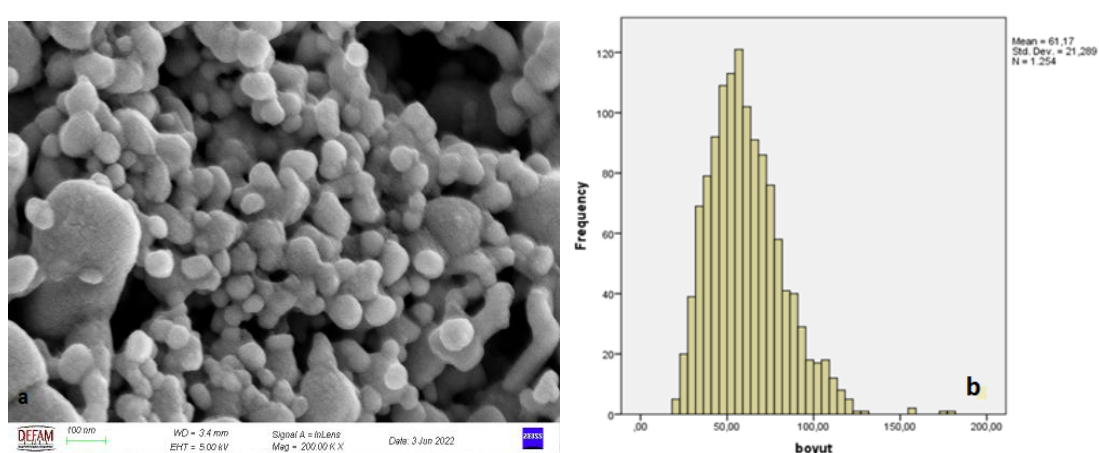


Figure 9- SEM results of nanoparticles obtained from the extract at 60 °C: (a) 200.00 K X, (b) histogram graph of nanoparticle size

The particle sizes of nanoparticles obtained from *Passiflora Edulis f. flavicarpa* leaves were reported to be between 50-100 nm, and their shapes were spherical in SEM and TEM analyses (Thomas et al. 2019). In the SEM analysis of AgNPs synthesized from *Vitis vinifera*, the particle sizes were reported to be between 30-70 nm, while in the TEM analysis, the sizes were found to be between 30-65 nm, and the shapes varied, including oval, triangular, and circular shapes (Hashim et al. 2020). In a study using *Berberis vulgaris* leaves and roots, the synthesized AgNPs were reported to have spherical shapes between 30-70 nm sizes in TEM analysis (Behravan et al. 2019). In TEM analysis, green-synthesized nanoparticles from Andean blackberry were reported to have spherical shapes and sizes between 12-50 nm (Kumar et al. 2017a).

Hernandez-Pinero et al. (2016) investigated the effects of different temperatures on the synthesis of AgNPs using basil, mint, marjoram, and peppermint. They observed that temperature had a significant impact on the synthesis process. They noted that varying heating rates resulted in AgNPs of different sizes, with higher heating rates leading to smaller AgNPs. In contrast, our study found that AgNPs synthesized at 60 °C were larger than those synthesized at 20 °C. However, as Hernandez-Pinero et al. (2016) pointed out, the choice of botanical species also influences the size of the AgNPs obtained. Therefore, it is possible to design a controlled system for synthesizing AgNPs with a specific diameter range by selecting particular plant species and heating rates to achieve nanoparticles of the desired size.

The scanning electron microscopy (SEM) images of the synthesized AgNPs reveal their length and homogeneity. These images indicate that the nanomaterials are spherical and of very small size. Due to their diminutive size, AgNPs can bind to cell membrane proteins and catalyze the generation of reactive oxygen species during bacterial growth, resulting in cell death due to oxidative stress (Alkhalaf et al. 2020). Consequently, the synthesized nanoparticles exhibited enhanced antimicrobial activity (Ramkumar et al. 2017; Lopes & Courrol 2018; Pallela et al. 2018).

EDX analysis was conducted to determine the elemental composition of AgNPs obtained from cornelian cherry extract at 20 °C and 60 °C. The findings of the EDX analysis are presented in Figure 3.5 and Figure 3.6. In the EDX results of the nanoparticles, strong peaks corresponding to silver at 3 eV were observed, confirming the formation of AgNP along with some weak peaks believed to originate from the fruit extract. The elemental composition of AgNPs synthesized after cornelian cherry

extraction at 20 °C was 82.82% Ag, 7.23% C, 1.40% O, and 8.55% Cl (Figure 10). The elemental composition of AgNPs obtained after extraction at 60 °C was determined as 83.64% Ag, 5.87% C, 1.26% O, and 9.24% Cl (Figure 11).

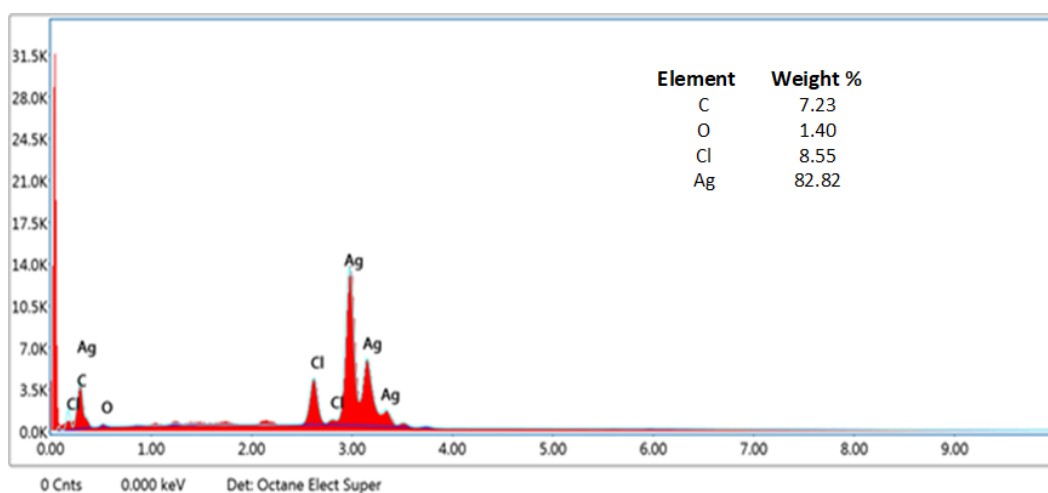


Figure 10- EDX result of the nanoparticles obtained from cornelian cherry extract at 20 °C

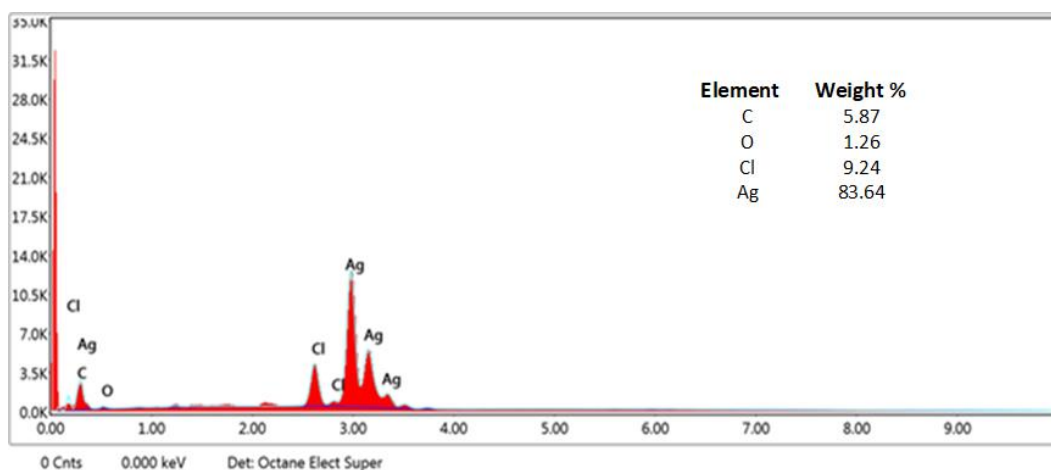


Figure 11- EDX result of the nanoparticles obtained from cornelian cherry extract at 60 °C

In the analysis using EDX, it was reported that nanoparticles obtained from garlic contained 75% Ag (Vijayakumar et al. 2019), nanoparticles obtained from *Mimusops elengi* fruit contained 47.6% Ag, 25.4% O, and 16.1% C (Korkmaz et al. 2020). AgNPs synthesized using *citrus sinensis* peels, *Capsicum annum*, *Mespilus germanica* fruit, and *Prunus japonica* leaves were reported to exhibit strong silver peaks (Kaviya et al. 2011; Saravanakumar et al. 2017; Baran et al. 2020; Diler & Leblebici 2020). In our study, the silver content of AgNPs obtained from both temperatures was relatively high.

Since the biological materials used in the synthesis of nanoparticles differ, each nanoparticle contains different components and functional groups, making it easier to determine the groups involved in reducing silver. FTIR analysis was conducted to identify the functional groups surrounding the nanoparticles and to determine the stabilizers (surface coatings) and reducing agents (Paiva-Santos et al. 2021).

The FTIR analysis results of cornelian cherry extract obtained at room temperature and the corresponding AgNPs are shown in Figure 12 and Figure 13. Regarding the peaks of the cornelian cherry obtained at 20 °C, the 2942 and 2884 cm^{-1} peaks were determined to be the C-H group (methyl, methylene and methoxy groups), the 1731 cm^{-1} peak as the C=O group (aldehyde), the 1585 cm^{-1} peak as the C=O group (carboxyl group), 1346 cm^{-1} peak as the N=O group, the 1245 cm^{-1} peak as the C-O group and the 1072 cm^{-1} peak as the C=C group (aromatic ring). The spectrum peaks of AgNPs were determined to be 2113 cm^{-1} , 1988 cm^{-1} , 1503 cm^{-1} and 1274 cm^{-1} . The comparison of cornelian cherry extract and AgNPs suggested that C=O and C-O groups are involved in the reduction of silver.

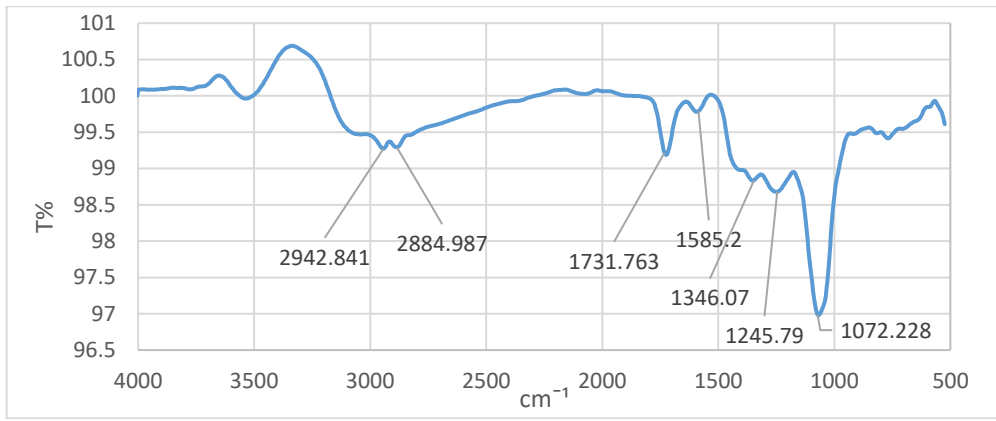


Figure 12- FTIR spectrum of the cornelian cherry extract obtained at 20 °C

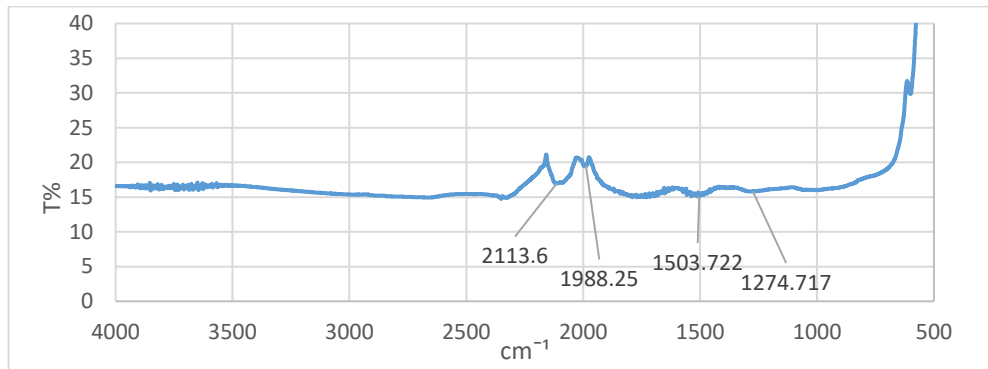


Figure 13- FTIR spectrum of the silver nanoparticles (AgNPs) obtained from cornelian cherry extract at 20 °C

The FTIR analysis results of cornelian cherry extract prepared by extraction at 60 °C and AgNP obtained from this extract are presented in Figures 14 and 15. In the FTIR spectrum of cornelian cherry extract obtained at 60 °C, the peak values correspond to 2917 and 2848 cm^{-1} for the C-H group, 1724 cm^{-1} for C=O, 1591 cm^{-1} for C=O group, 1343 cm^{-1} for N=O group, 1236 cm^{-1} for C-O group, and 1083 cm^{-1} for C=C groups. The spectrum peaks formed by AgNPs were observed at 2107 cm^{-1} , 1985 cm^{-1} , 1536 cm^{-1} , and 1046 cm^{-1} , and, comparing the spectrum peaks of *Cornus mas* L. extract with AgNPs, it was thought that the C=O and C=C groups play a role in reducing silver and contributing to AgNP formation.

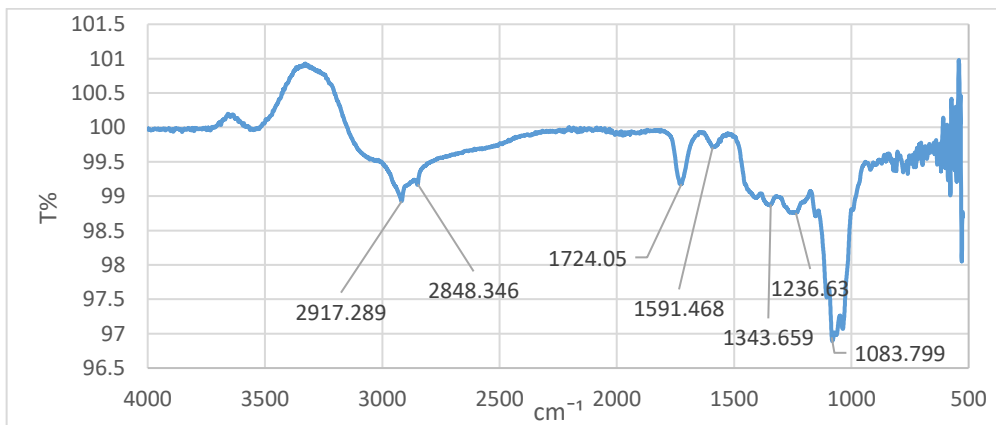


Figure 14- FTIR spectrum of the cornelian cherry extract obtained at 60 °C

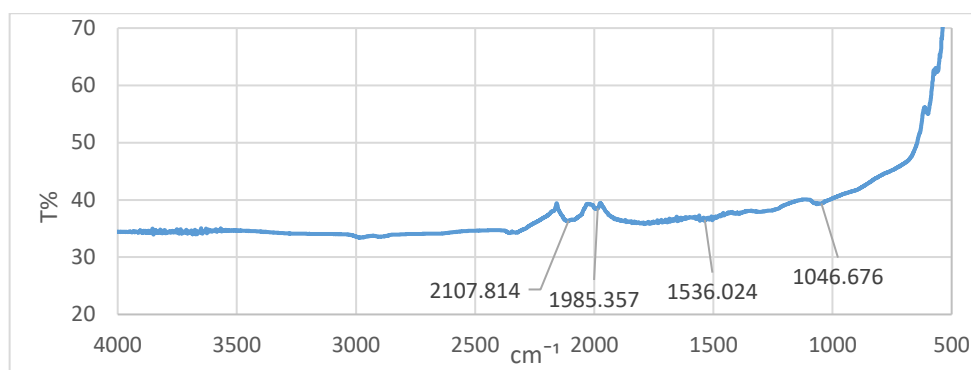


Figure 15- FTIR spectrum of the silver nanoparticles (AgNPs) obtained from cornelian cherry extract at 60 °C

The absorbance peaks of the extract and nanoparticle of silver nanoparticles synthesized using *Cornus sanguinea* fruit leaves were determined to be $3392\text{--}3434\text{ cm}^{-1}$ (O-H) and $1594\text{--}1618\text{ cm}^{-1}$ (C=O), indicating the presence of groups involved in Ag reduction (David et al. 2020). The FTIR analysis of the extract and synthesized AgNPs from *Cornus officinalis* fruit revealed peaks at 3352 and 3371 cm^{-1} (O-H), 2984 and 2983 cm^{-1} (C-H), 1655 and 1651 cm^{-1} (C=O), 1450 and 1448 cm^{-1} , 1273 and 1275 cm^{-1} , 1045 and 1049 cm^{-1} (C=C), indicating the presence of groups involved in Ag reduction (He et al. 2017). The extract derived from *Prunus japonica* exhibited peaks at 3284 cm^{-1} (N-H), 2927 cm^{-1} (C-H), 2363 cm^{-1} (C-H), 1598 cm^{-1} (C=O), 1384 cm^{-1} (alcohol, ethers, esters, carboxylic acids, and amino acids), and 1070 cm^{-1} (C-OH). A comparison of the peak values of the synthesized AgNPs from this extract revealed the involvement of C=O, N-H, and C-H groups in reduction (Saravanakumar et al. 2017). The peaks of AgNPs obtained from *Mangifera indica* extract were found to be at 3734 cm^{-1} (O-H), 2950 cm^{-1} (-CH), 2350 cm^{-1} (C-H), 1530 cm^{-1} (C-O), and 1030 cm^{-1} (N-O), indicating the involvement of these compounds in Ag reduction (Ameen et al. 2019). In the FTIR analysis of nanoparticles obtained from blackberry have been reported to be 3275 cm^{-1} (O-H) and 1634 cm^{-1} (C=O) groups, responsible for Ag reduction (Kumar et al. 2017a). The FTIR analysis of nanoparticles synthesized from cornelian cherry extract reported that the responsible groups for Ag reduction were 3159 cm^{-1} (O-H), 1717 cm^{-1} (C=O), and 1224 cm^{-1} (C=OO) (Filip et al. 2019).

Based on our results, the FTIR spectra obtained for both temperature applications were similar, and the groups involved in the reduction of silver and the formation of nanoparticles from cornelian cherry extract were determined to be C=C, C=O, and C-O (Figure 12, Figure 13, Figure 14, and Figure 15). These groups play a role as secondary metabolites in Ag reduction and the stability of nanoparticle formation (Arya et al. 2019; Paiva-Santos et al. 2021). Compared with previous studies, our results indicated the presence of similar groups of phytochemicals involved in Ag reduction.

The determination of the crystal structure and size of nanoparticles is provided by X-ray diffraction (XRD) analysis, which allows the identification of atom types through the diffraction of X-rays (Rana et al. 2020). In this context, XRD analysis was performed to determine the crystal structure and size of silver nanoparticles synthesized from cornelian cherry extract at $20\text{ }^{\circ}\text{C}$.

The average crystal sizes of AgNPs synthesized from the extract obtained at $20\text{ }^{\circ}\text{C}$ were determined to be 38.81 nm using the Debye-Scherrer equation, and their nanoparticle structures were found to be face-centered cubic. The peak points at 2θ angles were determined as 38.22° , 44.41° , 64.57° , 77.49° , and 81.61° , corresponding to the Bragg diffraction planes of (111), (200), (220), (311), and (222), respectively (Figure 16).

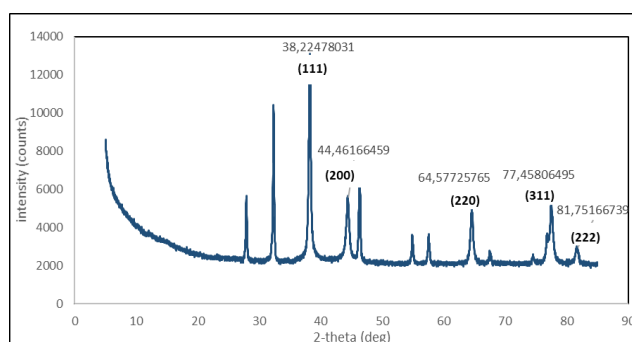


Figure 16- XRD result of AgNPs synthesized from cornelian cherry extract at 20 °C

The average crystal sizes of AgNPs synthesized from the extract obtained at $60\text{ }^{\circ}\text{C}$ were found to be 37.88 nm , and their nanoparticle structures were determined to be face-centered cubic. The peak points at 2θ angles were determined as 38.12° , 44.34° , 64.44° , 77.38° , and 81.52° , corresponding to the diffraction planes of (111), (200), (220), (311), and (222), respectively (Figure 17).

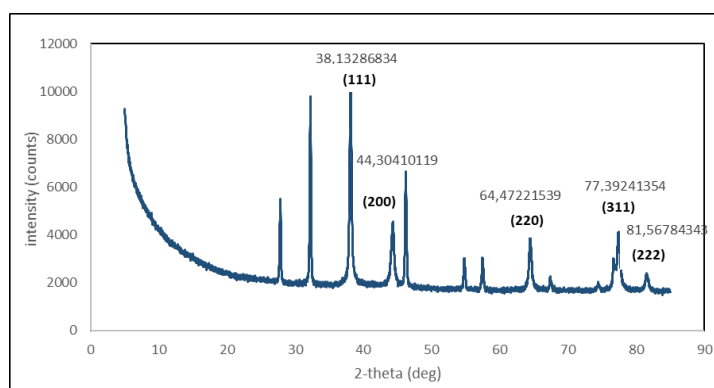


Figure 17- XRD result of AgNPs synthesized from cornelian cherry extract at 60 °C

The diffractions of AgNPs synthesized from *Rosa canina* were reported to be (111), (200), (220), (311), and (222), with a crystal size of 19.75 nm and a cubic crystal structure (Gulbagca et al. 2019). AgNPs synthesized from *Prunus persica* leaves showed diffractions of (111), (200), (220), (311), and (222), with a crystal size of 40 nm (Kumar et al. 2017b). AgNPs synthesized from *Mimusops elengi* exhibited 2θ values of 32.56°, 38.45°, 44.69°, 64.86°, 81.77°, and an average crystal size of 43 nm (Korkmaz et al. 2020). AgNPs synthesized from *Berberis vulgaris* leaves, and roots were determined to have crystal sizes of 50 nm (Behravan et al. 2019). AgNPs synthesized from apple showed 2θ values of 38.15°, 44.35°, 64.59°, 77.47°, 81.60°, corresponding diffractions of (111), (200), (220), (311), (222), and an average crystal size of 30 nm, with a cubic crystal structure [Ali et al. 2016]. AgNPs synthesized from *Forsythia suspensa* exhibited 2θ values of 38.23°, 46.31°, 64.58°, 77.50°, corresponding diffractions of (111), (200), (220), (311), and an average crystal size of 47.3 nm (Du et al. 2019).

In the present study, the crystal sizes of the nanoparticles synthesized from the extracts obtained at 20 °C and 60 °C were calculated as 38.81 nm and 37.88 nm, respectively (Figure 3.11 and Figure 3.12). It was determined that the shapes of the nanoparticles were cubic crystals for both temperature values. When compared with the SEM results, the average sizes of the nanoparticles synthesized from the extracts obtained at 20 °C and 60 °C were calculated as 50.86 nm and 61.17 nm, respectively, and these values were close to the crystal sizes obtained from XRD analysis. The comparison of our results with previous studies revealed similarities in crystal sizes, diffraction values, and peak points.

3.3. Antimicrobial activity of silver nanoparticles

The antimicrobial effects of AgNPs synthesized through green synthesis from cornelian cherry at two different extraction temperatures were investigated using the paper disk method against *Staphylococcus aureus*, *Listeria monocytogenes*, *Salmonella* Typhi, and *Escherichia coli* O157:H7. The concentrations of bacterial cultures used for determining the antimicrobial activity were found to be 9.9×10^8 CFU/mL for *Staphylococcus aureus*, 3.8×10^8 CFU/mL for *Listeria monocytogenes*, 5.7×10^8 CFU/mL for *Salmonella* Typhi, and 6.7×10^8 CFU/mL for *Escherichia coli* O157:H7.

The results of the antimicrobial activity of AgNPs synthesized from cornelian cherry extracts obtained at 20 °C and 60 °C are presented in Table 1.

Table 1- Antimicrobial activity of AgNPs synthesized from. cornelian cherry

Microorganism	AgNP (mg/mL)	Cornelian cherry (20 °C) (mm)			Cornelian cherry (60 °C) (mm)		
		CA	E	NP	CA	E	NP
<i>Staphylococcus aureus</i>	10	30	8	9	27	9	9
	25	28	9	9	30	7	9
<i>Listeria monocytogenes</i>	10	21	7	ND	19	ND	ND
	25	20	9	9	20	8	8
<i>Salmonella</i> Typhi	10	24	7	ND	21	ND	ND
	25	22	8	7	22	7	ND
<i>Escherichia coli</i> O157:H7	10	25	8	9	25	ND	7
	25	22	* ND	ND	21	ND	ND

*ND: not detected CA: Chloramphenicol (30µg), E: Extract, NP: Silver nanoparticle

The positive control, chloramphenicol antibiotic disks, created inhibition zones ranging from 19-30 mm in the Petri dishes. The negative control, cornelian cherry extract, exhibited inhibition zone diameters ranging from 7-9 mm against the tested pathogenic bacteria.

As shown in Table 1, AgNPs synthesized from extracts obtained at 20 °C formed a 9 mm inhibition zone against *Staphylococcus aureus* and *Escherichia coli* O157:H7 cultures at a concentration of 10 mg/mL. However, they did not show any significant activity against the other microorganisms ($P>0.05$). AgNPs prepared at a 25 mg/mL concentration also formed 9 mm inhibition zones against *Staphylococcus aureus* and *Listeria monocytogenes* cultures and a 7 mm inhibition zone against *Salmonella* Typhi culture ($P>0.05$). However, they did not exhibit antimicrobial activity against *Escherichia coli* O157:H7 (Figure 18).

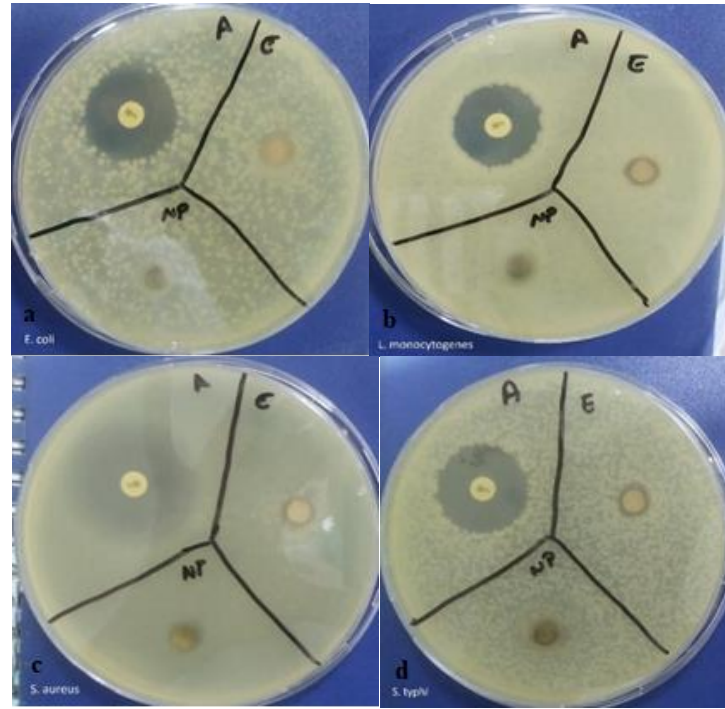


Figure 18- The antimicrobial results of AgNPs synthesized from cornelian cherry extract at 20 °C (25 mg/mL) as follows: (a) *E. coli* O157:H7, (b) *L. monocytogenes*, (c) *S. aureus*, (d) *S. Typhi*.

The antimicrobial activity of AgNPs synthesized from the extract at a temperature of 60 °C and prepared at a concentration of 10 mg/mL, as indicated in Table 1, resulting in the formation of a 9-mm-inhibition zone in *Staphylococcus aureus* culture and a 7-mm-inhibition zone in *Escherichia coli* O157:H7 cultures. However, the AgNPs at a 25 mg/mL concentration exhibited a 9 mm inhibition zone in the *Staphylococcus aureus* culture and an 8 mm inhibition zone in the *Listeria monocytogenes* culture. Notably, both concentrations of AgNPs showed no significant efficacy against *Salmonella* Typhi culture ($P>0.05$) (see Figure 19).

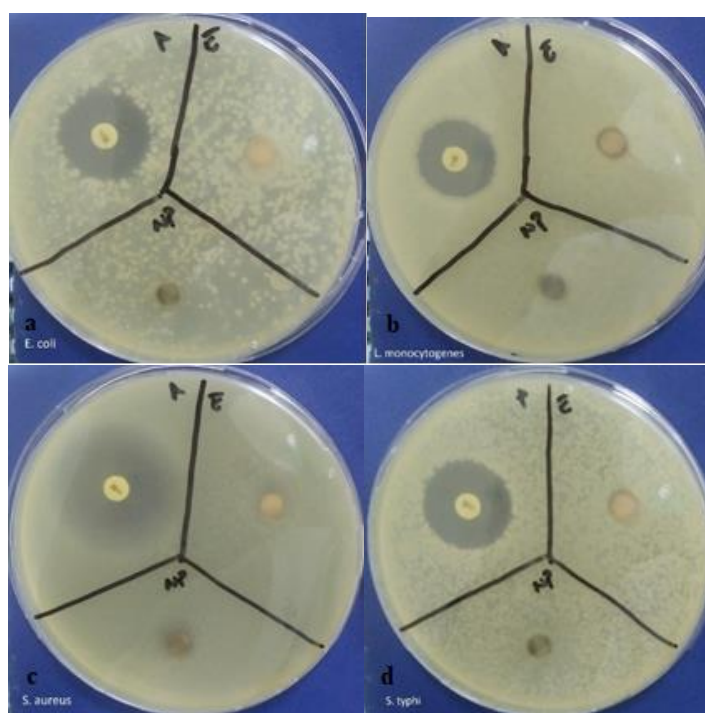


Figure 19- The antimicrobial results of AgNPs synthesized from cornelian cherry extract at 60 °C (25 mg/mL) as follows: (a) *E. coli* O157:H7, (b) *L. monocytogenes*, (c) *S. aureus*, (d) *S. Typhi*

The studies conducted have demonstrated the antimicrobial effects of AgNPs at various concentrations against certain bacteria. While antimicrobial effects have been observed in studies involving bacteria such as *Escherichia coli*, *Vibrio cholera*, *Bacillus subtilis*, *Bacillus vallismortis*, *Klebsiella pneumoniae*, *Proteus vulgaris*, *Staphylococcus aureus*, and *Aeromonas hydrophila* (Vignesh et al. 2013; Saravanakumar et al. 2017; Kumar et al. 2017b; Pirtarighat et al. 2019; Tailor et al. 2020;), Taghavizadeh Yazdi et al. (2019) reported no antibacterial effect on *Staphylococcus aureus*, and *Bacillus subtilis* at the concentration they utilized.

The results obtained in this study indicate that silver nanoparticles synthesized from cornelian cherry did not exhibit statistically significant activity against pathogenic bacteria ($P > 0.05$). It is suggested that the concentrations of 10 and 25 mg/mL used in the experiments may not have been sufficient, and therefore, higher concentrations should be considered in future research.

4. Conclusions

This study presents an innovative approach to nanoparticle synthesis using the environmentally friendly, low-cost, and simple method of utilizing cornelian cherry (*Cornus mas L.*) fruit with high polyphenol content for green synthesis. The observed color change during the formation of nanoparticles, the stable structure of the resulting nanoparticles, their spherical shape, and the silver content over 80% demonstrate the suitability of cornelian cherry, which is known for its high phenolic content, for this purpose. The microbiological study indicates the antimicrobial potential of the resulting nanoparticles and the need for further studies using plants known for their high phenolic content. The increasing resistance of bacteria worldwide to various agents leads to the search for new methods for controlling these bacteria, and studies conducted in this regard demonstrate the usability of AgNPs obtained through green synthesis.

In our research, we have observed that silver nanoparticles offer several advantages for synthesis, including ease of processing, measurability, and economic accessibility. Additionally, Cornelian cherry (*Cornus mas L.*) demonstrates the capability to form stable nanoparticles that can be stored for extended periods without molecular aggregation. Some studies have investigated the regulation of such nanoparticles through testing, whereas limited attention has been given to plant-based mechanisms. Subsequently, in our studies, it is imperative to identify the key components of *Cornus mas L.* extract and elucidate their roles in the production of AgNPs (silver nanoparticles). Numerous mechanisms have been proposed to account for the antibacterial activity of AgNPs. These mechanisms encompass the release of silver ions from AgNPs, the generation of reactive oxygen species, disruption of cellular morphology, inactivation of crucial enzymes, DNA condensation, and interference with DNA replication. Nevertheless, there is potential for further exploration to develop novel AgNP formulations. Furthermore, comprehensive research should be undertaken to assess the migration of silver ions into food products, and it is essential to establish migration limits to safeguard consumer health.

Acknowledgements

This study was supported by the Manisa Celal Bayar University Research Projects Management Unit (Project No. 2021-033).

References

- Abbasi E, Milani M, Fekri Aval S, Kouhi M, Akbarzadeh A, Tayefi Nasrabadi H, Nikasa P, Joo S.W Hanifehpour Y & Nejati-Koshki K (2016). "Silver nanoparticles: synthesis methods, bio-applications and properties". *Critical reviews in microbiology* 42: 173-180. <https://doi.org/10.3109/1040841x.2014.912200>
- Ali Z A, Yahya R, Sekaran S D & Puteh R (2016). "Green synthesis of silver nanoparticles using apple extract and its antibacterial properties". *Advances in Materials Science and Engineering* pp. 1-6. <https://doi.org/10.21275/sr231021141519>
- Alkhattaf F S (2021). "Gold and silver nanoparticles: Green synthesis, microbes, mechanism, factors, plant disease management and environmental risks". *Saudi Journal of Biological Sciences* 28(6): 3624-3631
- Alkhalaf M I, Hussein R H & Hamza A (2020). "Green synthesis of silver nanoparticles by *Nigellasativa* extract alleviates diabetic neuropathy through anti-inflammatory and antioxidant effects". *Saudi Journal of Biological Sciences* 27(9): 2410-2419. <https://doi.org/10.1016/j.sjbs.2020.05.005>
- Ameen F, Srinivasan P, Selvankumar T, Kamala-Kannan S, Al Nadhari S, Almansob A, Dawoud T & Govarthanan M (2019). "Phytosynthesis of silver nanoparticles using *Mangifera indica* flower extract as bioreductant and their broad-spectrum antibacterial activity". *Bioorganic Chemistry* 88: 102970
- Arshadi E, Sedaghat S & Moradi O (2018). "Green synthesis and characterization of silver nanoparticles using fructose". *Asian Journal of Green Chemistry* 2(1): 41-50
- Arya A, Mishra V & Chundawat T S (2019). "Green synthesis of silver nanoparticles from green algae (*Botryococcus braunii*) and its catalytic behavior for the synthesis of benziimidazoles". *Chemical Data Collections* 20: 100190
- Baran M F, Umaz A & Eren A (2020). "Antimicrobial applications of silver nanoparticles synthesized from plant origin against some microorganisms". *Fen Bilimleri ve Matematik Alanında Araştırma ve Derlemeler* 93-100. (In Turkish)
- Baysal G (2020). "The use of nanosystems in the food industry". *The Journal of Food* 45(3): 517-529. (In Turkish)
- Behravan M, Panahi A H, Naghizadeh A, Ziaee M, Mahdavi R & Mirzapour A (2019). "Facile green synthesis of silver nanoparticles using *Berberis vulgaris* leaf and root aqueous extract and its antibacterial activity". *International journal of biological macromolecules* 124: 148-154. <https://doi.org/10.1016/j.ijbiomac.2018.11.101>
- Cao Y, Jin R & Mirkin C A (2001). "DNA-Modified Core- Shell Ag/Au Nanoparticles". *Journal of the American Chemical Society* 123: 7961-7962
- Celep E, Aydın A & Yeşilada E (2012). "A comparative study on the in vitro antioxidant potentials of three edible fruits: Cornelian cherry, Japanese persimmon and cherry laurel". *Food and Chemical Toxicology* 50(9): 3329-3335. <https://doi.org/10.1016/j.fct.2012.06.010>
- Ceylan R, Demirbas A, Ocoşoş İ, & Aktumsek A (2021). "Green synthesis of silver nanoparticles using aqueous extracts of three *Sideritis* species from Turkey and evaluations bioactivity potentials". *Sustainable Chemistry and Pharmacy* 21: 100426
- David L, Moldovan B, Baldea I, Olteanu D, Bolfa P, Clichici S & Filip G A (2020). "Modulatory effects of *Cornus sanguinea* L. mediated green synthesized silver nanoparticles on oxidative stress, COX-2/NOS2 and NFkB/pNFkB expressions in experimental inflammation in Wistar rats". *Materials Science and Engineering: C*, 110: 110709. <https://doi.org/10.1016/j.msec.2020.110709>
- Diler D & Leblebici Y (2020). "Muşmula (*Mespilus germanica* L.) Silver nanoparticle (AgNP) synthesis and characterization studies in medlar (*Mespilus germanica* L.) extract biocatalyst". *Bilim Armonisi*, 3(1): 17-23. <https://doi.org/10.37215/bilar.595127> (In Turkish)
- Du J, Hu Z, Yu Z, Li H, Pan J, Zhao D & Bai Y (2019). "Antibacterial activity of a novel *Forsythia suspensa* fruit mediated green silver nanoparticles against food-borne pathogens and mechanisms investigation". *Materials Science and Engineering: C*, 102: 247-253. <https://doi.org/10.1016/j.msec.2019.04.031>
- Ekrikaya S, Yılmaz E, Celik C, Demirbuga S, Ildiz N, Demirbas A & Ocoşoş İ (2021). "Investigation of ellagic acid rich-berry extracts directed silver nanoparticles synthesis and their antimicrobial properties with potential mechanisms towards *Enterococcus faecalis* and *Candida albicans*". *Journal of Biotechnology* 341: 155-162
- Filip G A, Moldovan B, Baldea I, Olteanu D, Suharoschi R, Decea N, Cismaru C M, Gal E, Cenariu M, Clichici S & David L (2019). "UV-light mediated green synthesis of silver and gold nanoparticles using cornelian cherry fruit extract and their comparative effects in experimental inflammation". *Journal of Photochemistry and Photobiology B: Biology* 191: 26-37. <https://doi.org/10.1016/j.jphotobiol.2018.12.006>
- Ghaedi M, Yousefinejad M, Safarpour M, Khafri H Z & Purkait M K (2015). "Rosmarinus officinalis leaf extract mediated green synthesis of silver nanoparticles and investigation of its antimicrobial properties". *Journal of Industrial and Engineering Chemistry* 31: 167-172. <https://doi.org/10.1016/j.jiec.2015.06.020>
- Gulbagca F, Ozdemir S, Gulcan M & Sen F (2019). "Synthesis and characterization of *Rosa canina*-mediated biogenic silver nanoparticles for anti-oxidant, antibacterial, antifungal, and DNA cleavage activities". *Heliyon* 5(12): e02980
- Hashim N, Paramasivam M, Tan J S, Kernain D, Hussin M H, Brosse N, Gambier F & Raja P B (2020). "Green mode synthesis of silver nanoparticles using *Vitis vinifera*'s tannin and screening its antimicrobial activity/apoptotic potential versus cancer cells". *Materials Today Communications* 25: 101511. <https://doi.org/10.1016/j.mtcomm.2020.101511>
- He Y, Li X, Wang J, Yang Q, Yao B, Zhao Y, Zhao A, Sun W & Zhang Q (2017). "Synthesis, characterization and evaluation cytotoxic activity of silver nanoparticles synthesized by Chinese herbal *Cornus officinalis* via environment friendly approach". *Environmental Toxicology and Pharmacology* 56: 56-60
- Hernandez-Morales L, Espinoza-Gómez H, Flores-López L Z, SoteloBarrera E L, Núñez-Rivera A, Cadena-Nava R D, Alonso- Núñez G & Espinoza K A (2019). "Study of the green synthesis of silver nanoparticles using a natural extract of dark or white *Salvia hispanica* L. seeds and their antibacterial application". *Applied Surface Science* 489: 952-961. <https://doi.org/10.1016/j.apsusc.2019.06.031>
- Hernandez-Pinero J L, Terrón-Rebolledo M, Foroughbakhch R, Moreno-Limón S, Melendrez M F, Solís-Pomar F & Pérez-Tijerina E (2016). "Effect of heating rate and plant species on the size and uniformity of silver nanoparticles synthesized using aromatic plant extracts". *Applied Nanoscience* 6(8): 1183-1190

- Kaviya S, Santhanalakshmi J, Viswanathan B, Muthumary J & Srinivasan K (2011). "Biosynthesis of silver nanoparticles using *Citrus sinensis* peel extract and its antibacterial activity". *Spectrochimica Acta Part A: Molecular and Biomolecular Spectroscopy* 79(3): 594-598. <https://doi.org/10.1016/j.saa.2011.03.040>
- Korkmaz N, Ceylan Y, Hamid A, Karadağ A, Bülbül A S, Aftab M N, Çevik Ö & Şen F (2020). "Biogenic silver nanoparticles synthesized via *Mimusops elengi* fruit extract, a study on antibiofilm, antibacterial, and anticancer activities". *Journal of Drug Delivery Science and Technology* 59: 101864. <https://doi.org/10.1016/j.jddst.2020.101864>
- Kumar B, Smita K, Cumbal L & Debut A (2017a). "Green synthesis of silver nanoparticles using Andean blackberry fruit extract". *Saudi journal of biological sciences* 24(1): 45-50. <https://doi.org/10.1016/j.sjbs.2015.09.006>
- Kumar R, Ghoshal G, Jain A & Goyal M (2017b). "Rapid green synthesis of silver nanoparticles (AgNPs) using (*Prunus persica*) plants extract: exploring its antimicrobial and catalytic activities". *J. Nanomed. Nanotechnol.*, 8(4): 1-8
- Lopes C R B & Courrol L C (2018). "Green synthesis of silver nanoparticles with extract of *Mimusops coriacea* and light". *Journal of Luminescence*, 199: 183-187
- Paiva-Santos A C, Herdade A M, Guerra C, Peixoto D, Pereira-Silva M, Zeinali M, Mascarenhas-Melo F, Paranhos A & Veiga F (2021). "Plant-mediated green synthesis of metal-based nanoparticles for dermatopharmaceutical and cosmetic applications". *International Journal of Pharmaceutics* 597: 120311
- Pallela P N V K, Ummey S, Ruddaraju L K, Pammi S V N & Yoon S G (2018). "Ultra Small, monodispersed green synthesized silver nanoparticles using aqueous extract of *Sida cordifolia* plant and investigation of antibacterial activity". *Microbial Pathogenesis* 124: 63-69. <https://doi.org/10.1016/j.micpath.2018.08.026>
- Pirtarighat S, Ghannadnia M & Baghshahi S (2019). "Green synthesis of silver nanoparticles using the plant extract of *Salvia spinosa* grown in vitro and their antibacterial activity assessment". *Journal of Nanostructure in Chemistry* 9(1): 1-9
- Polat S & Fenercioğlu H (2014). "Nanotechnology applications in food packaging: Use of inorganic nanoparticles". *Gıda* 39(3): 187-194. (In Turkish)
- Rai V R & Bai J (2011). "Nanoparticles and their potential application as antimicrobials". Ed.: A. Méndez-Vilas, Microbiology Series No. 3 Vol. 1, Spain pp. 197-209
- Ramkumar V S, Pugazhendhi A, Gopalakrishnan K, Sivagurunathan P, Saratale G D, Dung T & Kannapiran E (2017). "Biofabrication and characterization of silver nanoparticles using aqueous extract of seaweed *Enteromorpha compressa* and its biomedical properties". *Biotechnology Reports* 14: 1-7
- Rana A, Yadav K & Jagadevan S (2020). "A comprehensive review on green synthesis of nature-inspired metal nanoparticles: mechanism, application and toxicity". *Journal of Cleaner Production* 272: 1-25. <https://doi.org/10.1016/j.jclepro.2020.122880>
- Rezvani E, Rafferty A, McGuinness C & Kennedy J (2019). "Adverse effects of nanosilver on human health and the environment". *Acta Biomaterialia* 94: 145-159
- Salejda A M, Kucharska A Z & Krasnowska G (2018). "Effect of cornelian cherry (*Cornus mas* L.) juice on selected quality properties of beef burgers". *Journal of Food Quality*, Article ID 1563651. <https://doi.org/10.1155/2018/1563651>
- Saravanakumar A, Peng M M, Ganesh M, Jayaprakash J, Mohankumar M & Jang H T (2017). "Low-cost and eco-friendly green synthesis of silver nanoparticles using *Prunus japonica* (Rosaceae) leaf extract and their antibacterial, antioxidant properties". *Artificial Cells, Nanomedicine, and Biotechnology* 45(6): 1165-1171
- Silver S (2003). "Bacterial silver resistance: Molecular biology and uses and misuses of silver compounds". *FEMS Microbiology Reviews* 27(2-3): 341-353
- Stankovic M S, Zia-Ul-Haq M, Bojovic B M & Topuzovic M D (2014). "Total phenolics, flavonoid content and antioxidant power of leaf, flower and fruits from cornelian cherry (*Cornus mas* L.)". *Bulgarian Journal of Agricultural Science* 20(2): 358-363.
- Sürengil G & Kılınc B (2011). "Gıda ambalaj sektöründe nanoteknolojik uygulamalar ve su ürünleri açısından önemi". *Journal of Fisheries Sciences* 5(4): 317-325
- Taghavizadeh Yazdi M E, Modarres M, Amiri M S & Darroudi M (2019). "Phyto-synthesis of silver nanoparticles using aerial extract of *Salvia leriifolia* Benth and evaluation of their antibacterial and photo-catalytic properties". *Research on Chemical Intermediates* 45(3): 1105-1116. <https://doi.org/10.1007/s11164-018-3666-8>
- Tailor G, Yadav B L, Chaudhary J, Joshi M & Suvalka C (2020). "Green synthesis of silver nanoparticles using *Ocimum canum* and their antibacterial activity". *Biochemistry and Biophysics Reports* 24: 100848. <https://doi.org/10.1016/j.bbrep.2020.100848>
- Thomas B, Vithiya B, Prasad T, Mohamed S B, Magdalane C M, Kaviyarasu K & Maaza M (2019). "Antioxidant and photocatalytic activity of aqueous leaf extract mediated green synthesis of silver nanoparticles using *Passiflora edulis* f. *flavicarpa*". *Journal of Nanoscience and Nanotechnology* 19(5): 2640-2648
- Vignesh, V, Anbarasi K F, Karthikeyeni S, Sathiyarayanan G, Subramanian P & Thirumurugan R (2013). "A superficial phyto-assisted synthesis of silver nanoparticles and their assessment on hematological and biochemical parameters in *Labeo rohita* (Hamilton, 1822)". *Colloids and Surfaces A: Physicochemical and Engineering Aspects* 439: 184-192. <https://doi.org/10.1016/j.colsurfa.2013.04.011>
- Vijayakumar S, Malaikozhundan B, Saravanakumar K, Durán-Lara E F, Wang M H & Vaseeharan B (2019). "Garlic clove extract assisted silver nanoparticle-Antibacterial, antibiofilm, antihelminthic, anti-inflammatory, anticancer and ecotoxicity assessment". *Journal of Photochemistry and Photobiology B: Biology* 198: 111558
- Wang S, Lawson R, Ray P C & Yu H (2011). "Toxic effects of gold nanoparticles on *Salmonella* Typhimurium bacteria". *Toxicology and Industrial Health* 27(6): 547-554





Aronia melanocarpa (Michaux) Elliot Fruit Juice Attenuates Acetaminophen-induced Hepatotoxicity on Larval Zebrafish Model

Çiğdem Bilgi^{a,b*} , Gülçin Çakan Akdoğan^{b,c} 

^aIstanbul University-Cerrahpaşa, Faculty of Pharmacy, Department of Pharmacognosy, Istanbul, TURKIYE

^bIzmir Biomedicine and Genome Center, Izmir, TURKIYE

^cDokuz Eylul University, Faculty of Medicine, Department of Medical Biology, Izmir, TURKIYE

ARTICLE INFO

Research Article

Corresponding Author: Çiğdem Bilgi, E-mail: cigdem.karakoyun@iuc.edu.tr

Received: 16 October 2023 / Revised: 15 January 2024 / Accepted: 10 February 2024 / Online: 23 July 2024

Cite this article

Bilgi Ç, Akdoğan Çakan G (2024). *Aronia melanocarpa* (Michaux) Elliot Fruit Juice Attenuates Acetaminophen-induced Hepatotoxicity on Larval Zebrafish Model. *Journal of Agricultural Sciences (Tarım Bilimleri Dergisi)*, 30(3):458-463. DOI: 10.15832/ankutbd.1375719

ABSTRACT

Aronia melanocarpa (Michaux) Elliot (chokeberry) is a natural medicinal plant with a rich content of phenolic compounds such as procyanidins, anthocyanins, and phenolic acids. Chokeberry fruits are gaining worldwide popularity due to the strong bioactivities of their phenolic constituents, such as antioxidant, anti-inflammatory, anticancer, and liver-protective effects.

In the present study, total phenolic, flavonoid, and anthocyanin contents of chokeberry juice were determined via the Folin-Ciocalteu method, a spectrophotometric method based on AlCl₃ complexation, and pH differential method, respectively. Anthocyanin content was determined as 1.14% (equivalent to cyanidin-3-glucoside), while phenolic and flavonoid contents were measured as 5060.87 and 331.03 mg per 100 g of freeze-dried juice (equivalent to gallic acid and quercetin), respectively.

Keywords: Anthocyanin, *Aronia*, Chokeberry, Hepatoprotective, Zebrafish

The hepatoprotective effects of chokeberry fruit juice were evaluated using a zebrafish *in vivo* model for acetaminophen (APAP)-induced liver injury. Zebrafish is an emerging *in vivo* liver injury model that enables hepatoprotective bioactivity screening of samples on live organisms.

The APAP-induced liver injury model was established by treating zebrafish larvae with 5 mM APAP from 2 days post fertilization (dpf) to 5 dpf. The hepatoprotective effect of chokeberry was evaluated via exposure to 1, 10, and 100 µg/mL of fruit juice. While chokeberry fruit juice did not cause any toxicity up to 100 µg/mL, it successfully reduced the injury induced by APAP when applied at 1 µg/mL concentration. To our knowledge, this is the first report evaluating the hepatoprotective effects of chokeberry using zebrafish *in vivo* liver injury model.

1. Introduction

Aronia melanocarpa (Michx.) Elliot, commonly known as black chokeberry, is a deciduous shrub belonging to the Rosaceae family (Gurçik et al. 2023). The plant typically grows up to 1 - 2 meters tall and can spread 1 - 2 meters. The fruits of the plant are black, pea-sized berries that are edible but have a very astringent taste (Shahin et al. 2019; Ekiert et al. 2021).

Chokeberry is native to eastern North America, from Canada to the central United States. It grows in various habitats, including wetlands, swamps, and woodland edges (Moorhead & Rossell 2019). The plant has been cultivated as an ornamental plant and for its berries, which are used to make juice, wine, and other food products (Çelik et al. 2022).

In Türkiye, research on chokeberry cultivation started in 2012 at the Atatürk Horticultural Central Research Institute, and commercial production of chokeberry began in 2017 with the establishment of large orchards in the Marmara and Black Sea Regions (Akdemir 2022; Akdemir et al. 2023). Chokeberry fruits can be consumed fresh or processed, and their high market value has led to growing interest in chokeberry production in Türkiye. As production increases, the chokeberry industry is expected to expand further in the country.

Phytochemical studies showed that chokeberry fruits are rich in various nutrients, including vitamins C, E, and K, as well as bioactive compounds such as anthocyanins, flavonoids, and phenolic acids (Platonova et al. 2021). Anthocyanins are the water-soluble plant pigments that give the deep purple-black color of the fruits and are potent antioxidants (Khoo et al. 2017). The hepatoprotective bioactivity of anthocyanins has been reported by several research groups using *in vivo* rodent models (Wang et al. 2020). Nevertheless, the hepatoprotective potential of chokeberry has not been explored in the zebrafish liver injury model.

The purpose of the present study was two-fold; 1) to assess bioactivity potential of chokeberries harvested in Türkiye, 2) to test the hepatoprotective effects of chokeberry fruit juice, in the zebrafish hepatic injury model. To this end, total phenol, flavonoid and anthocyanin content of chokeberry juice were analysed. Next, the hepatoprotective bioactivity of fruit juice was evaluated using an *in vivo* zebrafish model featuring acetaminophen-induced liver injury.

To our knowledge, this study represents the first report demonstrating the liver-protective bioactivity of locally harvested chokeberry fruit juice using the zebrafish experimental model, shedding valuable insights for hepatoprotective drug discovery research.

2. Material and Methods

2.1. Plant material

Chokeberries were collected during the fruiting season from Kamiloba region (Büyükçekmece/İstanbul) and deposited at Istanbul University-Cerrahpaşa Faculty of Pharmacy Herbarium (IUCPH; voucher no:220901). Fruits were crushed with a homogenizer (Stuart Scientific SHM2) and centrifuged at 3000 rpm for 3 min. The supernatant was freeze-dried and stored at -20 °C until the experiment.

2.2. Chemicals and reagents

APAP, Chem Cruz (Santa Cruz Biotechnology, Inc., Dallas, TX, USA) was commercially purchased. The main stock of APAP was prepared by solubilizing it in deionized water. All dilutions were carried out using E3 fish media. Low melting point agarose and tricaine methanesulfate (TMS) were purchased from Sigma (Sigma-Aldrich, DL, United States).

2.3. Total phenolic content

The total phenolic content was determined using the Folin-Ciocalteu method, as described previously by Singleton and Rossi (Singleton & Rossi 1965), with slight modifications incorporated as per the recommendations of Dewanto et al. (2002). Through the calibration curve of gallic acid, the phenolics were determined and expressed as gallic acid equivalents (GAE, mg gallic acid/100g freeze-dried sample).

2.4. Total flavonoid content

Quantitative determination of total flavonoids was performed spectrophotometrically at 425 nm, following complexation with aluminum chloride. The total flavonoid content was determined and expressed as quercetin equivalents (QE, mg quercetin/100g sample) through the utilization of the calibration curve of quercetin.

2.5. Total anthocyanin content (TAC)

The determination of TAC was carried out using the pH differential method, as previously outlined by researchers (Giusti & Wrolstad 2001). Results were expressed as mg of cyanidin 3-glucoside per 100 mg sample.

2.6. Zebrafish maintenance and embryo collection:

A transgenic zebrafish line *lfabp:mCherry*, which was generated in Izmir Biomedicine and Genome Center (IBG) Çakan Lab, was used (Kwan et al. 2007). All adult zebrafish were maintained under a 14:10 light: dark cycle at 28.5 °C under standard feeding conditions at the IBG zebrafish facility.

Adult zebrafish were paired for mating in breeding tanks the day before collecting embryos, using dividers to separate males and females. The dividers were then removed, allowing the fish to spawn on the experimental day. Periodic checks were conducted, and embryos were collected at 5–10-minute intervals within an hour to minimize age variation resulting from multiple spawning events. Transgenic larvae were determined under a fluorescent microscope, embryos and larvae were maintained at 28.5±1 °C during experiments, and treatment was refreshed daily.

2.7. Exposure of larvae to apap and chokeberry fruit juice

Larvae were treated with APAP at a dose of 5 mM (755.8 mg/L) from 2 to 5 days post-fertilization (dpf) to generate a hepatic injury model. APAP also served as the positive control for this experiment. Exposure to chokeberry fruit juice (1; 10; 100 µg/mL in E3 media) was performed both as a single treatment (C) or in combination with 5 mM APAP (DT, dual treatment) for each concentration. Untreated larvae were only treated with fresh E3 media and used as the negative control. All treatments were refreshed daily and stopped at 5 dpf. Stereo-fluorescent images were taken, and the liver protectant effect of chokeberry fruit juice was determined via liver size measurements.

2.8. Statistical analysis

Comparisons of liver size changes between groups (n=10) were carried out using One-way analysis of variance (ANOVA), and p-values less than 0.05 were considered significant.

3. Results and Discussion

The phytochemical analysis revealed varying levels of anthocyanin, total phenolic, and flavonoid contents present in chokeberry juice (equivalent to cyanidin-3-glucoside, gallic acid, and quercetin, respectively), as shown in Table 1.

Table 1- Phytochemical content of chokeberry juice

Content	Method	Reference compound	Determined*
Phenols	Folin-Ciocalteu	Gallic acid	5060.87
Anthocyanins	pH-differential method	Cyanidin-3-glucoside	1.14
Flavonoids	UV-spectroscopy	Quercetin	331.03

*. Determined concentrations are expressed as % (v/v) for anthocyanins and as mg/100g for phenolics and flavonoids

The anthocyanin content was determined as 1.14%, equivalent to cyanidin-3-glucoside, indicating a rich presence of these pigments responsible for the vibrant colors in fruits and also are known for their potential health benefits, including hepatoprotective bioactivities arising from the antioxidant and anti-inflammatory properties (Mohammed & Khan 2022). These findings align with prior research highlighting the potent antioxidant and anti-inflammatory properties of anthocyanins, suggesting a potential link to the observed hepatoprotective effects (Denev et al. 2018; Panjaitan et al. 2013).

The phenolic content was measured as 5060.87 mg per 100 g of chokeberry juice and expressed as gallic acid equivalents. Phenolics are well-known for their ability to scavenge free radicals and protect against oxidative stress, contributing to potential liver-protectant effects (Tan et al. 2012; Zhang & Tsao 2016). Flavonoid content in the chokeberry juice was measured as 331.03 mg per 100 g juice, equivalent to quercetin. Flavonoids are a large group of bioactive compounds with antioxidant and anti-inflammatory activities, offering potential protection against various liver diseases (Akhlaghi 2016). Also, recent investigations have indicated that flavonoids, including quercetin, can induce hepatoprotective effects (Singh et al. 2014).

In the context of *in vivo* bioactivity testing, it was observed that APAP significantly impaired liver function and reduced liver size, thereby confirming the suitability of the APAP-induced hepatotoxicity larval model for our experiment. Notably, dual treatment (DT) with 1 µg/mL chokeberry fruit juice and 5 mM APAP for 96 h between 2-5 dpf has led to a significant increase in liver size in zebrafish larvae (Figure 1D and 2) compared to the group treated with sole 5 mM APAP (positive control). This result suggests that consuming chokeberries may provide partial protection against liver injury induced by APAP.

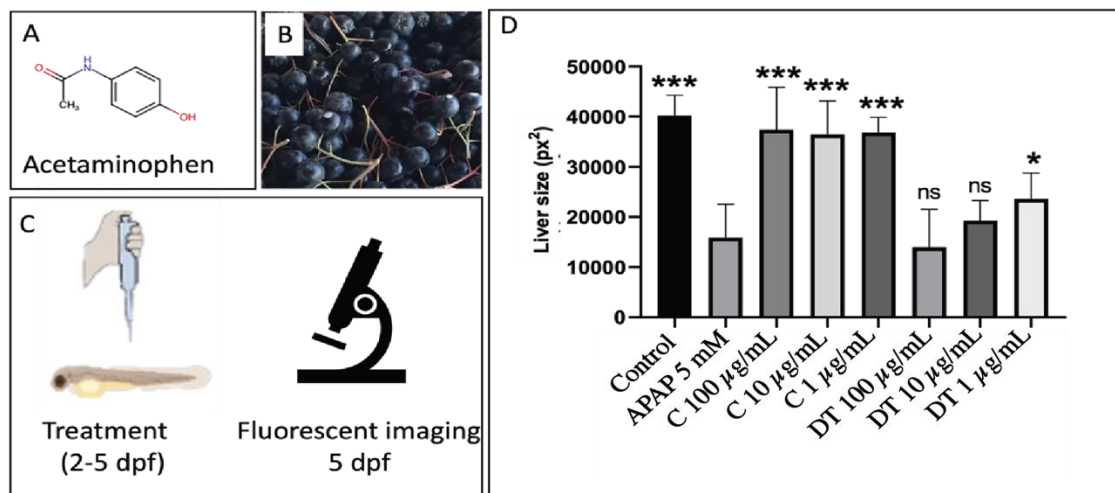


Figure 1- Treating zebrafish larvae between 2-5 days post-fertilization (dpf) with most-DILI agent, acetaminophen 5 mM, significantly decreased the liver size of which liver injury was alleviated with A) Chemical structure of APAP B) Chokeberry fruits C) Schematic illustration of experiment D) 2D measurement of liver size in different treatment groups. Control: untreated control group; APAP 5 mM: acetaminophen treated group; C: Chokeberries treated group; DT: Dual treatment with chokeberries in various concentrations and 5 mM APAP

The liver size of the untreated control was calculated as 40202.4 px² (square pixels), while the APAP 5 mM treated group had an average liver size of 15908.9 px², implying severe APAP-induced liver injury (Figure 1D). While all tested concentrations of chokeberry juice have shown more-less healed liver tissue, 1 µg/mL chokeberry juice demonstrated the best result with a statistically significant ($P < 0.05$) increase in liver area (23633.7 px²) compared to the APAP single-treated group. Single treatments of fruit juice seemed to be safe for liver health up to 100 µg/mL (Figure 1D and 2A).

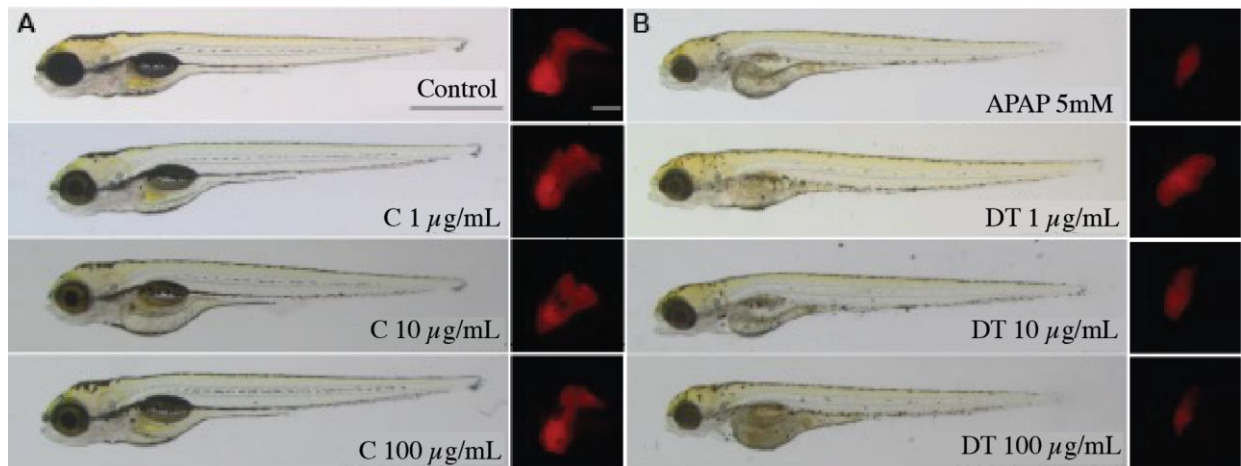


Figure 2- Chokeberry fruits displayed hepatoprotective bioactivity against APAP-induced liver injury on 5 dpf zebrafish larvae. The single treatment of APAP resulted in severe hepatic damage, while chokeberry dual treatment with APAP alleviated APAP-induced liver injury." A) The larvae treated with chokeberry fruit juice showed no discernible visual differences compared to the untreated control group. B) APAP (5mM=755.8 µg/mL) exposure severely reduced liver size and caused liver injury, while the combination of various concentrations of chokeberry fruit juice with the same dose of APAP partially reversed this injury. Control: untreated control group; APAP 5 mM: acetaminophen treated group; C: Chokeberries treated group; DT: Dual treatment with chokeberries and 5 mM APAP. Scale bars for whole larva and liver images: 1 mm and 200 µm, respectively

This study represents the first report to explore the hepatoprotective potential of chokeberry extract in a zebrafish model, despite previous evidence of its hepatoprotective bioactivity in rodents. Furthermore, our results present the potential utility of chokeberries grown in Türkiye due to their bioactivity.

Previously, the hepatoprotective effects of chokeberry extract against APAP-induced liver injury were established in a rat model, where daily oral administration of APAP at doses ranging from 2.5 to 10 mL/kg demonstrated notable mitigation of elevated liver serum biomarkers ALT and AST induced by APAP treatment (Valcheva-Kuzmanova et al. 2014). According to another research of same group, carbon tetrachloride (CCl₄)-induced elevation of AST and ALT activities in rats was reversed with anthocyanin administration (Valcheva-Kuzmanova et al. 2004). The co-administration of anthocyanins extracted from chokeberry was shown to decrease aspartate aminotransferase (AST), alanine aminotransferase (ALT) activities, bilirubin levels, and urea in the blood serum in rats with cadmium chloride-induced liver injury (Kowalczyk et al. 2003). Similarly, a study using a mouse model of chronic alcoholic liver injury, showed that chokeberries have hepatoprotective effects by restoring the AST/ALT ratio and reducing pathological damage to the liver and other organs (Wang et al. 2020).

Although the liver-protective activity of chokeberry has been demonstrated in other *in vivo* models, the use of the zebrafish model is reported for the first time. The zebrafish model aligns with the principles of the '3R' framework, which emphasizes the reduction, refinement, and replacement of animal experiments (Canedo et al. 2022). Zebrafish's genetic similarity to humans and its transparent embryos provide a useful screening platform for real-time visualization of liver function and response to treatments (Goessling & Sadler 2015). Moreover, zebrafish serve as a valuable model for studying liver diseases due to conserved tissue functions, shared liver cell types, and regulatory networks (Çakan-Akdoğan et al. 2023; Vliegthart et al. 2014).

This model is characterized by its rapid reproduction and cost-effectiveness, enabling us to conduct experiments on a large scale without incurring excessive costs. This scalability is particularly advantageous in hepatoprotection research, where the efficient screening of numerous plant extracts is paramount.

Our study addressed the issue of non-dose-dependent bioactivity of chokeberry within the tested concentrations (Figure 1D). The increasing amount of chokeberry juice with 5 mM APAP displayed gradually decreased hepatoprotection, implying a reverse-dose response relationship. Higher concentrations, 200, 400, and 800 µg/mL (data not shown) of chokeberry juice were lethal for larvae when applied as dual treatment with 5 mM APAP, while, interestingly, single treatments of the same concentrations did not cause any toxicity nor lethality. The safety of single treatments and toxicity in higher doses in dual treatment both imply the possibility of interactions between chokeberry and APAP (Yang et al. 1992). It can be speculated that the mechanism of this drug-nutrient interaction may arise from the competition of APAP and the phytochemical content of

chokeberry juice for the same metabolic pathway. APAP is primarily metabolized in the liver through two pathways, glucuronidation, and sulfation, which also have roles in metabolizing various components in chokeberry juice (Płatosz et al. 2021; van Rongen et al. 2016). It is known that sulfotransferases and glucuronidation enzymes catalyze the metabolic reactions of chokeberry fruits and APAP. However, when the dose of APAP exceeds the capacity of these pathways, a small amount of the drug is metabolized by the cytochrome P450 enzyme system, specifically CYP2E1, into a toxic metabolite called NAPQI (van Rongen et al. 2016). If glutathione levels are depleted, or NAPQI production is excessive, the toxic metabolite can bind to liver proteins and cause cell damage, leading to liver injury. The depletion of glutathione might have taken place in this study due to the high concentrations of chokeberry consumption. It is possible that chokeberry occupied the glutathione metabolic pathway, leading to increased competition for the same metabolic enzymes between APAP and chokeberry. As a result, APAP was forced to take the alternative metabolic pathway known as the CYP system, which results in toxic metabolites. Further investigation is needed to clarify the underlying mechanism of chokeberry fruit metabolism.

The chokeberry used in the present study was locally obtained from Büyükçekmece/İstanbul, a field located close to the city center, which provides advantages of transportation to national and international markets. The phenolic, flavonoid, and anthocyanin content of the chokeberry juice can be considered as medium-high level when compared to different juice and dry fruit samples in the literature and market (Tolić et al. 2015). According to our findings the hepatoprotective activity is strikingly high when the strong injury capacity of APAP in the liver is considered. It is plausible to think that optimization of harvest, juice extraction and bottling processes can increase the bioactivity potential of these locally sourced chokeberries and provide an advantage to local farmers. The zebrafish hepatic injury model used here can be used to assess the *in vivo* activity of end products to reach the ideal conditions.

4. Conclusions

We investigated the potential liver protective and healing effects of chokeberry juice using an *in vivo* zebrafish APAP-induced liver injury model (2-5 dpf) and observed promising outcomes, particularly the hepatoprotective effect of chokeberry juice with the concentration of 1 µg/mL. The total phenolic, anthocyanin, and flavonoid content of chokeberry tested here might play a crucial role in protecting liver cells from oxidative damage, thus contributing to the observed positive effects on liver health. These groups of compounds are known to modulate various cellular processes, reduce inflammation, and enhance antioxidant defense mechanisms, which could be beneficial in mitigating liver injury induced by APAP. Thus, the phytochemical findings and demonstration of chokeberries' hepatoprotective effects on zebrafish provide valuable insights into the potential mechanisms underlying their hepatoprotective properties, for which further investigations are needed. By harnessing the advantages of the zebrafish model, we not only expand the scope of our research on the hepatoprotective effects of chokeberry in relation to its phenolic content but also accelerate the screening of pure compounds and plant extracts for their bioactivity potential using liver-specific transgenic zebrafish models.

The chokeberries collected from Büyükçekmece/İstanbul showed promising potential for hepatoprotective activity due to their medium-high levels of phenolic, flavonoid, and anthocyanin content. Optimization of the harvest, juice extraction, and bottling processes has the potential to further increase the bioactivity of these chokeberries, providing a significant advantage to local farmers. Zebrafish is a useful model for screening the hepatoprotective activities of plant extracts and natural products.

References

- Akdemir S (2022). Determination of Variability in Ambient Conditions During Cold Storage of Aronia Fruits. *Tekirdağ Ziraat Fakültesi Dergisi* 19(2): 305–317
- Akdemir S, Torçuk A I & Uysal Seçkin G (2023). Determination of Quality Parameters of Aronia Melanocarpa During Cold Storage. *Erwerbs-Obstbau* 65(3): 531–537
- Akhlaghi M (2016). Non-alcoholic Fatty Liver Disease: Beneficial Effects of Flavonoids. *Phytotherapy Research* 30(10): 1559–1571
- Canedo A, Saiki P, Santos A L, Carneiro K S, Souza A M, Qualhato G, Brito R S, Mello-Andrade F & Rocha T L (2022). Zebrafish (Danio Rerio) Meets Bioethics: The 10Rs Ethical Principles in Research. *Ciência Animal Brasileira* 23: e-70884
- Çelik H, Karabulut B & Uray Y (2022). Growth-Development, Yield and Quality Characteristics of Aronia Varieties Grown in Pots. *International Journal of Innovative Approaches in Agricultural Research* 6(3): 246-254
- Denev P, Kratchanova M, Petrova I, Klisurova D, Georgiev Y, Ognyanov M & Yanakieva I (2018). Black Chokeberry (Aronia Melanocarpa (Michx.) Elliot) Fruits and Functional Drinks Differ Significantly in Their Chemical Composition and Antioxidant Activity. *Journal of Chemistry*.
- Dewanto V, Wu X, Adom K K & Liu R H (2002). Thermal Processing Enhances the Nutritional Value of Tomatoes by Increasing Total Antioxidant Activity. *Journal of Agricultural and Food Chemistry* 50(10): 3010–3014
- Ekiert H, Kubica P & Szopa A (2021). Successful Cultivation and Utilization of Aronia Melanocarpa (Michx.) Elliott (Black Chokeberry), a Species of North-American Origin in Poland and the Biosynthetic Potential of Cells from in Vitro Cultures. In: Ekiert H, Ramawat K G & Arora J (Eds.), *Medicinal Plants: Domestication, Biotechnology and Regional Importance*, Springer, India, pp. 69–111
- Giusti M M & Wrolstad R E (2001). Anthocyanins. Characterization and Measurement with UV-Visible Spectroscopy. *Current Protocols in Food Analytical Chemistry* 1: 1–13
- Goessling W & Sadler K C (2015). Zebrafish: An Important Tool for Liver Disease Research. *Gastroenterology* 149(6): 1361–1377
- Gurčík Ľ, Bajusová Z, Ladvenicová J, Palkovič J & Novotná K (2023). Cultivation and Processing of Modern Superfood—Aronia Melanocarpa (Black Chokeberry) in Slovak Republic. *Agriculture* 13(3): 604

- Khoo H E, Azlan A, Tang S T & Lim S M (2017). Anthocyanidins and Anthocyanins: Colored Pigments as Food, Pharmaceutical Ingredients, and the Potential Health Benefits. *Food & Nutrition Research* 61(1): 1361779
- Kowalczyk E, Kopff A, Fijałkowski P, Kopff M, Niedworok J, Błaszczak J, Kędziora J & Tyślerowicz P (2003). Effect of Anthocyanins on Selected Biochemical Parameters in Rats Exposed to Cadmium. *Acta Biochimica Polonica* 50(2): 543–548
- Kwan K M, Fujimoto E, Grabher C, Mangum B D, Hardy M E, Campbell D S, Parant J M, Yost H J, Kanki J P & Chien C B (2007). The Tol2kit: A Multisite Gateway-based Construction Kit for Tol2 Transposon Transgenesis Constructs. *Developmental Dynamics: An Official Publication of the American Association of Anatomists* 236(11): 3088–3099
- Mohammed H A & Khan R A (2022). Anthocyanins: Traditional Uses, Structural and Functional Variations, Approaches to Increase Yields and Products' Quality, Hepatoprotection, Liver Longevity, and Commercial Products. *International Journal of Molecular Sciences* 23(4): 2149
- Moorhead K K & Rossell I M (2019). Southern Mountain Fens. In: Messina M G & Conner W H (Eds.), *Southern Forested Wetlands*, Routledge pp. 379–403
- Panjaitan R G P, Handharyani E, Chairul & Manalu W (2013). Hepatoprotective activity of *Eurycoma longifolia* Jack. roots. *Indian Journal of Traditional Knowledge* 12(2): 225–230
- Platonova E Y, Shaposhnikov M V, Lee H Y, Lee J H, Min K J & Moskalev A (2021). Black Chokeberry (*Aronia Melanocarpa*) Extracts in Terms of Geroprotector Criteria. *Trends in Food Science & Technology* 114: 570–584
- Platosz N, Bączek N, Topolska J, Szawara-Nowak D, Skipor J, Milewski S & Wiczowski W (2021). Chokeberry Anthocyanins and Their Metabolites Ability to Cross the Blood-Cerebrospinal Fluid Barrier. *Food Chemistry* 346: 128730
- Rongen A V, Väilitalo P A J, Peeters M Y M, Boerma D, Huisman F W, Ramshorst B V, van Dongen E P A, van den Anker J N & Knibbe C A J (2016). Morbidly Obese Patients Exhibit Increased CYP2E1-Mediated Oxidation of Acetaminophen. *Clinical Pharmacokinetics* 55: 833–847
- Shahin L, Phaal S S, Vaidya B N, Brown J E & Joshee N (2019). *Aronia* (Chokeberry): An Underutilized, Highly Nutraceutical Plant. *Journal of Medicinally Active Plants* 8(4): 46–63
- Singh D, Arya P V, Aggarwal V P & Gupta R S (2014). Evaluation of antioxidant and hepatoprotective activities of *Moringa oleifera* Lam. leaves in carbon tetrachloride-intoxicated rats. *Antioxidants* 3(3): 569–591
- Singleton V L & Rossi J A (1965). Colorimetry of Total Phenolics with Phosphomolybdc-Phosphotungstic Acid Reagents. *American Journal of Enology and Viticulture* 16(3): 144–158
- Tan S A, Ramos S, Martín M A, Mateos R, Harvey M, Ramanathan S, Najimudin N, Alam M, Bravo L & Goya L (2012). Protective Effects of Papaya Extracts on Tert-Butyl Hydroperoxide Mediated Oxidative Injury to Human Liver Cells (An in-Vitro Study). *Free Radicals and Antioxidants* 2(3): 10–19
- Tolić M T, Landeka Jurčević I, Panjkota Krbavčić I, Marković K & Vahčić N (2015). Phenolic content, antioxidant capacity and quality of chokeberry (*Aronia melanocarpa*) products. *Food technology and biotechnology*, 53(2): 171–179
- Valcheva-Kuzmanova S, Borisova P, Galunska B, Krasnaliev I & Belcheva A (2004). Hepatoprotective Effect of the Natural Fruit Juice from *Aronia Melanocarpa* on Carbon Tetrachloride-Induced Acute Liver Damage in Rats. *Experimental and Toxicologic Pathology* 56(3): 195–201
- Valcheva-Kuzmanova, S., & Kuzmanov, K. (2014). Protective effect of *Aronia melanocarpa* fruit juice in a model of paracetamol-induced hepatotoxicity in rats. *Toxicological Problems*, Eds. Dishovsky C, Radenkova J, Military Publishing House, Sofia 160–166
- Vliegenthart A D B, Tucker C S, Del Pozo J & Dear J W (2014). Zebrafish as Model Organisms for Studying Drug-induced Liver Injury. *British Journal of Clinical Pharmacology* 78(6): 1217–1227
- Wang Z, Liu Y, Zhao X, Liu S, Liu Y & Wang D (2020). *Aronia Melanocarpa* Prevents Alcohol-Induced Chronic Liver Injury via Regulation of Nrf2 Signaling in C57BL/6 Mice. *Oxidative Medicine and Cellular Longevity*
- Yang C S, Brady J F & Hong J Y (1992). Dietary Effects on Cytochromes P450, Xenobiotic Metabolism, and Toxicity. *The FASEB Journal* 6(2): 737–744
- Zhang H & Tsao R (2016). Dietary Polyphenols, Oxidative Stress and Antioxidant and Anti-Inflammatory Effects. *Current Opinion in Food Science* 8: 33–42



Copyright © 2024 The Author(s). This is an open-access article published by Faculty of Agriculture, Ankara University under the terms of the [Creative Commons Attribution License](https://creativecommons.org/licenses/by/4.0/) which permits unrestricted use, distribution, and reproduction in any medium or format, provided the original work is properly cited.



Machine Learning-based for Automatic Detection of Corn-Plant Diseases Using Image Processing

Khaled Adil Dawood Idress^{a*} , Omsalma Alsadig Adam Gadalla^b , Yeşim Benal Öztekin^a ,
Geofrey Prudence Baitu^c 

^aOndokuz Mayıs University, Faculty of Agriculture, Department of Agricultural Machinery and Technologies Engineering, Samsun, TÜRKİYE

^bUniversity of Khartoum, Faculty of Agriculture, Department of Agricultural Engineering, Khartoum, SUDAN

^cUniversity of Dar es Salaam, College of Agriculture and Food Technology, Department of Agricultural Engineering, Dar es Salaam, TANZANIA

ARTICLE INFO

Research Article

Corresponding Author: Khaled Adil Dawood Idress, E-mail: adilkhaled850@gmail.com

Received: 26 April 2023 / Revised: 06 January 2024 / Accepted: 15 January 2024 / Online: 23 July 2024

Cite this article

Idress K A D, Gadalla O A A, Öztekin Y B, Baitu G P (2024). Machine Learning-based for Automatic Detection of Corn-Plant Diseases Using Image Processing. *Journal of Agricultural Sciences (Tarim Bilimleri Dergisi)*, 30(3):464-476. DOI: 10.15832/ankutbd.1288298

ABSTRACT

Corn is one of the major crops in Sudan. Disease outbreaks can significantly reduce maize production, causing huge damage. Conventionally, disease diagnosis is made through visual inspection of the damage in fields or through laboratory tests conducted by experts on the affected plant parts of the crop. This process typically requires highly skilled personnel, and it can be time-consuming to complete the necessary tasks. Machine learning methods can be implemented to rapidly and accurately detect disease and reduce the risk of crop failure due to disease outbreaks. This study aimed to use traditional machine learning techniques to detect maize diseases using image processing techniques. A

total of 600 images were obtained from the open-source Plant Village dataset for experimentation. In this study, image segmentation was done using K-means clustering, and a total of 4 GLCM texture features and two statistical features were extracted from the images. In this study, four traditional machine learning algorithms were applied to detect diseased maize leaves (common rust and gray leaf spot) and healthy maize leaves. The results showed that all the algorithms performed well in identifying the diseased and healthy leaves, with accuracy rates ranging from 90% to 92.7%. The highest accuracy scores were obtained with support vector machine and artificial neural networks, respectively.

Keywords: Maize Disease, Traditional Machine Learning, Image Processing, Feature Extraction

1. Introduction

Maize (*Zea mays* L.) is one of the most widely cultivated and consumed cereal crops worldwide, after wheat and rice, and is recognized as the "queen of cereals". It holds significant economic importance for resource-limited farmers in developing countries. Maize is not only utilized as a primary food source but also for industrial purposes, including biofuel production, starch, and oil extraction. Unfortunately, like other crops, plant diseases are a significant challenge that farmers face worldwide. Maize diseases occur yearly and significantly impede maize production (Subramanian et al. 2022). The diseases affecting maize crops have the potential to cause varying degrees of harm, from moderate to severe, to the overall production of the crop. Reports indicate that the annual damage caused by pathogenic diseases alone ranges from 4% to 14% of total maize production (Oerke & Dehne 2004). During its growth, maize leaves are exposed to several disease risks such as grey leaf spot, blight, and common rust. Early detection and management of these diseases are essential for maintaining the health of the maize crop and ensuring optimum yield. In order to manage diseases effectively, it is crucial to accurately diagnose and identify them before implementing any control measures. Conventionally, disease diagnosis is made through visual inspection of the damage in fields or through laboratory tests conducted by experts on the affected plant parts of the crop (Donatelli et al. 2017). Despite their effectiveness, the traditional approaches to disease diagnosis have some inherent limitations, which can make them impractical in some situations. These methods typically require highly skilled personnel and it can be time-consuming to complete the necessary tasks.

The most promising strategy for overcoming the limitations of traditional disease diagnosis methods and increasing production seems to be the development of automated systems based on computer vision (Subramanian et al. 2022). The progress made in artificial intelligence (AI) techniques has led to the development of highly advanced computerized systems that can accurately identify diseases (Jiang et al. 2017). Two classification techniques, machine learning (ML) and deep learning (DL), are used for categorizing crop leaf diseases. The key distinction between traditional machine learning and deep learning lies in how features are extracted. In traditional ML, features aren't automatically extracted, while in DL, feature extraction happens

automatically and is regarded as learning weights. Hence, in DL, the system learns the required features autonomously by being exposed to adequate data (Vasavi et al. 2022). The use of machine learning-based AI applications has experienced significant growth in recent times, aided by the development of computational systems, particularly processors with embedded graphical processing units (GPUs). Leaf diseases can be precisely identified and categorized by utilizing digital image processing approaches, support vector machine (SVM), neural networks, and other techniques (Zhang et al. 2018). Panigrahi et al. (2020) employed supervised machine learning methodologies such as Naive Bayes (NB), Decision Tree (DT), K-Nearest Neighbor (KNN), Support Vector Machine (SVM), and Random Forest (RF) to detect maize plant diseases, encompassing northern leaf blight, Common rust, and *Cercospora* leaf spot. The aforesaid classification techniques were analyzed and compared in order to select the most suitable model with the highest accuracy for plant disease prediction. Classification accuracies of 77.56%, 77.46%, 76.16%, 74.35%, and 79.23% were achieved using SVM, NB, KNN, DT, and RF, respectively. Padol & Yadav (2016) used a Linear Support Vector Machine classification approach to identify various types of diseases in grape leaves. They applied pre-processing techniques to the grape leaf images and employed K-means clustering to detect the affected regions. They extracted color and texture features from these regions. SVM yielded better results, with an accuracy of 93.33%, compared to an accuracy of 83.33% achieved with powdery class grape leaf images. Singh et al. (2015) introduced an automatic leaf disease detection method using genetic algorithms. The proposed approach involves pre-processing the input image using image processing techniques and segmenting it using genetic algorithms for disease classification. To enhance the recognition rate in the classification process, the authors suggest utilizing Artificial Neural Networks (ANN), fuzzy logic, and hybrid algorithms. They proposed that these techniques will be effective in improving the accuracy of the classification process. Linear SVM, medium tree, quadratic SVM, and cubic SVM were employed to identify diseases in maize leaves. The model was initially trained using labeled image data, and the classification model with the highest accuracy rate was chosen to test new image data for disease detection. After testing, quadratic SVM performed best in detecting maize disease, with an accuracy rate of 83.3% (Chokey & Jain 2019). Mukhopadhyay et al. (2021) demonstrated a method for classifying diseases on tea plant leaves. Their approach involved using a non-dominated sorting genetic algorithm (NSGA-II) based on image segmentation to identify the infected regions on tea leaves. Principal Component Analysis (PCA) and multi-class (SVM) were then applied to classify and detect disease in the tea leaves, respectively. The results showed that this algorithm was able to accurately identify the type of disease present in tea leaves, with an average accuracy of 83%. Ramakrishnan & Sahaya (2015) created a method for classifying diseases on groundnut leaves by utilizing the backpropagation algorithm. Mokhtar et al. (2015) utilized gray-level co-occurrence matrix (GLCM) texture features to differentiate between healthy and contaminated tomato leaves and classify their respective status. They applied the SVM algorithm along with established kernel functions for the classification process. Their dataset encompassed 800 samples, consisting of both healthy and diseased tomato leaves. To assess the effectiveness of their approach, they employed N-fold cross-validation, achieving impressive classification accuracy of 99.83%. Ramesh & Vydeki (2019) proposed a machine learning-based classification method employing KNN and ANN. They extracted statistical features such as mean and standard deviation and GLCM texture features to detect blast disease in Indian rice. Their experimentation led to 63% and 88% test accuracies for normal images using the KNN and ANN algorithms, respectively. Moreover, for blast-affected images, test accuracies were 79% with KNN and 90% with ANN algorithms, respectively. In another study SVM and a convolutional neural network (CNN) were used to detect and categorize various plant diseases. Data was sourced from the "new plant diseases dataset" on Kaggle, which includes a collection of more than 12,949 images displaying both healthy and unhealthy crop leaves. Initially, the diseased segment of the leaf was isolated from the image, and diverse features were extracted using a GLCM. This segmented portion is then identified using SVM, achieving an accuracy of 80%. In order to enhance accuracy further, they employed CNN for the identification of plant diseases, which notably improved performance, achieving an accuracy rate of 97.71% (Fulari et al. 2020).

In the literature, many studies have used deep-learning models to detect maize diseases. Waheed et al. (2020) introduced an optimized DenseNet architecture and conducted training on several models, including VGGNet, XceptionNet, EfficientNet, and NASNet, to identify and classify maize leaf diseases. Their study demonstrated that the proposed CNN architecture possessed fewer parameters, making it computationally efficient compared to other architectures. The accuracy achieved by the model proposed in their work stands at an impressive 98.06%. Subramanian et al. (2022) utilized pre-trained models, including VGG16, ResNet50, InceptionV3, and Xception, to classify three common maize leaf diseases using a dataset comprising 18 888 images of healthy and diseased leaves. Their methodology involved employing Bayesian optimization for hyperparameter tuning and implementing image augmentation techniques to enhance the models' ability to generalize. The study conducted a comparative analysis of the proposed models. The results revealed that all the trained models showcased an accuracy exceeding 93% in accurately classifying maize leaf diseases. Notably, VGG16, InceptionV3, and Xception stood out by achieving exceptional accuracy rates, surpassing 99% in their classification performance for these diseases. (Yang et al. 2023) proposed an adversarial training collaborating multi-path context feature aggregation network for maize disease density prediction. Their study focused on utilizing adversarial training to address issues related to network overfitting, thereby enhancing the robustness and generalization capabilities of the model. They conducted both quantitative analysis and interpretability analysis using the Plant Village dataset. The outcomes of their research demonstrated exceptional results with high-quality performance metrics. Specifically, their model achieved impressive recognition accuracies of 98.4%, 99.60%, 98.62%, and 99.80% for classifying leaf blight, gray leaf, healthy leaf, and leaf rust images, respectively. This signifies the effectiveness and accuracy of their approach in predicting maize disease densities across various categories within the dataset. Xu et al. (2021) introduced a multiscale convolutional global pooling neural network to enhance the accuracy of identifying maize diseases. By employing transfer learning techniques, they addressed the challenge of limited sample data leading to overfitting. The experimental results revealed

notable classification accuracies using different models: 86.17% for VGGNet-16, 88.8% for DenseNet, 90.48% for ResNet, 90.86% for AlexNet, and 93.28% for TCI-ALEXN. Their findings suggest that the proposed model exhibited superior performance compared to conventional convolutional neural network models like VGGNet-16, DenseNet, ResNet-50, and AlexNet in terms of recognition accuracy, signifying its efficacy in accurately identifying maize diseases. A new method was introduced to predict the severity of maize common rust disease using CNN deep learning models. The approach involved using threshold-segmentation on images of infected maize leaves to calculate the percentage of affected leaf area. This information was used to create fuzzy decision rules for categorizing the disease into four severity classes. A VGG-16 network was trained using these severity classes to automatically classify test images of common rust disease. The VGG-16 network achieved high validation accuracy (95.63%) and testing accuracy (89%) when tested on images categorized into early stage, middle stage, late stage, and healthy based on the proposed approach (Sibiya & Sumbwanyambe 2021). A proposed novel 15-layer deep convolutional neural network model was developed to distinguish images of three maize crop diseases - grey leaf spot (GLS), common rust (CR), and northern corn leaf blight (NCLB) - in addition to healthy images. The researchers utilized the maize dataset available in the Plant Village data repository for training, validation, and testing of their model. Their model was trained using 90% (1,376 images) of the dataset and then evaluated with the remaining 10% of the data. The experimental outcomes demonstrated strong performance in categorizing previously unseen maize images. The proposed model achieved an impressive overall classification accuracy of 99.10%, along with an F1-score of 97.49% on the testing set of the maize dataset (Haque et al. 2023). CNN was utilized for the automated detection of maize leaf diseases, trained on the Plant Village maize crop dataset. Various preprocessing techniques were applied to the dataset, and the efficiency of different model configurations was assessed based on metrics like accuracy, recall, precision, and F1 score. The proposed CNN model achieved a high accuracy of 96.76% by employing contrast limiting adaptive histogram equalization (CLAHE) on each RGB channel, subsequently converting the enhanced image into hue, saturation, value (HSV) color space (Jasrotia et al. 2023). From previous studies, we have noticed that using deep learning models to detect healthy and diseased maize leaves achieved very high accuracy, ranging from 79.74% to 99.84%. However, because of requiring a large amount of data, instead of just focusing on one approach, we focused on improving the accuracy of existing traditional machine learning methods to classify diseased and healthy maize leaves.

Plant diseases, such as grey leaf spot and common rust, can cause significant damage to corn crops, resulting in reduced yield and economic losses for farmers. Traditional methods for disease detection require trained professionals and can be time-consuming and expensive. In contrast, automated disease detection using machine learning-based techniques can provide a more efficient and cost-effective solution to this problem. Previous studies have used various image-processing techniques to detect plant diseases, including color, shape, and texture feature extraction, and classification algorithms. However, the proposed study differs from previous research in several ways. Firstly, statistical features such as mean and standard deviation were used, in addition to GLCM texture features, to improve the accuracy of the detection system. Secondly, a gap was noted in prior research; only two studies concentrated on utilizing GLCM texture features and statistical features for distinguishing between tomato and Indian rice leaves, with no studies conducted about classifying maize leaves.

The proposed study is needed to address the limitations of previous research and provide a more robust and accurate solution for automated plant disease detection. The study has the potential to benefit farmers and agricultural industries by enabling early detection and prevention of plant diseases, which can help to reduce crop losses and increase food security.

This study aims to evaluate the performance of various machine learning algorithms, including SVM, DT, RF, and ANN in detecting diseased maize leaves (common rust and gray leaf spot), as well as healthy maize leaves. MATLAB was employed to segment the images, extract the features, and perform the classification.

2. Material and Methods

2.1 Image acquisition

Image detection research requires a suitable dataset at every step, from training to evaluating the algorithms. A total of 600 images were obtained from the open-source Plant Village dataset (<https://github.com/spMohanty/PlantVillage-Dataset>) for experimentation. The images were divided into three categories, with two being diseased and one being healthy. The categories included 200 images each of healthy maize leaves, grey leaf spot, and common rust. Example images of disease symptoms for each class are presented in Figures 1, 2, and 3.



Figure1- Samples in healthy condition



Figure 2- Samples of leaves with common rust

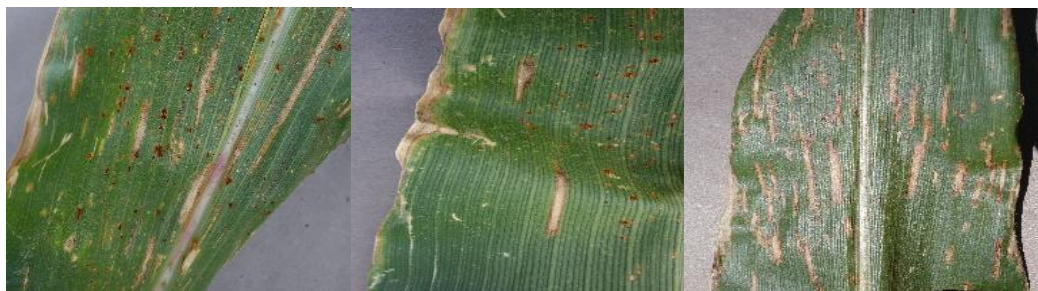


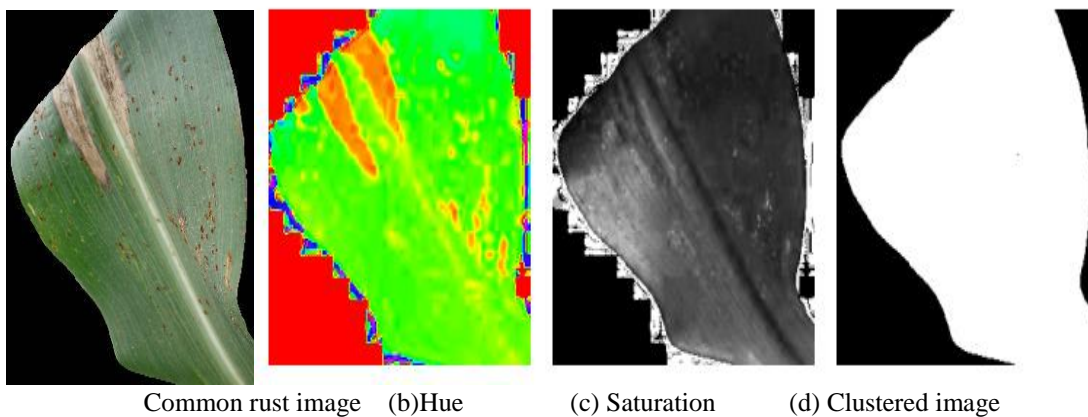
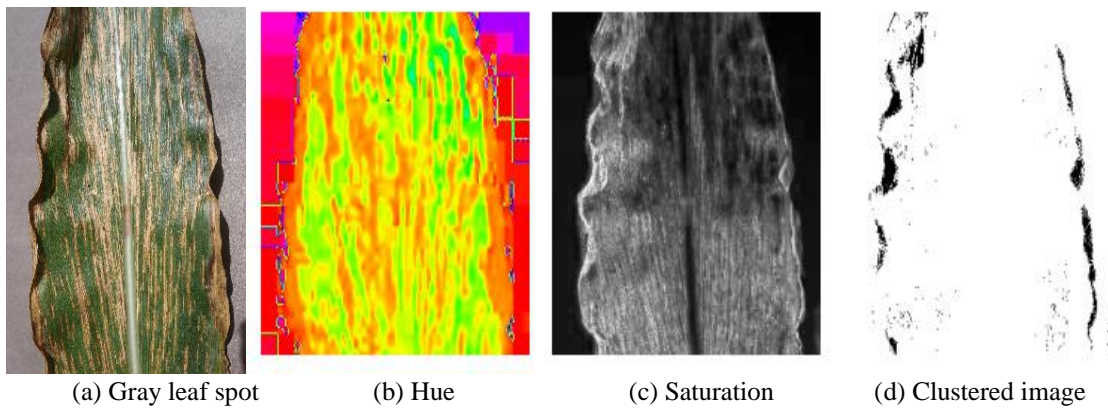
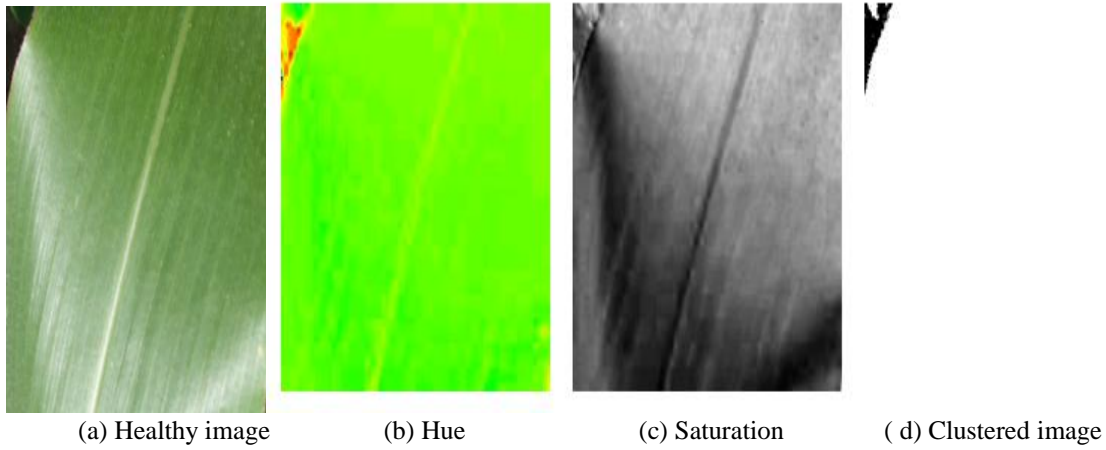
Figure 3- Samples of leaves with gray leaf spot

2.2 Image processing

The color of the leaves can indicate the overall health of a maize plant. Diseased plants often have leaves that turn yellow or brown or have spots or decaying areas. The goal is to gather this information from image data. In feature extraction, the aim is to obtain features that differentiate well in the feature space, have a low number of dimensions, and are resilient to data variability. Red-green-blue (RGB) features extract color information and are widely used for image processing and recognition. RGB is particularly useful for object detection in images that display significant color changes. For object detection in an image with significant color changes, it is recommended to use RGB as the color format. The values of RGB range from 1 to 255.

2.3 Image segmentation

K-means clustering, which is a computer vision approach for dividing an image into multiple segments or clusters based on the distribution of color and intensity among its pixels, was used in this study for image segmentation. Following the pre-processing of images, different K values were used for image segmentation with K-means clustering. According to experimental findings, K=3 produced a clearer and more precise image (Dhingra et al. 2019). Figure (a-d) shows the original images (healthy and infected images), hue, saturation, and K-means clustered images. In this study, the image was converted from RGB to gray-level color space. Then, the images were resized to 400 pixels, and finally, the images were clustered using K-means clustering.



2.4 Feature extraction

In this study, disease infection was detected using segmented images to extract various features. Statistical features such as mean and standard deviation were extracted along with GLCM texture features. The gray level co-occurrence matrix was utilized for the GLCM texture feature to identify the region affected by the disease. The study established the relationships between the features extracted with the GLCM algorithm for both the affected and normal regions. Furthermore, the average color value of the image was computed using the following equation.

1. Mean

$$\text{Mean} = E_i = \sum_{j=1}^N p_{ij}$$

Where; E_i , represents the mean of the dataset: N is the number of values in the dataset and \sum , denotes the summation of all values in the dataset: $P(i,j)$, denotes the probability of co-occurrence of pixel values i and j at a particular offset within the GLCM.

2. Standard Deviation

$$S.D. = \sqrt{\frac{1}{N} \sum_{j=1}^N (P_{ij} - E_i)^2}$$

Where; $S.D$, represents the standard deviation: N is the number of values in the dataset: \sum , denotes the summation of squared differences between each value P_{ij} and (E_i) is the mean.

3. Energy

$$\text{Energy} = \sum_{(i,j=0)}^{(N-1)} (P_{ij})^2$$

Where; $P(i,j)$, denotes the probability of co-occurrence of pixel values i and j at a particular offset within the GLCM. Energy represents the sum of squared elements in the GLCM.

4. Homogeneity

$$\text{Homogeneity} = \sum_{i,j=0}^{N-1} \frac{P_{ij}}{1 + (i - j)^2}$$

Where; $|i-j|$, represents the absolute difference between i and j .

5. Contrast

$$\text{Contrast} = \sum_{i,j=0}^{N-1} P_{ij}(i - j)^2$$

Where; $P(i,j)$, represents the probability of co-occurrence of pixel values i and j in the GLCM, and i and j are the gray levels.

6. Correlation

$$\text{Correlation} = \sum_{i,j=0}^{N-1} \frac{P_{ij} (i-\mu)(i-\mu)}{\sigma^2}$$

Where; $P(i,j)$, represents the probability of co-occurrence of pixel values i and j in GLCM: μ , denotes is the mean of GLCM, and σ is the standard deviation of GLCM.

2.5 Performance evaluation

The confusion matrix and area under the receiver operating characteristic (ROC) curve are two commonly used metrics for evaluating the performance of binary classification models. The confusion matrix provides detailed information about the model's predicted and actual classes, while the ROC curve provides a visual representation of the model's trade-off between sensitivity and specificity at different classification thresholds.

The confusion matrix consists of four values: true positives (TP), false positives (FP), true negatives (TN), and false negatives (FN). These values can be used to calculate various performance metrics, such as accuracy, precision, recall, and F1-score. The confusion matrix is beneficial for identifying which types of errors the model is making.

The ROC curve plots the true positive rate (TPR) against the false positive rate (FPR) at different classification thresholds. The TPR is the ratio of correctly predicted positive examples to the total number of positive examples, while the FPR is the ratio of incorrectly predicted positive examples to the total number of negative examples. The area under the curve (AUC) is a scalar value that summarizes the performance of a model across all possible classification thresholds. AUC represents the probability

that a randomly chosen positive example will be ranked higher than a randomly chosen negative example by the model. A perfect model would have an AUC of 1.0, while a completely random model would have an AUC of 0.5. The AUC metric has several advantages over other classification performance metrics, such as accuracy, precision, and recall. One advantage is that it is insensitive to class imbalance, which is a common problem in many real-world classification problems. Additionally, the AUC metric provides a single scalar value that summarizes the overall performance of a model, making it easy to compare different models or different settings of a single model (Géron 2019).

Using both the confusion matrix and ROC curve together provides a comprehensive evaluation of the model's performance. The confusion matrix provides detailed information on the model's errors, while the ROC curve provides a visual representation of the model's performance at different classification thresholds. AUC provides a single scalar value that summarizes the overall performance of the model.

3. Results and Discussion

The study collected a dataset of 600 images from the Plant Village dataset, which were categorized into three classes: healthy maize leaves (200 images), grey leaf spot (200 images), and common rust (200 images). K-means clustering was employed for image segmentation, and statistical features such as mean and standard deviation, along with GLCM texture features, were extracted after the segmentation process. The dataset was split into 75% for training and 25% for testing. Four conventional ML algorithms, DT, SVM, KNN, and ANN models, were employed to train and test the images. The algorithms performed well in classifying the diseased and healthy maize leaves, with accuracy rates ranging from 90% to 92.7%. SVM and ANN achieved the highest accuracy scores among the tested algorithms.

3.1 Decision tree classifier

A DT classifier is a type of machine learning algorithm that can be used for classification problems like classifying diseased and healthy maize leaves. The algorithm works by dividing the data into smaller subsets based on certain attributes and making decisions about the class label of each record based on the values of these attributes. The DT classifier was able to achieve an accuracy of 90% in the test dataset. Using decision tree models to classify common rust, gray leaf spot and healthy maize leaves can be a highly effective approach in the field of plant pathology. The high accuracy of 90% achieved in this study suggests that the decision tree model was able to distinguish between the three different categories of maize leaves accurately. The confusion matrix and ROC curve for the DT classifier are shown in Figures 3 and 4.

True Class	Common rust	48	1	1
	Gray leaf spot	1	45	4
	Healthy	1	7	42
		Common rust	Gray leaf spot	Healthy
		Predicted Class		

Figure 3- Decision Tree confusion matrix

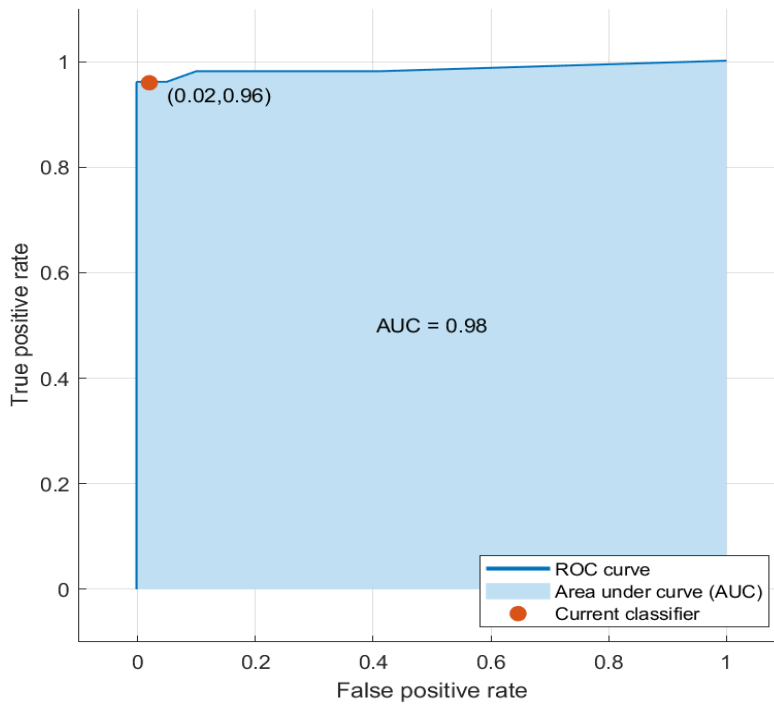


Figure 4- ROC curve for Decision Tree model

3.2. Support vector machine classifier

SVM is a popular machine learning algorithm that is used for classification problems. In the context of classifying maize leaves into common rust, gray spot, and healthy, SVM can be a viable solution. In this experiment, an SVM classifier was used to classify diseased maize leaves (common rust, gray leaf spot), and healthy maize leaves. The dataset was divided into a training and testing set, with the training set being used to train the model and the test set used to evaluate its accuracy. The results of the model show that it had 91.3% accuracy rate on the test dataset, indicating that it was able to classify diseased and healthy leaves correctly with a high degree of accuracy. The confusion matrix and ROC curve for the SVM classifier are shown in Figures 5 and 6.

	Common rust	Gray leaf spot	Healthy
Common rust	48		2
Gray leaf spot		46	4
Healthy		7	43
	Common rust	Gray leaf spot	Healthy
	Predicted Class		

Figure 5- SVM confusion matrix

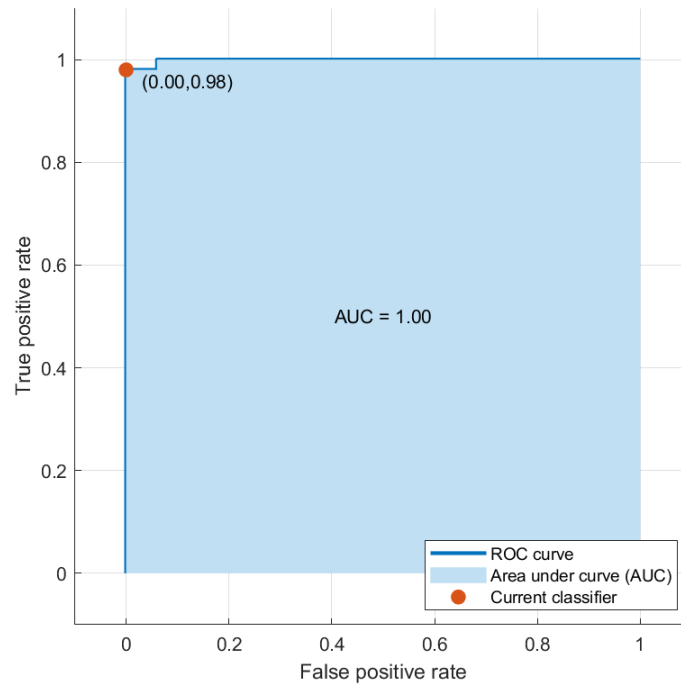


Figure 6- ROC curve for Support Vector Machine model

3.3 K- Nearest neighbor classifier

The KNN model is a machine learning algorithm that can be used to detect diseased leaves (common rust and gray leaf spot) and healthy maize leaves in images. The model works by classifying a test image based on the closest match to the images in the training dataset. The algorithm is simple and efficient, making it a popular choice for image classification tasks. To implement the KNN model for maize leaf detection, a dataset of images of diseased maize leaves and healthy images was used to train and test the model. The result showed that the KNN model was able to achieve an accuracy of 90% in the test dataset, indicating that it was able to classify diseased and healthy leaves correctly with a high degree of accuracy. The confusion matrix and ROC curve, shown in Figures 7 and 8, provide further insight into the performance of the KNN classifier.

	Common rust	Gray leaf spot	Healthy
Common rust	49	1	
Gray leaf spot		45	5
Healthy		9	41
	Common rust	Gray leaf spot	Healthy
	Predicted Class		

Figure 7- KNN confusion matrix

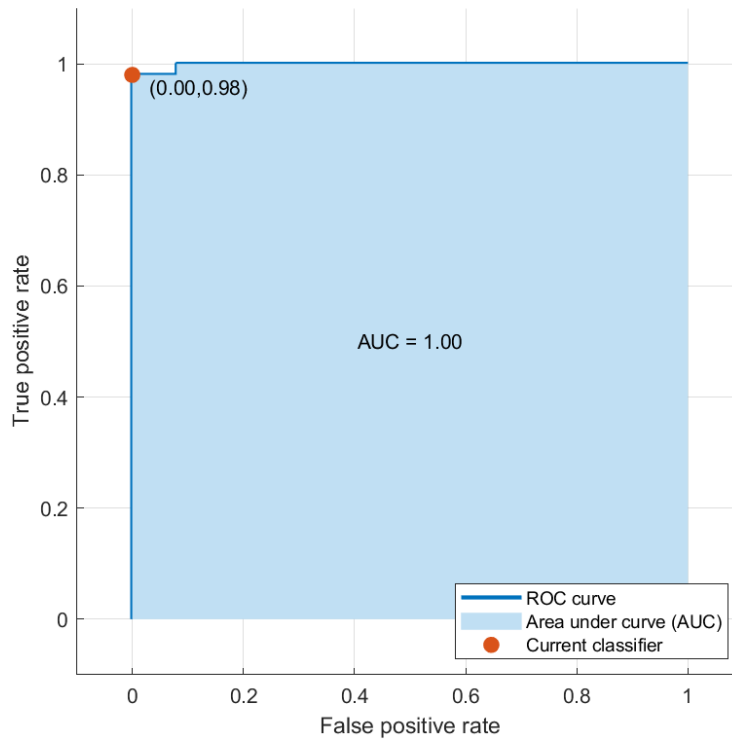


Figure 8- ROC curve for K-Nearest Neighbors model

3.4 Artificial neural network classifier

The ANN model is a machine learning technique that can be used to detect diseased leaves (common rust and gray leaf spot) and healthy maize leaves in images. The ANN model works by learning a mapping between inputs and outputs based on a training dataset. The mapping is represented by a network of interconnected nodes that process information and make predictions. The results indicated that the model achieved an accuracy rate of 92.7% for the test dataset, demonstrating its ability to accurately distinguish between healthy and diseased maize leaves. The confusion matrix and ROC curve for the ANN classifier are shown in Figures 9 and 10.

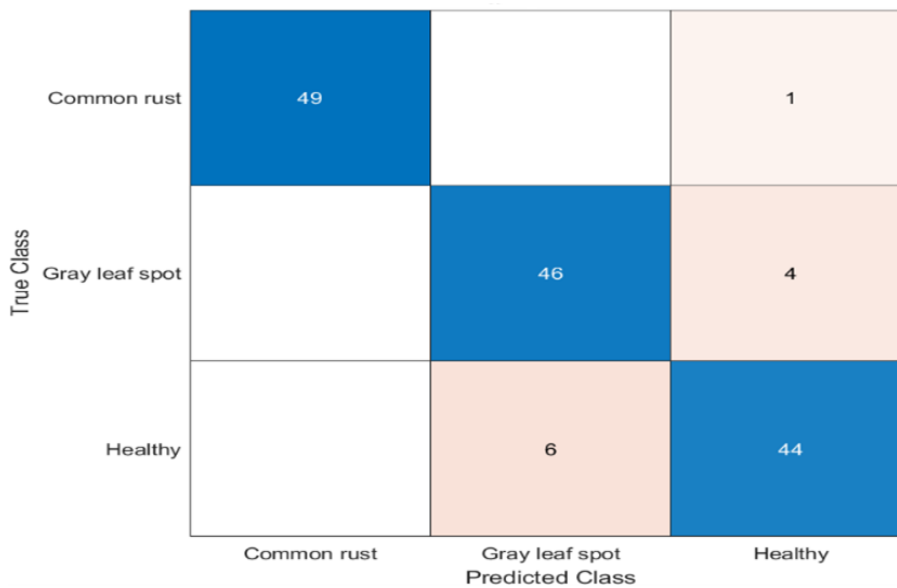


Figure 9- ANN confusion matrix

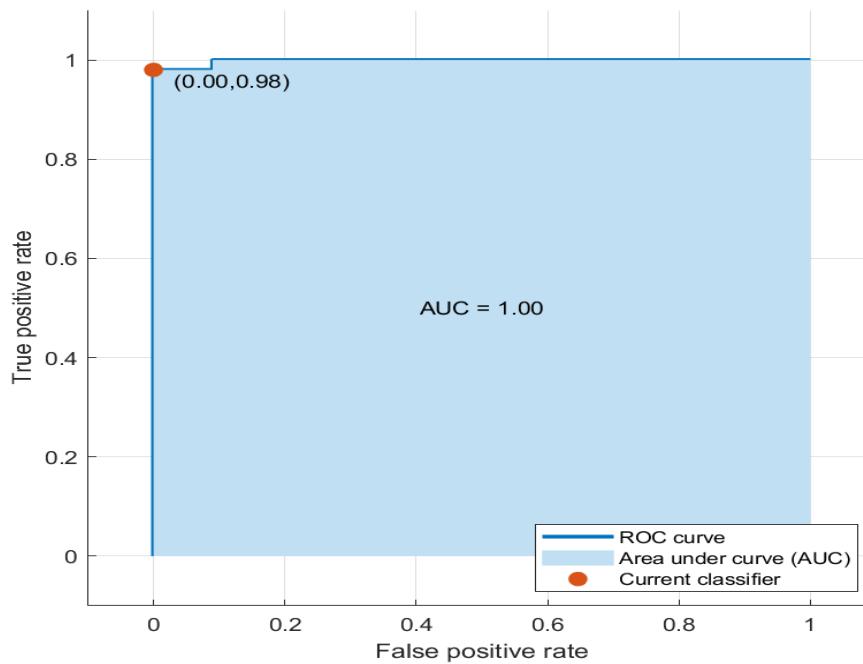


Figure 10- ROC curve for Artificial Neural Network model

4. Discussion

Many studies have been carried out to enhance the accuracy of detecting maize diseases by applying machine learning and deep learning algorithms. Table 1 presents the studies focused on classifying diseased and healthy maize, rice, grape, and tomato leaves. Table 1 also gives the diseases that were classified, the models used, and their accuracy rates.

Ramesh & Vydeki (2019) proposed a machine learning-based classification methodology that included KNN and ANN. Statistical features, including mean and standard deviation along with GLCM texture features, were extracted to detect blast disease in Indian rice. Test accuracies of 63 and 88% for normal images were achieved using KNN and ANN algorithms, respectively, and test accuracies of 79 and 90% were achieved for blast-affected images using KNN and ANN, respectively.

Table 1- Comparison of accuracy rates of classifying diseased and healthy maize, rice, grape, and tomato leaves using traditional machine learning and deep learning models

<i>Author(s)</i>	<i>Model architecture</i>	<i>Detected diseases</i>	<i>Accuracy</i>
Ramesh & Vydeki (2019)	KNN and ANN	Healthy images, blast affected images	63% and 88%. 79% and 90%.
Panigrahi et al. (2020)	SVM, NB, KNN, DT, and RF	Northern leaf blight, common rust, and Cercospora leaf spot	77.56%, 77.46%, 76.16%, 74.35%, and 79.23%.
Padol & Yadav (2016)	Linear SVM	Grape leaf images	93.33%
Chokey & Jain (2019)	Linear SVM, quadratic SVM, and cubic SVM	Common smut, common rust	79.5%, 73.1%, and 83.3%.
Mukhopadhyay et al. (2021)	SVM	Healthy or infected tomato leaves.	99.83%
Waheed et al. (2020)	XceptionNet, EfficientNet, VGG19Net, NASNet, and Optimized DenseNet	Common rust, Cercospora leaf spot, gray leaf spot, northern leaf blight, and healthy crop.	93.52%, 99.84%, 96.36%, 91.9%, and 98.06%.
Subramanian et al. (2022)	VGG16, ResNet50, InceptionV3, and Xception	Blight, common rust, grey leaf spot, healthy.	95.04%, 79.44%, 96.9%, and 95.45%.
Yang et al. (2023)	VGG11, EfficientNet, Inception-v3, MobileNet, and ResNet50. ViT, Improved ViT, and multi-path context feature aggregation network.	Leaf blight, gray leaf, healthy leaf, and leaf rust	97.9%, 91.6%, 97.2%, 90.2% and 96.6%. 93.9%, 98.7%, and 99.5%
Xu et al. (2021)	VGGNet-16, DenseNet, ResNet, AlexNet, and TCI-ALEXN.	Northern leaf blight, common rust, healthy, and gray leaf spot.	86.17, 88.8, 90.48, 90.86, and 93.28.
Our study	DT, SVM, KNN, and ANN.	Grey leaf spot, common rust, and healthy leaves.	90%, 91.3%, 90%, and 92.7%.

In this study, we focused on using traditional machine learning to detect healthy and diseased maize leaves. In our initial experiment, extracting statistical and GLCM texture features without processing resulted in a test classification accuracy ranging between 66.7% and 72.7%. Attempting to enhance the accuracy, initially color features were extracted, yet this did not yield improvement due to the close similarity in shape between the diseased classes. To address this challenge, K-means clustering was implemented to separate the diseased leaf portions. After applying K-means clustering, the test classification accuracy significantly improved from 66.7, 70.7, 70.7, and 72.7% to 90, 90, 91.3, and 92.7%, using DT, SVM, KNN, and ANN respectively.

From the previous studies presented in Table 1, few studies focused on detecting plant diseases using traditional machine learning techniques, especially extracting GLCM texture features along with statistical features. The highest accuracy (99.83%) was achieved in a study conducted by Mukhopadhyay et al. (2021) to classify healthy and infected tomato leaves. They obtained this high accuracy because they focused only on classifying tomato leaves as healthy or infected, so that the differences between these two classes were clear compared to our study, in which we focused on classifying two different diseases and healthy maize leaves. Another study was conducted by Ramesh & Vydeki (2019) to detect healthy and blast-affected images. GLCM texture features, along with statistical features, were extracted from the Indian rice images. They achieved test accuracies of 63%, 88%, 79%, and 90% for healthy and blast-affected rice images, which is less than the highest accuracy achieved in our study of 92% using the ANN model. This highlights the efficiency of our proposed traditional machine learning model in detecting different types of maize diseases effectively and with high accuracy. Also, from previous studies, the use of deep learning models to detect healthy and diseased maize leaves achieved very high accuracy, ranging from 79.74% to 99.84%, but requires a large amount of data. Instead of just focusing on one approach, it is necessary to improve the accuracy of existing traditional machine learning and see how they perform.

4. Conclusions

This study aimed to identify healthy and diseased maize leaves using traditional machine learning algorithms. For this purpose, six hundred images from the Plant Village dataset were used, which were categorized into three groups: healthy leaves (200 images), grey leaf spot (200 images), and common rust (200 images). K-means clustering was employed for image segmentation, and statistical features such as mean and standard deviation, along with GLCM texture features, were extracted after the segmentation process. Then the dataset was split into training and testing sets, where 75% of the images were used for training

and 25% for testing. Four conventional ML algorithms, DT, SVM, KNN, and ANN models, were employed to train and test the images.

The study findings showed that all four algorithms performed well in accurately detecting diseased and healthy maize leaves, with accuracy rates ranging from 90% to 92.7%. Support vector machines and artificial neural networks achieved the highest accuracy scores, which suggests that these algorithms are more effective in identifying diseased maize leaves.

References

- Chokey T & Jain S (2019). Quality Assessment of Crops using Machine Learning Techniques. *2019 Amity International Conference on Artificial Intelligence (AICAI)* pp. 259–263. <https://doi.org/10.1109/AICAI.2019.8701294>
- Dhingra G, Kumar V & Joshi H D (2019). A novel computer vision based neutrosophic approach for leaf disease identification and classification. *Measurement* 135: 782–794. <https://doi.org/10.1016/J.MEASUREMENT.2018.12.027>
- Donatelli M, Magarey R D, Bregaglio S, Willocquet L, Whish J P M & Savary S (2017). Modelling the impacts of pests and diseases on agricultural systems. *Agricultural Systems* 155: 213–224. <https://doi.org/10.1016/J.AGSY.2017.01.019>
- Fulari U, Shastri R & Fulari A (2020). Leaf Disease Detection Using Machine Learning. *Journal of Seybold Report* 15(9): 1828–1832
- Géron A (2019). *Hands-On Machine Learning with Scikit-Learn, Keras, and TensorFlow: Concepts, Tools, and Techniques to Build Intelligent Systems* (R. Roumeliotis & N. Tache, Eds.; 2nd ed.). O'Reilly Media, Inc.
- Haque M, Marwaha S, Deb C, Nigam S & Arora A (2023). Recognition of diseases of maize crop using deep learning models. *Neural Computing and Applications* 35(10): 7407–7421. <https://doi.org/10.1007/s00521-022-08003-9>
- Jasrotia S, Yadav J, Rajpal N, Arora M & Chaudhary J (2023). Convolutional Neural Network Based Maize Plant Disease Identification. *Procedia Computer Science* 218(1): 1712–1721. <https://doi.org/10.1016/J.PROCS.2023.01.149>
- Jiang F, Jiang Y, Zhi H, Dong Y, Li H, Ma S, Wang Y, Dong Q, Shen H & Wang Y (2017). Artificial intelligence in healthcare: past, present and future. *Stroke and Vascular Neurology* 2. <https://doi.org/10.1136/svn-2017-000101>
- Mokhtar U, El-Bendary N, Hassenian A, Emary E, Mahmood M, Hefny H & Tolba M (2015). SVM-Based Detection of Tomato Leaves Diseases. In D. Filev & J (Eds.), *Advances in Intelligent Systems and Computing* (Vol. 323, pp. 641–652). Springer, Cham. https://doi.org/10.1007/978-3-319-11310-4_55
- Mukhopadhyay Dr. S, Paul M, Pal R & De D (2021). Tea leaf disease detection using multi-objective image segmentation. *Multimedia Tools and Applications*, 80(1). <https://doi.org/10.1007/s11042-020-09567-1>
- Oerke E C & Dehne H W (2004). Safeguarding production—losses in major crops and the role of crop protection. *Crop Protection* 23(4): 275–285. <https://doi.org/10.1016/J.CROPRO.2003.10.001>
- Padol P B & Yadav A A (2016). SVM classifier based grape leaf disease detection. *2016 Conference on Advances in Signal Processing (CASP)* pp. 175–179. <https://doi.org/10.1109/CASP.2016.7746160>
- Panigrahi K P, Sahoo A K & Das H (2020). A CNN Approach for Corn Leaves Disease Detection to support Digital Agricultural System. *2020 4th International Conference on Trends in Electronics and Informatics (ICOEI)(48184)* pp. 678–683. <https://doi.org/10.1109/ICOEI48184.2020.9142871>
- Ramakrishnan M & Sahaya A N A (2015). Groundnut leaf disease detection and classification by using back propagation algorithm. *2015 International Conference on Communications and Signal Processing (ICCSP)* pp. 964–968. <https://doi.org/10.1109/ICCSP.2015.7322641>
- Ramesh S & Vydeki D (2019). Application of machine learning in detection of blast disease in South Indian rice crops. *Journal of Phytology* 11(1): 31–37. <https://doi.org/10.25081/jp.2019.v11.5476>
- Sibiya M & Sumbwanyambe M (2021). Automatic Fuzzy Logic-Based Maize Common Rust Disease Severity Predictions with Thresholding and Deep Learning. *Pathogens* 10(2): 131. <https://doi.org/10.3390/pathogens10020131>
- Singh V, Varsha & Misra A K (2015). Detection of unhealthy region of plant leaves using image processing and genetic algorithm. *2015 International Conference on Advances in Computer Engineering and Applications* pp. 1028–1032. <https://doi.org/10.1109/ICACEA.2015.7164858>
- Subramanian M, Shanmugavadivel K & Nandhini P S (2022). On fine-tuning deep learning models using transfer learning and hyper-parameters optimization for disease identification in maize leaves. *Neural Computing and Applications* 34: 13951–13968. <https://doi.org/10.1007/s00521-022-07246-w>
- Vasavi P, Punitha A & Rao V N T (2022). Crop leaf disease detection and classification using machine learning and deep learning algorithms by visual symptoms: A review. *International Journal of Electrical and Computer Engineering* 12(2): 2079–2086. <https://doi.org/10.11591/ijece.v12i2.pp2079-2086>
- Waheed A, Goyal M, Gupta D, Khanna A, Hassanien A E & Pandey H M (2020). An optimized dense convolutional neural network model for disease recognition and classification in corn leaf. *Computers and Electronics in Agriculture* 175(12): 105456. <https://doi.org/10.1016/j.compag.2020.105456>
- Xu Y, Zhao B, Zhai Y, Chen Q & Zhou Y (2021). Maize Diseases Identification Method Based on Multi-Scale Convolutional Global Pooling Neural Network. *IEEE Access* 9: 27959–27970. <https://doi.org/10.1109/ACCESS.2021.3058267>
- Yang W, Shen P, Ye Z, Zhu Z, Xu C, Liu Y & Mei L (2023). Adversarial Training Collaborating Multi-Path Context Feature Aggregation Network for Maize Disease Density Prediction. *Processes* 11(4): 1132. <https://doi.org/10.3390/pr11041132>
- Zhang X, Qiao Y, Meng F, Fan C & Zhang M (2018). Identification of Maize Leaf Diseases Using Improved Deep Convolutional Neural Networks. *IEEE Access* 6: 30370–30377. <https://doi.org/10.1109/ACCESS.2018.2844405>



Copyright © 2024 The Author(s). This is an open-access article published by Faculty of Agriculture, Ankara University under the terms of the [Creative Commons Attribution License](https://creativecommons.org/licenses/by/4.0/) which permits unrestricted use, distribution, and reproduction in any medium or format, provided the original work is properly cited.



Effects of 24-Epibrassinolide on Shoot Tip Cultures Under NaCl Stress in Tomato (*Solanum lycopersicum* L.)

Emel Yilmaz-Gokdogan^{a*} , Betul Burun^b 

^aMinistry of National Education, District Directorate of National Education, 48000, Mugla, TURKEY

^bMugla Sıtkı Kocman University, Faculty of Science, Department of Biology, 48000, Mugla, TURKEY

ARTICLE INFO

Research Article

Corresponding Author: Emel Yilmaz-Gokdogan, E-mail: emelyilmazgokdogan@gmail.com

Received: 28 April 2023 / Revised: 20 December 2023 / Accepted: 16 January 2024 / Online: 23 July 2024

Cite this article

Yilmaz-Gokdogan E, Burun B (2024). Effects of 24-Epibrassinolide on Shoot Tip Cultures Under NaCl Stress in Tomato (*Solanum lycopersicum* L.). *Journal of Agricultural Sciences (Tarim Bilimleri Dergisi)*, 30(3):477-487. DOI: 10.15832/ankutbd.1289108

ABSTRACT

The negative effects of salt stress on plants and their environment are increasing dramatically day by day, and it is crucial for plants to develop salt tolerance with various applications and biotechnological approaches. For this purpose, it is possible to improve salt tolerance in plants through different studies using controlled and uniform *in vitro* cultures, which are an alternative approach to greenhouse and pot experiments that affected by external environmental conditions. In this study, 24-epibrassinolide (24-epiBL) was used for increasing salt tolerance in *in vitro* shoot tip cultures of tomato M-28 hybrid cultivar. Shoot tips of 10-day sterile seedlings were placed in MS medium supplemented with 2 mg L⁻¹ K + 0.4 mg L⁻¹ NAA in a 12-day culture period, and 12-day plantlets soaked in 24-epiBL solutions (0, 1, 2 μM) were transferred to MS medium containing different concentrations of NaCl (0, 20, 40, 60, 80, 100 mM). After 20 days, the plantlets derived from *in vitro* cultures were used to

assess growth (length, fresh and dry weight of plantlets) and biochemical parameters (pigment, MDA, proline, total soluble protein contents, POX and SOD enzyme activities). All growth and biochemical parameters, including pigment and total soluble protein content, were adversely impacted by salt stress (particularly at 40, 60, 80, and 100 Mm NaCl concentrations). However, MDA, proline content, as well as SOD and POX enzyme activity, increased as a results of oxidative stress at the same NaCl concentrations. As a result, NaCl responses in plant differed between various NaCl and 24-epiBL concentrations, and the different defense strategies combine multiple tolerance mechanisms. Therefore, this study, indicates that pretreatment of 24-epiBL to plantlets derived from shoot tips of the tomato M-28 hybrid cultivar played crucial role in mitigating the effects of salt stress.

Keywords: Antioxidant enzymes, 24-epibrassinolide, *In vitro* culture, Proline, Salt tolerance, Tomato

1. Introduction

Salt stress in arid and semi-arid areas is one of the most important environmental problems that can majorly limits plant productivity in our country and around the world (Osman et al. 2011; Sriniegn et al. 2015). Therefore, the salinity of soils on irrigated lands decreases agricultural production, directly causing economic losses (Cristea et al. 2020; El-Sayed 2021). Salinity has impacted more than one-third of irrigated areas, and it estimated that approximately half of the world's cultivated land will be salinized by 2050 (Guo et al. 2022). Thus, soil salinity is a major abiotic constraint to crop yield and sustainable agricultural productivity (Ahmad et al. 2018).

Salinity negatively impresses plant growth by disturbing water balance, specific ion toxicity, creating an imbalance in plant nutrition, and combinations of these factors, and affecting plant physiological and biochemical processes (Loganayaki et al. 2020). Ionic effects related to NaCl stress induce damages of macromolecules and compartments of the cells such as cell membrane, cell wall, lipits, proteins, and nucleic acids as a result of nutritional disorders in leaves and meristems (Aly et al. 2012). In relation to ionic stress, the carbohydrate and protein levels vary among plants that are affected by salt stress. Additionally, proline has osmoregulatory properties and interacts with salt, drought and other stress factors (Abdel-Farid et al. 2020). The osmotic stress decreases cell expansion in the growing tissues of young plants, and also leads to stomatal closure, which helps to minimize water loss and plant damage (Rivera et al. 2022). Therefore, plants must cope with ionic and osmotic stress caused by salt stress, and plant responses must be formed against these secondary stresses. The response to ionic stress is slow, and Na⁺ is either excluded from the cell or compartmentalized within the cell. A rapid response is given to osmotic stress, and external osmotic pressure is increased (Sané et al. 2021).

NaCl, which has the ability to compete with the basic ions effective in plant development and leads to the inability of plants to benefit from nutrients, shows its destructive effect as the most vital factor of salt stress, with excessive production of Reactive

Oxygen Species (ROS) (Aazami et al. 2021). The production of ROS occurs at low concentrations in chloroplast, mitochondrion and peroxisome under unstressed conditions and increases under salt stress (Ashraf 2009). ROS such as superoxide, hydrogen peroxide, hydroxyl, singlet oxygen are free radicals that highly reactive in cells (Mudgal et al. 2010). ROS can be considered both a cellular signal of different stresses and a secondary messenger involved in complex signaling pathways of stress responses (Aazami et al. 2021). Plants have non-enzymatic and enzymatic defense systems against ROS that cause damage of biomolecules e.g. proteins, lipids and nucleic acids (Koca et al. 2007). Non-enzymatic antioxidants include ascorbic acid, glutathione, proline, carotenoids, flavonoids, and tocopherol and these antioxidants play a significant role in ROS detoxification and retrograde signaling (Guo et al. 2022). It was reported that the activities of enzymatic antioxidants such catalase (CAT), superoxide dismutase (SOD), peroxidase (POX) and glutathione reductase (GR) generally increased under different abiotic stress conditions (Sairam & Tyagi 2004).

It is accepted that salt tolerance of plants is their ability to accomplish their lives on soil that has high concentrations of soluble NaCl salt (Parida & Das 2005). Salt tolerance differs depending on the genotype of plants, and it is provided via changes in physiological and metabolic events such as uptake, transport, and exclusion of salt by the roots at the cellular level (Osman et al. 2011). Tomato is considered as moderately tolerant plant to salinity, and wild tomato species exhibit higher salt tolerance than cultivated tomato (Szczepaniak & Kulpa 2012). On the other hand, the responses to salinity is variable depending upon different tomato lines or cultivars commonly used in agriculture (Zaki & Yokoi 2016). Since different environmental conditions such as temperature, light intensity, humidity and climatic factors affect the response of tomato plants to salt stress, it is important to create and maintain controlled and uniform *in vitro* conditions with reliable experimental data to respond to salt stress (Khaliluev et al. 2022). Different *in vitro* culture techniques using seeds, cotyledons and hypocotyl explants were tested on tomato M-28 hybrid cultivar under salt stress conditions (Yilmaz-Gokdogan & Burun 2015; Yilmaz-Gokdogan & Burun 2017). *In vitro* shoot tip analyses of tomato seedlings at early first-true-leaf stage is frequently used to test for salt tolerance because of high genetic stability (Cano et al. 1998; Shibli et al. 2007). Shoot tip cultures comprison to seed, cell suspension, or callus cultures can be easily propogated *in vitro* and show the nearest stress responses to the whole plant under NaCl conditions (Lokhande et al. 2011).

The use of various biomolecules has been mentioned for the improvement of salt tolerance against the destructive effects of salt stress. Brassinosteroids (BRs), as one of these biomolecules that has antistress characteristic, structurally look like animal steroidal hormones, and promote growth in plants, are new phytohormones classes (Anwar et al. 2018). BRs, when exogenously applied in micro-level (micromolar and nanomolar) concentrations, affect many developmental processes in plants (Singh et al. 2021). It is revealed that BRs lead to distinct cell responses such as stem elongation, root and leaf development, leaf bending and epinasty, formation and development of the pollen tube, reproductive development, xylem differentiation, proton-pump activation, and regulation of gene expression (Yang et al. 2011; Ahmad et al. 2018). In addition to their roles in the development of plants, BRs confer stress tolerance on plants against different abiotic stresses such as salt, heat, cold, drought, and heavy metals (Surgun et al. 2012).

The present study was aimed to determine effects of short term exogeneous 24-epibrassinolide (24-epiBL) pretreatment against salt stress with physiological and biochemical parameters using *in vitro* shoot tip cultures in the tomato M-28 hybrid cultivar.

2. Material and Methods

2.1. Plant materials and *in vitro* culture

Seeds of tomato M-28 hybrid cultivar were obtained from Agrotek Seed Agriculture Industry and Commercial Limited Company, Antalya, Turkey. Seeds were sterilized with 50% dilute sodium hypochlorite (2.25% NaOCl) for 5 min, and then they were thoroughly washed with sterile deionized water three times (Yilmaz-Gokdogan & Burun 2017). Surface sterilized seeds were cultured on ½ Murashige-Skoog (½ MS) (1962) media containing 20 g L⁻¹ sucrose and 7 g L⁻¹ agar for germination (Murashige & Skoog 1962). *In vitro* shoot tips (5 mm) of 10-day sterile seedlings with a germination rate of 95% were transferred to MS medium supplemented with 2 mg L⁻¹ Kinetin (K) + 0.4 mg L⁻¹ Naphthalene Acetic Acid (NAA) for the production of the healthy plantlets (Yilmaz & Burun 2014). Plantlets derived from 12-day *in vitro* cultures soaked in 24-epiBL (0, 1, 2 μM) solutions that prepared by 70% acetone for 40 seconds, and then the plantlets were transferred to MS medium containing different NaCl concentrations (0, 20, 40, 60, 80, 100 mM) for 20 days. Cultures were maintained in culture room at temperature of 25 ± 2 °C with 16/8 hours light/dark photoperiod using cool white florescent tubes (~45 μmol m⁻² s⁻¹).

2.2. Determination of growth parameters

The lengths, fresh weight (FW), and dry weight (DW) of shoots and/or roots in randomly sampled plantlets were measured, and plant samples (shoots and/or roots) for dry weight determination were recorded after being oven dried at 70 °C for 48 hours.

2.3. Determination of biochemical parameters

2.3.1. Pigment content

The pigment content (chlorophyll a, chlorophyll b, total chlorophyll, and carotenoid) of 24-epiBL non-pretreated and pretreated plantlets was extracted from fresh leaf tissue (0.05 g) by acetone (80%) and determined by a spectrophotometer following the procedure reported by Strain & Svec (1966).

2.3.2. Malondialdehyde (MDA) content

MDA content for the determination of lipid peroxidation level in cell membrane was determined using the thiobarbituric acid reaction according to Heath & Packer (1968). The leaves of plantlets (0.5 g) were homogenised in 3 ml of trichloroacetic acid (TCA), (0.1%). TCA (20%) + thiobarbituric acid (TBA), (0.5%) mixture was added to the supernatant after centrifuging at $13\,000 \times g$ for 10 min at room temperature and the mixture was incubated at 95 °C in water bath for 30 min. The reaction stopped on an ice bath and the MDA concentration was calculated using the absorbance at 532 and 600 nm by spectrophotometer. The extinction coefficient (155 mM cm^{-1}) was used for the calculation of MDA concentration.

2.3.3. Proline content

For determination of proline content, the leaves of 24-epiBL pretreated plantlets under NaCl stress were extracted using the ninhydrin reagent according to Bates et al. (1973). The leaves of plantlets (0.5 g) were extracted with 10 ml aqueous sulfosalicylic acid (3%), and then samples were filtered through Whatmann (No. 2), 110 diameter filter paper. 1:1:1 solution of homogenate, ninhydrin reagent, and glacial acetic acid was incubated at 100 °C for 1 hour for colorimetric determinations of proline. The reaction in the tubes was stopped in an iced bath and the absorbance of the fraction aspirated with toluene from the liquid phase was read at 520 nm with a spectrometer. Proline content ($\mu\text{mol proline g}^{-1}\text{ FW}$) was calculated using a standard calibration curve.

2.3.4. Total soluble protein content

Total soluble protein content was determined by the Bradford (1976) method using known concentrations of bovine serum albumin as a standard curve. The leaves of plantlets (0.5 g) obtained *in vitro* culture were homogenized in sodium phosphate buffer (5 mL, 0.05 M Na-P buffer, pH: 7). The extraction process was carried out at 0-4 °C. The absorbance was read at 595 nm with a spectrophotometer after the homogenate was centrifuged at $13\,000 \times g$ for 15 min at 4 °C.

2.3.5. SOD and POX enzymes activity

SOD (E.C. 1.15.1.1) activity was measured using the method described by Beauchamp & Fridovich (1971). The leaves of plantlets (0.5 g) were homogenized in Na-P buffer solution (0.05 M pH: 7.8), and then the homogenate was centrifuged at $13\,000 \times g$ for 15 min at 4 °C. The supernatant was used for determining SOD activity, and the test tubes containing the reaction mixture (3 mL), were kept under white light intensity at $500\ \mu\text{E m}^{-2}\text{ s}^{-1}$ for 10 min. One unit of SOD activity was determined as the enzyme amount that inhibited 50% of NBT photoreduction at 560 nm wavelength and was expressed as unit SOD mg^{-1} protein.

POX (E.C. 1.11.1.7) was measured according to Chance & Maehly (1955) using guaiacol oxidation. The leaf samples of plantlets (0.5 g) were homogenized in Na-P buffer solution (0.05 M pH: 6.0), and the homogenate was centrifuged at $13\,000 \times g$ for 15 min at 4 °C. After the addition of H_2O_2 to the reaction mixture, an increase in absorbance was recorded every 30 seconds at 470 nm, and POX enzyme activity was calculated as $\Delta\text{A}470\ \text{min}^{-1}\ \text{mg}^{-1}$ protein.

2.4. Experimental design and statistical analysis

The study was set up based on a completely randomized design with a factorial arrangement in two replicates, and 15 shoot tip explants were used in each replication. The statistical analysis was subjected to one-way analysis of variance (ANOVA) using the Statistica 7 program. Data was presented as means \pm standart errors, and means were compared by Tukey's HSD (Honestly Significant Differences) test, and differences with P values ≤ 0.05 were considered statistically significant.

3. Results and Discussion

3.1. Growth parameters

3.1.1. Length, fresh weight and dry weight of shoots

The effect of 24-epiBL pretreatment on the physiological parameters such as length, fresh weight, and dry weight of the shoots of plantlets under NaCl stress is shown in Table 1. In general, shoot length and shoot dry weight were negatively affected by the

increasing salt stress. Whereas shoot fresh weight increased at a 20 mM NaCl dose, and then decreased gradually with increasing NaCl concentration in the culture media. It was found that shoot fresh weight in 24-epiBL non-treated *in vitro* plantlets was the highest (810 mg) in the 20 mM NaCl dose by showing an inducing effect on the plant development compared to the control (0 mM NaCl) (750 mg), and increasing NaCl concentrations negatively affected shoot fresh weight, ranging from 740 mg to 180 mg (from 40 mM NaCl to 100 mM NaCl, respectively). Since tomato plants are considered moderately tolerant to salt stress, 80 mM and 100 mM NaCl concentrations caused a dramatic decrease in developmental parameters for the M-28 hybrid cultivar we used for our study. Similar results related to development of shoots and roots of plantlets were also obtained in different works (Mercado et al. 2000; Shibli et al. 2007; Abu-Khadejeh et al. 2011; Sringeng et al. 2015; Khaliluev et al. 2022). Roşca et al. (2023) stated that reducing plant development under salt conditions may be an adaptive morphological strategy to limit water loss through transpiration. Aly et al. (2012) emphasized that the decrease in growth because of high salinity is due to several factors as water and nutritional deficiency, ionic imbalance, specific ion toxicity, Na⁺ and Cl⁻ excess might cause disorganize cell division, elongation and structure. Nutrients imbalance due to depressed uptake, shoot transport from roots and impaired internal distribution of nutritious minerals such as K⁺ and Ca⁺² can be explained the reduction in plant growth (Rashed et al. 2016). Sousa et al. (2022) also underlined that salt-induced declines in growth-related parameters primarily correlated with reduced water uptake, along with a negative interference in nutrient and ion ratios caused by the build-up of salts.

Table 1- Shoot length, fresh weight and dry weight of 24-epiBL pretreated plantlets under NaCl stress conditions

24-EpiBL (μ M)	NaCl (mM)					
	0	20	40	60	80	100
<i>Shoot Length (cm)</i>						
0	10.90 ± 0.43	10.25 ± 0.68	7.57 ± 0.60	7.40 ± 0.34	6.15 ± 0.45 ^a	3.33 ± 0.23 ^b
1	10.13 ± 0.42	10.98 ± 0.44	7.82 ± 0.74	7.35 ± 0.36	3.44 ± 0.31 ^b	3.89 ± 0.35 ^{ab}
2	9.94 ± 0.40	11.09 ± 0.51	7.45 ± 0.55	7.19 ± 0.43	4.74 ± 0.42 ^{ab}	4.29 ± 0.32 ^a
<i>Shoot Fresh Weight (mg)</i>						
0	750 ± 30	810 ± 60 ^b	740 ± 80	520 ± 40	410 ± 40 ^a	180 ± 30 ^b
1	730 ± 30	980 ± 60 ^{ab}	840 ± 80	520 ± 40	210 ± 30 ^b	250 ± 40 ^{ab}
2	700 ± 30	1100 ± 40 ^a	660 ± 70	550 ± 40	360 ± 50 ^{ab}	390 ± 50 ^a
<i>Shoot Dry Weight (mg)</i>						
0	31.10 ± 3.72	14.07 ± 3.18	11.07 ± 3.29 ^{ab}	8.30 ± 2.17	12.43 ± 0.61 ^a	2.53 ± 0.72 ^b
1	32.78 ± 4.05	24.45 ± 5.98	10.97 ± 3.84 ^b	8.34 ± 2.09	3.33 ± 1.52 ^b	3.35 ± 0.68 ^b
2	27.71 ± 3.09	26.80 ± 4.70	23.76 ± 2.76 ^a	9.36 ± 2.95	4.13 ± 0.95 ^b	7.26 ± 0.67 ^a

Values, means ± standard errors. In terms of the values in the same column, the letters show the statistical differences between 24-epiBL concentrations compared to the control at P≤0.05

When evaluating the effect of 24-epiBL pretreatment against salt stress on shoot growth, it was found that 24-epiBL used to reduce negative effect of NaCl stress improved development of plantlets. 24-EpiBL pretreatment (2 μ M) increased the shoot length, fresh and dry weight of the growing plantlets at a dose of 100 mM NaCl. Again, 24-epiBL pretreatment (2 μ M) caused an increase in the fresh weight of the shoots developed at 20 mM NaCl, and the increase was found to be statistically significant difference (P≤0.05) (Table 1). It is clear that salt stress negatively affects growth and development of *in vitro* plantlets and in this study, 24-epiBL pretreatment improved developmental parameters such as length, fresh weight, and dry weight of shoots under salt stress. The use of BR, especially 24-epiBL, was suggested to enhance for NaCl tolerance. Anuradha & Rao (2001; 2003) reported positive effects of 24-epiBL on parameters such as fresh weight, dry weight, and length of rice seedlings grown from seeds at salt stress condition. According to Anwar et al. (2018), plants showed very rapid responses upon BR application at very low concentrations by increasing shoot growth because of the elongation and expansion of cells under stress conditions. BRs obtained stress tolerance by enhancing the multiple plant defense systems through increasing the activities of antioxidant enzymes (APX, SOD, POD, CAT, and GR), and altering nutrient accumulation to enhance seedling growth. Ahmad et al. (2018) reported that 24-epiBL increased plant growth under salt stress by enhancing the photosynthetic efficiency and H⁺-ATPase enzyme activity that is directly responsible for the activation of cell wall loosening enzymes and therefore developing growth. The present study clearly reveals that pretreatment of 24-epiBL on shoot tips is sufficient to reduce the possible negative impacts of NaCl stress.

3.1.2. Length, fresh weight and dry weight of roots

The effect of 24-epiBL pretraetment on length, fresh weight and dry weight of the plantlets roots under NaCl stress is shown in Table 2. In general, the root development process was negatively affected under NaCl stress. Root length, fresh and dry weight decreased under salt conditions. The root length was 8.13 cm in the NaCl-free control medium, and it was also determined that it was 7.88, 7.03, 6.16, 7.43, 5.35 cm from 20 mM NaCl to 100 mM NaCl. Root fresh weight and dry weight were the highest (340 mg and 31.10 mg, respectively) in the control groups and they were the lowest (30 mg and 2.53 mg, respectively) at the 100 mM NaCl stress (Table 2).

Table 2- Root length, root fresh weight and root dry weight of 24-epiBL pretreated plantlets under NaCl stress conditions

24-EpiBL (μM)	NaCl (mM)					
	0	20	40	60	80	100
Root Length (cm)						
0	8.13 \pm 0.19 ^a	7.88 \pm 0.28	7.03 \pm 0.36	6.16 \pm 0.26	7.43 \pm 0.45	5.35 \pm 0.61
1	7.41 \pm 0.19 ^b	8.02 \pm 0.35	7.15 \pm 0.35	5.97 \pm 0.27	6.26 \pm 0.56	6.71 \pm 0.67
2	8.00 \pm 0.22 ^{ab}	8.71 \pm 0.25	7.10 \pm 0.53	6.12 \pm 0.29	7.24 \pm 0.53	5.94 \pm 0.59
Root Fresh Weight (mg)						
0	340 \pm 10 ^a	340 \pm 20 ^a	210 \pm 20	80 \pm 8	80 \pm 08	30 \pm 08
1	280 \pm 10 ^b	270 \pm 20 ^b	180 \pm 10	80 \pm 9	90 \pm 25	50 \pm 11
2	290 \pm 10 ^{ab}	330 \pm 10 ^{ab}	150 \pm 20	100 \pm 7	80 \pm 13	40 \pm 06
Root Dry Weight (mg)						
0	31.10 \pm 3.72	14.07 \pm 3.18	11.07 \pm 3.29 ^{ab}	8.30 \pm 2.17	12.43 \pm 0.61 ^a	2.53 \pm 0.72 ^b
1	32.78 \pm 4.05	24.45 \pm 5.98	10.97 \pm 3.84 ^b	8.34 \pm 2.09	3.33 \pm 1.52 ^b	3.35 \pm 0.68 ^b
2	27.71 \pm 3.09	26.80 \pm 4.70	23.76 \pm 2.76 ^a	10.57 \pm 3.47	4.13 \pm 0.95 ^b	7.26 \pm 0.67 ^a

Values, means \pm standard errors. In terms of the values in the same column, the letters show the statistical differences between 24-epiBL concentrations compared to the control at $P \leq 0.05$

Excessive levels of sodium chloride in the soil near the root system may affect cell division and enzyme activity in the root tips, leading to a reduction in root length due to reduced water uptake and toxicity of sodium chloride (Abdel-Farid et al. 2020). Seth & Kendurkar (2015) reported that the reduction in root length under salt stress is mainly due to low water potential and limited cell growth in the external environment. 24-epiBL (2 μM) used against NaCl stress showed a positive effect on root length and root dry weight at 20 mM and 100 mM NaCl. In this context, root dry weight improved by 24-epiBL pretreatment at 100 mM NaCl (Table 2).

3.2. Biochemical parameters

3.2.1. Pigment content

The effect of BRs on the pigment contents of plantlets grown *in vitro* shoot tips under salt stress is summarized in Table 3. Especially pigment contents are negatively affected by increasing salinity when compared to the control (0 mM NaCl). Similarly, El-Meleigy et al. (2004) and Mohamed et al. (2011) reported that chlorophyll a and total chlorophyll contents decreased under salt stress. Photosynthesis activity is connected to photosynthetic pigments, namely chlorophyll a, chlorophyll b, and carotenoids, which are pivotal to the photosynthetic process (Bressan 2010). Additionally, salt stress leads to a reduction in pigment biosynthesis or an increase in pigment degradation. Furthermore, the disruption of the chloroplast's ultrastructure, including thylakoids, may be caused by Na^+ toxicity or oxidative damage associated with salt stress (Aly et al. 2012).

Table 3- Chlorophyll pigment contents of 24-epiBL pretreated plantlets under NaCl stress conditions

24-EpiBL (μM)	NaCl (mM)					
	0	20	40	60	80	100
Chlorophyll a ($\mu\text{g mL}^{-1}$)						
0	5.40 \pm 0.48	3.66 \pm 0.14	3.22 \pm 0.31	3.23 \pm 0.39	2.81 \pm 0.10	2.63 \pm 0.017 ^b
1	3.62 \pm 0.85	4.32 \pm 0.51	2.05 \pm 0.09	2.46 \pm 0.12	3.19 \pm 0.52	3.04 \pm 0.005 ^a
2	3.91 \pm 0.08	4.72 \pm 0.24	2.18 \pm 0.02	1.86 \pm 0.47	1.90 \pm 0.01	1.93 \pm 0.011 ^c
Chlorophyll b ($\mu\text{g mL}^{-1}$)						
0	3.99 \pm 0.34 ^a	1.17 \pm 0.32	1.72 \pm 0.226 ^b	1.44 \pm 0.005 ^b	3.14 \pm 0.985 ^a	3.82 \pm 0.06 ^b
1	3.22 \pm 0.29 ^{ab}	1.49 \pm 0.01	2.57 \pm 0.531 ^{ab}	2.24 \pm 0.005 ^a	0.24 \pm 0.026 ^b	4.82 \pm 0.01 ^a
2	0.94 \pm 0.02 ^b	1.59 \pm 0.10	3.71 \pm 0.008 ^a	1.45 \pm 0.011 ^b	0.80 \pm 0.005 ^b	1.13 \pm 0.01 ^c
Total Chlorophyll ($\mu\text{g mL}^{-1}$)						
0	8.14 \pm 0.81	5.07 \pm 0.43 ^{ab}	5.11 \pm 0.10 ^b	4.50 \pm 0.58	7.02 \pm 0.03 ^a	6.55 \pm 0.060 ^b
1	5.55 \pm 1.10	5.03 \pm 0.03 ^b	5.92 \pm 0.25 ^a	3.89 \pm 0.65	2.77 \pm 0.20 ^b	8.07 \pm 0.028 ^a
2	4.77 \pm 0.28	6.50 \pm 0.37 ^a	5.74 \pm 0.10 ^{ab}	3.13 \pm 0.64	2.73 \pm 0.01 ^b	3.13 \pm 0.008 ^c
Carotenoid ($\mu\text{g mL}^{-1}$)						
0	1.07 \pm 0.24	0.72 \pm 0.15 ^{ab}	0.63 \pm 0.04	0.96 \pm 0.13	0.36 \pm 0.003 ^c	0.54 \pm 0.003
1	0.80 \pm 0.29	0.32 \pm 0.06 ^b	0.81 \pm 0.02	0.68 \pm 0.14	2.09 \pm 0.083 ^a	0.66 \pm 0.005
2	1.92 \pm 0.30	0.78 \pm 0.06 ^a	0.81 \pm 0.08	0.60 \pm 0.20	1.35 \pm 0.003 ^b	0.93 \pm 0.254

Values, means \pm standard errors. In terms of the values in the same column, the letters show the statistical differences between 24-epiBL concentrations compared to the control at $P \leq 0.05$.

24-EpiBL pretreatments under NaCl stress ameliorated the negative effect of salinity. Chlorophyll a content at 100 mM NaCl, chlorophyll b content at 40, 60, and 100 mM NaCl, total chlorophyll content at 40 and 100 mM NaCl, and carotenoid content at 80 mM NaCl were improved by 24-epiBL pretreatment, and increases in these pigment contents were found statistically significant ($P \leq 0.05$). Shahid et al. (2011) reported that 24-epiBL pretreatment against NaCl stress increased chlorophyll a and chlorophyll b content. Sharma et al. (2013) underlined that enhancement of the chlorophyll content with 24-epiBL might be due to BR-mediated transcriptional and translational regulations of genes related to the synthesis of photosynthetic pigments or due to their reducing roles in chlorophyll catabolism.

3.2.2. MDA content

MDA content, which determines lipid peroxidation in cell membranes, increased under NaCl stress. MDA content ranged from 0.73 to 4.48 $\mu\text{mol g}^{-1}$ FW between 0 mM-100 mM NaCl stress (Figure 1). MDA content, a decomposition product of unsaturated fatty acids called lipid peroxidation, is regarded as a biochemical marker for determining the oxidative damage in the cell and organelle membranes under salt stress conditions (Sharma et al. 2013). Lipid peroxidation changes membrane properties such as proteins, lipids, carbohydrates, membrane permeability, fluidity and bilayer thickness, and disorders the blayer structure of the cell membrane (Ahammed et al. 2012).

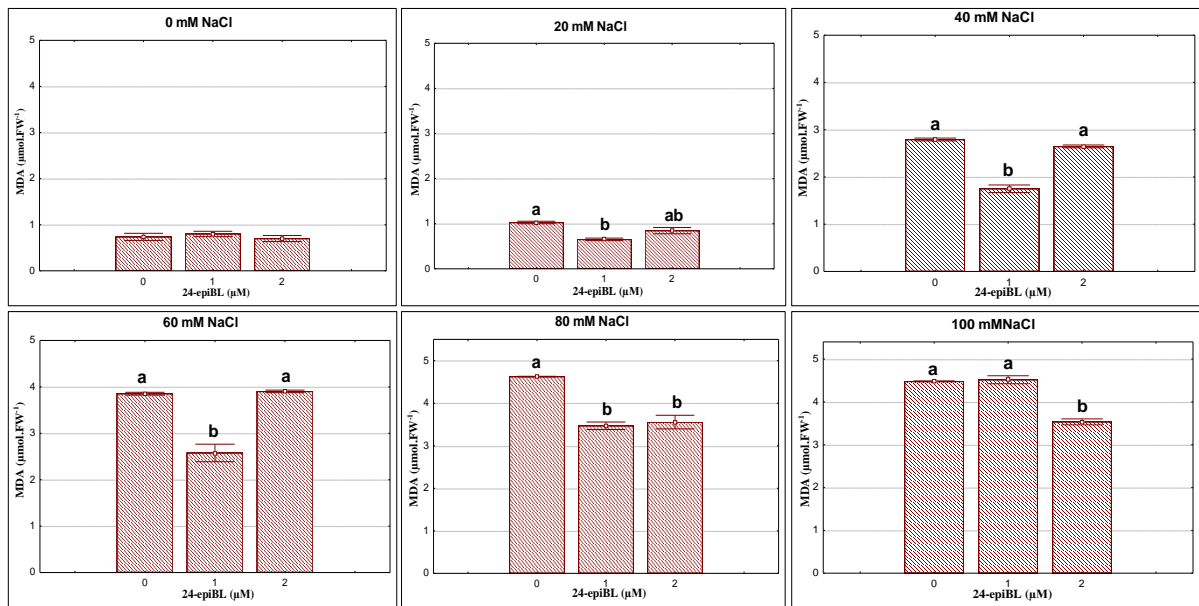


Figure 1- MDA contents ($\mu\text{mol g}^{-1}$ FW) of 30 day-old plantlets grown 24-epiBL non-pretreated and pretreated *in vitro* shoot tips against to salt stress

It was found that MDA content statistically decreased with 24-epiBL pretreatment (1 μM) at 20, 40, and 60 mM NaCl, 24-epiBL pretreatments (1 μM and 2 μM) at 80 mM NaCl, and 24-epiBL pretreatment (2 μM) at 100 mM NaCl. Thus, 24-epiBL pretreatment for all NaCl concentrations ameliorated lipid peroxidation and cell membrane damage due to decreased MDA content (Figure 1). Ding et al. (2012) in eggplant, Sharma et al. (2013) in rice and Hu et al. (2016) in potato reported that 24-epiBL application against NaCl stress decreased increasing MDA content. The strong antioxidative defense system combined with other physiological differences in the plants contributes to the various salt responses between *in vitro* materials like calli or shoot tips, and whole plants (Lokhande et al. 2011). Thus, this result showed that 24-epiBL regulate lipid peroxidation in the cellular membranes and improves salt tolerance in plants.

3.2.3. Proline content

Proline is one of the most important biochemical markers accumulating under salinity conditions. Proline content increased under NaCl stress in the study. The proline content of 24-epiBL non-pretreated shoots ranged from 9.83 $\mu\text{mol g}^{-1}$ FW (control) to 19.86 $\mu\text{mol g}^{-1}$ FW (100 mM NaCl) (Figure 2). Proline is accumulated in various plant species under salt stress and other abiotic stress factors (Szabados & Savoure 2009). Proline, which plays a protective function against salt stress in plants, acts as a compatible osmolyte, enzyme protectant, free radical scavenger, cell redox balancer, cytosolic pH buffer, and stabilizer for subcellular structures to obtain salt tolerance (Iqbal et al. 2014). Proline acts as a store of energy that can be quickly broken down and used under NaCl stress (Woodward & Bennett 2005). Aly et al. (2012) indicated that accumulation of proline under stress conditions is due to induction in the proline biosynthesis or inhibition in the proline oxidation. Accumulation of proline play a key role on stress tolerance and proline as an osmolyte contributes to the scavenging of ROS, keeping the configurations of proteins and store carbone and nitrogene resources in plants (Verbruggen & Hermans 2008). Proline maintain cellular redox

potential and serves to stabilize ultra-structural changes in cells. A higher accumulation of proline is reported to strengthen the ability of the cell to make ionic adjustments in the cell cytosol under stress conditions (Shahid et al. 2020).

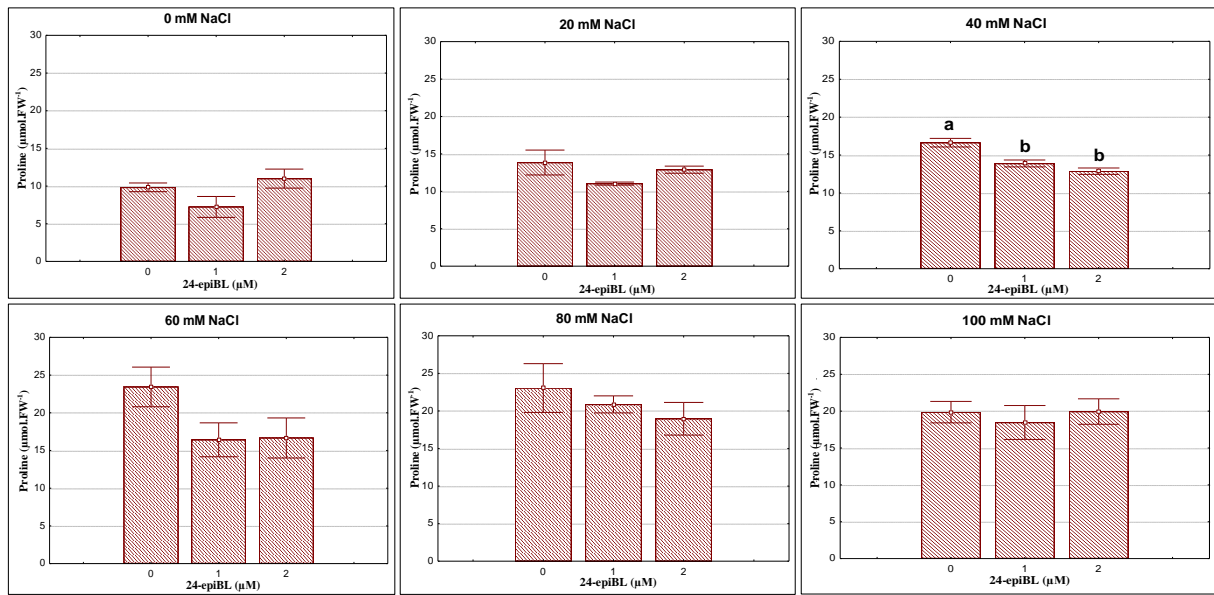


Figure 2- Proline contents ($\mu\text{mol g}^{-1}$ FW) of 30 day-old plantlets grown 24-epiBL non-pretreated and pretreated *in vitro* shoot tips against to salt stress

In this study, proline content increased under salt stress. Similarly, Abu-Khadejeh et al. (2011) reported that proline content increased in the shoots of JO112 and JO992 tomato cultivars under salt stress conditions. Results from the another study showed that proline in the tomato calli increased compared with the control (Hassanein 2004; Mohamed et al. 2007; Aazami et al. 2010). It was found that this parameter decreased with 24-epiBL pretreatments. This finding was in accordance with the results of study conducted in pepper plants (Houimli et al. 2010). The decrease in proline content by 24-epiBL pretreatments (1 μM and 2 μM) was statistically significant only at a 40 mM NaCl concentration (Figure 2). As a result, 24-epiBL alleviates the negative effects of NaCl stress through different mechanisms including regulation of cytoplasmic pH and stabilization of protein, DNA, RNA, and membranes with the protective effects of proline (Sabir et al. 2012).

3.2.4. Soluble protein content

One of the osmolytes accumulated in high concentrations to maintain the osmotic balance in the cells is the soluble protein, which has at low molecular weight inside the cell. Total soluble protein content in 24-epiBL non-pretreated shoots was induced at a low NaCl concentration (20 mM NaCl), but this parameter decreased with increasing NaCl stress. Amini & Ehsanpour (2006), Shibli et al. (2007), Mohamed et al. (2011) and Abu-Khadejeh et al. (2011) reported that protein content in tomato decreased under salt stress, similar to our study findings. The decrease in the protein content under NaCl stress might be due to protein degradation, denaturation, proteolysis, decreases in the protein synthesis and free amino acids (El-Mashad & Mohamed 2012). In this study, when the effect of 24-epiBL used against salt stress was evaluated, total protein content statistically increased by 24-epiBL (2 μM) only at 40 mM NaCl concentration. Sharma et al. (2013) and Khalid & Aftab (2016) emphasized that protein content decreased under NaCl stress in rice but it increased by 24-epiBL application against to NaCl. Proteins in the plant cells may supply a nitrogen storage form of that is reutilized and may serve as an osmotic adjustment under stress conditions (Mehr 2013).

3.2.5. SOD and POX enzymes activities

In our study, SOD activity in leaves of *in vitro* plantlets was increased under salt stress conditions. SOD enzyme activity in leaves of 24-epiBL non-pretreated shoots ranged from 10.18 unit SOD mg^{-1} protein (control, 0 mM NaCl) to 41.06 unit SOD mg^{-1} protein (100 mM NaCl), (Figure 3). Various antioxidant enzymes protect the cell against reactive oxygen species that are more likely to be produced under salt stress conditions. According to Roşca et al. (2023), in tomatoes exposed to salt stress, antioxidant production and antioxidant enzymes activities can vary depending on cultivar, salt concentration, plant age, or part of the plant.

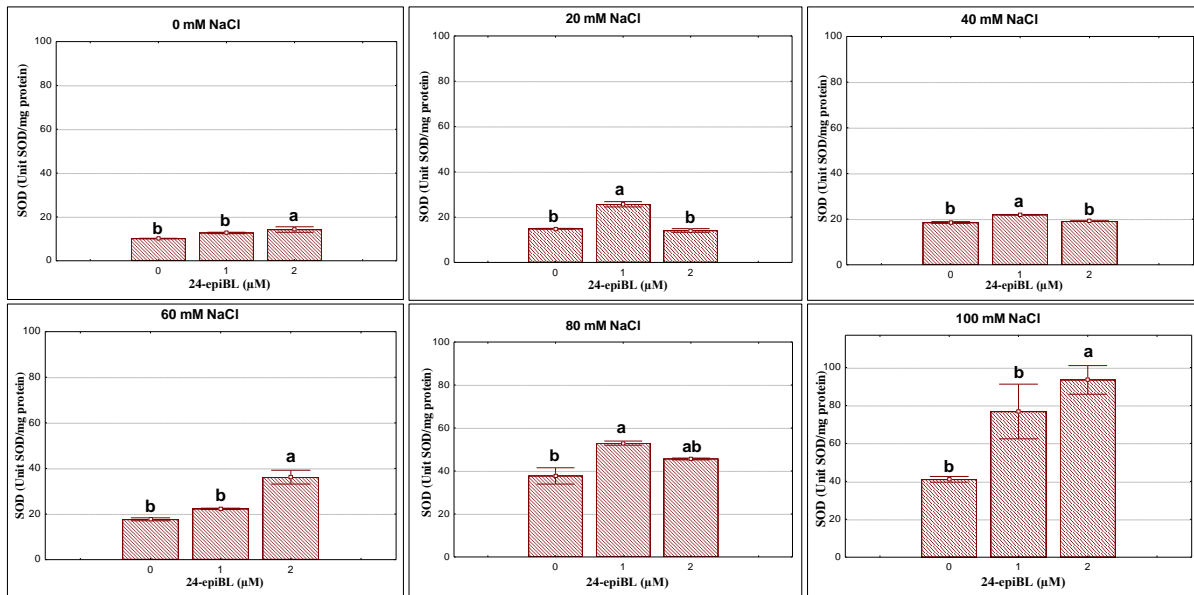


Figure 3- SOD enzyme activity (Unit SOD mg⁻¹ protein) of 30 day-old plantlets grown 24-epiBL non-pretreated and pretreated *in vitro* shoot tips against to salt stress

When the effects of SOD activity according to NaCl concentrations used were statistically evaluated, 24-epiBL (1 μM) had a significant difference on SOD activity at 20, 40 and 80 mM NaCl concentrations. 24-epiBL (2 μM) had a positive effect on SOD activity at 60 and 100 mM NaCl concentrations, and this increase was found statistically significant (Figure 3). Shahbaz et al. (2008) in wheat, Shahid et al. (2011) in pea, Ding et al. (2012) in eggplant, Sharma et al. (2013) in rice, Nafie et al. (2015) in common bean, and Upadhyaya et al. (2015) in potato reported that SOD enzyme activity increased by 24-epiBL under salt stress. ROS such as singlet oxygen, superoxide, hydrogen peroxide, hydroxyl are produced during aerobic metabolism, and ROS production under abiotic stress are much more than normal condition. However, plants generally can eliminate superoxide with the SOD activity which catalyzes the dismutation of superoxide into hydrogen peroxide and oxygen (Parida & Das 2005). BR-mediated ROS signal maintains the homeostasis which turns the activation of transcription factors that regulate stress responsive genes related to biosynthesis of SOD, POX, and CAT enzymes which enhance tolerance to different abiotic stresses by up-regulation of the antioxidant machinery system (Singh et al. 2021).

Hydrogen peroxide can be eliminated by POX (Ashraf & Harris 2004). In our study, POX enzyme activity increased under NaCl stress. POX enzyme activity in leaves of 24-epiBL non-pretreated shoots ranged from 1.65 ΔA470 min⁻¹ mg⁻¹ protein (control, 0 mM NaCl) to 5.12 ΔA470 min⁻¹ mg⁻¹ protein (100 mM NaCl) (Figure 4).

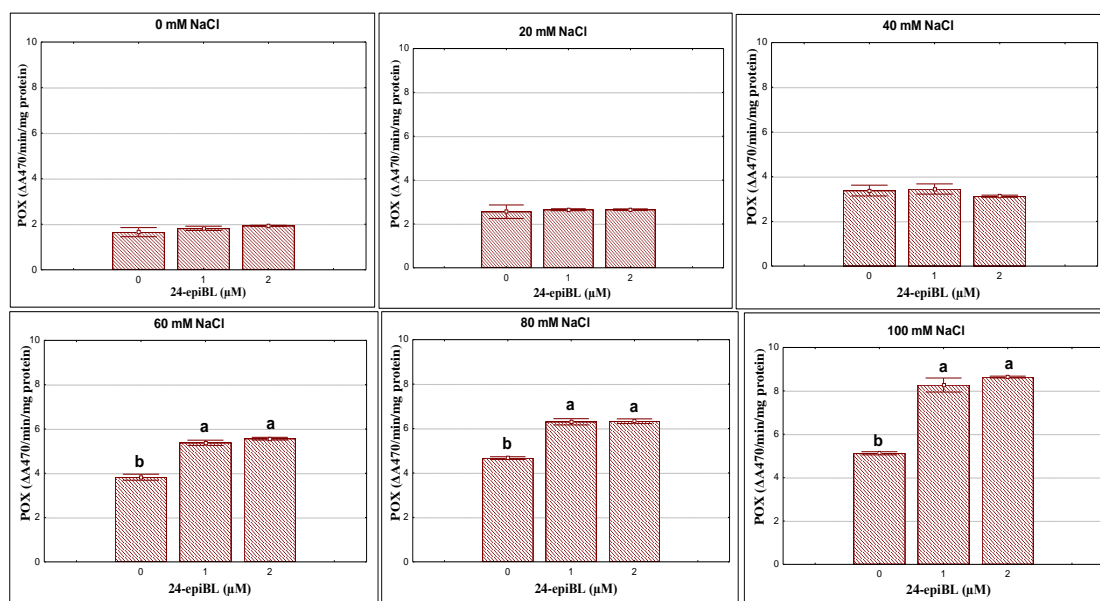


Figure 4- POX enzyme activity (ΔA470 min⁻¹ mg⁻¹ protein) of 30 day-old plantlets grown 24-epiBL non-pretreated and pretreated *in vitro* shoot tips against to salt stress

As a result, POX activity was increased by 24-epiBL (1 and 2 μM) at 60, 80, and 100 mM NaCl concentrations, and it was found that the increases were statistically significant (Figure 4). The reason for the increase in the SOD and POX enzymes activity might be the possible effects of BR on expressions of the genes coding for the biosynthesis of these enzymes, which resulted in enhanced oxidation of harmful reactive substances (El-Mashad & Mohamed 2012).

4. Conclusions

Soil salinity is one of environmental problems that affect plant development and productivity, causing great economic losses. Different biotechnological approaches are used to overcome the detrimental effects of salt stress that occur in plants. Among these approaches, it is important to use these cultivars in agricultural applications, identify plant species and cultivars that have high salt tolerance, increase the salt tolerance of plants and reduce the effects of salt stress by using different substances such as proline, glisine-betain, especially BRs and 24-epiBL. As a result, in the present study, the effect of 24-epiBL against NaCl stress was first studied using *in vitro* shoot tip culture in M-28 hybrid cultivar and positive effect on salt tolerance of tomato plants was determined by growth and biochemical parameters. 2 μM 24-epiBL pretreatment showed a reformative effect on shoot and root development of plantlets under 100 mM NaCl stress. 1 μM 24-epiBL increased the pigment content in plantlets at a 100 mM NaCl dose. The MDA content, which increased under stress conditions, decreased with 1 μM 24-epiBL pretreatment at 40-80 mM NaCl dose. Osmoregulant proline content decreased with 1 μM and 2 μM 24-epiBL at 40 mM NaCl dose. 1 μM 24-epiBL at 20, 40, and 80 mM NaCl stress and 2 μM 24-epiBL at 60, 100 mM NaCl stress increased the SOD activity even more, allowing the tomato M-28 hybrid cultivar to fight the oxidative stress. POX activity increased with the pretraetment of 1 μM and 2 μM 24-epiBL at 20, 80, and 100 mM NaCl stress. In our study, 24-epiBL at both doses (1 μM and 2 μM) exogenously applied to the shoot tips showed a positive effect at modarate (40-60 mM NaCl) and high salt doses (80-100 mM NaCl). Further studies are needed to determine the effects of 24-epiBL at molecular level as well as growth and biochemical parameters by using *in vitro* cultures against salt stress in different crop species and cultivars.

Declaration of conflicting Interest

The authors declared no conflicts of interest with respect to the research, authorship and publication of this article.

This study is the part of Emel YILMAZ-GOKDOGAN's PhD thesis. The study was supported by Mugla Sitki Kocman University, Scientific Research Projects Coordination Unit (Mugla, Turkey, project number: 2011/17).

References

- Aazami M A, Torabi M & Jalili E (2010). *In vitro* response of promising tomato genotypes for tolerance to osmotic stress. *African Journal of Biotechnology* 9(26): 4014-4017
- Aazami M A, Rasouli F & Ebrahimzadeh A (2021). Oxidative damage, antioxidant mechanism and gene expression in tomato responding to salinity stress under *in vitro* conditions and application of iron and zinc oxide nanoparticles on callus induction and plant regeneration. *BMC Plant Biology* 21: 597-620. doi: 10.1186/s12870-021-03379-7
- Abdel-Farid I B, Marghany M R, Rowezek M M & Sheded M G (2020). Effect of salinity stress on growth and metabolomic profiling of *Cucumis sativus* and *Solanum lycopersicum*. *Plants* 9: 1626-1645. doi:10.3390/plants9111626
- Abu-Khadejeh A, Makhadmeh I, Shibli R A & Mohammed M J (2011). Physiological responses of tomato microshoot cultures to *in vitro* induced salinity stress. *Jordan Journal of Agricultural Sciences* 7(2): 260-272
- Ahammed G J, Choudhary S P, Xiaojian Xia S C, Shi K, Zhou Y & Yu J (2012). Role of brassinosteroids in alleviation of phenanthrene-cadmium co-contamination-induced photosynthetic inhibition and oxidative stress in tomato. *Journal of Experimental Botany* 63(2): 695-709. doi: 10.1093/jxb/ers323
- Ahmad F, Singh A & Kamal A (2018). Crosstalk of brassinosteroids with other phytohormones under various abiotic stresses. *Journal of Applied Biology & Biotechnology* 6(1): 56-62. doi: 10.7324/JABB.2018.60110
- Ahmad P, Abd_Allah E F, Alyemeni M N, Wijaya L, Alam P, Bhardwaj R & Siddique K H M (2018). Exogenous application of calcium to 24-epibrassinosteroid pretreated tomato seedlings mitigates NaCl toxicity by modifying ascorbate-glutathione cycle and secondary metabolites. *Scientific Reports* 8(13515): 1-15. doi:10.1038/s41598-018-31917-1
- Aly A A, Khafaga A F & Omar G N (2012). Adverse effect of salt stress in Egyptian clover (*Trifolium alexandrinum* L.) by Asa application through some biochemical and RT-PCR markers. *Journal of Applied Phytotechnology in Environmental Sanitation* 1(2): 91-102
- Amini F & Ehsanpour A A (2006). Response of tomato (*Lycopersicon esculentum* Mill.) cultivars to MS, water agar and salt stress in *in vitro* culture. *Pakistan Journal of Biological Sciences* 9(1): 170-175. doi:10.3923/pjbs.2006.170.175
- Anuradha S & Rao S S R (2001). Effect of brassinosteroids on salinity stress induced inhibition of seed germination and seedling growth of rice (*Oryza sativa* L.). *Plant Growth Regulation* 33: 151-153. doi:10.1023/A:1017590108484
- Anuradha S & Rao S S R (2003). Application of brassinosteroids to rice seeds (*Oryza sativa* L.) reduced the impact of salt stress on growth, prevented photosynthetic pigment loss and increased nitrate reductase activity. *Plant Growth Regulation* 40: 29-32. doi:10.1023/A:1023080720374
- Anwar A, Liu Y, Dong R, Bai L, Yu X & Yansu L (2018). The physiological and molecular mechanism of brassinosteroid in response to stress: a review. *Biological Research* 51(46): 1-15. doi: 10.1186/s40659-018-0195-2
- Ashraf M (2009). Biotechnological approach of improving plant salt tolerance using antioxidants as markers. *Biotechnology Advances* 27: 84-93. doi: 10.1016/j.biotechadv.2008.09.003
- Ashraf M & Harris P J C (2004). Potential biochemical indicators of salinity tolerance in plants. *Plant Science* 166: 3-16. doi:10.1016/j.plantsci.2003.10.024

- Bates L S, Waldren R P & Teare I D (1973). Rapid determination of free proline for water stress studies. *Plant Soil* 39: 205-207
- Beaucamp C & Fridovich I (1971). Superoxide dismutase improved assays and an assay applicable to acrylamide gels. *Anal Biochem* 44: 276-287
- Bradford M M (1976). A rapid and sensitive method for the quantitation of microgram quantities of protein utilizing the principle of protein-dye binding. *Anal Biochem* 72: 248-254
- Bressan R A (2010). Stress physiology. In: L Taiz & E Zeiger (Eds.), *Plant Physiology*, Sinauer Associates, Sunderland, Massachusetts pp.782
- Cano E A, Perez-Alfocea F, Moreno V, Caro M & Bolarin M C (1998). Evaluation of salt tolerance in cultivated and wild tomato species through *in vitro* shoot apex culture. *Plant Cell, Tissue and Organ Culture* 53: 19-26
- Chance B & Maehly C (1955). Assay of catalase and peroxidases. *Method Enzymol* 11: 764-775
- Cristea T O, Iosob G A & Prisecaru M (2020). Studies regarding the interdependence between the cytogenetic aspects and the application of stress factors over the tissues cultivated "*in vitro*" at tomatoes. *Biologie* 29(1): 57-60
- Ding H-D, Zhu X-H, Zhu Z-W, Yang S-J, Zha D-S & Wu X-X (2012). Amelioration of salt-induced oxidative stress in eggplant by application of 24-epibrassinolide. *Biologia Plantarum* 56(4): 767-770. doi: 10.1007/s10535-012-0108-0
- El-Mashad A A & Mohamed H I (2012). Brassinolide alleviates salt stress and increases antioxidant activity of cowpea plants (*Vigna sinensis*). *Protoplasma* 249: 625-635. doi: 10.1007/s00709-011-0300-7
- El-Meleigy E-S A, Gabr M F, Mohamed F H & Ismail M A (2004). Responses to NaCl salinity of tomato cultivated and breeding lines differing in salt tolerance in callus cultures. *International Journal of Agriculture & Biology* 6(1): 19-26
- El-Sayed T R (2021). Production of tomato lines tolerating to salinity using *in-vitro* culture technique. *Journal of Plant Production* 12(12): 1351-1357. doi: 10.21608/JPP.2021.220184
- Guo M, Wang X-S, Guo H-D, Bai S-Y, Khan A, Wang X-M, Gao Y-M & Li J-S (2022). Tomato salt tolerance mechanisms and their potential applications for fighting salinity: a review. *Frontiers in Plant Science* 10:1-22. doi:10.3389/fpls.2022.949541
- Hassanein A M (2004). Effect of relatively high concentrations of mannitol and sodium chloride on regeneration and gene expression of stress tolerant (*Alhagi graecorum*) and stress sensitive (*Lycopersicon esculentum* L.) plant species. *Bulgarian Journal of Plant Physiology* 30(3-4): 19-36
- Heath R L & Packer L (1968). Photoperoxidation in isolated chloroplast. I. Kinetics and stoichiometry of fatty acid peroxidation. *Arch Biochem Biophys* 125: 189-198
- Houimli S I M, Denten M & Mouhanded B D (2010). Effects of 24-epibrassinolide on growth, chlorophyll, electrolyte leakage and proline by pepper plants under NaCl-stress. *EurAsian Journal BioSciences* 4: 96-104. doi:10.5053/ejobios.2010.4.0.12
- Hu Y, Xia S, Su Y, Wang H, Luo W, Su S & Xiao L (2016). Brassinolide increases potato root growth *in vitro* a dose-dependent way and alleviates salinity stress. *Biomed Research International* 2016: 1-11. doi:10.1155/2016/8231873
- Iqbal N, Umar S, Khanb N A & Khan M I R (2014). A new perspective of phytohormones in salinity tolerance: Regulation of proline metabolism. *Environmental and Experimental Botany* 100: 34-42. doi:10.1016/j.envexpbot.2013.12.006
- Khalid A & Aftab F (2016). Effect of exogenous application of 24-epibrassinolide on growth, protein contents, and antioxidant enzyme activities of *in vitro*-grown *Solanum tuberosum* L. under salt stress. *In Vitro Cellular & Developmental Biology-Plant* 52: 81-91. doi:10.1007/s11627-015-9745-2
- Khaliluev M R, Bogoudinova L R, Raldugina G N & Baranova E N (2022). A simple and effective bioassay method suitable to comparative *in vitro* study of tomato salt tolerance at early development stages. *Methods and Protocols* 5(11): 1-17. doi:10.3390/mps5010011
- Koca H, Bor M, Özdemir F & Türkan İ (2007). The effect of salt stress on lipid peroxidation, antioxidative enzymes and proline content of sesame cultivars. *Environmental and Experimental Botany* 60: 344-351. doi:10.1016/j.envexpbot.2006.12.005
- Loganayaki K, Tamizhmathi S, Brinda D, Gayathri S, Mary M C & Mohanlal VA (2020). *In vitro* evaluation of tomato (*Lycopersicon esculentum* Mill.), chilli (*Capsicum annum* L.), cucumber (*Cucumis sativus* L.) and bhendi (*Abelmoschus esculentus* L.) for salinity stress. *International Journal of Chemical Studies* 8(2): 2364-2367. doi:10.22271/chemi.2020.v8.i2aj.9104
- Lokhande V H, Nikam T D, Patade V Y, Ahire M L & Suprasanna P (2011). Effects of optimal and supra-optimal salinity stress on antioxidative defence, osmolytes and *in vitro* growth responses in *Sesuvium portulacastrum* L. *Plant Cell, Tissue and Organ Culture* 104: 41-49. doi:10.1007/s11240-010-9802-9
- Mehr Z S (2013). Salt-induced changes in germination and vegetative stages of *Anethum graveolens* L. *Journal of Stress Physiology & Biochemistry* 9(2): 189-198.
- Mercado J A, Sancho-Carrascosa M A, Jimenez-Bermudez S, Peran-Quesada R, Pliego-Alfaro F & Quesada M A (2000). Assessment of *in vitro* growth of apical stem sections and adventitious organogenesis to evaluate salinity tolerance in cultivated tomato. *Plant Cell, Tissue and Organ Culture* 62: 101-106. doi:10.1023/A:1026503603399
- Mohamed A N, Rahman M H, Alsadon A A & Islam R (2007). Accumulation of proline in NaCl-treated callus of six tomato (*Lycopersicon esculentum* Mill.) cultivars. *Plant Tissue Culture and Biotechnology* 17(2): 217-220. doi:10.3329/ptcb.v17i2.3242
- Mohamed A N, Ismail M R, Kadir M A & Saud H M (2011). *In vitro* performances of hypocotyl and cotyledon explants of tomato cultivars under sodium chloride stress. *African Journal of Biotechnology* 10(44): 8757-8764. doi:10.5897/AJB10.2222
- Mudgal V, Madaan N & Mudgal A (2010). Biochemical mechanism of salt tolerance in plant: a review. *International Journal of Botany* 6(2): 136-143.
- Murashige T & Skoog F (1962). A revised medium for rapid growth and bioassays with tobacco tissue cultures. *Physiol Plant* 15: 473-497.
- Nafie E M, Khalfallah A A & Mansur R M (2015). Syndrome effects of NaCl and epibrassinolide on certain molecular and biochemical activities of salt-sensitive *Phaseolus vulgaris* cv. Brunco L. grown under *in vitro* condition. *Life Science Journal* 12(7): 119-136.
- Osman M G, Elhadi E A & Khalafalla M M (2011). *In vitro* screening of some tomato commercial cultivars for salinity tolerant. *International Journal of Biotechnology and Biochemistry* 7(5): 543-552.
- Parida A K & Das A B (2005). Salt tolerance and salinity effects on plants: a review. *Ecotoxicology and Environmental Safety* 60: 324-349. doi:10.1016/j.ecoenv.2004.06.010
- Rashed M R U, Roy M R, Paul S K & Haque M (2016). *In vitro* screening of salt tolerant genotypes in tomato (*Solanum lycopersicum* L.). *Journal of Horticulture* 3(4): 1-8. doi: 10.4172/2376-0354.1000186
- Rivera P, Moya C & O'Brien J A (2022). Low salt treatment results in plant growth enhancement in tomato seedlings. *Plants* 11(807): 1-8. doi:10.3390/plants11060807
- Roşca M, Mihalache G & Stoleru V (2023). Tomato responses to salinity stress: from morphological traits to genetic changes. *Frontiers in Plant Science* 10:1-26. doi:10.3389/fpls.2023.1118383

- Sabir F, Sangwan R S, Kumar R & Sangwan N S (2012). Salt stressed-induced responses in growth and metabolism in callus cultures and differentiating *in vitro* shoots of Indian ginseng (*Withania somnifera* Dunal). *Journal of Plant Growth Regulation* 31: 537-548. doi:10.1007/s00344-012-9264-x
- Sairam R K & Tyagi A (2004). Physiology and molecular biology of salinity stress tolerance in plants. *Current Science* 86(3): 407-421. doi:10.1007/1-4020-4225-6
- Sané A K, Diallo B, Kane A, Sagna M, Sané D & Sy M O (2021). *In vitro* germination and early vegetative growth of five tomato (*Solanum lycopersicum* L.) varieties under salt stress conditions. *American Journal of Plant Sciences* 12: 796-817. doi: 10.4236/ajps.2021.1210105
- Seth R & Kendurkar S V (2015). *In vitro* screening: An effective method for evaluation of commercial cultivars of tomato towards salinity stress. *International Journal of Current Microbiology and Applied Sciences* 4(1): 725-730
- Shahbaz M, Ashraf M & Athar H-U-R (2008). Does exogenous application of 24-epibrassinolide ameliorate salt induced growth inhibition in wheat (*Triticum aestivum* L.)? *Plant Growth Regulation* 55: 51-64. doi:10.1007/s10725-008-9262-y
- Shahid M A, Pervez M A, Balal R M, Mattson N S, Rashid A, Ahmad R, Ayyub C M & Abbas T (2011). Brassinosteroid (24-epibrassinolide) enhances growth and alleviates the deleterious effects induced by salt stress in pea (*Pisum sativum* L.). *Australian Journal of Crop Science* 5(5): 500-510
- Shahid M A, Sarkhosh A, Khan N, Balal R M, Ali S, Rossi L, Gómez C, Mattson N, Nasim W & Garcia-Sanchez F (2020). Insights into the physiological and biochemical impacts of salt stress on plant growth and development. *Agronomy* 10(938): 1-34. doi:10.3390/agronomy10070938
- Sharma I, Ching E, Saini S, Bhardwaj R & Pati P K (2013). Exogenous application of brassinosteroid offers tolerance to salinity by altering stress responses in rice variety Pusa Basmati-1. *Plant Physiology and Biochemistry* 69: 17-26. doi:10.1016/j.plaphy.2013.04.013
- Shibli R A, Kushad M, Yousef G G & Lila M A (2007). Physiological and biochemical responses of tomato microshoots to induced salinity stress with associated ethylene accumulation. *Plant Growth Regulation* 51: 159-169. doi:10.1007/s10725-006-9158-7
- Singh A, Dwivedi P, Kumar V & Pandey D K (2021). Brassinosteroids and their analogs: Feedback in plants under *in vitro* condition. *South African Journal of Botany* 143: 256-265. doi:10.1016/j.sajb.2021.08.008
- Sousa B, Rodrigues F, Soares C, Martins M, Azenha M, Lino-Neto T, Santos C, Cunha A & Fidalgo F (2022). Impact of combined heat and salt stresses on tomato plants—Insights into nutrient uptake and redox homeostasis. *Antioxidants* 11(478): 1-21. doi:10.3390/antiox11030478
- Srinieng K, Saisavoey T & Karnchanat A (2015). Effect of salinity stress on antioxidative enzyme activities in tomato cultured *in vitro*. *Pakistan Journal of Botany* 47(1): 1-10.
- Surgun Y, Yilmaz E, Çöl B & Burun B (2012). Sixth class of plant hormones: brassinosteroids. *CBU Journal of Science* 8(1): 27-46 (in Turkish)
- Strain H H & Svec WA (1966). Extraction, separation, estimation and isolation of chlorophylls. In: V P Bernon & G R Seely (Eds). In *The Chlorophylls*, Academic Press, New York.
- Szabados L & Savoure A (2009). Proline: a multifunctional amino acid. *Trends in Plant Sciences* 15(2): 89-97. doi:10.1016/j.tplants.2009.11.009
- Szczepaniak M & Kulpa D (2012). Response of *Lycopersicon peruvianum* L. line to salinity *in vitro* culture. *Folia Pomeranae Universitatis Technologiae Stetinensis seria Agricultura, Alimentaria, Piscaria et Zootechnica* 295(22): 53-58
- Upadhyaya C P, Bagri D S & Upadhyay D C (2015). Ascorbic acid and/or 24-epibrassinolide trigger physiological and biochemical responses for the salt stress mitigation in potato (*Solanum tuberosum* L.). *Intenational Journal of Applied Sciences and Biotechnology* 3(4): 655-667. doi:10.3126/ijasbt.v3i4.13975
- Verbruggen N & Hermans C (2008). Proline accumulation in plants: a review. *Amino Acids* 35: 753-759. doi:10.1007/s00726-008-0061-6
- Woodward A J & Bennett I J (2005). The effect of salt stress and abscisic acid on proline production, chlorophyll content and growth of *in vitro* propagated shoots of *Eucalyptus camaldulensis*. *Plant Cell, Tissue and Organ Culture* 82: 189-200. doi:10.1007/s11240-005-0515-4
- Yang C-J, Zhang C, Lu Y-N, Jin J-Q & Wang X-L (2011). The mechanisms of brassinosteroids' action: from signal transduction to plant development. *Molecular Plant* 4(4): 588-600. doi:10.1093/mp/ssr020
- Yilmaz E & Burun B (2014). *In vitro* callus formation and shoot regeneration from hypocotyl and cotyledon explants of tomato (*Lycopersicon esculentum* Mill.). *SDU Journal of Natural and Applied Science* 18(3): 105-113 (in Turkish)
- Yilmaz-Gokdogan E & Burun B (2015). Development of seedling and germination of tomato (*Lycopersicon esculentum* Mill.) seeds pre-applied 24-epibrassinolide under NaCl stress conditions. *Afyon Kocatepe University Journal of Science and Engineering* 15: 18-27. doi:10.5578/fmbd.10187 (in Turkish)
- Yilmaz-Gokdogan E & Burun B (2017). The ameliorative effects of 24-epibrassinolide on shoot organogenesis inhibition occurring under NaCl-stressed conditions in cultures of cotyledon and hypocotyl explants of tomato (*Lycopersicon esculentum* Mill.). *Acta Botanica Croatica* 76(2): 163-170. doi:10.1515/botcro-2017-0006
- Zaki H E M & Yokoi S (2016). A comparative *in vitro* study of salt tolerance in cultivated tomato and related wild species. *Plant Biotechnology* 33: 361-372. doi: 10.5511/plantbiotechnology.16.1006a





The Photochemical and Antioxidant Defence Strategies of Two Maize Genotypes Exposed to Zinc Toxicity at the Seedling Stage

Yasemin Ekmekçi^{a*}, Şeküre Çulha Erdal^a, Şeniz Ünalın Okar^{b,c}, Nuran Çiçek^a, Deniz Tanyolaç^b

^aFaculty of Science, Department of Biology, Hacettepe University, 06800 Ankara, TURKEY

^bFaculty of Engineering, Department of Chemical Engineering, Hacettepe University, Beytepe Campus, 06800 Ankara, TURKEY

^cCurrent address: Pulver Chemistry Industry and Trade Inc. Gebze Organized Industrial Zone (GOSB) Tembelova Area 3200 Street No:3201 Gebze 41400 Kocaeli / TURKEY

ARTICLE INFO

Research Article

Corresponding Author: Yasemin Ekmekçi, E-mail: yase@hacettepe.edu.tr; ekmekciy@gmail.com

Received: 28 July 2023 / Revised: 08 January 2024 / Accepted: 16 January 2024 / Online: 23 July 2024

Cite this article

Ekmekçi Y, Çulha Erdal Ş, Ünalın Okar Ş, Çiçek N, Tanyolaç D (2024). The Photochemical and Antioxidant Defence Strategies of Two Maize Genotypes Exposed to Zinc Toxicity at the Seedling Stage. *Journal of Agricultural Sciences (Tarım Bilimleri Dergisi)*, 30(3):488-500. DOI: 10.15832/ankutbd.1333983

ABSTRACT

The main objective of the current study was to elucidate photochemical and antioxidant strategies in two maize genotypes, namely DK626 and 3223 at the early seedling stage under zinc (Zn^{2+}) toxicity. The seedlings were grown in a controlled growth room at a temperature regime of 25 ± 1 °C, with 40 ± 5 % humidity, 16 h photoperiod and at $300 \mu mol m^{-2} s^{-1}$ light intensity for 8 days. Then, the seedlings were exposed to toxic zinc concentrations (2, 5 and 8 mM $ZnSO_4 \cdot 7H_2O$) for 12 days. Both genotypes accumulated approximately the same amounts of Zn in leaves; however, the shoot and root lengths, and biomass decreased further in DK626 compared to 3223. The malondialdehyde content in the leaves increased gradually depending on the Zn concentrations, and the deterioration of the membrane structure was greater in DK626 compared to 3223 at highly toxic Zn levels. A reduction in photochemical activity was accompanied by non-photochemical quenching and excess energy was removed from

the reaction centers by fluorescence and non-radiative inactivation in genotypes under Zn toxicity. The chlorophyll and carotenoid contents were significantly decreased, and the anthocyanin accumulation was increased with increasing Zn levels, especially in DK626. In addition, the activities of antioxidant enzymes and isoenzymes were induced at different levels in genotypes depending on the Zn toxicity level. The seedlings exposed to toxic Zn concentrations had achieved to sustain their growth by regulating their photosynthetic efficiency and their antioxidant defence system. Consequently, these genotypes could potentially be successfully used for the phytoremediation of Zn-contaminated areas. However, further studies are required to screen all growth stages for Zn tolerance capacity before making a more informed decision regarding the phytoremediation potentials of these two genotypes.

Keywords: Antioxidant defence system, Chlorophyll *a* fluorescence induction, Growth characteristics, Maize (*Zea mays* L.), Photochemical activity, Zinc toxicity

1. Introduction

Heavy metal accumulation in terrestrial and aquatic environments disrupts the normal functioning of ecosystems by causing strong toxicological effects on all living forms, including microorganisms, plants, animals and humans (Anwaar et al. 2015; Paunov et al. 2018; Alsafran et al. 2023; Sharma et al. 2023). Due to industrial and agricultural activities, such as mining, electroplating, leather tanning, traffic, use of sewage sludge or agrochemicals and fertilizers (stable manure) obtained from animals fed with feed containing heavy metals has become a global environmental crisis (Glińska et al. 2016; Chen et al. 2017). Elements such as cadmium (Cd), aluminum (Al), copper (Cu), arsenic (As), manganese (Mn), iron (Fe), mercury (Hg), nickel (Ni), zinc (Zn), cobalt (Co) and lead (Pb) are among these heavy metals. However, some of these metals (Cu, Fe, Mn and Zn) are classified as essential nutrients for the many structural and biochemical functions of plants (Karahan et al. 2020; Dobrikova et al. 2022; Alsafran et al. 2023).

Zinc (Zn^{2+}) is the second transition metal after Fe according to its abundance in plants. The uptake of Zn by plants from the soil depends on its concentration, soil clay fraction and soil pH (Andrejić et al. 2018; Antoniadis et al. 2018). Zn takes charge of many metabolic processes including the maintenance of the integrity of cell walls and membranes, regulation of the activity of many enzymes (isomerases, hydrolases, oxidoreductases, transferases, carbonic anhydrase, etc.), photosynthesis, carbohydrate, lipids and nucleic acid metabolism, regulation of the activities of hormones, pigment synthesis, gene expression and regulation, protein synthesis, and defence against stressors (Diaz-Pontones et al. 2021; Dobrikova et al. 2022). However, if the physiological range is exceeded, zinc concentrations rise above tolerable levels and a toxic effect occurs. Meanwhile, acidic soil pH increases the Zn solubility and uptake by plants (Chaney 1993; Kaur & Garg 2021; Natasha et al. 2022). High Zn concentrations in soil,

leading to the accumulation of approximately 400-500 mg kg⁻¹ DW Zn in the leaf tissues (Chaney 1993; Marschner 1995), can induce disruptions in the morphological, physiological and biochemical processes, limiting plant growth and development. Major indications of Zn toxicity include decrease in yield, reduction in leaf area, a lower biomass accumulation, formation of chlorosis and necrotic areas on leaves, root damages, reduced germination and stunted growth (Anwaar et al. 2015; Chen et al. 2017; Dobrikova et al. 2021). Zn toxicity is also associated with water imbalance, altered uptake and translocation of nutrients (such as P, Fe, and Mg deficiency) and change in membrane permeability (Ramakrishna & Rao 2015; Petrovic & Krivokapic 2020; Seregin et al. 2023). Moreover, Zn toxicity can restrict photosynthesis at a range of different structural-functional levels by reducing pigmentation, transpiration rate and stomatal and mesophyll conductivity, increasing respiration, reducing the activity of Calvin cycle enzymes and/or limiting photochemical reactions (Andrejić et al. 2018; Szopiński et al. 2019). Studies have shown that the photosynthetic responses of plants exposed to Zn toxicity vary depending on the plant species, Zn concentration or genetic variance (Paunov et al. 2018; Szopiński et al. 2019; Fatemi et al. 2020). In addition, the imbalance between absorption and consumption of light energy in the photosynthetic pathway by Zn toxicity triggers the overproduction of reactive oxygen species [ROS - hydroxyl radical (OH[•]), superoxide radical (O₂^{-•}), and hydrogen peroxide (H₂O₂)]. Excessive ROS production disrupts redox homeostasis in cells and eventually causes oxidative stress in the plant (Chen et al. 2017). To cope with the destruction caused by ROS, plants have complex antioxidant protection systems consisting of enzymatic [superoxide dismutase (SOD), guaiacol peroxidase (POD), ascorbate–glutathione cycle enzyme (ascorbate peroxidase-APX and glutathione reductase-GR), etc.] and non-enzymatic (ascorbate, glutathione, anthocyanins, flavonoids, carotenoids, etc.) components (Miller et al. 2008; Yin et al. 2018).

Maize is one of the main cereal crops cultivated globally along with rice and wheat and is used as a raw material in the starch, syrup, industrial alcohol (ethanol for beer or whiskey) and bioplastic making industries as well as human and animal nutrition (Díaz-Pontones et al. 2021; Abedi et al. 2022). According to the 2021 data of FAOSTAT, maize is the most produced plant worldwide after sugarcane. Furthermore, due to its adaptability to many different environmental conditions, maize has a wide cultivation area from temperate to tropical regions (Saboor et al. 2021). As a consequence of its widespread use and enormous potential maize is sometimes referred to as the “miracle crop” and/or “queen of cereals” (Suganya et al. 2020). Unfortunately, maize kernels are naturally poor in zinc minerals, so maize is used as an indicator plant for the evaluation of Zn deficiency in soil (Ayyar & Appavoo 2017). Although most of the studies conducted with maize are related to the effects of Zn deficiency on plants and improving Zn deficiency, several studies have examined the effects of Zn toxicity on growth, photosynthesis, antioxidant system, yield and/or Zn content in different development stages as well as germination, stalk elongation and tassel formation, and reproductive stage (Alonso-Blázquez et al. 2015; Janeeshma et al. 2021). Despite relatively rich database on the effects of toxic Zn levels on plant metabolism, it is evident that there are still some unresolved issues. For example, the effect of toxic Zn levels on photochemical activity and antioxidant defence mechanisms at the cellular level is not sufficiently clear at the early seedling stage, when the organs necessary for maize to perform their vital functions begin to develop and mature. Considering the lack of information on this subject, the main objective of this study is to elucidate the photochemical and antioxidant defence strategies in the seedlings of two maize genotypes exposed to zinc toxicity. The relationship between Zn toxicity and tolerance of genotypes at the early seedling stage was comparatively investigated from the point of the membrane structure, photosynthetic pigment contents, functionality of photosystems and antioxidant defence mechanisms.

2. Material and Methods

2.1. Plant materials, growth and treatment conditions

The seeds of the maize (*Zea mays* L. namely DK626 and 3223) genotypes were used in this study. In previous studies conducted by Ünalán (2006), it was determined that DK626 was tolerant and 3223 was sensitive to Zn toxicity at the germination stage. The seeds were germinated onto filter papers wetted with distilled water in germination boxes (20 x 13.5 x 8 cm) at 23±2 °C in dark conditions for 5 days. Subsequently, the seedlings of the genotypes were transferred to plastic pots (14 x 13 cm) filled with perlite and watered with Hewitt's nutrient solution (N, 168; P, 41; K, 156; Mg, 36; Ca, 160; S, 48; Fe, 2.8, Mn, 0.55; B, 0.54; Cu, 0.064; Zn, 0.065 and Mo, 0.048 mg L⁻¹) every other day. The plants were grown in a controlled growth room at a temperature regime of 25±1 °C, with 40±5% humidity, 16 h photoperiod and at 300 µmol m⁻² s⁻¹ light intensity. On the 8th day after transfer, zinc treatment was initiated for the next 12 days by applying Hewitt's nutrient solution containing 2, 5 and 8 mM ZnSO₄·7H₂O to seedlings. At the end of the zinc treatment period, the seedlings were harvested for the morphological, physiological and biochemical analyses.

2.2. Growth parameters

The shoot (the distance from perlite surface to the tip of the longest leaves) and root lengths (the longest seminal roots) of the maize seedlings were measured (cm plant⁻¹) for each zinc treatments. In addition, three plants were randomly taken from shoot and root for each treatment and their fresh weight (g plant⁻¹) was measured and then kept in an oven at 80 °C for 48 hours to determine the dry weight of these plants (g plant⁻¹).

2.3. Zinc content

The leaves of the harvested seedlings were washed in deionized water, then dried in oven at 80 °C for 48 hours and subsequently mill ground to powder. The tissues powder was burned in a muffle furnace at 550 °C for 4 h. The ash was brought to a standard volume with 1 M HNO₃. The Zn content in the tissues was determined using flame atomic absorption spectrophotometer (Unicam, 929 AAS) and the Zn contents of the leaves was calculated (mg kg⁻¹ DW). Additionally, the bioaccumulation factor (BF) were calculated according to Roccotiello et al. (2010).

The bioaccumulation factor (BF): $\text{metal content}_{\text{shoot}}/\text{metal content}_{\text{soil}}$ (1)

2.4. Chlorophyll *a* fluorescence measurements

Chlorophyll *a* fluorescence measurements were performed with a portable, modulated fluorescence monitoring system (FMS2; Hansatech Ltd., Norfolk UK) on randomly selected leaves of the maize cultivars (6 replicates). Following at least 30 min of dark adaptation, the minimum chlorophyll *a* fluorescence (F_O) was determined using a measuring beam of 0.2 $\mu\text{mol m}^{-2} \text{s}^{-1}$ intensity. A saturation pulse (1 s of white light of 7500 $\mu\text{mol m}^{-2} \text{s}^{-1}$ intensity) was used to obtain the maximum fluorescence (F_M) after a dark-adapted state was reached. The maximal quantum efficiencies of PSII of dark-adapted plants (F_V/F_M and its more sensitive F_V/F_O) were calculated using Equation 2. F_V is known to be the variable fluorescence (Equation 3). Light-induced changes in chlorophyll *a* fluorescence following actinic illumination (300 $\mu\text{mol m}^{-2} \text{s}^{-1}$) were recorded prior to the measurement of F'_O (minimum chlorophyll *a* fluorescence in light-saturated state) and F'_M (maximum fluorescence in light-saturated state). The quantum efficiency of PSII open centers in the light-adapted state, referred to as ΦPSII (Equation 4), was determined from F'_M and F_S (steady-state fluorescence in the light-saturated state) values. The quantum efficiency of the excitation energy trapping of PSII (Equation 5) was calculated according to Genty et al. (1989). After the actinic light was shut off, the minimum fluorescence in the light-adapted state (F'_O) was determined by illuminating the leaves with far-red light (7 $\mu\text{mol m}^{-2} \text{s}^{-1}$). The photochemical quenching (Equation 6) and the nonphotochemical quenching (Equation 7) were calculated according to Genty et al. (1989). The electron transport rate (ETR) was determined by multiplying the quantum efficiency by incident photon flux density and an average factor of 0.84 for leaf absorbance and dividing by a factor of 2 to account for the sharing of absorbed photons between the two photosystems (PSI and PSII, Equation 8) (Genty et al. 1989). Additionally, the quantum yields of chlorophyll photophysical decay of light-adapted leaves referred to as Φ_C (Equation 9) were calculated (Guadagno et al. 2010; Calvo et al. 2017). Based on these, the energy partitioning in the PSII complex occurs in three parts; the photochemical processes, nonphotochemical quenching (heat dissipation) and chlorophyll photophysical decay. These three mechanisms are competitive and their sum is equal to 1 (Equation 10).

$$F_V/F_M = (F_M - F_O) / F_M \quad (2)$$

$$F_V = F_M - F_O \quad (3)$$

$$\Phi\text{PSII} = (F'_M - F_S) / F'_M \quad (4)$$

$$F_V'/F_M' = (F_M' - F_O') / F_M' \quad (5)$$

$$qP = (F'_M - F_S) / (F'_M - F'_O) \quad (6)$$

$$\text{NPQ} = F_M - F'_M / F'_M \quad (7)$$

$$\text{ETR} = (F'_M - F_S) / (F'_M) \times \text{PAR} \times 0.84 \times 0.5 \quad (8)$$

$$\Phi_C = F_S/F_M \quad (9)$$

$$\Phi\text{PSII} + \text{NPQ} + \Phi_C = 1 \quad (10)$$

2.5. Pigment analysis

The photosynthetic pigment [chlorophyll (Chl *a*, *b*) and carotenoids (Car *x*, *c*)] contents were determined from the leaf sample and calculated as mg g FW⁻¹ according to Lichtenthaler (1987). The absorbance values of the solutions were recorded at the 470, 644.8 and 661.6 nm and the pigment contents were calculated using the following equation:

$$\text{Chl } a = (11.24 \times A_{661.6}) - (2.04 \times A_{644.8}) \quad (11)$$

$$\text{Chl } b = (20.13 \times A_{644.8}) - (4.19 \times A_{661.6}) \quad (12)$$

$$\text{Total Chl} = (7.05 \times A_{661.6}) - (18.09 \times A_{644.8}) \quad (13)$$

$$\text{Car} = [(1000 \times A_{470}) - (1.9 \times \text{Chl } a) - (63.14 \times \text{Chl } b)] / 214 \quad (14)$$

In addition, the Chl *a/b* ratio was calculated from the Chl data. The anthocyanin content (mg g FW⁻¹) was determined according to the method of Mancinelli et al. (1975). The absorbances were recorded at the 530 and 657 nm and the content was calculated using the following equation:

$$\text{Anthocyanin content} = A_{530} - (A_{657}/3) \quad (15)$$

2.6. Antioxidant enzyme and isoenzyme activities

Fresh leaf samples (0.5 g and 3 replicates) were ground with liquid nitrogen and the soluble protein was extracted in the antioxidant enzyme related extraction buffer. Protein concentrations from leaf extracts were determined according to (Bradford 1976). Fine powder was homogenized in 1 mL of buffer containing 9 mM Tris-HCl buffer (pH 6.8) and 13.6% glycerol and SOD (EC 1.15.1.1) enzyme and isoenzyme activities were determined (Laemmli 1970; Beauchamp & Fridovich 1971; Beyer & Fridovich 1987). Guaiacol POD (EC 1.11.1.7) enzyme activity was based on the determination of guaiacol oxidation ($\epsilon = 26.6 \text{ mM cm}^{-1}$) at 470 nm by H₂O₂ (Pütter 1974). In addition, POD isoenzyme was assayed according to Rao et al. (1995). APX (EC1.11.1.11) enzyme and isoenzyme activities were assayed according to the method of Wang et al. (1991) and the staining of non-denatured polyacrylamide gels was performed according to Mittler & Zilinskas (1993). GR (EC 1.6.4.2) enzyme activity was determined by following the decrease in absorbance at 340 nm due to NADPH oxidation (Sgherri et al. 1994) and GR isoenzyme was determined to make the bands in non-denatured polyacrylamide gels apparent according to the method of Rao et al. (1995). SOD, POD, APX and GR isozyme bands were visualized and analyzed using the Bio-Profil V99 software program of the Vilber Lourmart imaging system (Marne la Vallee, France).

2.7. Statistical analysis

The experiments were performed in a completely randomized design by three replicates. Differences among the treatments as well as between the genotypes were analyzed using the SPSS 20.0 (Chicago, IL, USA). Statistical variance analysis of the data was performed using ANOVA and compared with the least significant differences (LSD) at the 5% level.

3. Result and Discussion

Zinc (Zn) plays a crucial role in various biological functions for all living organisms; however, plants employ different strategies to cope with the uptake, transport, and retention of high Zn concentrations, which can lead to toxicity (Anwaar et al. 2015; Petrovic & Krivokapic 2020; Kaur & Garg 2021; Stanton et al. 2022). In this study, it was investigated that the effects of Zn toxicity on the morphological structure, photochemical efficiency and antioxidant defence systems of maize genotypes. The bioaccumulation factor (BF) is accepted to be one of the important indexes for phytoremediation that imply the potential of plants to regulate the uptake, transport and accumulation of metals in their aerial parts (Rai et al. 2019; Wieczorek et al. 2023). Elevated toxic Zn concentration caused the decrease in BF of both maize genotypes (Figure 1). Although the amount of Zn required for optimum growth is universally assumed to be in the range of 30 to 200 $\mu\text{g g}^{-1}$ DW within plants, some species can accumulate zinc of more than 10.000 $\mu\text{g g}^{-1}$ DW without showing any indication of toxicity (Sofa et al. 2013; Sperdouli et al. 2022). By contrast, Zn is accepted to be toxic for plants when the tissue concentration is above 400 $\mu\text{g g}^{-1}$ DW (Sofa et al. 2013). The amount of Zn in the control leaves of DK626 and 3223 genotypes were measured as 342 and 347 $\mu\text{g g}^{-1}$ DW, respectively, and these values were below the threshold considered to be toxic (Figure 1). In all Zn treatments, both genotypes accumulated Zn significantly and similarly in their tissues, and this accumulation generally increased in parallel with the increase in application levels (41, 123 and 119-fold in DK626, and 47, 119 and 128-fold in 3223 at the 2, 5 and 8 mM compared to the control, respectively). This could be indicative that the leaves were approaching the saturation point in Zn uptake and accumulation under high toxicity conditions. When the results above are evaluated together, maize genotypes have exhibited almost similar tolerance to Zn toxicity, and these genotypes could be used as accumulator crops for contaminated soil with toxic zinc metal due to both genotypes having a bioaccumulation factor (BF) > 1. Wieczorek et al. (2023) have reported that if the BF values of plants are greater than 1 under zinc toxicity, it can be considered as a bioaccumulator plant.

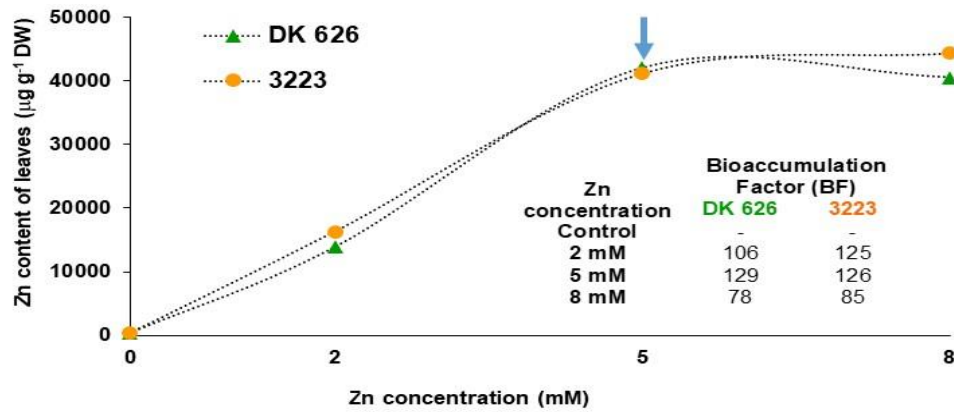


Figure 1 - Zinc content (g kg⁻¹ DW) in leaf tissue of maize genotypes

Zn accumulation in leaves caused growth restrictions by altering the ion balance and disrupting metabolic processes (Tiecher et al. 2017; M’Rah et al. 2023). The root and shoot lengths of maize genotypes were significantly declined in especially 5 and 8 mM Zn treatments (more than 8%) (Figure 2). In addition, a gradual reduction in biomass accompanied these alterations, and the fresh and dry weights of shoot and root decreased under all Zn treatments in DK626 (24-60% and 16-70% compared to control, respectively), whereas the decreases in biomass were more pronounced under the 5 and 8 mM Zn concentration in 3223 (21-54% and 35-67% compared to control, respectively) (Figure 2 and 3). Declines in biomass production and lengths are general responses of Zn toxicity and, therefore, these parameters are frequently a reliable indicator of the plant's susceptibility to stress (Glińska et al. 2016). Moreover, the root/shoot dry weight ratio and total biomass values indicated that root and shoot growth were similarly affected in DK626 under Zn toxicity, with the exception of the 2 mM Zn concentration, while the root growth was more inhibited in 3223 only at the highest toxicity (8 mM) (Figure 3). Many researchers have stated that roots are in direct contact with zinc toxicity, so the toxicity is first perceived by the roots, which triggers a reduction in cell division and a change in hormone balance and a retardation of minerals and water acquisition, thus limiting root growth (Glińska et al. 2016; Kaur & Garg 2021). In addition to these, all growth parameters values decreased more dramatically in DK626 compared to 3223, revealing that DK626 was slightly sensitive to zinc toxicity.

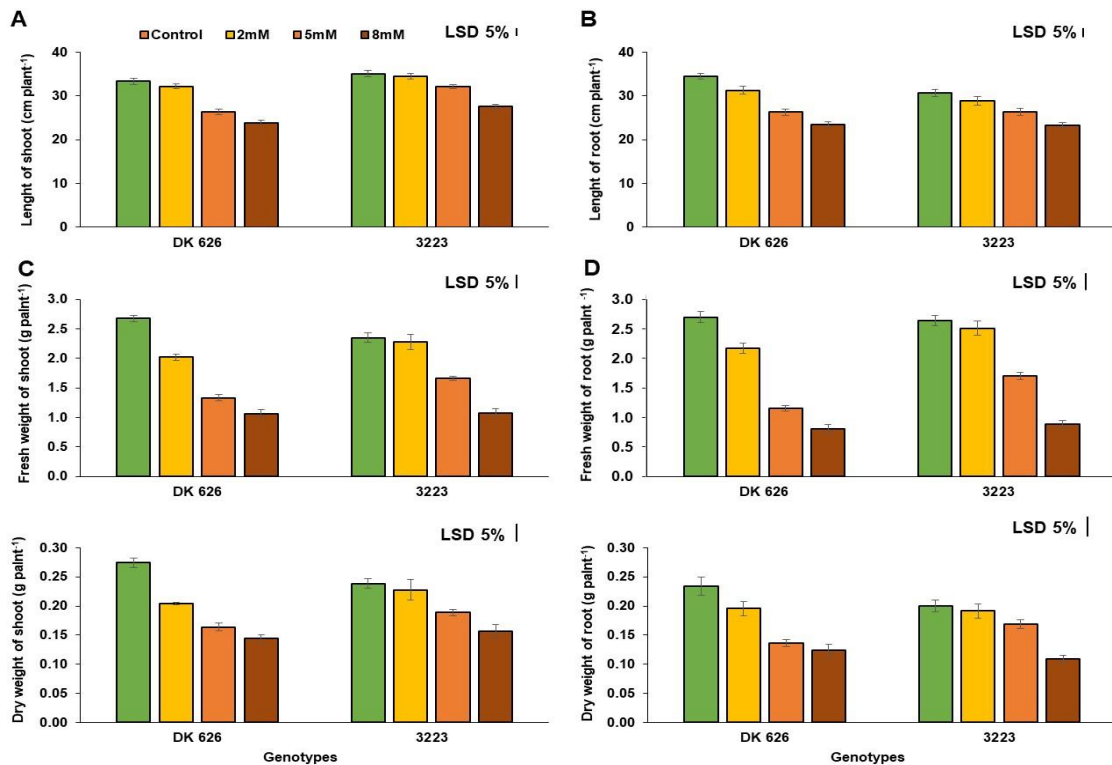


Figure 2- Length of shoot (A) and root (B), fresh weight of shoot (C) and root (D), and dry weight of shoot (E) and root (F) of maize genotypes exposed to Zn toxicity. The values are presented as the mean ± standard error (SE), n=15 for length of shoot and root and n=5 for fresh and dry weight of shoot and root. The bars and different letters indicate significant differences between treatments and cultivars at P<0.05 according to the LSD test

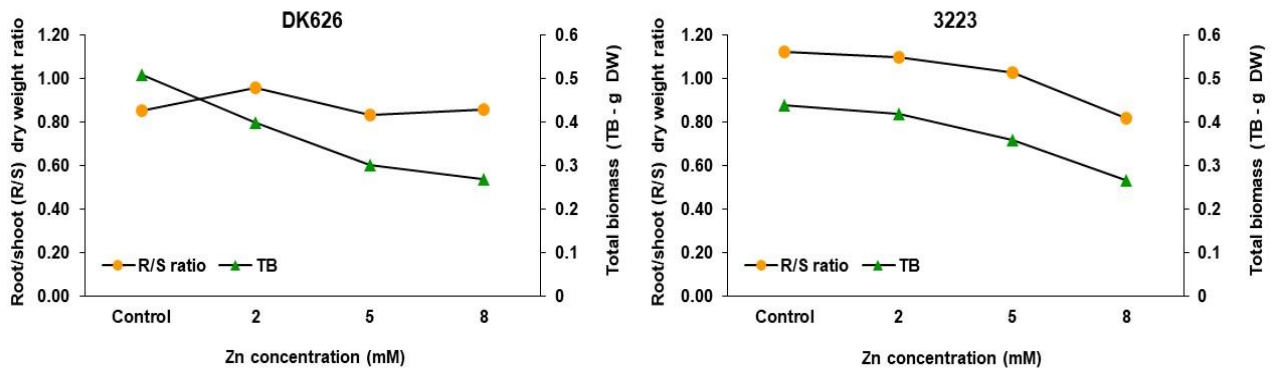


Figure 3 - The effects of Zn toxicity on root/shoot dry weight ratio and total biomass accumulation in maize genotypes. Values shown are mean \pm SE

Oxidative stress, which occurs due to uncontrolled and excessive production of reactive oxygen species (ROS), is among the main factors that impair metabolic function by affecting cellular structures in plants exposed to heavy metal stress conditions. The non-quenched ROS trigger peroxidation in cellular membranes, resulting in an increase in malondialdehyde (MDA), an indicator of lipid peroxidation (Ramakrishna & Rao 2015; Dobrikova et al. 2021; Kaur & Garg 2021). MDA content increased 3.0 and 6.3- fold in DK626 at 5 and 8 mM Zn concentrations, while it elevated gradually 1.4 to 3.1-fold in 3223 at all Zn treatments (Table 1). It has been reported that under toxic Zn conditions, ultrastructural alterations of cellular organelles such as chloroplasts and mitochondria occur due to the disruption of the membrane structures of these organelles (Mukhopadhyay et al. 2013). In addition, Jayasri & Suthindhiran (2017) have suggested that heavy metals such as Zn and Pb could demolish the structure and function of chloroplast by attaching to sulfhydryl (-SH) group of the chloroplast proteins and could limit the chlorophyll biosynthesis by targeting Fe and Mg. The increase in MDA content, which indicates degradation in the membrane structures, could have limited plant biomass production in maize genotypes by destroying the structure of chlorophyll pigments and photosynthetic apparatus (Figure 4 and 5).

Table 1 - Effects of elevated toxic zinc concentration on malondialdehyde (MDA) content in the leaves of two maize cultivars. Each value represents the mean \pm SE (n = 3)

Cultivars	Zn concentration			
	Control	2 mM	5 mM	8 mM
DK 626	3.84 \pm 0.03 ^a	3.66 \pm 0.06 ^a	11.38 \pm 0.03 ^b	23.12 \pm 0.20 ^c
3223	2.96 \pm 0.10 ^a	4.15 \pm 0.09 ^b	6.86 \pm 0.01 ^c	9.15 \pm 0.09 ^d
LSD 5%	0.39			

The novelty of this study is to address the lack of research data concerning the effects of zinc toxicity on photosynthetic functionality strategy of maize genotypes in the early seedling stage. For this purpose, the effect of Zn toxicity on energy fluxes of utilization and dissipation of light energy absorbed by PSII was evaluated by using the chlorophyll a fluorescence technique (Figure 4). The maximal quantum efficiency of PSII (F_v/F_m) slightly decreased in both maize genotypes at the 5 and 8 mM Zn treatments (Figure 4C). The alterations in F_v/F_m ratio reflect disruptions in the photochemical activity of PSII (Küpper & Andresen 2016). The F_v/F_o value, which provides information regarding the maximum quantum yield of PSII photochemistry (Lichtenthaler et al. 2005), was significantly decreased due to zinc toxicity compared to F_v/F_m (Figure 4D). Lichtenthaler et al. (2005) have also reported that F_v/F_o is more sensitive parameter than F_v/F_m . The decreases in F_v/F_m and F_v/F_o of genotypes were due to the increases in F_o and decrease in F_m , particularly under 5 and 8 mM Zn treatments (Figure 4A and B). The decline in F_m could indicate that the reduced Q_A ratio increases and accordingly the electron transfer from Q_A to the Q_B slows down (Andrejić et al. 2018) and could also imply PSII photoinhibition (Sapeta et al. 2023). In addition, Paunov et al. (2018) suggested that the decrease in F_m may be partially related to a decrease in the content of chlorophyll a. A similar relationship between Chl $a+b$ content and Chl a/b ratio was found in this study (Figure 5A and C). The increase of F_o could be a result of the decline in the transfer of excitation energy from the antenna complex to the reaction center of the PSII, but also to the direct effect of Zn on the reaction centers of PSII (Vaillant et al. 2005). These alterations in F_o and F_m of genotypes have indicated that there was damage to the acceptor and donor sides of PSII at high Zn concentrations. In a similar manner to F_v/F_m and F_v/F_o ratios, the value of F'_v/F'_m diminished marginally in both maize genotypes at 5 and 8 mM Zn concentrations (Figure 4E). The decline in F'_v/F'_m indicated that Zn toxicity also caused a deterioration in the efficiency of trapping the excitation energy by open PSII reaction centers. The observed decreases in F_v/F_m and F'_v/F'_m could be due to Zn-induced deterioration in the structure of PSII reaction centers or photoinhibition of PSII, which could trigger a decrease in the electron transfer rate from Q_A to Q_B and a subsequent reduce in electron flow from PSII to PSI (Paunov et al. 2018). Moreover, the ETR of both genotypes were also

adversely affected by elevated Zn toxicity (especially at higher Zn levels) (Figure 4J). Other studies have reported that photosynthetic electron transport was decreased in wheat, Arabidopsis and young bean by zinc toxicity (Paunov et al. 2018; Szopiński et al. 2019). It has been suggested that the detrimental effect of Zn on photosynthetic electron transport is due to the loss of membrane integrity, decreased permeability of biomembranes, and the disassembly of the thylakoid membrane due to the production of reactive oxygen species under stress (Balafrej et al. 2020). The Φ_{PSII} value which expresses the efficiency of the energy used to drive photosynthesis slightly declined only in DK626 at 5 and 8 mM Zn concentrations (Figure 4F). Despite the changes in F'_V/F'_M and ETR, photochemical quenching (qP) was not significantly affected in maize genotypes at any Zn concentrations (Figure 4G). The qP expresses the trapping photon energy that derives photosynthesis and also results from the activation of light-induced enzymes involved in carbon metabolism and the opening of stomata (Calvo et al. 2017). The stability of qP under Zn toxicity indicated that maize genotypes could protect a balance between the captured photon energy and the use of electrons passing through the photosynthetic electron transport chain (Çiçek & Çakırlar 2008). The excitation energy absorbed by plants is accomplished in the dissipation in three separate ways: it can be used in the photochemical pathway, it can be distributed in photophysical processes (fluorescence, inductive rezonans and radiationless transfer) or it can be dispersed by thermal deactivation (non-photochemical quenching) (Iriel et al. 2019). However, non-photochemical quenching (NPQ) markedly reduced at all Zn treatments in DK626 (16, 26 and 25% decrease at 2, 5 and 8 mM Zn concentrations, respectively) and only at 2 mM Zn concentration in 3223 (26%) (Figure 4H). The findings reveal that the excess excitation energy not used in the photochemical pathway was dissipated by using photophysical processes instead of the photoprotective pathway NPQ in maize genotypes, especially in DK626, under Zn toxicity. The Φ_C , expresses the quantum yield of chlorophyll photophysical decay, displays the efficiency of photophysical processes, and is associated with radiative degradation of chlorophyll (Guadagno et al. 2010). The Φ_C increased significantly at 5 and 8 mM Zn treatments in DK626 (17 and 14%, respectively), and only at the highest Zn concentration in 3223 (8%) (Figure 4I). These indicated that Zn toxicity induced a greater fraction of the excitation energy to be lost from the reaction centers as fluorescence and non-radiative inactivation of reaction centres (Cordon et al. 2018). Moreover, these three mechanisms are competitive in sharing the absorbed energy, and, therefore, any alteration in the quantum efficiency of one can typically induce changes in the efficiency of the others (Maxwell & Johnson 2000; Iriel et al. 2019). Consequently, all chlorophyll fluorescence results have revealed that the effects of toxic Zn levels on photochemical activity were minor. Also, along with somewhat occurrence of photoinhibition in the photosynthetic apparatus due to zinc toxicity, the results obtained may suggest that an adaptation mechanism has been working and a balance has been established.

Regarding pigments, exposure to Zn toxicity dramatically decreased chlorophyll and carotenoid concentrations in maize genotypes (Figure 5A and B). The Chl *a+b* content decreased by 35-71% and 23-56% with increasing Zn concentration in DK626 and 3223, respectively. The reduction of the chlorophyll content may be due to many possible and interrelated causes: obstruction of enzyme activities involved in chlorophyll biosynthesis such as δ -aminolevulinic acid dehydratase (ALA-D) and protochlorophyllide reductase as a result of interference to the functional sulfhydryl region of Zn and/or activation of the chlorophyll-degrading enzyme chlorophyllase as well as competition of Zn with Fe and Mg in the structure of the intermediate or final product during chlorophyll synthesis (Anwaar et al. 2015; Ramakrishna & Rao 2015; Kaur & Garg 2021) as well as lipid peroxidation, especially photosynthetic membrane damage.

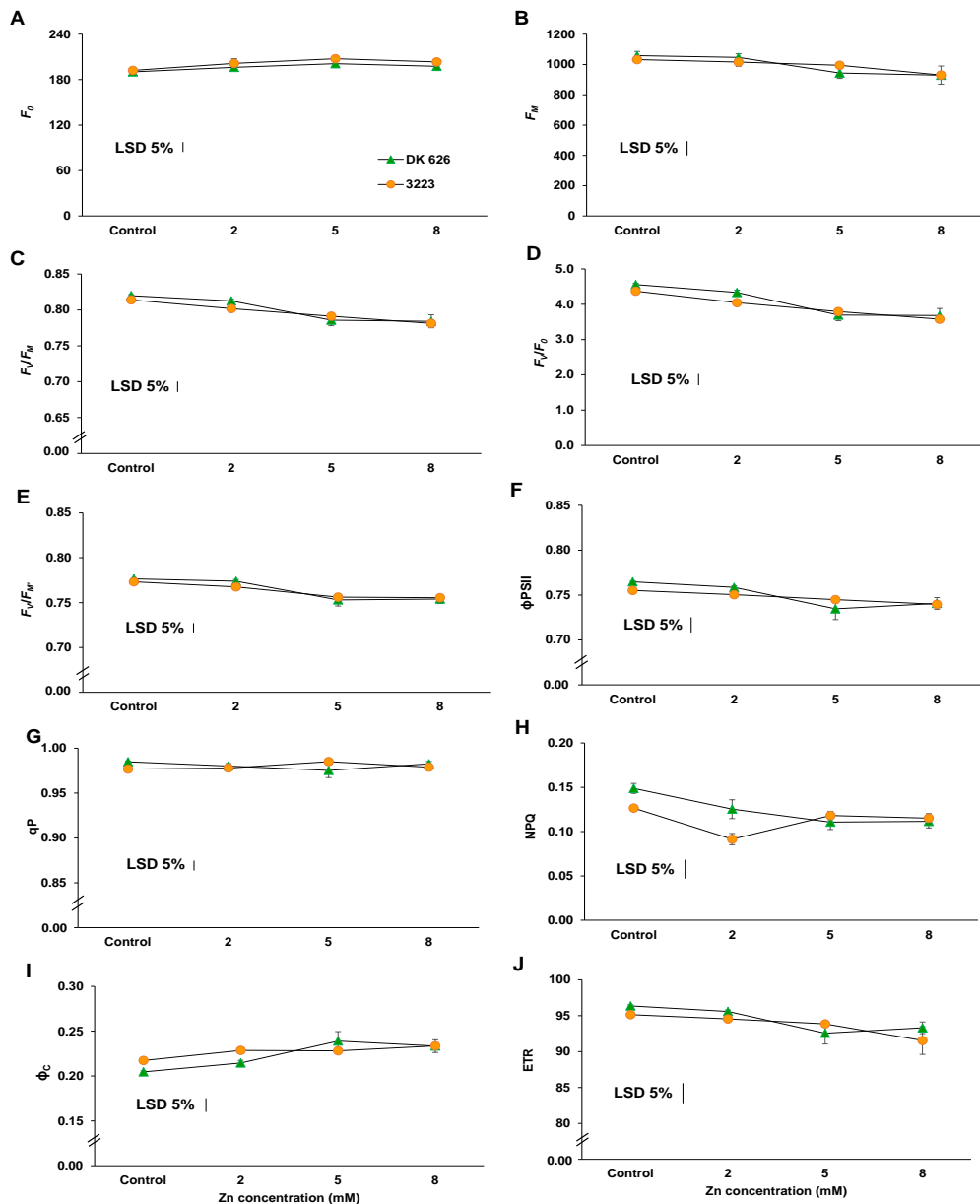


Figure 4 - F_0 , minimum fluorescence (A); F_M , maximum fluorescence (B); F_V/F_M and F_V/F_0 , maximum quantum yields of PSII (C and D); F_V'/F_M' , quantum efficiency of excitation energy trapping of PSII of light-adapted leaves (E); ϕ_{PSII} , efficiency of open reaction centre of light adapted state (F); qP , photochemical quenching (G); NPQ , nonphotochemical quenching (H); ϕ^C , quantum yields of chlorophyll photophysical decay of light-adapted leaves (I) and ETR , electron transport rate (J) of maize genotypes exposed Zn toxicity. The error bars represent the standard error ($\pm SE$) for six replicates

Zn toxicity caused a decrease in the Chl *a/b* ratio as well as reducing pigment content, and the reduction was remarkable in DK626 at 5 and 8 mM Zn treatments (17 and 25%, respectively) (Figure 5C). The decline indicated that Chl *a* had a higher sensitivity to Zn exposure than Chl *b*. Moreover, the Chl *a/b* ratio is an indicator that reveals the status of light harvesting complexes (LHC) and reaction center of PSs, because LHC contains Chl *a* and Chl *b*, whereas the reaction centers only contain Chl *a* (Çiçek & Çakırlar 2008). In addition, the Car content decreased by 37-71% in DK626 and 23-55% in 3223 under Zn toxicity. The ratio of Chl (*a+b*) / Car (*x+c*) was also decreased by zinc toxicity, indicating the Chl content declined more than the Car content (Figure 5D). Several studies show that excess Zn could induce the decrease in carotenoid content (Ramakrishna & Rao 2015; Paunov et al. 2018). In addition to chlorophylls and carotenoids, leaf colors in plants are associated with a change in the relative content of other pigments including anthocyanin (Pan et al. 2020). The anthocyanin content increased by 73 and 82% in DK626 at the 5 and 8 mM Zn concentrations, respectively, and 41% at 8 mM Zn treatments in 3223 compared to controls (Figure 5E). It has been reported that Zn-induced anthocyanin synthesis and accumulation may play a role in protecting cell macromolecules from oxidative stress and/or increasing metal chelation in plants (Sofa et al. 2018; Szopiński et al. 2019; Kaur & Garg 2021). Moustaka et al. (2018) have claimed that the biosynthesis of anthocyanin was strongly related to the redox state of plastoquinone pool in the red leaves of poinsettia under high light intensity conditions and this accumulation could serve a protective role, limiting the production of ROS.

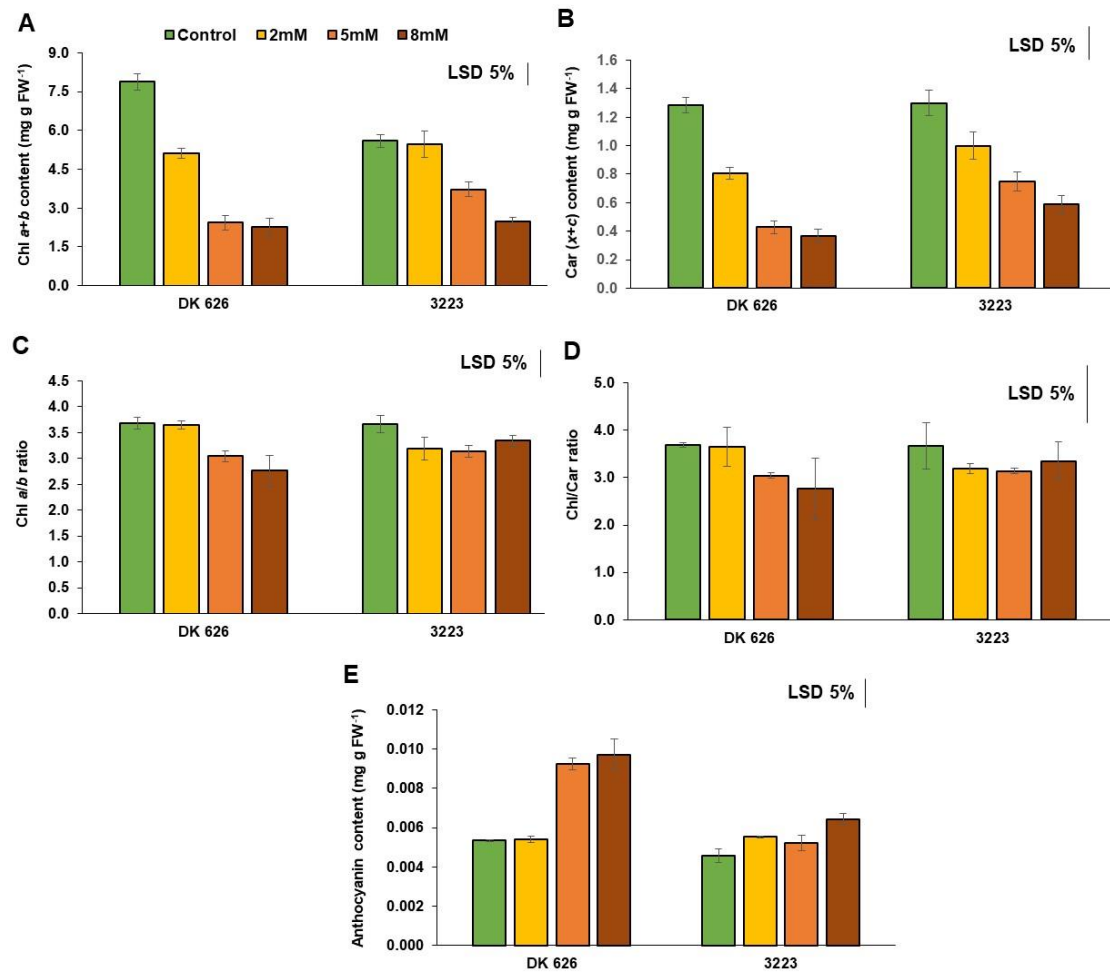


Figure 5 - Chlorophyll (Chl) *a* + *b* (A) and carotenoid (B) contents, Chl *a*/*b* ratio (C), Chl / Car ratio (D) and anthocyanin content (E) in leaves of maize genotypes at elevated toxic Zn concentrations. The values are presented as the mean \pm standard error (SE), $n=5$ for chlorophyll and carotenoid and $n=3$ for anthocyanin. The bars and different letters indicate significant differences between treatments and cultivars at $P<0.05$ according to the LSD test

Zinc is a redox-inert element that cannot carry out monovalent oxidation-reduction reactions, but it can indirectly induce the generation of ROS such as $O_2^{\cdot-}$ and H_2O_2 (Díaz-Pontones et al. 2021). However, Zn also plays a role in scavenging ROS due to its role as a component of antioxidant enzymes (Dalcorsio et al. 2014). In this way, excess zinc causes an imbalance between ROS and detoxification mechanism, and in this case, oxidative stress is triggered, which causes cellular damage (Ramakrishna & Rao 2015; Sofu et al. 2018). Oxidative stress is generally determined by the change in MDA content, a marker of lipid peroxidation (Sperdouli et al. 2021). In our study, the marked increase in Zn content and MDA contents, and the significant decrease in plant biomass and lengths at the highest Zn concentrations are an indication of triggering oxidative stress. The activities of four antioxidant enzymes and their isoenzymes in the cellular defence system of maize leaves under Zn toxicity were examined in this study: SOD, which catalyzes the conversion of $O_2^{\cdot-}$ radicals to H_2O_2 and O_2 ; subsequently; POD, APX and GR in detoxifying the formed H_2O_2 (Figure 6). Total SOD enzyme activity was increased in all Zn treatments compared to controls; however, it was statistically significant only at the highest Zn concentration in DK626 (2.2-fold) and at 5 mM Zn treatment in 3223 (1.8-fold) (Figure 6A). Also, three SOD isoforms were detected in leaves of both genotypes and the alteration in band intensity of the isoforms supported changes in total SOD isoenzyme activity (Figure 6A, right side). Total POD enzyme activity was increased only at 2 mM Zn concentration in DK626 and at 5 mM Zn treatment in 3223 (about 1.4 and 1.3-fold, respectively) compared to their controls (Figure 6B). As a comparison, four POD isoforms in maize leaves, with one different band in each genotype, were separated with non-denaturing PAGE. The band densities of POD isoforms enhanced at the same levels of Zn treatment that the total enzyme activities were increased. APX activity remained unchanged in the DK626 genotype (except 8mM), whereas it significantly increased in the 3223, especially under the highest zinc toxicity (Figure 6C). In addition, the alteration of GR activity in DK626 exposed to Zn toxicity was found to be similar to that in APX activity, and GR activities were found somewhat increased in DK626 under all Zn treatments (Figure 6D). For this reason, we suggest that POD may have played a more active role in H_2O_2 scavenging in DK626 under excess zinc treatments. In 3223, total APX activity was significantly upregulated at 5 and 8 mM Zn treatments (about 1.41 and 1.75-fold, respectively) whereas increased GR activity was detected at 2 and 5 mM Zn concentrations (approx. 1.7 and 2-fold, respectively). Moreover, alteration in the number of bands and/or band intensity of the isoforms in the gel images of APX and GR enzymes in 3223 supported the changes in the total enzyme activity (Figure 6C and D). These findings indicate that the 3223 genotype used the ascorbate-glutathione cycle to

detoxify H_2O_2 and in this pathway catalyzes ascorbate (AsA) to form monodehydroascorbate (increased APX activity) while increasing recuperation of GSH from GSSG (increased GR activity). Various studies have exhibited that the increases in POD and Asada-Halliwell pathway enzymes (APX, GR etc.) activities in plants were detoxified damaging effects of metal toxicity (Ekmeççi et al. 2008; Mukhopadhyay et al. 2013; Tiecher et al. 2017; Baran & Ekmeççi 2022).

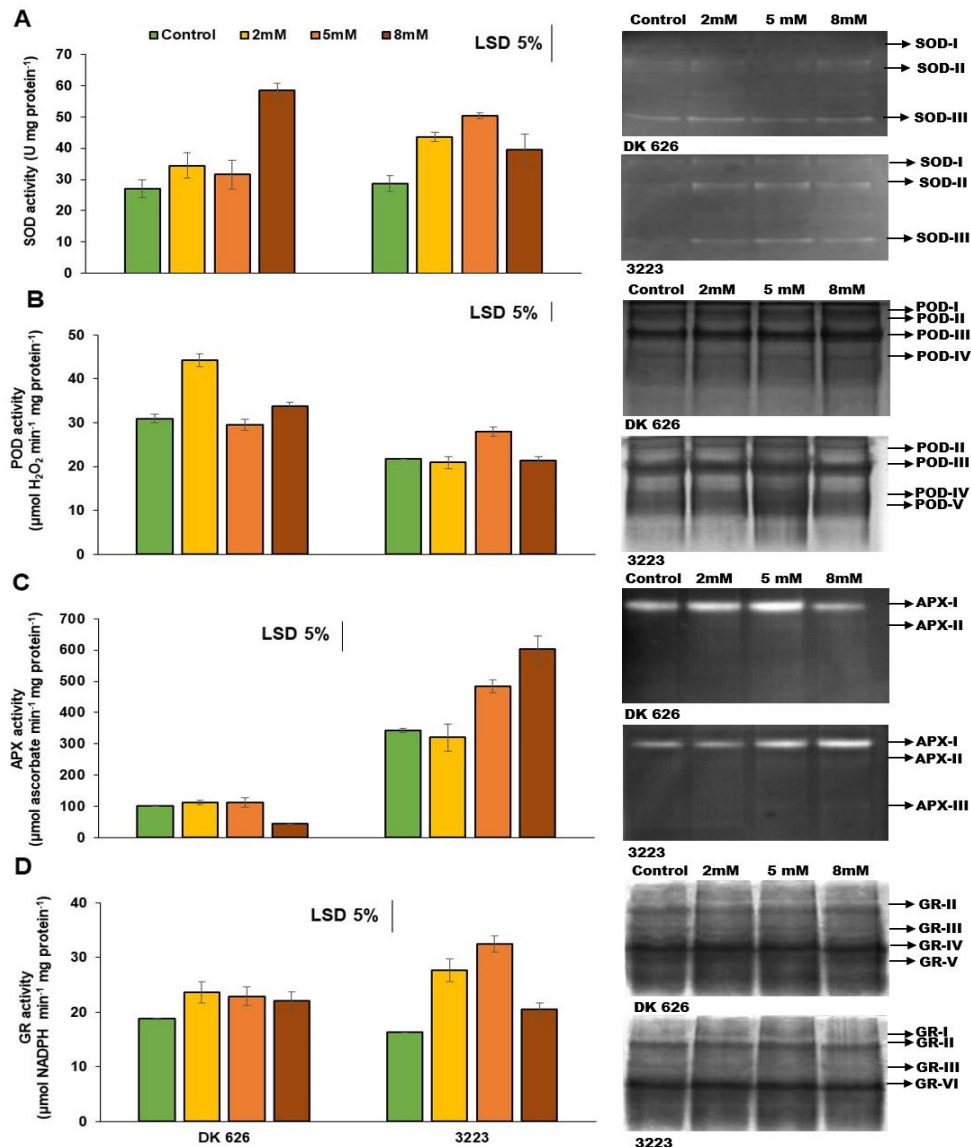


Figure 6 - Alteration induced by Zn toxicity in the activities of total enzymes and isoenzymes in leaves of maize genotypes: SOD (A), POD (B), APX (C) and GR (D). The error bars represent the standard error (\pm SE) for three replicates

4. Conclusions

The accumulation of excess Zn in leaves led to the restricted growth, loss of photosynthetic pigments and photochemical efficiency of the two maize genotypes. However, DK626 showed more membrane deterioration than 3223 with highly toxic Zn concentrations according to the MDA results. Furthermore, the decrease in photosynthetic pigment contents and the increase in anthocyanin contents reveal that DK 626 was more affected by Zn toxicity than the other genotype. However, by slightly increasing SOD and POD enzyme activities, DK626 overcome the damaging effects of oxidative stress induced by Zn toxicity compared to 3223. The genotypes achieved an adaptation to zinc toxicity by increasing the anthocyanin content, regulating antioxidant enzyme activities, and maintaining the functionality of the photosynthetic machineries.

In the previous study, the genotypes were identified as tolerant (DK626) and sensitive (3223) at the germination stage. However, the results of this study have shown that both genotypes the differentiation in tolerance responses to zinc toxicity between these genotypes disappeared during the early seedling stage. Therefore, tolerance levels to Zn toxicity of both genotypes were quite high and of a similar nature. It may be declared that both genotypes have exhibited tolerant responses to Zn toxicity, but with different strategies. Consequently, both genotypes of *Zea mays* L. might be suggested to be used for the phytoremediation of highly toxic Zn-contaminated areas. However, further studies are required to screen all growth stages for

Zn tolerance capacity before a more informed decision can be made regarding the phytoremediation potentials of these two genotypes.

Data availability: Data are available on request due to privacy or other restrictions.

Author Contributions: YE and DT took part in conceptualization, review and editing; YE and ŞÜO were involved in experimental data collection and analysis; ŞÇE and NÇ were involved in writing and the original draft.

Conflict of Interest: The authors declare that they have no conflicts of interest.

Financial Support: The authors are grateful to Hacettepe University, Scientific Research Unit (Project No. 02 02 602 013) for its financial support.

References

- Abedi T, Gavanji S & Mojiri A (2022). Lead and zinc uptake and toxicity in maize and their management. *Plants* 11: 1922. <https://doi.org/10.3390/plants11151922>
- Alonso-Blázquez N, García-Gómez C & Fernández MD (2015). Influence of Zn-contaminated soils in the antioxidative defence system of wheat (*Triticum aestivum*) and maize (*Zea mays*) at different exposure times: potential use as biomarkers. *Ecotoxicology* 24: 279-291. <https://doi.org/10.1007/s10646-014-1376-6>
- Alsafran M, Saleem MH, Al Jabri H, Rizwan M & Usman K (2023). Principles and applicability of integrated remediation strategies for heavy metal removal/recovery from contaminated environments. *Journal of Plant Growth Regulation* 42: 3419-3440. <https://doi.org/10.1007/s00344-022-10803-1>
- Andrejić G, Gajić G, Prica M, Dželetović Ž & Rakić T. (2018). Zinc accumulation, photosynthetic gas exchange, and chlorophyll a fluorescence in Zn-stressed *Miscanthus x giganteus* plants. *Photosynthetica* 56(4): 1249-1258. <https://doi.org/10.1007/s11099-018-0827-3>
- Antoniadis V, Shaheen S M, Tsadilas C D, Selim M H & Rinklebe J (2018). Zinc sorption by different soils as affected by selective removal of carbonates and hydrous oxides. *Applied Geochemistry* 88: 49-58. <https://doi.org/10.1016/j.apgeochem.2017.04.007>
- Anwaar S A, Ali S, Ali S, Ishaque W, Farid M, Farooq M A, Najeeb U, Abbas F & Sharif M (2015). Silicon (Si) alleviates cotton (*Gossypium hirsutum* L.) from zinc (Zn) toxicity stress by limiting Zn uptake and oxidative damage. *Environmental Science and Pollution Research* 22(5): 3441-3450. <https://doi.org/10.1007/s11356-014-3938-9>
- Ayyar S & Appavoo S (2017). Effect of graded levels of Zn in combination with or without microbial inoculation on Zn transformation in soil, yield and nutrient uptake by maize for black soil. *Environment & Ecology* 35(1): 172-176
- Balafrej H, Bogusz D, Triqui Z-E A, Guedira A, Bendaou N, Smouni A & Fahr M (2020). Zinc hyperaccumulation in plants: A review. *Plants* 9(562): 2-22. <https://doi.org/10.3390/plants9050562>
- Baran U & Ekmeççi Y (2022). Physiological, photochemical, and antioxidant responses of wild and cultivated *Carthamus* species exposed to nickel toxicity and evaluation of their usage potential in phytoremediation. *Environmental Science and Pollution Research* 29: 4446-4460. <https://doi.org/10.1007/s11356-021-15493-y>
- Beauchamp C & Fridovich I (1971). Superoxide dismutase: improved assays and an assay applicable to acrylamide gels. *Analytical Biochemistry* 44: 276-287. [https://doi.org/10.1016/0003-2697\(71\)90370-8](https://doi.org/10.1016/0003-2697(71)90370-8)
- Beyer W F & Fridovich I (1987). Assaying for superoxide dismutase activity: Some large consequences of minor changes in conditions. *Analytical Biochemistry* 161(2): 559-566. [https://doi.org/10.1016/0003-2697\(87\)90489-1](https://doi.org/10.1016/0003-2697(87)90489-1)
- Bradford M M (1976). A rapid and sensitive method for the quantitation of microgram quantities of protein utilizing the principle of protein-dye binding. *Analytical Biochemistry* 72(1-2): 248-254. [https://doi.org/10.1016/0003-2697\(76\)90527-3](https://doi.org/10.1016/0003-2697(76)90527-3)
- Calvo B O, Parapugna T L & Lagorio M G (2017). Variability in chlorophyll fluorescence spectra of eggplant fruit grown under different light environments: A case study. *Photochemical & Photobiological Sciences* 16: 711-720. <https://doi.org/10.1039/c6pp00475j>
- Chaney R L (1993). Zinc Phytotoxicity. In: Robson A D (ed) *Zinc in Soils and Plants*. Developments in Plant and Soil Sciences, 55. Springer, Dordrecht, pp 135-150. <https://doi.org/10.1007/978-94-011-0878-2-10>
- Chen Q, Zhang X, Liu Y, Wei J, Shen W, Shen Z & Cui J (2017). Hemin-mediated alleviation of zinc, lead and chromium toxicity is associated with elevated photosynthesis, antioxidative capacity; suppressed metal uptake and oxidative stress in rice seedlings. *Plant Growth Regulation* 81: 253-264. <https://doi.org/10.1007/s10725-016-0202-y>
- Çiçek N & Çakırlar H (2008). Effects of salt stress on some physiological and photosynthetic parameters at three different temperatures in six soya bean (*Glycine max* L. Merr.) cultivars. *Journal of Agronomy & Crop Science* 194: 34-46. <https://doi.org/10.1111/j.1439-037X.2007.00288.x>
- Cordon G, Iriel A, Cirelli A F & Lagorio M G (2018). Arsenic effects on some photophysical parameters of *Cichorium intybus* under different radiation and water irrigation regimes. *Chemosphere* 204: 398-404. <https://doi.org/10.1016/j.chemosphere.2018.04.048>
- DalCorso G, Manara A, Piasentin S & Furini A (2014). Nutrient metal elements in plants. *Metallomics* 6: 1770-1788. <https://doi.org/10.1039/c4mt00173g>
- Díaz-Pontones D M, Corona-Carrillo J I, Herrera-Miranda C & González S (2021). Excess zinc alters cell wall class III peroxidase activity and flavonoid content in the maize scutellum. *Plants* 10: 197. <https://doi.org/10.3390/plants10020197>
- Dobrikova A, Apostolova E, Adamakis I S & Han A (2022). Combined impact of excess zinc and cadmium on elemental uptake, leaf anatomy and pigments, antioxidant capacity, and function of photosynthetic apparatus in clary sage (*Salvia sclarea* L.). *Plants* 11: 2407. <https://doi.org/10.3390/plants11182407>
- Dobrikova A, Apostolova E, Hanć A, Yotsova E, Borisova P, Sperdouli I, Adamakis I-D S & Moustakas M (2021). Tolerance mechanisms of the aromatic and medicinal plant *Salvia sclarea* L. to excess zinc. *Plants* 10: 194. <https://doi.org/10.3390/plants10020194>
- Ekmeççi Y, Tanyolaç D & Ayhan B (2008). Effects of cadmium on antioxidant enzyme and photosynthetic activities in leaves of two maize cultivars. *Journal of Plant Physiology* 165: 600-611.
- Fatemi H, Zaghdoud C, Nortes P A, Carvajal M & Martínez-Ballesta M C (2020). Differential aquaporin response to distinct effects of two Zn concentrations after foliar application in pak choi (*Brassica rapa* L.) plants. *Agronomy* 10: 450. <https://doi.org/10.3390/agronomy10030450>

- Genty B, Briantais J M & Baker N R (1989). The relationship between the quantum yield of photosynthetic electron transport and quenching of chlorophyll fluorescence. *Biochimica et Biophysica Acta (BBA) - General Subjects* 990(1): 87-92. [https://doi.org/10.1016/S0304-4165\(89\)80016-9](https://doi.org/10.1016/S0304-4165(89)80016-9)
- Glińska S, Gapińska M, Michlewska S, Skiba E & Kubicki J (2016). Analysis of *Triticum aestivum* seedling response to the excess of zinc. *Protoplasma* 253: 367-377. <https://doi.org/10.1007/s00709-015-0816-3>
- Guadagno C R, Virzo De Santo A & D'Ambrosio N (2010). A revised energy partitioning approach to assess the yields of non-photochemical quenching components. *Biochimica et Biophysica Acta* 1797: 525-530. <https://doi.org/10.1016/j.bbabi.2010.01.016>
- Iriel A, Cordon G, Fernández Cirelli A & Lagorio M G (2019). Non-destructive methodologies applied to track the occurrence of natural micropollutants in watering: *Glycine max* as a biomonitor. *Ecotoxicology and Environmental Safety* 182: 109368. <https://doi.org/10.1016/j.ecoenv.2019.109368>
- Janeeshma E, Kalaji H M & Puthur J T (2021). Differential responses in the photosynthetic efficiency of *Oryza sativa* and *Zea mays* on exposure to Cd and Zn toxicity. *Acta Physiologiae Plantarum* 43: 12. <https://doi.org/10.1007/s11738-020-03178-x>
- Jayasri M A & Suthindhiran K (2017). Effect of zinc and lead on the physiological and biochemical properties of aquatic plant *Lemna minor*: its potential role in phytoremediation. *Applied Water Science* 7: 1247-1253. <https://doi.org/10.1007/s13201-015-0376-x>
- Karahan F, Ozyigit I I, Saracoglu I A, Yalcin I E, Ozyigit A H & Ilcim A (2020). Heavy metal levels and mineral nutrient status in different parts of various medicinal plants collected from eastern mediterranean region of Turkey. *Biological Trace Element Research* 197: 316-329. <https://doi.org/10.1007/s12011-019-01974-2>
- Kaur H & Garg N (2021). Zinc toxicity in plants: a review. *Planta* 253: 129. <https://doi.org/10.1007/s00425-021-03642-z>
- Küpper H & Andresen E (2016). Mechanisms of metal toxicity in plants. *Metallomics* 8: 269-285. <https://doi.org/10.1039/c5mt00244c>
- Laemmli U K (1970). Cleavage of structural proteins during the assembly of the head of bacteriophage T4. *Nature* 227: 680-685. <https://doi.org/10.1038/227680a0>
- Lichtenthaler H K, Buschmann C & Knapp M (2005). How to correctly determine the different chlorophyll fluorescence parameters and the chlorophyll fluorescence decrease ratio R_{Fd} of leaves with the PAM fluorometer. *Photosynthetica* 43(3): 379-393. <https://doi.org/10.1007/s11099-005-0062-6>
- Lichtenthaler H K (1987). Chlorophylls and carotenoids: Pigments of photosynthetic biomembranes. *Methods in Enzymology* 148: 350-382. [https://doi.org/10.1016/0076-6879\(87\)48036-1](https://doi.org/10.1016/0076-6879(87)48036-1)
- M'Rah S, Marichali A, M'Rabet Y, Chatti S, Saber C, Casabianca H & Hosni K (2023). Morphology, physiology, and biochemistry of zinc-stressed caraway plants. *Protoplasma* 260: 853-868. <https://doi.org/10.1007/s00709-022-01818-2>
- Mancinelli A L, Yang C P H, Lindquist P, Anderson O R & Rabino I (1975). Photocontrol of anthocyanin synthesis: III. The action of streptomycin on the synthesis of chlorophyll and anthocyanin. *Plant Physiology* 55(2): 251-257. <https://doi.org/10.1104/pp.55.2.251>
- Marschner H (1995). Mineral nutrition of higher plants. London: Academic Press.
- Maxwell K & Johnson G H (2000). Chlorophyll fluorescence-a practical guide. *Journal of Experimental Botany* 51(345): 659-668. <https://doi.org/10.1093/jxb/51.345.659>
- Miller G, Shulaev V & Mittler R (2008). Reactive oxygen signaling and abiotic stress. *Physiologia Plantarum* 133: 481-489. <https://doi.org/10.1111/j.1399-3054.2008.01090.x>
- Mittler R & Zilinskas B A (1993). Detection of ascorbate peroxidase activity in native gels by inhibition of the ascorbate-dependent reduction of nitroblue tetrazolium. *Analytical Biochemistry* 212: 540-546. <https://doi.org/10.1006/abio.1993.1366>
- Moustaka J, Panteris E, Adamakis I-D S, Tanou G, Giannakoula A, Eleftheriou E P & Moustakas M (2018). High anthocyanin accumulation in poinsettia leaves is accompanied by thylakoid membrane unstacking, acting as a photoprotective mechanism, to prevent ROS formation. *Environmental and Experimental Botany* 154: 44-55. <https://doi.org/10.1016/j.envexpbot.2018.01.006>
- Mukhopadhyay M, Das A, Subba P, Bantawa P, Sarkar B, Ghosh P & Mondal T D (2013). Structural, physiological, and biochemical profiling of tea plants under zinc stress. *Biologia Plantarum* 57(3): 474-480. <https://doi.org/10.1007/s10535-012-0300-2>
- Natasha N, Shahid M, Bibi I, Iqbal J, Khalid S, Murtaza B, Bakhat H F, Farooq A B U, Amjad M, Hammadd H M, Niazi N K & Arshad M, (2022). Zinc in soil-plant-human system: A data-analysis review. *Science of the Total Environment* 808: 152024. <https://doi.org/10.1016/j.scitotenv.2021.152024>
- Pan L, Li J, Yin H, Fan Z & Li X (2020). Integrated physiological and transcriptomic analyses reveal a regulatory network of anthocyanin metabolism contributing to the ornamental value in a novel hybrid cultivar of *Camellia japonica*. *Plants* 9: 1724. <https://doi.org/10.3390/plants9121724>
- Paunov M, Koleva L, Vassilev A, Vangronsveld J & Goltsev V (2018). Effects of different metals on photosynthesis: Cadmium and zinc affect chlorophyll fluorescence in durum wheat. *International Journal of Molecular Science* 19: 787. <https://doi.org/10.3390/ijms19030787>
- Petrovic D & Krivokapic S (2020). The effect of Cu, Zn, Cd, and Pb accumulation on biochemical parameters (proline, chlorophyll) in the water caltrop (*Trapa natans* L.), Lake Skadar, Montenegro. *Plants* 9: 1287. <https://doi.org/10.3390/plants9101287>
- Pütter J (1974). Peroxidases. In: Bergmeyer HU (ed) In *Methods of Enzymatic Analysis*, Academic P. Academic Press, NY, USA, pp. 685-690
- Rai P K, Lee S S, Zhang M, Tsang Y F & Kim K-H (2019). Heavy metals in food crops: Health risks, fate, mechanisms, and management. *Environment International* 125: 365-385. <https://doi.org/10.1016/j.envint.2019.01.067>
- Ramakrishna B & Rao S S R (2015). Foliar application of brassinosteroids alleviates adverse effects of zinc toxicity in radish (*Raphanus sativus* L.) plants. *Protoplasma* 252: 665-677. <https://doi.org/10.1007/s00709-014-0714-0>
- Rao M V, Hale B A & Ormrod D P (1995). Amelioration of ozone-induced oxidative damage in wheat plants grown under high carbon dioxide: Role of antioxidant enzymes. *Plant Physiology* 109(2): 421-432. <https://doi.org/10.1104/pp.109.2.421>
- Rocciotiello E, Manfredi A, Drava G, Minganti V, Mariotti M G, Berta G & Cornara L (2010). Zinc tolerance and accumulation in the ferns *Polypodium cambricum* L. and *Pteris vittata* L. *Ecotoxicology and Environmental Safety* 73: 1264-1271. <https://doi.org/10.1016/j.ecoenv.2010.07.019>
- Saboor A, Ali M A, Hussain S, Enshasy H A E, Hussain S, Ahmed N, Gafur A, Sayyed R Z, Fahad S, Danish S & Datta R (2021). Zinc nutrition and arbuscular mycorrhizal symbiosis effects on maize (*Zea mays* L.) growth and productivity. *Saudi Journal of Biological Sciences* 28: 6339-6351. <https://doi.org/10.1016/j.sjbs.2021.06.096>
- Sapeta H, Yokono M, Takabayashi A, Ueno Y, Cordeiro A M, Hara T, Tanaka A, Akimoto S, Oliveira M. M. & Tanaka R (2023). Reversible down-regulation of photosystems I and II leads to fast photosynthesis recovery after long-term drought in *Jatropha curcas*. *Journal of Experimental Botany* 74(1): 336-351. <https://doi.org/10.1093/jxb/erac423>

- Seregin I V, Ivanova T V, Voronkov A S, Kozhevnikova A D & Schat H (2023). Zinc- and nickel-induced changes in fatty acid profiles in the zinc hyperaccumulator *Arabidopsis halleri* and non-accumulator *Arabidopsis lyrata*. *Plant Physiology and Biochemistry* 197: 107640. <https://doi.org/10.1016/j.plaphy.2023.107640>
- Sgherri C L M, Loggini B, Puliga S & Navari-Izzo F (1994). Antioxidant system in *Sporobolus stapfianus*: Changes in response to desiccation and rehydration. *Phytochemistry* 35(3): 561-565. [https://doi.org/10.1016/S0031-9422\(00\)90561-2](https://doi.org/10.1016/S0031-9422(00)90561-2)
- Sharma J K, Kumar N, Singh N P & Santal A R (2023). Phytoremediation technologies and their mechanism for removal of heavy metal from contaminated soil: An approach for a sustainable environment. *Frontier in Plant Science* 14: 1076876. <https://doi.org/10.3389/fpls.2023.1076876>
- Sofo A, Moreira I, Gattullo C E, Martins L L & Mou M (2018). Antioxidant responses of edible and model plant species subjected to subtoxic zinc concentrations. *Journal of Trace Elements in Medicine and Biology* 49: 261-268. <https://doi.org/10.1016/j.jtemb.2018.02.010>
- Sofo A, Vitti A, Nuzzaci M, Tataranni G, Scopa A, Vangronsveld J, Remans T, Falasca G, Altamura M M, Degola F & di Toppi L S (2013). Correlation between hormonal homeostasis and morphogenic responses in *Arabidopsis thaliana* seedlings growing in a Cd/Cu/Zn multi-pollution context. *Physiologia Plantarum* 149: 487-498. <https://doi.org/10.1111/pp1.12050>
- Sperdouli I, Adamakis I D S, Dobrikova A, Apostolova E, Hanć A & Moustakas M (2022). Excess zinc supply reduces cadmium uptake and mitigates cadmium toxicity effects on chloroplast structure, oxidative stress, and photosystem II photochemical efficiency in *Salvia sclarea* plants. *Toxics* 10: 36. <https://doi.org/10.3390/toxics10010036>
- Sperdouli I, Mellidou I & Moustakas M (2021). Harnessing chlorophyll fluorescence for phenotyping analysis of wild and cultivated tomato for high photochemical efficiency under water deficit for climate change resilience. *Climate* 9:154. <https://doi.org/10.3390/cli9110154>
- Stanton C, Sanders D, Krämer U & Podar D (2022). Zinc in plants: Integrating homeostasis and biofortification. *Molecular Plant* 15: 65-85. <https://doi.org/10.1016/j.molp.2021.12.008>
- Suganya A, Saravanan A & Manivannan N (2020). Role of zinc nutrition for increasing zinc availability, uptake, yield, and quality of maize (*Zea Mays* L.) grains: an overview. *Communications in Soil Science and Plant Analysis* 51(15): 2001-2021. <https://doi.org/10.1080/00103624.2020.1820030>
- Szopiński M, Sitko K, Gieron Ż, Rusinowski S, Corso M, Hermans C, Verbruggen N & Małkowski E (2019). Toxic effects of Cd and Zn on the photosynthetic apparatus of the *Arabidopsis halleri* and *Arabidopsis arenosa* pseudo-metallophytes. *Frontier in Plant Science* 10: 748. <https://doi.org/10.3389/fpls.2019.00748>
- Tiecher T L, Tiecher T, Ceretta C A, Ferreira P A A, Nicoloso F T, Soriani H H, De Conti L, Kulmann M S S, Schneider R O & Brunetto G (2017). Tolerance and translocation of heavy metals in young grapevine (*Vitis vinifera*) grown in sandy acidic soil with interaction of high doses of copper and zinc. *Scientia Horticulturae* 222: 203-212. <https://doi.org/10.1016/j.scienta.2017.05.026>
- Ünalın Ş (2006) Response of antioxidant enzyme defence system on the maize cultivars under the heavy metal stress and investigation of maize's usability for removal of heavy metal. MSc thesis, Hacettepe University (in Turkish).
- Vaillant N, Monnet F, Hitmi A, Sallanon H & Coudret A (2005). Comparative study of responses in four *Datura* species to a zinc stress. *Chemosphere* 59: 1005-1013. <https://doi.org/10.1016/j.chemosphere.2004.11.030>
- Wang S Y, Jiao H J & Faust M (1991). Changes in ascorbate, glutathione, and related enzyme activities during thidiazuron-induced bud break of apple. *Physiologia Plantarum* 82(2): 231-236. <https://doi.org/10.1111/j.1399-3054.1991.tb00086.x>
- Wieczorek J, Baran A, Bubak A (2023). Mobility, bioaccumulation in plants, and risk assessment of metals in soils. *Science of The Total Environment* 882: 163574. <https://doi.org/10.1016/j.scitotenv.2023.163574>
- Yin J, Gentine P, Zhou S, Sullivan S C, Wang R, Zhang Y, & Guo S (2018). Large increase in global storm runoff extremes driven by climate and anthropogenic changes. *Nature communications* 9(1): 4389. <https://doi.org/10.1038/s41467-018-06765-2>



Copyright © 2024 The Author(s). This is an open-access article published by Faculty of Agriculture, Ankara University under the terms of the [Creative Commons Attribution License](https://creativecommons.org/licenses/by/4.0/) which permits unrestricted use, distribution, and reproduction in any medium or format, provided the original work is properly cited.



Instrumental use of Marine Bacteria to Stimulate Growth in Seaweed

Pham Thi Mien^{*a} , Phan Minh-Thu^{*a} , Bui Thi Ngoc Trieu^a , Nguyen Minh Hieu^a , Dao Viet Ha^a 

^aInstitute of Oceanography, Vietnam Academy of Science and Technology, Nha Trang, VIETNAM

ARTICLE INFO

Research Article

Corresponding Authors: Pham Thi Mien, Phan Minh-Thu, E-mail: mien.pham@gmail.com, phanminhthu@vnio.org.vn

Received: 04 November 2023 / Revised: 06 February 2024 / Accepted: 24 February 2024 / Online: 23 July 2024

Cite this article

Mien P T, Minh-Thu P, Trieu B T N, Hieu N M, Ha D V (2024). Instrumental use of Marine Bacteria to Stimulate Growth in Seaweed. *Journal of Agricultural Sciences (Tarim Bilimleri Dergisi)*, 30(3):501-512. DOI: 10.15832/ankutbd.1386116

ABSTRACT

Edible seaweed - *Caulerpa lentillifera* is being cultivated along the coast of Khanh Hoa province, Vietnam, and makes a relatively large contribution to the economic development of this region. Bacterial strains originating from marine sources such as those associated with seaweed and hard coral were screened for properties of promote plant growth with the capacity of indole-3-acetic acid (IAA) - a phytohormone belonging to auxin group, the phosphate solubilization ability and antibacterial activity of IAA-producing strains were also performed in this study. Robust strains were identified by morphological methods with biochemical tests and analysis of 16s RNA sequences. Isolate RN06 produced high amounts

of IAA, utilized inorganic phosphate, and inhibited *Bacillus subtilis* ATCC6633, *Escherichia coli* 0157, and *Serratia marcescens* PDL100. The IAA producer HRA5 isolated from hard coral demonstrated the ability to solubilize phosphate and exhibited antibacterial activity against *B. subtilis*. Morphological analysis and 16sRNA sequencing showed that isolate RN06 was the closest strain to *Bacillus amyloliquefaciens* and HRA5 was linked to *Pseudomonas* sp. This is the first report of isolated bacteria from seaweed and corals from the Vietnamese sea served as potential strains for further research of the application of biological inoculants specifically for seaweed farming.

Keywords: Indole-3-acetic acid-producing bacteria, Phosphate solubilizing bacteria, Antimicrobial activity, Marine potential bacteria

1. Introduction

Seaweeds are divided into three groups based on their pigment content: Green (Chlorophyta), brown (Phaeophyta), and red (Rhodophyta). They are a group of marine plant-like organisms distributed geographically, from tropical to polar regions, with ecoregions ranging from intertidal to submerged zones that are still exposed to sunlight (Tirtawijaya et al. 2022). The diversity of seaweed-associated bacteria, the role and the relationship between bacteria and their host as well as their production of bioactive compounds have been investigated for a long time. However, the research on the edible seaweed *Caulerpa lentillifera* was focused on the nutrient requirement, optimum cultivational conditions, and production of bioactive substances such as antioxidants, antimicrobials, antitumor compounds as well as pigments. Not much is known about the diversity of microorganisms associated with the sea grape *C. lentillifera*. Among phytohormones, indole-3-acetic acid (IAA) increased polysaccharide content in edible seaweed rather than other normal functions of phytohormones which induce the growth such as 6-benzyl aminopurine and gibberellin (Tao et al. 2017). It was worth that Polysaccharides exhibited anticoagulant, and immunomodulatory effects and prevented cancer activity (Chen et al. 2019). Auxin is a phytohormone that controls almost every aspect of growth and development in plants. They are the basic compounds that regulate the growth and development of plants. One of the most important natural auxins is IAA produced by plants, bacteria, fungi, and brown algae (Ali et al. 2009; Leyser 2010; Sunarpi et al. 2021). So far, auxin has also been found in the marine sediment (Maruyama et al. 1989), and IAA-producing marine microorganisms affected the growth of thallus of coenocytic alga *Caulerpa sertularioides* (Mishra & Kefford 1969). Indole-3-acetic acid was detectable in *Dictyota dichotoma* germlings and mature tissue and auxin play a role during the apical-basal patterning of the embryo of brown algae (Bogaert et al. 2019). Indole-3-acetic acid (IAA) was produced by a brown algae *Ectocarpus siliculosus* so far and affected the growth of its host (Le Bail et al. 2010). However, another paper showed that an un-culturable microbe associated with the alga might be the true producer of IAA instead of alga (Dittami et al. 2014). The plant hormone IAA from plant growth-promoting *Pseudomonas putida* UB1 was reported to play a major role in the development of the host plant root system (Bharucha et al. 2013). A *Sulfitobacter* isolate associated with the diatom *Pseudonitzschia* could promote diatom cell division via the secretion of indole-3-acetic acid. The hormone indole-3-acetic acid was synthesized by this bacterium using both diatom-secreted and endogenous tryptophan. Both IAA and tryptophan acted as biological signaling molecules in their interaction for nutrient exchanges (Amin et al. 2015). It was illustrated that an *Enterobacter* strain that overproduces IAA acts as a bio-herbicide (Park et al. 2015). In another paper, the marine bacterium *Ruegeria* sp. R11 was thought to be responsible for algal blooms (hosts) and produced IAA, but the role of IAA in the interaction between bacteria and algae

had not been clearly established (Mayers et al. 2016). Without a doubt IAA is an important substrate in the communication between algae and marine bacteria (Lin et al. 2022).

Although, phosphorus is one of the most important and major components of seawater. It is normally found in the form of both inorganic and organic phosphates. Microorganisms play a vital role in the phosphorus cycle both in terrestrial and aquatic ecosystems. Thus, many kinds of phosphate-solubilizing bacteria like *Bacillus*, *Pseudomonas*, *Nitrosomonas*, *Erwinia*, *Serratia*, *Rhizobium*, *Xanthomonas*, *Enterobacter*, and *Micrococcus* have been isolated from various habitats compassing of coastal, offshore, and mangrove (Rawat et al. 2021) *Pseudomonas aeruginosa* KUPSB12 isolated from the river Ganga west Bengal India was effective in phosphate solubilization with Pikovskaya's agar method and also was a good candidate for the production of antimicrobial substances. Crude extract from *P.aeruginosa* inhibited the growth of both Gram-negative and Gram-positive test strains (Paul & Sinha 2017). *Enterobacter* and *Serratia* strains isolated from *Mimosa pudica* root nodules have plant growth-promoting characters compassing auxin production, phosphate solubilization, and enzymatic activities. Moreover, *Serratia* strains had antimicrobial activity against plant pathogenic fungi *Fusarium* sp. and *Alternaria solani*. Other strains of *Enterobacteria* sp. strain NOD1 and NOD10 were very efficient in promoting shoot height and increasing the size of the legumes *Phaseolus vulgaris* and *Mimosa pudica* in vitro (Sánchez-Cruz et al. 2019). Recently the diversity and functional traits of actinobacteria from the coastal salt marsh soil from Jiangsun province have been investigated. The results from that paper showed that 2.8-43.0% of actinobacterial sequences belonged to rhizosphere bacterial communities by high throughput sequencing methods. Among all isolates, two strains were identified as plant growth-promoting and were inoculated into wheat seed under salt-stress conditions. Both strains promoted seed germination and significantly enhanced plant growth. They were identified as *Streptomyces* sp. KLBMP S0051 and *Micromonospora* sp. KLBMP S0019 (Gong et al. 2018). The diversity of seaweed-associated bacteria, the role and the relationship between bacteria and their host as well as their production of bioactive compounds have been investigated for a long time. Previously, we found that *Micrococcus* sp. strain A-2-28 associated with the soft coral *Alcyonium digitatum* showed antimicrobial activity and metabolite analysis showed the presence of IAA in the crude extract of this bacteria (Pham 2014). On the other hand, *Micrococcus* was the most common bacterium among the isolates from the soft corals, the natural compounds from this bacterium have also been reported so far (Palomo et al. 2013). In addition, we coincidentally detected that the most abundant *Enterobacter* and *Pseudomonas* from *Acropora* the majority species of building coral reefs in the center of Vietnam when PO_4 concentration in ambient seawater was lowest compared to those in three other sampling times (Pham et al. 2019).

The marine animals including corals, sponges, and muscles from Vietnamese seawater become interesting for investigation of bioactive compounds. Along the coast of ca 3000 km from the north to the south are many activities of aquaculture in open water. In addition, many coastal regions now are farming edible sea grapes for commercial trades, especially in Khanh Hoa province, which is the best place to grow green seaweed in Vietnam, developing sustainable farming both in soil and water is a challenge for Vietnamese, we need more and more basic research and application technology.

This present study is first searching for indigenous bacterial strains with benefit features such as the production of phytohormone IAA, solubilization of phosphate, and inhibition of pathogenic bacteria to use for further use as biological inoculants in seaweed farming.

2. Material and Methods

The living coral *Acropora hyacinthus* was collected from the Center of Vietnam by a diver with SCUBA at the station in Hang Rai (109°18'28" E and 11°67'71" N), Ninh Hai, Ninh Thuan province, Viet Nam. The living edible seaweed *C. lentillifera* cultivated in natural seawater in the VAST Key Lab for Food and Environment Safety in Center Vietnam was used to isolate bacteria for this study. After collecting, the samples were preserved in a sterile dark polyethylene bag, stored in an ice box, and transferred to the laboratory as soon as possible for further study. In the laboratory, samples were immersed in ethanol 70% for 30 seconds and then washed three times with sterile filtered seawater. At the laboratory, samples were immersed in the ethanol 70% for 30 seconds and then washed three times with sterile filtered seawater. The wet weight of 2 g of each sample was homogenized in 18 mL of sterile 0.45 μ m (Whatman) filtered seawater collected at the sampling sites and diluted samples were used to isolate until a pure strain (Pham et al. 2018). The pure isolates were long time preserved in TM medium (Tryptone: 1 g/L, Yeast extract: 1 g/L, Agar: 15 g/L, NaCl: 5 g/L) plus 50% glycerol at room temperature (approx. 30 °C) at Marine Ecology Department, Institute of Oceanography, VAST.

2.1. Screening of IAA producer strains

Total of 50 pure microorganisms derived from corals and edible seaweed were screened for IAA production in modified LB broth medium (LBM g/L) consisting of KH_2PO_4 : 1, Na_2HPO_4 : 1, $MgSO_4 \cdot 7H_2O$: 0.2, pH= 7.0, glucose: 10; yeast extract: 5, NaCl: 5, Tryptone: 5, L-tryptophan: 0.5 at 30 ± 1 °C on a rotary shaker at 120 rpm. After 3 incubated days, broth cultures were centrifuged at 10,000 rpm for 10 min and the supernatant was collected for testing of IAA production by using Salkowski's reagent after keeping for 30 min at 30 °C in the dark, the development of pink to reddish color was noted as slight pink (+), pink (++) and dark pink (+++) for increment IAA producing levels. The positive control of pink color development was added by using 1 μ g/mL of authentic IAA (Sigma) and negative control was performed with distilled water instead of cultured broth in the same manner (Gupta et al. 2012).

2.2. Quantitative of IAA

All IAA production strains were inoculated in LB-modified broth medium and incubated at 30 ± 1 °C for 10 days on a rotary shaker at 120 rpm. Each 2 mL broth culture was harvested and centrifuged at 10,000 rpm for 15 min. The cell pellets were dried at 70 °C in a hot oven to get dry weight for biomass values of triplicate samples. Then 1 mL of supernatant sample of day 4, day 7, and day 10 was taken and mixed with 2 mL of Salkowski's reagent and kept for 30 min to develop color. Color intensity was assayed with a spectrophotometer at 530 nm by the colorimetric method (Gordon & Paleg 1957) and calculated based on the curve of standard IAA (Sigma) with a series of concentrations of 0, 5, 10, 20, 50, and 100 µg/mL. Two-time distilled water was used as a blank sample.

2.3. Detection of phosphate solubilizing activity of IAA-producing strains

The IAA-producing bacterium was screened on Pikovskaya's agar (PKV) medium for phosphate solubilization by the Agar Spot method. PKV consisted of 2.5 g/L calcium triphosphate $\text{Ca}_3(\text{PO}_4)_2$ as phosphate source, glucose 10 g/L, $(\text{NH}_4)_2 \text{SO}_4$ 0.5 g/L, $\text{MgSO}_4 \cdot 7\text{H}_2\text{O}$ 0.1 g/L, KCl 0.2 g/L, NaCl 2 g/L, FeSO_4 0.002 g/L, Yeast extract 0.5 g/L, MnSO_4 0.002 g/L, Agar 15 g/L. The pH was adjusted to 7.0 ± 0.2 before sterilization. The cultured plates were incubated at 30 ± 1 °C for 5 days and colonies with a clear halo marked positive for phosphates solubilization (Gupta et al. 2012). The Agar Spot method yielded the results in terms of solubilization index (SI). The phosphate solubilization index was calculated by the ratio of the sum of colony diameter and halo zone diameter divided by colony diameter or the ratio of total zone over colony zone (Paul & Sinha, 2017) as the equation (1). PKV broth medium was used for pH drop check daily for 10 incubation days at 30 ± 1 °C on a rotary shaker at 120 rpm with a glass electrode (Ahmad et al. 2013).

$$SI = \frac{CD+HSD}{CD} \quad (1)$$

Where; SI: Solubilization index, CD: Colony diameter, and HSD: Halo zone diameter.

2.4. Antibacterial testing

The isolated strains were streaked in Marine Agar (Himedia) plates for 3-5 days and then inoculated into 300 mL Erlenmeyer flasks containing 100 mL BM medium (yeast extract: 1 g/L, beef extract: 1 g/L, tryptone 2 g/L, glucose 10 g/L, 1000 mL filtered seawater). After 72 h of incubation at 30 °C with shaking at 120 rpm, the bacterial cells and the supernatants were homogenized by using of Ultrasonic processor for breaking the cells in 30 s. The homogenized broth was extracted by ethyl acetate 1/1 (v/v). Crude extracts were dried and re-suspended in 1 mL of methanol (Merck). The methanolic extracts were applied for antimicrobial activities by agar well diffusion method on Mueller Hinton Agar (MHA-Himedia, India) according to Bauer et al. (1966). A total of 30 µL methanolic extract of each isolated bacteria was inoculated into four available wells on MHA-containing indicator bacteria. The same amount of methanol without extract was used as a negative control. All the plates tested with *Bacillus subtilis* ATCC6633, *Salmonella typhimurium* ATCC6994, and *Escherichia coli* 0157 were incubated at 37 °C for 24 h. The plates tested with *Serratia marcescens* PDL100 were incubated at 25 °C for 24 h. The zone of inhibition was measured and expressed in the mean of the four wells excluding the well diameter.

2.5. Identification of potential marine bacteria

The potent plant growth-promoting strains were identified by traditional methods with biochemical tests and commercial identification compassing of API 20E, API-ZYM, and API 50CH (BioMérieux, France) as well. Individual tests were performed according to West and Colwell (1984), and Cowan and Steel (1970), as cited in (Buller 2014), Gram determination was decided based on the result of the KOH reaction (Halebian et al. 1981). Some antibiotic-producing strains were identified by the 16sRNA gene analysis according to Pham (2014).

2.6. Statistical analysis

One-way ANOVA statistical analysis of the results was carried out by using the Statgraphics Centurion XV software. Multiple Range Least Significant Difference was used to measure specific differences between pairs of means. Significant differences between the two treatments were tested using t-test: Paired Two Sample for Means with a significance level of $P \leq 0.05$ and compared t Stat and t Critical one-tail, t Stat and t Critical two-tail.

3. Results

3.1. Screening of IAA producer and phosphate solubilization strains

Out of 50 tested strains, six cultures isolated from edible algae *C. lentillifera* cultured at the Key Lab for Food and Environment Safety in Center Vietnam, and five other strains isolated from *Acropora* sp. from a coral reef in the center of Viet Nam produced IAA into screening broth medium. The phosphate solubilization screening and IAA-producing marine isolates are listed in Table 1.

Table 1- Microorganisms producing IAA and solubilizing phosphate

No	Isolates	Sources of isolation	Development of pink color	Phosphates solubilization
RN02	Gram-positive, rod-shape	<i>C. lentillifera</i>	+++	Positive
RN04	Gram-positive rod shape	<i>C. lentillifera</i>	++	Negative
RN05	Gram-positive rod shape	<i>C. lentillifera</i>	+	Positive
RN06	Gram-positive rod shape	<i>C. lentillifera</i>	+++	Positive
RN07	Gram-negative, coccus	<i>C. lentillifera</i>	++	Negative
RN08	Gram-positive rod shape	<i>C. lentillifera</i>	+	Negative
HRA1	Gram-negative rod shape	<i>Acropora</i> sp.	+++	Positive
HRA2	Gram-negative rod shape	<i>Acropora</i> sp.	+++	Positive
HRA3	Gram-negative rod shape	<i>Acropora</i> sp.	+++	Negative
HRA4	Gram-negative rod shape	<i>Acropora</i> sp.	+++	Negative
HRA5	Gram-negative rod shape	<i>Acropora</i> sp.	+++	Positive

+: Slight pink color development, ++: pink color development, +++ : dark pink color

The strains derived from edible algae showed dark pink color development including RN02, and RN06, other strains RN04, RN07 possessed pink color development (++) , whereas two other strains RN05, RN08 produced IAA slightly (+). All cultures from hard corals (HRA1, HRA2, HRA3, HRA4, HRA5) were considered as potential IAA producers with dark pink color development.

3.2. Production of IAA

The IAA production of isolates is shown in Table 2 and biostatistics of signification for means of treatment with the range of different letters. Most of the isolates revealed the highest IAA production on day 7 of cultivation. Strains RN02 and RN06 revealed dark pink color development (Table 1) and also yielded high levels of IAA production (Table 2). In the same manner, two isolates from the edible seaweed strain RN05 and RN08 produced very low amounts of IAA. The biostatistics analysis showed that those values were not significantly different. It inferred the two mentioned strains produced the same amount of IAA with the same trend.

Table 2- Biostatistics analysis of the significantly different treatment of IAA producers from marine-derived bacteria. The values are the mean of triplicate samples. The significantly different values are identified with different letters (P<0.05)

STRAINS	IAA ($\mu\text{g/mL}$)		
	Day 4	Day 7	Day 10
RN02	17.80 ^{fg}	12.15 ^{ghi}	14.70 ^{gh}
RN04	9.63 ^{hijk}	12.82 ^{gh}	4.99 ^{lmnop}
RN05	1.12 ^{pq}	6.08 ^{klmn}	1.62 ^{opq}
RN06	8.75 ^{ijkl}	25.75 ^{ab}	12.82 ^{gh}
RN07	7.71 ^{ijklm}	11.39 ^{ghij}	3.56 ^{nopq}
RN08	0.63 ^q	1.24 ^{opq}	1.31 ^{opq}
HRA1	5.23 ^{lmno}	18.93 ^{dfg}	18.37 ^{defg}
HRA2	4.08 ^{mnpq}	27.42 ^a	15.00 ^{gh}
HRA3	4.38 ^{mnpq}	23.73 ^{abc}	5.99 ^{klmn}
HRA4	21.82 ^{bcde}	21.36 ^{cdef}	1.88 ^{opq}
HRA5	2.79 ^{nopq}	18.00 ^{efg}	23.00 ^{bc}

Three strains HRA1, HRA2, and HRA3 from hard corals were good IAA producing (+++) in the screening step and also produced a high amount of IAA after 7 days of cultivation with 18.93 $\mu\text{g/mL}$ 27.42 $\mu\text{g/mL}$ and 23.73 $\mu\text{g/mL}$, respectively. Particularly, the strain HRA2 showed the highest amount of IAA on day 7 with 27.42 $\mu\text{g/mL}$. The best producer seaweed derived strain RN06 also yielded 25.75 $\mu\text{g/mL}$ IAA on day 7. Those values of IAA produced from HRA2 and RN06 were significantly different from IAA from day 4 and day 10 for both strains.

As shown in Table 3, the edible seaweed isolates RN02, RN05, RN08, and HRA3 reached the highest biomass on day 7 and the lowest biomass on day 10, the differences in biomass values between days 4 and 7, also days 7 and 10 were statistically significant. However, differences in biomass on days 4 and 10 were not statistically significant (Table 3). Both edible seaweed isolates RN06 and RN07 reached the maxima biomass on day 7 and the lowest on day 10. Biomass of strain RN06 on day 7 (14.22 mg/mL) had a statistically significant difference with biomass on day 4 (5.92 mg/mL) but there was no significant difference with biomass from day 10 (11.85 mg/mL). In contrast, the sea grape-associated isolate RN07 reached the highest

amount of biomass on day 7 with 10.67 mg/mL and there was a significant difference in biomass on day 10 with 6.89 mg/mL while there was no significant difference in biomass on day 4 (7.63 mg/mL).

Table 3- Biostatistics analysis of the significantly different treatment of biomass producers from marine-derived bacteria. The significantly different values are identified with different letters ($P= 0.05$).

STRAINS	BIOMASS (mg/mL)		
	Day 4	Day 7	Day 10
RN02	10.81 ^{abcdefg}	14.96 ^a	9.04 ^{bcdefghi}
RN04	7.29 ^{ghij}	8.17 ^{defghij}	7.67 ^{ghij}
RN05	7.85 ^{efghij}	11.63 ^{abcde}	5.26 ⁱ
RN06	5.93 ^{ij}	14.22 ^{ab}	11.85 ^{abcd}
RN07	7.63 ^{ghij}	10.67 ^{bcdefg}	6.89 ^{hij}
RN08	7.78 ^{fghij}	11.41 ^{abcdef}	5.93 ^{ij}
HRA1	11.48 ^{abcde}	10.15 ^{bcdefgh}	12.37 ^{abc}
HRA2	11.85 ^{abcd}	11.26 ^{abcfe}	7.78 ^{fghij}
HRA3	8.52 ^{cdefghij}	12.15 ^{abc}	8.15 ^{defghij}
HRA4	11.26 ^{abcdef}	12.15 ^{abc}	10.52 ^{bcdefg}
HRA5	8.29 ^{cdefghij}	9.55 ^{bcdefgh}	11.85 ^{abcd}

Most strains reached maxima of biomass on day 7, except HRA1, HRA2, and HRA5 isolates (Table 3). The isolates HRA1 and HRA5 had the highest biomass on day 10, but there were no statistically significant differences. The coral associate isolates HRA2 reached the highest biomass on day 4 with 11.85 mg/mL and slightly dropped a non-significant difference on day 7 with 11.26 mg/mL. The biostatistics analysis showed that only biomass yielded on day 4 (11.85 mg/mL) and day 10 (7.78 mg/mL) was a statistically significant difference (Table 3). Comparing of single strain, among isolates from seaweed RN02 produced the highest biomass and the total biomass produced from this strain was significantly different from other edible algae isolates except RN06. The results from the IAA screening step (Table 1) and quantitative IAA production looked like proof that RN04 and RN07 should be grouped in the moderate IAA producer strains whereas the strains RN05, and RN08 revealed rather weak IAA producer group and two other strains RN02 and RN06 showed as good IAA producers. Other coral-associated strains compassing HRA1, HRA2, HRA3, HRA4, and HRA5 should be placed in the last group for IAA producer.

3.3. Qualitative estimation of phosphate solubilization

Three out of six isolates from edible algae strains RN02, RN05, and RN06, and other three from coral strains HR1, HR2, and HR5 revealed phosphate soluble activities (Table 1, Figure1). Five strains consisting of RN02, RN06, HRA1, HRA2, and HRA5 could be considered as potential strains for both IAA producing and phosphate solubilization.

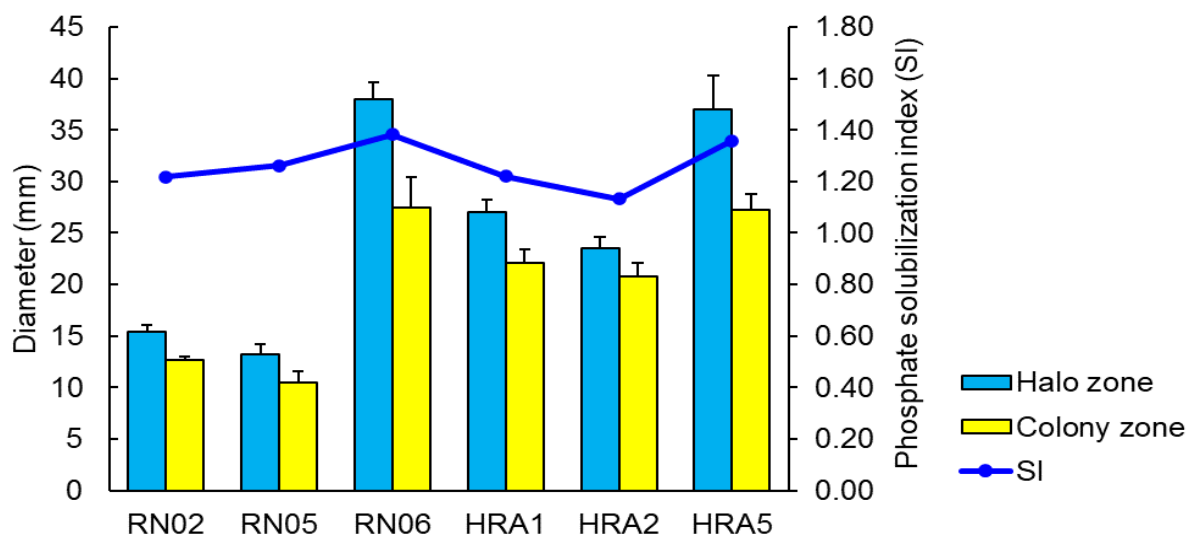


Figure 1- Phosphate solubilization of potential strains

The results of the Agar spot and pH drop methods are shown in Table 1 and Figure2. From these results of the comparison of the two methods revealed that isolates HRA1 showed a maximum of SI in the agar spot whereas minimum in the pH drop method, it showed a significant drop of pH in the incubation medium, it referred that HRA1 has the highest phosphate solubilizing potential. The pH drop was usually company with the phosphate solubilization, the pH was slightly dropped in the first days of incubation and reached the lowest point of 3.4 on day 5 and then remained stable. This trend of pH in broth medium for all strains in this present study.

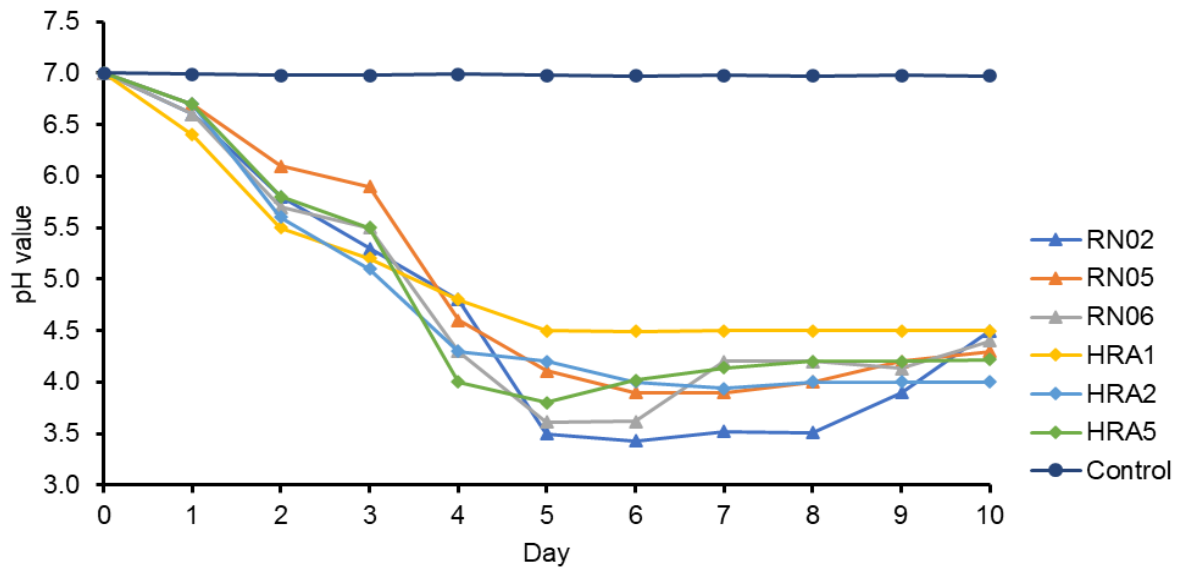


Figure 2- The pH change over cultivation time

As can be seen from Figure1, the most effective phosphate solubilization isolates are RN06 and HRA5 with SI equal to 1.38 and 1.35, respectively, both strains showed a pH drop from 7.00 to 3.61 and 3.80 in sequences on day 5 of incubation then the pH increased slightly up to ca. 5 on day 10. The pH drop in liquid media was thought to be a company with the solubilization of inorganic phosphate.

3.4. Antimicrobial activities

Antimicrobial activities of the IAA producer strains are shown in Figure3 with the mean and standard deviation. There were four strains RN04, RN06, RN07, and HRA5 showed inhibition of Gram-positive *B. subtilis*, the strain HRA5 had the strongest activity with a diameter of 7.85 mm and RN06 showed the lowest antibacterial activity with an average inhibition zone of 4.70 mm in diameter. The strain RN06 showed active against both two Gram-negative tested *E. coli* and coral pathogenic *S. marcescens* PDL100, whereas the strain RN04 had no inhibition of *E. coli*

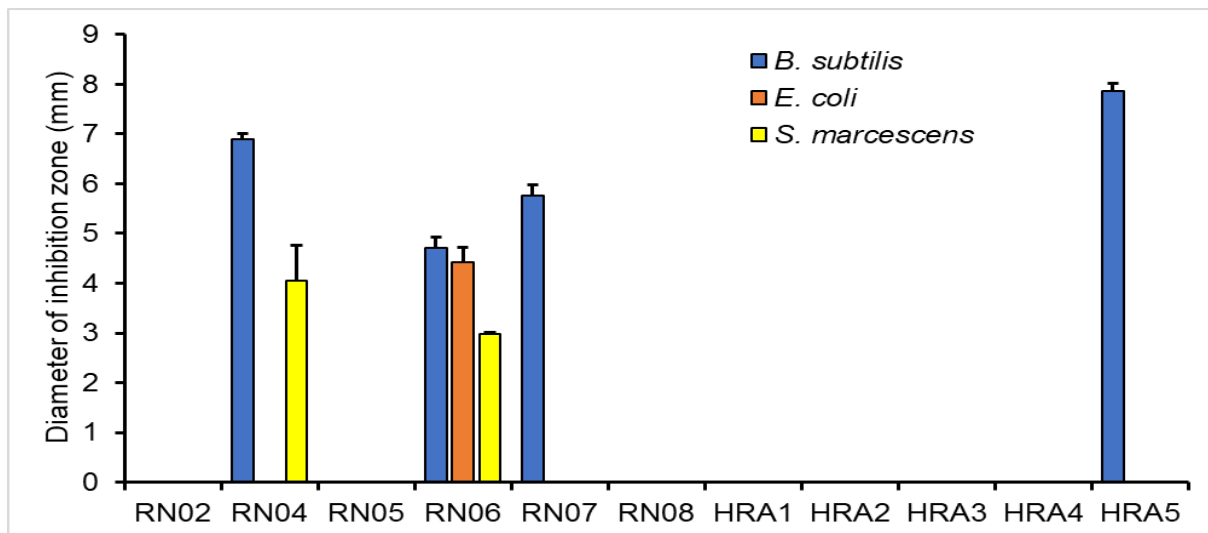


Figure 3- Antimicrobial activity of IAA producer strains

3.5. Identification of RN06 and HRA5

The potential strains RN06 and HRA5 from this study were closest to *Bacillus* and *Pseudomonas* respectively. The results of morphological and chemical tests are shown in Table 4 and the results of 16sRNA sequencing analysis are shown in Table 5, and Figure 4.

Table 4- Basic biochemical tests of potent strains RN06 and HRA5

<i>Characteristics</i>		<i>RN06</i>	<i>HRA5</i>
Morphological and supplementary tests			
1	Gram Staining	Positive	Negative
2	Cell width	0.8	0.2
3	Shape	Rods	Rods
4	Motility	Motile	Motile
5	Spore	Sporing	Non-Sporing
6	Catalase	Positive	Positive
7	Oxidase	Positive	Positive
8	MCA	-	+
9	TCBS	w	+
10	NaCl (%)	0/6	0/6
11	Methyl Red	+	-
12	V-P (Acetoin production)	+	-
13	Indole production	-	-
14	Citrate utilization	+	+
15	Nitrate reduction	+	+
16	H ₂ S production	-	-
17	Acetate utilization	+	-
18	Gelatin hydrolysis	+	-
Fermentation			
19	GLU (Glucose)	+	-
20	MAN (Mannitol)	+	w
21	INO (Inositol)	+	-
22	SOR (Sorbitol)	+	-
23	RHA (L-rhamnose)	-	-
24	SAC (Sucrose)	+	-
25	MEL (Melibiose)	w	+
26	AMY (Amygdalin)	+	-
27	ARA (Arabinose)	+	-
28	SAL (Salicin)	+	-
29	Starch	+	-
30	LAC (Lactose)	w	-
31	MAL (Maltose)	+	-
Enzymatic Reactions			
32	ONPG (Galactosidase)	+	-
33	ADH (Arginine decarboxylase)	-	+
34	LDC (Lysine decarboxylase)	-	-
35	ODC (Ornithine decarboxylase)	-	-
36	TDA (Tryptophane deaminase)	-	w
37	Urease	-	w

Vp: Voges-Proskauer, MCA: Growth on MacConkey, w: weak, +: positive reaction, -: negative, TCBS: thiosulfate-citrate-bile-sucrose agar, NaCl%: Growth in 0% and 6% salt in LBM medium.

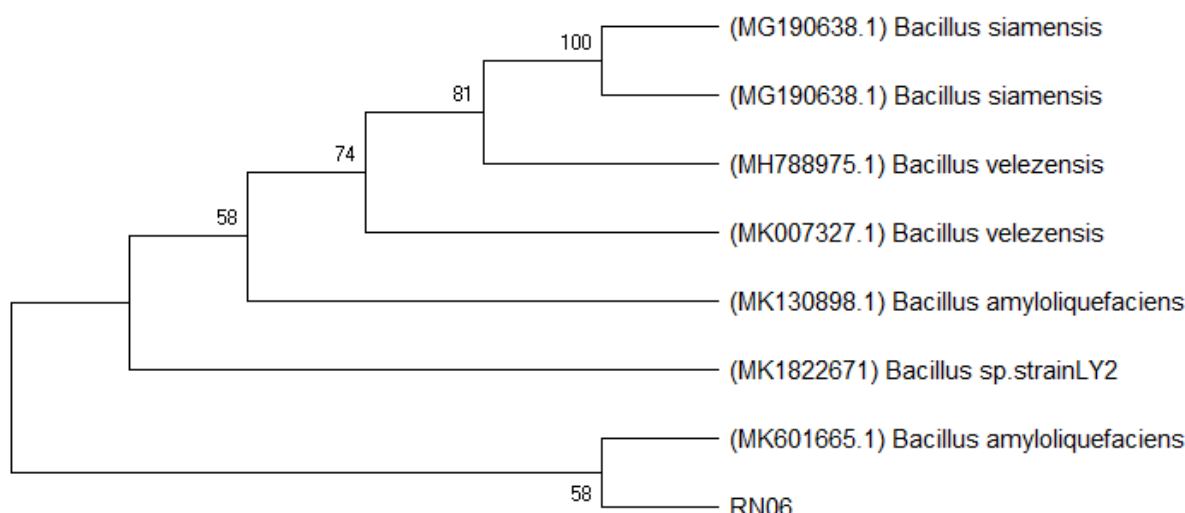


Figure 4- Neighbor-joining phylogenetic tree based on 16S rRNA gene sequences. Evolutionary relationships of taxa: The evolutionary history was inferred using the Neighbor-Joining method. The bootstrap consensus tree inferred from 1000 replicates is taken to represent the evolutionary history of the taxa analyzed. There were a total of 1342 positions in the final dataset. Evolutionary analyses were conducted in MEGA X

It was clear that the strain RN06 belonged to the genera *Bacillus*, however, the results from the analysis of 16s rRNA have been given some different results. Compared to other results for the identification of *Bacillus* with conventional biochemical tests with API kit (Logan & Berkeley 1984). The results from the biochemical test strongly suggested that this strain could be affiliated with *Bacillus amyloliquefaciens* rather than other *Bacillus* species (Table 5). In addition, the phylogenetic analysis showed that the strain RN06 was the closest to *Bacillus amyloliquefaciens* strain CIFTMFBB7 (Figure 4).

Both two potent strains from this study can grow at no salt concentration and 6% NaCl as well (Table 4). It could be due to the sources of isolation, the strain RN06 and HRA5 were associated with sea grapes and hard coral respectively and the salinity of seawater in the ambient sampling site was less than 35‰. However, this test was done here for getting a basic chemical test (up to 6% NaCl only) rather than a salt tolerance test, so all potential strains in this study were suggested to further experiment including salt tolerance, other plant-hormone producing or antifungals test with plant pathogens.

Table 5- Identification of RN06 and HRA5

Strains	Most closed relative strains from GenBank (NCBI)	Query cover (%)	Identify (%)	Possible genus
RN06	<i>Bacillus amyloliquefaciens</i> (MK130898.1)	99	99.93	<i>Bacillus</i> sp. strain RN06
	<i>Bacillus siamensis</i> (MG190638.1)	99	99.93	
	<i>Bacillus</i> sp. LY2 (MK182267.1)	99	99.93	
	<i>Bacillus velezensis</i> (MH788975.1)	99	99.93	
	<i>Bacillus amyloliquefaciens</i> (MH788971.1)	99	99.93	
	<i>Bacillus amyloliquefaciens</i> (MK601665.1)	99	99.93	
	<i>Bacillus velezensis</i> (MK007327.1)	99	99.93	
HRA5	<i>Pseudomonas fluorescens</i> (CP032618.1)	97	100	<i>Pseudomonas</i> sp. strain HRA5
	<i>Pseudomonas</i> sp. LG1D9 (CP026881.1)	97	100	
	<i>Pseudomonas chlororaphis</i> (CP011020.1)	97	99.93	
	<i>Pseudomonas fluorescens</i> (CP008896.1)	97	99.93	
	<i>Pseudomonas fluorescens</i> (GU198103.1)	97	100	
	<i>Pseudomonas gessardii</i> (NR_024928.1)	97	99.86	
	<i>Pseudomonas synxantha</i> (LR590482.1)	97	99.86	

4. Discussion & Conclusions

4.1. IAA producers

Compared to other results the marine-derived bacteria from this present study produced rather low amounts of IAA (maxima ca 30 µg/mL). These results are likely to be the same as those of Jeon et al. (2003) when using L-tryptophan as a precursor with a

concentration of 500 mg/L at initial cultivation, the *Pseudomonas fluorescens* strain M45 produced 17.7 µg/mL IAA, and *P. fluorescens* strains MCO7 yielded 22.7 µg/mL IAA. The results from this study reflected the reliability of those methods which were applied successfully in other studies (Gutierrez et al. 2009). They also revealed that when the strain was strongly acted with Salkowski's reagent, it inferred that they could be a good IAA-producing strain. This study was the first report of a good source of IAA produced from marine bacteria isolated from edible algae and hard coral from the Vietnamese sea. All isolates showed good growth in modified LB medium and cultivation conditions. This medium was desired for marine strains with some marine element components such as marine salts. However, the concentration of IAA was not always parallel to the amount of high biomass. The results from this study were similar to those of results from other studies of screening estuary *Vibrio* strains for IAA production. It was shown that the bacterial cells in the cultured broth of the highest IAA (21.43 µg/mL) producing strain J-S2-8 were similar to quite low IAA (5.52 µg/mL) producing strain J-S2-26 with 3.64×10^9 cell/mL and 3.42×10^9 cell/mL, respectively (Gutierrez et al. 2009). The other study of screening IAA producers from bacteria associated with sponges from the Gulf of Mannar, southeast coast of India showed that many associated bacteria could produce IAA in rather low concentration with a maximum of 0.41 µg/mL in LB plus tryptophan medium. The most abundant IAA-producer bacteria belonged to *Pseudomonas fluorescens*, *P. aeruginosa*, *P. putida*, *B. subtilis*, *B. licheniformis*, and *B. megaterium* (Vasanthabharathi & Jayalakshmi 2017). It is worth noting that the IAA amount produced from isolates in this study is in low concentration. Indeed, the high concentration of auxin could be toxic to plants, when IAA is the principal natural auxin in higher plants and overdose effects of IAA involve the use of herbicides for weed control (Grossmann 2003). On the other hand, the IAA produced from bacteria should be lower in vivo if they are considered biofertilizers. This phytohormone also is induced from the host plants and tryptophan was not usually found in vast amounts from soils.

4.2. Phosphate solubilization strains

The pH drop in liquid media was thought to be a company with the solubilization of inorganic phosphate. The phosphate-soluble bacteria produced organic acids in the media and induced the pH drops to dissolve phosphorus-containing minerals or insoluble phosphates (Cooper 1959). The pH drop on the first five days of bacterial incubation was significantly correlated with phosphate solubilization. The group of very good phosphate solubilization bacteria was all strains with a significant drop in pH at the first five days; the group bacteria were decided as good phosphate solubilization when the pH dropped to 4 and remained for the whole last time of incubation, whereas other bacteria group showed the pH still a decrease of the pH up to 3 along with the experimental time were poor phosphate solubilization (Sánchez-Cruz et al. 2019). However, all isolates from this present study showed a pH trend like the group of very good phosphate solubilization bacteria (Sánchez-Cruz et al. 2019). The results of phosphate solubilization with low SI values inferred that all tested strains possessed weak phosphate solubilization capacity in comparison with *P. aeruginosa* strain KUPSB12 with phosphate solubilization index of 2.85 in screening Pikovskaya's agar and a high amount of phosphate production of 219.64 ± 0.330 mg/mL in liquid medium as well (Paul & Sinha 2017).

The pH values and phosphate solubilization of all isolates were not found to be strictly correlated, thus the pH drop in the liquid medium was effective by other aspects such as the type of microorganisms and the cultivation media. It was shown in the study of phosphate solubilization by fungal isolates from the Brazilian soils (de Oliveira Mendes et al. 2014), that result showed that *Aspergillus niger* FS1 was able to solubilize 71, 36, 100, and 14% of the phosphate from AlPO_4 , FePO_4 , $\text{Ca}_3(\text{PO}_4)_2$, and RPs, respectively. The phosphate solubilization was effective by medium acidification, particularly for $\text{Ca}_3(\text{PO}_4)_2$.

The microorganisms associated with corals in this study were decided as the most dominant bacteria in *Acropora muricata* isolated in August 2016 (Pham et al. 2019). The pH value and PO_4^{4-} in ambient seawater were measured with 7.61 ± 0.03 and 4.77 ± 1.29 µgP/L, respectively, at the same time of collecting sample. While those parameters measured in May 2016 were 8.10 ± 0.00 and 15.89 ± 2.30 µgP/L, respectively, it could be seen at the time of sample collection, the concentration of PO_4^{4-} in seawater was rather low. The data also revealed that the number of phosphate solubilization bacteria was strongly correlated with the pH values in ambient seawater (Pham et al. 2019). In some cases, phosphate deficiency has accelerated bacteria to dissolve insoluble phosphate (Gyaneshwar et al. 1999). One of the most effective inorganic phosphorus solubilizers was the genera of *Enterobacter* and *Pseudomonas* (Yazdani et al. 2009).

4.3. Antimicrobial activities

The inhibition level of bacteria in this study is similar to those of isolates from the hard coral (Nguyen et al. 2016) when the clear zones received in both studies were quite weak. However, the results of other studies reported that many coral-derived bacteria had strong antimicrobial activities against the growth of several tested strains (de Castro et al. 2010; Zhang et al. 2012). Three strains P9, P11, and P20 belonged to *Pseudomonas* and showed inhibition against nine tested strains. Those strains were most effective against the test strains *S. aureus*, *S. typhimurium*, and *Micrococcus* sp. However, there was no inhibition against *Candida albicans*. The isolate P8 identified as *Bacillus pumilus* had antimicrobial activity against 12 tested bacteria (*Aeromonas salmonicida*, *A. hydrophila*, *Enterobacter xiangfangensis*, *Enterococcus faecium*, *E. coli*, *Micrococcus* sp., *S. typhimurium*, *Staphylococcus aureus*, *Streptococcus* sp., *Vibrio alginoliticus*, *V. proteolyticus*, *V. vulnificus*) and the yeast *C. albicans*. The results emphasized the potential use of epiphytic bacteria isolated from brown algae *Padina pavonica* (Peacocks tail) from the northern coast of Tunisia as producers of novel antibacterial compounds (Ismail et al. 2016). *Bacillus licheniformis* strain A2

isolated from the halotolerant plant *Suaeda fruticosa* from the saline desert, Gujarat (India) was reported to solubilize phosphate, produce IAA, and inhibit pathogenic fungus against *Fusarium oxysporum* (Goswami et al. 2014).

In addition, the potential strain RN06 isolated from sea grape possessed antimicrobial capacity against human pathogen *E. coli* 0157. It is inferred that this strain is very powerful in use for aquaculture or agriculture when it is applied in the field, it is very effective in preventing microbial contamination from human activities. The results from the basic chemical test and analysis of the 16S rRNA gene showed that the strain RN06 was most relative to *Bacillus* sp. and isolates HRA5 were identified as *Pseudomonas* sp. It could be seen that both genera were good candidates for PGP so far. A strain of *Bacillus subtilis* LK14 isolated from a medical plant *Moringa peregrina* growing in the arid region of Arabia has shown significant prospects in phosphate solubilization after 5 days of cultivation, *B. subtilis* LK14 produced IAA with the highest concentration of 8.7 μM after 14 days of growth. This strain was applied to *Solanum lycopersicum* and it significantly increased the shoot and root biomass as well as chlorophyll contents as compared to control plants (Khan et al. 2016). On the other hand, the estuary bacteria *Pseudomonas aeruginosa* strain KUPSB12 was illustrated as a potential strain for antimicrobial capacity against Gram-negative tested strains including *E. coli*, *Shigella flexneri*, *V. cholerae*, and three Gram-positive tested strains *Bacillus subtilis*, *Micrococcus luteus* and *Staphylococcus aureus* (Paul & Sinha 2017). None of the total of 11 strains which were IAA producer strains in this study were actinomycetes according to the morphological results. However, actinomyces was thought to be a good candidate for plant growth promotion. Both strains produced a bit low amount of IAA with $3.04 \pm 0.16 \mu\text{g/mL}$ from *Streptomyces* and $4.24 \pm 0.21 \mu\text{g/mL}$ from *Micromonospora*. The actinobacteria isolated from salt marsh soil have been shown to have tolerance of NaCl up to 5 and 11%, respectively, the ability of nitrogen-fixing, produce some hydrolytic enzymes, and could able to serve as plant growth promoting with proof in application in wheat plants under salt stress (Gong et al. 2018).

Macroalgae were reported as good sources of marine microorganisms, the microorganisms are beneficial and harmful partners as well. The *Bacillus* spp. and *Pseudomonas* spp. were the most commonly associated bacteria which were confirmed from algae (del Olmo et al. 2018; Karthick & Mohanraju 2018). The strain RN06 was an IAA producer, phosphate solubilization also possessed antimicrobial activity against three out of four tested strains including of human pathogenic strain *E. coli* 0157. It is worth noting that this bacterium was isolated from edible seaweed so that it could be a potent strain for use as a biological inoculant in commercial aquaculture of seaweed when the demand for seaweed as a healthy food has been increasing recently, especially in Southeast Asia (Chen et al. 2019). The results from the basic chemical test and analysis of the 16S rRNA gene showed that the strain RN06 was most relative to *Bacillus* sp., and isolate HRA5 was identified as *Pseudomonas* sp. It could be seen that both genera were good candidates for plant growth promotion so far (Comeau et al. 2021). Noteworthy, the strain *S. marcescens* strain PDL100 known to cause a severe disease named "white spot" on reef-building coral *Acropora palmate* in the Florida Keys, United States was used as a tested strain (Gyaneshwar et al. 1999).

The estuary bacteria *P. aeruginosa* strain KUPSB12 illustrated as a potential strain for plant growth-promoting when it showed high effectiveness with phosphate solubilization and possessed antimicrobial capacity against *E. coli*, *S. flexneri*, *Vibrio cholerae*, *B. subtilis*, *Micrococcus luteus* and *Staphylococcus aureus* (Paul & Sinha 2017).

Both two potent strains from this study can grow at no salt concentration and 6% NaCl as well (Table 2). It could be due to the sources of isolation, the strain RN06 and HRA5 were associated with sea grapes and hard coral respectively and the salinity of water in the ambient sampling site was less than 35‰. However, this test was done here for getting of basic chemical test (up to 6% NaCl only) rather than a salt tolerance test, so all potential strains in this study were suggested to further experiment including salt tolerance, other plant hormone-producing or antifungals test with plant pathogens.

Seaweed-associated bacteria *Bacillus amyloliquefaciens* strain RN06 produced high amounts of IAA, solubilized inorganic phosphate, and produced antibiotics including antimicrobial agent against human pathogen *E. coli* 0157, and coral pathogen *S. marcescens* PDL100. The derived hard coral bacterium HRA5 was identified as *Pseudomonas* genera. Both two marine potent isolates from this study were identified as *Bacillus* and *Pseudomonas* at the general level. Interestingly, they have been well-known plant growth-promoting bacteria in soils so far. Although the results from this work are still limited, it can clearly pave the way for research on the application of biological inoculants of original marine isolates to seaweed farming as the demand for this food has been increasing rapidly in recent years.

Acknowledgments

This research was supported by the project of the Vietnam Academy of Science and Technology, grant number CSCL17.02/23-24. We would like to thank Mr Phan Kim Hoang for sampling and identification of corals. We acknowledge VAST Key Lab for Food and Environment Safety in Center Viet Nam, Institute of Oceanography - VAST for providing facilities to conduct this experiment.

Conflicts of Interest

The authors declare no conflict of interest. The funders had no role in the design of the study; in the collection, analyses, or interpretation of data; in the writing of the manuscript, or in the decision to publish the results.

References

- Ahmad B, Nigar S, Malik N A, Bashir S, Ali J, Yousaf S, Bangash J A & Jan I (2013). Isolation and Characterization of Cellulolytic Nitrogen Fixing Azotobacter species from Wheat Rhizosphere of Khyber Pakhtunkhwa. *World Applied Sciences Journal* 27 (1): 51-60. [10.5829/idosi.wasj.2013.27.01.81120](https://doi.org/10.5829/idosi.wasj.2013.27.01.81120)
- Ali B, Sabri A N, Ljung K & Hasnain S (2009). Auxin production by plant associated bacteria: impact on endogenous IAA content and growth of *Triticum aestivum* L. *Lett Appl Microbiol* 48(5): 542-547. <https://doi.org/10.1111/j.1472-765X.2009.02565.x>
- Amin S A, Hmelo L R, van Tol H M, Durham B P, Carlson L T, Heal K R, Morales R L, Berthiaume C T, Parker M S, Djunaedi B, Ingalls A E, Parsek M R, Moran M A & Armbrust E V (2015). Interaction and signalling between a cosmopolitan phytoplankton and associated bacteria. *Nature* 522: 98-101. <https://doi.org/10.1038/nature14488>
- Bauer A W, Kirby W M, Sherris J C & Turck M (1966). Antibiotic susceptibility testing by a standardized single disk method. *American Journal of Clinical Pathogens* 45: 493-496.
- Bharucha U, Patel K & Trivedi U B (2013). Optimization of Indole Acetic Acid Production by *Pseudomonas putida* UB1 and its Effect as Plant Growth-Promoting Rhizobacteria on Mustard (*Brassica nigra*). *Agricultural Research* 2(3): 215-221. <https://doi.org/10.1007/s40003-013-0065-7>
- Bogaert K A, Blommaert L, Ljung K, Beeckman T & De Clerck O (2019). Auxin Function in the Brown Alga *Dictyota dichotoma*. *Plant Physiol* 179(1): 280-299. <https://doi.org/10.1104/pp.18.01041>
- Buller N B (2014). *Bacteria and Fungi from Fish and Other Aquatic Animals*. ISBN-13: 978 1 84593 805 5 ed. Centre for Agriculture and Bioscience International (CABI), Oxfordshire, UK.
- Chen X, Sun Y, Liu H, Liu S, Qin Y & Li P (2019). Advances in cultivation, wastewater treatment application, bioactive components of *Caulerpa lentillifera* and their biotechnological applications. *PeerJ* 7: e6118-e6118. <https://doi.org/10.7717/peerj.6118>
- Comeau D, Balthazar C, Novinscak A, Bouhamdani N, Joly D L & Filion M (2021). Interactions Between *Bacillus* Spp., *Pseudomonas* Spp. and *Cannabis sativa* Promote Plant Growth. *Frontiers in Microbiology* 12. <https://doi.org/10.3389/fmicb.2021.715758>
- Cooper R (1959). Bacterial fertilizers in the Soviet Union. *Soils Fertil.* 22: 327-333.
- de Castro A P, Araujo S D J, Reis A M, Moura R L, Francini-Filho R B, Pappas G, Jr, Rodrigues T B, Thompson F L & Kruger R H (2010). Bacterial community associated with healthy and diseased reef coral *Mussismilia hispida* from eastern Brazil. *Microb. Ecol* 59: 658-667. <https://doi.org/10.1007/s00248-010-9646-1>
- de Oliveira Mendes G, Moreira de Freitas A L, Liparini Pereira O, Ribeiro da Silva I, Bojkov Vassilev N & Dutra Costa M (2014). Mechanisms of phosphate solubilization by fungal isolates when exposed to different P sources. *Annals of Microbiology* 64(1): 239-249. <https://doi.org/10.1007/s13213-013-0656-3>
- del Olmo A, Picon A & Nuñez M (2018). The microbiota of eight species of dehydrated edible seaweeds from North West Spain. *Food Microbiology* 70: 224-231. <https://doi.org/10.1016/j.fm.2017.10.009>
- Dittami S M, Barbeyron T, Boyen C, Cambefort J, Collet G, Delage L, Gobet A, Groisillier A, Leblanc C, Michel G, Scornet D, Siegel A, Tapia J E & Toton T (2014). Genome and metabolic network of "Candidatus *Phaeomarinobacter ectocarpi*" Ec32, a new candidate genus of Alphaproteobacteria frequently associated with brown algae. *Frontiers in Genetics* 5: 241-254. <https://doi.org/10.3389/fgene.2014.00241>
- Gong Y, Bai J L, Yang H T, Zhang W D, Xiong Y W, Ding P & Qin S (2018). Phylogenetic diversity and investigation of plant growth-promoting traits of actinobacteria in coastal salt marsh plant rhizospheres from Jiangsu, China. *Syst Appl Microbiol* 41(5): 516-527. <https://doi.org/10.1016/j.syapm.2018.06.003>
- Gordon S A & Paleg L G (1957). Observations on the Quantitative Determination of Indoleacetic Acid. *Physiol. Plant* 10: 39-47
- Goswami D, Dhandhukia P, Patel P & Thakker J N (2014). Screening of PGPR from saline desert of Kutch: growth promotion in *Arachis hypogea* by *Bacillus licheniformis* A2. *Microbiol Res* 169(1): 66-75. <https://doi.org/10.1016/j.micres.2013.07.004>
- Grossmann K (2003). Mediation of Herbicide Effects by Hormone Interactions. *Journal of Plant Growth Regulation* 22(1): 109-122. <https://doi.org/10.1007/s00344-003-0020-0>
- Gupta M, Kiran S, Gulati A, Singh B & Tewari R (2012). Isolation and identification of phosphate solubilizing bacteria able to enhance the growth and aloin-A biosynthesis of *Aloe barbadensis* Miller. *Microbiol Res* 167(6): 358-363. <https://doi.org/10.1016/j.micres.2012.02.004>
- Gutierrez C K, Matsui G Y, Lincoln D E & Lovell C R (2009). Production of the phytohormone indole-3-acetic acid by estuarine species of the genus *Vibrio*. *Appl Environ Microbiol* 75(8): 2253-2258. <https://doi.org/10.1128/AEM.02072-08>
- Gyaneshwar P, Parekh L J, Archana G, Poole P S, Collins M D, Hutson R A & Kumar G N (1999). Involvement of a phosphate starvation inducible glucose dehydrogenase in soil phosphate solubilization by Enterobacter asburiae. *FEMS Microbiology Letters* 171(2): 223-229. <https://doi.org/10.1111/j.1574-6968.1999.tb13436.x>
- Halebian S, Harris B, Finegold S M & Rolfe R D (1981). Rapid method that aids in distinguishing Gram-positive from Gram-negative anaerobic bacteria. *Journal of clinical microbiology* 13(3): 444-448. <https://doi.org/10.1128/jcm.13.3.444-448.1981>
- Ismail A, Ktari L, Ahmed M, Bolhuis H, Boudabbous A, Stal L J, Cretoiu M S & El Bour M (2016). Antimicrobial Activities of Bacteria Associated with the Brown Alga *Padina pavonica*. *Front Microbiol* 7: 1072-1085. <https://doi.org/10.3389/fmicb.2016.01072>
- Jeon J-S, Lee S-S, Kim H-Y, Ahn T-S & Song H-G (2003). Plant Growth Promotion in Soil by Some Inoculated Microorganisms. *The Journal of Microbiology* 41(4): 271-276.
- Karthick P & Mohanraju R (2018). Antimicrobial Potential of Epiphytic Bacteria Associated With Seaweeds of Little Andaman, India. *Front Microbiol* 9: 611. <https://doi.org/10.3389/fmicb.2018.00611>
- Khan A L, Halo B A, Elyassi A, Ali S, Al-Hosni K, Hussain J, Al-Harrasi A & Lee I-J (2016). Indole acetic acid and ACC deaminase from endophytic bacteria improves the growth of *Solanum lycopersicum*. *Electronic Journal of Biotechnology* 21: 58-64. <https://doi.org/10.1016/j.ejbt.2016.02.001>
- Le Bail A, Billoud B, Kowalczyk N, Kowalczyk M, Gicquel M, Le Panse S, Stewart S, Scornet D, Cock J M, Ljung K & Charrier B (2010). Auxin metabolism and function in the multicellular brown alga *Ectocarpus siliculosus*. *Plant physiology* 153(1): 128-144. <https://doi.org/10.1104/pp.109.149708>
- Leyser O (2010). The power of auxin in plants. *Plant Physiol* 154(2): 501-505. <https://doi.org/10.1104/pp.110.161323>
- Lin H, Li Y & Hill R T (2022). Microalgal and bacterial auxin biosynthesis: implications for algal biotechnology. *Current Opinion in Biotechnology* 73: 300-307. <https://doi.org/10.1016/j.copbio.2021.09.006>
- Logan N A & Berkeley R C (1984). Identification of *Bacillus* Strains Using the API System. *Journal of General Microbiology* 130(7): 1871-1882

- Maruyama A, Maeda M & Simidu U (1989). Microbial production of auxin indole-3-acetic acid in marine sediments. *Marine Ecology Progress Series* 58(1/2): 69-75. <http://www.jstor.org/stable/24842169>
- Mayers T J, Bramucci A R, Yakimovich K M & Case R J (2016). A Bacterial Pathogen Displaying Temperature-Enhanced Virulence of the Microalga *Emiliana huxleyi*. *Frontiers in Microbiology* 7. 10.3389/fmicb.2016.00892
- Mishra A K & Kefford N P (1969). Developmental studies on the coenocytic alga, *Caulerpa sertularioides*. *J Phycol* 5(2): 103-109. <https://doi.org/10.1111/j.1529-8817.1969.tb02586.x>
- Nguyen K H, Pham T M, Bui H H & Vo H T (2016). Screening of coral associated bacteria with antimicrobial activities from scleractinian coral *Acropora muricata* in the Nha Trang bay. *The Collection of Marine Work (in Vietnamese)* 22: 83-95
- Palomo S, González I, de la Cruz M, Martín J, Tormo J R, Anderson M, Hill R T, Vicente F, Reyes F & Genilloud O (2013). Sponge-derived *Kocuria* and *Micrococcus* spp. as sources of the new thiazolyl peptide antibiotic kocurin. *Marine drugs* 11(4): 1071-1086. <https://doi.org/10.3390/md11041071>
- Park J-M, Radhakrishnan R, Kang S-M & Lee I-J (2015). IAA Producing *Enterobacter* sp. I-3 as a Potent Bio-herbicide Candidate for Weed Control: A Special Reference with Lettuce Growth Inhibition. *Indian journal of microbiology* 55(2): 207-212. <https://doi.org/10.1007/s12088-015-0515-y>
- Paul D & Sinha S N (2017). Isolation and characterization of phosphate solubilizing bacterium *Pseudomonas aeruginosa* KUPSB12 with antibacterial potential from river Ganga, India. *Annals of Agrarian Science* 15(1): 130-136. <https://doi.org/10.1016/j.aasci.2016.10.001>
- Pham T M (2014). Community of soft coral *Alcyonium digitatum* associated bacteria and their antimicrobial activities. PhD Thesis, Christian-Albrecht University of Kiel, GEOMAR in Kiel, Germany.
- Pham T M, Nguyen K H, Nguyen M H, Phan M T, Hoang T D, Vo H T, Nguyen T D H, Le T D & Nguyen H H (2019). A study on bacteria associated with three hard coral species from Ninh Thuan by epifluorescence and most diluted culture method. *Vietnam Journal of Marine Science and Technology* 19(2): 271-283. <https://doi.org/10.15625/1859-3097/19/2/10814>
- Pham T M, Nguyen N T & Nguyen K H (2018). *Bacillus* sp. VK2 isolated from *Acropora hyacinthus* from Ninh Thuan and its antimicrobial activities against cause of white pox disease in *Acropora palmate*. *Vietnam Journal of Marine Science and Technology* 18(2): 197-204. <https://doi.org/10.15625/1859-3097/18/2/8766>
- Rawat P, Das S, Shankhdhar D & Shankhdhar S C (2021). Phosphate-Solubilizing Microorganisms: Mechanism and Their Role in Phosphate Solubilization and Uptake. *Journal of Soil Science and Plant Nutrition* 21(1): 49-68. <https://doi.org/10.1007/s42729-020-00342-7>
- Sánchez-Cruz R, Tpia Vázquez I, Batista-García R A, Méndez-Santiago E W, Sánchez-Carbente M d R, Leija A, Lira-Ruan V, Hernández G, Wong-Villarreal A & Folch-Mallol J L (2019). Isolation and characterization of endophytes from nodules of *Mimosa pudica* with biotechnological potential. *Microbiological Research* 218: 76-86. <https://doi.org/10.1016/j.micres.2018.09.008>
- Sunardi H, Nikmatullah A, Ambana Y, Ilhami B T K, Abidin A S, Ardiana N, Kirana I A P, Kurniawan N S H, Rinaldi R, Jihadi A & Prasedya E S (2021). Phytohormone content in brown macroalgae *Sargassum* from Lombok coast, Indonesia. *IOP Conference Series: Earth and Environmental Science* 712(1): 012042. <https://doi.org/10.1088/1755-1315/712/1/012042>
- Tao C, Yuan C, Ruan C, Chen Q & Lin W (2017). Effects of different phytohormones on the growth of *Caulerpa lentillifera*. *Journal of Fuzhou University (Natural Science Edition)* 45(2): 291-295
- Tirtawijaya G, Negara B F S P, Lee J-H, Cho M-G, Kim H K, Choi Y-S, Lee S-H & Choi J-S (2022). The Influence of Abiotic Factors on the Induction of Seaweed Callus. *Journal of Marine Science and Engineering* 10(4): 513. <https://doi.org/10.3390/jmse10040513>
- Vasanthabharathi V & Jayalakshmi S (2017). Diversity and Distribution of Indole Acetic Acid Producing Marine Sponge Associated Bacteria from Gulf of Mannar, Southeast Coast of India. *Global Veterinaria* 19(1): 487-490. <https://doi.org/10.5829/idosi.gv.2017.487.490>
- Yazdani M, Bahmanyar M A, Pirdashti H & A E M (2009). Effect of phosphate solubilization microorganisms (PSM) and plant growth promoting rhizobacteria (PGPR) on yield and yield components of corn (*Zea mays* L.). *Proc. World Acad. Science* 37: 90-92. <https://doi.org/10.5281/zenodo.1080014>
- Zhang X, Sun Y, Bao J, He F, Xu X & Qi S (2012). Phylogenetic survey and antimicrobial activity of culturable microorganisms associated with the South China Sea black coral *Antipathes dichotoma*. *FEMS Microbiol. Lett* 336: 122-130. <https://doi.org/10.1111/j.1574-6968.2012.02662.x>



Copyright © 2024 The Author(s). This is an open-access article published by Faculty of Agriculture, Ankara University under the terms of the [Creative Commons Attribution License](https://creativecommons.org/licenses/by/4.0/) which permits unrestricted use, distribution, and reproduction in any medium or format, provided the original work is properly cited.



A comprehensive Assessment of Sunflower Genetic Diversity Against *Macrophomina phaseolina*

Nemanja Ćuk^a , Sandra Cvejić^{a*} , Velimir Mladenov^b , Milan Jocković^a , Miloš Krstić^a , Brankica Babec^a ,
Siniša Jocić^a , Boško Dedić^a 

^aDepartment of Sunflower, Institute of Field and Vegetable Crops, Novi Sad, SERBIA

^bFaculty of Agriculture, University of Novi Sad, SERBIA

ARTICLE INFO

Research Article

Corresponding Author: Sandra Cvejić, E-mail: sandra.cvejic@ifvcns.ns.ac.rs

Received: 27 April 2023 / Revised: 21 December 2023 / Accepted: 25 January 2024 / Online: 23 July 2024

Cite this article

Ćuk N, Cvejić S, Mladenov V, Jocković M, Krstić M, Babec B, Jocić S, Dedić B (2024). A comprehensive Assessment of Sunflower Genetic Diversity Against *Macrophomina phaseolina*. *Journal of Agricultural Sciences (Tarim Bilimleri Dergisi)*, 30(3):513-525. DOI: 10.15832/ankutbd.1288528

ABSTRACT

The sunflower is a significant oil crop that can be cultivated in various environmental conditions. Due to the changing climate, the pathogen profile has been altered, posing a threat to sunflower production. Among the various threats, charcoal rot, caused by the soil-borne fungus *Macrophomina phaseolina* (Tassi) Goid, is one of the most significant pathogen. This study aimed to investigate the resistance of 80 sunflower inbred lines to this pathogen using two inoculation methods and naturally infested area under field conditions in two years, 2019 and 2020. The results showed that both inoculation methods and occurrence of disease in naturally infested area (DNI) effectively differentiated between resistant and susceptible inbred lines, with the toothpick method being the

most effective. Thirteen inbred lines were resistant according to all inoculation methods, and the others were moderately resistant moderately susceptible or susceptible regarding to inoculation method. The study identified five inbred lines (Ha 74, L1, LIV 10, MA SC 2 and PB 21) as the most resistant, making them important sources for breeding sunflower hybrids resistant to *M. phaseolina*. Their resistance was confirmed in 2020, highlighting their potential to combat the impact of climate change on sunflower production. This study represents a valuable insight into the control of *M. phaseolina* using sunflower resistant genotypes, especially since resistance findings have been lacking in other plant species.

Keywords: Charcoal rot, Disease severity, Inbred lines, Inoculation methods, Sunflower

1. Introduction

Sunflower (*Helianthus annuus* L.) is an important oil crop that is grown on more than 28 million hectares worldwide, primarily in temperate, semi-dry regions (Miklić 2022). The major producers of sunflower seeds are Russia, Ukraine, the European Union, and Argentina, which collectively account for over 75% of total sunflower seed production (USDA 2023). Sunflower has advantages over other oil crops due to its adaptation, i.e., its ability to grow in different agroecological conditions, and its moderate drought tolerance attributed to a well-developed root system (Debaeke et al. 2017). However, the changing climate is affecting the pathogen profile, jeopardizing sunflower production. One of the severe threats to sunflower production is charcoal rot caused by a soil-borne fungus, *Macrophomina phaseolina* (Tassi) Goid. Unlike most pathogens, *M. phaseolina* prefers in warm and dry conditions, and can spread within the host within 24 to 48 hours after infection (Khan 2007), especially in conditions of water deficient yields can be significantly reduced (Özelçi et al. 2022). The severity of the disease can be extremely high, and the changing climate has led to the emergence of this pathogen in other European countries with continental climates. Isolates from these countries are more adapted to lower temperatures than those from tropical and subtropical regions (Veverka 2008). Moreover, *M. phaseolina* is a worldwide crop pathogen that can affect over 700 plant species and has a broad geographic distribution (Schroeder et al. 2019; Dell'Olmo et al. 2022).

In field production of sunflower, symptoms of *M. phaseolina* infestation can be visible after seed filling, resulting in premature ripening and complete yield loss (Mahmoud 2010; Chattopadhyay et al. 2015). The infestation can cause a reduction in seed yield of up to 20% (Jordaan et al. 2019; Qamar & Ghazanfar 2019), and in severe cases, yield can be reduced by 75% or 90% (Mahmoud 2010; Ijaz et al. 2013). The stems of affected plants lose their green colour, and grey discoloration appears from the lower part of the stem and spreads to the upper parts, making it challenging to intervene in crops towards the end of the vegetation period (Bokor 2007). Other symptoms on sunflower that can confirm presence of disease are, reduced head diameter, premature ripening, absence or compression of pith in the lower part of the stem, and microsclerotia presence in the middle area

of stem and on the main root (Mahmoud & Budak 2011). Therefore, it is essential to develop suitable field screening methods for *M. phaseolina* to obtain accurate information on its impact on sunflower plants.

Controlling the pathogen is a difficult task due to its ability to survive in various conditions, and no existing fungicides are available. Therefore, the most effective way to control the disease is by using resistant genotypes (Cotuna et al. 2021). To ensure ecologically acceptable sunflower production, it is necessary to use highly resistant hybrids to economically important pathogens (Seiler et al. 2017). The production of high-quality sunflower genetic material requires constant monitoring of the interactions between the sunflower as a host, economically significant diseases, and the environment, as well as the type of existing resistance (Škorić 2016; Tančić-Živanov et al. 2021). Successful breeding for disease resistance involves monitoring the interactions between the sunflower, specific pathogens, and the environment, assessing the stability of sunflower resistance to certain pathogens, and applying general principles of resistance breeding. However, genetics of resistance against *M. phaseolina* has not been fully elucidated and different findings have been reported. Talukdar et al. (2009) reported a continuous distribution of soybean reaction to *M. phaseolina*, ranging from highly susceptible through moderately resistant, to highly resistant. This suggests that disease resistance is influenced by multiple loci, thus making breeding for resistance difficult. Khan (2007) reported that sunflower tolerance to *M. phaseolina* has been horizontal, controlled by polygenes and completely resistant genes do not exist. All commercial sunflower cultivars are susceptible, especially expressed among hybrids with short vegetation and for genotypes in arid areas (Kaya 2016). Thus, only a moderate resistance level has been found in cultivated sunflower germplasm (Tančić et al. 2012; Ijaz et al. 2013; Jalil et al. 2013) and the wild relatives (Tančić et al. 2012; Seiler et al. 2017; Warburton et al. 2017; Shehbaz et al. 2018).

The rising abiotic and biotic stresses associated with global climate change necessitate the development of climate-ready sunflower capable of withstanding stress and providing stable yields (Radanović et al. 2022). Climate changes deliver unpredictable rainfall patterns resulting in more extended and more frequent periods of drought (Masalia et al. 2018). Environmental factors are limiting for the disease appearance caused by *M. phaseolina*, and high humidity immediately after infection could completely stop the disease development, while dry and warm period will boost formation of microsclerotia in the stem and finally lead to symptoms appearing at the plant maturity stage.

The aim of this study was to assess the response of 80 sunflower inbred lines to *M. phaseolina* infection, by analyzing disease symptoms, disease incidence, and McKinney index. Two primary goals were to identify potential sources of resistance to *M. phaseolina* and to evaluate different inoculation methods during two-year trial to determine the most effective approach. The identification of sunflower inbred lines with resistance to *M. phaseolina* would enable the timely improvement of preferred hybrids through resistance introgression, leading to the production of high-quality sunflower.

2. Material and Method

2.1. Plant material

Eighty sunflower inbred lines were selected from the sunflower broad gene pool at the Institute of Field and Vegetables Crops (IFVC) Novi Sad, Serbia (Anđelković et al. 2020). Ensuring divergence among the lines in terms of various characteristics such as origin, maturity, morphological traits, disease tolerance, type, and general agronomic properties (Table 1). Some of the inbred lines were previously evaluated for resistance to *M. phaseolina*, and only those exhibiting a certain level of resistance were selected for this study (Tančić-Živanov et al. 2021).

Table 1- List of 80 sunflower inbred lines inoculated in Rimski Šančevi Novi Sad, 2019, with three inoculation method and evaluated for resistance to *Macrophomina phaseolina*

No	Inbred lines	Traits of interest	No	Inbred lines	Traits of interest
1	AB-OR-8*	Medium early, OR	41	IMI AB 24 PR	IMI
2	AB-OR-ST-50	Medium early	42	KINA-B-5	Medium late
3	AB-OR-ST-62	Medium early	43	KINA-H-25	Late
4	AR-KOR-10	Medium early	44	L1 *	Medium early, good GCA
5	AR-7	Bright leaves	45	LIP P 16	Early
6	AS 1 PR	HO	46	LIP P 32	resistant to <i>O. cumana</i>
7	AS 87*	Medium early, good GCA	47	LIP P 98*	ultra-early, resistant to <i>O. cumana</i>
8	AS 95 PR	High 1000 seed mass	48	LIV 10	Medium early, OR
9	AZDO-2	Late	49	LIV 17	OR
10	BT-VL-24	OR	50	MA-SC-2*	Medium late, good GCA
11	BT-VL-17-SU	SU	51	NS BW 3	White seed colour, birds
12	CMS 1-90	Good GCA, PH	52	NS KOD 10	OR
13	CMS1 122	Late	53	OD-DI-32	Early
14	CMS1 30*	Medium early	54	OD-DI-47	Early
15	CMS-III-8	PH	55	OD-DI-49	Medium early
16	DEJ-10	Dwarf	56	OD-DI-80	Good GCA
17	DF AB 2 *	Late, good GCA	57	OD-DI-83	Good GCA
18	DI-42	Medium late	58	ODESSA 4*	Medium early
19	DM 3	Resistance to rust	59	OR 26 PL	OR
20	DOP 27 08	HO	60	PB-21*	Medium early, resistant to rust
21	DOP 32 08	HO, tolerant to <i>Phoma macdonaldi</i>	61	PH BC1 92	PH
22	FE 49	Late	62	PH BC2 67	PH
23	FE 54	OR	63	PL-DI-25*	Early, good GCA, <i>Pl6</i> gene
24	FE 7	OR	64	POP 3	Resistance to rust
25	Ha 22	PH, good GCA	65	PR-ST-3	PH, good GCA
26	HA 26*	Medium early, good GCA	66	PR ST 28	Late
27	Ha 26 OL ARG	HO	67	PR-2648-2	Good GCA
28	Ha 267	OR	68	RNS P 10	Ultra-early
26	Ha 412 HO	HO	69	RNS P 2	Ultra-early
30	Ha 431	Resistant to rust	70	RS O 2	Ultra-early
31	HA 441	Tolerant to <i>Sclerotinia spp.</i>	71	RUB-3 *	Medium early
32	HA 444	High oleic	72	SAM-INTER-3	Dwarf
33	HA 465	High tolerant to <i>Sclerotinia spp.</i>	73	SAN 3	Ultra-early maturity
34	Ha 48	Late	74	SAN 35	Ultra-early maturity
35	Ha 74*	Medium early, PH	75	SC MI 4	Good GCA
36	Ha R 3	Resistant to rust	76	SU-AB-4-PR	SU
37	Ha 458	HO	77	UK 58 ST	HO
38	Ha-98	PH	78	V 8931-3-4-OL	HO
39	IMI AB 12 PR*	Late, IMI	79	VL A 8 PR	OR
40	IMI AB 14 PR	IMI	80	VL-3	Early

GCA-general combining ability; IMI-tolerant to imidasolinone herbicides; SU-tolerant to sulphonyl urea herbicide; HO - high oleic OR-resistant to *O. cumana*; PH-tolerant to *Phomopsis spp.*; HO-high oleic line

2.2. Isolate characteristics

The isolate of *M. phaseolina*, was selected from collection of 50 isolates based on pathogenicity test. Infected plant tissue was placed in paper bag for air drying, after that plant samples were stored at 4 °C. Before of testing the isolate, the stems were washed under running tap water for half our and left to dry on sterile filter papers. Subsequently, small cuts from stems exhibiting

visible microsclerotia underwent surface sterilization in two steps: in 70% ethanol (C₂H₅OH) for three minutes, and in 1% sodium hypochlorite (NaOCl) for an extra three minutes. These sterilized stem sections were plated onto potato dextrose agar (PDA) and incubated at 30 °C for 24 hours. The isolated hyphal tips were then transferred to new PDA plates to establish fresh, uncontaminated fungal colonies.

To determine the most aggressive *M. phaseolina* isolate, a pathogenicity test was conducted. A 4 mm mycelial disc from a colony was placed at the center of a PDA plate and allowed to incubate for four days. Once the PDA plate was entirely colonized by *M. phaseolina*, ten de-hulled sunflower seeds from the inbred line Ha 26 were introduced onto each colony. After six day seed were evaluated according to Rayatpanah et al. (2012) scale: 0= completely healthy seed, 1= seedling discoloration on the contact with the mycelium, 2= seed teguments covered with and healthy seedling, 3= seed teguments covered with microsclerotia and infected seedlings 4= bouth tegument and seedling infected 5= infected seed, not germinated.

2.3. Trial setup and plant material

The experiments were conducted at the Sunflower Department's disease testing nursery of the Institute of Field and Vegetable Crops in Rimski Šančevi, Novi Sad, in 2019 and 2020. On April 18th, 2019, the 80 selected inbred lines from the sunflower gene pool at the IFVC Novi Sad, Serbia were planted. However, inbred line PR-ST-28 was eliminated due to its low emergence, leaving 79 inbred lines for *M. phaseolina* resistance screening at the end of the growing season. Based on their resistance levels, 15 inbred lines were chosen for the following year's trial, which were planted on May 5th, 2020. The meteorological data analysis for the two-year weather conditions is presented in Figure 1 (RSRHZ 2023).

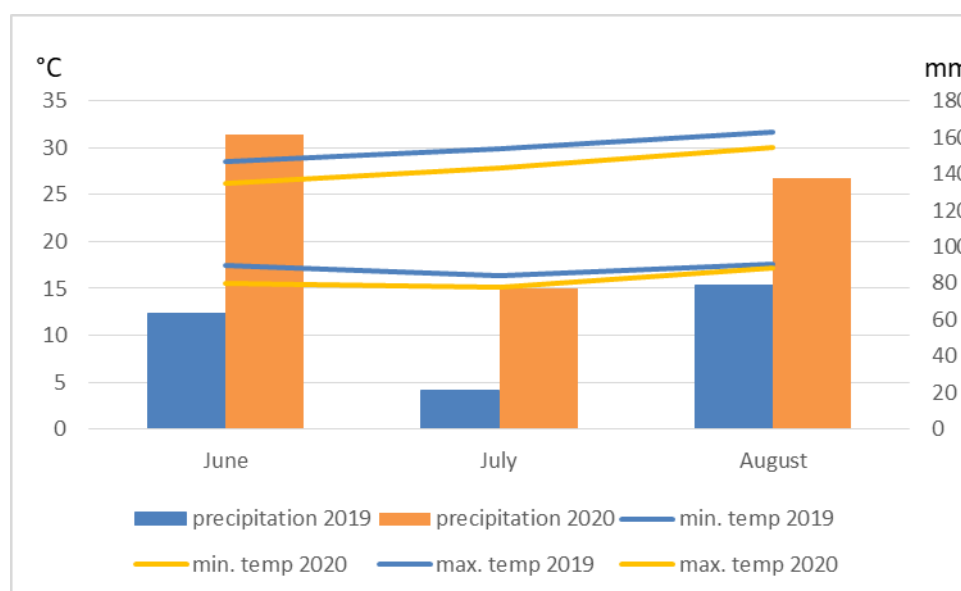


Figure 1- Meteorological data for the vegetation season (june-august) 2019 and 2020 in Novi Sad, Serbia
Min t - minimal temperature, Max t - maximal temperature

2.4. Inoculation methods

Two inoculation methods, the Unwounded Stem Base Inoculation (USBI) method and the toothpick (TP) method, were used to artificially inoculate the sunflower inbred lines. These two inoculation methods are different from each other since toothpick method represents an aggressive method, which requires artificial tissue penetration, and plants show the reaction to stop pathogen which is already in the plant. The USBI method is less aggressive and this method doesn't require artificial plant injury, and pathogen itself struggles autonomously to penetrate the plant tissue. The trials were set up as a Complete Randomized Block Design (CRBD), with each inbred line planted in three replications and each replication comprising three rows, resulting in a total of 36 plants per replication (3 x 12 plants). The plants were spaced at 0.7 m between rows and 0.3 m within rows, and no irrigation was applied.

In the first group (12 plants per inbred line and replication), the USBI method was applied 30 days after emergence, and each plant was inoculated by digging area around plant where is 2g mixture of maize flour and microsclerotia evenly distributed all around the plant stem. This mixture was contains: maize flour and sand medium in a ratio of 1:20, which was also contain 5 discs (4 mm in diameter) from the edge of the 4 day old *M. phaseolina* colony grown on PDA incubated at 30°C. In order to obtain quality distribution of microsclerotia mixture was shaken every second day, until 14th day, when mixture was prepared for use (Mihaljčević 1980). The second group (12 plants per inbred line and replication) was inoculated using the TP method by inserting infected toothpicks into the stem tissue 1 cm above the plant's first node (Jiménez -Díaz et al. 1983). Toothpicks were

sterilized and placed in laboratory glass cup and then PDA was a poured all over toothpicks. This glass was incubated on 30 °C in order to microclerotinia cover all toothpicks. Incubation of toothpicks lasted for 7 days. The third group (12 plants per inbred line and replication) was grown in natural conditions, marked as a disease in naturally infested area (DNI). In this group of plants disease occurrence without artificial inoculation was observed.

2.5. Data analyses

At the maturity stage (R8) of sunflower, symptoms of *M. phaseolina* infection were evaluated (Schneiter & Miller 1981). Each plant stem was longitudinally cut (photo 1), and the length of the tissue with visible microsclerotia was measured and evaluated with grades from 0 to 8: (0-(0-5 cm); 1-(5-10 cm), 2-(10-20 cm); 3-(20-30 cm); 4-(30-40 cm), 5-(40-50 cm); 6-(50-60 cm); 7-(60-70 cm); 8-(more than 70 cm). Any plants displaying symptoms of other diseases were removed before the end of the growing season.



Photo 1: Longitudinally cut of sunflower stem with visible multiple microsclerotia and damages of infection with *Macrophomina phaseolina*

Disease incidence and McKinney index were calculated for each inbred line in each year, method, and DNI (McKinney 1923). Disease incidence (I) was calculated as the proportion of diseased plants, which represents percents of plants with symptoms:

$$I = \frac{x}{N} \times 100$$

The number of plants with symptoms (x) divided by the total number of plants examined (N), multiplied by 100.

McKinney index is estimated as a value on the interval scale and has been used to determine a disease severity index on a percentage basis. (M) was calculated according to the formula:

$$M = \frac{\sum x_i}{n_i n} \times 100$$

Where; x represents the disease grade according to the area covered with microsclerotia $\sum x_i$ represents the sum of every plant's grade; n_i represents the highest grade of the scale – 8, and n represents the total number of diseased plants evaluated. The results were expressed as a percentage (%).

The inbred line reaction to *M. phaseolina* was evaluated MPR (*M. phaseolina* reaction) using the proposed scale for each tested method. The obtained data were used to classify inbred lines McKinney index (Table 2).

Table 2- Proposed scale of sunflower inbred lines to *Macrophomina phaseolina* reaction according to McKinney index

<i>MPR of inbred lines</i>	<i>McKinney index</i>
Resistant (R)	0-5%
Moderately resistant (MR)	5.1-20%
Moderately susceptible (MS)	20.1-40%
Susceptible (S)	40.1-100%

MPR -*Macrophomina phaseolina* reaction;

The Kruskal-Wallis test together with pot hoc Dunn's test was used to analyze statistical differences in the resistance of inbred lines to *M. phaseolina*. In order to control the familywise error rate, it was used Holm stepwise adjustment (Dinno 2015). To visualize the experimental results, a UPGMA cluster analysis of previously standardized data by z-score was performed by using IBM SPSS 25, and PAST 4.10. Cluster graphic was followed by a heat map that categorized the inbred lines into according to resistance, implicating that inbred lines with dark blue colour are more resistant than others, while brighter colours are representing lower level of resistance and eventually red colour represent sensitive inbred lines. Levels of resistance to *M. phaseolina* and highlighted differences between inoculation methods and disease in naturally infested area. Additionally, a Kurskal-Wallis test was conducted to compare the values of McKinney index in 2019 and 2020 for the 15 selected lines.

3. Results and Discussion

3.1. *Macrophomina phaseolina* characteristic and isolate pathogenicity

In order to choose the most aggressive *M. phaseolina* isolate for the field experiments, we tested 50 isolates collected from sunflower production areas in Serbia. According to the pathogenicity test, the isolate with the highest grade (Indjija, Serbia 45°4'8"N, 20°3'21"E – named MPIN18) of aggressiveness was chosen for further work (Ćuk et al. 2022). This isolate was obtain grade 5 for every examined seed, which is maximal grade (data not shown).

3.2. Weather conditions

Relying on natural infestation and pathogen attack for testing breeding material is unreliable due to dependence on environmental conditions and non-homogeneous inoculum distribution in the soil (Van der Heyden et al. 2021). In that context, the two-year weather conditions varied during the vegetation season, having an unusual relationship between rainfall distribution and average daily temperature. Average temperatures were lower in 2020, followed by heavy rains but distributed in fewer days. The temperature range for the optimal development of *M. phaseolina* can vary between 25 to 35 °C, so the temperatures for *M. phaseolina* were optimal for both years (Parmar et al. 2018). However, higher temperatures in 2019 and less rainfall were more suitable for *M. phaseolina* development, affecting the sunflower's infestation level of inbred lines.

3.3. Filed experiment in 2019

Inbred line PR-ST-3 was eliminated due to its low emergence, leaving 79 inbred lines for *M. phaseolina* resistance screening at the end of the growing season. According to every plant disease grade, the variability of these inbred lines to *M. phaseolina* was

confirmed using Kruskal-Wallis test showing significant differences for both tested methods and DNI (for all methods, $p < 0.01$). However, the reaction of inbred lines varied due to the inoculation method. Therefore, it is necessary to examine in more detail the reaction of inbred lines depending on the infection of a particular method.

In this study, 79 sunflower inbred lines were evaluated for their resistance to *M. phaseolina*, and disease incidence and McKinney index of every inbred line were calculated (Table 3). According to the strictest MPR, that inbred lines obtain in table 3. Thirteen inbred lines were found to be resistant, while 16 were susceptible, and the remaining lines were classified as moderately resistant or moderately susceptible in year 2019. Inbred lines (FE 49, HA 74, HA 458, L1, LIV 10, LIV 17, MA-SC-2, PB 21, PH BC 1 92, SAM INTER 3, SAN 35, AR-7, VL A 8 PR) were resistant and they also showed low disease incidence and low McKinney index value, indicating high resistance level or slowed disease progress due to the complexity of interaction between host and pathogen. The biotrophy-necrotrophy switch in pathogen evokes differential response results, showing that the host tailored its defence strategy to meet the changing situation (Chowdhury et al. 2017).

Table 3- Disease incidence and McKinney index for *M. phaseolina* resistance of 79 sunflower inbred lines inoculated using Toothpick (TP) method and Unwounded Stem Base Inoculation (USBI) method and in disease in naturally infested area (DNI) obtained in Rimski šančevi, Novi Sad in 2019

Inbred lines	Disease incidence (%)			McKinney index (%)					
	TP	USBI	DNI	TP	grade	USBI	grade	DNI	grade
AB-OR-8	92.59	80.57	42.90	52.15	S	34.09	MS	12.23	MR
AB-OR-ST-50	80.30	58.96	45.79	46.74	S	40.94	S	25.40	MS
AB-OR-ST-62	79.17	35.25	4.76	42.71	S	8.20	MR	1.19	R
AR-7	0.00	6.36	0.00	0.00	R	2.01	R	0.00	R
AR-KOR-10	25.76	12.12	3.03	9.70	MR	2.27	R	0.76	R
AS 87	83.33	53.33	38.74	45.23	S	22.08	MS	19.15	MS
AS 95 PR	61.95	68.89	25.00	26.30	MS	26.18	MS	7.19	MR
AS-1-PR	51.85	25.62	22.22	26.60	MS	9.56	MR	9.72	MR
AZDO 2	29.55	43.33	24.09	20.50	MS	29.93	MS	13.40	MR
BT VL 24	18.52	14.11	0.00	1.39	R	5.56	MR	0.00	R
BT-VL-17-SU	38.55	37.68	14.44	11.03	MR	16.53	MR	4.79	R
CMS 1-90	69.26	52.42	50.34	37.04	MS	30.18	MS	25.69	MS
CMS1 122	72.22	66.69	88.89	45.83	S	28.47	MS	18.06	MR
CMS1 30	100	77.77	33.33	27.08	MS	27.08	MS	4.17	R
CMS-3-8	34.43	23.23	15.34	11.40	MR	11.33	MR	3.74	R
DEJ-10	52.02	5.56	5.81	22.38	MS	1.39	R	2.56	R
DF AB 2	57.15	46.67	73.16	29.63	MS	26.62	MS	45.89	S
DI-42	28.24	25.45	28.55	12.96	MR	5.19	MR	8.23	MR
DM 3	70.37	51.82	64.88	27.43	MS	6.48	MR	41.36	S
DOP 27 08	30.95	33.59	31.82	13.10	MR	17.80	MR	16.77	MR
DOP 32 08	43.81	32.07	12.12	24.48	MS	9.34	MR	3.79	R
FE 49	14.95	9.09	2.78	4.84	R	2.35	R	0.69	R
FE 54	70.00	43.33	32.59	30.31	MS	16.59	MR	15.32	MR
FE 7	12.50	15.76	0.00	5.24	MR	3.11	R	0.00	R
Ha 22	85.71	38.85	36.72	44.40	S	11.99	MR	12.54	MR
HA 26	38.96	22.41	18.33	13.69	MR	4.10	R	3.65	R
Ha 26 OL ARG	47.62	29.63	43.96	16.07	MR	10.19	MR	13.76	MR
Ha 267	76.67	24.07	55.00	38.47	MS	6.89	MR	28.54	MS
HA 412 HO	66.45	43.45	51.85	37.17	MS	21.21	MS	22.57	MS
HA 431	65.74	30.81	17.5	17.49	MR	9.09	MR	0.83	MR
HA 441	35.21	33.81	19.47	13.66	MR	22.26	MS	7.29	MR
HA 444	23.54	4.17	5.56	6.71	MR	1.04	R	2.08	R
HA 465	30.97	36.29	3.03	6.02	MR	10.77	MR	0.38	R
Ha 48	50.51	21.06	24.05	27.78	MS	10.43	MR	22.94	MS
Ha 74	6.67	3.03	0.00	0.83	R	2.65	R	0.00	R
HA458	12.50	13.33	0.00	4.17	R	1.67	R	0.00	R
Ha-98	95.83	48.11	45.96	56.04	S	16.12	MR	14.74	MR
HA-R-3	67.58	81.53	73.57	33.03	MS	54.80	S	42.00	S
IMI AB 12 PR	69.44	61.82	51.91	47.43	S	43.07	S	42.94	S
IMI AB 14 PR	31.06	25.4	25.00	9.28	MR	12.57	MR	13.72	MR
IMI AB 24 PR	47.81	23.08	38.89	21.00	MS	8.97	MR	10.56	MR
KINA-B-5	88.90	83.33	48.26	73.49	S	53.54	S	30.79	MS
KINA-H-25	65.99	49.49	44.44	25.59	MS	12.25	MR	22.69	MS
L1	0.00	0.00	26.67	0.00	R	0.00	R	0.42	R
LIP P 16	81.67	64.47	56.75	33.75	MS	23.70	MS	13.75	MR
LIP P 32	27.94	9.09	7.04	8.29	MR	2.27	R	1.81	R
LIP P 98	72.62	57.43	91.11	9.67	MR	13.87	MR	11.81	MR
LIV 10	23.91	5.56	0.00	3.37	R	0.35	R	0.00	R

Table 3 (Continue)- Disease incidence and McKinney index for *M. phaseolina* resistance of 79 sunflower inbred lines inoculated using Toothpick (TP) method and Unwounded Stem Base Inoculation (USBI) method and in disease in naturally infested area (DNI) obtained in Rimski Šančevi, Novi Sad in 2019

Inbred lines	Disease incidence (%)			McKinney index (%)					
	TP	USBI	DNI	TP	grade	USBI	grade	DNI	grade
LIV 17	12.12	0.00	2.78	1.52	R	0.00	R	0.00	R
MA-SC-2	0.00	0.00	4.76	0.00	R	0.00	R	0.00	R
NS KOD 10	83.33	50.00	62.50	47.01	S	23.96	MS	36.98	MS
NS W 3	63.30	46.27	36.10	31.31	MS	16.46	MR	12.99	MR
OD-DI-32	40.68	29.6	6.48	9.09	MR	9.25	MR	4.40	R
OD-DI-47	31.61	16.67	4.76	12.49	MR	5.21	MR	1.79	R
OD-DI-49	68.35	49.95	67.09	41.2	S	24.39	MS	28.91	MS
OD-DI-80	76.72	53.41	43.81	22.29	MS	16.38	MR	11.79	MR
OD-DI-83	60.42	18.84	24.44	22.12	MS	5.54	MR	14.31	MR
ODESA 4	86.11	100	66.67	49.65	S	48.05	S	4.17	R
OR 26 PL	69.44	22.42	33.94	36.67	MS	9.36	MR	10.34	MR
PB-21	0.00	2.78	3.70	0.00	R	0.69	R	0.42	R
PH BC1 92	9.72	10.74	3.70	1.35	R	1.85	R	0.00	R
PH BC2 67	31.67	5.56	22.23	6.88	MR	0.52	R	0.00	R
PL-DI-25	84.40	79.55	67.58	41.27	S	43.53	S	29.17	MS
POP 3	72.22	54.88	35.00	40.97	S	24.37	MS	16.67	MR
PR ST 28	8.33	19.45	0.00	1.04	R	5.90	MR	0.00	R
PR-2648-2	64.65	58.12	26.01	25.13	MS	5.38	MR	11.55	MR
RNS P 10	53.59	42.07	39.29	31.19	MS	23.10	MS	15.43	MS
RNS P 2	44.17	18.84	0.00	14.38	MR	3.95	R	0.00	MR
RS O 2	78.15	9.09	6.67	29.89	MS	0.76	R	1.25	R
RUB-3	96.3	75.76	62.5	59.96	S	48.83	S	38.19	MS
SAM-INTER-3	42.41	29.07	12.96	3.45	R	2.57	R	0.69	R
SAN 3	60.00	57.41	63.89	15.21	MR	7.64	MR	12.15	MR
SAN 35	9.52	7.41	14.03	2.00	R	0.00	R	0.00	R
SC MI 4	27.27	8.33	11.11	5.68	MR	0.35	R	0.00	R
SU-AB-4-PR	31.11	36.11	47.42	11.20	MR	14.58	MR	16.23	MR
UK 58 ST	40.53	18.65	16.67	17.29	MR	10.42	MR	7.29	MR
V 8931-3-4-OL	25.00	41.33	37.9	5.00	MR	7.40	MR	4.03	MR
VL A 8 PR	8.89	3.03	0.00	1.25	R	0.76	R	0.00	R
VL-3	67.22	42.73	36.57	31.11	MS	15.80	MR	13.78	MR
Min	0.00	0.00	0.00	0.00		0.00		0.00	
Max	100.00	100.00	91.10	73.49		54.80		45.89	
CV	55.96	68.81	79.84	78.21		97.26		105.76	

The most severe disease severity score level obtain from disease severity of TP and USBI method and from DNI is bolded; R – resistant; MR - moderately resistant; MS - moderately susceptible; S - susceptible; Min - minimal value; Max - maximal value; CV - Coefficient of variation

Both the USBI and TP methods were employed for testing sunflower inbred lines for resistance to *M. phaseolina*, in order to avoid the uncertainties that may arise from adverse weather conditions or inadequate inoculum distribution in the field. While the USBI method mimics the natural path of pathogen infestation and is easy to handle, there is always a risk of failure due to unfavorable environmental conditions (Tančić Živanov et al. 2021). The TP method, on the other hand, produces a high infection rate but does not imitate the pathogen’s natural infestation path and require artificial wounding of the plant, which can lead to disease incidence skipping and increased plant severity. According to Mc Kinney index, only one inbred line, MA SC 2, exhibited complete resistance, while the other resistant lines showed slight infestation in one of the artificial inoculation methods or even in DNI. Among resistant inbred lines, the highest McKinney index was observed in inbred lines FE 49, HA458, LIV 10, SAM-INTER 3, and SAN 35 when tested using the TP method. Overall, it can be concluded that the TP method is more reliable in obtaining high disease incidence even under unfavorable environmental conditions for the pathogen development. While artificial inoculation methods are expected to be highly efficient, natural disease occurrence can be influenced by various factors and may be highly variable, as demonstrated in the study of Dedić et al. (2011) in the inoculation of sunflower with *Sclerotinia sclerotiorum* where natural infection did not occur due to environmental factors. Additionally, it was observed that the TP method elicited the most aggressive reaction in the tested inbred lines. This was expected, as this method requires tissue injury, making it the most aggressive and most suitable inoculation method which require growing sunflower through whole vegetation (Tančić et al. 2012; Tančić-Živanov et al. 2021; Aydođdu et al. 2022).

3.4. Cluster analysis

Additionally, a cluster analysis of disease severity followed by a heat map was used to better classify the 79 tested sunflower inbred lines based on the inoculation method (Figure 1). The resistant and moderately resistant inbred lines were represented by shades of blue, while susceptible inbred lines were indicated by red, orange, and yellow colours. The inbred lines Ha 74, L1, MA SC 2, PB 21 PH-BC 1 92, SAN 35, LIV 17, AR-7 and VL-A 8-PR were found to be similar to each other, with a dark blue

colour indicating that they were the most resistant inbred lines, not only to *M. phaseolina* but also for other desirable traits such as resistance to *Phomopsis* spp. (Ha 74 and PH BC 1-92), *Puccinia* spp. (PB 21), broomrape resistance (LIV 17 and VL-A-8-PR), earliness (SAN 35), and good combining abilities (L1, MA-SC-2). Combining desirable traits in one genotype can make the breeding process more efficient and less time-consuming (Qi & Ma 2022). The cluster graph also showed that the TP and USBI methods were more similar to each other than DNI, which was expected as the contact of inoculum and sunflower plants was provided. However, using different inoculation methods resulted in significant variations in colour for certain inbred lines, indicating that the method of inoculation can affect the level of resistance observed in different sunflower inbred lines (Figure 2).

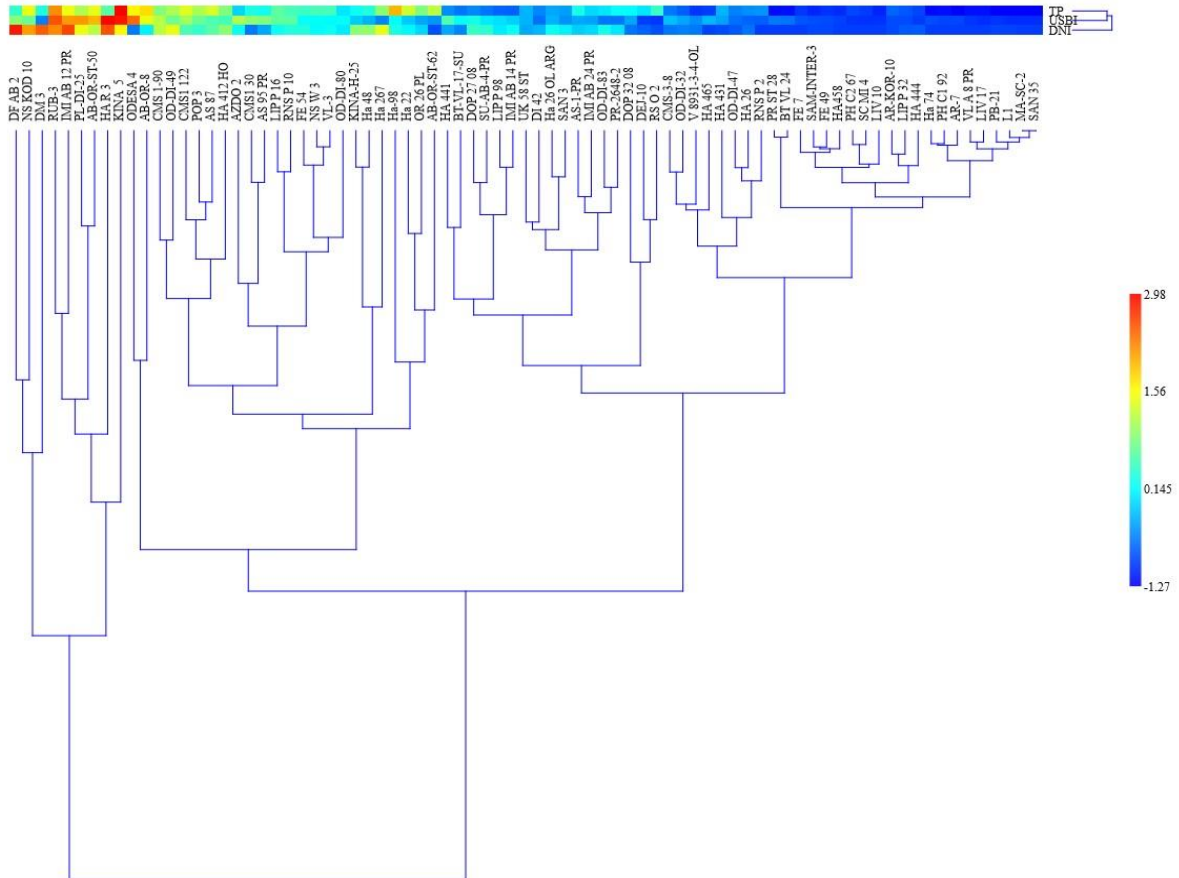


Figure 2- UPMGA cluster analysis followed by a heat map showing relationships among 79 sunflower inbred lines inoculated with *M. phaseolina* isolate using two different inoculation methods toothpick (TP) and Unwounded Stem Base Inoculation (USBI) method and disease in naturally infested area (DNI) without artificial inoculation based on McKinney index

3.5. Comparison of field trials in 2019 and 2020

Fifteen sunflower inbred lines were retested in 2020 for their resistance to *M. phaseolina* (Table 4). In order to check variability among those examined inbred lines, it was noticed that in 2019, inbred lines Ha 74, MA SC 2, L1, LIV 10, PB 21 were the most resistant among every inoculation method according to disease incidence and McKinney index. These lines showed low McKinney index, indicating high resistance which candidate them as resistance sources for further breeding (Laidig et al. 2021).

Table 4- Disease incidence and McKinney index for *M. phaseolina* resistance of 15 sunflower inbred lines inoculated using Toothpick (TP) method and Unwounded Stem Base Inoculation (USBI) method and in disease in naturally infested area (DNI) obtained in Rimski Šančevi, Novi Sad in 2020

Inbred lines	Disease incidence			McKinney index					
	TP	USBI	DNI	TP	grade	USBI	grade	DNI	grade
AB OR 8	87.71	83.33	47.78	42.23	S	53.82	S	38.19	MR
AS 87	70.00	59.60	20.45	15.42	MR	12.31	MR	0.76	R
CMS 1-30	94.44	45.83	0	29.34	MR	20.83	MS	0	R
DF-AB-2	20.83	3.33	0	0.52	R	1.67	R	0	R
Ha 26	55.56	25.00	16.67	34.03	MS	15.63	MR	8.33	MR
Ha 74	9.52	28.04	0	0	R	0.46	R	0	R
IMI-AB-12-PR	22.73	15.15	37.04	15.96	MR	9.85	MR	3.70	R
L1	9.76	3.33	0	1.39	R	0	R	0	R
LIP P 98	68.89	58.15	22.22	9.17	MR	8.65	MR	3.47	R
Liv 10	55.96	15.25	28.24	11.81	MR	0.76	R	3.07	R
MA-SC-2	27.78	8.33	13.33	1.39	R	1.85	R	3.33	R
Odessa 4	91.67	88.64	77.78	49.48	S	63.05	S	25.60	MS
PB 21	64.82	0	0	6.25	MR	0	R	0	R
PL-DI-25	100.00	89.26	64.29	61.20	S	67.64	S	36.68	MS
RUB-3	20.95	21.21	8.33	7.38	MR	3.41	R	0.52	R
Min	9.76	0	0	0		0		0	
Max	100	89.26	77.78	61.20		67.64		38.19	
CV	60.7	88.53	101.21	102.90		137.63		163.93	

By comparing these inbred lines to each other they did not have statistically significant difference in all years regarding to inoculation method (Figure 3). Similar reaction of these inbred lines was confirmed also in 2020. Inbred lines which were sensitive, AB OR 8, ODESSA 4 and PL-DI 25 were also similar to each other. Comparing these inbred lines regarding to reaction in 2019 and 2020, resistant inbred lines did not show statistically different reaction in these two years, while sensitive inbred lines AB OR 8, ODESSA 4 and PL-DI 25, had statistically different reaction regarding at least one inoculation method. Sharma et al. (2016) also confirms that resistant genotypes of pigeon pea have more stable reaction to Fusarium wilt than sensitive ones. Different reaction to *M. phaseolina* confirms that climate conditions had large impact on disease progress in these two years, since location of the trial was the same (Veverka 2008). Beside these inbred lines, other lines showed similar reactions in 2020 as in 2019 (Table 5).

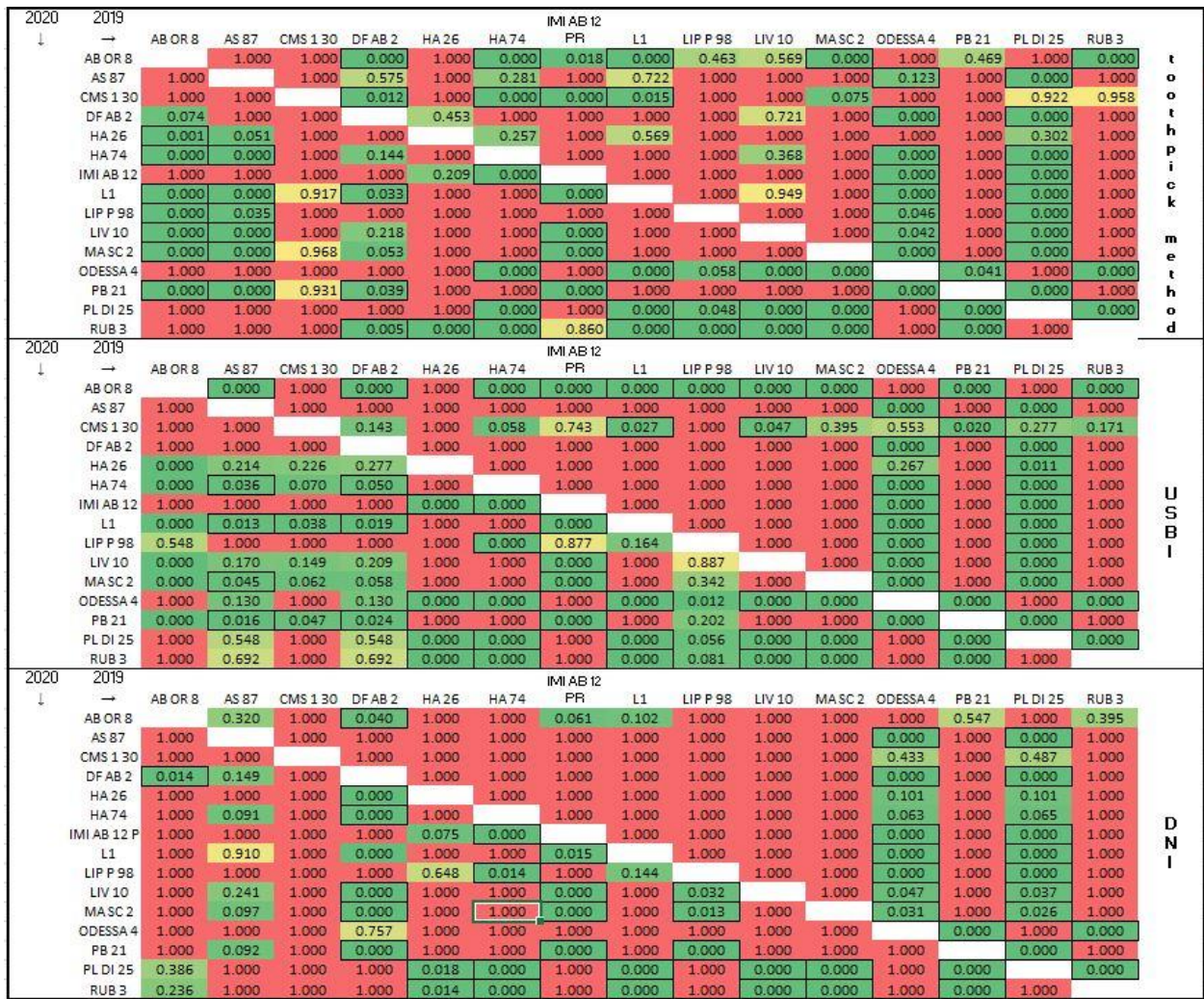


Figure 3- Pairwise comparisons of disease grade of inbred lines tested with Kruskal Wallis and Dunn’s test, in 2019 and 2020. Intensity of colour implicate the significance of the association among inbred lines, only dark green and squared associations are statistically significant (P<0.05)

Table 5- Differences between *M. phaseolina* reactions (MPR) inoculated with toothpick (TP) method and Unwounded Stem Base Inoculation (USBI) method and disease in naturally infested area (DNI) of selected sunflower inbred lines in 2019 and 2020 using Kruskal Wallis test

Sunflower inbred lines	TP	USBI	DNI
AB-OR 8	0.28	0.13	0.05*
AS 87	0.05*	0.51	0.05*
CMS 1-30	0.66	0.83	0.11
DF-AB 2	0.05*	0.05*	0.04*
Ha 26	0.13	0.66	0.82
Ha 74	0.32	0.8	1.00
IMI AB 12 PR	0.05*	0.13	0.05*
L1	0.13	1.00	0.32
LIP-P-98	0.83	0.28	0.26
LIV 10	0.28	0.35	0.12
MA-SC 2	0.32	0.32	0.32
ODESSA 4	0.05*	0.268	0.121
PB 21	0.32	0.32	0.32
PL-DI 25	0.13	0.05*	0.52
RUB 3	0.05*	0.05*	0.05*

*Significance at level $\alpha=0.05$

The significant differences in disease incidence and McKinney index in all inoculation methods between 2019 and 2020 were observed for inbred lines DF-AB-2 and RUB-3. Inbred line RUB-3 was highly susceptible in 2019 but much more resistant in

2020, while inbred line DF-AB-2 showed a high level of susceptibility, especially in the DNI method, in 2020. In 2019, inbred line DF-AB-2 was positioned with highly resistant inbred lines, while inbred line RUB 3 showed a noticeably lower level of susceptibility in 2020.

Although some of the tested inbred lines showed high levels of resistance in certain inoculation methods, previous studies have not found any sunflower genotypes that are completely resistant to *M. phaseolina* (Beg 1992; Aboutalebi et al. 2014; Taha et al. 2018; Siddique et al. 2020). However, other authors (Tančić-Živanov et al. 2021) have found hybrids and inbred lines that did not develop symptoms of *M. phaseolina*. The differences in these results may be due to the large variability among *M. phaseolina* isolates (Aboshosha et al. 2007; Tančić et al. 2012).

4. Conclusions

The study identified four sunflower inbred lines (Ha 74, L1, LIV 10, MA-SC 2 and PB 21) as potential sources of resistance to *M. phaseolina*, with the ability to limit the spread of infection even under high disease pressure. Both inoculation methods (TP and USBI) were effective in differentiating between resistant and susceptible inbred lines, with the TB method being the most aggressive and precise. Further research is needed to understand the mechanisms underlying resistance in these inbred lines and to develop novel resistant lines for sunflower breeding programs.

Acknowledgements

This work is supported by the Ministry of Education, Science and Technological Development of the Republic of Serbia, grant number 451-03-68/2022-14/ 200032, by the Science Fund of the Republic of Serbia through IDEAS project “Creating climate smart sunflower for future challenges” (SMARTSUN), grant number 7732457, by the European Commission through Twinning Western Balkans project CROPINNO, grant number 101059784, by Centre of Excellence for Innovations in Breeding of Climate-Resilient Crops - Climate Crops, Institute of Field and Vegetable Crops, Novi Sad, Serbia, and based upon work from COST Actions PlantEd (CA18111) and EPI-CATCH (CA19125), supported by COST (European Cooperation in Science and Technology). www.cost.eu.

References

- Aboshosha S S, Attaalla S I, El-Korany A E & El-Argawy E (2007). Characterization of *Macrophomina phaseolina* isolates affecting sunflower growth in El-Behera governorate, Egypt. *International Journal of Agriculture and Biology* 9(6): 807-815
- Aboutalebi R, Dalili A, Rayatpanah S & Andarkhor A (2014). Evaluation of sunflower genotypes against charcoal rots disease in vitro and in vivo condition. *World Applied Sciences Journal* 31(4): 649-653
- Anđelković V, Cvejić S, Jocić S, Kondić-Špika A, Marjanović Jeromela A, Mikić S, Prodanović S, Radanović A, Savić Ivanov S, Trkulja D & Miladinović D (2020). Use of plant genetic resources in crop improvement—example of Serbia. *Genetic Resources and Crop Evolution* 67(8): 1935-1948
- Aydoğdu M, Kurbetli İ & Sülü G (2022). Occurrence of charcoal rot in globe artichoke and assessment of inoculation techniques for pathogenicity and management. *Brazilian Archives of Biology and Technology* 65: e22210254
- Beg A (1992). Screening sunflower inbred lines for charcoal rot (*Macrophomina phaseolina*) resistance. *Helia* 15(16): 91-96
- Bokor P (2007). *Macrophomina phaseolina* causing a charcoal rot of sunflower through Slovakia. *Biologia* 62(2): 136-138
- Chattopadhyay C, Kolte S J & Waliyar F (2015). *Diseases of edible oilseed crops*. Taylor & Francis, Oxfordshire
- Dell’Olmo E, Tripodi P, Zaccardelli M & Sigillo L (2022). Occurrence of *Macrophomina phaseolina* on Chickpea in Italy: Pathogen Identification and Characterization. *Pathogens* 11(8): 84
- Chowdhury S, Basu A & Kundu S (2017). Biotrophy-necrotrophy switch in pathogen evoke differential response in resistant and susceptible sesame involving multiple signaling pathways at different phases. *Scientific reports* 7(1): 1-17
- Cotuna O, Paraschivu M & Sărățeanu V (2021). Charcoal rot of the sunflower roots and stems (*Macrophomina phaseolina* (Tassi) Goid.)-An overview. *Scientific Papers* 22(1): 107-116
- Ćuk N, Cvejić S, Mladenov V, Miladinović D, Babec B, Jocić S & Dedić B (2022). Introducing a cut-stem inoculation method for fast evaluation of sunflower resistance to *Macrophomina phaseolina*. *Phytoparasitica* 50(4): 775-788
- Debaeke P, Casadebaig P, Flenet F & Langlade N (2017). Sunflower crop and climate change: vulnerability, adaptation, and mitigation potential from case-studies in Europe. *OCL Oilseeds and fats crops and lipids* 24(1): 15
- Dedić B, Miladinović D, Jocić S, Terzić S, Tančić S, Dušanić N & Miklič V (2011). Sunflower inbred lines screening for tolerance to white rot on stalk. *Ratarstvo i povrtarstvo/Field and Vegetable Crops Research* 48(1): 167-172
- Dinno A (2015). Nonparametric pairwise multiple comparisons in independent groups using Dunn's test. *The Stata Journal* 15(1), 292-300
- Ijaz S, Sadaqat H A & Khan M N (2013). A review of the impact of charcoal rot (*Macrophomina phaseolina*) on sunflower. *The Journal of Agricultural Science* 151(2): 222-227
- Jalil S, Sadaqat H A, Tahir H N, Shafaulah H A & Ali N (2013). Response of sunflower under charcoal rot (*Macrophomina phaseolina*) stress conditions. *International Journal of Scientific and Engineering Research* 1(3): 89-92
- Jiménez-Díaz R M Blanco-López M A & Sackston C (1983). Incidence and Distribution of Charcoal Rot of Sunflower Caused by *Macrophomina phaseolina* in Spain. *Plant Disease* 67: 1033-1036
- Jordaan E, Van der Waals J E & McLaren N W (2019). Effect of irrigation on charcoal rot severity, yield loss and colonization of soybean and sunflower. *Crop Protection* 122(2) 63-69
- Kaya Y (2016). Sunflower In S Gupta (Eds.) *Breeding oilseed crops for sustainable production*, Elsevier Inc, Amsterdam, pp. 55-88
- Khan S N (2007). *Macrophomina phaseolina* as causal agent for charcoal rot of sunflower. *Mycopathology* 5(2): 111-118

- Laidig F, Feike T, Hadasch S, Rentel D, Klocke B, Miedaner T & Piepho HP (2021). Breeding progress of disease resistance and impact of disease severity under natural infections in winter wheat variety trials. *Theoretical and Applied Genetics* 134: 1281-1302
- Mahmoud A (2010). Molecular and biological investigations of damping-off and charcoal-rot diseases in sunflower. (Thesis), Sabanci University, Turkey
- Mahmoud A & Budak H (2011). First report of charcoal rot caused by *Macrophomina phaseolina* in sunflower in Turkey. *Plant disease* 95(2): 223-223
- Masalia R R, Temme A A, Torralba N D L & Burke J M (2018). Multiple genomic regions influence root morphology and seedling growth in cultivated sunflower (*Helianthus annuus* L.) under well-watered and water-limited conditions. *PLoS One* 13(9): e0204279
- McKinney H H (1923). Influence of soil, temperature and moisture on infection of wheat seedling by *Helminthosporium sativum*. *Journal of Agricultural Research* 31(9): 827-840
- Mihaljčević M (1980). Sources of resistance to *Sclerotium bataticola* Taub. in sunflower inbred lines and hybrids. (Thesis) University of Novi Sad, Serbia
- Miklić V (2022). Introduction to the Special Issue Sunflower. *OCL* 29(16) 1-2
- Özelçi D, Akbulut G B & Yiğit E (2022). Effects of Melatonin on *Morus nigra* cv.' Eksi Kara' Exposed to Drought Stress. *Journal of Agricultural Sciences* 28(4): 555-569
- Parmar H, Kapadiya H J, Bhaliya C M & Patel R C (2018). Effect of Media and Temperature on the Growth and Sclerotial Formation of *Macrophomina phaseolina* (Tassi) Goid causing Root Rot of Castor. *International Journal of Current Microbiology and Applied Sciences* 7(2): 671-675
- Qamar M I & Ghazanfar M U (2019) Effect of charcoal rot (*M. phaseolina*) on yield of sunflower (*Helianthus annuus* L.). *Pakistan Journal of Phytopathology* 31(2): 221-228
- Qi L & Ma G (2019). Marker-assisted gene pyramiding and the reliability of using SNP markers located in the recombination suppressed regions of sunflower (*Helianthus annuus* L.). *Genes* 11(1): 10
- Radanović A, Cvejić S, Luković J, Jocković M, Jocić S, Dedić B, Gvozdenac S, Ćuk N, Hladni N, Jocković J, Hrnjaković O & Miladinović D (2022). Creating climate smart sunflower for future challenges—the SMARTSUN multidisciplinary project. In Proceedings, 20th International Sunflower Conference, 20-23 June, Novi Sad, pp. 252-252
- RSRHZ (2023). Meteorološki godišnjak - klimatološki podaci Retrieved in April, 24, 2023 from https://www.hidmet.gov.rs/latin/meteorologija/klimatologija_godisnjaci.php.
- Schneider A & Miller J F (1981). Description of Sunflower Growth Stages. *Crop Science* 21: 901-903
- Schroeder M M, Lai Y, Shirai M, Alsalek N, Tsuchiya T, Roberts P & Eulgem T (2019). A novel *Arabidopsis* pathosystem reveals cooperation of multiple hormonal response-pathways in host resistance against the global crop destroyer *Macrophomina phaseolina*. *Scientific reports* 9(1): 1-14
- Seiler G J, Qi L L & Marek L F (2017). Utilization of sunflower crop wild relatives for cultivated sunflower improvement. *Crop Science* 57(3): 1083-1101
- Sharma M, Ghosh R, Telangre R, Rathore A, Saifulla M, Mahalinga DM, Saxena DR & Jain YK (2016). Environmental influences on pigeonpea-*Fusarium udum* interactions and stability of genotypes to Fusarium wilt. *Frontiers in plant science* 7: 253
- Shehbaz M, Rauf S, Al-Sadi A M, Nazir S, Bano S, Shahzad M & Hussain M M (2018). Introgression and inheritance of charcoal rot (*Macrophomina phaseolina*) resistance from silver sunflower (*Helianthus argophyllus* Torr. and A. Gray) into cultivated sunflower (*Helianthus annuus* L.). *Australasian Plant Pathology* 47(4):413-420
- Siddique S, Shoaib A, Khan S N & Mohy-Ud-Din A (2020). Screening and histopathological characterization of sunflower germplasm for resistance to *Macrophomina phaseolina*. *Mycologia* 113 (1):1-16
- Škorić D (2016). Sunflower breeding for resistance to abiotic and biotic stresses. In: A K Shanker & C Shanker (Eds.), *Abiotic and Biotic Stress in Plants-Recent Advances and Future Perspectives*. IntechOpen, London, pp. 585-635
- Taha M M, Mahmoud A F, Hassan M A, Mahmoud A M & Sallam M A (2018). Potential resistance of certain sunflower cultivars and inbred lines against charcoal rot disease caused by *Macrophomina phaseolina* (Tassi) Goid. *Journal of Phytopathology and Pest Management* 5(3): 55-66
- Talukdar A, Verma K, Gowda D S, Lal S K, Sapra R L, Singh K P, Singh R & Sinha P (2009). Molecular breeding for charcoal rot resistance in soybean I. Screening and mapping population development. *Indian Journal of Genetics and Plant Breeding* 69(04): 367-370
- Tančić S, Terzić S, Dedić B, Atagić J, Jocić S & Miklić V (2012). Resistance of wild sunflower species to *Macrophomina phaseolina*. In: Proceedings of the forth joint UNS-PSU international conference on bioscience: biotechnology and biodiversity, 18-20 June, Novi Sad, pp. 34-37
- Tančić-Živanov S, Dedić B, Cvejić S, Jocić S & Miklić V (2021). Sunflower genotypes tolerance to charcoal rot (*Macrophomina phaseolina* (Tassi) Goid.) under the field conditions. *Genetika* 53(3): 1117-1131
- USDA (2023). Sunflower seed 2022World Production: 50,442 (1000 MT) Retrieved in April, 21, 2023 from <https://ipad.fas.usda.gov/cropeplorer/cropview/commodityView.aspx?cropid=2224000>
- Van der Heyden H, Dutilleul P, Charron J B, Bilodeau G J & Carisse O (2021). Monitoring airborne inoculum for improved plant disease management. A review. *Agronomy for Sustainable Development*, 41(3): 1-23
- Veverka K, Palicová J & Křížková I (2008). The incidence and spreading of *Macrophomina phaseolina* (Tassi) Goidanovich on sunflower in the Czech Republic. *Plant Protection Science* 44(4) :127-137
- Warburton M L, Rauf S, Marek L, Hussain M, Ogunola O & Gonzalez D S J (2017). The use of crop wild relatives in maize and sunflower breeding. *Crop Science* 57(3): 1227-1240





Agricultural Land-based Functional Model for Effective Rural Land Management in Türkiye

Orhan Ercan^{a*}

^aFaculty of Applied Sciences, Department of Real Estate Development and Management Ankara University, TÜRKİYE

ARTICLE INFO

Research Article

Corresponding Author: Orhan Ercan, E-mail: orhanercan@ankara.edu.tr

Received: 14 August 2023 / Revised: 21 January 2024 / Accepted: 25 January 2024 / Online: 23 July 2024

Cite this article

Ercan O (2024). Agricultural Land-based Functional Model for Effective Rural Land Management in Türkiye. *Journal of Agricultural Sciences (Tarım Bilimleri Dergisi)*, 30(3):526-545. DOI: 10.15832/ankutbd.1342935

ABSTRACT

Rapid urbanization and industrial expansion exert escalating pressure on rural areas, resulting in the inappropriate utilization of agricultural lands for non-farming purposes. This misuse is notably prevalent across industry, urban development, tourism, mining, and transportation infrastructure sectors. The challenges associated with this issue include land fragmentation, the underutilization of agricultural lands, a lack of effective agricultural land-use planning, identification and reclamation of abandoned agricultural lands, improvement of land acquisition and banking practices, land consolidation, land valuation, digitalization in agriculture, and the imperative for effective governance. In this study, agricultural land management in Türkiye was evaluated from legal,

technical, and managerial aspects, and the article proposes a functional model based on agricultural land that integrates rural land management into a broad framework of land policy and agricultural land-use planning. This model encompasses components related to land ownership, value, use, development, and spatial data infrastructure. Successful implementation necessitates the restructuring of existing institutions or the establishment of new ones. This study aims to address the above-mentioned issues and, with the proposed model, achieve a sustainable agricultural infrastructure by resolving the land-based problems of rural areas, and positioning them as a crucial component of rural land management.

Keywords: Agricultural land management, Agricultural land use planning, Land fragmentation, Land banking, Land use, Land development, Land value

1. Introduction

In rural areas, the management of rural lands presents a multifaceted challenge, combining various sectors, interests, and demands. This complex field of activity necessitates collaboration among practitioners, spanning policy, governance, the economy, and civil society, along with contributions from scientists (Masum 2017; Weith et al. 2019).

Rural areas are typically characterized by low population density and economies that are primarily based on agriculture and forestry. These areas, situated beyond urban centres, often face limitations in accessing essential services like education, healthcare, and infrastructure. Despite their geographical distance, they maintain direct connections with urban areas in economic, social, environmental, and production aspects, thus taking on administrative significance. Rural areas encompass small and medium-sized towns in rural regions, village settlements, agricultural lands, forests, pastures, plateaus, meadows, and natural resources. For instance, Magel (2022) notes that Germany remains a predominantly rural country, with over 2 000 of its 2 300 cities and municipalities in the Bavarian region characterized as rural. In contrast, in Türkiye, out of its 81 provinces, 973 districts, and 32 125 neighbourhoods, approximately 93.4% of the population resides in urban areas, while the remaining 6.6% inhabits the 18 211 villages (TURKSTAT 2023). This demographic distribution highlights Türkiye's departure from rural attributes, positioning it as a country significantly distinct from such characteristics.

Due to the significance of agricultural land in rural land management, the European Union's Rural Development Policy for the 2007-2013 period identified three main axes that necessitate preventive measures: competitiveness, rural development, and the management of agricultural and forested areas. It emphasized the sustainable use of 'agricultural and forested lands,' as one of the sub-components under the main axis of land management (EC 2008).

The development of rural areas, amid the trends of globalization and localization, relies on supporting essential economic activities like agriculture and forestry, alongside fostering continuous ecological interaction with urban areas (SCR 2018). In Türkiye, the economic sectoral management policy for rural areas primarily focuses on the agriculture sector to promote

development, aiming to develop the regions where the rural population lives and works (Kayıkçı 2009). Among the vital components in rural area management are agricultural infrastructure, agriculture, and agricultural governance.

Land management practices, focusing on spatially-oriented horizontal domains, have been integral to Türkiye's rural development policies over the past five decades, with significant projects like Village-Town in 1973 and Agriculture-Town in 1997 (Çolakoğlu 2007). Despite these efforts, the anticipated benefits have proven elusive. Addressing irregular and unauthorized urban development within Turkish urban areas required a systematic approach. This involved meticulous cadastral surveys to unravel land ownership intricacies, culminating in the formalization of land titles within the national land registry. Subsequently, spatial planning was orchestrated and complemented by the design and implementation of appropriate real estate financing models. This comprehensive strategy streamlined land ownership for citizens, catalysing the eradication of informal settlements and fostering the creation of well-structured urban centres.

Similarly, within the realm of land management, establishing an efficient rural land management system in Türkiye necessitates measures such as institutional restructuring, legislative regulations, capacity augmentation, prudent technology utilization, and management strategies focused on constructive resolutions (GDAR 2014).

The primary considerations in agricultural land management encompass various factors, including urban expansion pressures leading to the encroachment upon agricultural lands, land fragmentation due to factors like inheritance, and the revitalization of abandoned lands for agricultural production. Additional priorities involve the regulation of non-agricultural land use permissions, land consolidation processes, effective irrigation strategies, on-farm development services, agricultural information systems, soil databases, digital technologies, the establishment of a well-functioning rural land market, comprehensive agricultural land use planning, the restructuring of relevant institutions, and the imperative need for good governance. In 2013, the Workshop on the Future of Land Consolidation in National Public Investments organized by the General Directorate of Agricultural Reform (GDAR) proposed the establishment of a dynamic and effective land acquisition and land banking institution (GDAR 2014).

In the 11th Development Plan (2019) and the Working Group report spanning 2019-2023 (SCR 2018), specific emphasis was placed on the adverse effects of land fragmentation due to inheritance, hindering the efficient utilization of agricultural lands. The plan included policies to address this issue (SCR 2014; 2018; Küsek et al. 2019; MOF 2019; Türker 2019; 2023; Ercan 2020; Kurugöllü et al. 2021; Akkul 2022; Arslan et al. 2022; Demirbaş 2023; Şanlı et al. 2023). The identification and revitalization of abandoned lands for agricultural production, coupled with effective land acquisition for agricultural enterprises and related land banking practices, were underscored as priorities for developing agricultural land markets. These priorities were also highlighted in the 2019 Presidential Annual Program (SCR 2014; SCR 2018; PAP 2019; MOF 2019; AFC 2019; Türker 2019; 2023).

In the country, integrating land consolidation efforts with irrigation investments is advisable, coupled with a simultaneous call for regulations to streamline the registration processes for consolidation projects (SCR 2018; Akkul 2022). Experts suggest expediting consolidation projects, aiming for completion within a ten-year timeframe (Demirbaş 2023; Türker 2023). A proposition has been put forth advocating the concurrent implementation of land consolidation, land acquisition, and land banking to achieve more efficient and multifunctional land usage (Hartvigsen 2022; Türker 2023).

Within the agricultural sector, advancing agricultural information systems through digitalization, leveraging technologies like artificial intelligence and data-driven business models, is imperative. Ensuring the accessibility of these systems to all stakeholders is vital. A key requirement is enhancing the Land Parcel Identification System (LPIS), aligning with the Integrated Administration and Control System (IACS) and the priorities of the European Union acquis. Recommendations regarding digitization in agriculture and the Integrated Administration and Control System have been focal points in the 10th and 11th development plans (SCR 2014; SCR 2018).

Crucial to the functioning of a well-managed agricultural system is the development of agricultural land use plans grounded in soil information systems (Ercan et al. 2013; 2016; SCR 2018; Ercan 2019; MOF 2019; Türker 2023). Additionally, the distinct treatment of rural settlements in spatial planning and construction compared to urban settlements, alongside the creation of specialized solutions to address challenges in rural areas, stands out as a top priority (Zengin 2015; Çopuroğlu 2017; Ercan 2019; GIS 2023).

Çopuroğlu (2017) and Zengin (2015) emphasize that Law No. 6360, enacted in 2014, resulted in the transfer of services aimed at rural areas in provinces designated as metropolitan municipalities to these municipalities. This shift has introduced significant challenges in the management of rural areas. They underscore that the law has posed legal, demographic, governance, budgetary, institutional, and spatial planning challenges. One notable consequence is the change in administrative boundaries, with metropolitan municipal boundaries being redefined. As a result, the proportion of the town and village population within the total population has disproportionately decreased since 2013 (AFC 2019).

Addressing these changes necessitates a comprehensive and integrated perspective, led by the Ministry of Agriculture and Forestry, concerning rural life. Furthermore, there is a need to reclassify villages that have been transformed into neighbourhoods

in rural areas back to their 'village' status. It's also essential to revise the definition of rural areas. Simultaneously, metropolitan municipalities must provide services such as infrastructure, roads, and drinking water in rural areas while delegating services related to the agricultural sector to the Ministry of Agriculture and Forestry. These discussions took place during the Agricultural and Forestry Summit, and proposed solutions have been integrated into the objectives of the Development Plan (SCR 2018; AFC 2019).

The complexity introduced by the law underscores the urgency of promptly addressing the legal, juridical, and technical aspects related to agricultural land. The effectiveness of land management relies not only on the laws enacted in this field but also on the institutions established. Achieving harmony across various components can only occur through effective coordination and a well-structured organizational framework, ensuring such coordination (SCR 2018; 2019)

2. Conceptual Overview

Global factors, disruptive technologies, and the digital products they offer create significant societal demand in land management within societies. The growing role of the United Nations and the World Bank in implementing digital transformation has sparked discussions about current land use policies, land use systems, sustainable rural land management, and future options.

UNECE (1996) emphasized that the land management system should include multi-purpose cadastre and land information systems based on spatial databases. UNECE (2005) highlighted the importance of registering land property rights and good governance in land management. The land hierarchy, as modelled by Williamson et al. (2010), starts from land policy at the top and goes through the land management paradigm, land administration, spatial data infrastructure, cadastre, and finally the cadastral parcel, forming a six-stage inverted pyramid. UNECE (2005) and Williamson et al. (2010) presented land management as the process of managing the use and development of land resources and emphasizing its significance. FAO (2012) defined land administration as the implementation and operationalization of rules related to land use rights. Land administration involves various systems and processes for managing rights on land, land use regulation, land valuation, and taxation.

Land management represents the process of using the physical resources of land effectively, supporting and implementing sound land policies, and facilitating social, economic, and environmental sustainability (Enemark 2005; 2006; 2010). In the context of the importance of land management in the implementation of the Sustainable Development Goals (SDGs), the Framework for Effective Land Administration UNGGIM (2020) document prepared by the Land Administration Experts Group established by the UN defines effective land management as "how," "what," "who," "when," and "where" in relation to land policy, land ownership, land use, land value, land development, and integrated geospatial information components. It supports the SDGs and is defined as the process of determining, recording, and disbursing the relationship between people and land.

Land management considers interactions among diverse land use categories and sectors, explicitly considering the demands of rural and urban areas, as well as the economic, social, and ecosystem functions of the land (Repp et al. 2015). The focus of land management is the procedural aspect of supervising land use and development to ensure effective coordination of spatial, sectoral, and temporal elements in multi-level governance processes. It entails adapting a range of tools and utilizing technological, political, and legal measures and activities. Management involves adjusting the set of tools and employing technological, political, and legal measures and activities (Haber et al. 2010). Rural land management involves the systematic planning, utilization, and conservation of land in rural areas, which encompasses a range of factors including agriculture, water resources, forests, pastures, natural resources, conservation, and development. The aim is to ensure the sustainable use and development of rural land, by considering factors such as environmental, economic, and social factors.

Land governance refers to the policies, processes, and institutions involved in the management of land, property, and natural resources. It encompasses decisions related to access to land, land rights, land value, land use, and land development (FIG 1995). The governance system comprises several distinct components, namely the institutional environment, market governance, private governance, and public governance (Bachev 2020). Land issues are at the core of agrarian governance (Wu et al. 2022). Agricultural governance refers to the system and processes through which agricultural resources and activities are managed and regulated. It encompasses the policies, laws, institutions, and practices that govern land, water, forests, and other natural resources used for agricultural purposes. The objective of agricultural governance is to achieve sustainable and fair management of agricultural resources while fostering agricultural productivity, rural development, and addressing social, economic, and environmental issues in rural areas. It entails decision-making processes that involve diverse stakeholders, such as farmers, landowners, government agencies, and civil society organizations.

Epidemic diseases, conflicts, climate change, demographic and economic challenges arising from rural migration, soil degradation, conflicts arising from the urban-rural balance, and global trends are factors that influence current land management, land use systems, and land use policies. With this awareness, the conservation and efficient use of land, water, agriculture, forests, and natural resources have become part of the Sustainable Development Goals (SDGs). SDG 1 (No poverty), SDG 2 (No Hunger), SDG 3 (Good Health and Well-Being), SDG 6 (Clean Water and Sanitation), SDG 9 (Industry, Innovation, and Infrastructure), SDG 11 (Sustainable cities and communities), SDG 13 (Climate Action), and SDG 15 (Life on Earth) directly involve objectives related to changes in land use and rural land management. The implementation of these objectives takes place

at the regional and local levels, necessitating changes in governance processes (Weith et al. 2019). In this regard, the FAO Strategic Framework for 2022-2031 (2023) aims to support the 2030 Agenda by transforming agri-food systems into more efficient, inclusive, resilient, and sustainable systems. The objective is to achieve better production, nutrition, a healthier environment, and an enhanced quality of life for all, with a commitment not to leave anyone behind.

Land use undergoes continuous change depending on the social, economic, and environmental impacts size and spatial distribution of the population. Urbanization is one of the fundamental reasons for the balance or conflict between economy and ecology in today's world (Ercan 2019). Urbanization will continue to exert pressure on land, causing a transformation from rural to urban areas (GLTN 2021). As cities continue to grow, rural areas are being converted into urban spaces, directly affecting the urban-rural balance in a negative way.

There are various definitions related to land use planning which are very close and related to each other. Metternich (2017) defines land use planning as the most appropriate tool that can help develop policies that harmonize human activities and environmental sustainability. Mattsson et al. (2021) define it as the process of determining future land use, while Williamson et al. (2010) describe it as the integration of land policies and land information into land use management to achieve sustainable development. According to Metternich (2017), Erdoğan et al. (2020), and the FAO guide (1993), land use planning encompasses the systematic evaluation of land and water potential, land use alternatives, and economic and social conditions to select and adopt the best land use options. Without the establishment of effective governance systems, agricultural land management, and consequently, agricultural reforms and their impact on food security and poverty reduction will remain ineffective. In recent years, various land use policies and approaches have been developed based on countries and institutional priorities, such as spatial land use planning, integrated land use planning, participatory land use planning, village land use planning, rural territorial land use planning, regional land use planning, and ecological land use planning. However, it is observed that there is insufficient emphasis on the need for a detailed agro-based macro-level spatial land use planning approach in these approaches and policies.

3. Rural Land Management in Türkiye

The efficiency of land administration in a country serves as a significant indicator of both the effectiveness of land management and the underlying land policy. Successful land management hinges not only on well-established laws but also on the institutions specifically created to implement these policies.

3.1. Land policy

In Türkiye, the legal foundation for land policy is rooted in the Constitution of the Republic of Türkiye and the Turkish Civil Code. According to Article 35 of the Constitution, every individual holds the right to property and inheritance, albeit with the stipulation that the exercise of this right should not contravene the public interest. Furthermore, Article 44 of the Constitution places the duty on the state to take measures for the protection and enhancement of fertile land cultivation, erosion prevention, and the provision of land to farmers engaged in agriculture but lacking adequate land. In situations where the public interest takes precedence, expropriation can be initiated in accordance with Article 46, and state ownership can be established, as outlined in Article 47. These constitutional provisions grant the legislator the authority to restrict property rights when it is deemed to be in the service of social welfare and the public interest. The safeguarding and development of forests are guaranteed by Article 169 of the Constitution. Notably, state forests cannot change ownership; they remain under state management and operation, subject to relevant legislation. Ownership of state forests cannot be acquired through adverse possession, and no easement right can be granted except for circumstances related to the public interest. Settlement within forest areas, pastures, and special conservation areas is prohibited.

The legal framework for rural land management practices in Türkiye is primarily constituted by various laws, including Law No. 5403 on Soil Conservation and Land Use, Law No. 2644 on Land Registry, Law No. 3402 on Cadastre, Law No. 6831 on Forestry, Law No. 4342 on Pastures, Law No. 3213 on Mining, Law No. 442 on Villages, Law No. 6360 on Metropolitan Municipalities, Law No. 3194 on Zoning, Law No. 2863 on the Protection of Cultural and Natural Resources, Law No. 3202 on Services for Villages, along with related Ministry Regulations, bylaws, regulations, and guidelines.

Notably, there is no single organization in Türkiye exclusively responsible for rural land management. Instead, various governmental entities have specific responsibilities. For instance, the General Directorate of Land Registry and Cadastre (GDLRC) is tasked with managing real estate and handling rights, responsibilities, and restrictions related to properties recorded in the land registry through cadastre. The General Directorate of Forestry (GDF) is responsible for overseeing forests, while GDAR manages agricultural lands, pastures, highland and lowland grazing areas, soil conservation, and rural land use. The General Directorate of National Estate manages properties owned by the state treasury, and various other public institutions are responsible for natural resource management based on their respective areas of relevance. It is essential to note that GDLRC is authorized and responsible for registering all types of properties, whether private or public, in the land registry.

3.2. Land administration

Land registry and cadastre services in Türkiye are carried out under the Ministry of Environment, Urbanization, and Climate Change within the structure of GDLRC. GDLRC has a two-tier organizational structure, consisting of central and provincial offices, and conducts its activities through 24 Regional Directorates, 973 Land Registry Offices, and 81 Cadastre Offices (in addition to licensed cadastre bureaus).

GDLRC is responsible for conducting the country's cadastre works, tracking changes, renewing and updating the cadastre. It is also responsible for maintaining the land registries under the state's responsibility in an organized manner, handling all kinds of registered and unregistered land transactions, as well as registration procedures related to real estate. Besides these, GDLRC is also responsible for tracking changes in the registries, conducting inspections, and archiving and preserving the records and documents. Additionally, GDLRC is authorized and responsible for producing or commissioning large-scale cadastral and topographic cadastral maps, controlling the map production process, and establishing the fundamental principles. Moreover, it creates the infrastructure for the spatial information system, allowing real and legal persons, as well as public institutions, to benefit from its data. Cadastre and land registry services are the responsibility of the state, and the state is objectively liable for any losses that may arise from the maintenance of land registers.

The initial cadastre of Türkiye has been completed (Ercan 2021). According to data from GDLRC in July 2023 (GDLRC 2023), the total number of cadastral parcels is 58.8 million. As of 2022, approximately fifteen million cadastral parcels in rural areas have been renewed, improving the spatial data infrastructure in rural regions (Ercan 2023). The automation of land registry activities was completed in 2004 and subsequently expanded in the following years. Cadastral data is provided to both local and foreign individuals and legal entities through mobile applications with a parcel inquiry system, free of charge.

3.3. Rural land use categories, rural population, and seasonal variations

Creating an effective and functioning land management system for the development and progress of urban and rural areas has become not just a necessity but an essential requirement. Especially during the Covid-19 pandemic, conflicts, and climate change, it has become evident that the management of semi-rural areas, situated between urban and rural regions, is just as crucial as urban area management. Rural land, in its simplest form, encompasses village settlements, agricultural lands, forested areas, and public properties like pastures, meadows, and highland areas.

According to TURKSTAT, a new approach at the neighbourhood-village level has been introduced, aligning with the Degree of Urbanization (DEGURBA) system developed by the European Statistical Office. Under this approach, densely populated urban settlements, which account for 1.6% of Türkiye's land area, house 67.9% of the population. In areas classified as rural, comprising 93.5% of the country's land area, 17.3% of the population resides. Additionally, in settlements categorized as moderately dense cities, making up 4.9% of the country's land area, 14.8% of the population resides (TURKSTAT 2022). These demographic distributions have significant implications for governance, social dynamics, and the development of rural settlements, emphasizing the need for policy and legislative frameworks that can effectively address the unique challenges and opportunities within these diverse areas.

Based on the recalculated data from the General Directorate of Geographic Information Systems website (2023), the per capita total agricultural land, which was 0.76 hectares in 1990, witnessed a decline to 0.46 hectares by 2018. Considering the total agricultural land in 2022 (23.864 million hectares), the per capita agricultural area has further diminished to 0.28 hectares.

Among the 58.8 million existing cadastral parcels, 32.5 million are classified as agricultural parcels in Türkiye. Türkiye accommodates 3.1 million agricultural enterprises, and due to various factors, the amount of abandoned agricultural land totals 2 million hectares, with an approximate shareholder count of 40 million (MT 2019). Furthermore, 7.66-million-hectare non-agricultural land rural areas are occupied by structures, including buildings and graveyards (TURKSTAT 2016). Along with these, 7.66 million hectares of non-agricultural land (rocky land, swamp, arid land, etc.), and 2.01 million hectares of land occupied by buildings in rural settlements (graveyards, etc.), are included in the land use category.

Approximately one-third of Türkiye's total land area, amounting to 23.864 million hectares, is identified as cultivable agricultural land, as outlined in Table 1. This comprises a significant proportion of the country's 78-million-hectare total land area.

In Türkiye, an expanse of 23.864 million hectares of land is designated as cultivable and falls under the status of permanent crops. The aggregate arable land encompasses 20.194 million hectares, with 16.510 million hectares dedicated to active cultivation. Additionally, 81.088 hectares are placed under protective cover according to their respective types. Notably, the total expanse left fallow amounts to 2.960 million hectares. The nation boasts 23.11 million hectares of forested land, with an additional 14.617 million hectares designated as permanent meadows and pastures (Table 1).

Table 1- Land use categories and amounts in Türkiye (ha)

Total utilized agricultural land	38 482 000
Total arable land and land under permanent crops	23 864 000
Total arable land	20 194 000
Sown area	16 510 000
Fallow area	2 960 000
Areas of vegetables and gardens	718 000
Area of ornamental plants	6 000
Total land under permanent crops	3 671 000
Areas of fruits, beverages and spices crops	2 385 000
Area of vineyards	385 000
Area of olive trees	901 000
Land under permanent meadows and pastures	14 617 000
Forest area	23 110 000
Areas for land under protective cover by type	810 881 000
Ornamental plants production for land under protective cover	1 599 706 562 (plants)

Source: TURKSTAT, 2022

Regarding the number of parcels, a significant 98.2% of holdings consist of land areas ranging from 5 to 499 hectares, with 77.5% falling within the 20-to-499-hectare range. On average, each agricultural holding contains 5.9 parcels of land, and the average parcel size for agricultural land is 12.9 decare (Table 2). This fragmentation results in each farmer cultivating, on average, 11 separate land parcels. Moreover, a single piece of land is jointly owned by an average of 13 individuals, leading to a fragmented ownership structure and a complex land use system. Consequently, agricultural holdings tend to be small, scattered, and divided into numerous parcels, often not generating sufficient income.

Table 2- Number of parcels of agricultural land per holding and average parcel size of agricultural land

<i>Holding size (decare)</i>	<i>Number of parcels of agricultural land per holding</i>	<i>Average parcel size of agricultural land (decare)</i>
Total	5.9	12.9
-5	1.5	1.6
5 – 9	2.4	2.7
10 – 19	3.4	3.8
20 – 49	4.7	6.4
50 – 99	6.9	9.4
100 – 199	10.1	12.9
200 – 499	13.7	20.6
500 – 999	21.1	30.3
1000+	36.9	60.3

Source: TURKSTAT 2016

Out of the total 6 189 351 households in the country, 4 106 983 (66.34%) are engaged in agricultural activities, while 2 082 368 (33.66%) do not participate in agricultural activities. These figures indicate that one out of every three households, despite residing in rural areas, is not involved in agriculture. Therefore, there is a need to reassess the agricultural infrastructure, particularly in terms of agricultural land, alongside other factors (Table 3).

Table 3- Rural settlement number, population structure, and seasonal population changes

Total number of households	6 189 351
Total number of households engaged in agricultural activity	4 106 983
Total number of households not engaged in agricultural activity	2 082 368

Source: TURKSTAT 2016

Among the 37 036 rural settlements in Türkiye, 61% of the residents choose to relocate from their villages, rural neighbourhoods, or towns to district centres or cities during the winter months, as reported by DAGD 2020. Among the rural population, 22.0% derive their livelihood from agricultural production activities, 22.0% from livestock activities, 20.4% from retirement pensions and social assistance, 7.9% from leasing activities, 6.5% from agricultural labour, 2.3% from forestry, and others engage in construction labour, guarding, mining labour, mushroom cultivation, transportation, and the service sector

(DAGD 2020). Only 42.4% of rural residents rely on agriculture and livestock for their livelihoods, highlighting the significance of more than half leaving their villages during the winter to live in provincial and district centres. This underscores the inadequacy of agricultural production and the agricultural economy in rural areas (Table 4).

Table 4- Rural settlement number, population structure, and seasonal population changes

Type of settlement	Period	Average	Median	Total	Rural settlement count	Population Change According to Winter Period (%)
Village	Winter	275	145	4 994 167	18 186	66
	Summer	457	250	8 315 167		
Rural neighbourhood	Winter	698	300	12 880 413	18 464	58
	Summer	1 102	400	20 345 925		
Township	Winter	3 052	2.5	1 178 015	386	68
	Summer	5 138	3.5	1 983 378		
Overall	Winter	514	207	19 052 429	37 036	61

Source: DAGD 2020

These statistical data underscore the imperative to address the institutional structure and functional model of Türkiye's agricultural administration within the framework of rural land management. This finding highlights a crucial concern for agricultural administration, emphasizing the concrete identification, modelling, resolution, and effective management of issues related to agricultural lands. The generation of these findings and solutions forms the foundational rationale for the preparation of this article.

3.4. Institutions and activities for rural land

Rural land management inherently involves various disciplines, spanning agriculture, water, biodiversity, climate change, demographics, and the economy. Similar to other countries, Türkiye lacks a single organization exclusively responsible for rural land management. We have constructed a 25x14 matrix, presented in Table 5, illustrating activities related to rural land management and their corresponding responsible institutions. This matrix highlights which technical components, among the 14 defined, are carried out by each organization, denoted by an 'x' in the respective field.

An analysis of Table 5 reveals that in the field of rural land management, 25 different institutions and organizations play various roles and possess distinct authorities. Given that rural land management is a holistic concept, these institutions should be integral components of the whole. Being part of the whole can only be possible through effective coordination within an institutional framework that facilitates such coordination. However, in Türkiye, there is no authorized and responsible administration for rural land activities. Consequently, a single activity may be carried out by multiple institutions, resulting in the duplication of work and the wastage of resources and labour.

The exclusive authority responsible for registration in the land registry is GDLRC. Although forest demarcation and cadastre, as well as pasture cadastre activities, are undertaken by their respective institutions as illustrated in Table-5 (GDF 2021; 2023), the cadastre, property-related controls, and registration fall under GDLRC's purview. Map production and spatial data management are conducted by all institutions according to their needs.

GDAR, as the authorized institution, is responsible for defining rural areas, developing agricultural infrastructure, enhancing productivity, and managing them. In its current form, GDAR continues to function as an organization responsible for executing a substantial portion of the Ministry's duties. Therefore, the restructuring of the institution to address land-related issues in the agricultural sector has become not only a necessity but an obligation.

Table 5- Matrix of institutions and activities for rural land

	<i>INSTITUTIONS</i>	<i>Mapping</i>	<i>Expropriation</i>	<i>Environment and Soil</i>	<i>Land valuation</i>	<i>Spatial Planning</i>	<i>Infrastructure</i>	<i>State Land Management</i>	<i>Land and Housing Production</i>	<i>Cadastral</i>	<i>Forest</i>	<i>Land Consolidation</i>	<i>Spatial Data Management</i>	<i>Land Registry</i>	<i>Coastal Management</i>
1	General Directorate of Land Registry and Cadastre	X			X			X		X	X		X	X	
2	General Directorate of Agriculture Reform	X	X	X	X	X	X	X	X			X	X		
3	General Directorate of Forestry	X	X	X	X			X		X	X		X		
4	General Directorate of Spatial Planning.	X	X		X	X			X						X
5	Municipalities	X	X	X	X	X	X	X	X			X	X		
6	General directorate for state hydraulic works	X	X	X	X		X	X				X	X		
7	Mass Housing Administration	X	X		X	X	X		X				X		
8	Disaster and emergency management presidency	X	X			X	X		X				X		
9	Petroleum pipeline corporation	X	X	X	X	X	X						X		
10	General directorate for highways	X	X	X	X		X						X		
11	Provincial Banks	X	X	X		X	X						X		
12	General Directorate of Turkish Coal Enterprises	X	X	X	X								X		
13	General Directorate for Foundations	X	X		X			X					X		
14	General Directorate of Mining Affairs	X	X	X				X					X		
15	General Directorate of Cultural Heritage and Museums	X	X	X		X		X					X		
16	South-eastern Anatolia Regional Development Administration	X				X	X						X		
17	Directorate General of Investments and Enterprises.		X	X		X							X		
18	General Directorate of Mineral Research and Exploration	X	X	X									X		
19	General Directorate of Turkish Electricity Distribution Corporation		X		X								X		
20	Directorate of Privatization Administration	X			X	X							X		
21	General Directorate of National Property		X		X			X					X		
22	General Directorate for Environmental Management			X									X		
23	General Directorate for Water Management			X									X		
24	General Directorate of GIS	X											X		
25	National Mapping Agency	X											X		

Source: Developed with inspiration from SCR 2014, GDAR 2014 and AFC 2019

4. Legal regulations and technical studies

4.1. Key legal regulations

In 2005, the General Directorate of Agricultural Reform formulated and enacted Law No. 5403, commonly known as the Law on Soil Conservation and Land Use. This legislation aimed to achieve several objectives, including the scientific classification of land and soil resources, the establishment of minimum sizes for agricultural land, and the promotion of income-generating agricultural practices. The law also sought to prevent land fragmentation, establish land use plans, and consider social, economic, and environmental dimensions in conservation and development, utilizing participatory methods. Furthermore, it aimed to deter unauthorized and improper land uses while developing methods for ensuring land protection.

In 2014, the Regulation on the Transfer of Agricultural Lands was introduced to address inheritance-based transfers of agricultural lands. This regulation incorporated provisions related to valuation, land use changes, minimum agricultural land size, sufficient income-generating land size, economic integrity, and procedures and principles for determining the qualifications of competent heirs. In response to evolving needs, the regulation underwent revisions in 2021.

The Medium-Term Plan for 2018-2020, endorsed by the Council of Ministers' Decision in September 2017, featured a provision aimed at bringing abandoned agricultural lands into production. This was to be achieved through models like land banking. Additionally, the "2018 Program" placed emphasis on developing models for utilizing abandoned agricultural lands and ensuring the efficient operation of agricultural enterprises. The "Agriculture and Food" section of the 2019 Presidential Annual Program (PAP 2019) highlighted efforts to utilize abandoned agricultural lands and develop land acquisition practices for the effective operation of agricultural enterprises, with a specific focus on land banking. These provisions elevated the identification and utilization of abandoned agricultural lands, land acquisition, and land banking as strategic objectives.

4.2. Land related activities and implementation project

Land consolidation projects in Türkiye were initiated in 1961. Since 2002, there has been a growing demand for land consolidation, making it a priority area for the government, particularly between 2009 and 2014. As of the end of 2022, the total area suitable for consolidation in the country is 14.3 million hectares. Out of the 8.78 million hectares of land tendered for consolidation projects, 6.78 million hectares have been completed and registered, while work is ongoing on the remaining 2 million hectares (SHW 2022; Demirtaş 2023). In addition to soil graduation and block design, land consolidation projects also offer services such as reducing land fragmentation, improving local road infrastructure, addressing irrigation and drainage issues, and providing on-field land development services like levelling and stone collection.

The 'Agricultural Monitoring and Information System' (TARBIL) was developed as part of the Integrated Administration and Control System (IACS). TARBIL is an integrated system that records all aspects of the country's agriculture, stores data, generates reports, and monitors results. One of the primary goals of the TARBIL project was to establish an information system for continuous and real-time data collection, rather than relying on periodic estimations. TARBIL is based on two main pillars: the production and utilization of accurate real-time data and the Agriculture Information System, which includes mobile applications.

The LPIS project, a requirement for candidate countries in the process of transition with the European Union, was implemented in 2014. As part of the project, orthophoto maps of the entire country were created and integrated with digitized agricultural parcels. In this context, a digital geospatial database for reference parcels was established, serving as a unique, homogeneous, reliable, and accurate LPIS database to support application administration.

In the permitting process for lands intended for agricultural and non-agricultural purposes, the Agricultural Lands Assessment and Information System (TAD Portal) was established to centralize the management of land and soil studies, assessments, inquiries, and archiving processes. With the TAD Portal, agricultural parcel inquiries can be conducted through the e-Government platform.

In recent years, a project has been developed to enhance and implement the existing soil database primarily using satellite imagery. Additionally, the institution has achieved a significant accomplishment by protecting large plains with high agricultural potential and facing erosion and degradation risks through a Council of Ministers decision. However, despite pilot project implementations for rural land valuation, the results have not been communicated to relevant professionals.

GDAR, with its authority in rural management and land use planning, has endeavoured to establish a nationwide model called the "Agro-Based Macro Level Land Use Planning" approach. Unfortunately, due to certain institutional reasons, the project could not be implemented.

4.3. Legal changes made by other institutions affecting rural land management

4.3.1. Transfer of land consolidation works to state hydraulic works

In 2018, a regulation was enacted that transferred the responsibility for implementing land consolidation and on-field development services from GDAR to State Hydraulic Works (DSİ). Other institutions and organizations now have the authority to act as project administrators for these services, subject to approval from DSİ.

4.3.2. Enactment of the metropolitan municipality law

In accordance with Law No. 6360, enacted in 2012 and amended in 2013, the number of Metropolitan Municipalities was increased to 30. This law expanded the boundaries of Metropolitan Municipalities to align with provincial administrative boundaries and equalized the boundaries of metropolitan district municipalities with district administrative boundaries (see Figure 1).

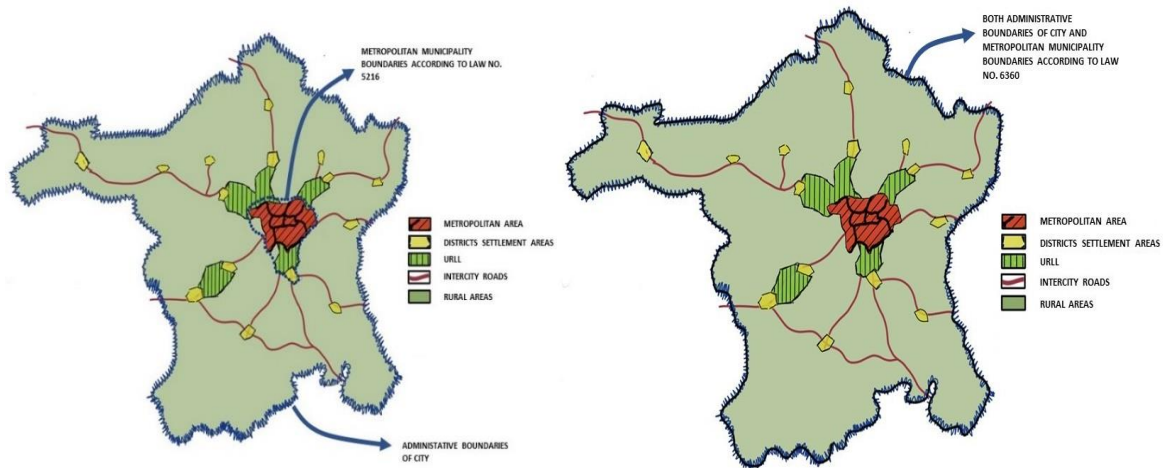


Figure 1- Before (left) and after (right) the Law No. 6360

The legal identity of villages situated within the boundaries of metropolitan municipalities was annulled by the law and transformed into neighbourhoods. This transformation resulted in the reclassification of a total of 18 211 areas, previously designated as villages, into neighbourhood status (Tekeli 2018). In 2012, approximately 22.7% of the Turkish population resided in villages. However, following the implementation of the aforementioned legal changes, this proportion significantly decreased to 8.2% in 2014 (see Table 6). Subsequently, in 2021, the percentage of individuals residing in provincial and district centres, initially at 93.2%, saw a slight rise to 93.4% in 2022. At the same time, the percentage of the population living in towns and villages experienced a reduction from 6.8% to 6.6% during this period (TURKSTAT 2023).

Table 6- Distribution of Rural and Urban Population between 1927-2022

Year	Total	Rural Population	Urban Population	Rural (%)	Urban (%)
1927	13 648 270	10 342 391	3 305 879	75.8	24.2
1950	20 947 188	15 702 851	5 244 337	75.0	25.0
1970	35 605 176	21 914 075	13 691 101	61.5	38.5
1980	44 736 957	25 091 950	19 645 007	56.1	43.7
1990	56 473 035	23 146 684	33 326 351	41.0	59.0
2000	67 803 927	23 797 653	44 006 274	35.1	64.9
2010	73 722 988	17 500 632	56 222 356	23.7	76.2
2012	75 627 384	17 178 953	58 448 431	22.7	77.2
2014	77 695 904	6 409 722	71 286 182	8.2	91.8
2015	78 741 053	6 220 543	72 520 510	7.9	92.1
2016	79 814 871	6 145 745	73 669 126	7.7	92.3
2017	80 810 525	6 060 789	74 749 736	7.5	92.5
2018	82 003 882	6 314 298	75 689 583	7.7	92.3
2019	83 154 997	5 987 159	77 167 837	7.2	92.8
2020	83 614 362	5 853 005	77 761 357	7.0	93.0
2021	84 680 273	5 758 258	78 922 014	6.8	93.2
2022	85 279 553	5 628 450	79 651 102	6.6	93.4

Source: Simplified from TURKSTAT data.

The reclassification of rural settlements, particularly villages within provincial boundaries, has resulted in substantial legal changes. In this restructuring, these settlements have undergone a legal transition from being self-governing villages to becoming neighbourhoods of the districts to which they were previously affiliated. This transformation has introduced numerous urban-oriented approaches, projects, programs, and practices that were primarily designed for urban environments. Moreover, the municipal and zoning legislation governing urban areas has been directly applied to rural environments. These changes have given rise to various challenges and issues in rural regions (Zengin 2015; Çopuroğlu 2017). Consequently, the traditional self-governing rural administrations, often deeply rooted in local customs and practices, have been entirely abolished. This transition marks a significant shift in the governance and administration of rural areas, imposing urban-centric models and regulations on communities accustomed to more autonomous modes of governance.

5. Discussion and Results

5.1. Discussion

The increasing migration from rural to urban areas in Türkiye is influenced by multiple factors, primarily rapid industrialization and urban expansion. This migration is a response to various challenges faced by rural communities, including limited income from agriculture, suboptimal living conditions, fragmentation of agricultural lands due to inheritance practices, and a growing need for social services such as education and healthcare. Consequently, agricultural lands in rural areas are being abandoned.

To tackle these challenges, the GDAR is actively engaged in comprehensive legal and strategic planning. The main objective is to rejuvenate abandoned agricultural lands through a process known as land banking. This strategy also aims to address the problem of agricultural land fragmentation caused by inheritance laws. Despite the introduction of the Regulation on the Transfer of Agricultural Lands in 2014, with subsequent revisions in 2021, certain ambiguities still impede its effective implementation. The fragmentation of agricultural lands poses a significant obstacle to efficient land use, leasing, inheritance management, and the success of land banking initiatives.

Moreover, the challenge of achieving an economically viable size for agricultural land, large enough to manage the complexities of rural land, remains unresolved. This challenge is rooted in issues such as land parcel fragmentation, intricate land tenure arrangements, and complex regulatory matters.

The existing challenges in valuing rural and agricultural lands, evident in institutional practices, pose a significant hurdle to the establishment of a functional rural land market. Moreover, the absence of a comprehensive and effective model for land banking hampers practical implementation, despite the potential utilization of existing technologies to identify and reintegrate abandoned lands into agricultural production. The lack of concerted efforts to execute project-based approaches further exacerbates these issues. Addressing these challenges is imperative for ensuring the sustainability of Türkiye's agricultural sector and the equitable and effective use of its crucial agricultural resources.

Despite the substantial legal transformation introduced by Law 6360, aimed at improving rural land management, no substantial progress has been made in amending this law. This has resulted in inter-institutional challenges that complicate rural land management. The transfer of authority and responsibilities for land consolidation to the DSİ has weakened GDAR, adding to the complexities.

The transfer of the TARBİL project to a different ministry unit has removed GDAR's jurisdiction and accountability over the project, hindering its contribution to GDAR's efforts. Conversely, the TAD portal, a valuable tool for agricultural inquiries, maintains its significance within e-government applications. The successful nationwide completion of the orthophoto production project forming the basis of the Land Parcel Identification System (LPIS) benefits not only GDAR but also various other governmental entities.

The preparation of Agricultural Land Use Plans, especially lacking at a micro scale in rural areas with prevalent agricultural activities, should align with the provisions of Soil Conservation and Land Use Law No. 5403. GDAR, a pivotal institution in rural development, rural land management, and the formulation of rural and regional planning regulations, aims to establish a nationwide Agro-Based Macro Level Land Use Planning model. However, the project's implementation, initially planned for three provinces, faces challenges due to complex institutional dynamics.

Over the past ten years, frequent rotations of senior officials within the institution's decision-making bodies have cast a shadow over the process, adversely affecting the implementation of evolving corporate strategies and technical projects. This has contributed to a persistent lack of success in these endeavours. Ongoing legal and institutional challenges call for collaborative and innovative solutions to facilitate more effective rural land management in Türkiye.

5.2. Results

The findings from the evaluation of land use categories, land use, legal regulations, ongoing projects, and institutional structure have been summarized as follows:

- I. The Soil Conservation and Land Use Law is identified as not adequately responsive to practical needs, highlighting the necessity for improvement.
- II. Measures are required to prevent the fragmentation of agricultural lands through inheritance, address land fragmentation and multiple ownership issues, and spatially identify and repurpose abandoned agricultural lands for agricultural production.
- III. There is a need for the establishment of a rural land valuation model integrated into legislation.
- IV. Clear definitions of competent farmers in agricultural management are essential, addressing issues related to tenancy, partnership, and joint cultivation.
- V. Immediate initiation of land acquisition and banking practices is recommended.
- VI. The expansion of the content of land consolidation projects, along with their implementation in conjunction with irrigation projects and land acquisition/banking, is deemed necessary.
- VII. The development of macro and micro-level land use plans for agricultural purposes, with a focus on urban-rural land interlinkages and small-scale agricultural enterprises, is suggested.
- VIII. The restructuring of the existing institutional framework into rural land management administration is proposed.
- IX. Emphasis on good governance, capacity building, and digitalization in agriculture is underscored.
- X. The development of an effective functioning rural land market in the country is identified as a crucial need.
- XI. The necessity to resolve technical, legal, and administrative problems related to agricultural land is acknowledged.
- XII. Metropolitan municipalities with expertise in infrastructure projects, including infrastructure, road, and drinking water projects, must expand their services to rural areas and transfer services related to the agricultural sector to the rural land management administration.

All these findings address issues related to rural land management, and it is believed that these problems can be effectively addressed through the proposed functional model and, consequently, institutional restructuring.

6. Rural Land Management Functional Model Proposal

In Türkiye, the primary issues related to agricultural land involve challenges in land transfers due to inheritance and shared ownership, inadequacy of farming land (scale problem), and land fragmentation. Secondary issues include the aging of the agricultural population, rural-to-urban migration, lack of farm capital, and the limited adoption of modern agricultural technologies. To effectively tackle these challenges, there is a need for the establishment of legal regulations pertaining to property, the creation of a comprehensive and efficient agricultural information system, the development of an agricultural land market, and the establishment of a dynamic institution to provide these services.

The persisting problems concerning agricultural land and its management remain at the forefront of the country's agenda. The framework for rural land management is depicted in Figure 2, encompassing key components aligned with the Sustainable Development Goals. These components include digital land data (ownership, value, use, and development), land policy, institutional framework, agricultural land use planning, and the establishment of an effective rural land market.

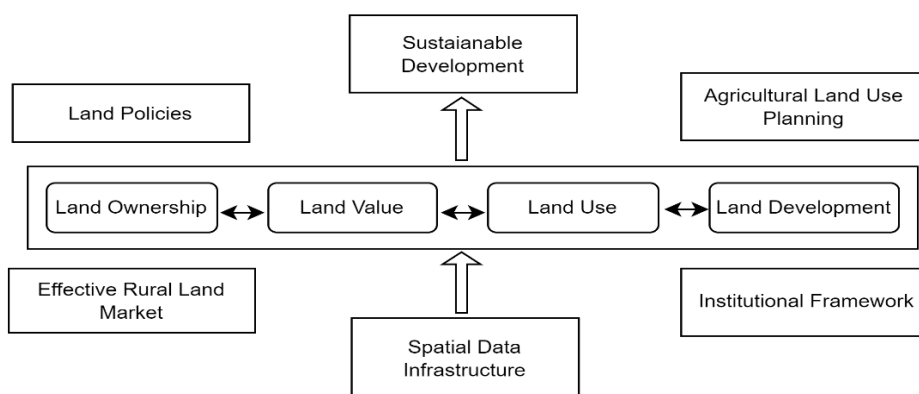


Figure 2- Rural land management framework (Source: modified based on Govender (2018))

In Türkiye, discussions on rural land management often gravitate towards the concept of land consolidation. Unfortunately, this association has contributed to a lack of clarity in understanding the broader scope of rural land management. Consequently,

there is an urgent need to develop a comprehensive paradigm for rural land management structured around a functional model centred on agricultural land, encompassing all relevant parameters.

As depicted in Figure 3, the Framework for Effective Land Administration (UN 2020) highlights the foundational elements of land management, including land ownership, use, value, development, and spatial data infrastructure. The hierarchical model of land management proposed by Williamson et al. outlines a series of activities situated between cadastral parcels and land policy, as illustrated in Figure 4. This research aims to formulate a land-based functional model that serves as the foundation for rural land management. The developed model strives to integrate the intricate processes and procedures between land policy and agricultural land use planning in rural areas. The subsequent sections elaborate on the proposed model, elucidating its components and the functional relationships between them.

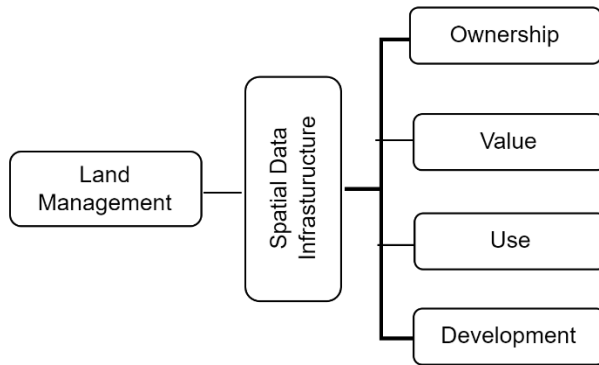


Figure 3- Land management components

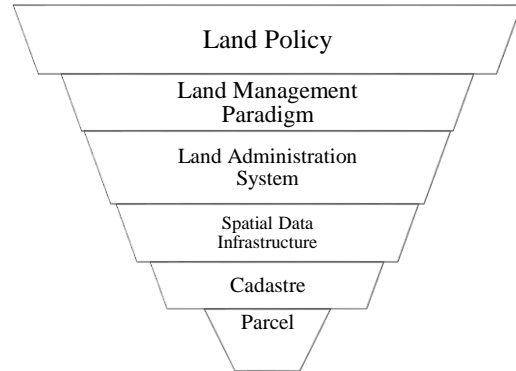


Figure 4- Land management hierarchy

6.1. Land policy, land administration, and rural land definition

Rural land management, a crucial subcomponent within the broader land management framework (depicted in Figures 3 and 4), constitutes a parcel-based system grounded in the principles of land policy, land administration, and rural land. This multidimensional domain demands a comprehensive and holistic approach. Through the implementation of effective land management strategies and a careful consideration of the urban-rural equilibrium, rural areas can thrive, preserving agricultural lands, forests, natural resources, and cultural heritage for the benefit of future generations.

In the realm of rural land management, land policy plays a central role. It involves the formulation, implementation, and regulation of guidelines, rules, and laws governing land ownership, utilization, and development in rural areas. The overarching goal of these policies is to ensure the sustainable and equitable exploitation of rural land resources, considering economic, social, and environmental factors. Effective land policy requires a balanced approach that harmonizes the diverse needs and interests of various stakeholders, including rural communities, government bodies, investors, and environmental organizations.

Key aspects integral to land policy in the context of rural land management include the regulatory framework, land ownership and value, land use, development, institutions and services, agricultural lands and village settlements, community development and empowerment, and digital land data and its dissemination (as illustrated in Figure 5).

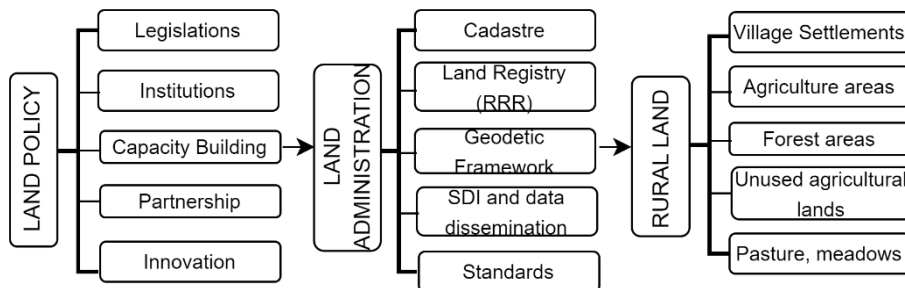


Figure 5- Rural land management paradigm

Land administration in rural land management involves the systematic organization, regulation, and oversight of land-related activities, encompassing functions such as land registration, tenure systems, geodetic framework, cadastre, and land records (Rights, Restrictions, and Responsibilities) as well as the establishment of spatial data infrastructure. The fundamental objective

of this framework is to ensure the efficient utilization of land, safeguard land rights, mitigate disputes, and facilitate sustainable rural development.

Rural land management, in particular, constitutes an integrated system aimed at preserving the economic, social, and environmental functions of land. It also entails fostering interaction among diverse land-use types and related sectors. This intricate coordination is realized within the spatial planning projections and spatial data infrastructure associated with village settlements, urban-rural transition zones, and agricultural lands. It is noteworthy that forests, pastures, and highlands are excluded from this model due to their status as public lands.

Türkiye has made notable strides in the realms of land policy, land administration, and the delineation of rural land, forming the legal and institutional foundation of rural land management. However, a significant challenge lies in the absence of a dedicated institution tasked with the responsibility of rural land management.

6.2. Key drivers and spatial planning strategies for sustainable rural development

Agriculture, forests, natural resources, the environment, climate change, biodiversity, rural infrastructure, demographic dynamics, and rural development serve as pivotal drivers for promoting sustainable rural land management. These factors exert a profound influence on decision-making and actions related to land utilization, management, and development. They are intricately interconnected, often entailing complex interlinkages that significantly shape practices within rural land management. Understanding these interconnections is of paramount importance in effective rural land management planning and policymaking. It allows for the cultivation of a balanced approach that carefully considers economic, social, environmental, and cultural dimensions.

Spatial plans and land use projects are acknowledged as potent technical instruments for achieving harmony and equilibrium between the natural environment and the built environment. These plans encompass social and economic activities, providing a visual representation of the spatial distribution of these activities within land use plans. Successful plans meticulously integrate the natural environment, encompassing biological elements such as soil, water, and air, with the human-made, socio-economic, and physical (constructed) environment, all while adhering to sustainability principles. Within this framework, there's an imperative need to harmoniously unify various factors, including:

- Natural Environment Factors: These factors involve elements such as soil, agriculture, pastures, forests, water, and underground resources.
- Economic Environment Factors: This category encompasses industry, trade, service, and tourism activities.
- Social Environment Factors: Here, we consider components related to education, health, culture, and housing activities.
- Technical Infrastructure Factors: This involves addressing transportation and logistics activities in the execution of spatial plans.
- When implementing spatial plans, it becomes evident that gaps exist in the production of national and regional spatial macro plans across various levels, including local and communal micro-level land use plans in Türkiye. To address these deficiencies, it is imperative to adhere to specific principles:
 - Establish Spatial Arrangements: This should be done within the framework of Agricultural Land Use Plans, with the aim of fulfilling the designated functions of rural and agricultural settlements, thereby enhancing their overall efficiency.
 - Comprehensive Integration of Agricultural Resources: Ensure that agricultural resources are thoroughly integrated into urban physical plans.
 - Optimize the Distribution of Urban Centres: Focus on optimizing the distribution of urban centres that support agricultural activities, spanning national, regional, sub-regional, provincial, district, and community scales.
 - Incorporate Spatial and Physical Dimensions: Include spatial and physical dimensions into agricultural and rural development plans and policies to foster integrated planning.
 - In conjunction with planning policies that emphasize the development of spatial plans and land use plans within agricultural areas and rural settlements, which inherently possess the characteristics of "bottom-up" planning approaches, the following strategies should be pursued:
 - Emphasis on Natural Environmental Elements: Emphasize the significance of natural environmental elements within the context of man-made socio-economic and physical environmental planning, with due consideration to agriculture.

- Utilization of Agropolitan and Integrated Rural Development Models: Ensure the optimal distribution of metropolitan, large urban, middle urban centres, sub-urban centres, urban service centres in rural areas, and agro-industrial focus areas within the framework of agropolitan and integrated rural development models.
- Addressing the Lack of Physical Dimensions: Address the deficiency in physical dimensions within development plans, particularly as they relate to socio-economic aspects on a sectorial basis.

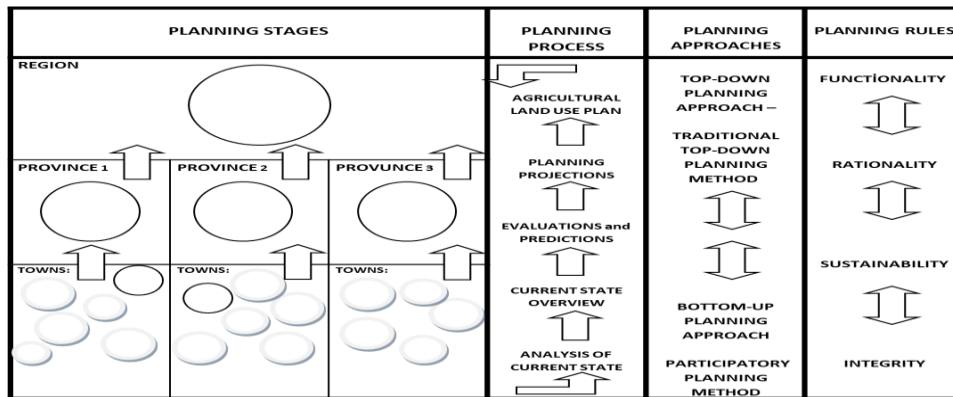


Figure 6- Planning processes, approaches, and rules

In the domain of land use planning, a multi-tiered approach is essential, integrating systems at the local, provincial, sub-regional, regional, and national levels. These systems functionally interconnect vertically and are spatially organized horizontally (Figure 6).

Decisions and practices in land use planning hinge upon the identification of local resources and the establishment of specific thresholds. In this context, lands subject to planning can be categorized as follows (Table 7):

- I. Suitable areas for development and urbanization,
- II. Areas demanding absolute protection and preservation,
- III. Areas that necessitate both protection and balanced utilization simultaneously.

To establish a rational 'protection and use' mixed land allocation plan, several methodological steps must be undertaken. First, a set of criteria is indispensable for determining construction and protection rates, ratios, and allocations for land use decisions within planning areas. Subsequently, conditions for protection and construction activities must be defined, alongside enforcement and control mechanisms. Completing these steps is paramount to achieving a well-balanced land use plan that prioritizes the equilibrium between economic and ecological considerations, thereby contributing to sustainable development.

The reduction of conflicts in rural areas, especially within urban-rural transition zones, aimed at fostering a more sustainable and habitable rural environment, is depicted in Table 7. As illustrated in Table 7, this approach constitutes the central element of the model proposed in this article. It seamlessly integrates both top-down and bottom-up planning approaches and policies, aligning with the recommendations put forth by Kleemann et al. (2023) for European contexts.

Table 7- Methodology for a balanced development of natural (ecological) and man-made (build-up) environments

<i>BUILT-UP AREAS</i>	<i>PROTECTION & LAND USE PATTERN</i>			<i>ABSOLUTE PROTECTION AREAS</i>
	<i>Determination of criteria Determination of land use characteristics Determination of conditions for protection Opening the land for use in respect to the conditions of protection Defining audit and sanction mechanisms</i>			
Residential Areas Production Areas Service Areas Transportation Lines Infrastructure Facilities and Utilities	Pre-Dominantly Built Up and Subsidiary Protected Areas	Equivalently Protected and Built-Up Areas	Pre-Dominantly Protected and Subsidiary Built-Up Areas	Ecological Production Areas Vegetation Areas Absolute Agricultural Production Areas. Irrigated Agricultural Production Areas. Natural Conservation Areas Juridical Status Areas

6.3. Integration of land management components with rural land

The components of land management, encompassing land ownership, value, use, and development, are pivotal parameters within the proposed functional model. Land ownership plays a central role in rural land management, fostering stakeholder engagement and empowerment. It incentivizes sustainable land use, facilitates wealth creation, and promotes asset building. Land ownership also opens pathways to credit access, land transfers, and conflict resolution. Moreover, it encourages responsible land stewardship, compliance with regulations, the establishment of a vibrant rural land market, and private investment for rural development. It further strengthens community cohesion, preserves cultural identity, and ensures the sustainable management of natural resources. In practice, land ownership constitutes the legal foundation of rural land, governing property law and daily transactions, including land transfers, inheritance, mortgages, and subsidies.

Rural land valuation assumes paramount importance in rural land management, as it determines the market value for transactions and informs decision-making. It serves as a crucial tool for asset management, taxation, revenue generation, rental fee assessments, insurance and risk evaluations, land use planning, agricultural and rural development, natural resource management, land conservation, land preservation, land transaction negotiations, and policy formulation and regulation. Therefore, there is an imperative need to develop and implement a feasible model for rural land valuation, distinct from urban land valuation.

Land use and management serve as the driving forces behind rural land management. Proper planning efficiently allocates resources, thereby enhancing agricultural productivity, ensuring food security, and promoting sustainable farming practices. This approach contributes to environmental sustainability by preserving ecosystems, managing natural resources, and mitigating climate change. Additionally, rural-urban linkages, community development, disaster risk reduction, tourism promotion, and infrastructure development are key benefits. Rural land use aligns with various Sustainable Development Goals (SDGs), including property rights, zero hunger, clean water and sanitation, sustainable cities and communities, responsible consumption and production, climate action, and life on land, fostering equitable land use. Rural land use management practices, such as conservation easements, land trusts, and zoning regulations, play a vital role in protecting natural landscapes, historic sites, and cultural heritage.

In the Turkish context, land use manifests through the establishment of build-up areas, achieving a balance between urban and rural land, and preserving natural areas. Rural build-up areas primarily encompass settlement areas in villages and semi-rural regions. Village settlement areas are associated with village settlement plans, construction permits, residence permits, and agricultural land use planning. The urban-rural perspective emphasizes new land use developments through agricultural land use planning, resulting in village-district development axes, planning and plan decisions, and the provision of social and economic amenities, all from a rural standpoint. Rural land uses are determined through detailed soil analyses and land use protection patterns, which include decisions about which lands are to be preserved for agricultural purposes and which are allocated for other uses.

Within the realm of rural land management, rural land development plays a critical role. This encompasses planning, design, and execution to optimize land use and its value. The significance of rural land development lies in promoting economic growth, enhancing infrastructure, creating livelihood opportunities, expanding agriculture, developing tourism, and fostering community growth. Practical applications of rural land development are carried out through land use planning, land acquisition and banking, land consolidation, and expropriation.

Agricultural land use planning is a fundamental component of rural land management, facilitating the sustainable and balanced development of agriculture. It plays a central role in shaping a resilient and sustainable future for rural areas and the broader agricultural sector. The planning process focuses on the efficient allocation of land resources, taking into account factors such as soil quality, climate, topography, and water availability. Beyond these fundamental considerations, it addresses crucial aspects such as climate change mitigation, support for rural livelihoods, infrastructure planning and development, adaptation to evolving market demands, conflict resolution, and the protection of land rights. In essence, agricultural land use planning is instrumental in charting a resilient and sustainable path for the agricultural sector and rural areas by ensuring responsible and balanced land resource utilization. In summary, the objective is to determine the most suitable land use for each parcel and the most suitable land for each use within rural areas.

6.4. Urban-rural land linkages

The relationship and interdependence between urban and rural lands hold significant importance in terms of land use and development. These interactions and dynamic connections play a critical role in sustainable development and community well-being.

Rural areas are indispensable as primary sources of essential resources, including agriculture, water resources, energy production, and forest resources. Cities primarily meet their fundamental resource requirements from rural areas, encompassing agricultural products, water, and energy production. Furthermore, cities offer opportunities for trade with rural regions,

supporting the sale of rural products. Rural areas provide the workforce and certain services required by urban centres. Additionally, rural areas can serve as vital recreational and tourist destinations for urban residents. Urban areas, in turn, rely on rural regions for services such as housing, infrastructure, transportation networks, and energy production. These services and resources originate in rural areas and are supplied to urban centres.

This symbiotic relationship between urban and rural areas underscores the essential role they play in each other's sustainability and development.

The intricate relationship and interactions between urban and rural areas should be integral considerations in land use planning. An integrated planning approach holds the potential to foster sustainable growth and development in both urban and rural regions. Such comprehensive planning should encompass topics like agricultural production, environmental protection, and the sustainable utilization of natural resources.

In essence, acknowledging the interdependence and interactions between urban and rural areas is crucial for a sustainable future. In this context, agricultural land use planning and balanced land use play a pivotal role in achieving economic and ecological equilibrium. To establish this equilibrium, it is essential to employ detailed soil maps, soil threshold analyses, and land use and protection patterns, as outlined in Figure 7 and Table 7.

Addressing the challenges of urban and rural areas collectively and implementing urban-rural integrated development strategies is essential (GLTN 2021; Wu et al. 2022). As evident from the proposed functional model tailored to Turkish conditions, which is based on agricultural land, it encompasses components such as land valuation, land use, and land development, all directly or indirectly interconnected with land ownership and spatial data. These relationships can be established, integrated into agricultural land use plans, and facilitated through spatial data infrastructure. In line with the GLTN recommendations, recognizing the urban-rural land relationship as a valuable land management tool allows for the leveraging of each other's strengths. The proposed functional model, the focal point of this article, developed to enhance this relationship, is illustrated in Figure 7.

6.5. Proposed functional model

Based on the research findings, it is evident that effective rural land management is influenced by a combination of political, legal, administrative, and technical factors. Rural land management is centered to the implementation of a functional model referred to as the 'land-based' model. Figure 7 illustrates the proposed agricultural land-based functional model for enhancing rural land management. This model is constructed on the principle of transforming rural land ownership, value, use, development, and spatial data infrastructure into an integrated economic, social, and environmental entity. Practical implementation of this model is anticipated to contribute significantly to achieving a harmonious balance between economic and ecological considerations. It will aid in enhancing agricultural infrastructure, fostering the development of liveable rural settlements, advancing agricultural practices, and facilitating the growth of robust rural land markets. Consequently, we recommend restructuring the GDAR into the General Directorate of Rural Land Management to spearhead this transformative process.

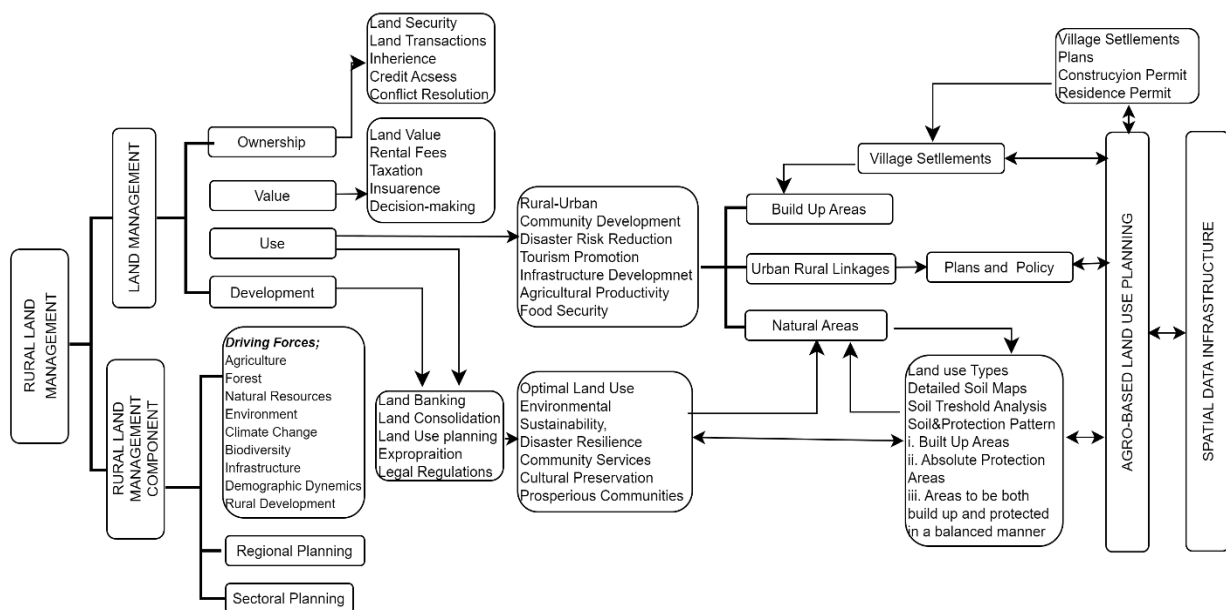


Figure 7- Proposed rural land management functional model

7. Conclusions

Based on the legal and technical activities conducted by the GDAR between 2005 and 2023, this research aimed to develop an effective rural land management system, primarily focusing on agricultural infrastructure. Taking national conditions into account within the context of global approaches, the study has yielded several significant conclusions:

The most remarkable outcome of this research is the identification of the predominant driving forces for change in rural land management within the proposed rural land functional model. These driving forces are grounded in policies regulating agriculture, spatial development, property rights, land use, value, land development, and good governance. In addition to technical, political, and institutional factors, these elements have emerged as significant driving forces, emphasizing the necessity for change in rural land management. The proposal of the functional model is structured around land management components in rural areas, involving the determination of the ownership, value, use, and development of each parcel, as well as agricultural land use planning. Another component of the model is the provision of data through spatial data infrastructure. The issues of land transfers due to inheritance and shared ownership, which we define as the primary problem in agriculture, can be addressed technically under the "land development" component, which includes land acquisition and land banking, land consolidation practices, and the essential component of agricultural land use planning. Administratively, these issues can be resolved through the coordination of the Rural Land Management Administration with the General Directorate of Land Registry and Cadastre and the General Directorate of Census and Citizenship. Land consolidation projects should be carried out in coordination with irrigation, land acquisition and banking, land valuation, and agricultural land use planning, thus eliminating the issue of land fragmentation. Abandoned lands can be easily identified using modern image processing technologies such as remote sensing and unmanned aerial vehicles, and brought into agricultural production.

Another significant finding of this research is the absence of an authoritative and responsible institution for rural land management. Therefore, the establishment of a Rural Land Management General Directorate has become a necessity. The primary activities outlined in the agricultural land-based functional model should be the core responsibilities of this proposed directorate. In this context, the transformation of the GDAR into the Rural Land Management General Directorate will be a crucial step in laying the foundation for agricultural development.

Furthermore, the research underscores the urgent need for new regulations in the agricultural land market, especially within the framework of the proposed model. These regulations should focus on land ownership, land value, land use, and development, with the aim of strengthening the agricultural infrastructure in Türkiye.

References

- 11th Development Plan (2019). Onbirinci Kalkınma Planı (2019-2023), Republic of Türkiye Presidency, Strategy and Budget Directorate, 2019, Ankara.605-7599-08-7, Kasım 2019, Ankara
- AFC (2019). Tarım ve Orman Bakanlığı, III. Tarım Orman Şurası, Şûra Kitabı (III. Agriculture Forest Summit, Council Book), ISBN: 978-605-7599-08-7, Kasım 2019, Ankara
- Akkul M (2022). Sürdürülebilir Arazi Yönetimi Açısından Kırsal Arazi Düzenlemesi Uygulamalarında Mülkiyete Yönelik Sorunların İrdelenmesi: Kop Bölgesi Örneği, Doktora Tezi, (Examination of Property-Related Issues in Rural Land Arrangement Practices from the Perspective of Sustainable Land Management: The Case of the KOP Region, Doctoral Thesis Necmettin Erbakan Üniversitesi Fen Bilimleri Enstitüsü, Harita Mühendisliği Anabilim Dalı, Konya
- Arslan F, Kartal S, Ünal S & Ayata Ü (2022). Arazi Bankacılığı, Ziraat & Orman, Su Ürünlerinde Araştırma ve Değerlendirmeler (Land Banking, Research and Evaluations in Agriculture & Forestry, Fisheries), Book, ISBN: 978-625-430-565-8, Gece Publishing
- Bachev H I (2020). Level of agrarian Governance sustainability in Bulgaria, Journal of Social and Administrative Sciences, Volume 7 Issue 3, September 2020
- Çolakoğlu E (2007). Kırsal Kalkınma Problemine Bir Çözüm Arayışı Olarak Köy- Kent Projesi (A Village-Town Project as a Search for a Solution to Rural Development Issue), *ZKÜ Sosyal Bilimler Dergisi* Cilt 3, Sayı 6, ss. 187-202.
- Çopuroğlu M A (2017). Büyükşehir Belediye Sınırları İçinde Yer Alan Kırsal Yerleşmelerin Sorunları Üzerine Bir Değerlendirme (An Evaluation on the Problems of the Rural Settlements in the Metropolitan Municipal Boundaries), Süleyman Demirel University Journal of Architecture Sciences and Applications Research article JASA2017, 2(2):18-32. e-ISSN: 2548-0170
- Demirbaş S (2023). Land Consolidation Studies İn Türkiye, III International Conference on Real Estate Development and Management, Ankara Üniversitesi Gayrimenkul Geliştirme ve Yönetimi Bölümü, ISBN:978-605-136-626-5, Ankara Üniversitesi Basımevi, 2023
- EC (2008). The EU Rural Development Policy 2007-2013, http://ec.europa.eu/agriculture/publi/fact/rurdev2007/2007_en.pdf. (access date: May 21, 2023)
- Enemark S (2005). Understanding the Land Management Paradigm, FIG Commission 7 Symposium on Innovative Technologies for Land Administration, Madison, Wisconsin, USA, 19-25 June 2005
- Enemark S (2006). Understanding the Land Management Paradigm, GIM International, January 2006, https://www.researchgate.net/publication/228342504_Understanding_the_land_management_paradigm
- Enemark S (2010). The Evolving Role of Cadastral Systems in Support of Good Land Governance, The Digital Cadastral Map, FIG Commission 7 Open Symposium Karlovy Vary, Czech Republic, 9 September 2010
- Ercan O (2019). Essentials of a Sustainable Land Use Planning Approach for Rural Areas and a Model Proposal to be Applied Under Turkish Conditions, Turkish Journal of Engineering (TUJE) Vol. 4, Issue 3, pp. 154-163, July 2020 ISSN 2587-1366, Turkey, DOI: 10.31127/tuje.650238 Research Article
- Ercan O (2020). Arazi Yönetimi Sistemi ve Kırsal Boyutu (The Land Management System and Rural Dimension), ICREDM2020 Conference, Ankara

- Ercan O (2021). A closer look at Turkish cadastre and its successful completion, *Land Use Policy*, Volume 110, November 2021, <https://doi.org/10.1016/j.landusepol.2020.104951>
- Ercan O (2023). Evolution of the cadastre renewal understanding in Türkiye: A fit-for-purpose renewal model proposal, *Land Use Policy*, Volume 131, August 2023, 106755, <https://doi.org/10.1016/j.landusepol.2023.106755>
- Erdoğan E H & Bastidas S (2020). FAO, Framework for Integrated Land Use Planning: an Innovative Approach, Technical Report · July 2020, DOI: 10.13140/RG.2.2.20078.23365
- FAO (2012). Voluntary Guidelines on the Responsible Governance of Tenure of Land, Fisheries, and Forests in the Context of National Food Security. Food and Agriculture Organization of United Nations (FAO), Rome
- FAO (2023). Strategic Framework 2022-2031, www.fao.org/strategic-framework/en (access date: 29 June, 2023)
- FIG (1995). The FIG Statement on the Cadastre. International Federation of Surveyors (FIG) Publication No. 11
- GDAR (2014). Final Report on the Workshop on the Future of Land Consolidation in National Public Investments, GDAR, Ankara
- DAGD (2020). Türkiye’de Kırsal Yerleşimler Saha Çalışması Raporu, Kalkınma Ajansları Genel Müdürlüğü Yayını Sayı: 8 Araştırma Raporu Sayı : 6 Aralık 2020, Ankara ISBN : 978-605-7679-06-2 (Rural Settlements Field Study Report in Turkey, Development Agencies General Directorate Publication Number: 8 Research Report Number: 6 December 2020, Ankara ISBN: 978-605-7679-06-2)
- GIS (2023). <https://csb.gov.tr/>, (access date: 13 June, 2023)
- GDLRC (2023). <https://GDLRC.gov.tr/>, (access date: 12 June, 2023)
- GLTN (2021). Report3, Author: Uchendu Eugene Chigbu, Urban-Rural Land Linkages: A Concept and Framework for Action, HS Number: HS/003/21E, Kenya
- GDF (2021). Türkiye Orman Varlığı 2020, (Turkish Forest Asset), Published by General Directorate of Forest, ISBN 978-605-7599-68-1, 2021, Ankara
- GDF (2023). Orman Genel Müdürlüğü 2022 Yılı İdare Faaliyet Raporu, Strateji Geliştirme Dairesi Başkanlığı Ankara/2023(The General Directorate of Forestry 2022 Administrative Activity Report, Strategy Development Department) Ankara/2023
- Govender W (2018). IOT/AI Disruption in Land Administration, (access date: 26 October, 2023). <https://geospatialworldforum.org/speaker/SpeakersImages/WillyGovender-iot.pdf>
- Haber W, Bückmann W & Endres E (2010): Anpassung des Landmanagements in Europa an den Klimawandel, *Natur und Recht* (32): 377-383
- Hartvigsen M (2022). The potential of multi-purpose land consolidation in Eastern Europe, FIG Congress 2022, Warsaw, Poland, 11–15 September 2022
- Kayıkcı S (2009). Türkiye’de Kırsal Alan Yönetimi, Ankara Üniversitesi Sosyal Bilimler Enstitüsü Kamu Yönetimi ve Siyaset Bilimi (Yönetim Bilimleri) Anabilim Dalı, Doktora Tezi (Rural Area Management in Türkiye, Ankara University Institute of Social Sciences, Department of Public Administration and Political Science (Management Sciences), PhD Thesis), Ankara
- Kleemann J, Struve B & Spyra M (2023). Conflicts in Urban Peripheries in Europe, *Land Use Policy*, Volume 133, October 2023, 106849, <https://doi.org/10.1016/j.landusepol.2023.106849>
- Kurugöllü S & Ünel F B (2021). Ekonomik Katkısı Olmayan Tarım Arazilerinin Araştırılması ve Değerlendirilmesi (Investigation and Evaluation of Agricultural Lands Without Economic Contribution), *Türkiye Arazi Yönetimi Dergisi*–2021; 3(2): 58-65, DOI: 10.51765/tayod.906612
- Küsek G, Akdemir Ş, Türker M, Hayran S & Berk A (2019). The Effects of Land Consolidation and Farmer Satisfaction: Cases of Adana and Mersin Provinces, *Fresenius Environmental Bulletin*, January 2019
- Magel H (2022). Urban - Rural - Partnership - It's a matter of territorial justice and status of mind!, FIG Congress 2022, Plenary session II, Warsaw, 12 October 2022
- Masum F (2017). Rural Land Management in Bangladesh: Problems and Prospects, *Geomatics, Landmanagement and Landscape* No: 4, pp. 79-93
- Mattsson H, Lindner G & Mansberger R (2021). Higher Education on Land Management and Land Administration, (access date: 12 February, 2021)
- Metternich G (2017). UN Convention to Combat Desertification, Global Land Outlook Working Paper Land Use Planning.
- MOF (2019). Tarım ve Orman Bakanlığı Tarım Reformu Genel Müdürlüğü, Atıl Tarım Arazilerinin Üretime Kazandırılması İle Arazi Bankacılığı Kurumsal Altyapı Oluşturma Bölge ve Merkez Çalıştayı Sonuç Ve Değerlendirme Raporu (Ministry of Agriculture and Forestry, General Directorate of Agricultural Reform, Regional and Central Workshop Results and Evaluation Report on Establishing Institutional Infrastructure for Bringing Unused Agricultural Lands into Production and Land Banking), Ankara 2019
- PAP (2018). 2019 Yılı Cumhurbaşkanlığı Yıllık Programı, (2019 Presidential Annual Program, published in the Official Gazette with the number 30578, dated October 27, 2018).
- Repp A & Weith T (2015). Building Bridges across Sectors and Scales: Exploring Systemic Solutions towards A Sustainable Management of Land—Experiences from 4th Year Status Conference on Research for Sustainable Land Management, *Land* 2015, 4(2): 325-336. doi.org/10.3390/land40203225
- SCR (2014). Kalkınma Bakanlığı Tarım Özel İhtisas Komisyonu, Tarım Arazilerinin Sürdürülebilir Kullanımı Çalışma Grubu Raporu (Sustainable Use of Agricultural Lands Working Group Report), Ankara.
- SCR (2018). Kalkınma Bakanlığı Kalkınma Planı on Birinci (2019-2023), Kırsal Kalkınma Özel İhtisas Komisyonu Raporu (Ministry of Development, Eleventh Development Plan (2019-2023), Report of the Specialized Commission on Rural Development), Ankara 2018
- SHW (2022). Faaliyet Raporu, Strateji Geliştirme Dairesi Başkanlığı, Ankara (Activity Report, General Directorate of State Hydraulic Works, Head of Strategy Development Department, Ankara)
- Şanlı H, Özdemir Ş & Türker M (2023). Türkiye’de Arazi Bankacılığı Uygulamaları ve Sürdürülebilir Tarımsal Üretim (Land Banking Practices and Sustainable Agricultural Production in Türkiye), III International Conference on Real Estate Development and Management, Ankara Üniversitesi Gayrimenkul Geliştirme ve Yönetimi Bölümü, ISBN:978-605-136-626-5, Ankara Üniversitesi Basımevi, 2023
- Tekeli, İ (2018). İzmir İli/Kenti İçin Bir Tarımsal Gelişme ve Yerleşme Stratejisi (ikinci baskı) (An Agricultural Development and Settlement Strategy for the Province/City of Izmir) (Second Edition), Akdeniz Akademisi Yayınları, DOI: 10.32325/iaak.1802217, İzmir, 2018
- Türker M (2019). In Turkey Land Abandonment and the Combat Activities (Land Banking Services), 6-8 November 2019/ Santiago.
- Türker M (2023). Türkiye’de Tarımsal Arazi Yönetimi ve Geleceği (Agricultural Land Management and its Future in Türkiye), III International Conference on Real Estate Development and Management, Ankara Üniversitesi Gayrimenkul Geliştirme ve Yönetimi Bölümü, ISBN:978-605-136-626-5, Ankara Üniversitesi Basımevi, 2023
- UNECE (1996). Land Administration Guidelines. ECE/HBP/96. United Nations: New York, Geneva

- UNECE (2005). Land Administration in the UNECE Region. Development trends and main principles Economic Commission for Europe. New York and Geneva, ECE/HBP/140. UNECE Information Services
- UNGGIM (2020). Framework for Effective Land Administration (draft)
- Weith T, Barkmann T, Gaasch N, Rogga S, Strauß C & Zscheischler J (2019). Sustainable Land Management in a European Context, A Co-Design Approach, Springer, Human-Environment Interactions, ISSN 2214-2339 ISSN 2452-1744 (electronic), ISBN 978-3-030-50840-1, ISBN 978-3-030-50841-8 (eBook)
- Williamson I, Enemark S, Wallace J & Rajabifard A (2010), Land Administration for Sustainable Development, Esri Press, 380 New York Street, Redlands, California 92373-8100
- Wu Y, Long H, Zhao O & Hui E C (2022). Land use policy in urban-rural integrated development, Land Use Policy, Volume 115, April 2022, 106041, <https://doi.org/10.1016/j.landusepol.2022.106041>
- Zengin O (2015), Büyükşehir Belediyesi Reformu ve Kırsal Alana Etkisi (Metropolitan Municipality Reform and Its Impact on Rural Areas), 21. Yüzyıl İçin Planlama Semineri (Planning Seminar for the 21st Century, in Ankara), Ankara



Copyright © 2024 The Author(s). This is an open-access article published by Faculty of Agriculture, Ankara University under the terms of the [Creative Commons Attribution License](#) which permits unrestricted use, distribution, and reproduction in any medium or format, provided the original work is properly cited.



Health Risk Assessment of Metals via Consumption of Rapa Whelk (*Rapana venosa*) from the Black Sea

Baris Bayrakli^{a*}, Murat Yigit^b, Mutlu Altuntas^c, Masashi Maita^d

^aDepartment of Fisheries, Vocational School, Sinop University, 57100 - Sinop, TÜRKİYE

^bDepartment of Fisheries Industry Engineering, Faculty of Marine Science and Technology, Canakkale Onsekiz Mart University, 17100 - Canakkale, TÜRKİYE

^cDepartment of Statistics, Faculty of Arts and Science, Sinop University, 57100 - Sinop, TÜRKİYE

^dCourse of Applied Biosciences, Graduate School of Marine Science and Technology, Tokyo University of Marine Sciences and Technology, 108-0075 - Tokyo, JAPAN

ARTICLE INFO

Research Article

Corresponding Author: Baris Bayrakli, E-mail: barisbayrakli@gmail.com

Received: 12 October 2023 / Revised: 02 January 2024 / Accepted: 25 January 2024 / Online: 23 July 2024

Cite this article

Bayrakli B, Yigit M, Altuntas M, Maita M (2024). Health Risk Assessment of Metals via Consumption of Rapa Whelk (*Rapana venosa*) from the Black Sea. *Journal of Agricultural Sciences (Tarim Bilimleri Dergisi)*, 30(3):546-561. DOI: 10.15832/ankutbd.1374919

ABSTRACT

The present study investigated the bioaccumulation of metals in raw, heat treated -and sterilized Rapa whelk, and evaluated the consumer risks for human consumption. All of the metals, with the exception of Mn, were found to be lower than the permissible FAO standards. A remarkable amount of metal was released into the boiling water (Al, Cr, Cu, Fe, Hg, Pb, Sb, Se, Zn) after heat treatment and hypochlorite solution (Al, As, Cu, Hg, Mn, Pb, Se, Zn). After sterilization, the levels for As, Mo, Cd, Sb, Cr, Zn, Se, Cu, and Hg in Rapa whelk were reduced by 47.4%, 40.1%, 24.9%, 20.3%, 17.5%, 4.5%, 3.6%, 0.93%, and 0.68%, respectively. The metals in Rapa whelk exposed to hypochlorite immersion were found to be below

permissible upper limits. The target hazard quotients for the non-carcinogenic risks of consuming sterilized Rapa whelk were below “1” (THQ<1), showing “no potential health risks” for adult men, women and children when consuming sterilized Rapa whelk. Indeed, Rapa whelk could be a good source of Cr, Cu, Fe, Mn, Mo, Se, and Zn to meet the daily recommended quantities in food, when consumed regularly. However, the cancer risks of As, Cd, Ni, and Pb proved to be over “acceptable levels”; hence, the safe consumption limits determined in this study are advisable when consuming Rapa whelk.

Keywords: Cancer risk, Hazard index, *Rapana venosa*, Toxic metals, Trace elements

1. Introduction

The precise line between whether a metal should be considered beneficial or harmful is dependent on dose limits and exposure frequencies (Alkan et al. 2016; Leonard et al. 2022; Yildiz et al. 2023). Trace elements such as copper, manganese, zinc, iron are essential for the metabolic activities in humans and other living organisms, which however can be toxic and cause severe damage at high levels of bioaccumulation in tissues (Çağlak & Karsli 2014; Makedonski et al. 2017). Metals such as arsenic, lead, cadmium and mercury with high bioaccumulation potentials in aquatic animals are certainly toxic (Duyar et al. 2023; Mol et al. 2019), with possible impacts on central nervous system functions, damage on blood composition, kidneys, lungs, and liver with severely reduced energy levels (Hajeb et al. 2014).

The sea snail “Rapa whelk” is a good bioindicator for metals, and its bioaccumulation is highly dependent on the level of metal pollution in the ecosystem (Liang et al. 2004; Terzi & Civelek 2021), possibly because of their low motion on the sea floor (Hwang et al. 2017). Despite being a seafood with notable health benefits, when Rapa whelk is consumed at high intake levels it can be seriously detrimental to health (Stancheva et al. 2012). Therefore, monitoring demersal marine species for possible environmental contaminations (Hwang et al. 2017) is crucial for any signs of toxic contamination and to ensure seafood safety. Since raw meat of Rapa whelk spoils quickly under inappropriate temperature conditions, heat treatment and sterilization are common applications prior to cold storage and marketing (Bayrakli et al. 2016). inconvenient conditions, heat treatment and sterilization are common preprocesses in Rapa whelk marketing prior to cold storage (Bayrakli et al. 2016). Joyce and Bo highlighted that cooking methods such as boiling, steaming, and frying can alter the toxicity level of metals in meat through various mechanisms, including the evaporation of water and volatile components, solubilization of the element, and metal binding to other macronutrients present in the food (Joyce & Bo 2016).

This study aimed to investigate consumer risks for adult men, women and children via consumption of Rapa whelk exposed to heat treatment and sterilization, and to evaluate possible reduction levels of metals in Rapa whelk through boiling and hypochlorite soaking.

2. Material and Methods

2.1. Study area and sampling

The Rapa whelk samples were collected from the nature from the southern coast of the Black Sea (Türkiye; 41°44'18.87"N, 35°55'09.69"E) (Figure 1) and immediately transferred to the commercial processing facilities (Sadıklar Seafood Company) in Dikmen-Sinop, Türkiye.

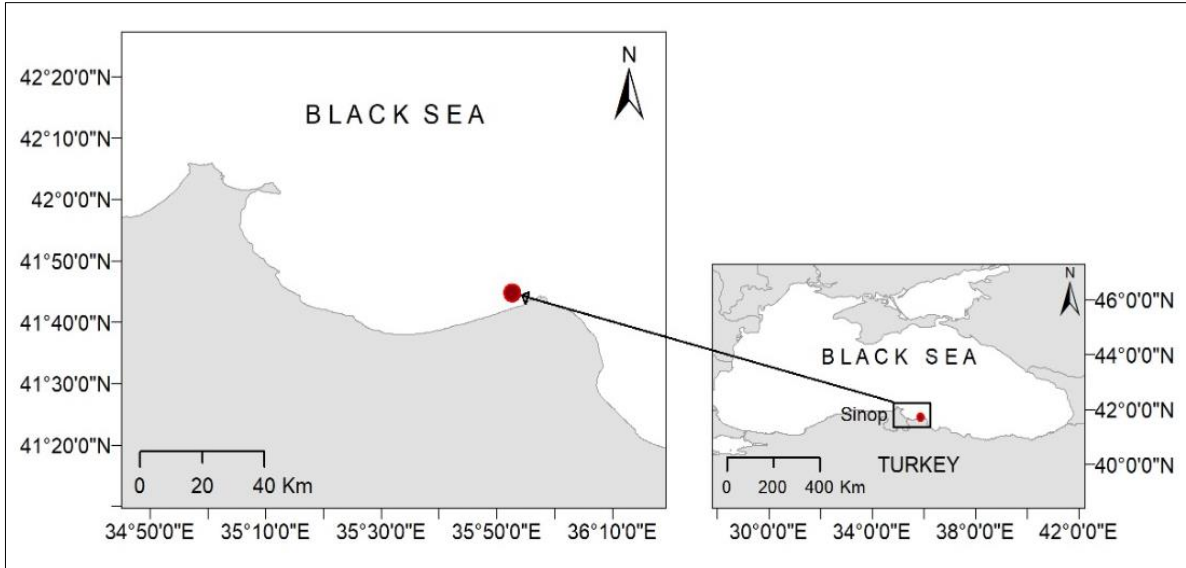


Figure 1- Study area, southern coast of the Black Sea

In total, 40 individuals of Rapa whelk were randomly selected from the harvest batch, and the shells of 20 individuals were carefully cracked using a hammer to obtain the raw meat with the precaution of preventing metal contamination. This group served as an untreated control group with no further processing. Wet weight of raw Rapa whelk was measured in a range between 13.90-38.02 g (mean weight 22.10 ± 7.88 g). The other group of 20 individuals was consecutively exposed to heat treatment and sterilization. Initially, the Rapa whelk was kept in an industrial boiler (2-ton) at 130 °C for 5 minutes; afterwards, the meat was separated from the shells using a fork. It is important to note that metal contamination was disregarded during this fork separation process. The operculum and intestines were removed, and the edible parts were pressure-washed. After heat treatment via boiling, the meat was sterilized in tubs containing 1% sodium hypochlorite (NaOCl) solution for 30 minutes, and then homogenized with a blender, shocked in plastic bags at -80 °C and cold-stored at -20 °C for further analyzes. Metal analyses in raw, heat treated, - and sterilized Rapa whelk were performed in order to evaluate a possible reduction of the metals in the meat. Additionally, the possible transfer of metals from the meat into the boiling water (heat treatment phase) or hypochlorite solution (sterilization phase) were also evaluated prior to -and after the treatments. Thereafter, all samples were transferred to the laboratories of the Department of Fisheries, Vocational School at Sinop University (Türkiye) under cold-chain within three hours of transport time.

2.2. Analyses of metal contents

All metal analyses in the present study were performed in triplicates following the EPA Method 200.3. Samples weighing 1.5 g were digested in Teflon vessels including a mixture of concentrated supra pure grade HNO₃ and H₂O₂ (7:1) according to (HPR-FO-67) temperature and pressure profile using a microwave digestion system (Milestone SK10). After adding the acid, Teflon bombs were closed and heated at 200 °C for 15 minutes and kept at same temperature for another 15 minutes. The digested solution was transferred into 50 mL polypropylene falcon tubes and made up to 50 mL by adding pure water. Standard Reference Material (CRM) and blank solutions were prepared using the same procedures. The CRM materials UME CRM 1201 and SEM 2016 mix were used to evaluate the precision and accuracy of the analyses. Inductively Coupled Plasma Spectrometry (ICP-MS Agilent 7700X) was used to measure the concentration for Arsenic (As), Aluminum (Al), Copper (Cu), Iron (Fe), Manganese (Mn), Mercury (Hg), Cadmium (Cd), Lead (Pb), Zinc (Zn), Selenium (Se), Chromium (Cr), Nickel (Ni), Molybdenum (Mo), Sb (Antimony) and Cobalt (Co) through multi-element techniques. During these experiments, all glassware and Teflon bombs were soaked overnight in 10% HNO₃, rinsed twice with distilled water and air dried to avoid contamination before use.

2.3. Estimations of consumer health risks

The health risks from metals via oral intake have been assessed as non-carcinogenic -and carcinogenic risks for adult men (AM, 70 kg, aged 19-30), adult women (AW, 57 kg, aged 19-30), and children (C, 36 kg, aged 9-13), according to reference classification by IOM (2006). The total mollusc consumption in Europe is around 1.7 kg/year per capita (4.66 g/day per person), that is nearly 7% of total seafood consumption of 23 kg per person in Europe (Failler et al. 2007). The estimated daily intake (EDI, mg/kg body weight/day) of metals was calculated by the formula according to Yigit et al. (2018a b), and Bayrakli (2021; Duyar et al. 2023).

$$EDI = \frac{MC \times MS}{BW}$$

Where; MC, metal concentration (mg kg⁻¹ ww) in meat; MS, meal size (kg/day), average daily intake of molluscs in the EU; BW, body weight (kg) for adults (men 70 kg, women 57 kg), or children (37 kg)

2.4. Non-carcinogenic risk

Non-carcinogenic risks were evaluated through a comparison of the exposure level with a reference dose suggested for the same exposure duration. Target hazard quotient (THQ), representing non-carcinogenic risk, is the ratio of estimated daily intake (EDI) and reference dose (RfD), an assumption of human exposure below which that substance is unlikely to pose measurable health risks. If the exposure level exceeds this threshold, there may be potential noncancerous health effects. Risk evaluation for As has been performed with the assumption that the toxic inorganic arsenic was 3% of the total (FSA 2004). The THQ caused by a single element within a single exposure route over a lifetime duration of 70 years has been estimated through the following equation(US-EPA 1989):

$$THQ = \frac{EDI}{RfD} \times 10^{-3}$$

Where; EDI, estimated daily intake (mg/kg body weight/day); RfD, reference doses (mg kg⁻¹ day⁻¹) for metals (EFSA, 2010; US-EPA, 2013)

There is no potential harmful effect when THQ is below "1" (THQ<1) (US-EPA, 1989), but a cumulative reaction of health effects may occur when the value is over "1" (THQ>1) (Hallenbeck 1993). For this reason, the arithmetic sum of each THQ is the total target hazard quotients (TTHQ), represented as hazard index (HI). When the hazard index exceeds unity, there may be potential health risks. For the evaluation of potential risks from multiple metals, noncancerous hazard index (HI) was estimated using the equation below (US-EPA 1989):

$$HI (TTHQ \sum_n) = (EDI_1/RfD_1) + (EDI_2/RfD_2) + (EDI_3/RfD_3) + \dots + (EDI_n/RfD_n)$$

$$HI = \sum_n THQ_m$$

Where; EDI_n, estimated intake level for the nth metal, n=15 in the present study.

2.5. Carcinogenic risks for toxic metals

The carcinogenic risk defines the incremental probability of any kind of cancer in the lifetime of an individual as a result of exposure to potential carcinogens. The cancer slope factor (CSF) converts EDI averaged over a lifetime of exposure directly to the incremental risk of an individual developing cancer. Among the measured metals, As, Cd, Ni, Pb are known to potentially cause cancer in humans (IARC 2012). The lifetime cancer risk (CRR) was estimated using the equation below (US-EPA 1989; 2010):

$$CRR = EDI \times CSF$$

Where; EDI, estimated daily intake (mg/kg/day); CSF, cancer slope factor (As: 1.5mg/kg/day, Cd: 6.3mg/kg/day, Ni: 0.84mg/kg/day, Pb: 0.0085mg/kg/day) (Liang et al. 2017).

Despite the fact that methylmercury (MeHg) is classified as possibly carcinogenic to humans (IARC, 2012), the CSF for Hg has not been issued by the US-EPA; therefore, the cancer risks for Hg were not estimated here. The level of cancer risk for carcinogens ranges between 10⁻⁴ and 10⁻⁶, that is a lifetime cancer risk level of 1/10.000, and 1/1.000.000, respectively. This means that a risk factor lower than 10⁻⁶ is acceptable and can be ignored, but a risk factor exceeding 10⁻⁴ is considered to be unacceptable. Hence, an average cancer benchmark of 10⁻⁵ was considered as the threshold in this study (US-EPA 2010).

2.6. Safe consumption limits

The safe daily consumption limit (SDC) was calculated using the following formulae (US-EPA 2000):

$$SDC = \frac{RfD \times BW}{MC}$$

Where; RfD, reference doses (mg kg⁻¹ day⁻¹) for metals (EFSA 2010); BW, body weight (kg) for adults (men 70 kg, women 57 kg), or children (37 kg); MC, metal concentration (mg kg⁻¹ ww) in meat

The safe weekly consumption rate (SWC, meals per week) was calculated by converting the SDC into MS, that is 0.227 kg/day for adult men and women, and 0.114 kg/day for children (US-EPA 1989, 2000). The safe weekly consumption (SWC, meals per week) was calculated according to the equation reported by (Yigit et al. 2018a):

$$SWC = \frac{SDC \times 7}{MS}$$

Where; SDC, safe daily consumption rate (US-EPA 2000); MC, analyzed metal concentration (mg kg⁻¹ ww) in meat

2.7. Compensation of daily requirements for essential trace elements

The percent compensation of minimum daily requirements (CDR_{min}) for essential trace elements in mollusc consumption was calculated using the following formulae according to Yiğit et al. (2020):

$$CDRmin = \frac{EDI \times 100}{EAR}$$

Where; EDI, estimated daily intake (mg/kg/day); EAR, estimated average daily requirement for a healthy human (IOM 2006).

2.8. Statistical analysis

Statistical analyses were conducted using metal analyses data from Rapa whelk samples during the pre-processing treatment prior to cold-storage. The statistical significance of the data was evaluated by ANOVA (Analysis of Variance). The Tukey comparison test was used to determine the differences between the experimental groups. The statistical analyzes were performed using the PAST computer program - 1.95 version (Hammer et al. 2001). The results were accepted as significantly different at P<0.05 level. Linear relationships between the metal elements were appraised using Pearson's rank correlation test. As a result of this evaluation, a Principal Component Analysis (PCA), which allows for dimension reduction in the data set, was applied in case of a high degree of correlation between the metal elements. The PCA was performed using 2 components for the examination of percentages of variance explanations. Standardized loadings based upon the correlation matrix for the PCA are presented in Table 1. Rv4.0.5 statistical software was used in the PCA analyses, and again the level of significance was considered as P<0.05.

Table 1- Standardized loadings based upon correlation matrix for Principal Component Analysis

Al	0.94	0.28	0.97	0.0285	1.2
Cr	-0.55	0.79	0.93	0.0715	1.8
Mn	0.96	0.22	0.98	0.0220	1.1
Fe	1.00	0.03	0.99	0.0079	1.0
Co	0.91	-0.19	0.87	0.1337	1.1
Ni	0.91	0.38	0.98	0.0176	1.3
Cu	0.46	0.78	0.82	0.1769	1.6
Zn	0.10	0.88	0.78	0.2218	1.0
As	-0.47	0.81	0.88	0.1210	1.6
Se	-0.26	-0.44	0.26	0.7386	1.6
Mo	-0.23	0.89	0.85	0.1548	1.1
Cd	-0.49	0.58	0.58	0.4233	1.9
Sb	0.67	0.37	0.59	0.4105	1.6
Hg	0.92	0.07	0.86	0.1412	1.0
Pb	0.64	-0.42	0.59	0.4075	1.7

PC: Principal Component

3. Results

3.1. Statistical evaluation

The Pearson correlation test results (Figure 2) and the correlogram (Figure 3) indicated strong positive significant correlations between Cu-Zn, Cd-As, As-Mo, Hg-Al, Hg-Fe, Mn-Fe, Mn-Al, Mn-Ni, Fe-Al, Fe-Ni, and Al-Ni. Moreover, strong negative significant correlations were found between Cr-Co, Zn-Se and Cu-Se (Figure 2, Figure 3). There were no relations between Cu-Cd, Zn-Hg, As-Se, Mo-Hg, Se-Hg, and Se-Co (Figure 3).

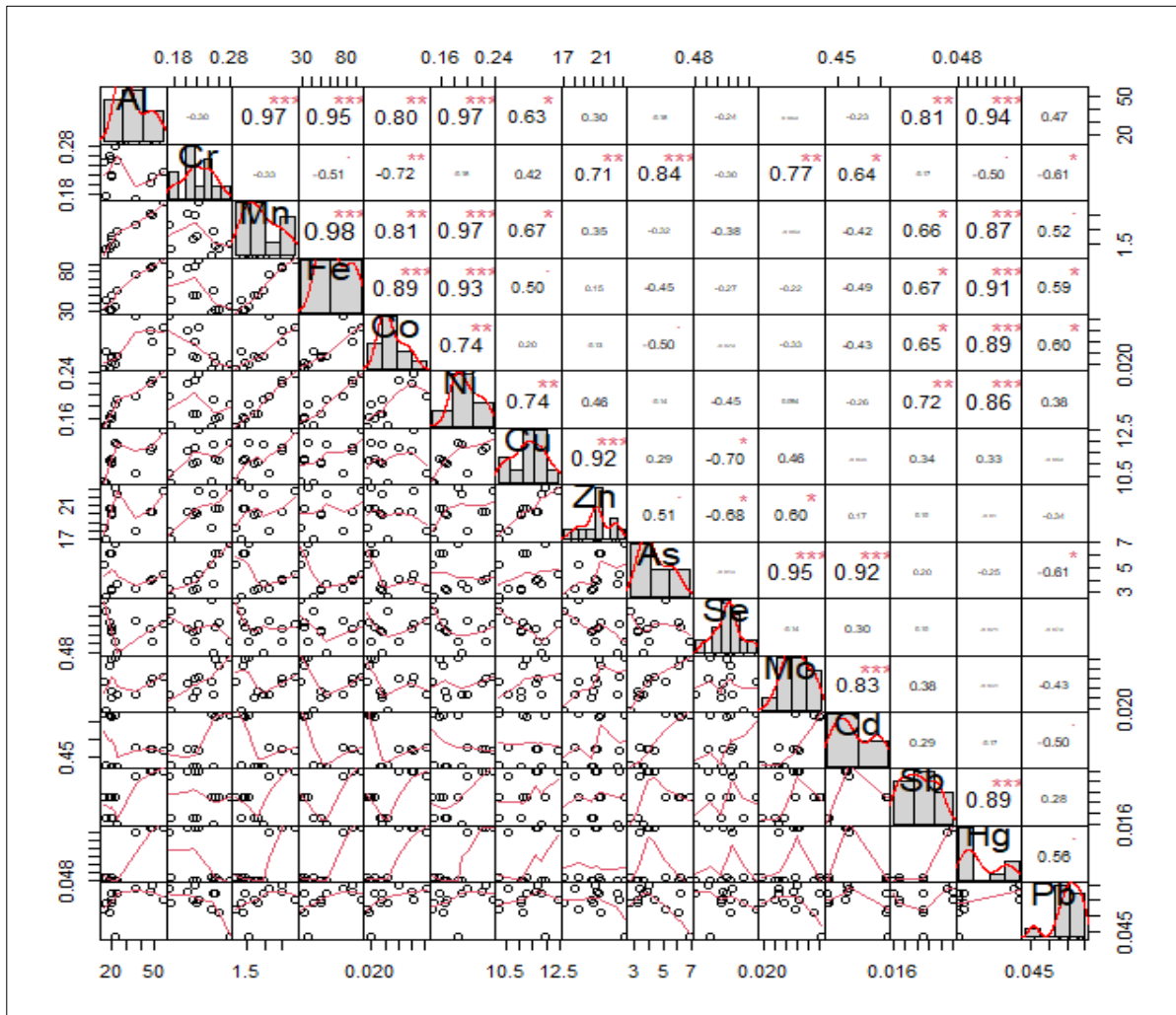


Figure 2- Pearson correlation results (top diagram) with bivariate scatter (bottom diagram) and density (diagram) plots (Each significance level is associated to a symbol: p-values (0, 0.001, 0.01, 0.05, 0.1, 1) => symbols ("***", "**", "*", ".", " "))

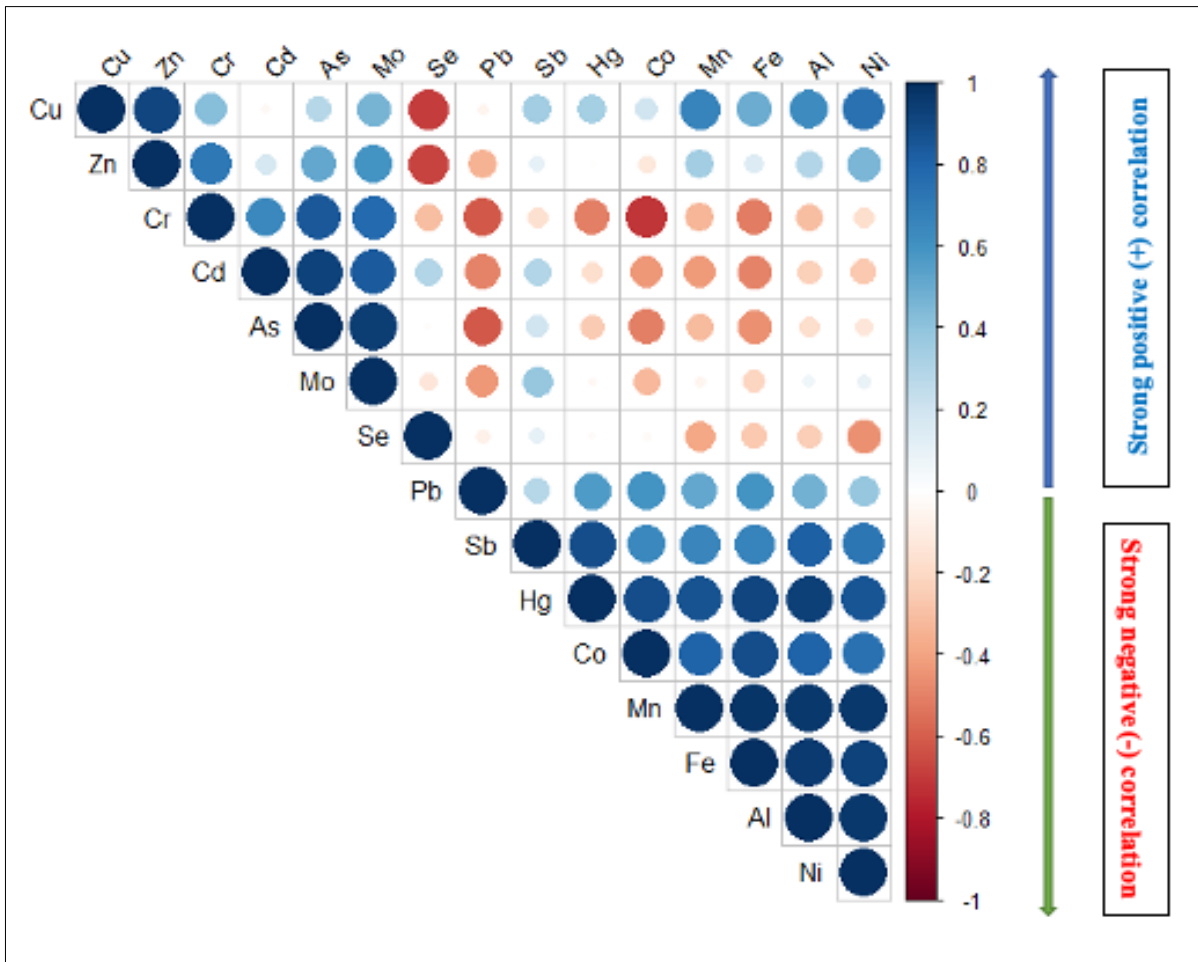


Figure 3- Correlogram of Pearson correlation results for each metal elements

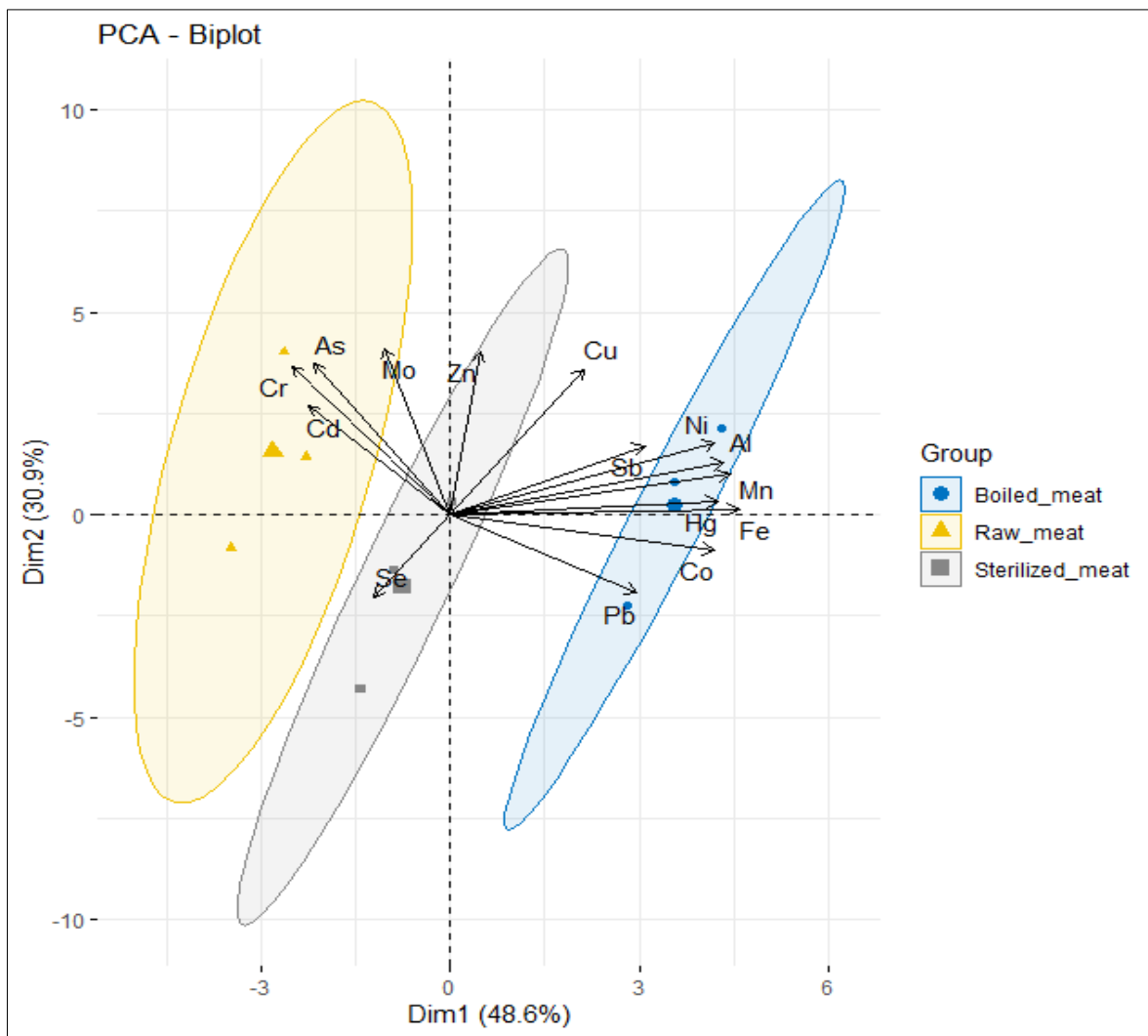


Figure 4- Biplot for principal component analysis of metal element levels represented

The PCA analyses performed between the metal elements showed that the size of the data could be represented by two components. The PC-1 and PC-2 principal components explained 49% and 31% (80% of total) of the total variation in the data, respectively (Table 2). The metals Al, Mn, Fe, Co, Ni and Hg were positively and strongly explained by PC1, while Cr, Cu, Zn, As and Mo were positively and strongly explained by PC2. Mo and Se were poorly explained as negatively by PC1. Co, Se and Pb were negatively and poorly explained by PC2. Fe and Hg are the weakest metals explained by PC2 compared to the other metals. Se was negatively and poorly explained by both the PC1 and PC2 components. It was observed that the proportion of common variance (community) was high for all metals except Se, and it was revealed that there was a high level of correlation between metals with a common variance close to “1” (one) and other metals (Table 1). The biplot of the principal components were plotted based on raw, heat treated, -and sterilized meat groups. The levels of As, Cd, Cr and Mo in raw meat were higher than the other metals. Concentrations of Al, Co, Fe, Hg, Mn, Ni, Pb and Sb were quite high compared to other metals in heat treated meat. Additionally, there was a high degree of correlation between these metals and the variation in metals was explained by PC1. Concentrations of Cu, Se and Zn were high in the sterilized meat group. Se is negatively correlated with Cu and Zn. The variation in Se cannot be also fully explained by both major components compared to variations among other metals (Figure 4).

Table 2- Accounted variance for each principal component (PC)

<i>Variations</i>	<i>PC-1</i>	<i>PC-2</i>
SS loadings	7.30	4.63
Proportion Variance	0.49	0.31
Cumulative Variance	0.49	0.80
Proportion Explained	0.61	0.39
Cumulative Proportion	0.61	1.00

3.2. Concentrations of metal in rapa whelk versus international standards

Metal concentrations in raw, heat treated, -and sterilized Rapa whelk are shown in Table 3. Remarkable variations have been observed in heavy metal levels among groups at different processing stages. Considering all the metal levels in raw Rapa whelk meat collected from the same marine area, average metal levels decreased in the order of Fe>Zn>Al>Cu>As>Mn>Cd>Se>Cr>Ni>Pb>Hg>Mo>Sb>Co; whereas metal levels in the heat treated and sterilized meat showed a declining order as Fe>Al>Zn>Cu>As>Mn>Se>Cd>Ni>Cr>Hg>Pb>Co>Mo>Sb, and Fe>Al>Zn>Cu>As>Mn>Se>Cd>Cr>Ni>Pb>Hg>Mo>Co>Sb, respectively. All average values (mg/kg wet weight basis) of the elements analyzed in the Rapa whelk meat, with the exception of Mn, were lower than the permissible FAO standard's upper limits in marine products for healthy food (FAO 1983) (Table 3).

Table 3- Metal contents and data on metal reduction in Rapa whelk meat after heat treatment (boiling) and sterilization (hypochlorite immersion) in comparison to permissible upper limits of FAO standards. Metals with no reduction but increment after sterilization are grey highlighted

Elements	Permissible limit (mg/kg ww)	Metal contents in Rapa whelk (mg/kg) means \pm SD, ww (wet weight) basis (min – max range in parenthesis)			Metal Reduction			
		Raw meat	Boiled meat	Sterilized meat	after heat treatment (boiling)		after sterilization (hypochlorite immersion)	
	FAO (1983)				weight (mg/kg)	percent (%)	weight (mg/kg)	Percent (%)
Al	NA	18.65 \pm 3.27 ^a (14.16 - 21.86)	46.71 \pm 8.32 ^b (35.98 - 56.26)	20.08 \pm 3.52 ^a (15.66 - 24.27)	-28.06	-150,48	-1,43	-7,67
As	10.0	6.10 \pm 0.69 ^b (5.24 - 6.92)	3.94 \pm 0.45 ^a (3.34 - 4.44)	3.21 \pm 0.41 ^a (2.67 - 3.66)	2.17	35.53	2.89	47.44
Cd	1.0	0.566 \pm 0.003 ^c (0.563 - 0.569)	0.472 \pm 0.004 ^b (0.468 - 0.479)	0.425 \pm 0.003 ^a (0.423 - 0.429)	0.09	16.62	0.14	24.86
Co	0.26	0.019 \pm 0.001 ^a (0.018 - 0.021)	0.035 \pm 0.004 ^b (0.030 - 0.041)	0.024 \pm 0.001 ^a (0.023 - 0.026)	-0,02	-81,90	-0,01	-25,47
Cr	1.0	0.261 \pm 0.014 ^a (0.247 - 0.281)	0.203 \pm 0.024 ^b (0.170 - 0.223)	0.215 \pm 0.031 ^{ab} (0.175 - 0.251)	0.06	22.01	0.05	17.50
Cu	30	11.15 \pm 0.69 ^a (10.27 - 11.94)	11.58 \pm 0.76 ^a (10.60 - 12.46)	11.05 \pm 0.67 ^a (10.21 - 11.84)	-0.43	-3.86	0.10	0.93
Fe	100	32.44 \pm 3.35 ^a (28.33- 36.54)	85.91 \pm 7.76 ^c (76.04 - 95.50)	49.98 \pm 5.23 ^b (43.37 - 56.16)	-53,47	-164,80	-17,54	-54,07
Hg	1.0	0.048 \pm 0.0004 ^a (0.048 - 0.049)	0.061 \pm 0.0003 ^b (0.060 - 0.061)	0.048 \pm 0.001 ^a (0.048 - 0.049)	-0.01	-25.56	0.0003	0.68
Mn	1.0	1.38 \pm 0.18 ^a (1.14 - 1.55)	2.52 \pm 0.31 ^b (2.14 - 2.89)	1.69 \pm 0.26 ^a (1.34 - 1.96)	-1,14	-82,16	-0,31	-22,67
Mo	NA	0.042 \pm 0.005 ^b (0.035 - 0.046)	0.033 \pm 0.004 ^b (0.027 - 0.036)	0.025 \pm 0.005 ^a (0.019 - 0.029)	0.01	21.52	0.02	40.09
Ni	80	0.163 \pm 0.016 ^a (0.147 - 0.184)	0.220 \pm 0.016 ^b (0.198 - 0.237)	0.169 \pm 0.018 ^a (0.149 - 0.192)	-0,06	-34,97	-0,01	-3,76
Pb	2.0	0.051 \pm 0.0061 ^a (0.043 - 0.057)	0.058 \pm 0.002 ^a (0.055 - 0.060)	0.055 \pm 0.001 ^a (0.054 - 0.057)	-0,01	-14,45	-0,01	-8,94
Sb	1.0	0.021 \pm 0.0001 ^a (0.0207 - 0.021)	0.026 \pm 0.0006 ^b (0.025 - 0.026)	0.017 \pm 0.0002 ^a (0.016 - 0.017)	-0.01	-23.09	0.004	20.27
Se	2.0	0.546 \pm 0.037 ^a (0.506 - 0.594)	0.532 \pm 0.021 ^a (0.503 - 0.550)	0.526 \pm 0.037 ^a (0.479 - 0.571)	0.01	2.46	0.02	3.63
Zn	40	20.73 \pm 1.95 ^a (18.43 - 23.20)	20.30 \pm 1.93 ^a (17.99 - 22.73)	19.80 \pm 2.24 ^a (16.95 - 22.41)	0.43	2.07	0.94	4.52

FAO: Food and Agriculture Organization–UN; NA: not available

Table 5- Estimated daily intake per meal size, safe daily consumption rate (SDC), safe weekly consumption (SWC), target hazard quotient, total target hazard index, and cancer risk rate for the studied metals in adult men (AM), adult women (AW), and children (C) consuming boiled -and sterilized Rapa whelk based on cancer slope factor and reference dose

Element	RfD (mg/kg/day)	CSF (mg/kg/day)	EDI (mg/kg/day, ww)			SDC (kg/day)			SWC (meals/week)			THQ			Cncer Risk (CRR)		
			AM	AW	C	AM	AW	C	AM	AW	C	AM	AW	C	AM	AW	C
As	0.0003	1.5	0.00021	0.00026	0.00042	0.22	0.18	0.11	6.73	5.48	6.89	0.021	0.026	0.042	3.2x10 ⁻⁴	3.9x10 ⁻⁴	6.2x10 ⁻⁴
Cd	0.001	6.3	0.000028	0.000035	0.000055	0.16	0.13	0.08	5.07	4.13	5.20	0.028	0.035	0.055	1.8x10 ⁻⁴	2.2x10 ⁻⁴	3.5x10 ⁻⁴
Ni	0.02	0.84	0.000011	0.000014	0.000022	8.27	6.73	4.25	255.0	207.7	261.2	0.0006	0.0007	0.0011	1.2x10 ⁻⁵	1.5x10 ⁻⁵	2.3x10 ⁻⁵
Pb	0.002	0.0085	0.0000037	0.0000045	0.0000071	2.53	2.06	1.30	78.17	63.65	80.05	0.0018	0.0023	0.0036	3.1x10 ⁻⁸	3.8x10 ⁻⁸	6.1x10 ⁻⁸
Al	1.0	N/A	0.0013	0.0016	0.0026	3.49	2.84	1.79	107.5	87.54	110.1	0.0013	0.0016	0.0026	For carcinogenic exposure; no cancer risk if value: > 0.000001 (10 ⁻⁶) cancer risk if value: < 0.000001 (10 ⁻⁶) benchmark: < 0.00001 (10 ⁻⁵) (US-EPA, 2010)		
Co	0.0003	N/A	0.0000016	0.0000020	0.0000032	0.86	0.70	0.44	26.49	21.57	27.12	0.0054	0.0067	0.0105			
Cr	0.003	N/A	0.000014	0.000018	0.000028	0.98	0.79	0.50	30.10	24.51	30.82	0.0048	0.0059	0.0093			
Cu	0.04	N/A	0.00074	0.00090	0.00143	0.25	0.21	0.13	7.82	6.36	8.00	0.018	0.023	0.036			
Fe	0.7	N/A	0.0033	0.0041	0.0065	0.98	0.80	0.50	30.23	24.62	30.96	0.0048	0.0058	0.0092			
Hg	0.0001	N/A	0.0000032	0.0000039	0.0000062	0.15	0.12	0.07	4.48	3.65	4.59	0.032	0.039	0.062			
Mn	0.14	N/A	0.00011	0.00014	0.00022	5.78	4.71	2.97	178.4	145.2	182.7	0.0008	0.0010	0.0016			
Mo	0.005	N/A	0.0000017	0.0000020	0.0000032	14.0	11.4	7.21	432.1	351.8	442.4	0.0003	0.0004	0.0006			
Sb	0.0004	N/A	0.0000011	0.0000014	0.0000022	1.68	1.37	0.86	51.80	42.18	53.04	0.0028	0.0034	0.0054			
Se	0.005	N/A	0.000035	0.000043	0.000068	0.67	0.54	0.34	20.52	16.71	21.02	0.0070	0.0086	0.0136			
Zn	0.3	N/A	0.0013	0.0016	0.0026	1.06	0.86	0.55	32.71	26.63	33.50	0.0044	0.0054	0.0085			
HAZARD INDEX (HI)												0.134	0.165	0.261			

RfD (mg kg⁻¹ day⁻¹): reference dose (EFSA 2010; US-EPA 201); CSF: cancer slope factors for As, Pb (US-EPA 1996), and Cd, Ni (Y. Liang et al. 2017); EDI (mg kg⁻¹ day⁻¹): Estimated daily intake per meal size; ww (wet weight) basis; THQ: target hazard quotient; CRR: cancer risk rate; HI: hazard index representing arithmetic sum of THQs

3.3. Concentrations of metal in raw, heat treated -and sterilized meat of Rapa whelk

The levels of As, Cd, Cr, and Mo were highest in the raw meat of Rapa whelk (6.10 ± 0.69 , 0.566 ± 0.003 , 0.261 ± 0.014 , and 0.042 ± 0.005 mg/kg, respectively), compared to those exposed to heat treatment -and sterilization (3.94 ± 0.45 , 0.472 ± 0.004 , 0.203 ± 0.024 , 0.033 ± 0.004 , mg/kg, and 3.21 ± 0.41 , 0.425 ± 0.003 , 0.215 ± 0.031 , 0.025 ± 0.005 mg/kg, respectively). The decrease of levels of As, Cd, and Cr after both heat treatment and sterilization were statistically significant ($P < 0.05$), but the decline in Mo was significant in the sterilized treatment group ($P < 0.05$) compared to the raw meat. Concentrations of Cu, Pb, Se, and Zn did not alter ($P > 0.05$) when the Rapa whelk was exposed to heat treatment (11.58 ± 0.76 , 0.058 ± 0.002 , 0.532 ± 0.021 , and 20.30 ± 1.93 mg/kg) or sterilization (11.05 ± 0.67 , 0.055 ± 0.001 , 0.526 ± 0.037 , and 19.80 ± 2.24 mg/kg) and remained similar to the non-treated meat (11.15 ± 0.69 , 0.051 ± 0.0061 , 0.546 ± 0.037 , and 20.73 ± 1.95 mg/kg). In contrast however, elevated levels of Al, Co, Fe, Hg, Mn, Ni, and Sb were recorded in Rapa whelk exposed to heat treatment, which thereafter declined to significant lower levels when further treated with sterilization through hypochlorite immersion ($P < 0.05$). Overall, As, Mo, Cd, Sb, Cr, Zn, Se, Cu, and Hg concentrations in the meat reduced by 47.44%, 40.09%, 24.86%, 20.27%, 17.50%, 4.52%, 3.63%, 0.93%, and 0.68%, respectively after the final processing phase of sterilization through hypochlorite immersion (1% NaOCl solution) (Table 3). The mean concentrations of metals found in the boiling water after heat treatment, and in the hypochlorite solution after sterilization, are given in Table 4. Overall, it was evidenced that a remarkable amount of Al, Cr, Cu, Fe, Hg, Pb, Sb, Se, and Zn were released into the boiling water during the heat treatment, and Al, As, Cu, Hg, Mn, Pb, Se, and Zn were concentrated in hypochlorite solution during the sterilization process.

3.4. Non-carcinogenic and carcinogenic consumer risks

The EDI per meal size ($\text{mg kg}^{-1} \text{day}^{-1}$), SDC (kg day^{-1}), SWC (meal/week), THQs and HI, and CRR for the studied metals in adults (men and women) and children upon consuming Rapa whelk, along with reference dose and cancer slope factor are presented in Table 5.

3.5. Compensation of minimum daily requirements for essential elements via Rapa whelk consumption

The compensation level of minimum daily requirements for the essential elements through Rapa whelk intake in human being has been given in Table 6. The findings show that 0.041%, 0.105%, 0.055%, 0.005%, 0.005%, 0.078%, and 0.014% of the daily requirements for Cr, Cu, Fe, Mn, Mo, Se, and Zn for adult men could be compensated by eating Rapa whelk, whereas these levels were found to be 0.070%, 0.129%, 0.050%, 0.008%, 0.006%, 0.096%, 0.024%, and 0.121%, 0.265%, 0.112%, 0.013%, 0.012%, 0.195%, 0.037%, for adult women and children, respectively.

Table 6- Percent compensation of minimum daily requirements (CDR_{min}) for essential trace elements in adult men (AM), adult women (AW), and children (C) via consuming sterilized Rapa whelk, based on estimated daily average requirement levels according to IOM (2006)

Element	EAR (mg/day, person ww)			EDI (mg/kg/day, ww)			CDR _{min} (%)		
	AM	AW	C	AM	AW	C	AM	AW	C
Cr	0.035	0.025	0.023	0.000014	0.000018	0.000028	0.041	0.070	0.121
Cu	0.70	0.70	0.54	0.00074	0.00090	0.00143	0.105	0.129	0.265
Fe	6.00	8.10	5.80	0.0033	0.0041	0.0065	0.055	0.050	0.112
Mn	2.30	1.80	1.75	0.00011	0.00014	0.00022	0.005	0.008	0.013
Mo	0.034	0.034	0.026	0.0000017	0.0000020	0.0000032	0.005	0.006	0.012
Se	0.045	0.045	0.035	0.000035	0.000043	0.000068	0.078	0.096	0.195
Zn	9.40	6.80	7.00	0.0013	0.0016	0.0026	0.014	0.024	0.037

EAR: estimated average daily requirement (mg/day) for a healthy human; ww (wet weight) basis; EDI ($\text{mg kg}^{-1} \text{day}^{-1}$): Estimated daily intake per meal size; ww (wet weight) basis; CDR_{min} (%): compensation of minimum daily requirement calculated according to Yigit et al.(2020).

4. Discussion

Both heat treatment and sterilization directly affected the metal levels in Rapa whelk. The levels of As, Cd, Cr, Mo, Se, and Zn reduced by 35.53%, 16.62%, 22.01%, 21.52%, 2.46%, and 2.07%, respectively in heat treated meat compared to the raw Rapa whelk, which is in line with the findings of Laparra et al. (2004). The reduction of metal levels in seafood after boiling can be attributed to solubilization in boiling water, as a result of broken chain between As and the food molecules as suggested by Hajeb et al. (2014). Results of the present study are also in close agreement with Ersoy (2011) and Devesa et al. (2001), who presented considerable reduction of Cr and Ni in fish exposed to microwave cooking. This was in line with Jorhem et al. (1994), who underlined severe decline in Cd, Ni, Co levels in crayfish after heat treatment. Further support was found in a study by and Atta et al. (1997), with a reduction in Cd, Cu, Pb, Zn levels in Tilapia niloticus following heat treatment. Perelló et al. (2008) reported decreased levels of Hg and As in hake fish after heat treatment, which supported our results in this study for As, but Hg showed

a decline after further treatment of sterilization. The reduction of some metals in cooked food might be attributed to the solubilization of metals from the soft tissue into the boiling water, as was earlier reported for the As solubilization from rice to water (Sengupta et al., 2006). In contrast, however, increased level of As in fish and molluscs after heat treatment was reported by Devesa et al. (2001). It seems there are inconsistencies among different reports regarding the effects of heat treatment on metals in seafood. This was the case for Al, Co, Fe, Hg, Mn, Ni, and Sb, which increased by heat treatment; however, As, Cd, Cr, Mo, Se, and Zn levels in heat treated Rapa whelk meat in the present study reduced remarkably. It has been reported that several factors could play important roles in the cooking process (Houlbrèque et al. 2011), such as time, temperature, and cooking medium (Hajeb et al. 2014). Juniawanti (2020) found that the duration of treatment may play a critical role. There 2020 study reported a 12%, 76%, and 83% reduction for Pb in Kupang shellfish after heat treatment for 15, 20, and 45 minutes, and over 83% after 60 minutes of boiling. In the present study, the initial preparations of samples prior to the analyses were conducted at the facilities of a commercial seafood processing company, where stainless steel metal benches and forks were used in the removal of meat from the shell. It is possible that a certain amount of metal contamination occurred during this process. While the degree of possible contamination was not determined here, it is still advisable to use non-metal materials during preprocessing in order to minimize any possible metal contamination. The decline in Al, Co, Fe, Hg, Mn, Ni, and Sb levels in this study may be attributed to the loss of moisture as has been earlier underlined by Protasowicki et al. (2008), or to the transfer of some metals from the shell into the meat. The shell of Rapa whelk is an efficient accumulator for metals (Richardson et al. 2001), and can be used as an indicator for metal accumulation records in the aquatic environment (Protasowicki et al. 2008).

Eventhough increased Hg was found in heat treated fish, the bio-accessibility of Hg was reduced by 24% compared to the raw fish (Maulvault et al., 2011). This was also reported for other metals with increased Cd, Se, and Zn levels in heat treated mussels, which however showed less bio-accessibility for these metals compared to raw mussels (Metian et al., 2009). Similarly, Houlbrèque et al. (2011) found increased Cd with significantly lowered bio-accessibility in mussels after heat treatment. It is interesting to underline that the inclusion of black coffee, black tea or green tea into the boiling media might decrease the bio-accessibility of Hg by up to 50-60% in raw fish, underlining a combined effect of heat treatment and the incorporation of tea or coffee for the reduction of Hg bio-accessibility in seafood (Ouédraogo & Amyot 2011). In the present study, the boiling process resulted in concentrating Al, Cr, Cu, Fe, Hg, Pb, Sb, Se, and Zn in the boiling water, which was in agreement with Metian et al. (2009), who reported that the heat treatment process concentrated the elements in the mussel soft tissue, and an important part of the elements were released into the boiling water, that eventually decreased their bio-accessibility when consumed. Hence, considering the findings in the present study regarding increased levels of Al, Cr, Cu, Fe, Hg, Pb, Sb, Se, and Zn in the boiling water, it could be possible that the bio-accessibility of these metals have been reduced as well, which however needs further clarification.

According to the findings in this study, the global intake of metals could be reduced by around 20% in Cd, Mo, Cr, and up to 35.5% in As, when the boiling water of Rapa whelk is discarded before eating. This is in close agreement with Metian et al. (2009), who noted that the consumption of heat treated mussels might contribute to a reduction in Cd intake by 65%, globally. Further studies are required to investigate possible reductions in metals from seafood with norm-exceeding levels to lower contents that may allow “safe food marketing” with reduced consumer risks in heat treated products.

Several processing methods applied in the industry, such as skinning, trimming, fat removal or cooking (frying, microwaving, broiling) may not always reduce metal concentrations in fish meat. For instance, Burger et al. (2003) found that the Hg in heat treated fish was higher than that of raw fish. Further, the heavy metals of As, Cd, and Hg could not be removed from the meat by common cooking methods such as frying, microwaving, or boiling (Morgan et al. 1997; Perelló et al. 2008). Various different kinds of solutions and complex agents such as acid and alkaline solutions, cysteine and homocysteine have been used for metal removal from seafood (Hajeb & Jinap 2009; 2012; Okazaki et al. 1984; Schab et al. 1978). In the present study, it was noteworthy that Rapa whelk released significant amounts of elements (Al, As, Cu, Hg, Mn, Pb, Se, Zn) into the hypochlorite solution during the sterilization process. Some earlier investigations provided evidence for reduced metal concentrations from fish by cysteine, the most reactive amino acid with Hg (Aizpurfa et al. 1997; Hajeb & Jinap 2012; Okazaki et al. 1984). A removal of 40% Hg from minced shark meat treated by salt solution (0.1 M NaCl) was reported by Aizpurfa et al. (1997). Similarly, Lipre (1980) found a 40% to 44% removal of Hg from cod fillets using 0.1% and 1% cysteine solutions for 24 h, respectively. And Danesh (1974) reported a 50% removal of Hg, Pb, and Cd from seafood through washing with 1% cysteine hydrochloride solution followed by heating at 100 to 132 °C for 1 to 30 min that enabled the evaporation of heavy metal ions. Yannai & Saltzman (1973) removed Hg from raw tuna by 55% in 2-2.2 pH and 79% at 1.5 pH though 0.33% cysteine hydrochloride immersion.

Further, Suprapti et al. (2016) found that soaking mussels in an acetic acid solution of 25% concentration for 90 min reduced Pb, Cr, and Cd to nearly half their original levels. Semenov et al. (2001) underlined that 0.1% citric acid solution can be used for Hg removal. The authors noted that Hg removal from fish was higher in a shorter soaking time, likely due to the reductive property of citric acid over time. Despite the increase of some metals after heat treatment in the present study, the levels for As, Cd, Mo, Sb, Cr, Se, Zn, Cu, and Hg reduced by 47.44%, 24.86%, 40.09%, 20.27%, 17.50%, 3.63%, 4.52%, 0.93%, and 0.68%, respectively, when the heat treated meat was immersed for 5 minutes in hypochlorite solution (1% NaOCl), which was comparable with findings from earlier investigations. Nevertheless, the discrepancies between removal efficiency among earlier studies could be attributed to the type of leaching agents, application times, pH and several other conditions, or a combination of all.

In the present study, the biplot analysis for the principal component of metals plotted by raw, heat treated, and sterilized meat groups showed a strong correlation between metals with high level of common variance close to “1”. From the results of principle component analyses it was noteworthy to see that the processing treatments affected metal distributions with principal elements of As, Cd, Cr, Mo in raw meat, Al, Co, Fe, Hg, Mn, Ni, Pb, Sb in heat treated meat, and Cu, Se, Zn in sterilized meat groups. This is a clear indication of lowering trends of toxic elements in raw meat towards essential elements in sterilized meat of Rapa whelk. Indeed, trace elements such as Cu, Mn, Zn, Fe are essential for human health, supporting metabolic activities; however, these trace elements can be toxic when consumed at high doses (Makedonski et al. 2017). In contrast however, metals such as As, Pb, Cd and Hg have high bioaccumulation capability in aquatic animals and are certainly toxic with severe health risks in human (Mol et al. 2019).

Considering non-carcinogenic health risks for children, adult men, and adult women, the THQs for all investigated metals remained below safety limit “1” (US-EPA 1989), showing that none of these metals pose non-carcinogenic risks for the three population groups when consuming sterilized Rapa whelk from the Turkish Black Sea coast. This is in line with the findings for Rapa whelk from the Bulgarian Black Sea coast (Peycheva et al. 2017). Major risk contributors among the cumulative metal concentrations in the present study were Hg, Cd, As, and Cu with HI rates of 23.9%, 23.6%, 25.8%; 20.9%, 21.2%, 21.1%; 15.7%, 15.8%, 16.1%; and 13.4%, 13.9%, 13.8% for adult men, women, and children, respectively. In accordance with this study, highest HI contribution with 23% in fish was reported for Cd by Akoto et al. (2014). The EDIs in Rapa whelk collected from the Bulgarian Black Sea coast were much lower than the recommendations by international organisations (Peycheva et al. 2017), which was in agreement with the findings of the present study. Mean EDIs for the investigated metals in Rapa whelk in this study were far below the RfD provided by EFSA (2010), with the exception for As (0.0003 mg/kg/day), that was very close to the RfD for adult men (0.00021 mg/kg/day), women (0.00026 mg/kg/day), but higher for children (0.00042 mg/kg/day). Hence for the children, it is advised to handle with caution. Assuming that the toxic inorganic arsenic was 3% of the total, EDIs and hazard risks for the toxic inorganic arsenic were estimated by multiplying the total arsenic with 0.03 (3% toxic inorganic arsenic of the total), following the suggestions of the FSA (2004). The element As is naturally found in the earth’s crust together with other elements. The arsenic combined with elements such as oxygen, chlorine, and sulfur, is referred to as “inorganic arsenic”. When the arsenic combined with carbon and hydrogen is referred to “organic arsenic”, which is found in seafood (fish and shellfish) and are less toxic or relatively nontoxic to human health. Overall lower EDIs found for the investigated metals compared to the RfDs (except As), strongly indicates that consumers would not experience significant health risks when eating Rapa whelk from the Turkish coast of Black Sea. A direct comparison of EDIs among various studies might result in erroneous predictions, due to variations in parameters such as exposure time, frequency, consumption rate, average body weight (Peycheva et al. 2017) or even a combination of all these factors. Hence, comparing EDIs with international reference values for specific conditions might be suggested.

For carcinogenic risks, estimations were made only for the following five metals: As, Cd, Ni, Pb, because of a lack of carcinogenic slope factors for the other metals investigated. The estimated CRRs of As for all three populations were higher than the acceptable range from 10^{-6} to 10^{-4} , with 3.2×10^{-4} for men, 3.9×10^{-4} for women, and 6.2×10^{-4} for children. The CRRs of Cd, Ni, and Pb were found to be 1.8×10^{-4} , 2.2×10^{-4} , 3.5×10^{-4} for men, 1.2×10^{-5} , 1.5×10^{-5} , 2.3×10^{-5} for women and 3.1×10^{-8} , 3.8×10^{-8} , 6.1×10^{-8} children, respectively. These values were overall higher than the acceptable range given by US-EPA (2010), and ranked in the order of As>Cd>Ni>Pb, showing that that As was the main contaminant creating a relatively high CRR among these metals.

In regards to the reference dose levels (RfD) of the international guidelines (EFSA 2010) for different body weight, age and gender groups, the highest level of safe daily consumption (SDC) per person adult men, women and children were found to be 14.01, 11.41, 7.21 kg/day for Mo; 8.27, 6.73, 4.25 kg/day for Ni; and 5.78, 4.71, 2.97 kg/day for Mn, respectively, which were followed by the remaining metals in the order of Al>Pb>Sb>Zn>Fe>Cr>Co>Se>Cu>As>Cd>Hg. The safe weekly consumption rates (SWC) per person followed the same trend with the highest values for Mo (432.0, 351.8, and 442.4 kg/day), and lowest for Hg (4.48, 3.65, and 4.59 meals/week) in adult men, women and children, respectively. This means that consuming Rapa whelk at these levels would not pose any significant health risk to consumers in all three populations. According to the results in this study, the level of safe consumption rates (SCR) were 32 to 3006 times higher than the “actual daily mollusc consumption” per person in European countries, which corresponds to 4.66 g capita per day (Failler et al. 2007). Similar to the findings in the present study, Yigit et al. (2018b) reported reasonably high levels of SCR (152.8, 64.3, 43.1, 12.9 kg/day person for Cu, Zn, Fe, and Mn, respectively) in Mediterranean mussels (*Mytillus galloprovincialis*) that did not have any hazardous effect on humans when consumed.

Regards the compensation levels of elements needed for a healthy human body, an adult man, woman or a child could only meet about 0.041-0.121% of the minimum daily requirement for Cr, 0.105-0.265% for Cu, 0.05-0.112% for Fe, 0.005-0.013% for Mn and Mo, 0.078-0.195% for Se, and 0.014-0.037% for Zn by consuming Rapa whelk, based on the estimated daily average requirement levels provided by IOM (2006). This was in line with Yigit et al. (2018b), who indicated that an individual would compensate only 0.013-0.94% of the minimum daily requirement for Cu, Zn, Fe, or Mn when consuming Mediterranean mussels collected near a Cu-alloy cage farm.

5. Conclusions

The present study reveals that levels of Hg, Cu, Se, Zn were reduced by 0.68 to 4.52% in Rapa whelk, whereas Cr, Sb, Cd were lowered by around 20%. Over a 40% reduction of Mo and As in Rapa whelk was achieved through heat treatment coupled with sterilization. Metals in Rapa whelk exposed to hypochlorite immersion were below permissible upper limits without any risks to consumers. THQs were below “1”, an indication of “no potential health risks” for human when consuming sterilized Rapa whelk. However, As, Cd, Ni, and Pb should be considered with caution, since these were close to or over the acceptable range provided by international organisations. Hence, it is highly advisable not to exceed the safe consumption limits for Rapa whelk estimated in this study. Further, regular the consumption of Rapa whelk would contribute the minimum daily requirement levels for Cr, Cu, Fe, Mn, Mo, Se, and Zn. These findings indicate that the per capita consumption of seafood in Turkey is below the global average (6.5 kg/year) (TUIK 2023).

References

- Aizpurfa I C M, Tenuta-Filho A, Sakuma A M & Zenebon O (1997). Use of cysteine to remove mercury from shark muscle. *International Journal of Food Science and Technology*, 32(4): 333–337. <https://doi.org/10.1046/j.1365-2621.1997.00407.x>
- Akoto O, Bismark Eshun F, Darko G & Adei E (2014). Concentrations And Health Risk Assessments Of Heavy Metals In Fish From The Fosu Lagoon. *International Journal of Environmental Research (IJER)*, 8(2): 403–410.
- Alkan A , Alkan N & Akbaş U (2016). The Factors Affecting Heavy Metal Levels in the Muscle Tissues of Whiting *Merlangius merlangus* and Red Mullet *Mullus barbatus* . *Journal of Agricultural Sciences* 22 (3): 349-359 . DOI: 10.1501/Tarimbil_0000001393
- Atta M B, El-Sebaie L A, Noaman M A & Kassab H E (1997). The effect of cooking on the content of heavy metals in fish (*Tilapia nilotica*). *Food Chemistry* 58(1–2): 1–4. [https://doi.org/10.1016/0308-8146\(95\)00205-7](https://doi.org/10.1016/0308-8146(95)00205-7)
- Bayrakli B, Özdemir S & Duyar H A (2016). Seasonal Variation in Biochemical Composition of the Veined Rapa Whelk , *Rapana venosa* (Valenciennes , 1846) Caught By Beam Trawl (Algarna) in The Black Sea. *Alinteri Journal of Agriculture Science* 31(2): 72–76.
- Bayrakli B (2021). Concentration and potential health risks of trace metals in warty crab (*Eriphia verrucosa* Forskal, 1775) from Southern Coasts of the Black Sea, Turkey. *Environmental Science and Pollution Research* 28(12): 14739–14749. <https://doi.org/10.1007/s11356-020-11563-9>
- BN S, AB O, & JAB S (2001). Method for isolation of heavy metals form, for instance mercury, from fish stock (Patent No. 2167541).
- Burger J, Dixon C, Boring S & Gochfeld M (2003). Effect of Deep-Frying Fish on Risk from Mercury. *Journal of Toxicology and Environmental Health, Part A*, 66(9): 817–828. <https://doi.org/10.1080/15287390306382>
- Çağlak E & Karsli B (2014). Investigation of Some Heavy Metals Accumulation in Muscle of Pike Perch (*Stizostedion lucioperca*, Linnaeus 1758) from Lake Beyşehir, Turkey. *Journal of Agricultural Sciences* 20(2): 203-214 . DOI: 10.15832/tbd.25388
- Danesh A (1974). Process for treating seafood (Patent No. US Patent 3958022).
- Devesa V, Macho M L, Jalón M, Urieta I, Muñoz O, Súnier M A, López F, Vélez D & Montoro R (2001). Arsenic in Cooked Seafood Products: Study on the Effect of Cooking on Total and Inorganic Arsenic Contents. *Journal of Agricultural and Food Chemistry* 49(8): 4132–4140. <https://doi.org/10.1021/jf0102741>
- Duyar H A, Bayrakli B & Altuntas M (2023). Effects of floods resulting from climate change on metal concentrations in whiting (*Merlangius merlangus* euxinus) and red mullet (*Mullus barbatus*) and health risk assessment. *Environmental Monitoring and Assessment* 195(8). <https://doi.org/10.1007/s10661-023-11534-w>
- EFSA (European Food safety Authority) (2010). Scientific Opinion on Lead in Food. In EFSA Journal (Vol. 8, Number 4). <https://doi.org/10.2903/j.efsa.2010.1570>
- Ersoy B (2011). Effects of cooking methods on the proximate, mineral and fatty acid composition of European eel (*Anguilla anguilla*). *International Journal of Food Science & Technology* 46(3): 522–527. <https://doi.org/10.1111/j.1365-2621.2010.02546.x>
- Failler P, Walle G Van de, Lecrivain N, Himbes A & Lewins R (2007). Future prospects for fish and fishery products. 4. Fish consumption in the European Union in 2015 and 2030. Part 1. European overview.FAO Fisheries Circular. No. 972/4 (Number FAO Fisheries Circular. No. 972/4).
- FAO (1983).Fishery Circular No. 764 Complation of Legal for Hazardous Substances in Fish and Fishery Product.
- FSA (2004). 1999 total diet study: total and inorganic arsenic in food.In: Agency, F.s. (Ed.), Food Surveillance Informat.
- Hajeb P & Jinap S (2009). Effects of washing pre-treatment on mercury concentration in fish tissue. *Food Additives & Contaminants: Part A*, 26(10): 1354–1361. <https://doi.org/10.1080/02652030903150567>
- Hajeb P & Jinap S (2012). Reduction of mercury from mackerel fillet using combined solution of cysteine, EDTA, and sodium chloride. *Journal of Agricultural and Food Chemistry* 60(23): 6069–6076. <https://doi.org/10.1021/jf300582j>
- Hajeb P, Sloth J J, Shakibzadeh S, Mahyudin N A & Afsah-Hejri L (2014). Toxic elements in food: Occurrence, binding, and reduction approaches. *Comprehensive Reviews in Food Science and Food Safety* 13(4): 457–472. <https://doi.org/10.1111/1541-4337.12068>
- Hallenbeck H W (1993). Risk assessment occupational health. *Risk Assessment and Occupational Health* 4, 254. <https://content.taylorfrancis.com/books/download?dac=C2009-0-23830-0&isbn=9781482264494&format=googlePreviewPdf>
- Hammer Ø, Harper D A T & Ryan P D (2001). Past: Paleontological Statistics Software Package for Education and Data Analysis. *Palaeontologia Electronica* 4(1): 9. https://palaeo-electronica.org/2001_1/past/past.pdf
- Houlbrèque F, Hervé-Fernández P, Teyssié J-L, Oberhaensli F, Boisson F, & Jeffree R (2011). Cooking makes cadmium contained in Chilean mussels less bioaccessible to humans. *Food Chemistry* 126(3): 917–921. <https://doi.org/10.1016/j.foodchem.2010.11.078>
- Hwang D-W, Choi M, Lee I-S, Shim K B & Kim T-H (2017). Concentrations of trace metals in tissues of Chionoecetes crabs (*Chionoecetes japonicus* and *Chionoecetes opilio*) caught from the East/Japan Sea waters and potential risk assessment. *Environmental Science and Pollution Research* 24(12): 11309–11318. <https://doi.org/10.1007/s11356-017-8769-z>
- IARC (International Agency for Research on Cancer) (2012). Monograph on Cadmium, Chromium, Copper, Iron, Plumbum and Zinc.
- IOM (Institute of Medicine) (2006). Dietary Reference Intakes. National Academies Press. <https://doi.org/10.17226/11537>
- Jorhem L, Engman J, Sundström B & Thim A M (1994). Trace elements in crayfish: Regional differences and changes induced by cooking. *Archives of Environmental Contamination and Toxicology* 26(2): 137–142. <https://doi.org/10.1007/BF00224796>

- Juniawanti D R (2020). Decreased Lead Levels, Kupang, and Boiling. *Journal of Public Health Science Research* 1(1): 1. <https://doi.org/10.30587/jphsr.v1i1.1178>
- Laparra J M, Vélez D, Montoro R, Barberá R, & Farré R (2004). Bioaccessibility of inorganic arsenic species in raw and cooked *Hizikia fusiforme* seaweed. *Applied Organometallic Chemistry* 18(12): 662–669. <https://doi.org/10.1002/aoc.732>
- Leonard L S, Mahenge A & Mudara N C (2022). Assessment of heavy metals contamination in fish cultured in selected private fishponds and associated public health risk concerns, Dar es Salaam, Tanzania. *Marine Science and Technology Bulletin* 11(2): 246– 258. <https://doi.org/10.33714/masteb.1108314>
- Liang L, He B, Jiang G, Chen D & Yao Z (2004). Evaluation of mollusks as biomonitors to investigate heavy metal contaminations along the Chinese Bohai Sea. *Science of The Total Environment* 324(1–3): 105–113. <https://doi.org/10.1016/j.scitotenv.2003.10.021>
- Liang Y, Yi X, Dang Z, Wang Q, Luo H & Tang J (2017). Heavy Metal Contamination and Health Risk Assessment in the Vicinity of a Tailing Pond in Guangdong, China. *International Journal of Environmental Research and Public Health* 14, 1557. <https://doi.org/10.3390/ijerph14121557>
- Lipre E (1980). Removal of mercury from fish. Tallinna Politechnilise Instituudi Toimetised, 489: 41–47
- Makedonski L, Peycheva K & Stancheva M (2017). Determination of heavy metals in selected black sea fish species. *Food Control* 72: 313–318. <https://doi.org/10.1016/j.foodcont.2015.08.024>
- Maulvault A L, Machado R, Afonso C, Lourenço H M, Nunes M L, Coelho I, Langerholc T & Marques A (2011). Bioaccessibility of Hg, Cd and As in cooked black scabbard fish and edible crab. *Food and Chemical Toxicology* 49(11): 2808–2815. <https://doi.org/10.1016/j.fct.2011.07.059>
- Metian M, Charbonnier L, Oberhaensli F, Bustamante P, Jeffree R, Amiard J-C & Warnau M (2009). Assessment of metal, metalloid, and radionuclide bioaccessibility from mussels to human consumers, using centrifugation and simulated digestion methods coupled with radiotracer techniques. *Ecotoxicology and Environmental Safety* 72(5): 1499–1502. <https://doi.org/10.1016/j.ecoenv.2008.10.009>
- Mol S, Kahraman A E & Ulusoy S (2019). Potential Health Risks of Heavy Metals to the Turkish and Greek Populations via Consumption of Spiny Dogfish and Thornback Ray from the Sea of Marmara. *Turkish Journal of Fisheries and Aquatic Sciences* 19(2): 19–27. https://doi.org/10.4194/1303-2712-v19_2_03
- Morgan J N, Berry M R & Graves R L (1997). Effects of commonly used cooking practices on total mercury concentration in fish and their impact on exposure assessments. *Journal of Exposure Analysis and Environmental Epidemiology* 7(1): 119–33. <http://www.ncbi.nlm.nih.gov/pubmed/9076613>
- Okazaki E, Kanna K, Suzuki T & Kikuchi T (1984). Elimination of mercury from shark flesh. *Bulletin of Tokai Regional Fisheries Research Laboratory (Japan)* 114: 125–132
- Ouédraogo O & Amyot M (2011). Effects of various cooking methods and food components on bioaccessibility of mercury from fish. *Environmental Research* 111(8): 1064–1069. <https://doi.org/10.1016/j.envres.2011.09.018>
- Perelló G, Martí-Cid R, Llobet J M & Domingo J L (2008). Effects of Various Cooking Processes on the Concentrations of Arsenic, Cadmium, Mercury, and Lead in Foods. *Journal of Agricultural and Food Chemistry* 56(23): 11262–11269. <https://doi.org/10.1021/jf802411q>
- Peycheva K, Panayotova V & Stancheva M (2017). Trace Elements Concentrations in Black Sea Mussel (*Mytilus galloprovincialis*) and Rapa Whelks (*Rapana venosa*) from Bulgarian Black Sea Coast and Evaluation of Possible Health Risks to Consumers. *Chemistry Research Journal* 2(6): 236–250
- Protasowicki M, Dural M & Jaremek J (2008). Trace metals in the shells of blue mussels (*Mytilus edulis*) from the Poland coast of Baltic sea. *Environmental Monitoring and Assessment* 141(1–3): 329–337. <https://doi.org/10.1007/s10661-007-9899-4>
- Richardson C, Chenery S & Cook J (2001). Assessing the history of trace metal (Cu, Zn, Pb) contamination in the North Sea through laser ablation-ICP-MS of horse mussel *Modiolus modiolus* shells. *Marine Ecology Progress Series* 211: 157–167. <https://doi.org/10.3354/meps211157>
- Schab R, Sachs K & Yannai S (1978). A proposed industrial method for the removal of mercury from fish. *Journal of the Science of Food and Agriculture* 29(3): 274–280. <https://doi.org/10.1002/jsfa.2740290313>
- Sengupta M K, Hossain M A, Mukherjee A, Ahamed S, Das B, Nayak B, Pal A & Chakraborti D (2006). Arsenic burden of cooked rice: Traditional and modern methods. *Food and Chemical Toxicology* 44(11): 1823–1829. <https://doi.org/10.1016/j.fct.2006.06.003>
- Stancheva M, Ivanova V & Peycheva K (2012). Determination of heavy metals in black sea *Mytilus galloprovincialis* and *Rapana venosa*. *Scripta Scientifica Medica* 44(2): 27. <https://doi.org/10.14748/ssm.v44i2.353>
- Suprapti N H, Bambang A N, Swastawati F & Kurniasih R A (2016). Removal of Heavy Metals from a Contaminated Green Mussel [*Perna Viridis* (Linnaeus, 1758)] Using Acetic Acid as Chelating Agents. *Aquatic Procedia* 7: 154–159. <https://doi.org/10.1016/j.aqpro.2016.07.021>
- Terzi E & Civelek F (2021). Cu, Cd, As and Hg resistance levels in *Escherichia coli* isolated from Mediterranean mussel and sea snail in the Southeastern Black Sea. *Marine Science and Technology Bulletin* 10(1): 36–41
- TUIK (2023). Türkiye Fishery Statistics, Ankara. <https://data.tuik.gov.tr/Kategori/GetKategori?p= Tarim-111>
- US-EPA (United States Environmental Protection Agency) (1989). Risk assessment guidance for superfund Vol I Human health evaluation manual (Part A).
- US-EPA (United States Environmental Protection Agency) (1996). United States Environmental Protection Agency, Soil Screening Guidance: User's Guide.
- US-EPA (United States Environmental Protection Agency) (2000). Guidance for assessing chemical contaminant data for use in fish advisories, volume II Risk assessment and fish consumption limits (EPA 823-B-00-008).
- US-EPA (United States Environmental Protection Agency) (2010). Risk assessment guidance for superfund volume I human health evaluation manual (Part A) I.
- US-EPA (United States Environmental Protection Agency) (2013). Regional screening level (RSL) fish ingestion table.
- Yannai S & Saltzman R (1973). Elimination of mercury from fish. *Journal of the Science of Food and Agriculture* 24(2): 157–160. <https://doi.org/10.1002/jsfa.2740240207>
- Yigit M, Celikkol B, Yilmaz S, Bulut M, Özalp H, Dwyer R, Maita M, Kizilkaya B, Yiğit Ü, Ergün S, Gürses K & Büyükkateş Y (2018). Bioaccumulation of trace metals in Mediterranean mussels (*Mytilus galloprovincialis*) from a fish farm with copper-alloy mesh pens and potential risk assessment. *Hum Ecol Risk Assess Int J* 24(2): 465–481. <https://doi.org/https://doi.org/10.1080/1080703920171387476>




- Yigit M, Dwyer R, Celikkol B, Yilmaz S, Bulut M, Buyukates Y, Kesbic O S, Aca Ü, Ozalp B, Maita M & Ergün S (2018). Human exposure to trace elements via farmed and cage aggregated wild Axillary seabream (*Pagellus acarne*) in a copper alloy cage site in the Northern Aegean Sea. *Journal of Trace Elements in Medicine and Biology* 50(May), 356–361. <https://doi.org/10.1016/j.jtemb.2018.07.020>
- Yigit M, Dwyer R, Yilmaz S, Bulut M, Ozalp B, Buyukates Y, Ergun S, Celikkol B, Kizilkaya B, Yigit Ü & Maita M (2020). Health Risks Associated with Trace Metals in Gilthead Seabream (*Sparus aurata*) from Copper Alloy and Antifouling-Coated Polymer Nets. *Thalassas* 36(1): 95–101. <https://doi.org/10.1007/s41208-019-00186-8>
- Yildiz H, Bayrakli B, Altuntas M & Celik I (2023). Metal concentrations, selenium-mercury balance, and potential health risk assessment for consumer of whiting (*Merlangius merlangus euxinus* L., 1758) from different regions of the southern Black Sea. *Environmental Science and Pollution Research* 30(24): 65059–65073. <https://doi.org/10.1007/s11356-023-26511-6>



Copyright © 2024 The Author(s). This is an open-access article published by Faculty of Agriculture, Ankara University under the terms of the [Creative Commons Attribution License](https://creativecommons.org/licenses/by/4.0/) which permits unrestricted use, distribution, and reproduction in any medium or format, provided the original work is properly cited.



Hemp Seed Priming via Different Agents to Alleviate Temperature Stress

Sibel Day^{a*} , Nilüfer Koçak-Şahin^a , Burak Öno^a 

^aAnkara University, Faculty of Agriculture, Department of Field Crops, 06110, Dışkapı, Ankara, TÜRKİYE

ARTICLE INFO

Research Article

Corresponding Author: Sibel Day, E-mail: day@ankara.edu.tr

Received: 15 November 2023 / Revised: 17 January 2024 / Accepted: 25 January 2024 / Online: 23 July 2024

Cite this article

Day S, Şahin-Koçak N, Öno^B (2024). Hemp Seed Priming via Different Agents to Alleviate Temperature Stress. *Journal of Agricultural Sciences (Tarım Bilimleri Dergisi)*, 30(3):562-569. DOI: 10.15832/ankutbd.1391194

ABSTRACT

Hemp (*Cannabis sativa* L.) seeds were treated with different priming agents (water, -0.8 MPa PEG 6000, 50 mMol thiamine and 10 mMol mannitol) and subjected to different temperatures (10, 15, 20, 25 and 30 °C). The impacts of low and high temperature on germination and initial growth, along with optimal conditions, were evaluated with priming agents. Results revealed that seed treatment accelerated mean germination time and increased emergence percentage at lower temperatures. The minimum mean germination times of 1.38 and 1.39 days were obtained at 20 °C with hydro priming and mannitol priming. The maximum germination percentages of 89.5 and 90% were observed with mannitol and hydro priming at 20 °C. Retarded seedling emergence was noted at 10 °C. Minimum emergence percentage at 10 °C was 46%

in control samples. Seed pre-treatments also promoted shoot length at all temperatures. However, root length promoting effects of seed treatments were more evident at 10, 15 and 20 °C. The minimum root length was 3.04 cm in controls at 30 °C. Seedling fresh and dry weight reached maximum values at 20 °C with water, thiamine and mannitol treatments. Chlorophyll and leaf proline content reached their highest values at 20, 25 and 30 °C. Overcoming temperature stress and promoting germination is important for hemp development. It was concluded that hemp seeds primed with water, thiamine, and mannitol had the highest biomass values for low, optimum, and high temperatures in this study. This indicates that these seed treatments are suitable for hemp plants that could experience low or high temperatures during germination and early growth stages.

Keywords: *Cannabis sativa* L., Hydro priming, Mannitol, Osmo priming, Thiamine

1. Introduction

Cannabis sativa L. (hemp) has been cultivated for more than 5000 years for its fibre, seeds and phytochemicals used in ethno-medicines and pharmacotherapy (Odieka et al. 2022). It is highly resistant against a large number of insect pests, and has a well-developed root system (Visković et al. 2023).

Hemp is cultivated in a wide range of climatic areas in Türkiye and the world with diversity in sowing time and temperatures depending on the longitude (day length), latitude, and altitude (meteorological parameters). The cultivation area in Türkiye is increasing due to increasing demand for hemp fibre. The most important factor in hemp cultivation is temperature. The seeds germinate best when the soil temperature is above 15 °C (Geneve et al. 2022). Most crops exhibit temperature-dependent seed germination. The temperature has an effect on both the percentage of seed germination and the time it takes for the first root to emerge. It is important to study seed germination in hemp at different temperatures. The temperature limits for hemp are important and global warming has motivated scientists to research the impacts of high temperatures. Exposure of seeds to high temperature stress during germination leads to delayed mobilisation of storage reserves, protein degradation, loss of enzyme activity, de novo protein synthesis, and membrane integrity resulting in cellular damage and collapse after prolonged exposure (Essemine et al. 2010). Although, hemp is a multifunctional medicinal plant and an alternative crop like sweet basil (Day 2021), safflower (Day et al. 2017) and black cumin (Day et al. 2022), studies about its germination, emergence and early seedling growth stages are rare.

Therefore, it is desirable to determine the right time and climate to ensure appropriate and good yield. There are a limited number of cultivars and little knowledge about the impact of temperature on seed germination, which is generally genotype dependent. Slow and reduced germination or late sowing could lead to low yield (Day 2022). The uncertain Central Anatolian climatic conditions, with low moisture, low temperature and frequently changing meteorological conditions, leave farmers with many problems during seed sowing and emergence.

Several strategies are employed by farmers in soil to improve germination and emergence. Seed treatments before sowing are widely used as an easy way to biofortify seeds with different chemicals or nutrient elements to stimulate their germination and emergence and inhibit the effects of external stresses, such as temperature or water deficit (Day & Koçak-Şahin 2023a).

Seed priming is a technique inducing pre-germinative metabolism via controlled rehydration (Paparella et al. 2015). The advantages of seed priming were revealed in both optimal and unfavourable conditions for many oil seed crops such as corn, sunflower and canola (Shrestha et al. 2019; Bouriou et al. 2020; Day 2022). This technique could also be used in industrial hemp to improve germination performance. Hemp seeds were primed with GA3 to alleviate drought stress and enhancing impacts were reported with 400 and 600 mg L⁻¹ GA3 doses (Du et al. 2022).

The detrimental impact of hydro priming could be reduced by inducing high osmotic pressure, so polyethylene glycol (PEG 6000) is one of the solutes frequently used for seed priming (Lemmens et al. 2019). Thiamine (vitamin B1) is produced by microbes and plants (Suohui et al. 2022) and it is well known that both thiamine and its phosphate esters are modulated by stress factors, which end up increasing total contents in many plant species (Rapala-Kozik et al. 2008; Tunc-Ozdemir et al. 2009). Many studies reported that the continuous synthesis of thiamine or enhanced endogenous levels could to improve the health of plants and their tolerance against harsh stressful conditions (Jabeen et al. 2022).

In plants, mannitol provides resistance under abiotic stress conditions (Hema et al. 2014). Increased concentrations improve resistance against salinity or drought stress conditions, as evident in peach (Lo Bianco et al. 2000), transgenic wheat, sugarcane, rice and sorghum (Cha-um et al. 2009). Improving effects of mannitol were also observed on *Zea mays* L. under saline conditions and Cr toxicity with exogenous application (Kaya et al. 2013; Habiba et al. 2019).

Overall, the purpose of the experiment was to evaluate the effect of several priming agents at different temperatures on the germination of industrial hemp seeds and to reduce the germination time. Furthermore, the study evaluated the use of substantially different agents to improve hemp seed germination and seedling growth at different temperatures.

2. Material and Methods

The hemp seeds used in this study belonged to the Narlısaray population procured from the Directorate of Agricultural Management at Gökhöyük, Amasya, Türkiye. The hemp seeds were primed using following treatments:

- I. Control: The seeds were germinated without any pre-treatment.
- II. Hydro priming: The seeds were soaked in distilled water at 20 °C for 8 h.
- III. Polyethylene glycol: The seeds were soaked in -0.8 MPa PEG 6000 solution at 20 °C for 8 h. Osmotic potential of PEG 6000 was adjusted according to Michel & Kaufmann (1973).
- IV. Thiamine: The seeds were soaked in 50 mMol thiamine solution for 8 h.
- V. Mannitol: The seeds were soaked in 10 mMol mannitol solution for 8 h.

After priming with PEG, thiamine and mannitol, the seeds were rinsed with distilled water to remove any traces of the respective chemicals from the surface of the seeds, followed by drying to initial weight.

2.1 Germination test

The experiment was conducted with four replications using 50 seeds in each replicate. Seeds from each treatment were placed into three layers of filter paper moistened with 21 mL of deionized water to check their seed viability. The rolled papers were put into sealed plastic bags and placed in an incubator in the dark. The seeds with a radicle length of 2 mm were counted as germinated. The germinated seeds were recorded daily for 14 days to calculate the mean germination time (MGT), and the germination percentage (GP). Germination and early seedling growth of control and primed seeds were evaluated at low temperatures (10±1 and 15±1 °C), room temperatures (20±1 and 25±1 °C) and high temperature (30 °C).

Germination speed was evaluated according to mean germination time (MGT) using the formula given below (ISTA 2017):

$$MGT = \frac{\sum(n \times t)}{N}$$

Where; n is the number of germinated seeds on each day, t is the days from planting and N is the total number of germinated seeds.

The germination percentage was calculated with the following equation (Day and Koçak-Şahin 2023b):

$$GP = \frac{NG}{NT} \times 100$$

Where; *GP* is the emergence percentage, *NG* is the number of germinated seeds and *NT* is the total number of seeds.

Germination index (GI) calculation was done according to the equation given below (Abdul-Baki & Anderson (1973):

$$GI = \text{Number of germinated seeds/day of first count} + \dots + \text{Number of germinated seeds/day of final count.}$$

2.2 Emergence tests

Four replicates of 50 seeds ($50 \times 4 = 200$ seeds) were sown at a depth of 2 cm in plastic trays ($30 \times 21 \times 9$ cm) containing peat and placed in a growth chamber (Sanyo versatile growth chamber, Japan) at 10 ± 1 , 15 ± 1 , 20 ± 1 , 25 ± 1 , and 30 ± 1 °C under $45 \mu\text{M}$ photons $\text{m}^{-2} \text{s}^{-1}$ light intensity for 16 h with 45% humidity. The peat used in the study had pH of 6.5 and EC of 40 mS m^{-1} , with porosity of around 69% (v w^{-1}).

The number of emerged seedlings (unfolding cotyledons on the surface) was counted daily up to 25 days, along with the emergence percentages of the respective seedlings. The plants were irrigated with 50 ml water 5 times during the 26 days of the experiment. The mean emergence time (MET, days), emergence percentage and emergence index were calculated according to the formulas given in the germination test.

Chlorophyll contents were measured on the 25th day. Shoot length, root length, seedling fresh and dry weight were measured for all seedlings from each replicate after the 26th day. Fresh weights of seedlings were measured soon after harvest to avoid weight loss (Day 2016). The dry weight of the seedlings was measured after drying the samples in an oven at 70 °C for 48 h (Yildiz et al. 2010).

2.3 Chlorophyll index and proline content determination

Chlorophyll measurements were done with SPAD-502 Plus (Konica Minolta) using five leaves per seedling. Ten seedlings from each replicate were used for sampling.

Free proline quantification in the shoots was determined following Bates et al. (1973). Proline was extracted from 100 mg of leaf samples by using ninhydrin reagent in 3% (w/v) aqueous sulfosalicylic acid. The organic toluene phase was separated and the absorbance of the red colour was read at 520 nm. Concentration of proline ($\mu\text{mol g}^{-1} \text{FW}$) was determined using a calibration curve prepared with L-proline.

2.4 Experimental design and statistical analysis

The design of the study was based on two factorials (5×5) arranged in a randomized complete block design with four replicates. The main factor was temperature and the sub-factor was seed priming treatments. Data for the emergence percentage were subjected to arcsine transformation before ANOVA. The differences between the means were compared using Duncan's multiple range test ($P < 0.01$).

3. Results

3.1 Germination and emergence test

Significant differences between priming agents were determined particularly at 10, 15 and 20 °C for mean germination time and germination percentage (Table 1). Decreased temperature led to an increase in MGT. The germination percentage and mean germination time were closely affected by temperature. PEG increased the mean germination time (6 days) compared to other treatments at 10 °C. However mean germination time of control treatments at other temperatures was longer than with the priming treatments. The lowest mean germination time for control and other treated seeds was observed at 30 °C with non-significant numerical differences of 1.67-1.82 d to germinate. Overall, the minimum mean germination time was observed with hydro priming (1.38 day) and mannitol priming (1.39 day) at 20 °C.

The maximum germination percentage values (89.5 and 90%) were recorded for mannitol based osmo priming and hydro priming at 20 °C (Table 1). Mannitol based osmo primed seeds failed to induce similar germination behaviour at 10-15 °C when compared with their performance at 20-25 °C.

Table 1- Impact of priming on MGT and germination percentages for hemp at different temperatures

Priming	Mean germination time (day)					Germination percentage (%)				
	10 °C	15 °C	20 °C	25 °C	30 °C	10 °C	15 °C	20 °C	25 °C	30 °C
Control	5.21 ^b	4.10 ^c	2.87 ^{ef}	2.92 ^{ef}	1,80 ^g	80.0 ^{bcd}	77.5 ^{bcd}	85.5 ^{abc}	83.0 ^{abc}	84.5 ^{abc}
Water	5.29 ^b	3.04 ^e	1.38 ^g	2.56 ^{ef}	1,67 ^g	83.5 ^{abc}	86.0 ^{ab}	90.0 ^a	85.5 ^{abc}	86.5 ^{ab}
PEG	6.00 ^a	3.02 ^e	2.70 ^{ef}	2.57 ^{ef}	1,78 ^g	77.5 ^{bcd}	86.0 ^{ab}	81.0 ^{bcd}	83.5 ^{abc}	72.0 ^d
Thiamine	5.26 ^b	2.90 ^{ef}	2.45 ^f	2.66 ^{ef}	1,82 ^g	80.5 ^{bcd}	84.5 ^{abc}	80.0 ^{bcd}	84.0 ^{abc}	77.5 ^{bcd}
Mannitol	4.89 ^b	3.50 ^d	1.39 ^g	2.53 ^{ef}	1,74 ^g	78.0 ^{bcd}	76.5 ^{cd}	89.5 ^a	85.0 ^{abc}	77.5 ^{bcd}

**, All values shown in a block with different letters are dissimilar according to DMRT at P<0.01 level of significance

Mean emergence time under different temperatures showed diversity (Table 2). Retarded seedling emergence was noted at 10 °C among the temperatures. All priming treatments at 10 °C had insignificant differences. At 15 °C, control seeds emerged earlier than treated seeds. Increased temperature shortened the emergence days of hemp with all treatments. At 25 °C, particularly PEG 6000 osmo primed seeds showed early emergence compared to controls, whereas at 30 °C PEG 6000, thiamine and mannitol-based priming treatments had earlier seedling emergence compared to the control and hydro priming treatments. The results clearly demonstrate that all types of priming treatments could not reduce the emergence time below 7.41 days at 10, 15 and 20 °C.

Table 2- Impact of priming on MET and emergence percentage of hemp at different growing temperatures

Priming	Mean emergence time (day)					Emergence percentage (%)				
	10 °C	15 °C	20 °C	25 °C	30 °C	10 °C	15 °C	20 °C	25 °C	30 °C
Control	13.03 ^a	8.00 ^{def}	7.69 ^{ef}	7.78 ^{ef}	8.08 ^{c-f}	46.00 ^d	47.50 ^{cd}	83.00 ^a	63.50 ^b	27.00 ^e
Water	12.99 ^a	9.32 ^{bcd}	8.06 ^{c-f}	6.84 ^{fg}	8.24 ^{b-f}	51.00 ^{cd}	53.50 ^{bcd}	76.00 ^a	56.00 ^{bcd}	29.00 ^e
PEG	13.45 ^a	9.52 ^{bc}	9.16 ^{b-e}	6.01 ^g	6.82 ^{fg}	52.50 ^{cd}	48.00 ^{cd}	75.00 ^a	48.00 ^{cd}	31.50 ^e
Thiamine	13.01 ^a	9.65 ^b	7.92 ^{def}	7.29 ^{fg}	6.74 ^{fg}	58.00 ^{bc}	49.00 ^{cd}	82.50 ^a	52.00 ^{cd}	32.50 ^e
Mannitol	13.97 ^a	9.07 ^{b-e}	7.41 ^{fg}	7.00 ^{fg}	6.77 ^{fg}	50.00 ^{cd}	56.00 ^{bcd}	79.00 ^a	54.50 ^{bcd}	32.00 ^e

**, All values shown in a block with different letters are dissimilar according to DMRT at P<0.01 level of significance

Seed treatments provided advantages for emergence percentage at 10 and 15 °C compared to controls but insignificant differences were observed (Table 2). At 10 °C, the minimum emergence percentage (46%) was obtained for control seeds. Emergence percentage had the highest results with all priming treatments at 20 °C. The minimum emergence percentages for all priming treatments were observed at 30 °C.

The germination index is a measure of the vigorousness of seeds, and a higher germination index indicates more vigorous seeds. At 10 °C, the best results were obtained from hydro priming with 36.56 and the hydro primed seeds also showed more vigour at 20, 25 and 30 °C. The maximum germination vigour was observed in mannitol-primed seeds at 20 °C (Table 3).

The emergence index values for all treatments reached their highest level at 20 °C and seeds osmo primed with PEG showed difference compared to other treatments (Table 3).

Table 3- Impact of priming on germination index and emergence index of hemp at different growing temperatures

Priming	Germination index					Emergence index				
	10 °C	15 °C	20 °C	25 °C	30 °C	10 °C	15 °C	20 °C	25 °C	30 °C
Control	20.44 ⁱ	29.77 ^{ghi}	38.97 ^{fg}	30.68 ^{ghi}	56.90 ^{bc}	7.86 ^{fg}	11.65 ^{efg}	30.71 ^a	14.56 ^{cde}	7.86 ^{fg}
Water	36.56 ^{fgh}	39.57 ^{fg}	80.58 ^a	46.16 ^{c-f}	65.65 ^b	7.96 ^{fg}	12.48 ^{def}	28.83 ^a	18.56 ^{bc}	8.22 ^{fg}
PEG	27.33 ^{hi}	40.76 ^{efg}	43.27 ^{def}	43.53 ^{def}	51.87 ^{cde}	8.45 ^{fg}	11.25 ^{efg}	21.50 ^b	17.61 ^{bcd}	11.34 ^{efg}
Thiamine	25.77 ⁱ	52.28 ^{cd}	46.21 ^{c-f}	41.79 ^{def}	53.10 ^{cd}	10.22 ^{efg}	9.73 ^{efg}	30.84 ^a	14.59 ^{cde}	11.21 ^{efg}
Mannitol	22.92 ⁱ	37.31 ^{fgh}	82.21 ^a	47.19 ^{c-f}	56.19 ^{bc}	6.04 ^g	13.00 ^{def}	27.40 ^a	17.49 ^{bcd}	12.71 ^{def}

**, All values shown in a block with different letters are dissimilar according to DMRT at P<0.01 level of significance

3.2 Seedling growth parameters

Smaller shoot length was noted in control treatments regardless of temperature (Table 4). The shoot length in all priming treatments had significant differences compared to control at 10, 15 and 20 °C. The largest shoots were noted at 20 °C with all priming treatments, including the mannitol-based priming, without sharp differences among them. The minimum shoot length with all priming treatments was observed at 30 °C. It is clear and established that increasing temperatures (25 - 30 °C) encouraged reductions in shoot length. Improved shoot lengths were noted for hydro primed, thiamine, and mannitol-based osmo primed seedlings at all temperatures.

Table 4- Impact of priming on shoot length and root length of hemp seedlings at different growing temperatures

Priming	Shoot length (cm)					Root length (cm)				
	10 °C	15 °C	20 °C	25 °C	30 °C	10 °C	15 °C	20 °C	25 °C	30 °C
Control	9.19 ^{g-j}	9.84 ^{e-h}	12.60 ^{bc}	8.59 ^{h-k}	7.27 ^k	3.78 ^{f-i}	3.99 ^{e-h}	5.06 ^{a-d}	4.34 ^{d-g}	3.04 ⁱ
Water	11.13 ^{cde}	11.00 ^{def}	14.20 ^a	9.99 ^{d-h}	7.94 ^{jk}	4.56 ^{c-f}	5.11 ^{a-d}	5.54 ^{ab}	3.50 ^{ghi}	3.67 ^{ghi}
PEG 6000	10.34 ^{d-g}	10.44 ^{d-g}	13.47 ^{ab}	8.73 ^{h-k}	7.70 ^{jk}	5.54 ^{ab}	4.62 ^{c-f}	4.68 ^{b-e}	3.08 ⁱ	3.38 ^{hi}
Thiamine	11.48 ^{cd}	11.34 ^{cde}	13.66 ^{ab}	9.51 ^{f-i}	7.85 ^{jk}	5.12 ^{a-d}	5.34 ^{abc}	5.22 ^{a-d}	3.41 ^{hi}	3.28 ^{hi}
Mannitol	10.80 ^{def}	11.42 ^{cd}	14.36 ^a	10.82 ^{def}	8.15 ^{ijk}	5.21 ^{a-d}	5.69 ^a	5.85 ^a	4.55 ^{c-f}	3.23 ^{hi}

** , All values shown in a block with different letters are dissimilar according to DMRT at P<0.01 level of significance

The longest roots with mannitol priming for all temperature levels are shown in Table 4. Hydro priming, PEG 6000 and thiamine-based priming also clearly enhanced root length at 10 and 15 °C. Significant drops in root length were observed for all priming treatments at 25 and 30 °C. The minimum root length (3.04 cm) was obtained in control at 30 °C.

Seedling fresh weight had maximum values at 20 °C for all priming treatments (Table 5). The heaviest seedling fresh weight (582.5 mg plant⁻¹) was recorded after mannitol priming at 20 °C.

Table 5- Impact of priming on fresh and dry weights of hemp seedlings at different growing temperatures

Priming	Fresh weight (mg plant ⁻¹)					Dry weight (mg plant ⁻¹)				
	10 °C	15 °C	20 °C	25 °C	30 °C	10 °C	15 °C	20 °C	25 °C	30 °C
Control	205.0 ^{ghi}	292.5 ^{c-g}	395.0 ^{bc}	220.0 ^{f-i}	160.0 ^{hi}	14.50 ^j	24.50 ^{f-j}	35.75 ^{cde}	34.00 ^{d-g}	17.25 ^{ij}
Water	230.0 ^{e-h}	297.5 ^{c-g}	487.5 ^b	322.5 ^{c-f}	197.5 ^{ghi}	21.50 ^{hij}	28.25 ^{e-h}	45.00 ^{abc}	41.50 ^{a-d}	22.25 ^{hij}
PEG6000	257.5 ^{e-h}	247.5 ^{e-h}	285.0 ^{d-g}	207.5 ^{ghi}	122.5 ⁱ	16.75 ^{ij}	24.00 ^{g-j}	39.00 ^{bcd}	36.50 ^{b-e}	17.50 ^{ij}
Thiamine	240.0 ^{e-h}	237.5 ^{e-h}	380.0 ^{cd}	272.5 ^{d-g}	300.0 ^{c-g}	17.75 ^{hij}	26.75 ^{e-i}	46.00 ^{ab}	46.25 ^{ab}	24.75 ^{f-j}
Mannitol	330.0 ^{c-f}	335.0 ^{cde}	582.5 ^a	250.0 ^{e-h}	295.0 ^{c-g}	17.00 ^{ij}	34.50 ^{def}	51.00 ^a	34.00 ^{d-g}	18.50 ^{hij}

** , All values shown in a block with different letters are dissimilar according to DMRT at P<0.01 level of significance

Dry weight gains at low and high temperatures (10 and 30 °C) were reduced in all priming treatments compared to their weight at other temperatures. Seedling dry weights with all priming treatments reached their highest values at 20 and 25 °C. The maximum dry weight (51.00 mg plant⁻¹) was obtained at 20 °C after mannitol priming treatment.

3.3 Leaf chlorophyll index and proline content

The minimum chlorophyll index values were observed for all treatments at 10 °C (Table 6). Only seedlings of PEG 6000 primed seeds with 34.83 SPAD value had significant differences compared to control and other osmo priming treatments. Chlorophyll index reached its highest value at 25 °C and the maximum value was obtained for thiamine priming with 56.03 SPAD value. Especially seedlings obtained from thiamine priming at 25 °C had the highest chlorophyll index. Thiamine and mannitol priming especially at 25 and 30 °C resulted in better chlorophyll index compared to controls.

Table 6- Impact of priming on chlorophyll and proline content in seedling leaves of hemp at different growing temperatures

Priming	Chlorophyll index (SPAD)					Leaf proline content (μmol g ⁻¹)				
	10 °C	15 °C	20 °C	25 °C	30 °C	10 °C	15 °C	20 °C	25 °C	30 °C
Control	29.64 ⁱ	35.81 ^g	49.19 ^{b-e}	46.59 ^{cde}	46.21 ^{de}	0.96 ^{ij}	1.49 ^{ghi}	1.94 ^{d-h}	2.43 ^{bcd}	1.39 ^{hi}
Water	31.49 ^{hi}	34.99 ^{gh}	48.22 ^{b-e}	50.05 ^{bcd}	49.77 ^{bcd}	0.55 ⁱ	1.34 ^{hi}	1.76 ^{e-h}	2.79 ^b	1.48 ^{ghi}
PEG6000	34.83 ^{gh}	35.94 ^g	45.31 ^e	48.87 ^{b-e}	48.90 ^{b-e}	0.97 ^{ij}	1.49 ^{ghi}	2.38 ^{bcd}	2.09 ^{c-f}	1.67 ^{fgh}
Thiamine	30.79 ⁱ	36.40 ^g	50.00 ^{bcd}	56.03 ^a	50.87 ^{bc}	0.59 ⁱ	1.40 ^{ghi}	2.27 ^{b-e}	2.48 ^{bcd}	1.93 ^{d-h}
Mannitol	30.38 ⁱ	41.17 ^f	50.37 ^{bcd}	51.95 ^b	51.30 ^b	0.71 ^j	1.99 ^{d-g}	2.37 ^{bcd}	3.94 ^a	2.59 ^{bc}

** , All values shown in a block with different letters are dissimilar according to DMRT at P<0.01 level of significance

Proline level increased at room temperatures of 20 and 25 °C and decreased at 30 °C. The minimum proline levels were noted in all treatments at 10 °C. The maximum proline level 3.94 μmol g⁻¹ was obtained in seedlings from mannitol-primed seedlings at 20 °C. The seed treatments did not improve leaf proline contents at 10 and 15 °C compared to the control treatment.

4. Discussion

4.1 Germination and Emergence tests

The study's results revealed that increasing temperatures shortened the mean germination time. Seed treatments including hydro priming, -0.8 Mpa PEG 6000, thiamine, and mannitol priming at 10, 15, 20, and 30 °C had positive impacts on the acceleration

of germination, and mobilized responses for the early growth of hemp seedlings under low temperatures. Decreasing time of germination using hydro priming under the low and room temperature conditions is very encouraging and similar enhancing results were reported for canola (Day 2022). The impact of temperature on germination was similar to results by Geneve et al. (2022) who reported that seed germination of hemp was highest at 19 °C.

Seedling emergence is directly influenced by vigour because this shows the ability of seeds to emerge under optimal or adverse field conditions (Kandasamy et al. 2020). All treatments were effective in enhancing germination and emergence indexes. Emergence index values were found to be statistically significant, with values at 20 °C superior to other temperatures. Osmo priming with PEG 6000 decreased the emergence index and this treatment led to retarded emergence at 20 °C compared to control and other treatments.

It was noteworthy that increasing temperatures shortened the time to emergence of the hemp seeds. However, the results suggest taking care in the selection of chemicals for priming treatments because dissimilar chemical agents were not equally effective to shorten the seedling emergence time at different temperatures.

Although hydro primed seeds at 10 °C had a reduced time of 12.99 d for emergence, the control treatment and emergence due to other priming treatments and control treatments had insignificantly different emergence times. It is well known that low temperatures may have full or partial negative delaying effects on seed germination and seedling emergence at low temperatures. In this study, the accelerating impact of seed pre-treatments on seedling emergence, especially for low temperatures, was not seen.

Emergence percentage was enhanced by seed treatments at 10 °C, it increased from 46% in control to 58% with thiamine treatment. All the treatments were effective to improve emergence at 10 °C but there was no significant difference in priming treatments. At all other temperatures, seed pre-treatments did not show significant differences compared to control. Particularly at 20 °C higher germination percentage values were observed compared to lower or higher temperatures. The promoting effects seen with thiamine (incipient thiol) and mannitol priming could be explained by the increased activity of thiol-dependent physiological reactions during germination and seedling growth. In plants, mannitol is an osmolyte and protects thiol-regulated enzymes (e.g., phosphoribulokinase) against hydroxyl radicals, which are abundant during the oxidative stress process and remobilization of stored nutrients during germination (Neumann et al. 1999; Shen et al. 1997).

4.2 Seedling growth parameters

Seed priming promoted seedling growth of hemp at all temperatures. Particularly while mannitol priming at low temperatures and 20 °C helped seedlings to gain more weight, thiamine and hydro priming supported weight gain at 25 and 30 °C. Thiamine efficiency increasing at 25 and 30 °C due to thiamine priming is clearly demonstrated in this study. Thiamine biosynthesis is light dependent and photosynthetic tissues are the main process area (Mozafar & Oertli 1993). The thiamine reserves are stored in seed embryos (Sherwood et al. 1941; Belanger et al. 1995) and influence their elongation and growth, facilitating early and prolonged growth of crop plants and improving chlorophyll pigmentation along with photosynthesis.

Mannitol enrichment of seeds via priming in the present study significantly increased seedling growth parameters and biomass, especially at low temperatures. This enhancement could be attributed to the role of mannitol in cellular osmotic adjustments and its role in scavenging hydroxyl radicals ($\bullet\text{OH}$) (Srivastava et al. 2010; Kaya et al. 2013). During seed priming or seed germination in field conditions, seeds face stress factors related to the seed itself or the environment. Mannitol was shown to have a supporting impact on hemp seed germination and early growth at low temperatures in this study.

4.3 Leaf chlorophyll index and proline content

Chlorophyll pigments are the main constituents of chloroplasts, which regulate the rate and the process of photosynthesis. It is reported that the SPAD value used in chlorophyll measurement is mainly related with nitrogen in plants and is sensitive to environmental stress. Thiamine priming of hemp, especially at 25 and 30 °C, significantly influenced the relative greenness (SPAD value) due to thiamine's role in carbon assimilation (photosynthesis) and respiration. Furthermore, thiamine-based priming led to increased thiamine reserves in hemp seeds and less energy was used for thiamine biosynthesis in chloroplasts. Previous studies also reported a positive impact of exogenous thiamine and thiamine priming on photosynthetic pigments (Bahuguna et al. 2012). Apart from thiamine accumulation in plants during abiotic stress, its exogenous application could provide resistance against abiotic stresses (Kaya et al. 2015; Ghaffar et al. 2019).

Chloroplasts and mitochondria are the main places where proline catabolism occurs (Raza et al. 2023). During the development of chloroplasts, the number, size and composition of plastids change depending on the environmental factors. Particularly, low temperature is an adverse environmental signal that alters processes during development of chloroplasts and influences other issues such as chlorophyll biosynthesis, light energy absorption, and photosynthetic electron transport occurring in chloroplasts (Liu et al. 2018). The low level of chlorophyll index and proline contents at low temperatures could be attributed to retarded and decreased chloroplast development during early seedling growth of hemp.

5. Conclusions

Germination and early seedling growth stages are the most important stages in all crops. Hemp is globally important due to its fibre and chemical constituents, which makes its cultivation important. Its cultivation area is expanding due to changing climate conditions and increasing demand. With increasing cultivation area, hemp could experience different temperature stresses during germination and early seedling growth. The plant is vulnerable to temperature stress in these stages. Overcoming temperature stress is important for hemp development. Hemp seeds primed with water, thiamine, and mannitol had the highest biomass values at low, optimum, and high temperatures in this research, which makes these seed treatments suitable for hemp plants that could experience low or high temperatures during germination and early growth stages.

In conclusion, the following results were observed; accelerated mean germination time and increases in emergence percentage at lower temperatures. Root length promoting effects of seed pre-treatments were more evident at 10, 15, and 20 °C. Seedling fresh and dry weight reached maximum values at 20 °C with water, thiamine and mannitol treatments. Chlorophyll and leaf proline content reached their highest values at 20, 25 and 30 °C.

References

- Abdul-Baki A A & Anderson J D (1973). Vigor determination in soybean by multiple criteria. *Crop Science* 13: 630-633
- Bahuguna R N, Joshi R, Shukla A, Pandey M & Kumar J (2012). Thiamine primed defense provides reliable alternative to systemic fungicide carbendazim against sheath blight disease in rice (*Oryza sativa* L.). *Plant Physiology and Biochemistry* 57: 159-167. <https://doi.org/10.1016/j.plaphy.2012.05.003>
- Bates L S, Waldren R A & Teare I D (1973). Rapid determination of free proline for water-stress studies. *Plant and Soil* 39: 205-207
- Belanger F C, Leustek T, Chu B & Kriz A L (1995). Evidence for the thiamine biosynthetic pathway in higher-plant plastids and its developmental regulation. *Plant Molecular Biology* 29: 809-821. <https://doi.org/10.1007/BF00041170>
- Bourioug M, Ezzaza K, Bouabid R, Alaoui-Mhamdi M, Bungau S, Bourgeade P, Alaoui-Sossé L, Alaoui-Sossé B & Aleya L (2020). Influence of hydro- and osmo-priming on sunflower seeds to break dormancy and improve crop performance under water stress. *Environmental Science and Pollution Research* 27: 13215–13226. <https://doi.org/10.1007/s11356-020-07893-3>
- Cha-um S, Thadavong S & Kirdmanee C (2009). Effect of mannitol-induced osmotic stress on proline accumulation, pigment degradation, photosynthetic abilities and growth characters in C3 rice and C4 sorghum. *Frontiers of Agriculture in China* 3: 266–273. <https://doi.org/10.1007/s11703-009-0063-5>
- Day S (2016). Determining the impact of excessive boron on some growth characters and some nutrients at the early growth stage of sunflower (*Helianthus annuus* L.). *Fresenius Environmental Bulletin* 25(10): 4294-4298
- Day S, Çıkılı Y & Aasim M (2017). Screening of three safflower (*Carthamus tinctorius* L.) cultivars under boron stress. *Acta Scientiarum Polonorum Hortorum Cultus* 16: 109-116. <https://doi.org/10.24326/asphc.2017.5.11>
- Day S (2021). Secondary metabolites of *Ocimum basilicum* L. In: Walton AA (ed) *Ocimum basilicum*: Taxonomy, cultivation and uses. Nova Science pp. 1–30
- Day S (2022). Impact of seed priming on germination performance of fresh and aged seeds of Canola. *Journal of Agriculture Environment and Food Sciences* 6(1): 37-40. <https://doi.org/10.31015/jaefs.2022.1.6>
- Day S, Abay G, Özgen Y & Önel B (2022). Effect of sulphur treatments on growth parameters and oil yield of black cumin (*Nigella sativa* L.). *Gesunde Pflanzen* 75: 1355-1360. <https://doi.org/10.1007/s10343-022-00793-1>
- Day S & Koçak-Şahin N (2023a). Seed priming with MgCl₂, CaCl₂, and ZnCl₂ as a biofortification based-approach induces changes in anise seedlings emergence. *Phyton-International Journal of Experimental Botany* 92(8): 2461-2471. <https://doi.org/10.32604/phyton.2023.029920>
- Day S & Koçak-Şahin N (2023b). Identification and morphologic characterization of some salt resistant exotic safflower (*Carthamus tinctorius* L.) lines during seedling growth. *Polish Journal of Environmental Studies* 32(4): 1-7. <https://doi.org/10.15244/pjoes/161982>
- Du G, Zhang H, Yang Y, Zhao Y, Tang K & Liu F (2022). Effects of gibberellin pre-treatment on seed germination and seedling physiology characteristics in industrial hemp under drought stress condition. *Life* 12: 1907. <https://doi.org/10.3390/life12111907>
- Essemine J, Ammar S & Bouzid S (2010). Impact of heat stress on germination and growth in higher plants: Physiological, biochemical and molecular repercussions and mechanisms of defence. *Journal of Biological Sciences* 10(6): 565-572
- Geneve R L, Janes E W, Kester S T, Hildebrand D F & Davis D (2022). Temperature limits for seed germination in industrial hemp (*Cannabis sativa* L.). *Crops* 2(4): 415-427. <https://doi.org/10.3390/crops2040029>
- Ghaffar A, Akram NA, Ashraf M, Ashraf M Y & Sadiq M (2019). Thiamin-induced variations in oxidative defense processes in white clover (*Trifolium repens* L.) under water deficit stress. *Turkish Journal of Botany* 43(1): 58–66. <https://doi.org/10.3906/bot-1710-34>
- Habiba U, Ali S, Rizwan M, Ibrahim M, Hussain A, Shahid M R, Alamri SA, Alyemeni MN & Ahmad P (2019). Alleviative role of exogenously applied mannitol in maize cultivars differing in chromium stress tolerance. *Environmental Science and Pollution Research* 26: 5111–5121. <https://doi.org/10.1007/s11356-018-3970-2>
- Hema R, Vemanna R S, Sreeramulu S, Reddy C P, Senthil-Kumar M & Udayakumar M (2014). Stable expression of mtID gene imparts multiple stress tolerance in finger millet. *PLoS ONE*, 9: e99110. <https://doi.org/10.1371/journal.pone.0099110>
- ISTA (2017). International Rules for Seed Testing, International Seed Testing Association, Basserdorf, Switzerland

- Jabeen M, Akram N A, Ashraf M, Tyagi A, El-Sheikh M A & Ahmad P (2022). Thiamin stimulates growth, yield quality and key biochemical processes of cauliflower (*Brassica oleracea* L. var. *Botrytis*) under arid conditions. *PLoS ONE* 17(5): e0266372. <https://doi.org/10.1371/journal.pone.0266372>
- Kandasamy S, Weerasuriya N, Gritsiouk D, Patterson G, Saldias S, Ali S & Lazarovits G (2020). Size variability in seed lot impact seed nutritional balance, seedling vigor, microbial composition and plant performance of common corn hybrids. *Agronomy* 10(2): 157. <https://doi.org/10.3390/agronomy10020157>
- Kaya C, Sonmez O, Aydemir S, Ashraf M & Dikilitas M (2013). Exogenous application of mannitol and thiourea regulates plant growth and oxidative stress responses in salt-stressed maize (*Zea mays* L.). *Journal of Plant Interaction* 8(3): 234-241. <https://doi.org/10.1080/17429145.2012.725480>
- Kaya C, Ashraf M, Sonmez O, Tuna A L, Polat T & Aydemir S (2015). Exogenous application of thiamine promotes growth and antioxidative defense system at initial phases of development in salt-stressed plants of two maize cultivars differing in salinity tolerance. *Acta Physiologicae Plantarum* 37: 1741–1753. <https://doi.org/10.1007/s11738-014-1741-3>
- Lemmens E, Deleu L J, De Brier N, De Man W L, De Proft M, Prinsen E & Delcour J A (2019). The impact of hydro-priming and osmo-priming on seedling characteristics, plant hormone concentrations, activity of selected hydrolytic enzymes, and cell wall and phytate hydrolysis in sprouted wheat (*Triticum aestivum* L.). *ACS Omega* 4(26): 22089-22100. <https://doi.org/10.1021/acsomega.9b03210>
- Liu X, Zhou Y, Xiao J & Bao F (2018). Effects of chilling on the structure, function and development of chloroplasts. *Frontiers in Plant Science* 9: 1715. <https://doi.org/10.3389/fpls.2018.01715>
- Lo Bianco R, Rieger M & Sung S J S (2000). Effect of drought on sorbitol and sucrose metabolism in sinks and sources of peach. *Physiologia Plantarum* 108: 71–78. <https://doi.org/10.1034/j.1399-3054.2000.108001071.x>
- Michel B E & Kaufmann M R (1973). The osmotic potential of polyethylene glycol 6000. *Plant Physiology* 51(5): 914-6. <https://doi.org/10.1104/pp.51.5.914>
- Mozafar A & Oertli J J (1993). Thiamin (vitamin B1): translocation and metabolism by soybean seedling. *Journal of Plant Physiology* 142(4): 438-445. [https://doi.org/10.1016/S0176-1617\(11\)81249-6](https://doi.org/10.1016/S0176-1617(11)81249-6)
- Neumann G, Preißler M, Azaizeh H A & Römheld V (1999). Thiamine (vitamin B1) deficiency in germinating seeds of *Phaseolus vulgaris* L. exposed to soaking injury. *Zeitschrift für Pflanzenernährung und Bodenkunde* 159(5): 491-498. <https://doi.org/10.1002/jpln.1996.3581590512>
- Odieka A E, Obuzor G U, Oyedeji O O, Gondwe M, Hosu Y S & Oyedeji A O (2022). The medicinal natural products of *Cannabis sativa* Linn.: A Review. *Molecules* 27(5): 1689. <https://doi.org/10.3390/molecules27051689>
- Rapala-Kozik M, Kowalska E & Ostrowska K (2008). Modulation of thiamine metabolism in *Zea mays* seedlings under conditions of abiotic stress. *Journal of Experimental Botany* 59: 4133-4143. <https://doi.org/10.1093/jxb/ern253>
- Raza A, Charagh S, Abbas S, Hassan M U, Saeed F, Haider S, Sharif R, Anand A, Corpas F J, Jin W & Varshney R K (2023). Assessment of proline function in higher plants under extreme temperatures. *Plant Biology* 25(3): 379-395. <https://doi.org/10.1111/plb.13510>
- Shen B O, Jensen R G & Bohnert H J (1997). Increased resistance to oxidative stress in transgenic plants by targeting mannitol biosynthesis to chloroplasts. *Plant Physiology* 113(4): 1177-1183. <https://doi.org/10.1104/pp.113.4.1177>
- Sherwood R C, Nordgren R & Andrews J S (1941). Thiamin in the products of wheat milling and in bread. *Cereal Chemistry* 18: 811-819
- Shrestha A, Pradhan S, Shrestha J & Subedi M (2019). Role of seed priming in improving seed germination and seedling growth of maize (*Zea mays* L.) under rain fed condition. *Journal of Agriculture and Natural Resources* 2(1): 265-273. <https://doi.org/10.3126/janr.v2i1.26088>
- Srivastava A K, Ramaswamy N K, Suprasanna P & D'Souza S F (2010). Genome-wide analysis of thiourea-modulated salinity stress responsive transcripts in seeds of *Brassica juncea*: identification of signalling and effector components of stress tolerance. *Annals of Botany* 106: 663-74. <https://doi.org/10.1093/aob/mcq163>
- Suohui T, Yanping C, Shuhui Z, Zhihua L, Honggang J, Jun L & Tao L (2022). Thiamine induces resistance in tobacco against black shank. *Australasian Plant Pathology* 51(2): 231-243. <https://doi.org/10.1007/s13313-021-00848-3>
- Tunc-Ozdemir M, Miller G, Song L, Kim J, Sodek A, Koussevitzky S, Misra A N, Mittler R & Shintani D (2009). Thiamine confers enhanced tolerance to oxidative stress in *Arabidopsis*. *Plant Physiology* 151: 421–432. <https://doi.org/10.1104/pp.109.140046>
- Visković J, Zheljajzkov V D, Sikora V, Noller J, Latković D, Ocamb C M & Koren A (2023). Industrial Hemp (*Cannabis sativa* L.) agronomy and utilization: A Review. *Agronomy* 13(3): 931. <https://doi.org/10.3390/agronomy13030931>
- Yildiz M, Ozcan S, Telci C, Day S & Ozat H (2010). The effect of drying and submersion pretreatment on adventitious shoot regeneration from hypocotyl explants of flax (*Linum usitatissimum* L.). *Turkish Journal of Botany* 34(4): 323-328. <https://doi.org/10.3906/bot-0912-276>





Creation of Gold Nanoparticles with the Use of *Nigella sativa* L. Plant Extract Derived from Agricultural Waste Components and Its Potential as a Biomedical Agent

Mehmet Fırat Baran^{a*} 

^aBatman University, Vocational School of Technical Sciences, Food Technology program, 72000, Batman, TÜRKİYE

ARTICLE INFO

Research Article

Corresponding Author: Mehmet Fırat Baran, E-mail: mfiatbaran@gmail.com

Received: 24 October 2023 / Revised: 10 February 2024 / Accepted: 11 February 2024 / Online: 23 July 2024

Cite this article

Baran M F (2024). Creation of Gold Nanoparticles with the Use of *Nigella sativa* L. Plant Extract Derived from Agricultural Waste Components and Its Potential as a Biomedical Agent. *Journal of Agricultural Sciences (Tarim Bilimleri Dergisi)*, 30(3):570-583. DOI: 10.15832/ankutbd.1380667

ABSTRACT

In this study, gold nanoparticles were rapidly synthesized with a low-cost and environmentally friendly approach through the extract prepared using agricultural waste parts of the *Nigella sativa* L. plant. Properties of gold nanoparticles from *N. sativa* leaf extract UV-visible Spectrophotometer, X-ray diffraction, Electron Disperse X-ray, Zeta potential and Zetasizer, Field Emission Scan Electron Microscopy (FESEM), Atomic Power Microscopy, Transmission Electron Microscopy (TEM), thermogravimetric and differential thermal analysis characterized by its data. It was observed that the morphologies of the synthesized gold nanoparticles (AuNPs) exhibited a spherical appearance with an average size distribution of 107 nm and a monodisperse. In addition, they were found to be stable structures at -17.7 mV surface charge, and maximum

absorbance at 538.41 nm. For the usability of AuNPs as biomedical agents, antimicrobial and anticancer effects were evaluated using Microdilution and MTT methods, respectively. It was determined that AuNPs were effective in suppressing the proliferation of 0.02-1.00 µg/mL concentration range on *Staphylococcus aureus* ATCC 29213, *Bacillus subtilis* ATCC 11774, *Escherichia coli* ATCC25922, *Pseudomonas aeruginosa* (ATCC27833) and *Candida albicans* pathogenic strains. The viability of CaCo-2, Skov-3, and U118 cancer cells was effectively inhibited by the produced AuNPs by, respectively, 66.73%, 30.93%, and 23.23%. It has been determined that AuNPs have significant antimicrobial and anticancer effects on hospital pathogens and cancer cell lines.

Keywords: Antimicrobial, Gold nanoparticles, FESEM, MTT, TEM analysis

1. Introduction

The field of nanotechnology is continuously expanding at a rapid pace. Within this domain, there is a growing interest in the study that focuses on the construction of structures that possess superior qualities at the nanoscale. Of particular importance in this sector is the research and development of technologies for the manufacturing of metallic nanoparticles as well as the application areas for these nanoparticles. Metallic nanoparticles contribute a lot to these fields with their superior qualities such as chemical, thermal, optical, magnetic, conductivity, and electronics in nano science and technological fields (Jafarizad et al. 2019; Firdhouse & Lalitha 2020; Punnoose & Mathew 2022). AuNPs, which are nanoscale structures, have many uses in medical applications (Attar & Yapaoz 2018; Donga et al. 2020; Rautray & Rajananthini 2020; Padalia & Chanda 2021) and theranostic applications of various diseases (Parida et al. 2011; Velmurugan et al. 2014; Patra et al. 2015; Kumar et al. 2017; Baran 2019; Mohammadi et al. 2019; Latha et al. 2019; Abu-Dief et al. 2020; Arroyo et al. 2020; Rautray & Rajananthini 2020), in catalysis studies (Zayadi et al. 2019), and in dye removal (Latha et al. 2019).

The manufacture of AuNPs calls for the utilisation of a wide range of methodologies, including biological, chemical, and physical approaches. The use of biological sources in synthesis research has a number of advantages over other approaches, including the ones listed above (Al-ogaidi et al. 2017; Patil et al. 2018; Rolim et al. 2019; Baran & Saydut 2019; Barabadi et al. 2020; Korani et al. 2021). Synthesis studies with plant parts (such as leaves, fruits, and flowers) are among the biologically sourced methods that are simpler, do not pose a threat to human health due to the absence of pathogenicity risk and toxic chemicals, do not require special conditions for welding, obtain more products as a result of synthesis, have a structure that is biocompatible, and bring about low cost advantages. A considerable deal of curiosity is generated by these, not just within the realm of biological approaches but also among other methods (Mythili et al. 2018; Parveen et al. 2019; Nor Azlan et al. 2020; Baran et al. 2021; Chen et al. 2021; Ercan 2023).

In the process of forming AuNPs, the extract that is prepared from plants contains a variety of components that act as reducing agents. These components include flavonoids, vitamins, phenolics, amino acids, polysaccharides, and so on. Following the combination of the extract obtained from plant sources of AuNPs and the metal salt solution, the ionised Au^{+3} valence form in the aqueous structure undergoes bioreduction through the phytochemicals present in the extract, resulting in the transformation of the ionised Au^{+3} valence form into Au^0 (AuNPs) (Shankar et al. 2016; Some et al. 2019; Donga et al. 2020; Korani et al. 2021).

Ranunculaceae is the family that includes the herbaceous, annual, self-growing, trichome-covered plant known as *N. sativa*. This plant can grow anywhere from 40 to 90 centimetres in height. This herb, which has been around for two thousand years, has made its way from Asia to Europe and Africa. A perennial plant native to Southern Europe and Western Asia, *N. sativa* is a member of the Ranunculaceae family and is grown in many regions of the globe. This medicinal plant, which has been used and considered sacred for thousands of years in traditional medicine systems like Unani, Ayurveda, Siddha, and Tibb-ā Nebevī, is used not only as a spice in cuisines around the world but also for gastrointestinal disorders, skin diseases, diabetes, cancer diseases, hair loss, and cosmetic purposes. Utilized in skin care products that fight aging and hair loss. In addition to its use as a spice, it has also been employed in the treatment of a variety of ailments, including bronchitis, asthma, hypertension, eczema, and the flu (Davoudi-Kiakalayeh et al. 2017). In terms of its phytochemical composition, it is distinguished by the presence of over one hundred beneficial chemicals, including thymoquinone, thymol, carvacrol, and nigellidine (Ariamanesh et al. 2019).

The purpose of this research was to characterise the properties of AuNPs produced using an extract derived from agricultural waste parts of the *N. sativa* plant cultivated in the Mardin Kızıltepe region, as well as to assess their potential as biomedical agents (antimicrobial and anticancer). The synthesis of AuNPs using an environmentally friendly method was the primary objective of this study.

2. Material and Methods

2.1. *N. sativa* extract preparation

The plant samples were collected from Mardin (Kızıltepe) in July. Dr. Cumali Keskin from Mardin Artuklu University confirmed the plant samples taxonomic identification. Plant samples were stored in the Herbarium (Voucher No. MAU: 2023-29) of the same institution (İş & Beyathı 2023). Post-harvest agricultural waste parts of the *N. sativa* plant were washed several times in the Mardin Kızıltepe Station region in June. It was kept on blotting paper in room condition. After drying, 100 g leaf sample was taken and boiled in a 1000 mL glass beaker with 400 mL distilled water. It was then cooled and, filtered. The obtained extract was prepared for synthesis.

2.2. Preparation of hydrogen tetrachloroaurate (III) hydrate (HAuCl_4) solution

A metal solution with a concentration of 50 millimolar (mM) was prepared to obtain AuNPs by bioreduction from the solid compound of Alfa Aesar, HAuCl_4 , 99.9% (Kandel, Germany).

2.3. Synthesis of AuNPs

The waste components of the *N. sativa* were utilised in the green synthesis process to produce AuNPs. The straightforward application processes and extremely low cost are two of the benefits of this environmentally safe technology that does not contain any hazardous chemicals. The synthesis of AuNPs in this bottom-up technique is facilitated by redox reactions involving Au^{+3} ions ionised in an aqueous environment; this is possible due to the bioactive components in the plant extract that include amine and hydroxyl groups. Additionally, these components effectively ensure stability and coating. 250 mL of the plant extract and 350 mL of 50 mM HAuCl_4 solution were mixed at 200 RPM at 25 °C for five minutes. It was kept without heat treatment, shaking, etc. The maximum absorbance bands of the structure that caused the color change were examined between 300-800 nm by taking samples from the synthesis medium over time, taking into account the intensity of the color change that occurred over time.

2.4. Characterization of AuNPs

To examine the formation of AuNPs with the color change occurring in the synthesis medium and the characteristic maximum absorbance bands associated with it, scans were made for maximum absorbances in the wavelength range of 300-800 nm in the Perkin Elmer One UV-vis device. The crystal structures of the synthesized AuNPs were evaluated using the Rigaku Miniflex 600 model X-Ray Diffraction Diffractometer (XRD) with measurements taken in the range of 20-80 at 2θ . Using the data obtained from these measurements, the calculation was made using the Debye-Scherrer equation to calculate the crystal nano dimensions (Rautray & Rajananthini 2020; Perveen et al. 2021; Uzma et al. 2021). Element contents of the synthesized particles were determined using RadB-DMAX II computer-controlled Electron Disperse X-ray (EDX). In the examination of mass losses of AuNPs against temperature changes, evaluation was made using Shimadzu TGA-50 Thermogravimetric and Differential Thermal Analysis (TGA-DTA) results at 25-900 °C. In the examination of the morphological structures of the synthesized AuNPs, Jeol Jem 1010 Field Emission Scan Electron Microscopy (FE-SEM) and Transmission Electron Microscopy (TEM)

were additionally identified using Park System XE-100 Atomic Power Microscopy (AFM) micrograph images. To determine the stability of AuNPs, Zeta potential, and Zetasizer analysis data were evaluated, respectively, in examining the surface charges and size distributions through a Marvin. The functional groups of the phytochemicals responsible for the reduction and stability of the synthesized AuNPs were evaluated by the frequency changes of the spectra read between 4000-650 cm^{-1} by Perkin Elmer One Fourier Transformation Infrared spectroscopy (FTIR).

2.5. Antimicrobial suppressing effects of synthesized AuNPs on hospital pathogens

Nosocomial pathogens of AuNPs synthesized by *N. sativa* plant extract, *Staphylococcus aureus* ATCC 29213 (*S. aureus*), *Bacillus subtilis* ATCC 11774 (*B. subtilis*), *Escherichia coli* (*E. coli*) ATCC25922, *Pseudomonas aeruginosa* (ATCC27833) and *Candida albicans* (*C. albicans*) microorganisms on their growth were determined using the Microdilution method (Baran 2018; Baran et al. 2021a; Baran et al. 2021b). Minimum Inhibition Concentration (MIC) values, which play a role in the antimicrobial effect on these microorganisms, were evaluated with this method. All microorganisms were obtained from Artuklu University Microbiology Research Laboratory, Mardin, Turkey. From the synthesised AuNPs, antibiotics, and HAuCl_4 , solutions with a concentration of 32 mg/mL were formed. In the first well of each microplate, microdilutions were performed till a final concentration of 2^{10} . To clarify, each dilution phase involved a reduction in concentration of 50% from the prior well, commencing from the initial well. After mixing the media and AuNPs prepared at different concentrations into the microplate wells, microdilution was performed starting from the first well. Some wells were reserved for other control steps of growth. With the same method, in addition, the suppressive effects of antibiotic and HAuCl_4 solution on the growth of pathogenic strains were examined for comparison purposes. Vancomycin was used for gram positive *S. aureus* and *B. subtilis* strains, colistin for gram negative *P. aeruginosa* and *E. coli* strains, and additionally floconazole antibiotics were used for *C. albicans*. After applying the microdilution method, the microplates were incubated at 37 °C for 24 hours. At the end of the period, reproduction control was performed and MIC was defined.

2.6. Anticancer effects of synthesized AuNPs on cancer cell lines that suppress viability

Cytotoxic effects of synthesized AuNPs on cancer cells were investigated by 3-(4,5-dimethylthiazol-2-yl)-2,5-diphenyl tetrazolium bromide assay (MTT) method (Aktepe et al. 2021; Atalar et al. 2021; Baran et al. 2021a; Baran et al. 2021b) in Dicle University Scientific Research Center, Diyarbakır, Turkey. In the application, Colorectal Adenocarcinoma (Caco-2), Glioblastoma (U118), and Human Ovarian sarcoma (Skov-3) lines were used as cancerous cell lines. In addition to these, cytotoxic effects on the Dermal Fibroblast (HDF) healthy cell line were also evaluated. Experimental applications were carried out in 75 t-flasks. Skov-3 cell line was allowed to grow in RPMI medium, other cell lines were allowed to grow in DMEM medium (Dulbecco Modified Eagle), in an oven at 37 °C with 5% CO_2 and 95% air where humidity conditions were provided. Hemocytometer-controlled cell lines were transferred to 96-well microplate wells and left overnight. Then, AuNPs prepared in varying concentrations were added to the wells and the cells were left to interact with the nanoparticles in an oven at 37 °C for 48 hours. After the interaction, MTT and DMSO solutions were waited for 3 and 15 minutes, respectively. Then, the absorbance spectrum of the cells was examined using MultiScan Go Thermo adjusted to a wavelength of 540 nm. By using these absorbances, the concentrations of AuNPs that suppressed the percent viability on the cells and the IC₅₀ (Concentration that constitutes half of the maximum inhibition) values were calculated using the formulas given below (Ahmed et al. 2019; Awad et al. 2019; Baran et al. 2021; Chen et al. 2021; Kumari et al. 2023)

$$\% \text{ Viability} = G/N \times 100 \quad (1)$$

$$\text{IC}_{50} = (G-N)/N \times 100 \quad (2)$$

In the equality; G= was used instead of absorbance values of cells after interaction with AuNPs, and N= absorbance values of cells in the absence of AuNPs.

3. Results and Discussion

3.1. Characterization of AuNPs

3.2. UV-vis Data of AuNPs

10 minutes after *N. sativa* extract and HAuCl_4 solution were mixed, a color change from yellow to pink-red occurred. With the increase in the intensity of the color change over time, samples were taken from the reaction medium periodically and scans were made for maximum wavelength absorbances using UV-vis (Figure 1). The color change from yellow to pink red occurred due to the formation of AuNPs (Gopinath et al. 2016; Latha et al. 2019; Parveen et al. 2019; Firdhouse & Lalitha 2020). The maximum absorbances obtained in the data were determined at a wavelength of 538.41 nm. These maximum absorbance bands confirmed the formation and existence of Surface Plasma Resonance (SPR) AuNPs, which are formed by the vibrations occurring on the plasma surface due to the formation of AuNPs (González-Ballesteros et al. 2017; Umamaheswari et al. 2018; Latha et al. 2019; Usman et al. 2019; Satpathy et al. 2020a; Chen et al. 2021; Korani et al. 2021; Mandhata et al. 2021).

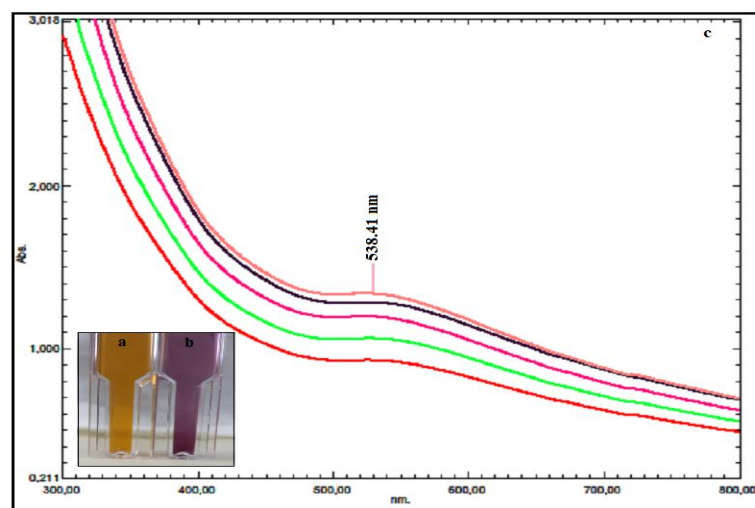


Figure 1- *N. sativa* extract (a), color change due to the formation of synthesized AuNPs (b), and (c) maximum absorbance bands of AuNPs in wavelength scan data

3.3. Crystal pattern and dimensions of synthesized AuNPs via XRD data

Determination of the crystal patterns and nano sizes of the synthesized AuNPs In the analysis performed between 20 and 80 at 2θ using XRD, the presence of Bragg angle expansions taken at the points (111), (200), (220), and (311) in the data, the crystal pattern of AuNPs showed the cubic centered face (fcc) (Figure 2) (Seku et al. 2019; Singh et al. 2019; Kp et al. 2020; Uzma et al. 2021). It has been observed that the structure of the synthesised AuNPs is compatible with the reference card number 05-2870 issued by the Joint Committee on Powder Diffraction Standards (JCPDS). The FWHM values of Bragg angles at points (111), (200), (220), and (311) were found to be 38.45, 44.42, 64.26, and 77.46, respectively. The crystal nanosizes of the synthesized AuNPs were calculated as 20.60 nm using the FWHM value of the high peak (belonging to Bragg's angle) by the Debye-scherrer equation. In the green synthesis studies, it was shown that the crystal nanosizes of AuNPs were calculated as 22.76 nm (Hatipođlu 2021b) and 27.91 nm (Uzma et al. 2021) through the Debye scherrer equation.

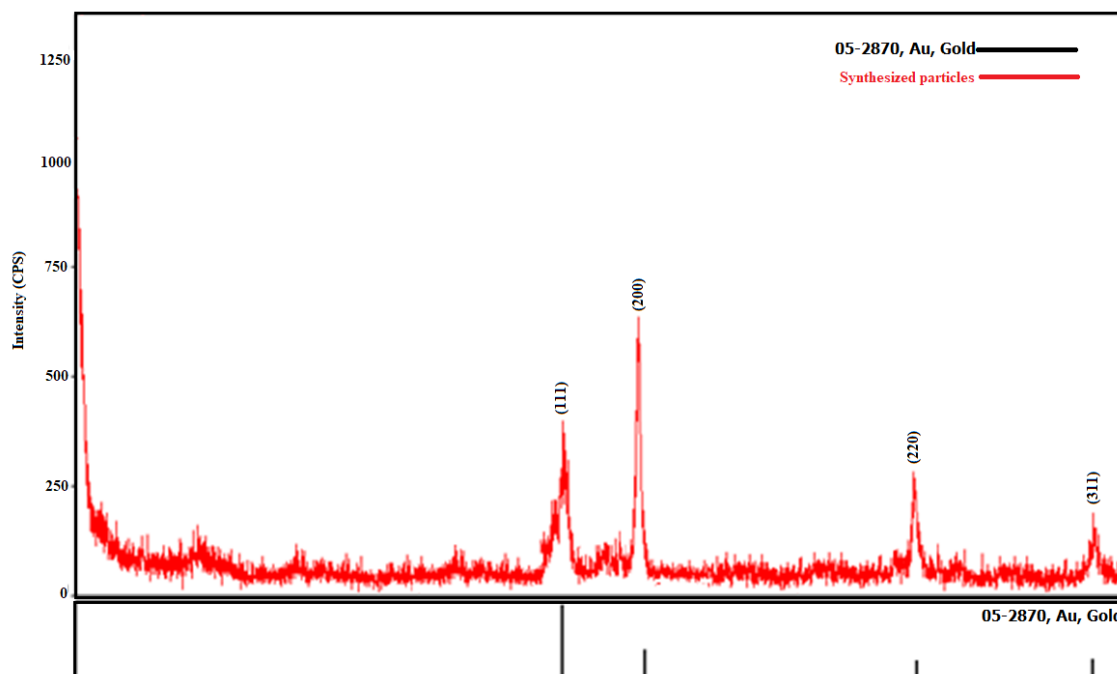


Figure 2- XRD data of the crystal structures of AuNPs synthesized with *N. sativa* extract at 2θ

3.4. Elemental profile of synthesized particles

The EDX profile given in Figure 3 was examined in the analysis of the elemental compositions of the particles synthesized by *N. sativa* extract. The presence of the Au element in the majority of the profile showed that AuNPs were formed. Weak peaks

such as O, and C in the profile were also due to the presence of phytochemicals (Gopinath et al. 2016; Doan et al. 2020; Chen et al. 2021; Hosny et al. 2021; Mandhata et al. 2021; Hosny et al. 2022a).

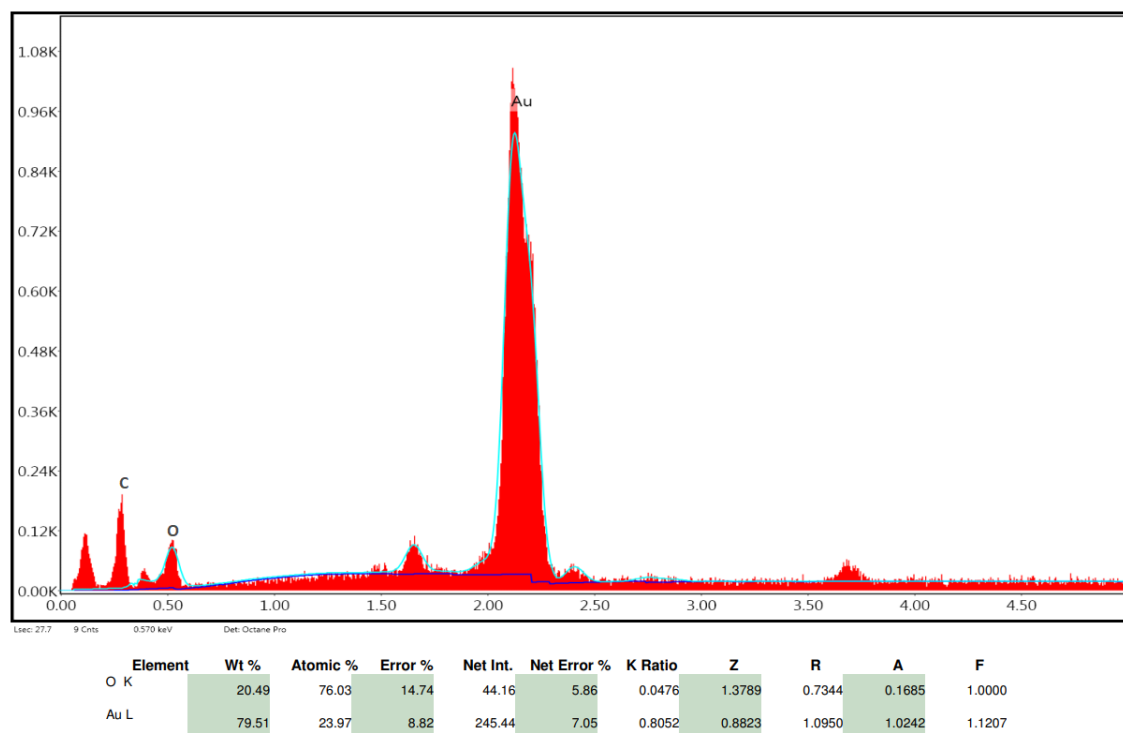


Figure 3- Elemental compositions of *N. sativa* plant extract green post-synthesis particles

3.5. TGA-DTA analysis of AuNPs obtained using *N. sativa* extract

The data obtained by performing TGA-DTA between 0 and 1000 °C for mass losses that may occur with the temperature change of the synthesized particles were evaluated. In the graph given in Table 1 and Figure 4, mass losses were observed at four different temperature points. The first mass loss occurred in the range of 27.10-225.29 °C, and the 3.86% mass loss occurred due to the loss of adsorbed water. Mass losses at 226.33 and 800.45 °C were due to the presence of phytochemicals, which are bioorganic compounds (Baran & Saydut 2019; Doan et al. 2020; Sepahvand et al. 2020; Padalia & Chanda 2021). The negative surface charge of -17.7 mV given in Figure 6 also supported the presence of phytochemicals around the synthesized AuNPs. In addition, the presence of peaks belonging to organic compounds in the EDX data given in Figure 5 confirmed this situation.

Table 1- Temperature points where mass losses occur against the resistance of the synthesized AuNPs to heat treatments ($n=3, \bar{X} \pm S\bar{X}$)

<i>Mass Loss Point</i>	<i>Temperature (°C)</i>	<i>Mass Loss (%)</i>
First	27.10-225.29	3.86±0.28
Second	226.33-350.16	26.59±0.74
Third	351.10-508.90	27.58±0.36
fourth	507.95-800.45	8.20±0.12

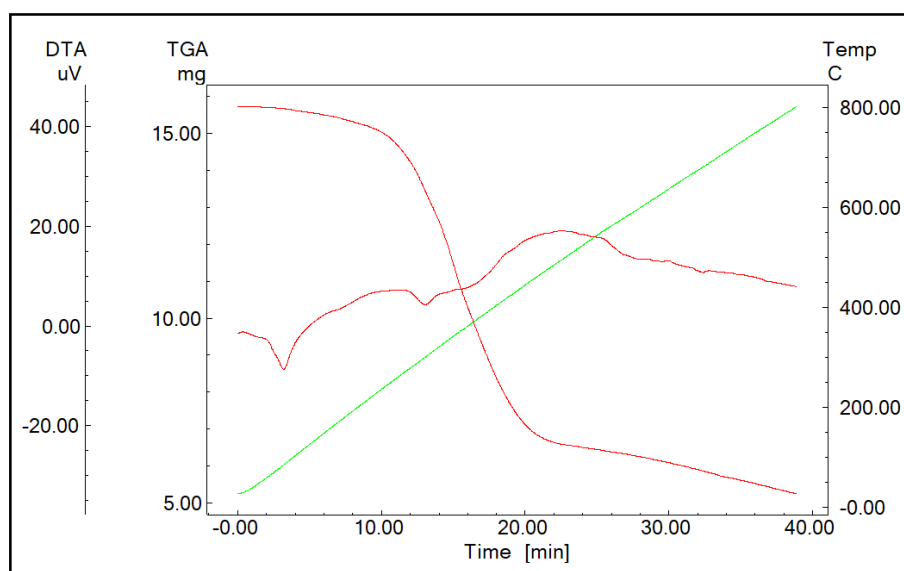


Figure 4- Mass loss points revealed by temperature change in TGA-DTA data of AuNPs obtained as a result of synthesis

3.6. Morphological structures of AuNPs

The morphologies of the synthesized AuNPs were observed spherical in appearance and in a single distribution in the FESEM and TEM images given in Figure 5. AuNPs synthesized with *Annona squamosa* L fruit extract were shown to be spherical and monodisperse in TEM images (Dadigala et al. 2018). In a synthesis study obtained with market plant wastes, it was seen that AuNPs were in spherical morphology (Mythili et al. 2018). In FESEM images of a study with *Elaeis guineensis* leaf extract, AuNPs were spherical in morphology (Ahmad et al. 2018). Similar findings were also found in other environmentally friendly synthesis studies (Ahmad et al. 2018; Usman et al. 2019; Jafarizad et al. 2019; Mousavi-Kouhi et al. 2022). In addition, in the AFM micrograph taken for the morphological structures and topographic distributions of the synthesized AuNPs in Figure 2, it was seen that they had dimensions below about 100 nm, exhibited a monodisperse, and were spherical (Francis et al. 2017; Vinita et al. 2018; Ullah et al. 2019; Rauf et al. 2021).

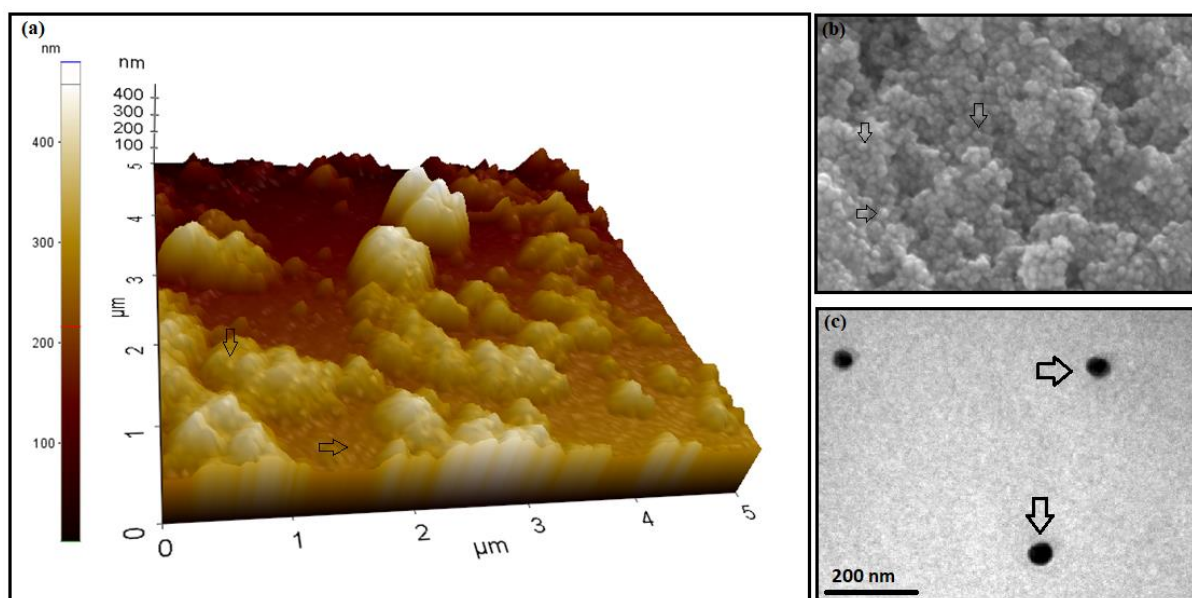


Figure 5- Showing the morphological structures of the synthesized AuNPs; a. AFM, and b. FESEM, and c. TEM micrograph images

3.7. FTIR spectroscopy data

FTIR spectroscopy analysis data were analyzed to examine the functional groups of phytochemicals responsible for bioreduction. In the spectroscopy data given in Figure 6, frequency shifts were observed at 3 different points, $3335.46\text{-}3319.70\text{ cm}^{-1}$, $2124.05\text{-}2115.41\text{ cm}^{-1}$, and $1635.63\text{-}1634.95\text{ cm}^{-1}$. These shifts, respectively, belong to alcohol or phenol groups (O-H), alkyne groups (-

C=C-), and amine groups (-NO), and their reduction of Au⁺³ valent metal in aqueous medium to Au⁰, that is, AuNPs. The findings indicated that hydroxyl/phenol groups, amine groups, and alkyne groups are some of the functional groups that may be involved in the creation and stability of gold nanoparticles (AuNPs) (Usman et al. 2019; Donga et al. 2020; Babu et al. 2020; Baran et al. 2021a).

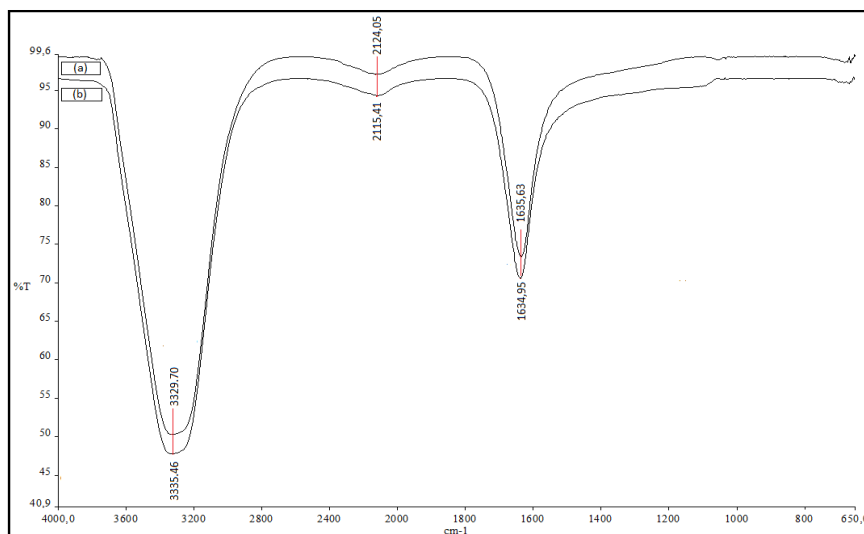


Figure 6- FTIR spectra of functional groups of phytochemicals that are responsible for bioreduction and stability; (a) *N. sativa* and (b) the liquid fraction that was formed as a result of the reaction

3.8. Charge distribution of the surface structures of synthesized AuNPs

The surface charges of AuNPs obtained using *N. sativa* extract are given in Figure 7. The results showed that they had a charge of -17.7 mV. A green synthesis study with *Elaeis guineensis* extract showed AuNPs to be -14.7 mV (Ahmad et al. 2018). In a synthesis study with *Cystoseira baccata* extract, it was shown to be -30.7 mV (González-Ballesteros et al. 2017). In addition, a graph of -19.2 mV surface charges of AuNPs was given in a study conducted with *Cyanthillium cinereum* extract (Punnoose & Mathew 2022).

Phytochemicals (such as alcoloids, and flavonoids) found in plant sources play an important role in stabilization and stability in the negative surface charge formation of AuNPs. The fact that the synthesized particles have only negative surface charges ensures that they are stable and prevents the formation of negative conditions such as aggregation and fluctuation that affect the stability. In addition, AuNPs, which have a negative surface charge, also contribute positively to pH stability, helping them to be effective in challenging circulatory or intracellular physiological conditions. The stable structure of AuNPs also has an important place in medical applications as therapeutic agents (Giljohann et al. 2010; Khan et al. 2019; Webster 2020; Hosny et al. 2022b).

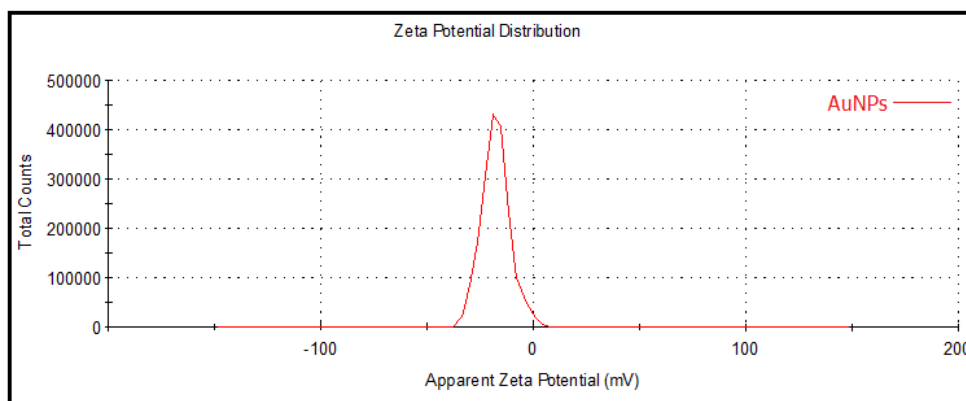


Figure 7- Distribution of surface charges of synthesised AuNPs according to their zeta potential's.

3.9. Density-dependent size distributions of synthesized AuNPs

The hydrodynamic size distributions of the AuNPs that were generated by the extract that was made using waste fractions from *N. sativa* and acquired through DLS are presented in Figure 8. After analysing the data, it was found that the diameters of the

senized AuNPs had a distribution that was, on average, 107 nm. In studies for the synthesis of plant-derived AuNPs, mean zetasize distributions were reported as 96.46 nm (Hatipoğlu 2021b) and 118 nm (Mousavi-Kouhi et al. 2022).

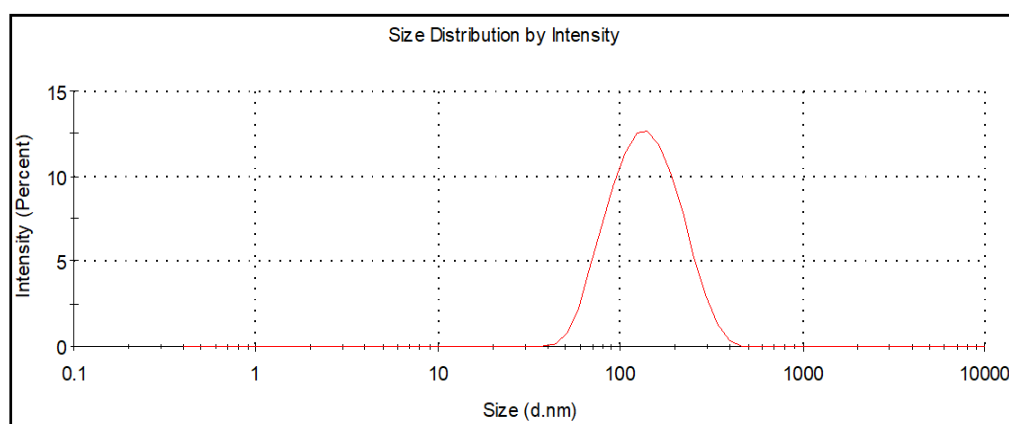


Figure 8- Distribution of density-dependent sizes of synthesized AuNPs

3.10. Antimicrobial suppressing effects of synthesized AuNPs on hospital pathogens

MIC values of AuNPs synthesized using *N. sativa* extract were analyzed by microdilution method in suppressing the growth of hospital pathogen microorganisms. MIC values of 0.02-0.03 $\mu\text{g/mL}$ and 0.50-1.00 $\mu\text{g/mL}$ were determined on the growth of Gram-positive strains and Gram-negatives, respectively. In addition, the MIC value of the synthesized AuNPs on the growth of *C. albicans* was found to be 0.25 $\mu\text{g/mL}$. AuNPs synthesized in all microorganisms except *P. aeruginosa* showed suppression at very low concentrations from both the antibiotic and HAuCl₄ solution. AuNPs, colistin antibiotic, and HAuCl₄ solution showed antimicrobial activity at the same concentration on *Paeruginosa* strain (Figure 9 and Table 2).

The AuNPs may exert antimicrobial effects at different concentrations on different strains. Cell wall structure, components, etc. of some strains cause AuNPs to be effective at different concentrations (Donga et al. 2020). In addition to the concentration, properties such as surface charge, shape, and size also play an important role in the antimicrobial effects of AuNPs (Jha et al. 2017). Since microorganisms and NPs are negatively and positively charged in a liquid medium, respectively, NPs interact with electrostatic attraction (Ahmed et al. 2016; Ferreyra Maillard et al. 2018; Babu et al. 2020). Subsequently, adverse changes occur in wall and membrane morphology, such as disruption of membrane potential and permeability. In addition, AuNPs block ATPase functional activity and cause a decrease in ATP level. AuNPs interact with structures where nitrogen, phosphate, sulfur, and oxygen atoms are highly concentrated, such as proteins (Cui et al. 2012; Donga et al. 2020). Another negative effect of NPs is that by increasing the expression of genes involved in redox reactions, they increase the level of Reactive Oxygen Species (ROS) such as -OH, -SO, and -NO. These species bind to important molecules such as proteins, DNA, lipids, and enzymes and adversely affect their structure and functions. All this accelerates biodegradation and causes the death of microorganisms (Cui et al. 2012; Ahmed et al. 2016; Jha et al. 2017; Donga et al. 2020). It was stated that AuNPs obtained in the green synthesis study with *Jatropha integerrima Jacq* extract were effective MICs at 10.00, 5.00, and 2.5 $\mu\text{g/mL}$ concentrations on *S. aureus*, *B. subtilis*, and *E. coli*, respectively (Suriyakala et al. 2022). In a similar study conducted with the *Paecilomyces variotii* bacterial strain, they found that the MIC VALUE was below 0.064 $\mu\text{g/mL}$. In another synthesis study with *Prunus cerasifera* extract, *S. aureus*, *B. subtilis*, *E. coli*, *P. aeruginosa*, and *C. albicans* 0.25, 0.12, 1.00, 0.50, and 0.50 $\mu\text{g/mL}$ concentrations were reported to be effective in MIC (Hatipoğlu 2021a).

Table 2- MIC values of synthesized AuNPs, antibiotics used for each strain in practice, and HAuCl₄ solution have antimicrobial effects on their growth (n=3, $\bar{X} \pm \bar{Sx}$, 24 Hours)

TESTED ORGANISM	AuNPs* $\mu\text{g/mL}$	HAuCl ₄ Solution** $\mu\text{g/mL}$	Antibiotic*** $\mu\text{g/mL}$
<i>S. aureus</i>	0.02±0.001	0.50±0.007	1.00±0.017
<i>B.subtilis</i>	0.03±0.001	0.25±0.002	1.00±0.015
<i>E. coli</i>	0.50±0.018	1.00±0.069	2.00±0.120
<i>P. aeruginosa</i>	1.00±0.067	1.00±0.032	1.00±0.058
<i>C. albicans</i>	0.25±0.004	0.50±0.016	2.00±0.082

*: Solution containing AuNPs synthesized via extract from *N. sativa* waste parts; **: Solution prepared from HAuCl₄ solid compound salt; ***: Solutions prepared from the antibiotics colistin for gram-negatives, vancomycin for gram-positives, and fluconazole for fungi.

Note: The concentration of each solution used in the preparation was 32 $\mu\text{g/mL}$.

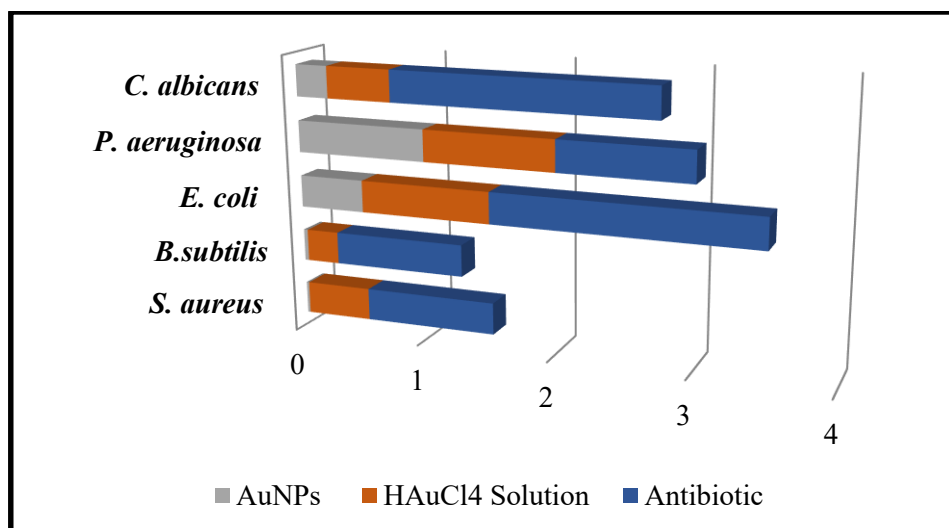


Figure 9- MIC values of AuNPs, HAuCl₄ solution, and antibiotics synthesized on the growth of microorganisms. (AuNPs; AuNPs synthesized through extract obtained from *N. sativa* waste parts, HAuCl₄ Solution; Solution prepared from HAuCl₄ solid compound salt at 32 µg/mL concentration, Antibiotic; Solutions prepared from the antibiotics colistin for gram-negatives, vancomycin for gram-positives, and fluconazole for fungi at a concentration of 32 µg/mL)

3.11. Anticancer effects of synthesized aunps on cancer cell lines that suppress viability

After the interaction of AuNPs synthesized by *N. sativa* extract with cancer cell lines and healthy cell lines for 48 hours, the percent viability of the cells was evaluated. The concentrations of U118, CaCo-2, and Skov-3 cancer cells as well as percent viability suppressing on HDF healthy cell line were determined by the MTT method. As seen in Table 3 and Figure 10, 56.52% viability at 100 µg/mL concentration in the healthy cell line showed that the synthesized AuNPs had no toxic effect. The same concentration caused suppression of 39.93%, 66.73%, and 23.23% in Skov-3, CaCo-2, and U118 cancer cells. It was observed that the concentration of 100 µg/mL was the most effective on the cancer cell CaCo-2 with 66.73% suppression. Even 25 µg/mL concentration produced 30.76% suppression on CaCo-2 cells. The IC₅₀ values of AuNPs synthesized on HDF, Skov-3, CaCo-2, and U118 cell lines were calculated as 118.88, 429.92, 174.83, and 632.11, respectively.

Some properties of nanoparticles such as concentration, shape, size, surface charge, interaction time, degree of deposition, etc. play an important role in toxicity (Remya et al. 2015; Swamy et al. 2015; Rolim et al. 2019). AuNPs contact cells through chemical adsorption, electrostatic attraction, hydrophobic interaction, or chemical bonds (Doan et al. 2020; Webster 2020; Mehravani et al. 2021). Tumorous and inflammatory tissues have large vascular vessels and their large pores that allow the passage of substances such as nutrients and oxygen to these areas. It allows nanoparticles to easily collect and pass to these points through these pores (Chen et al. 2021; Hosny et al. 2021). AuNPs that pass through the cell membrane cause some negative changes in both the structure and functions of some important biomolecules (such as DNA, Proteins). As a result of these interactions, they activate Caspase enzymes, which play a role in cell death mechanisms such as apoptosis, with the increase of ROS. In addition, they affect mitochondrial permeability and increase cytochrome c release, increasing the propagation of signals to cause apoptosis and causing cell death (Rolim et al. 2019; Webster 2020; Barabadi et al. 2020; Donga et al. 2020; Hosny et al. 2022a).

Table 3- Percent viability rates as a result of cytotoxic effects of synthesized AuNPs on 48 h cell lines (n=3, $\bar{X} \pm S\bar{X}$, 48 Hours)

Cell Lines	25 µg/mL	50 µg/mL	100 µg/mL	200 µg/mL
HDF	86.74±0.011	80.07±0.012	56.52±0.013	14.64±0.030
U118	87.82±0.090	83.78±0.042	76.77±0.044	73.43±0.049
CaCo-2	69.24±0.008	43.17±0.003	33.27±0.003	12.25±0.019
Sk-ov-3	73.90±0.003	66.85±0.008	60.07±0.006	52.15±0.019

Cancer cells: **CaCo-2**; Human Colorectal Adenocarcinoma, **U118**; Human Glioblastoma, and **Skov-3**; Human Healthy cells: **HDF**; Human Dermal Fibroblast

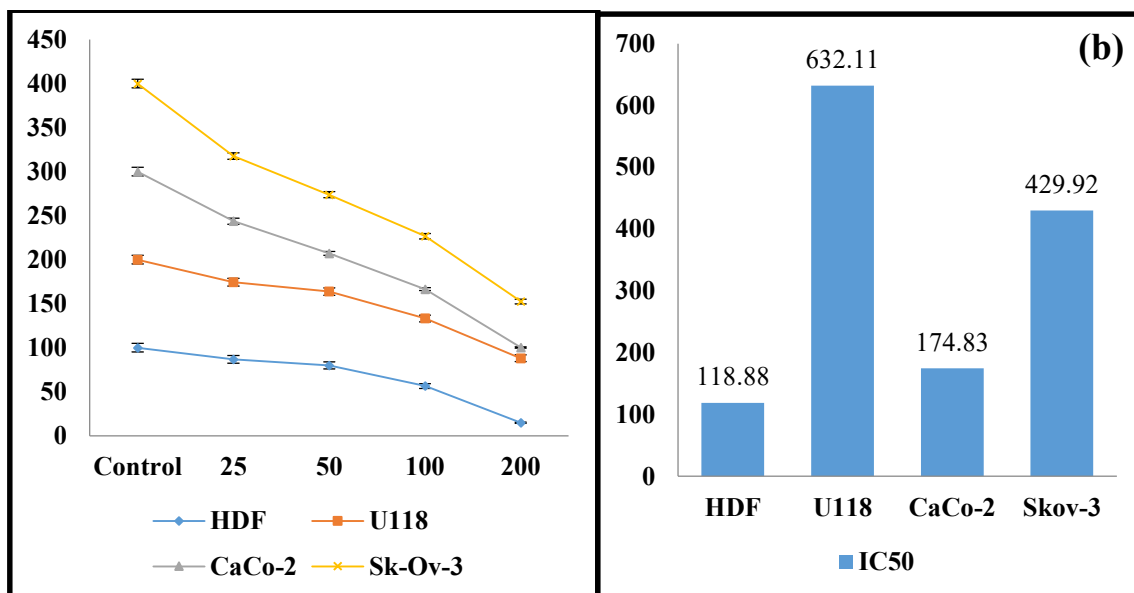


Figure 10- (a) Percent survival rates as a result of the interaction of the synthesized AuNPs with the cell lines for 48 hours via the MTT method, (b) IC50 values of the AuNPs on the cell lines

It was stated that AuNPs synthesized using *Cystoseira baccata* extract were effective on CaCo-2 cancer cells at a concentration of 400 $\mu\text{g/mL}$ (González-Ballesteros et al. 2017). It has been reported that AuNPs synthesized with *Hygrophila spinosa* extract at a concentration of 47.5 $\mu\text{g/mL}$ have a role in suppression of percent viability (Satpathy et al. 2020b). In addition, in some studies, it was reported that AuNPs obtained by green synthesis on different cancer cell lines showed anticancer effects with the MTT method (Chellamuthu et al. 2019; Chellapandian et al. 2019; Webster 2020).

4. Conclusions

N. sativa plant has many medicinal benefits. For this reason, the demand for its production continues to increase day by day. As a result of the products, a large part of the green parts of the plant remains as agricultural waste. In this study, AuNPs were rapidly synthesized with a low-cost, environmentally friendly approach by using the extract prepared from these parts of the plant to recycle these agricultural waste parts into a useful area. The characterization of AuNPs from *N. sativa* leaf extract was determined by UV-vis, XRD, EDX, Zeta potential and Zetasizer, FESEM, AFM, and TGA-DTA. It was observed that the morphology of AuNPs with a maximum absorbance of 538.41 nm was spherical, with a size distribution of 107 nm and monodisperse. The AuNPs synthesized with a surface charge of -17.7 mV were stable. For the usability of AuNPs as biomedical agents, antimicrobial and anticancer effects were investigated using microdilution and the MTT methods, respectively. AuNPs were effective on hospital pathogens at very low concentrations in the range of 0.02-1.00 $\mu\text{g/mL}$ concentrations. The percent viability on cancer cell lines especially CaCo-2 significantly suppressed on cancer cells.

The significant suppression that AuNPs synthesised with the waste parts of *N. sativa* extract show on the pathogenic strains and cancer cells used in practise demonstrates that they have the potential to make a significant contribution to the search for anticancer and antimicrobial agents by improving the conditions under which they are synthesised. It is possible that the evaluation of this in-vitro study in vivo will be of major value to the medical field. It is also possible to undertake a large number of research to investigate its impact on various cancer cells and pathogenic strains.

References

- Abu-Dief A M, Abdel-Rahman L H, Abd-El Sayed M A, Zikry M M & Nafady A (2020). Green Synthesis of AgNPs Utilizing Delonix Regia Extract as Anticancer and Antimicrobial Agents. *Chemistry Select* 5(42): 13263–13268. <https://doi.org/10.1002/slct.202003218>
- Ahmad T, Bustam M A, Irfan M, Moniruzzaman M, Anwaar Asghar H M, & Bhattacharjee S (2018). Green synthesis of stabilized spherical shaped gold nanoparticles using novel aqueous *Elaeis guineensis* (oil palm) leaves extract. *Journal of Molecular Structure* 1159: 167–173. <https://doi.org/10.1016/j.molstruc.2017.11.095>
- Ahmed K B A, Raman T & Veerappan A (2016). Future prospects of antibacterial metal nanoparticles as enzyme inhibitor. *Materials Science and Engineering C* 68: 939–947. <https://doi.org/10.1016/j.msec.2016.06.034>
- Ahmed M J, Murtaza G, Rashid F & Iqbal J (2019). Eco-friendly green synthesis of silver nanoparticles and their potential applications as antioxidant and anticancer agents. *Drug Development and Industrial Pharmacy* 45:1682–1694. <https://doi.org/10.1080/03639045.2019.1656224>
- Aktepe N, Baran A, Atalar M N, Baran M F, Düz M Z, Yavuz Ö, İrtegin Kandemir S & Kavak D E (2021). Biosynthesis of Black Mulberry Leaf Extract and Silver NanoParticles (AgNPs): Characterization, Antimicrobial and Cytotoxic Activity Applications. *MAS Journal of Applied Sciences* 8(8): 685–700. <https://doi.org/10.52520/masjaps.120>

- Al-ogaidi I, Salman M I, Mohammad F I, Aguilar Z, Al, M, Hadi Y A, & Al-rhman R M A (2017). Antibacterial and Cytotoxicity of Silver Nanoparticles Synthesized in Green and Black Tea. *World Journal of Experimental Biosciences* 5(1): 39–45. <https://wjebio.com/index.php/journal/article/view/118>
- Ariamanesh H, Tamizi N, Yazdinezhad A, Salah S, Motamed N & Amanloo S (2019). The Effectiveness of *Nigella Sativa* Alcoholic Extract on the Inhibition of *Candida Albicans* Colonization and Formation of Plaque on Acrylic Denture Plates: an In Vitro Study. *Journal of Dentistry* 20(3): 171–177. <https://doi.org/10.30476/dentjods.2019.44911>
- Arroyo G V, Madrid A T, Gavilanes A F, Naranjo B, Debut A, Arias M T & Angulo Y (2020). Green synthesis of silver nanoparticles for application in cosmetics. *Journal of Environmental Science and Health - Part A Toxic/Hazardous Substances and Environmental Engineering* 55(11): 1304–1320. <https://doi.org/10.1080/10934529.2020.1790953>
- Atalar M N, Baran A, Baran M F, Keskin C, Aktepe N, Yavuz Ö & Irtegun Kandemir S (2021). Economic fast synthesis of olive leaf extract and silver nanoparticles and biomedical applications. *Particulate Science and Technology* 2021: 1–9 <https://doi.org/10.1080/02726351.2021.1977443>
- Attar A & Yapaoz M A (2018). Biosynthesis of palladium nanoparticles using Diospyros kaki leaf extract and determination of antibacterial efficacy. *Preparative Biochemistry and Biotechnology* 48(7): 629–634. <https://doi.org/10.1080/10826068.2018.1479862>
- Awad M A, Eisa N, Virk P, Hendi A A, Ortashi K, Mahgoub A A, Elobeid M M & Eissa F (2019). Green synthesis of gold nanoparticles: Preparation, characterization, cytotoxicity, and anti-bacterial activities. *Materials Letters* 256: 126608. <https://doi.org/10.1016/j.matlet.2019.126608>
- Babu B, Palanisamy S, Vinosha M, Anjali R, Kumar P, Pandi B, Tabarsa M, You S G & Prabhu N M (2020). Bioengineered gold nanoparticles from marine seaweed *Acanthophora spicifera* for pharmaceutical uses: antioxidant, antibacterial, and anticancer activities. *Bioprocess and Biosystems Engineering* 43(12): 2231–2242. <https://doi.org/10.1007/s00449-020-02408-3>
- Barabadi H, Webster T, Vahidi H, Sabori H, Damavandi Kamali K, Jazayeri Shoushtari F, Mahjoub M A, Rashedi M, Mostafavi E, Medina Cruz D, Hosseini O & Saravana M (2020). Green nanotechnology-based gold nanomaterials for hepatic cancer therapeutics: A systematic review. *Iranian Journal of Pharmaceutical Research* 19(3): 3–17. <https://doi.org/10.22037/ijpr.2020.113820.14504>
- Baran M F (2018). Green Synthesis Of Silver Nanoparticles (AgNPs) Using *Pistacia terebinthus* Leaf: Antimicrobial Effect And Characterization. *EJONS International Journal on Mathematic, Engineering and Natural Sciences* 2: 67–75
- Baran M F (2018). Green Synthesis Of Silver Nanoparticles (AgNPs) Using *Pistacia terebinthus* Leaf: Antimicrobial Effect And Characterization. *EJONS International Journal on Mathematic, Engineering and Natural Sciences* 2: 67–75
- Baran M F (2019). Evaluation of Green Synthesis and Anti-Microbial Activities of AgNPs Using Leaf Extract of Hawthorn Plant. *Research and Evaluations in Science and Mathematics* 2019(3): 110–120
- Baran M F & Saydut A (2019). Gold nanomaterial synthesis and characterization. *Dicle University Journal of Engineering* 10(3): 1033–1040. <https://doi.org/10.24012/dumf.551865>
- Baran M F, Keskin C, Atalar M N & Baran A (2021). Environmentally Friendly Rapid Synthesis of Gold Nanoparticles from Artemisia absinthium Plant Extract and Application of Antimicrobial Activities. *Journal of the Institute of Science and Technology* 11(1): 365–375. <https://doi.org/10.21597/jist.779169>
- Baran A, Baran M F, Keskin C, Kandemir S I, Valiyeva M, Mehraliyeva S, Khalilov R & Eftekhari A (2021 a). Ecofriendly/Rapid Synthesis of Silver Nanoparticles Using Extract of Waste Parts of Artichoke (*Cynara scolymus L.*) and Evaluation of their Cytotoxic and Antibacterial Activities. *Journal of Nanomaterials* 2021: 1–10. <https://doi.org/10.1155/2021/2270472>
- Baran A, Keskin C, Baran M F, Huseynova I, Khalilov R, Eftekhari A, Irtegun-Kandemir S & Kavak D E (2021b). Ecofriendly Synthesis of Silver Nanoparticles Using Ananas comosus Fruit Peels: Anticancer and Antimicrobial Activities. *Bioinorganic Chemistry and Applications* 2021: 058149. <https://doi.org/10.1155/2021/2058149>
- Chellamuthu C, Balakrishnan R, Patel P, Shanmuganathan R, Pugazhendhi A & Ponnuchamy K (2019). Gold nanoparticles using red seaweed *Gracilaria verrucosa*: Green synthesis, characterization and biocompatibility studies. *Process Biochemistry* 80(2):58-63 0–1. <https://doi.org/10.1016/j.procbio.2019.02.009>
- Chellapandian C, Ramkumar B, Puja P, Shanmuganathan R, Pugazhendhi A & Kumar P (2019). Gold nanoparticles using red seaweed *Gracilaria verrucosa*: Green synthesis, characterization and biocompatibility studies. *Process Biochemistry* 80(2): 58–63. <https://doi.org/10.1016/j.procbio.2019.02.009>
- Chen J, Li Y, Fang G, Cao Z, Shang Y, Alfarraj S, Ali Alharbi S, Duan X, Yang S & Li J (2021). Green synthesis, characterization, cytotoxicity, antioxidant, and anti-human ovarian cancer activities of *Curcuma kwangsiensis* leaf aqueous extract green-synthesized gold nanoparticles. *Arabian Journal of Chemistry* 14(3): 103000. <https://doi.org/10.1016/j.arabjc.2021.103000>
- Chen X, Xue Z, Ji J, Wang D, Shi G, Zhao L & Feng S (2021). Hedysarum polysaccharides mediated green synthesis of gold nanoparticles and study of its characteristic, analytical merit, catalytic activity. *Materials Research Bulletin* 133(7): 111070. <https://doi.org/10.1016/j.materresbull.2020.111070>
- Cui Y, Zhao Y, Tian Y, Zhang W, Lü X & Jiang X (2012). The molecular mechanism of action of bactericidal gold nanoparticles on *Escherichia coli*. *Biomaterials* 33(7): 2327–2333. <https://doi.org/10.1016/j.biomaterials.2011.11.057>
- Dadigala R, Guttana V, Kotu G M, Bandi R, Gangapuram B R & Alle M (2018). Microwave assisted rapid green synthesis of gold nanoparticles using *Annona squamosa L* peel extract for the efficient catalytic reduction of organic pollutants. *Journal of Molecular Structure* 1167: 305–315. <https://doi.org/10.1016/j.molstruc.2018.05.004>
- Davoudi-Kiakalayeh A, Mohammadi R, Pourfathollah A A, Siery Z & Davoudi-Kiakalayeh S (2017). Alloimmunization in thalassemia patients: New insight for healthcare. *International Journal of Preventive Medicine* 8(101): 1–7. <https://doi.org/10.4103/ijpvm.IJPVM>
- Doan V D, Thieu A T, Nguyen T D, Nguyen V C, Cao X T, Nguyen T L H & Le V T (2020). Biosynthesis of Gold Nanoparticles Using *Litsea cubeba* Fruit Extract for Catalytic Reduction of 4-Nitrophenol. *Journal of Nanomaterials* 2020(1): 1–10. <https://doi.org/10.1155/2020/4548790>
- Donga S, Bhadu G R & Chanda S (2020). Antimicrobial, antioxidant and anticancer activities of gold nanoparticles green synthesized using *Mangifera indica* seed aqueous extract. *Artificial Cells, Nanomedicine and Biotechnology* 48(1): 1315–1325. <https://doi.org/10.1080/21691401.2020.1843470>
- Ercan L (2023). Investigation of Antibacterial and Antifungal Efficacy of Zinc and Silver Nanoparticles Synthesized from *Nasturtium officinale*. *Journal of Agricultural Sciences* 29(3): 788-799. <https://doi.org/10.15832/ankutbd.1163132>
- Ferreira Maillard A P V, Dalmasso P R, López de Mishima B A & Hollmann A (2018). Interaction of green silver nanoparticles with model membranes: possible role in the antibacterial activity. *Colloids and Surfaces B: Biointerfaces* 171(7): 320–326. <https://doi.org/10.1016/j.colsurfb.2018.07.044>

- Firdhouse M J & Lalitha P (2020). Facile synthesis of anisotropic gold nanoparticles and its synergistic effect on breast cancer cell lines. *IET Nanobiotechnology* 14(3): 224–229. <https://doi.org/10.1049/iet-nbt.2019.0279>
- Francis S, Joseph S, Koshy E P & Mathew B (2017). Green synthesis and characterization of gold and silver nanoparticles using Mussaenda glabrata leaf extract and their environmental applications to dye degradation. *Environmental Science and Pollution Research* 24: 17347–17357. <https://doi.org/10.1007/s11356-017-9329-2>
- Giljohann D A, Seferos D S, Daniel W L, Massich M D, Patel P C & Mirkin C A (2010). Gold nanoparticles for biology and medicine. *Angewandte Chemie - International Edition* 49(19): 3280–3294. <https://doi.org/10.1002/anie.200904359>
- González-Ballesteros N, Prado-López S, Rodríguez-González J B, Lastra M & Rodríguez-Argüelles M C (2017). Green synthesis of gold nanoparticles using brown algae *Cystoseira baccata*: Its activity in colon cancer cells. *Colloids and Surfaces B: Biointerfaces* 153: 190–198. <https://doi.org/10.1016/j.colsurfb.2017.02.020>
- Gopinath K, Kumaraguru S, Bhakayaraj K, Mohan S, Venkatesh K S, Esakkirajan M, Kaleeswaran P, Alharbi N S, Kadaikunnan, S, Govindarajan M, Benelli G & Arumugam A (2016). Green synthesis of silver, gold and silver/gold bimetallic nanoparticles using the *Gloriosa superba* leaf extract and their antibacterial and antibiofilm activities. *Microbial Pathogenesis* 101:1 1–11. <https://doi.org/10.1016/j.micpath.2016.10.011>
- Hatipoğlu A (2021a). Green synthesis of gold nanoparticles from *Prunus cerasifera pissardii nigra* leaf and their antimicrobial activities on some food pathogens. *Progress in Nutrition* 23(3): e2021241. <https://doi.org/10.23751/pn.v23i3.11947>
- Hatipoğlu A (2021b). Rapid green synthesis of gold nanoparticles: synthesis, characterization, and antimicrobial activities. *Progress in Nutrition* 23(3): e2021242. <https://doi.org/10.23751/pn.v23i3.11988>
- Hosny M, Fawzy M, Abdelfatah A M, Fawzy E E & Eltaweil A S (2021). Comparative study on the potentialities of two halophytic species in the green synthesis of gold nanoparticles and their anticancer, antioxidant and catalytic efficiencies. *Advanced Powder Technology* 32(9): 3220–3233. <https://doi.org/10.1016/j.apt.2021.07.008>
- Hosny, M., Fawzy, M., El-Badry, Y. A., Hussein, E. E., & Eltaweil, A. S. (2022b). Plant-assisted synthesis of gold nanoparticles for photocatalytic, anticancer, and antioxidant applications. *Journal of Saudi Chemical Society* 26(2): 101419. <https://doi.org/10.1016/j.jscs.2022.101419>
- Hosny M, Fawzy M, El-Borady O M & Mahmoud A E D (2021). Comparative study between *Phragmites australis* root and rhizome extracts for mediating gold nanoparticles synthesis and their medical and environmental applications. *Advanced Powder Technology* 32(7): 2268–2279. <https://doi.org/10.1016/j.apt.2021.05.004>
- İş Ş & Beyatlı A (2023). Biological and Pharmacological Properties of Black Cumin (*Nigella sativa*). *Mersin University Faculty of Medicine Lokman Hekim Journal of Medical History and Folkloric Medicine* 13(3): 543–552. <https://doi.org/10.31020/muftfd.1310960> (In Turkish)
- Jafarizad A, Safaee K, Vahid B, Khataee A & Ekinci D (2019). Synthesis and characterization of gold nanoparticles using *Hypericum perforatum* and *Nettle* aqueous extracts: A comparison with turkevich method. *Environmental Progress and Sustainable Energy* 38(2): 508–517. <https://doi.org/10.1002/ep.12964>
- Jha P, Saraf A, Rath D & Sharma D (2017). Green Synthesis and Antimicrobial Property of Gold Nanoparticles: a Review. *World Journal of Pharmaceutical and Medical Research* 3(8): 431–435.
- Khan A U, Khan M, Malik N, Cho M H & Khan M M (2019). Recent progress of algae and blue-green algae-assisted synthesis of gold nanoparticles for various applications. *Bioprocess and Biosystems Engineering* 42(1): 1–15. <https://doi.org/10.1007/s00449-018-2012-2>
- Korani S, Rashidi K, Hamelian M, Jalalvand A R, Tajehmiri A, Korani M, Sathyapalan T & Sahebkar A (2021). Evaluation of Antimicrobial and Wound Healing Effects of Gold Nanoparticles Containing *Abelmoschus esculentus* (L.) Aqueous Extract. *Bioinorganic Chemistry and Applications* 2021(1): 1–13. <https://doi.org/10.1155/2021/7019130>
- Kumar V, Singh D K, Mohan S, Gundampati R K & Hasan S H (2017). Photoinduced green synthesis of silver nanoparticles using aqueous extract of *Physalis angulata* and its antibacterial and antioxidant activity. *Journal of Environmental Chemical Engineering* 5(1): 744–756. <https://doi.org/10.1016/j.jece.2016.12.055>
- Kumar V, Singh S, Srivastava B & Bhadouria R (2019). Journal of Environmental Chemical Engineering Green synthesis of silver nanoparticles using leaf extract of *Holoptelea integrifolia* and preliminary investigation of its antioxidant, anti-inflammatory, antidiabetic and antibacterial activities. *Journal of Environmental Chemical Engineering* 7(3): 103094. <https://doi.org/10.1016/j.jece.2019.103094>
- Kumari A, Naveen Dhatwalia J, Thakur S, Radhakrishnan A, Chauhan A, Chandan G, Choi B H & Neetika N (2023). Antioxidant, antimicrobial, and cytotoxic potential of *Euphorbia royleana* extract-mediated silver and copper oxide nanoparticles. *Chemical Papers* 77(8): 4643–4657. <https://doi.org/10.1007/s11696-023-02814-3>
- Küp F Ö, Coşkunçay S & Duman F. (2020). Biosynthesis of silver nanoparticles using leaf extract of *Aesculus hippocastanum* (horse chestnut): Evaluation of their antibacterial, antioxidant and drug release system activities. *Materials Science and Engineering C* 107: 110207. <https://doi.org/10.1016/j.msec.2019.110207>
- Latha D, Prabu P, Gnanamoorthy G, Munusamy S, Sampurnam S, Arulvasu C & Narayanan V (2019). Size-dependent catalytic property of gold nanoparticle mediated by *Justicia adhatoda* leaf extract. *SN Applied Sciences* 1(134): 1–14. <https://doi.org/10.1007/s42452-018-0148-y>
- Mandhata C P, Sahoo C R, Mahanta C S & Padhy R N (2021). Isolation, biosynthesis and antimicrobial activity of gold nanoparticles produced with extracts of *Anabaena spiroides*. *Bioprocess and Biosystems Engineering* 44(8): 1617–1626. <https://doi.org/10.1007/s00449-021-02544-4>
- Mehravani B, Ribeiro A I & Zille A. (2021). Gold nanoparticles synthesis and antimicrobial effect on fibrous materials. *Nanomaterials* 11(5): 1–37. <https://doi.org/10.3390/nano11051067>
- Mohammadi F, Yousefi M & Ghahremanzadeh R (2019). Green Synthesis, Characterization and Antimicrobial Activity of Silver Nanoparticles (AgNps) Using Leaves and Stems Extract of Some Plants. *Advanced Journal of Chemistry-Section A* 2(4): 266–275. <https://doi.org/10.33945/SAMI/AJCA.2019.4.1>
- Mousavi-Kouhi S M, Beyk-Khormizi A, Mohammadzadeh V, Ashna M, Es-haghi A, Mashreghi M, Hashemzadeh V, Mozafarri H, Nadaf M & Taghavizadeh Yazdi M E (2022). Biological synthesis and characterization of gold nanoparticles using *Verbascum speciosum* Schrad. and cytotoxicity properties toward HepG2 cancer cell line. *Research on Chemical Intermediates* 48(1): 167–178. <https://doi.org/10.1007/s11164-021-04600-w>
- Mythili R, Selvankumar T, Srinivasan P, Sengottaiyan A, Sabastinraj J, Ameen F, Al-sabri A, Kamala-kannan S, Govarthanan M & Kim H (2018). Biogenic synthesis, characterization and antibacterial activity of gold nanoparticles synthesised from vegetable waste. *Journal of Molecular Liquids* 262(7): 318–321. <https://doi.org/10.1016/j.molliq.2018.04.087>
- Nor Azlan A Y H, Katas H, Jalluddin N Q & Fauzi Mh Busra M (2020). Gold nanoparticles biosynthesized using *Lignosus rhinocerotis* extracts: comparative evaluation of biostatic and cytotoxicity Effects. *Sains Malaysiana* 49(7): 1697–1712. <https://doi.org/10.17576/jsm-2020-4907-20>

- Padalia H & Chanda S (2021). Antioxidant and Anticancer Activities of Gold Nanoparticles Synthesized Using Aqueous Leaf Extract of *Ziziphium nummularia*. *BioNanoScience* 11(2): 281–294. <https://doi.org/10.1007/s12668-021-00849-y>
- Parida U K, Bindhani B K & Nayak P (2011). Green Synthesis and Characterization of Gold Nanoparticles Using Onion (*Allium cepa*) Extract. *World Journal of Nano Science and Engineering* 01(04): 93–98. <https://doi.org/10.4236/wjnse.2011.14015>
- Parveen R, Ullah S, Sgarbi R & Tremiliosi-Filho G (2019). One-pot ligand-free synthesis of gold nanoparticles: The role of glycerol as reducing-cum-stabilizing agent. *Colloids and Surfaces A: Physicochemical and Engineering Aspects* 565(10): 162–171. <https://doi.org/10.1016/j.colsurfa.2019.01.005>
- Patil M P, Singh R D, Koli P B, Patil, K T, Jagdale B S., Tipare A R & Kim G (2018). Antibacterial potential of silver nanoparticles synthesized using *Madhuca longifolia* flower extract as a green resource. *Microbial Pathogenesis* 121(8): 184–189. <https://doi.org/10.1016/j.micpath.2018.05.040>
- Patra S, Mukherjee S, Kumar A, Ganguly A, Sreedhar B & Ranjan C (2015). Green synthesis, characterization of gold and silver nanoparticles and their potential application for cancer therapeutics. *Materials Science & Engineering C* 53(8): 298–309. <https://doi.org/10.1016/j.msec.2015.04.048>
- Perveen K, Husain F M, Qais F A, Khan A, Razak S, Afsar T, Alam P, Almajwal A M & Abulmeaty M M A (2021). Microwave-assisted rapid green synthesis of gold nanoparticles using seed extract of *Trachyspermum ammi*: Ros mediated biofilm inhibition and anticancer activity. *Biomolecules* 11(2): 1–16. <https://doi.org/10.3390/biom11020197>
- Punnoose M S & Mathew B (2022). Microwave-assisted green synthesis of *Cyanthillium cinereum* mediated gold nanoparticles: Evaluation of its antibacterial, anticancer and catalytic degradation efficacy. *Research on Chemical Intermediates* 48(3): 1025–1044. <https://doi.org/10.1007/s11164-021-04641-1>
- Rauf A, Ahmad T, Khan A, Maryam Uddin G, Ahmad B, Mabkhot Y N, Bawazeer S, Riaz N, Malikovna B K, Almarhoon Z. M & Al-Harrasi A (2021). Green synthesis and biomedical applications of silver and gold nanoparticles functionalized with methanolic extract of *Mentha longifolia*. *Artificial Cells, Nanomedicine and Biotechnology* 49(1): 194–203. <https://doi.org/10.1080/21691401.2021.1890099>
- Rautray S & Rajananthini A U (2020). Therapeutic potential of green, synthesized gold nanoparticles. *BioPharm International*, 33(1): 30–38.
- Remya R R, Rajasree S R R, Aranganathan L & Suman T Y (2015). An investigation on cytotoxic effect of bioactive AgNPs synthesized using *Cassia fistula* flower extract on breast cancer cell MCF-7. *Biotechnology Reports* 22(8): 110–115. <https://doi.org/10.1016/j.btre.2015.10.004>
- Rolim W R, Pelegrino M T, de Araújo Lima B, Ferraz L S, Costa F N, Bernardes J S, Rodrigues T, Brocchi M & Seabra A B (2019). Green tea extract mediated biogenic synthesis of silver nanoparticles: Characterization, cytotoxicity evaluation and antibacterial activity. *Applied Surface Science* 463(1): 66–74. <https://doi.org/10.1016/j.apsusc.2018.08.203>
- Satpathy S, Patra A, Ahirwar B & Hussain M D (2020a). Process optimization for green synthesis of gold nanoparticles mediated by extract of *Hygrophila spinosa* T. Anders and their biological applications. *Physica E: Low-Dimensional Systems and Nanostructures* 121(3): 113830. <https://doi.org/10.1016/j.physe.2019.113830>
- Seku K, Gangapuram B R, Pejjai B, Hussain M, Hussaini S S, Golla N & Kadimpati K K (2019). Eco-friendly synthesis of gold nanoparticles using carboxymethylated gum *Cochlospermum gossypium* (CMGK) and their catalytic and antibacterial applications. *Chemical Papers* 73(7): 1695–1704. <https://doi.org/10.1007/s11696-019-00722-z>
- Sepahvand M, Buazar F & Sayahi M H (2020). Novel marine-based gold nanocatalyst in solvent-free synthesis of polyhydroquinoline derivatives: Green and sustainable protocol. *Applied Organometallic Chemistry* 34(12): 1–11. <https://doi.org/10.1002/aoc.6000>
- Shankar P D, Shobana S, Karuppasamy I, Pugazhendhi A, Ramkumar V S, Arvindnarayan S & Kumar G (2016). A review on the biosynthesis of metallic nanoparticles (gold and silver) using bio-components of microalgae: Formation mechanism and applications. *Enzyme and Microbial Technology* 95(1): 28–44. <https://doi.org/10.1016/j.enzmictec.2016.10.015>
- Singh A K, Tiwari R, Singh V K, Singh P, Khadim S R, Singh U, Laxmi Srivastava V, Hasan S H & Asthana R K (2019). Green synthesis of gold nanoparticles from *Dunaliella salina*, its characterization and *in vitro* anticancer activity on breast cancer cell line. *Journal of Drug Delivery Science and Technology* 51(6): 164–176. <https://doi.org/10.1016/j.jddst.2019.02.023>
- Some S, Bulut O, Biswas K, Kumar A, Roy A, Sen I K, Mandal A, Franco O L, İnce İ A, Neog K, Das S, Pradhan S, Dutta S, Bhattacharjya D, Saha S, Das Mohapatra P. K, Bhuimali A, Unni B G Kati A & Ocoy I (2019). Effect of feed supplementation with biosynthesized silver nanoparticles using leaf extract of *Morus indica* L. V1 on *Bombyx mori* L. (Lepidoptera: Bombycidae). *Scientific Reports* 9(1): 1–13. <https://doi.org/10.1038/s41598-019-50906-6>
- Suriyakala G, Sathiyaraj S, Babujanathanam R, Alarjani K M, Hussein D S, Rasheed R A & Kanimozhi K (2022). Green synthesis of gold nanoparticles using *Jatropha integerrima* Jacq. flower extract and their antibacterial activity. *Journal of King Saud University - Science* 34(3): 101830. <https://doi.org/10.1016/j.jksus.2022.101830>
- Swamy M K, Akhtar M S, Mohanty S K & Sinniah U R (2015). Synthesis and characterization of silver nanoparticles using fruit extract of *Momordica cymbalaria* and assessment of their *in vitro* antimicrobial, antioxidant and cytotoxicity activities. *Spectrochimica Acta - Part A: Molecular and Biomolecular Spectroscopy* 151(12): 939–944. <https://doi.org/10.1016/j.saa.2015.07.009>
- Ullah N, Odda A H, Li D, Wang Q & Wei Q (2019). One-pot green synthesis of gold nanoparticles and its supportive role in surface activation of non-woven fibers as heterogeneous catalyst. *Colloids and Surfaces A: Physicochemical and Engineering Aspects* 571(January): 101–109. <https://doi.org/https://doi.org/10.1016/j.colsurfa.2019.03.076>
- Umamaheswari C, Lakshmanan A & Nagarajan N S (2018). Green synthesis, characterization and catalytic degradation studies of gold nanoparticles against congo red and methyl orange. *Journal of Photochemistry and Photobiology B: Biology* 178(8): 33–39. <https://doi.org/10.1016/j.jphotobiol.2017.10.017>
- Usman A I, Aziz A A & Noqta O A (2019). Green sonochemical synthesis of gold nanoparticles using palm oil leaves extracts. *Materials Today: Proceedings* 7(3): 803–807. <https://doi.org/10.1016/j.matpr.2018.12.078>
- Uzma M, Prasad D, Sunayana N, Vinay R & Shilpashree H (2021). Studies of *in vitro* antioxidant and anti-inflammatory activities of gold nanoparticles biosynthesized from a medicinal plant, *Commiphora wightii*. *Materials Technology* 37(9): 915–925. <https://doi.org/10.1080/10667857.2021.1905206>
- Velmurugan P, Anbalagan K, Manosathyadevan M, Lee K J, Cho MinJung-Hee Park Sae-Gang Oh K S B, Oh B-T & Lee S M. (2014). Green synthesis of silver and gold nanoparticles using *Zingiber officinale* root extract and antibacterial activity of silver nanoparticles against food pathogens. *Bioprocess and Biosystems Engineering* 37(10): 1935–1943. <https://doi.org/10.1007/s00449-014-1169-6>
- Vinita Nirala N R & Prakash R (2018). One step synthesis of AuNPs@MoS₂-QDs composite as a robust peroxidase- mimetic for instant unaided eye detection of glucose in serum, saliva and tear. *Sensors and Actuators, B: Chemical* 263(6): 109–119. <https://doi.org/10.1016/j.snb.2018.02.085>




- Webster T J (2020). Recent Developments in the Facile Bio-Synthesis of Gold Nanoparticles (AuNPs) and Their Biomedical Applications. *International Journal of Nanomedicine* 2020(15): 275–300. <https://doi: 10.2147/IJN.S233789>
- Zayadi R A, Abu Bakar F & Ahmad M K (2019). Elucidation of synergistic effect of eucalyptus globulus honey and *Zingiber officinale* in the synthesis of colloidal biogenic gold nanoparticles with antioxidant and catalytic properties. *Sustainable Chemistry and Pharmacy* 13(March): 100156. <https://doi.org/10.1016/j.scp.2019.100156>



Copyright © 2024 The Author(s). This is an open-access article published by Faculty of Agriculture, Ankara University under the terms of the [Creative Commons Attribution License](#) which permits unrestricted use, distribution, and reproduction in any medium or format, provided the original work is properly cited.



Molecular Characterization and Dose-Response to 2,4-D Herbicide in *Convolvulus arvensis* Populations in Türkiye

Yücel Karaman^{a*} , Nihat Tursun^a , Hikmet Murat Sipahioğlu^b 

^aPlant Protection Department, Agricultural Faculty, Malatya Turgut Ozal University, Malatya, 44210, TURKEY

^bPlant Protection Department, Agricultural Faculty, Malatya Turgut Ozal University, Malatya, 44210, TURKEY (Retired)

ARTICLE INFO

Research Article

Corresponding Author: Yücel Karaman, E-mail: yucel.karaman@ozal.edu.tr

Received: 19 December 2023 / Revised: 15 February 2024 / Accepted: 16 February 2024 / Online: 23 July 2024

Cite this article

Karaman Y, Tursun N, Sipahioğlu H M (2024). Molecular Characterization and Dose-Response to 2,4-D Herbicide in *Convolvulus arvensis* Populations in Türkiye. *Journal of Agricultural Sciences (Tarım Bilimleri Dergisi)*, 30(3):584-593. DOI: 10.15832/ankutbd.1407008

ABSTRACT

Field bindweed (*Convolvulus arvensis* L.) is an important weed species in agricultural areas in Türkiye and worldwide. The study, conducted in 2018-2019, involved collecting seeds from 16 different provinces in Türkiye (Adana, Ankara, Çanakkale, Denizli, Diyarbakır, Erzurum, Hatay, İzmir, Karaman, Kayseri, Konya, Malatya, Samsun, Şanlıurfa, Tekirdağ and Uşak). These seeds were then germinated under greenhouse conditions (29/19°C day/night), and molecular characterization of the samples was performed. As a result of comparing the samples with a specific reference from NCBI GenBank, it was found that the similarity ratios were close to each other but formed different groups. The study

revealed that samples from Adana, Konya and Samsun belonged to different groups in terms of similarity. Subsequently, the dose-response rates of these samples to 2,4-D, a herbicide licensed against field bindweed, were determined. In the dose-response analysis of the herbicides, ED₅₀ values of 131.93, 115.42 and 141.89 g.a.i/ha were determined for Adana, Konya and Samsun, respectively. The study concluded that the dose-response of field bindweed in Adana, Konya and Samsun provinces, belonging to different molecular groups, to 2,4-D herbicide is close to each other but exhibits different values.

Keywords: Field bindweed, Weed, Molecular characterization, Herbicide

1. Introduction

Weeds in agricultural areas are one of the biggest problems in the world, as they lead to yield and product losses (Jabran et al. 2015). Around 1800 weed species in the world cause a 31.5% decline in agricultural productivity (Kubiak et al. 2022). Weeds in agricultural areas negatively impact crop development by competing for water, light, and nutrients with crops, ultimately reducing the quality and quantity of the product (Güncan & Karaca 2023). On the other hand, weeds also serve as hosts for plant diseases and pests (Mourellos et al. 2014; Üremiş et al. 2020).

Field bindweed (*Convolvulus arvensis* L.) was first classified by Linnaeus in 1753 (Güncan 1979). Native to Europe and Asia and it thrives in temperate, tropical and Mediterranean climates (Lyons 1998; Gubanov et al. 2004). Originating from the European continent, field bindweed is widespread in temperate regions of Western Asia, North America and Europe. However, it causes more damage in Europe in terms of cultivated area (Holm et al. 1977). In Türkiye, it is widespread throughout the country and is observed in both temperate and arid regions (Coruh & Zengin 2007; Özkil & Üremiş 2020; Kuru & Üremiş 2021). Field bindweed competes with other species in the vicinity for water and nutrients. It climbs on surrounding plants, hindering their development and causing yield losses. The weed reduces the available water at a soil depth of 60 cm, leading to plants withering due to water deficiency. Additionally, it poses challenges in pruning by overgrowing shrubs and small trees (Vogelsgang 1998). Field bindweed serves a breeding ground for insect pests and an alternative host for viruses causing plant diseases (Tamaki et al. 1975). The seeds, leaves and especially the roots of field bindweed contain the glycoside convolvulin. This resinous, water-insoluble compound induces severe hyperemia (blood rush), peristalsis, and diarrhea in the stomach and intestinal tract of animals (Lubenov 1985).

Pesticides, commonly utilized for controlling diseases, pests and weeds in agricultural areas worldwide, play a significant role as pollutants. The continuous and improper use of these substances unnecessarily increases production costs, disrupts the balance of nature, diminishes sustainable agriculture, and negatively impact human health (Pimentel et al. 1992; Pimentel & Greiner 1997; Dogan et al. 2004). As human health is endangered by pollution, there has been an increasing pressure to reduce and ban the use of herbicides in agricultural areas (Matteson 1995). However, chemical control, specifically the use of herbicides

remains the primary method for easy and practical weed control in agricultural areas (Uygur & Şekeroğlu 1993). The application of herbicides such as 2,4-dichlorophenoxyacetic acid (2,4-D), dicamba and glyphosate in the chemical control of field bindweed can effectively manage this weed (Vogelgsang 1998). The primary objective of weed control in a given agricultural area is to maintain the weed population below the economic damage threshold rather than eradicating it completely. Even low doses of herbicide applications have been found to have a significant effect on weeds (Steckel et al. 1990). It has been proven that weeds can be controlled with lower those licensed (Salonen 1992; Zhang et al. 2000; Boström & Fogelfors 2002; Busi et al. 2016; Vranjes et al. 2019). Integrated weed control in agricultural areas should be carefully managed. If herbicides are needed in the integrated control method, determining the application dose is an important step (Kudsk & Streibig 2003).

The process of classifying living organisms into specific groups according to their degree of similarity and relatedness is called classification. The classification process helps us determine the relationships between weeds and crops and to obtain information about them. If the individuals of a particular species are similar in terms of their competitive ability and developmental characteristics, they also have similar habitats (Hoffmann & Frodsham 1993). Classifications based on the external appearance of living beings and their relationships with the environment are referred to as artificial or empirical classifications. However, this classification has lost its validity today. The scientific (natural or phylogenetic) classification is based on the physiological, anatomical and ancestral similarities of organisms and the degree to which they are related. The main feature of this classification is the use of molecular techniques (genetic markers), and it has recently taken an important place in the classification of living organisms (Hoffmann & Frodsham 1993). Chloroplast trnL-F and ribosomal ITS gene regions are frequently used to determine phylogenetic relationships in different plant groups (Brouat et al. 2001; Soejima & Nagamasu 2004). In recent years, in addition to morphological traits, molecular traits are increasingly used to identify plant species (Mummenhoff et al. 1997). In molecular characterization, many regions of genomic DNA (gDNA), chloroplast DNA (cpDNA) and mitochondrial DNA (mtDNA) are used to classify plants. In phylogenetic analyses, molecular characters are employed when morphological characters are insufficient (Yokoyama et al. 2000). Internal transcribed regions (ITS) on nuclear DNA (nrDNA), intergenic regions (trnL-F) and protein coding (ndhF) regions on cpDNA are used to determine intraspecific diversity (Kellogg 1998). Since more variation can occur in the ITS region, it is possible to distinguish between closely related species and to characterize different populations of the same species by examining this region (White et al. 1990).

In this study, field bindweed seeds collected from different provinces of Türkiye (Malatya, Erzurum, Diyarbakır, Şanlıurfa, Kayseri, Konya, Karaman, Ankara, Samsun, Adana, Hatay, Denizli, İzmir, Uşak, Tekirdağ and Çanakkale) were grown in controlled greenhouse environments, and molecular characterization was performed with the obtained plant samples. After molecular processing, the aim of this study was to determine the phylogenetic similarity rates among the samples and to assess the responses of the samples found in different groups to the 2,4-D herbicide.

2. Material and Methods

2.1. Specimen collection

The seeds of field bindweed were collected between 2016 and 2017 from agricultural land in various provinces of Türkiye. (Malatya, Erzurum, Diyarbakır, Şanlıurfa, Kayseri, Konya, Karaman, Ankara, Samsun, Adana, Hatay, Denizli, İzmir, Uşak, Tekirdağ and Çanakkale). The collected seeds, which were 1-2 years old, were stored at +4 °C until the start of the studies. The studies were conducted in 2018-2019 in greenhouses and laboratories of Malatya Turgut Özal University Faculty of Agriculture, Malatya, Türkiye.

2.2. Genomic DNA isolation

For DNA isolation, field bindweed seeds collected from fields in different provinces were first subjected to a dormancy-breaking study (the seeds were immersed in water at 90 °C for 5 seconds and then removed (Karaman & Tursun 2021). Following this study, the seeds were sown in the greenhouse under conditions of 29 °C±1 14 hours during the day and 19 °C±1 10 hours at night. When the seedlings had reached the 4-6 leaf stage, 100 mg leaf samples were taken from each sample. The Bioline DNA extraction kit was used to isolate the plant DNAs. To obtain high-quality and high-density total DNA, the extraction methods specified by the respective company were used. The samples for the PCR application were stored at -20 °C and taken out of the freezer and used when needed.

2.3. PCR amplification of the ITS region and electrophoresis

The universal ITS4 (5'-TCCTCCGCTTATTGATATGC-3') and ITS5 (5'-GGAAGTAAAAGTCGTAACAAG G - 3') primers were used to amplify the ITS regions on the isolated ribosomal DNA. The components for the PCR reaction, using the enzyme GoTaq G2 Flexi DNA Polymerase (Cat:M780B) from Promega with a total volume of 50 µl for the ITS region, are listed in Table 1.

Table 1- PCR components, amounts or ratios used in the amplification of ribosomal DNA by the PCR method

PCR Components	For 1 sample (μ l)	For 16 samples (μ l)
5X PCR Buffer	10	160
dNTP (20 mM)	1	16
MgCl ₂ (25 mM)	3	48
Mould DNA	2	32
Primer F (ITS4) (100 mM)	1	16
Primer R (ITS5) (100 mM)	1	16
GoTaq G2 Flexi DNA poly. enzyme	0,4	6,4
Sterile water	31.6	505.6

After adding all PCR parameters to the sterile tubes, a brief cycle was performed to ensure that all liquids were collected at the bottom of the tubes. The prepared PCR mixture was tested in 36 thermal cycles (Table 2).

Table 2- PCR thermal cycles used in the amplification of ribosomal DNA

94 °C/de ...2 min DNA double strand separation	} Total 36 cycles
94 °C/de ...1 min DNA double strand separation	
55 °C/de ...1 min primer binding	
72 °C/de ...2 min DNA synthesis	
72 °C/de ...10 min final elongation	

The PCR applications were conducted using the Prima-96plusTM Thermal Cycler device. The products obtained after the PCR process were prepared for electrophoresis as 1.5% agarose gel. For this, 100 mL of sterile distilled water and 3 μ l of fluorescent dye were added to a suitable container and run at 85 V for 45 minutes. Imaging was performed using the Gel Imaging and Analysis System to visualize the stained DNA.

2.4. DNA sequencing of ITS regions

DNA sequencing of ITS regions, amplified from genomic DNA using universal primers, was carried out by BM Laboratory Systems (Ankara) in a single direction.

2.5. Phylogenetic analyzes and entry of DNA sequences into the GenBank

The phylogenetic analysis of the sequenced DNA samples was completed, and the DNA sequences were registered in the GenBank (NCBI). The access numbers can be found in the Results section. The programs Unipro UGENE, Unipro UGENE, MEGA11 and CLC Main Workbench 20 were used. A different function of each program was used for the sequence analysis and the creation of the phylogenetic tree. The creation of the phylogenetic tree was repeated 100 times using the neighbor-joining algorithm and the Bootstrap method (Felsenstein 1985; Saitou & Nei 1987; Nei & Kumar 2000; Tamura et al. 2021; Ateş 2022)

2.6. Dose-response studies of field bindweed (*Convolvulus arvensis*) samples to 2,4-D herbicide

In the study, the efficacy of the herbicide containing the active ingredient 2,4-D (Hektas Ester'h 480 g/l 2,4-D acid equivalent isooctylester), licensed for the control of field bindweed, was investigated for the samples in different groups resulting from phylogenetic analyses. For this purpose, the experiments were conducted in a fully automated greenhouse under controlled conditions at a temperature of 29 °C \pm 1 14 hours during the day and 19 °C \pm 1 10 hours at night. The area of the glass greenhouse in the study is 25 m², and the humidity inside was maintained at around 60 \pm 10 % depending on the automation system.

2.7. Pot trials

Field bindweed seeds from three provinces (Adana, Konya and Samsun), which were in distinct groups based on molecular characterization, were used for the study. The seeds were immersed in 90 °C hot water for 5 seconds before sowing to break the dormancy of the seeds (Karaman & Tursun 2021). Following dormancy breaking, a prepared 1:1/3 peat:perlite mixture was placed in plastic pots measuring 25 cm height and 15 cm width, and sowing (5 seeds in each pot) was performed. Despite the humid greenhouse environment, irrigation was carried out at regular intervals to maintain moisture balance in the pots. After germination, the seedlings were thinned to one per pot at the stage of two true leaves. Since field bindweed tends to wrap 1 m long, stakes were driven into the pots to serve as controls. The study was conducted with four replications and two repetitions according to a randomized plots experimental design.

2.8. Effect of 2,4 D herbicide on *convolvulus arvensis* samples

Different doses of the herbicide containing the active ingredient 2,4 D-amine were applied post-emergence to field bindweed samples in Adana, Konya and Samsun provinces, which were categorized into different groups based on molecular studies, during the 2-6 leaf stage. The calibration of the electronic spray booth for herbicide application was set at 300 L of water per ha, 304 kPa pressure and 5 km/h. Various doses of herbicide 2,4-D were used in the trial: 0 g.a.i /ha (unsprayed control), N/4 (180 g.a.i /ha), N/2 (360 g.a.i /ha), N (recommended dose – 720 g.a.i /ha), 2N (1440 g.a.i /ha), 4N (2880 g.a.i /ha) and 8N (5760 g.a.i /ha). After the spraying process, the pots were again left under the same conditions. Percentage/symptom values (Table 3) were monitored weekly for 4 weeks after herbicide application (Bajwa et al. 2019). Finally, harvesting was conducted at the end of the 4th week (28th day). During harvesting, the aerial parts of the plants were removed. Subsequently, the plant materials were dried in paper bags in an oven set at 105 °C for 24 hours (Yusriah et al. 2012), their weight was determined using a precision scale.

Table 3- Herbicide damage assessment system based on morphological symptoms in the degree of damage in field bindweed (*Convolvulus arvensis* L.)

Damage rating	Morphological responses
0	Not evident
10	Negligible discoloration, distortion and/or stunting barely seen
20	Slight damage discoloration, distortion and or stunting clearly seen
30	Moderate damage: moderate discoloration, marked distortion and/or stunting. Recovery expected
40	Substantial damage: much discoloration, distortion, and stunting: some damage probably irreversible
50	Majority of plant tissue is damaged, mostly irreversibly: substantial necrosis; discoloration and distortion
60	Nearly all the plant tissue damaged, mostly irreversibly some plants killed (<40%): substantial necrosis and distortion
70	Sever damage, necrosis and wilting
80	Very severe damage, heavy necrosis and wilting
90	Extreme irreversible damage with <10% green tissue visible, most tissue discolored and distorted permanently or desiccated
100	Complete loss of plant

2.9. Statistical analysis

The significance of the differences in the recorded data was determined by analysis of variance (ANOVA) using IBM SPSS STATISTICS 25.0 software with a general linear model (GLM). Initially, the differences between treatments were analyzed with ANOVA and then with the Duncan test for a multiple-range test ($P \leq 0.05$).

Data on visual reduction (%) and dry matter (DM) reduction (%) of the effect of 2,4-D herbicide on field bindweed were subjected to nonlinear regression analysis on herbicide dose using the four-parameter log-logistic model (Knezevic et al. 2007; Ulloa et al. 2011):

$$Y = C + \frac{(D - C)}{\{1 + \exp[B(\log X - \log E)]\}}$$

Where; Y is the response (e.g., percent DM reduction), C is the lower limit, D is the upper limit, B is the slope of the line at the inflection point (also known as the rate of change), and E is the dose that results in a 50% response between the upper and lower limit (also known as the inflection point, ED₅₀).

The ED₅₀ values were used to compare visual (%) and dry matter (DM) reduction of each field bindweed under 2,4-D (Matzenbacher et al. 2015; Chen et al. 2015). The analyzes of the dose-response curves were performed using the software R (R version 2.15.3, R Development Core Team 2013) using the statistical add-on package drc (dose-response curves) (Knezevic et al. 2007; Knezevic & Datta 2015). When determining the effect of 2,4 D on field bindweed, the ED₅₀ (dose controlling 50% of field bindweed) and ED₉₀ (dose controlling 90% of field bindweed) values were also determined.

3. Results and Discussion

3.1. Identification of samples of field bindweed (*Convolvulus arvensis*) from different provinces by molecular methods

For the phylogenetic studies, field bindweed the samples from different provinces (Malatya, Erzurum, Diyarbakır, Şanlıurfa, Kayseri, Konya, Karaman, Ankara, Samsun, Adana, Hatay, Denizli, İzmir, Uşak, Tekirdağ, and Çanakkale) were grown from seeds, and their relationships were determined by molecular methods. It has been found that morphological characteristics are not sufficient to determine the degree of similarity between plant species, and some sequence analyzes are useful for phylogenetic analyzes (Yokoyama et al. 2000). For example, one of the methods used to determine the relationships among plant species is ITS (Internal Transcribed Spacers) PCR of the nrDNA region (Baldwin et al. 1995). This method has become a commonly used in molecular systematic studies of plants, enabling the identification of plant species by determining species-specific gene regions (Baldwin et al. 1995; Tursun et al. 2021; Saric-Krsmanović et al. 2022). Ribosomal DNA internal transcribed spacers (rDNA ITS), known as one of the most reliable methods in phylogenetic studies, are used for plant systematics and identification due to genomic segments' functionally. The high percentage of conservative genes and their belonging to the ITS sections provide an advantage in their use (Baldwin et al. 1995).

The ITS has been widely utilized in systematic studies to determine genus and species levels in many plant varieties. The two internal regions ITS-1 and ITS-2 are located between the genes coding for the subunits of 5.8S, 18S and 26S nuclear ribosomal RNA (nrRNA). In this study, genomic DNA was isolated from each field bindweed in the provinces and universal primers ITS4 (5'- TCCTCCGCTTATTGATATGC-3') and ITS5 (5'GGAAGTAAAAGTCGTAACAAG G - 3') were used to amplify the ITS regions. Using these primers, the ITS1, 5.8S and ITS2 regions in the rDNA were amplified by PCR. The consensus sequences were determined by comparing the sequence data obtained with reference sequences. The genome information of the field bindweed species, for which DNA sequencing was performed was analyzed using the CLC Main Workbench 20.0.1 program. After DNA sequencing, a search for the cloned region in GenBank was performed with the BLAST program. The DNA sequences of field bindweed samples from different provinces were registered in the National Center for Biotechnology Information (NCBI) GenBank, making them available to researchers worldwide. The GenBank accession numbers and gene lengths (bp) are shown in Table 4.

Table 4- GenBank accession numbers of field bindweed samples

Provinces	GenBank Accession Numbers	Length (bp)
Malatya	MT071458	667
Erzurum	MT071459	678
Diyarbakır	MT071460	684
Şanlıurfa	MT071461	678
Ankara	MT071462	675
Karaman	MT071463	678
Kayseri	MT071464	673
Konya	MT071465	660
Samsun	MT071466	635
Adana	MT071467	677
Hatay	MT071468	677
Denizli	MT071469	678
İzmir	MT071470	669
Uşak	MT071471	656
Tekirdağ	MT071472	678
Çanakkale	MT071473	681

The relationships of field bindweed samples from different provinces of Türkiye both with each other and with other field bindweed individuals worldwide, were revealed through phylogenetic analysis. When comparing specimens from different provinces of Türkiye, it was found that the specimens from Adana and Diyarbakır provinces formed a distinct group due to the genetic differences. While specimens collected from other provinces were grouped together, it was determined that the plant sample collected from Samsun province, despite being in the same group, was genetically more distant from the plant samples collected from other provinces.

When comparing field bindweed samples from different provinces of Türkiye with other plant specimens worldwide, it was observed that the plant specimens in Türkiye were divided into two distinct groups. Specifically, Samsun, Konya, Kayseri, Uşak, Çanakkale, Karaman and Şanlıurfa were identified as forming one group, while Denizli, Ankara, Hatay, Adana, Diyarbakır,

Erzurum, Malatya, İzmir and Tekirdağ provinces constituted another group. Additionally, it was noted that the plant specimens belonging to other field bindweed species worldwide formed a separate group distinct from the plant specimens in Türkiye, indicating a significant degree of relatedness. The phylogenetic tree of the ITS gene region of the biotypes of *Convolvulus arvensis* was constructed by repeating 100 times with the distance-based method (neighbour-joining) and the bootstrap method in the programme CLC Main Workbench 20. As a result of the phylogenetic analyses, all studied *Convolvulus arvensis* biotypes were classified as I. and II. They are divided into two main groups: Group I is divided into subgroups Ia and Ib, and group II into subgroups IIa and IIb. Turkey's biotypes are distributed among subgroups Ia, Ib and IIb, in contrast to other countries (Figure 1). Sunar et al. (2015) utilized random amplified DNA markers (RAPD) in another molecular study on field bindweed. In this experiment, field bindweed samples were collected from five locations in Erzurum province (Aşkale, Erzurum (centre), İspir, Oltu and Tortum). Comparative analysis of populations revealed that the populations of Erzurum and Aşkale as well as the populations of Tortum and Oltu showed similar clustering. The study suggested that the similarity in these populations, forming a common group, could be attributed to geographical reasons. The findings indicated a significant correlation between the proximity of geographical regions and the genetic proximity of the populations within those regions. Several studies have also reported a significant correlation between geographical and genetic distance (Xia et al. 2005; Nianxi et al. 2006; Qian et al. 2008). The phylogenetically distant grouping of field bindweed samples collected from different locations in Türkiye and other field bindweed species worldwide aligns with the outcomes of these studies.

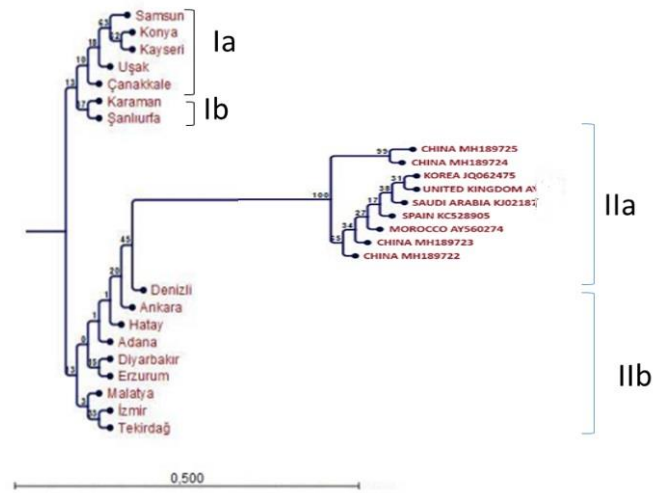


Figure 1- Phylogenetic analysis of field bindweed from different provinces in Türkiye and other field bindweed specimens from around the world

In the study, the CLC Main Workbench 20.0.1 program was used to determine the relationships among field bindweed species in different provinces of Türkiye and other field bindweed species in the world. It was observed that the degree of similarity among field bindweed samples in Türkiye varies among provinces and that their relationships to species globally are distant. Utilizing a specific reference from the NCBI GenBank, the similarities of field bindweed from different provinces were grouped in the study. As a result, it was determined that a total of four main groups were formed, except for the reference KJ021876.1 Saudi Arabia (Figure 2).



Figure 2- Similarities and grouping of field bindweed from different provinces with a specific reference via NCBI GenBank

Molecular diagnostic studies are used by researchers to identify species. Sarić-Krsmanović et al. (2022) entered the sequence results of the ITS1 and ITS2 5.8S ribosomal RNA gene regions of 24 of the 26 populations of *Cuscuta campestris* into NCBI GenBank. When compared with other samples in the database, all samples were found to belong to the species *Cuscuta campestris* Yunck. with a similarity level of 95%. When creating the phylogenetic tree, the genetic diversity between the species is divided into clusters. Keskin et al. (2017) conducted taxonomic identifications of species belonging to the genus *Cuscuta*. ITS primers were used to determine the relationships among the species of the genus *Cuscuta*, and the PCR products obtained were subjected to DNA sequencing. Phylogenetic analyzes were performed using CLC DNA Workbench software and Vector NTI programs. Plant samples with known DNA sequencing were registered in the GenBank of the National Center for Biotechnology Information (NCBI). The species registered in the GenBank included *C. approximata* Babington (GenBank accession no. KU686677), *C. lupuliformis* Krockner (GenBank accession no. KU707914), *C. campestris* Yuncker (GenBank accession no. KU725869), *C. babylonica* Aucherex Choisy (GenBank accession no. KU725870), *C. babylonica* (GenBank accession no. KU761258), as well as *C. approximata* (GenBank accession no. KU725873). The studies emphasized the importance of using the ITS region in species identification and in assessing the similarities of samples belonging to the species.

3.2. Effect of 2,4 D herbicide on field bindweed samples

ITS primers were used to identify the samples of field bindweed collected in different provinces for molecular characterization. All collected samples were identified as belonging to the field bindweed species, and the similarities between these samples were grouped using bioinformatics analysis. As a result, a total of four main groups were formed among the field bindweed samples of all provinces except the reference value. Since the samples of Adana, Konya and Samsun belonged to different groups, they were used in herbicide experiments. When the dose responses of Adana, Konya and Samsun samples to the herbicide 2,4-D were evaluated by their dry weight values 28 days after spraying, the ED₅₀ values were 131.93, 115.42 and 141.89 g.a.i/ha, respectively, and the ED₉₀ values were 728.0, 876.4 and 913.0 g.a.i/ha, respectively (Table 5 and Figure 3). In the trial, the herbicide 2,4-D produced similar dose-response results on three different samples of field bindweed (Adana, Konya and Samsun).

Table 5- Dose-response curves for the field bindweed (*Convolvulus arvensis* L.) grown under glass greenhouse conditions (dry matter) (2,4-D) (g.a.i /ha)

Locations	Regression parameters (\pm SE)			ED ₅₀ (\pm SE)	ED ₉₀ (\pm SE)
	B	C	D		
Adana	-1.29 (0.3)	-0.1 (2.3)	87.73 (2.12)	131.93 (15.3)	728.0 (98.3)
Konya	-1.08 (0.23)	-0.1 (1.9)	87.76 (2.43)	115.42 (14.7)	876.4 (30.5)
Samsun	-1.18 (0.17)	0.03 (2)	91.22 (1.94)	141.89 (13.1)	913.0 (81.2)

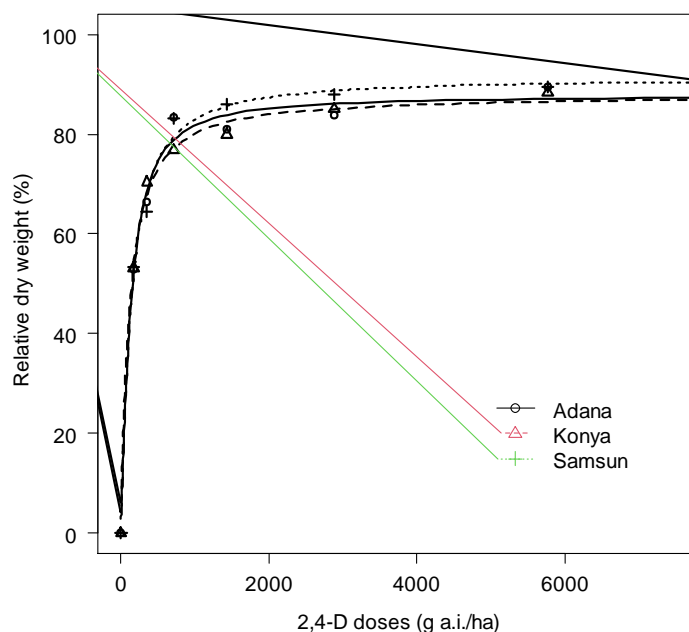


Figure 3- Dose-response curve of field bindweed in Adana, Konya and Samsun locations against herbicide with 2,4-D active ingredient

In addition to the dry matter of field bindweed, percentage symptom values were visually recorded each week, and differences between the samples of field bindweed in the provinces of Adana, Konya and Samsun were determined. When assessing the lethality of the normal dose of 2,4-D on the plants of Adana sample, results of 33%, 55%, 95% and 100% were obtained in the 1st, 2nd, 3rd and 4th weeks, respectively. Examining the lethality of the normal dose of 2,4-D on Konya sample plants yielded results of 22%, 70%, 90% and 95% in the 1st, 2nd, 3rd and 4th weeks, respectively. For the Samsun sample plants, results of 37%, 74%, 95% and 100% were observed in the 1st, 2nd, 3rd and 4th weeks, respectively. Mortality of 70% or more was observed in the Konya and Samsun samples in the 2nd week, while mortality in the Adana sample occurred slightly later and was determined to be 55%. In all three samples, a mortality rate of 90% or more was observed in the 3rd week. Other studies also indicate that the 2,4-D herbicide used in the experiment had a positive effect on the control of field bindweed (Flint & Barrett 1998; Bayat & Zargar 2020).

4. Conclusions

The result of the study indicates that the field bindweed populations originating from different provinces of Türkiye formed close groups in terms of their genetic similarity and also exhibited similar reaction to the herbicide 2,4-D, which was used for weed control. Based on these findings, it was determined that the herbicide 2,4-D had a positive effect on field bindweed as a weed control agent. Importantly, the genetic proximity or distance of field bindweed samples did not alter the efficacy of the herbicide.

References

- Ateş A (2022). Determination of the critical period for weed control in wheat (*Triticum aestivum* L.) and investigation of control possibilities of wild mustard (*Sinapis arvensis* L.). PhD Thesis, Malatya Turgut Özal University, Malatya. 117pp (In Turkish)
- Bajwa A A, Wang H, Chauhan BS & Adkins S (2019). Effect of elevated carbon dioxide concentration on growth, productivity and glyphosate response of parthenium weed (*Parthenium hysterophorus* L.). *Pest Manag. Sci.* 75: 2934–2941. <https://doi.org/10.1002/ps.5403>
- Baldwin B G, Sanderson M J, Porter J M, Wojciechowski M F, Campell C S & Donoghue M J (1995). The ITS Region of Nuclear Ribosomal DNA: Valuable Source of Evidence on Angiosperm Phylogeny. *Annals of the Missouri Botanical Garden* pp. 250-272. <https://doi.org/10.2307/2399880>
- Bayat M & Zargar M (2020). Field bindweed (*Convolvulus arvensis*) control and winter wheat response to post herbicides application. *Journal of Crop Science and Biotechnology* 23: 149-155. DOI No. 10.1007/s12892-019-0213-0
- Boström U & Fogelfors H (2002). Response of Weeds and Crop Yield to Herbicide Dose Decision-Support Guidelines. *Weed Science* 50:186-195. <https://doi.org/10.1614/0043>
- Brouat C, Gielly L & Mckey D (2001). Phylogenetic relationships in the genus *Leonar doxa* (Leguminosae: Caesalpinioideae) inferred from chloroplast trnL into nan dtrnL-trnF intergenic spacer sequences. *American Journal of Botany* 88: 143-149. <https://doi.org/10.2307/2657134>
- Busi R, Giroto M & Powles S B (2016). Response to low-dose herbicide selection in self-pollinated *Avena fatua*. *Pest Management Science* 72(3): 603-608
- Chen Z Y, Xiong Z J, Pan X Y, Shen S Q, Geng Y P, Xu C Y, Chen J K & Zhang W J (2015). Variation of genome size and the ribosomal DNA ITS region of *Alternanthera philoxeroides* (Amaranthaceae) in Argentina, the USA, and China. *Journal of Systematics and Evolution* 53(1): 82-87. DOI: 10.1111/jse.12118.

- Coruh I & Zengin H (2007). Determination of economic threshold of field bindweed (*Convolvulus arvensis* L.) in spring wheat in Erzurum, Türkiye. *Journal of Ataturk University Agricultural Faculty* 38: 151-157
- Dogan M N, Unay A, Boz O & Albay F (2004). Determination of optimum weed control timing in maize (*Zea mays* L.). *Turk J Agric.* 28: 349- 354
- Felsenstein J (1985). Confidence limits on phylogenies: An approach using the bootstrap. *Evolution* 39:783-791
- Flint J L & Barrett M (1998). Effects of glyphosate combinations with 2, 4-D or dicamba on field bindweed. *Weed Science*, 37: 12-18. <https://doi.org/10.1017/S0043174500055776>
- Gubanov I A, Kiseleva K V, Novikov V S & Tihomirov V N (2004). An illustrated identification book of the plants of Middle Russia, Vol. 3: Angiosperms (dicots: archichlamy deans). Moscow: Institute of Technological Researches; 520 pp In Russian
- Güncan A (1979). Research on the Biology of Field Bindweed (*Convolvulus arvensis* L.) and its Control Possibilities in Wheat. Ataturk University Publications No. 515. Faculty of Agriculture Publications No. 234. Research Series No. 151 (In Turkish).
- Güncan A & Karaca M (2023). Weed control. Selçuk University Publications 379pp (In Turkish)Hoffmann MP & Frodsham AC (1993). Natural enemies of vegetable insect pests. Cooperative Extension, Cornell University, Ithaca, NY 63 pp
- Holm L G, Plunknett D L, Pancho J V & Herberger J P (1977). *The World's Worst Weeds*. University Press of Hawaii, Honolulu, Hawaii. USA. pp. 98-104
- Jabran K, Mahajan G, Sardana V & Chauhan BS (2015). Allelopathy for weed control in agricultural systems. *Crop. Prot.* 72: 57–65
- Karaman Y & Tursun N (2021). Germination biology of field bindweed seeds collected from different provinces. *Bulgarian Journal of Agricultural Science* 27(6): 1168-1177
- Kellogg EA (1998). "Who's Related to Whom? Recent Results from Molecular Systematic Studies". *Current Opinion in Plant Biology* 1/2: 149. [https://doi.org/10.1016/S1369-5266\(98\)80017-4](https://doi.org/10.1016/S1369-5266(98)80017-4)
- Keskin F, Kaya İ, Usta M, Demir İ, Sipahioğlu H M & Nemli Y (2017). Molecular Cloning and Sequence Analysis of The its Region of Nuclear Ribosomal DNA for Species Identification in Dodders (*Cuscuta*; Convolvulaceae). *International Journal of Agriculture & Biology*, Issn Print: 1560–8530; Issn Online: 1814–9596 17–0384/2017/19–6–1447–1451 Doi: 10.17957/Ijab/15.0442 <http://www.fsublishers.org>
- Knezevic S Z, Streibig J C & Ritz C (2007). Utilizing R software package for dose-response studies: the concept and data analysis. *Weed Technology* 21: 840–848. <https://doi.org/10.1614/WT-06-161.1>
- Knezevic S Z & Datta A (2015). The critical period for weed control: revisiting data analysis. *Weed Science* 63: 188–202. <https://doi.org/10.1614/WS-D-14-00035.1>
- Kubiak A, Wolna-Maruwka A, Niewiadomska A & Pilarska A A (2022). The Problem of Weed Infestation of Agricultural Plantations vs. the Assumptions of the European Biodiversity Strategy. *Agronomy*, 12, 1808.
- Kudsk P & Streibig J C (2003). Herbicides a two edged sword. *Weed Research* 43(2): 90–102. <https://doi.org/10.1046/j.1365-3180.2003.00328.x>
- Kuru H H & Üremiş İ (2021). “ Determination of density and frequency of field muskmelon (*Cucumis melo* var. *agrestis* Naudin) and field bindweed (*Convolvulus arvensis* L.) in Çukurova Region” *MKU Journal of Agricultural Sciences* 26(2): 461-471 (In Turkish)
- Lubenov Y (1985). Noxious Weeds are the Source of Death and Life. Çev, B. Makaklı, M. Dinçer. Cag Printing House. Ankara. (In Turkish)Lyons K E (1988). Element steward ship abstract for *Convolvulus arvensis* L. In: Field bindweed. Arlington: The Nature Conservancy pp.1-21
- Matteson P C (1995). The 50% Pesticide cuts in Europe: A Glimpse of our future? *American Entomology* 41: 210-220. <https://doi.org/10.1093/ae/41.4.210>
- Matzenbacher F O, Bortoly E D, Kalsing A & Merotto A Jr (2015). Distribution and analysis of the mechanisms of resistance of barnyard grass (*Echinochloa crus-galli*) to imidazolinone and quinclorac herbicides. *Journal of Agricultural Science* 153: 1044–1058. <https://doi.org/10.1017/S0021859614000768>
- Mourellos C A, Malbran I, Balatti P A, Ghiringhelli P D & Lori GA (2014). Gramineous and non-gramineous weed species as alternative hosts of *Fusarium graminearum*, causal agent of *Fusarium* head blight of wheat, in Argentina. *Crop Protection*, 65: 100-104
- Mummenhoff K, Franzke A & Koch M (1997). “Molecular phylogenetic of *Thlaspis*. I. (Brassicaceae) Based on Chloroplast DNA Restriction Site Variation and Sequences of the Internal Transcribed Spacers of Nuclear Ribosomal DNA” *Cand. J. Botany*, 75, (1997): 469–487. <https://doi.org/10.1139/b97-051>
- Nei M & Kumar S (2000). *Molecular Evolution and Phylogenetics*. Oxford University Press, New York.
- Nianxi Z, Yubao G, Wang J, Ren A & Xu H (2006). RAPD diversity of *Stipa grandis* populations and its relationship with some ecological factors. *Acta Ecologica Sinica* 26(5): 1312–1319. [https://doi.org/10.1016/S1872-2032\(06\)60023-1](https://doi.org/10.1016/S1872-2032(06)60023-1)
- Özkil M & Üremiş İ (2020). “ The Situation Of Morningglory (*Ipomoea* spp.) and Field Bindweed (*Convolvulus* spp.) Species And Their Frequency And Density In The Agricultural Areas Of The Mediterranean Region” *Ege University Faculty of Agriculture Journal* 57(2): 229-237 (In Turkish)
- Pimentel D, Acquay H, Biltonen M, Rice P, Silva M, Nelson J, Lipner V, Giordano S, Horowitz A & D'amore M (1992). Environmental and Economic Costs of Pesticide Use. *Bioscience* 42: 750-760. <https://doi.org/10.2307/1311994>
- Pimentel D & Greiner A (1997). Environmental and Socio-Economic Costs of Pesticide Use. (Ed.:D. Pimentel), *Techniques For Reducing Pesticide Use: Economic and Environmental Benefits*. John Wiley and Sons, Chichester (UK), pp. 51-78
- Qian Z Q, Xu L, Wang Y L, Yang J & Zhao G F (2008). Ecological genetics of *Reaumuria songorica* Pall. Maxim. population in the oasis-desert ecotone in Fukang, Xinjiang, and its implications for molecular evolution. *Biochemical Systematics and Ecology* 36: 593–601. <https://doi.org/10.1016/j.bse.2008.01.008>
- Saitou N & Nei M (1987). The neighbor-joining method: A new method for reconstructing phylogenetic trees. *Molecular Biology and Evolution* 4: 406-425
- Sarić-Krsmanović M, Zagorchev L, Gajić Umiljendić J, Rajković M, Radivojević L, Teofanova D & Vrbničanić S (2022). Variability in Early Seed Development of 26 Populations of *Cuscuta campestris* Yunck.: The Significance of Host, Seed Age, Morphological Trait, Light, Temperature, and Genetic Variance. *Agronomy* 12(3): 559
- Salonen J (1992). Efficacy of Reduced Herbicide Doses in Spring Cereals of Different Competitive Ability. *Weed Research* 32(6):483-491. <https://doi.org/10.1111/j.1365-3180.1992.tb01909.x>
- Soejima A & Nagamasu H (2004). Phylogenetic analysis of Asian *Symplocos* (*Symplocaceae*) based on nuclear and chloroplast DNA sequences. *Journal of Plant Research* 117(3):199-207

- Steckel LE, Defelice MS & Sims BD (1990). Integrating Reduced Doses of Post Emergence Herbicides and Cultivation for Broad Leaf Weed Control in Soybeans (*Glycine max*). *Weed Science* 38: 541-545. <https://doi.org/10.1017/S0043174500051456>
- Sunar S, Agar G & Nardemir G (2015). Analysis of genetic diversity in bindweed (*Convolvulus arvensis* L.) populations using random amplified polymorphic DNA (RAPD) markers. *Journal of Biodiversity and Environmental Sciences (JBES)*. ISSN: 2220-6663 (Print) 2222-3045 (Online). Vol. 7, No. 1, pp. 197-204
- Tamaki G, Moffitt H R & Turner J E (1975). The influence of perennial weeds on the abundance of the red backed cutworm on asparagi. *Environmental Entomology* 4: 274-276
- Tamura K, Stecher G & Kumar S (2021). MEGA 11: Molecular Evolutionary Genetics Analysis Version 11. *Molecular Biology and Evolution* <https://doi.org/10.1093/molbev/msab120>.
- Tursun A O, Sipahioglu H M & Telci I (2021). Genetic relationships and diversity within cultivated accessions of *Salvia officinalis* L. in Turkey. *Plant Biotechnology Reports* 15(5): 663-672
- Ulloa SM, Datta A, Bruening C, Neilson B, Miller J, Gogos G & Knezevic S Z (2011). Maize response to broadcast flaming at different growth stages: effects on growth, yield and yield components. *European Journal of Agronomy* 34: 10–19. <https://doi.org/10.1016/j.eja.2010.09.002>
- Uygur N & Şekeroğlu E (1993). Agricultural Development and Nature Conservation in the Göksu Delta, Proceedings of the International Göksu Delta Environmental Development Seminar. Natural Life Protection Association, Istanbul, p. 162 (In Turkish)
- Üremiş İ, Soylu S, Kurt Ş, Soylu E M & Sertkaya E (2020). Evaluation of Weed Species, Their Frequencies, Densities and Current Status in Carrot Fields in Hatay Province. *Tekirdağ Faculty of Agriculture Journal* 17(2): 211-228. <https://doi.org/10.33462/jotaf.645336> (In Turkish)
- Vogelgsang S (1998). Pre-emergence Efficacy of Phomopsis *C. arvensis* Ormeno to Control Field Bindweed (*C. arvensis* L.). Ph.D. thesis, Department of Plant Science, Macdondd Campus of McGU University Montr6al. QC. Canada.
- Vranjes F, Vrbnicanin S, Nedeljkovic D, Savic A & Bozic D (2019). The response of *Chenopodium album* L. and *Abutilon theophrasti* Medik. to reduced doses of mesotrione. *Journal of Environmental Science and Health, Part B*, 54(7): 615-621
- White TJ, Bruns T, Lee S & Taylor J (1990). Amplification and direct sequencing of fungal ribosomal RNA genes for phylogenetics. Pages 315-322 in M. A. Innis, D. H. Gelfand, J. J. Sninsky, and T. J. White, eds. *PCR Protocols-A Guide to Methods and Application*. San Diego: American Press.
- Xia T, Chen SL, Chen SY & Ge XJ (2005). Genetic variation within and among populations of *Rhodiolaalsia* (Crassulaceae) native to the Tibetan Plateau as detected by ISSR markers. *Biochemical Genetics* 43(3–4): 87–101. DOI: 10.1007/s10528-005-1502-5
- Yusriah L, Sapuan S M, Zainudin E S & Mariatti M (2012). Exploring the potential of betel nut husk fiber as reinforcement in polymer composites: effect of fiber maturity. *Procedia Chemistry* 4: 87-94
- Yokoyama J, Suzuki M, Iwatsuki K & Hasebe M (2000). Molecular Phylogeny of *Coriaria* with Special Emphasis on the Disjunct Distribution, *Molecular Phylogenetics and Evolution* 14(1): 11. <https://doi.org/10.1006/mpev.1999.0672>
- Zhang J, Weaver SE & Hamill AS (2000). Risks and Reliability of Using Herbicides at Below-labeled Rates. *Weed Technology* 14:106-115. <https://doi.org/10.1614/0890-037X>



Copyright © 2024 The Author(s). This is an open-access article published by Faculty of Agriculture, Ankara University under the terms of the [Creative Commons Attribution License](https://creativecommons.org/licenses/by/4.0/) which permits unrestricted use, distribution, and reproduction in any medium or format, provided the original work is properly cited.



Comparative Assessment of Solar Dryer with Thermal Energy Storage System and Heat Pump Dryer in Terms of Performance Parameters and Food Analysis

Özlem Timurtas^a , Gökhan Gürlek^{b*} 

^aGraduate School of Natural and Applied Science, Ege University, Izmir, TÜRKİYE

^bFaculty of Engineering, Department of Mechanical Engineering, Ege University, Izmir, TÜRKİYE

ARTICLE INFO

Research Article

Corresponding Author: Gökhan Gürlek, E-mail: gokhan.gurlek@ege.edu.tr

Received: 15 November 2023 / Revised: 18 February 2024 / Accepted: 22 February 2024 / Online: 23 July 2024

Cite this article

Timurtas Ö, Gürlek G (2024). Comparative Assessment of Solar Dryer with Thermal Energy Storage System and Heat Pump Dryer in Terms of Performance Parameters and Food Analysis. *Journal of Agricultural Sciences (Tarim Bilimleri Dergisi)*, 30(3):594-605. DOI: 10.15832/ankutbd.1391447

ABSTRACT

Striving for the highest quality food product in the shortest time with the least energy expenditure is the cornerstone of the food drying process. Furthermore, the geometric properties of the product significantly influence the efficiency of the drying process. Therefore, in this study, peach slices of three different thicknesses were dried in three different dryer types. The drying of peaches was carried out using a solar energy drying system, a thermal energy storage solar dryer, and a dryer with a heat pump. The drying performances of peach slices of three different thicknesses were investigated. Moisture extraction rates (MER), specific moisture extraction rates (SMER), and specific energy consumption

(SEC), which relate to the amount of removed moisture and the amount of consumed energy at the end of the drying studies, were calculated. Food analyses, such as moisture content, color, texture, and water activity were performed. Considering the amount of energy consumed, it is seen that the heat pump system consumes more energy than the solar energy system. In addition, by using the heat storage system, the drying time is shortened, and the energy consumption is reduced. A decrease in SEC values was observed with the activation of the heat storage solar dryer.

Keywords: Solar assisted dryer, Basalt stone, Thermal energy storage, Heat pump dryer

1. Introduction

Since drying is a highly energy-demanding process, various drying systems have been developed to increase energy efficiency and reduce energy costs. Solar dryers are systems that provide higher energy savings compared to other drying technologies. However, the great disadvantage of these systems is that their operation is restricted to sunlight. Energy storage methods have been developed to store solar energy as heat energy to continue drying even without the sun. When there is little or no sunlight, this stored energy is converted into usable energy. Thus, while shortening the total drying time, economical and hygienic drying is provided (Atalay 2019). Considering these circumstances, the significance of energy storage mediums in industrial drying processes is steadily growing. Many studies on solar-powered dryers and thermal storage systems have been carried out. While agricultural products and seafood were dried by Fudholi et al., within the scope of solar drying studies (Fudholi et al. 2014), drying models were obtained by drying mint leaves in another study (Akpınar 2010). Pepper (Akin et al. 2014), tomato (Gürlek et al. 2009), bitter melon slices (Vijayan et al. 2020), apple, and mint (Şevik et al. 2019) were dried using solar air collectors. The drying of asparagus roots was examined in a distinct study by Kohli et al., using four different drying methods at 40, 50, 60, and 70 °C in sun drying, tray drying, fluidized bed drying, and vacuum drying (Kohli et al. 2021).

Energy storage systems offer a solution to the discontinuity problem encountered in renewable energy applications. Thus, the operating costs of the system used are reduced (Gunerhan & Hepbasli 2005). Heat storage materials are expected to have certain thermo-physical qualities such as high thermal conductivity and heat storage capacity. Many studies have been done on the capacity of materials to store thermal energy. As thermal energy storage (TES) material, sand, rock, aluminium (Natarajan et al. 2017), pebble (Atalay 2020; Chaouch et al. 2018), paraffin wax (Atalay 2020), concrete, sand, and rock bed (Ayyappan et al. 2016) were used. Apricot (Baniasadi et al. 2017), apricot, onion, pea (Rehman et al. 2023), radish, pepper, mushroom (Qiu et al. 2016), wheat seeds (Singh et al. 2022), and crop (Abubakar et al. 2018) drying studies were also dried using heat storage materials.

Since the drying process is an intense energy consuming process, the use of heat pumps has emerged as an alternative in drying operations. It is stated that energy consumption will decrease with the increase in efficiency in heat pump systems used

in drying applications (Goh et al. 2011). Evaluation of the physical attributes of heat-pump-dried food reveals its consistently superior quality compared to conventionally dried counterparts. According to the research with tray dryer, microwave dryer, heat pump dryer and freeze dryer conducted by Baysal et al. (2015), the heat pump dryer had the lowest energy consumption and the highest MER and SMER values (Baysal et al. 2015). Also, sliced apple (Aktaş et al. 2019), tomato (Queiroz et al. 2004) cereals (Liu et al. 2019), sliced radishes (Lee & Kim 2009), plums (Hepbasli et al. 2010), cotton cloth (Ganjehsarabi et al. 2014), and apple (Gürlek et al. 2015) drying studies were carried out using a dryer with a heat pump.

The drying method and drying system affect the product quality. Properties of the dried product, such as color, odor, final moisture content, water activity value, aroma, nutritional value, and content of harmful substances such as aflatoxin, determine the quality of the product. Exposing the products to high temperatures during the drying process degrades the quality. The process temperature can be lowered to increase product quality, attention should be paid to the increase in drying time and drying costs (Nindo et al. 2003). Different drying processes affect product quality directly. For example, long exposure to the hot air generated by electrical resistance decreases the quality of the products. On the other hand, high operating costs also arise in the freeze-drying process where high-quality products are obtained (Huang et al. 2011). It was determined that dried apple slices produced by freeze drying and microwave methods are of higher quality compared to those produced by tray and heat pump drying methods (Baysal et al. 2015). In another study, kiwi fruit was air-dried at four different temperatures and its drying properties were determined (Orikasa et al. 2008). Using a combined convection-microwave dryer, Kesbi et al. studied the drying of lemon slices. Measurements of L^* , a^* , b^* , a total color difference, chroma, and rehydration capability were used to assess the dried lemon slices' quality (Mirzabeigi Kesbi et al. 2016). In their study to dry Brussels sprouts, Nakilcioğlu-Taş and Ötleş determined that a^* , ΔE and browning index increased with increasing microwave output power during drying (Nakilcioğlu-Taş & Ötleş 2018). Polat et al. carried out drying studies of peach puree using microwave dryer, convective dryer, and combined convective-pulsed microwave dryer. They examined the drying curves, color, pH and microstructure of the dried products (Polat et al. 2021).

Inspired by the fact that heat pump dryers and solar dryers are cheaper than other dryers, we hypothesize that low energy consumption and high-quality drying can be realized in a shorter drying time by using three different types of dryers: solar energy drying systems (SEDS), thermal energy storage drying systems (TESDS), and heat pump drying systems (HPDS). The results obtained from the solar-powered dryer when the storage unit is active, and passive were compared with the results of the experiments made with the dryer with a heat pump at the same temperature. In SEDS, drying was carried out during the hours of solar radiation, while continuous drying was carried out in TESDS and HPDS. The results include an evaluation of the positive effects of the thermal energy storage (TES) system on system performance, energy consumption, and drying time. Additionally, the study examines the quality characteristics of the dry products obtained through the drying process in different dryers. Thus, besides the amount of energy consumed, quality criteria were also evaluated. It is expected that the effect of the TES system on the drying time, the performance parameters of three different drying systems, and the product quality characteristics discussed in the study will contribute significantly to the literature.

2. Material and Methods

2.1. Dried material

The peach was used in the drying study. Peach (*Prunus Persica*) fruit is a downy fruit from the Rosaceae family of the order Rosales and is mostly grown in tropical-subtropical regions in the world. It contains vitamins A and C, fiber, potassium minerals, and phytochemical compounds such as anthocyanin, total phenol, and flavonoid (Saidani et al. 2017).

2.2. TES material

Unlike the literature (Kant et al. 2016) that uses many energy storage materials in solar drying systems, basalt stone was used as an energy storage material in this study. Basalt, along with granite, is one of the two most common rocks in nature. It is an extrusive rock with fine grains and contains more iron and magnesium with respect to granite. It usually consists of minerals such as olivine, pyroxene, and feldspar. Basalt has a hard, dark, and dense texture. Being a hard material provides superior abrasion resistance in basalt. It was formed by the solidification of magma and its melting point temperature is above 1050 °C. It has a density between 2800 and 2900 kg/m³. Thermo-physical properties related to basalt stone are shown in Table 1 (Gunerhan & Hepbasli 2005; Hartlieb et al. 2016; Nahhas et al. 2019).

Table 1-Physical properties of basalt rocks (Hartlieb et al. 2016).

<i>Physical properties of basalt stone</i>	
Density (kg/m ³)	2870
Specific Heat Capacity (J/kg K)	898
Thermal Capacity (MJ/m ³ K)	2.58
Diffusivity (mm ² /s)	0.79
Thermal Conductivity (W/mK)	1.55

2.3. Experimental setup of solar dryer With/Without TES system

Three types of dryers were used for experimental studies: SEDS, TESDS, and HPDS. The designed and produced solar dryer with a TES unit is shown schematically in Figure 1-a. The system consists of basic elements such as solar air collectors (2), drying cabinet (1), perforated shelves to accelerate the heat transfer mechanism (3), fans (5,6), waste heat recovery unit (7), and TES unit (14). The TES unit consists of three solar air collectors (8), fans (11,12), and basalt stone (13). In addition, the crossflow heat exchanger (7) installed in the drying system allows the waste heat to be recovered at a certain rate. The drying cabinet is surrounded by insulation material (0.030 W/mK) with a low heat conduction coefficient to prevent heat loss. The five solar air collectors used in the system are made of double-layer polycarbonate cover material and polystyrene insulation material surrounding the main body.

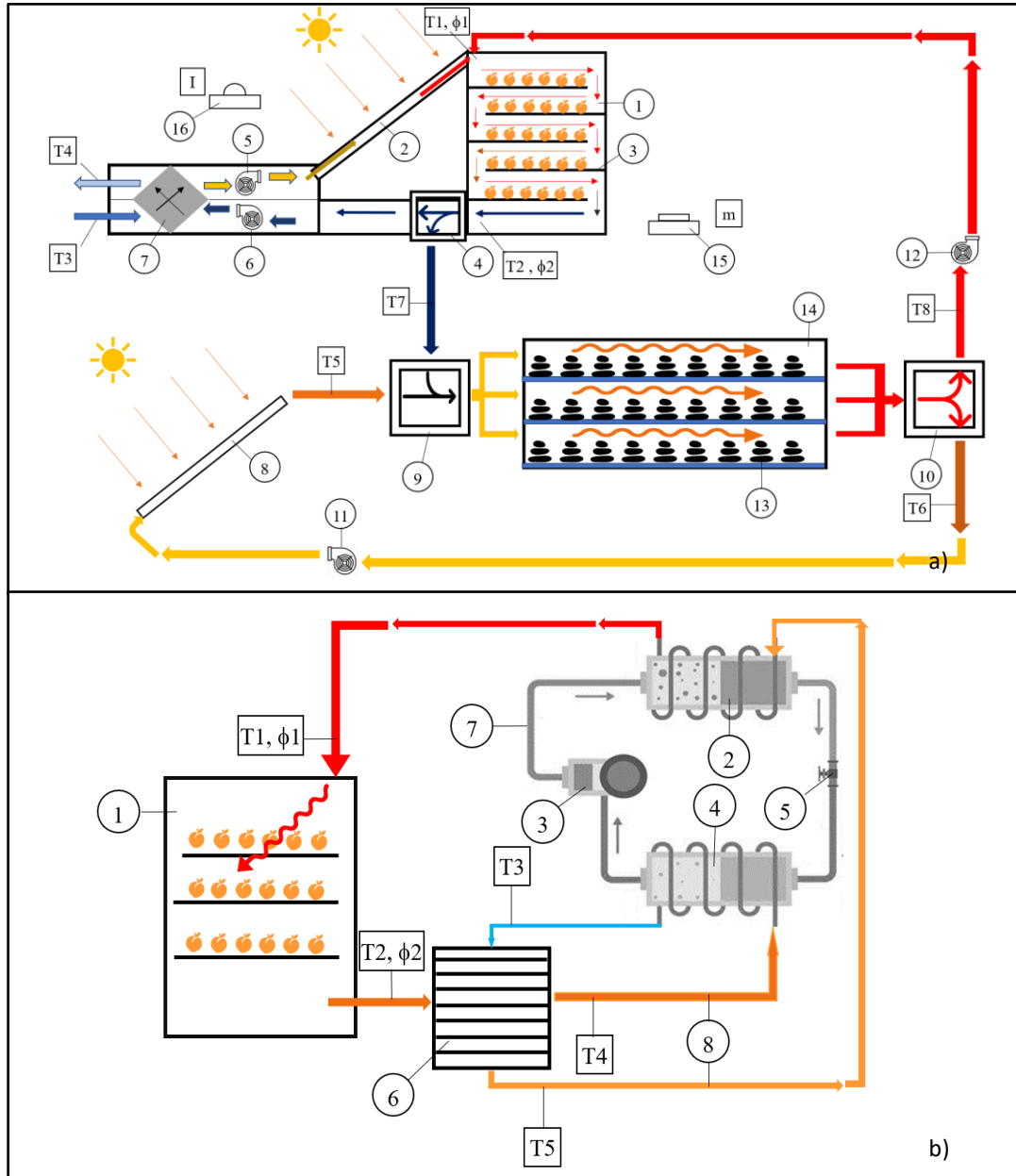


Figure 1-Schematic representations a) the solar assisted thermal energy storage dryer, b) the dryer with a heat pump

Fresh air taken from the outside is heated by passing through solar energy collectors (2). The air, whose temperature is brought to drying temperature, is contacted with the product to be dried in the drying cabinet (1). The air, whose temperature decreases, and humidity increases, leaves the drying cabin, and is sent to the crossflow heat exchanger (7) in the waste heat recovery unit. The energy in the air leaving the drying cabin is transferred to the fresh air taken from outside through this heat recovery. Thus, the temperature of the fresh air is slightly increased before it enters the solar energy collector, and heat recovery is achieved. During daylight hours, the energy storage unit (14) works in parallel with the drying unit but independently of each other. In the three solar energy collectors (8) in this system, the heated air enters the energy storage cabinet (13). The air transfers

its energy to the basalt stones and is sent to the collectors with a reduced temperature. The energy obtained during the hours of sunlight is stored in basalt stones. When the solar radiation values are insufficient for the drying process, the airflow direction is changed with dampers (4,9,10). Thus, the low-temperature air leaving the drying cabinet enters the energy storage cabin via dampers (4, 9). Drying air temperature increases with the stored energy it receives from basalt stones. The drying air, whose temperature increases, is sent back to the drying cabinet by the damper (10). Thus, the drying process is carried out continuously during the hours when there is no sunlight.

During the drying process, anemometer was used for air velocity measurement at the entrance of the drying cabinet and similarly pyranometer was used for solar radiation (I) measurement in the system. The product mass (m) loss was recorded at 30 minutes intervals by means of a precision balance. The humidity of the drying air was measured at the entrance and exit of the drying cabinet. Drying cabinet inlet and outlet temperatures (T1, T2), waste heat recovery unit inlet and outlet air temperatures (T3, T4), inlet and outlet air temperatures (T7, T8) when the energy storage system is active and energy storage unit inlet and outlet air temperatures (T5, T6) were measured every five minutes.

2.4. Experimental setup of the HPDS

Another system used is the HPDS shown schematically in Figure 1-b. The heat pump unit, drying cabinet (1), drying air ducts (8), and heat recovery unit (6) are the main components of the HPDS. The heat pump unit, on the other hand, consists of the compressor (3), condenser (2), evaporator (4), refrigerant channel (7), and expansion valve (5).

The drying cabinet is constructed from panels that are 8 cm thick and have polyurethane insulation. The shelf arrangement is made gradually and the passage of the drying air through the entire product surface is provided. The shelves are made of perforated steel wires for maximum contact of the drying air with the product. Air ducts are made of 0.6 mm thick galvanized sheet material. Insulation is made to prevent heat loss from air ducts. The heat pump unit used in the drying system allows drying to a maximum of 55 °C.

The HPDS is a two-fluid system. R404 refrigerant is used as the fluid. The refrigerant evaporated by the heat drawn from the drying air in the evaporator part of the heat pump unit is compressed up to the condenser pressure with the compressor. In the condenser, the thermal energy within the refrigerant transfers to the drying air, and the temperature of the drying air increases up to the drying temperature. The temperature of the refrigerant decreases a little after transferring its energy to the drying air. The refrigerant leaving the condenser at a relatively low temperature and high pressure is throttled in the expansion valve until the evaporator pressure. Thus, the cycle of the refrigerant is completed. The drying air enters the drying cabinet after being heated in the condenser. After the drying process, it comes to the heat exchanger with a decrease in temperature and an increase in moisture. Here, the temperature of the low temperature drying air leaving the evaporator is slightly increased before it enters the condenser. Thus, system efficiency is increased by preheating.

Temperature values (T2, T3, T4, T5) from the inputs and outputs of the waste heat recovery unit and the temperature (T1, T2) and humidity values (ϕ_1 , ϕ_2) at the entrance and exit of the drying cabin were measured and recorded. Sizing information for both drying systems is shown in Table 2.

Table 2-Dimensions and capacities of dryer equipment's

<i>Dryer systems dimension and capacity</i>	
<i>Solar dryer with thermal energy storage system</i>	
Drying Cabin (length x width x height)	2.3 m x 2.3 m x 2.3 m
Solar Air Collector (length x width)	2 m x 1 m
Distance Between Perforated Shelves	0.4 m
Waste Heat Recovery Unit (length x width x height)	1.1 m x 0.4 m x 0.4 m
Thermal Energy Storage System (length x width x height)	2 m x 1 m x 1 m
<i>Heat pump dryer</i>	
Compressor	1300 W
Condenser	4800 W
Evaporator	3500 W
Drying cabin (length x width x height)	0.86 m x 0.86 m x 1.20 m
Air Vent (length x width)	0.40 m x 0.20 m
Perforated Shelves (length x width x height)	0.70 m x 0.70 m x 0.02 m

2.4. Determination of energy efficiency in drying systems

The efficiency of drying systems was assessed using moisture extraction rates (MER), specific moisture extraction rates (SMER), and specific energy consumption (SEC). SMER is defined as kilograms of moisture removed (MoR) per kilowatt-hour of energy

consumed during drying (EC). Consumed energy relates to the total power of the dryer, including the power of the fan and electrical equipment. The amount of moisture evaporating in drying time (DT), or MER, is a indicator of drier capacity. The total energy needed to remove one kilogram of water is known as SEC, which is the opposite of SMER (Baysal et al., 2015). SMER, MER, and SEC values are calculated with the following equations respectively.

$$SMER = \frac{MoR}{EC}, \left(\frac{kg}{kW} \right) \quad (1)$$

$$MER = \frac{MoR}{DT}, \left(\frac{kg}{h} \right) \quad (2)$$

$$SEC = \frac{EC}{MoR}, \left(\frac{kWh}{kg} \right) \quad (3)$$

2.5. Food analysis of dried products

In this study, dried peach slices of different thicknesses were subjected to various food analyses such as moisture, water activity, color, and texture profile.

2.6. Determination of moisture content

The moisture content determination of dried peach slices was made in a vacuum oven (Wisd, WiseVen, Germany). Three grams of samples were kept in a vacuum oven at 67 °C until they reached constant weight in petri dishes. The amount of moisture was calculated as a percentage based on the dry base.

2.7. Determination of water activity

A water activity measuring instrument (Testo AG 400) with an accuracy of ± 0.001 was used to calculate the water activity value, which is defined as the ratio of the product's equilibrium vapor pressure to pure water's equilibrium vapor pressure at the same temperature. To determine the water activity (aw), approximately 3-4 g of sliced peach sample was placed into the instrument's sealed chamber made of stainless steel. When there is a change of less than 0.001 in the water activity value, it is assumed that the system has reached the balance, and the water activity value is read from the indicator of the device. Fruits with an aw value below 0.7 were considered dried fruit (Bourdoux et al. 2016). The basis of the measuring device is to calculate the water activity value of the product using the following equation:

$$a_w = \frac{P}{P_0} \quad (4)$$

Where; P and P₀ denote the vapor pressure of the water in the product and the vapor pressure of pure water, respectively.

2.8. Color determination

A Hunter Lab Color Flex (CFLX 45-2) was used to measure the color values of dried peach slices. The values of the color parameters L*, a*, and b* were established. The product's brightness, redness, and yellowness are indicated by the values L*, a*, and b* respectively. After standardization, fresh and dried product a*, L*, and b* values were determined. The subscript "ref" states the color of the fresh peach slices accepted as a reference in equation 5 and equation 6. The L* value takes values starting from 0 for dark colors and continuing up to 100 for light colors. Total color difference (ΔE) and color intensity (chroma, ΔC) are calculated according to the following equations respectively. Total color difference, a calorimetric statistic that combines a*, b*, and L* is frequently used to describe the color change in foods during drying processing. Chroma value refers to the saturation degree of the color and changes in proportion to the strength of the color (Baysal et al. 2015).

$$\Delta E = \sqrt{(L^* - L^*_{ref})^2 + (a^* - a^*_{ref})^2 + (b^* - b^*_{ref})^2} \quad (5)$$

$$\Delta C = \sqrt{(a^* - a^*_{ref})^2 + (b^* - b^*_{ref})^2} \quad (6)$$

2.9. Tissue profile (shearing) analysis

Tissue profile analyzes of dried peach slices were performed using TAXT Express tissue analyzer (Stable Microsystems, Surrey, UK) and shear forces were calculated.

2.10. Statistical analysis

Statistical analysis was applied to results from the triplicate trials. In the statistical evaluation of food analysis results, the differences between samples were determined using one-way ANOVA analysis. Tukey test was used to determine significant differences at $P < 0.05$.

2.11. Experimental drying processes

Peaches were sliced in thicknesses of 3, 5, and 10 mm using a slicing machine. The sliced peaches were dried in three drying options (SEDS, TESDS, HPDS) and the data during drying were examined. Experiments have been started by using solar energy-assisted TES system. Measurements were taken at the determined points in the system. Data was collected at regular intervals to monitor the drying process of peach slices. Solar radiation levels were measured every 10 minutes, the mass loss of the peach slices was recorded every 30 minutes, and temperature and humidity values were captured every 5 minutes. Temperature and humidity were measured and recorded at various locations throughout the dryer with heat pump. The mass loss in peach products during drying was determined by regularly weighing the product. According to the data obtained during the studies, temperature and humidity distributions, air velocity changes, solar radiation values during the day, drying rate, and moisture content curves were analyzed.

In SEDS, drying was carried out during the hours when solar radiation was present, while continuous drying was carried out in TESDS and HPDS. Thus, total drying times for different drying options were determined. Based on the energy consumed for drying, SMER, MER, and SEC values were compared. The quality properties of the dry products were obtained. Thus, besides the amount of energy consumed, quality criteria were also evaluated.

3. Results and Discussion

At first, peach slices of 3-, 5-, and 10-mm thickness were dried in SEDS. Figure 2 shows the radiation values of these drying processes and the inlet - outlet air temperatures of the drying chamber. In all three experiments, the irradiance values were around 1000 W/m^2 at noon. Sudden changes in radiation values in the 5 mm peach drying study can be explained by the cloudiness. In all drying studies, the difference between the temperature of the inlet air (T1) and the temperature of the outlet air (T2) is maximum at noon and is the lowest in the morning and evening hours. The ambient air temperature (T3) varied in the range of 25-30 °C throughout the experiments. The data obtained revealed that the experiments were carried out in similar weather conditions. Each experiment was started at 11:00 am and continued until the products were dry. 3 mm peach slices were dried until 17:00, 5 mm peach slices were dried until 19:00, and the drying process of 10 mm peach slices was finished on the second day. 3 mm slices dried in 6 hours, 5 mm slices dried in 8 hours, and 10 mm slices dried in 14 hours are shown in Figure 2.

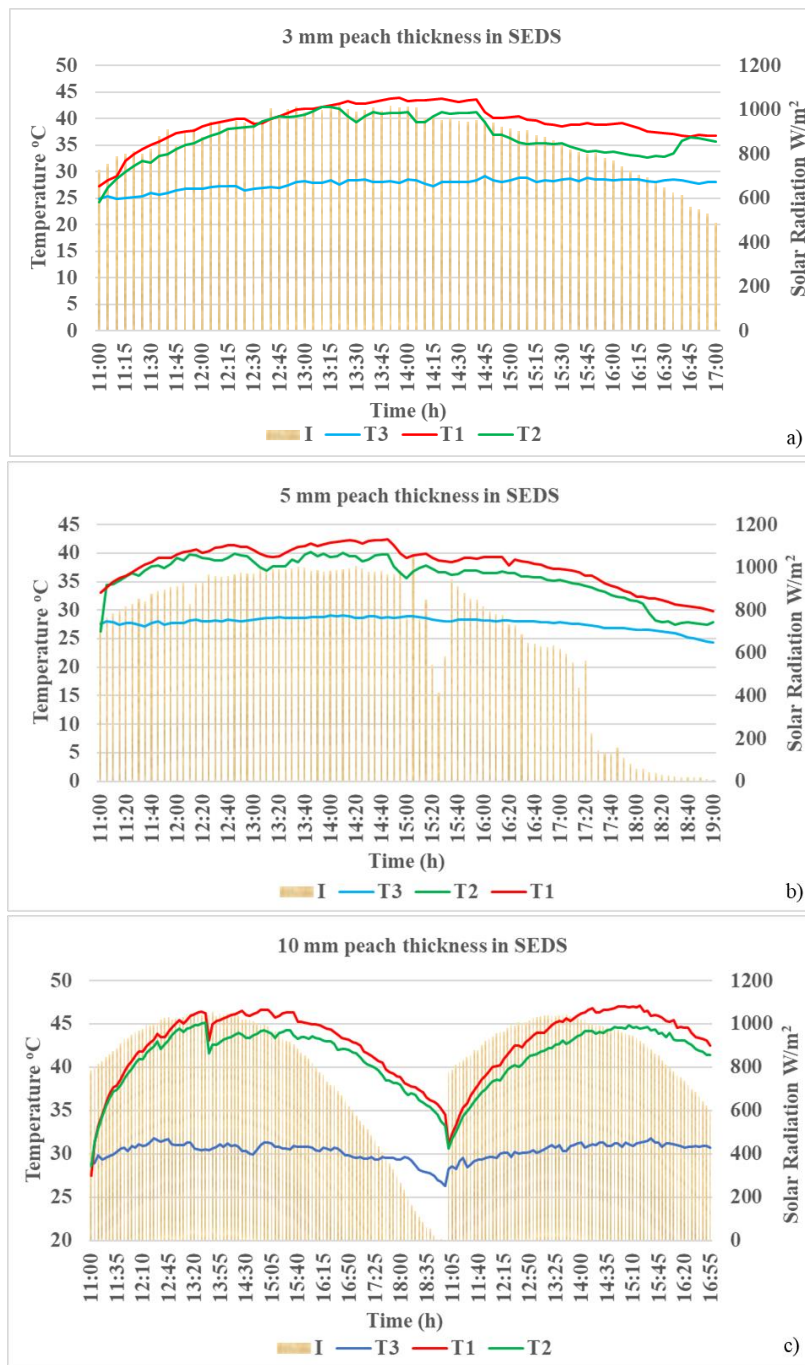


Figure 2-Solar radiation and drying temperatures for different peach thicknesses a)3 mm, b)5 mm, c)10 mm in SEDS

It was observed that as the peach thickness increased, the drying times were prolonged and even delayed to the second day. Reducing drying times is important for system performance and costs. For this reason, new studies have been carried out by including the TES unit using basalt stone in the drying system. Firstly, drying was applied to 3 mm thick peach slices. The drying was started at 11:00 and was completed at 17:00. During the experiment, there was no need to activate the TES unit by opening the dampers during the drying of 3 mm-thick products.

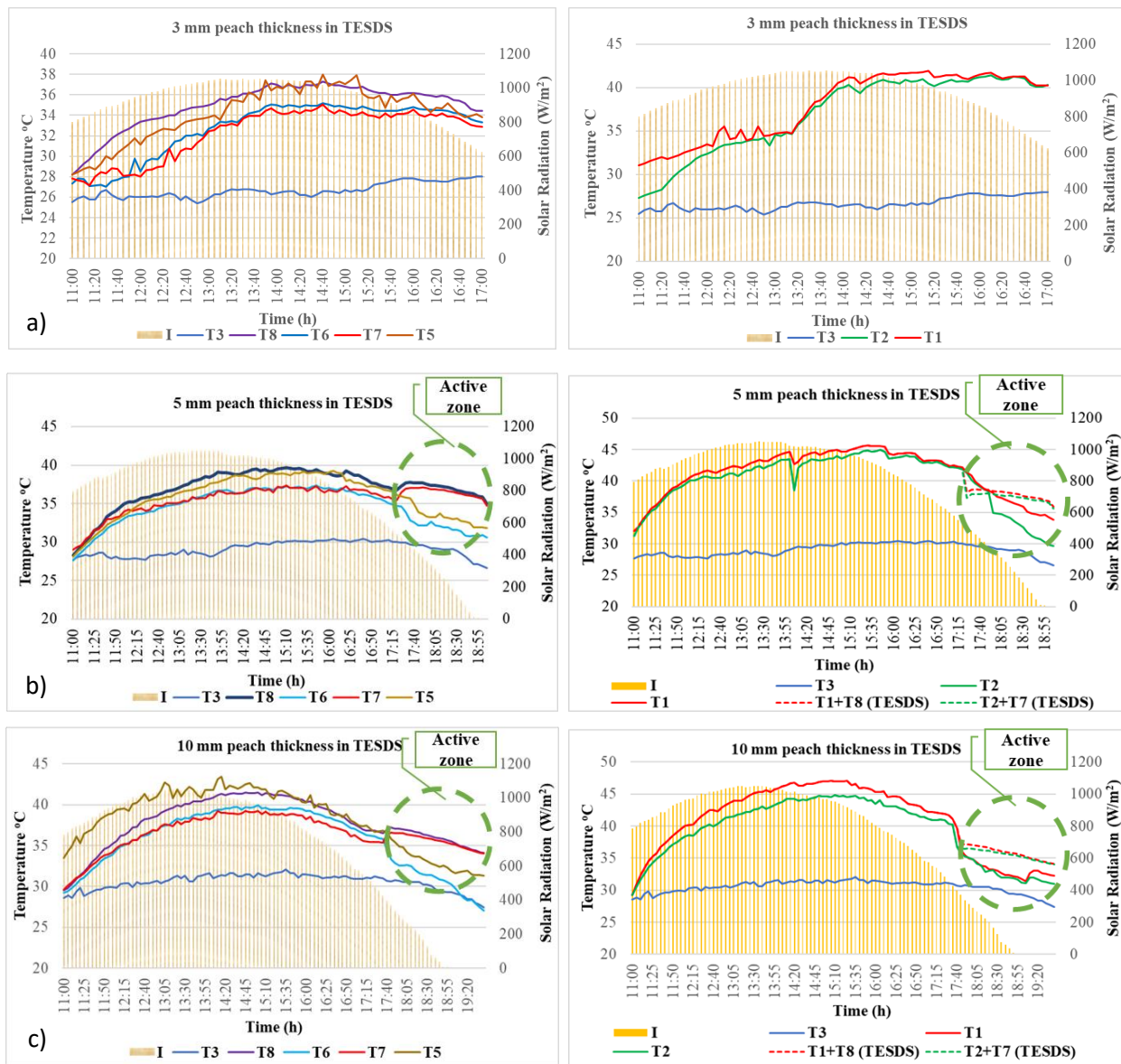


Figure 3-Solar radiation and drying temperatures for a) 3 mm peach in TESDS, b)5 mm peach in TESDS, c) 10 mm peach in TESDS

In Figure 3-a, daily solar radiation values (I), ambient air temperature (T3), drying cabinet inlet (T1) and outlet (T2) temperatures, and temperature changes at the inlet - outlet points of the TES unit (T5, T6, T7, and T8) are given. The air circulating in the TES unit during the day provided the storage of thermal energy in the basalt stones. The temperature (T5) of the air circulating in the storage unit increased at the exit of the solar air collectors, and the air temperature (T6) decreased after transferring the thermal energy to the basalt stone. Thus, energy is stored in the basalt stone during the day. Since the TES unit was not activated in this drying study, the air at T7 and T8 points was stagnant and changed depending on the radiation value.

The daily radiation values (I), ambient air temperature (T3), inlet (T1), and outlet (T2) temperatures of the drying cabinet and the temperature changes at the inlet-outlet points of the TES unit (T5, T6, T7, T8) during the experiments carried out for the drying of 5 mm peach slices are given in Figure 3-b. Unlike Figure 3-a, in these trials, the TES unit was activated as of 17:30 and the thermal energy required for drying was obtained from the heat stored in the basalt stone. In the figure, the air temperature entering the drying cabinet (T1+T8) and the air temperatures (T2+T7) leaving the drying cabinet are shown with dashed lines for the active and de-active states of the TES unit. The change in the temperature of the air entering the drying cabinet when the TES unit is not used and the temperature change of the air entering the drying cabinet when the storage unit is active is shown in the circular active zone with dashed lines. When the active zone in the circle is examined, it is seen that the air at the desired temperature is supplied to the drying cabinet by using the storage system during the evening hours when the solar radiation values are very low. From the moment the TES unit was activated with the control of the dampers depending on the solar radiation, a sudden increase was observed in the T7 and T8 temperatures due to the energy taken from the basalt stone. Figure 3-c shows the temperatures in the drying of 10 mm thick peach slices using a TESDS. When the TES unit was not used, 10 mm thick peach samples were dried in two days, while when the storage unit was activated, they dried at 19:40. The fact that drying

continues even during hours when there is no solar radiation shortened the total drying time and enabled the desired dryness level to be reached more quickly.

In addition to the solar dryer, peach slices with 3-, 5- and 10-mm thicknesses were dried in a HPDS. Since it was not exposed to solar radiation, the system worked at constant temperature values. The system was set so that the temperature of the air entering the drying cabinet was 40 °C. Temperatures of 40-41 °C, 39-40 °C, 14 °C, 26 °C, and 26-27 °C were measured at T1, T2, T3, T4, and T5 points, respectively, in three drying experiments (Figure 1-b).

The time-dependent moisture content changes obtained from the experiments with three different drying methods are given in Figure 4. When the graph is examined, it is a natural result that as the thickness of the peach samples increases, the drying time is prolonged due to the high moisture content.

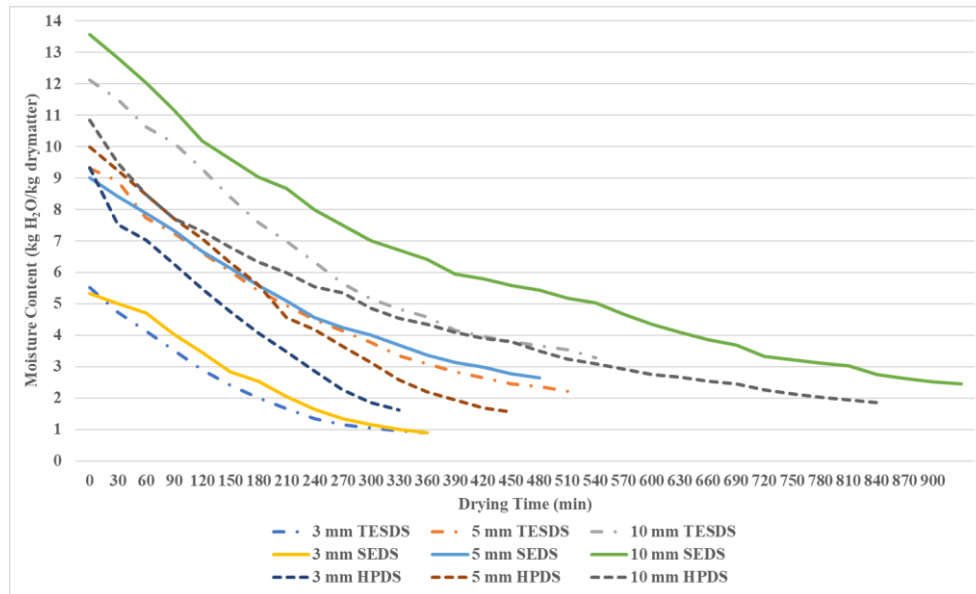


Figure 4-The time-dependent moisture content changes for experiments with three different drying methods

The most significant difference occurred during the drying of 10 mm thick peach samples. It has been observed that the drying studies performed with HPDS and SEDS are delayed to the second day, whereas in the drying performed with TESDS, the drying period ends at the end of the first day with the use of the heat stored during the day. It has been determined once again that the TESDS makes a positive contribution to the drying time.

The weight of the peach slices was measured in each experiment before and after drying, and the overall amount of moisture removed from the products was calculated. The drying system's electricity meter was used to calculate the consumption of electrical energy. For each experiment, the SMER, MER, and SEC values are shown in Table 3-a. In the 10 mm peach drying trials where the heat storage system was activated, it was observed that the MER value increased, and the SEC value decreased with the shortening of the drying time. On the other hand, in terms of the amount of moisture removed per unit of energy consumed, SEDS and TESDS systems seem to be quite successful compared to the heat pump drying system. It is seen that the highest energy consumption occurs with the heat pump drying system. Results similar to the SMER value range of 0.13 kg/kWh to 0.40 kg/kWh found in the study (Yahya et al. 2018) using a solar-assisted heat pump dryer were obtained.

Moisture content, water activity, color, and texture profile analyses of dried peach slices were made. Food analysis results for peach slices are given in Table 3-b. The moisture content of dried peach slices varies between 0.90 kg_{water}/kg_{drymatter} and 3.29 kg_{water}/kg_{drymatter}. When the drying methods were compared with each other, they were found to be statistically different ($P < 0.05$). Karaaslan et al., in their three different drying studies of peach in a solar dryer, found the final moisture content similar to our study (Karaaslan et al. 2021). Water activity has a direct relationship with equilibrium moisture content. As seen in Table 3-b, water activity results varied between 0.52 - 0.91. It was found that the water activity of 10 mm TESDS samples was the greatest and was significantly different from other samples ($P < 0.05$).

Color analyses of fresh and dried peaches were made, and the results were compared with each other. The color of peach slices before processing was determined as $L^* = 61.82 \pm 0.15$, $a^* = 15.09 \pm 0.07$, $b^* = 41.85 \pm 0.11$. L^* values, which indicate the lightness of the product, vary between 51.61 and 77.00. The L^* value of the 5 mm SEDS sample is very similar to that of fresh peach samples. The highest L^* values were obtained in products dried with a heat pump. When the a^* values were examined, it was seen that the products dried with solar energy turned red due to the browning that occurred during the drying process. The b^* values of the dried products varied between 34.03 - 56.33. The differences in L^* , a^* , and b^* values between the different

drying methods were found to be statistically significant ($P<0.05$). For each drying method, the increase in slice thickness and drying time caused a darkening in the product color, and L^* values decreased. The a^* and b^* values showed that the color change occurred mostly in yellow tones. Total color differences (ΔE) were calculated between 3.48 and 21.57. Minimum ΔE values were evaluated for 5 mm SEDS samples, and the highest ΔE values were evaluated for 5 mm HPDS samples. There was no significant change in ΔE values for 3 mm SEDS and 5 mm SEDS ($P>0.05$). In a study conducted in a solar dryer (García-Moreira et al. 2023), the color change values of peaches dried at different drying air speeds were found to be 13.28 ± 7.6 and 17.13 ± 4.4 . These results are especially similar to those from TESDS drying experiments. It was understood that the drying time due to the drying methods is effective on the color change value. The minimum ΔC was calculated for 3 mm SEDS.

The shear forces of fresh and dried peach slices were examined. Depending on the amount of drying and slice thickness, increases in shear force were observed. As can be seen from literature research, it has been revealed that food analysis results differ in peach drying studies (Tan et al. 2022). These differences between studies can be attributed to factors such as dryer type, drying time, drying temperature, and product type.

Table 3- a) Performance parameters of drying experiments and b) food analysis results of peach slices

<i>Performance parameters of drying experiments</i>								
	Dried Peach (g)	Consumed Energy (kW)	Evaporated Moisture (g)	MER (kg _w /h)	SMER (kg _w /kWh)	SEC (kWh/kg _w)	Drying Time (h)	
3 mm SEDS	2789.62	5.430	2344.90	0.39	0.43	2.32	6.00	
5 mm SEDS	3760.00	7.240	2895.13	0.35	0.40	2.50	8.16	
10 mm SEDS	6191.05	13.57	3901.47	0.26	0.29	3.44	14 (30.5)	
3 mm TESDS	2193.42	7.150	1817.24	0.29	0.25	4.00	6.16	
5 mm TESDS	3106.76	9.280	2538.04	0.32	0.27	3.70	8.00	
10 mm TESDS	5093.38	9.470	3359.92	0.41	0.35	2.85	8.16	
3mm HPDS	2310.92	9.548	1914.00	0.35	0.20	5.00	5.50	
5 mm HPDS	2490.28	12.60	2118.35	0.28	0.17	5.88	7.50	
10 mm HPDS	3048.00	24.64	2507.53	0.18	0.10	10.0	14.0	

<i>Food analysis results of peach slices</i>								
	Moisture content (kg _{water} /kg _{drymatter})	Water Activity (aw)	L^* (Brightness)	a^* (redness)	b^* (yellowness)	ΔE	ΔC	Shear Force (N)
Color values of fresh peach			61.82±0.15	15.09±0.07	41.85±0.11	0	0	2.94
3 mm SEDS	0.91±0.87 ^e	0.536±0.016 ^b	63.96±0.03 ^c	12.92±0.57 ^d	43.75±0.50 ^d	3.59±0.27 ^g	2.88±0.45 ^f	15.57
5 mm SEDS	2.64±0.55 ^b	0.522±0.102 ^b	60.33±0.13 ^f	16.38±0.16 ^c	38.98±0.20 ^e	3.48±0.27 ^g	3.14±0.15 ^f	43.86
10 mm SEDS	2.75±0.38 ^b	0.520±0.099 ^b	58.78±0.43 ^g	20.37±0.26 ^a	44.02±0.13 ^d	6.46±0.19 ^f	5.70±0.25 ^e	91.81
3 mm TESDS	0.90±0.37 ^e	0.639±0.024 ^b	74.54±0.19 ^c	16.81±0.67 ^{bc}	50.79±0.22 ^b	15.64±0.33 ^c	9.10±0.14 ^c	35.95
5 mm TESDS	2.23±0.27 ^c	0.659±0.007 ^b	57.55±0.28 ^h	20.43±0.22 ^a	34.03±0.09 ^f	10.38±0.41 ^e	9.45±0.33 ^c	86.83
10 mm TESDS	3.29±0.45 ^a	0.912±0.035 ^a	51.61±0.44 ⁱ	21.41±0.43 ^a	38.59±0.34 ^e	12.44±0.55 ^d	7.11±0.15 ^d	68.43
3mm HPDS	1.63±0.93 ^d	0.658±0.053 ^b	77.00±0.12 ^a	8.77±0.60 ^c	51.35±0.34 ^b	18.98±0.47 ^b	11.41±0.32 ^b	45.85
5 mm HPDS	1.56±0.37 ^d	0.659±0.006 ^b	75.48±0.27 ^b	7.66±0.35 ^c	49.73±0.20 ^c	21.57±0.44 ^a	10.83±0.26 ^b	40.63
10 mm HPDS	1.87±0.75 ^d	0.587±0.026 ^b	72.15±0.20 ^d	17.9±0.47 ^b	56.33±0.15 ^a	18.01±0.25 ^b	14.75±0.04 ^a	87.77

a - 1 Different letters within rows are significantly different ($P<0.05$)

4. Conclusions

Three different dryer types have been investigated in this study. Solar air-heated, solar with thermal energy storage, and heat-pump dryers were used to dry the peach slices. The heat storage unit loaded with basalt stone was put into operation for the continuity of drying during the hours when there is no daylight.

In the drying process using SEDS, the drying times of 3-, 5-, and 10-mm thicknesses were determined as 6, 8, and 14 hours, respectively. A 10 mm-thick peach slice was kept in the system for a total of 30.5 hours, and drying took place within 14 hours of this time. The remaining times passed as the period when drying was unavailable during the night. The drying was spread over two days. In the drying process with TESDS, the heat storage system was activated at the time when the solar radiation values were insufficient for drying. In 5- and 10-mm-thick peach slices, the drying air temperature increased with the heat taken from the heat storage system, and drying was carried out at low radiation values. In the dryer with a heat pump, drying times of 5.5, 7.5, and 14 hours were obtained, respectively, for all three thicknesses at constant drying temperatures.

Considering the amount of energy consumed, it is seen that the heat pump system consumes more energy than the solar energy system. The advantage of solar energy systems in terms of energy consumption has clearly emerged. In addition, the

drying time was shortened using the heat storage system, which resulted in savings in energy consumption. A decrease in SEC values was observed with the commissioning of the heat storage solar dryer.

This study not only demonstrates the effects of different dryer types on drying performance but also offers guidance on the use of thermal energy storage systems in drying applications. Drying food products of high quality in the shortest time with the lowest energy consumption should be the main target, and studies should be continuously improved in this direction.

Abbreviations

SEDS	Solar energy drying system
TESDS	Thermal energy storage drying system
HPDS	Heat pump drying system
SMER	Specific moisture extraction rate, kg _w /kWh
MER	Moisture extraction rate, kg _w /h
SEC	Specific energy consumption, kWh/kg _w
MoR	Moisture removed
EC	Energy consumed during drying
DT	Drying time
Nomenclature	
aw	Water activity
P	Vapor pressure of product, Pa
P ₀	Vapor pressure of pure water, Pa
L*	Brightness value
a*	Redness value
b*	Yellowness value
ΔE	Total color difference
ΔC	Color intensity

References

- Abubakar S, Umaru S, Kaisan M U, Umar U A, Ashok B & Nanthagopal K (2018). Development and performance comparison of mixed-mode solar crop dryers with and without thermal storage. *Renewable Energy* 128: 285–298. <https://doi.org/10.1016/j.renene.2018.05.049>
- Akin A, Gurlek G & Ozbalta N (2014). Mathematical model of solar drying characteristics for pepper (*Capsicum Annuum*). *Journal of Thermal Science and Technology* 34(2): 99-109
- Akpinar E K (2010). Drying of mint leaves in a solar dryer and under open sun: Modelling, performance analyses. *Energy Conversion and Management* 51(12): 2407–2418. <https://doi.org/10.1016/j.enconman.2010.05.005>
- Aktaş M, Koşan M, Çatalbaş C & Gök M (2019). Drying of Sliced Apple and Carrot with Heat Pump Technique: Performance Analysis (In Turkish). *Journal of Polytechnic* 22(3): 523-529. <https://doi.org/10.2339/politeknik.534443>
- Atalay H (2019). Comparative assessment of solar and heat pump dryers with regards to exergy and exergoeconomic performance. *Energy* 189: 116180. <https://doi.org/10.1016/j.energy.2019.116180>
- Atalay H (2020). Assessment of energy and cost analysis of packed bed and phase change material thermal energy storage systems for the solar energy-assisted drying process. *Solar Energy* 198: 124–138. <https://doi.org/10.1016/j.solener.2020.01.051>
- Ayyappan S, Mayilsamy K & Sreenarayanan V V (2016). Performance improvement studies in a solar greenhouse drier using sensible heat storage materials. *Heat and Mass Transfer* 52(3): 459–467. <https://doi.org/10.1007/s00231-015-1568-5>
- Baniasadi E, Ranjbar S & Boostanipour O (2017). Experimental investigation of the performance of a mixed-mode solar dryer with thermal energy storage. *Renewable Energy* 112: 143–150. <https://doi.org/10.1016/j.renene.2017.05.043>
- Baysal T, Ozbalta N, Gokbulut S, Capar B, Tastan O & Gurlek G (2015). Investigation of effects of various drying methods on the quality characteristics of apple slices and energy efficiency. *Journal of Thermal Science and Technology* 35(1): 135–144
- Bourdoux S, Li D, Rajkovic A, Devlieghere F & Uyttendaele M (2016). Performance of Drying Technologies to Ensure Microbial Safety of Dried Fruits and Vegetables. *Comprehensive Reviews in Food Science and Food Safety* 15(6): 1056-1066. <https://doi.org/10.1111/1541-4337.12224>
- Chaouch W B, Khellaf A, Mediani A, Slimani M E A, Loumani A & Hamid A (2018). Experimental investigation of an active direct and indirect solar dryer with sensible heat storage for camel meat drying in Saharan environment. *Solar Energy* 174: 328–341. <https://doi.org/10.1016/j.solener.2018.09.037>
- Fudholi A, Sopian K, Othman M Y & Ruslan M H (2014). Energy and exergy analyses of solar drying system of red seaweed. *Energy and Buildings* 68: 121–129. <https://doi.org/10.1016/j.enbuild.2013.07.072>
- Ganjehsarabi H, Dincer I & Gungor A (2014). Exergoeconomic Analysis of a Heat Pump Tumbler Dryer. *Drying Technology* 32(3): 352–360. <https://doi.org/10.1080/07373937.2013.829853>
- García-Moreira D P, Hernández-Guzmán H, Pacheco N, Cuevas-Bernardino J C, Herrera-Pool E, Moreno I & López-Vidaña E C (2023). Solar and Convective Drying: Modeling, Color, Texture, Total Phenolic Content, and Antioxidant Activity of Peach (*Prunus persica* (L.) Batsch) Slices. *Processes* 11(4): 1280. <https://doi.org/10.3390/pr11041280>

- Goh L J, Othman M Y, Mat S, Ruslan H & Sopian K (2011). Review of heat pump systems for drying application. *Renewable and Sustainable Energy Reviews* 15(9): 4788–4796. <https://doi.org/10.1016/j.rser.2011.07.072>
- Gunerhan H & Hepbasli A (2005). Utilization of Basalt Stone as a Sensible Heat Storage Material. *Energy Sources* 27(14): 1357–1366. <https://doi.org/10.1080/009083190523253>
- Gürlek G, Akdemir Ö & Güngör A (2015). Usage of Heat Pump Dryer in Food Drying Process and Apple Drying Application. *Pamukkale University Journal of Engineering Sciences* 21(9): 398–403. <https://doi.org/10.5505/pajes.2015.35761>
- Gürlek G, Özbalta N & Güngör A (2009). Solar tunnel drying characteristics and mathematical modelling of tomato. *Journal of Thermal Science and Technology* 29(1): 15–23
- Hartlieb P, Toifl M, Kuchar F, Meisels R & Antretter T (2016). Thermo-physical properties of selected hard rocks and their relation to microwave-assisted comminution. *Minerals Engineering* 91: 34–41. <https://doi.org/10.1016/j.mineng.2015.11.008>
- Hepbasli A, Colak N, Hancioglu E, Icier F & Erbay Z (2010). Exergoeconomic Analysis of Plum Drying in a Heat Pump Conveyor Dryer. *Drying Technology* 28(12): 1385–1395. <https://doi.org/10.1080/07373937.2010.482843>
- Huang L, Zhang M, Mujumdar A S & Lim R (2011). Comparison of four drying methods for re-structured mixed potato with apple chips. *Journal of Food Engineering* 103(3): 279–284. <https://doi.org/10.1016/j.jfoodeng.2010.10.025>
- Kant K, Shukla A, Sharma A, Kumar A & Jain A (2016). Thermal energy storage based solar drying systems: A review. *Innovative Food Science & Emerging Technologies* 34: 86–99. <https://doi.org/10.1016/j.ifset.2016.01.007>
- Karaaslan S, Ekinci K, Ertekin C & Kumbul B S (2021). Thin layer peach drying in solar tunnel drier. *Erwerbs-Obstbau* 63(1): 65–73. <https://doi.org/10.1007/s10341-020-00536-4>
- Kohli D, Champawat P S, Jain S K, Mudgal V D & Shahi N C (2021). Mathematical modelling for drying kinetics of asparagus roots (*Asparagus Racemosus* L.) and determination of energy consumption. *Biointerface Research in Applied Chemistry* 12(3): 3572–3589. <https://doi.org/10.33263/BRIAC123.35723589>
- Lee J H & Kim H J (2009). Vacuum drying kinetics of Asian white radish (*Raphanus sativus* L.) slices. *LWT - Food Science and Technology* 42(1): 180–186. <https://doi.org/10.1016/j.lwt.2008.05.017>
- Liu M, Wang S, Liu R & Yan J (2019). Energy, exergy and economic analyses on heat pump drying of lignite. *Drying Technology* 37(13): 1688–1703. <https://doi.org/10.1080/07373937.2018.1531883>
- Mirzabeigi Kesbi O, Sadeghi M & Mireei S A (2016). Quality assessment and modeling of microwave-convective drying of lemon slices. *Engineering in Agriculture, Environment and Food* 9(3): 216–223. <https://doi.org/10.1016/j.eaef.2015.12.003>
- Nahhas T, Py X & Sadiki N (2019). Experimental investigation of basalt rocks as storage material for high-temperature concentrated solar power plants. *Renewable and Sustainable Energy Reviews* 110: 226–235. <https://doi.org/10.1016/j.rser.2019.04.060>
- Nakilcioğlu-Taş E & Ötleş S (2018). Colour change kinetics of the inner and outer surface of brussels sprouts during microwave drying process. *Journal of Agricultural Sciences* 24(4): 488–500.
- Natarajan K, Thokchom S S, Verma T N & Nashine P (2017). Convective solar drying of *Vitis vinifera* & *Momordica charantia* using thermal storage materials. *Renewable Energy* 113: 1193–1200. <https://doi.org/10.1016/j.renene.2017.06.096>
- Nindo C I, Sun T, Wang S W, Tang J & Powers J R (2003). Evaluation of drying technologies for retention of physical quality and antioxidants in asparagus (*Asparagus officinalis*, L.). *LWT - Food Science and Technology* 36(5): 507–516. [https://doi.org/10.1016/S0023-6438\(03\)00046-X](https://doi.org/10.1016/S0023-6438(03)00046-X)
- Orikasa T, Wu L, Shiina T & Tagawa A (2008). Drying characteristics of kiwifruit during hot air drying. *Journal of Food Engineering* 85(2): 303–308. <https://doi.org/10.1016/j.jfoodeng.2007.07.005>
- Polat A, Taşkin O & İzli N (2021). Application of drying techniques on peach puree. *Tarım Bilimleri Dergisi* <https://doi.org/10.15832/ankutbd.595857>
- Qiu Y, Li M, Hassanien R H E, Wang Y, Luo X & Yu Q (2016). Performance and operation mode analysis of a heat recovery and thermal storage solar-assisted heat pump drying system. *Solar Energy* 137: 225–235. <https://doi.org/10.1016/j.solener.2016.08.016>
- Queiroz R, Gabas A L & Telis V R N (2004). Drying kinetics of tomato by using electric resistance and heat pump dryers. *Drying Technology* 22(7): 1603–1620. <https://doi.org/10.1081/DRT-200025614>
- Rehman H U, Naseer F & Ali H M (2023). An experimental case study of solar food dryer with thermal storage using phase change material. *Case Studies in Thermal Engineering* 51: 103611. <https://doi.org/10.1016/j.csite.2023.103611>
- Saidani F, Giménez R, Aubert C, Chalot G, Betrán J A & Gogorcena Y (2017). Phenolic, sugar and acid profiles and the antioxidant composition in the peel and pulp of peach fruits. *Journal of Food Composition and Analysis* 62: 126–133. <https://doi.org/10.1016/j.jfca.2017.04.015>
- Şevik S, Aktaş M, Dolgun E C, Arslan E & Tuncer A D (2019). Performance analysis of solar and solar-infrared dryer of mint and apple slices using energy-exergy methodology. *Solar Energy* 180: 537–549. <https://doi.org/10.1016/j.solener.2019.01.049>
- Singh D, Mishra S & Shankar R (2022). Drying kinetics and performance analysis of indirect solar dryer integrated with thermal energy storage material for drying of wheat seeds: an experimental approach. *Energy Sources, Part A: Recovery, Utilization, and Environmental Effects* 44(3): 7967–7985. <https://doi.org/10.1080/15567036.2022.2118907>
- Tan S, Miao Y, Zhou C, Luo Y, Lin Z, Xie R & Li W (2022). Effects of hot air drying on drying kinetics and anthocyanin degradation of blood-flesh peach. *Foods* 11(11): 1596. <https://doi.org/10.3390/foods11111596>
- Vijayan S, Arjunan T V & Kumar A (2020). Exergo-environmental analysis of an indirect forced convection solar dryer for drying bitter gourd slices. *Renewable Energy* 146: 2210–2223. <https://doi.org/10.1016/j.renene.2019.08.066>
- Yahya M, Fahmi H, Fudholi A & Sopian K (2018). Performance and economic analyses on solar-assisted heat pump fluidised bed dryer integrated with biomass furnace for rice drying. *Solar Energy* 174: 1058–1067. <https://doi.org/10.1016/j.solener.2018.10.002>



